CONFERENCE PROCEEDINGS

Third International Conference on Advances in Concrete and Construction Engineering for Sustainability (ICACC 2024)



HYBRID MODE

April 26-27, 2024



SCOPUS Indexed Publication

IOP Conference Series Earth and Environmental Science

Issue 1 - Volume 1409 : IOP Conference Series: Earth and Environmental Science IOP Science

Accepted papers received: October 23, 2024 • Published online: November 26, 2024



Organized by

Department of Civil Engineering

VASAVI COLLEGE OF ENGINEERING, HYDERABAD, INDIA

(Private Un-aided Non-minority Autonomous Institution)

ACCREDITED BY NAAC WITH 'A++' GRADE

Affiliated to Osmania University and Approved by AICTE

44 YEARS OF EXCELLENCE

In association with

POORNIMA COLLEGE OF ENGINEERING

Affiliated to RTU, Kota • Approved by AICTE & UGC under 2(f) • NAAC A+ Accredited

CELEBRATING 25 YEARS OF EXCELLENCE

SITAPURA, JAIPUR-302022 (RAJASTHAN), INDIA

Proceedings Link: **https://iopscience.iop.org/issue/1755-1315/1409/1**

PROCEEDINGS EDITOR(S)



Dr. K.V.L. Subramaniam
Professor, Dept. of Civil, IIT Hayderabad, India
Chief Editor: ICACCES 2024



Dr. S. Vijaya Kumar
Associate Professor
Dept. of Civil, VCE, India
Organizing Chair: ICACCES 2024



Dr. M.V.S.S. Sastri
Associate Professor
Dept. of Civil, VCE, India
Organizing Chair: ICACCES 2024



Dr. Raj Kumar Satankar
Associate Professor
ME, PCE. Jaipur, India
Organizing Secretary: ICACCES 2024

EDITORIAL BOARD



Dr. S.V. Ramana
Principal, VCE, Hyderabad, India
General Chair, ICACCES 2024



Prof. (Dr.) Mahesh M. Bundele
Director & Principal, PCE, Jaipur, India
General Chair, ICACCES 2024



Dr. B Sridhar
Prof. & Head, Dept. of CE, VCE, India
Organizing Chair, ICACCES 2024



Dr. Pankaj Dhemla
Vice Principal, PCE, Jaipur, India
Organizing Chair, ICACCES 2024



Dr. Narayan Lal Jain
HOD, ME, PCE, Jaipur, India
Organizing Chair, ICACCES 2024



Vasavi College of Engineering
(Private Un-aided Non-minority Autonomous Institution)
ACCREDITED BY NAAC WITH 'A++' GRADE
Affiliated to Osmania University and Approved by AICTE.







Third International Conference on Advances in Concrete and Construction Engineering for Sustainability (ICACC 2024)

April 26-27, 2024

(HYBRID MODE)

Editor(s)

Dr. Kolluru V.L. Subramaniam
Professor, Department of Civil Engineering, IIT Hyderabad, India

Dr. Raj Kumar Satankar
Associate Professor, Department of Mechanical Engineering, Poornima College of Engineering, Jaipur, India

Dr. S. Vijaya Kumar
Associate Professor, Department of Civil Engineering, Vasavi College of Engineering, Hyderabad, India

Dr. M.V.S.S. Sastri
Associate Professor, Department of Civil Engineering, Vasavi College of Engineering, Hyderabad, India

ORGANISING INSTITUTE

Vasavi College of Engineering, Hyderabad, India
in association with
Poornima College of Engineering, Jaipur, India

Content from this work may be used under the terms of the Creative Commons Attribution 4.0 licence. Any further distribution of this work must maintain attribution to the author(s) and the title of the work, journal citation and DOI.
Published under licence by IOP Publishing Ltd

PREFACE

This volume contains selected articles from the Third International Conference on Advances in Concrete and Construction Engineering for Sustainability (ICACC 2024) held on 26-27th April 2024 at Vasavi College of Engineering (A), Hyderabad, Telangana, India and jointly organized by Poornima College of Engineering, Jaipur, India. The eminent gatherings are meticulously organized by the Vasavi College of Engineering and the Poornima College of Engineering. The ICACC 2024 conference offered a great opportunity to bring together professors, researchers, consultants, and scholars around the globe as a great platform to deliver the latest innovations. Sustainability is crucial for mitigating environmental challenges like climate change, resource depletion, and pollution. The conference explores how innovation in construction methods, materials, and emerging technologies can mitigate these challenges by reducing greenhouse gas emissions, minimizing waste generation, optimizing resource use, and enhancing infrastructure resilience. The conference's themes have been selected accordingly so that it could foster communication among researchers and practitioners working in a wide variety of the above areas in Civil and Environmental Engineering. The potential number of participants gather at ICACC 2024 to present research results, share visions and ideas, obtain updates on the latest technologies, and expand professional and social networking. One of the notable objectives of these conferences is to construct a robust scientific communication bridge, connecting researchers in India and abroad in engineering sciences. This bridge is designed to facilitate the exchange of ideas, experiences, and expertise, promoting collaboration and knowledge sharing on an international scale.

The articles covered a wide spectrum of themes in civil engineering, including but not limited to Infrastructure, geotechnical, sustainability, and environmentally friendly applications. The contributing authors are researchers in their respective fields from several universities and Colleges belonging to different countries. This book will prove a valuable resource for practicing engineers and researchers in the fields of geotechnical engineering, environmental engineering, structural engineering, construction materials, and management of projects.

International Conference on Advances in Concrete and Construction Engineering for Sustainability (ICACC 2024) kicked off with great enthusiasm and anticipation in a hybrid mode, with an invocation of blessings from God Vigneshwara. This conference brought together experts, researchers, practitioners, and industry professionals from around the globe to delve into the latest advancements in concrete and construction engineering aimed at fostering sustainability. In the beginning, Dr. S. Vijayakumar, the Organising Secretary informed them about the conference, and its outline to the guest and participants. The ceremony commenced with a welcome address by the conference

Patron Dr. S, V. Ramana, Principal, of Vasavi College of Engineering, highlighting the significance of sustainable practices in the construction industry and the role of innovation in achieving these goals. Dr. Mahesh Bundele, Principal & Director, of Poornima College of Engineering has shared his insights on emerging trends, challenges, and opportunities in concrete and construction engineering. Dr. B. Sridhar, Professor and Head of Civil Engineering, VCE, also addressed the audience and expressed his views about the conference theme and its organizational motives. The Chief Guest of the inaugural session Professor Ir. Dr U. Johnson Alengaram, Professor & Director, Centre for Innovative Construction Technology, University of Malaya, Kuala Lumpur, Malaysia commends the organizers for convening this important event, which provides a platform for collaboration, knowledge sharing, and the exchange of ideas. Professor stated Concrete, as one of the most widely used construction materials, plays a pivotal role in shaping the sustainability of our infrastructure. As we strive to mitigate the environmental impact of construction activities, it is essential to explore innovative approaches to concrete production, design, and utilization. This includes embracing alternative materials, optimizing mix designs, and adopting advanced construction techniques that minimize resource consumption and carbon emissions. Moreover, sustainability encompasses not only environmental considerations but also social and economic dimensions.

Subsequently, the inaugural session transitioned into two keynote presentations delivered by Dr U. Johnson Alengaram, Professor & Director, Centre for Innovative Construction Technology, University of Malaya, Kuala Lumpur, Malaysia. Dr. U. Johnson Alengaram's presentation centered on "Valorisation of Low-Carbon Footprint Materials and Construction of Low-cost Model House & Cement-Free Geopolymer Concrete House for Bus Drivers". In the second keynote speech by Dr. Bindumadhava Aery, Technical Director, Infrastructure, Aurecon, Greater Brisbane Area, Australia, on "Sustainability in Geotechnical Engineering" Following the inaugural events, the first day featured the organization of three parallel technical sessions, wherein authors and participants actively engaged in presenting their research papers. The research papers in this conference were invited considering these three tracks:

- Advances and Sustainability in Structural Engineering
- Sustainability in Transportation and Geotechnical Engineering
- Environment and Sustainability.

The first technical session in offline mode was chaired by Dr. M.V. Rama Rao, Professor, Vasavi College of Engineering, Hyderabad, Telangana, India, and the session moderator was Dr. S. Vijaya Kumar and a total of 15 authors presented their papers. The second technical session was chaired by Dr. A. Ramesh, Professor, Department of Civil

Engineering, VNRVJIT, Hyderabad, India, and the session moderator was Dr. C. Mohan Lal, Vasavi College of Engineering, Hyderabad, India. In the second session total of 11 presenters were allowed to present their papers. Dr. Ashish Kumar Nayak, PVPSIT, Vijayawada, Andhra Pradesh, India chaired the third technical session and the session moderators were Dr. B. Narender, Anurag University, Hyderabad, India, and the second Moderator Dr Raj Kumar Satankar. Poornima College of Engineering, Jaipur, India. In the last session, a total of 15 papers were presented.

The second day of the ICACC 2024 conference commenced with a keynote session delivered by Dr. Meghna Sharma, Assistant Professor at the National Institute of Technology Hamirpur, Himachal Pradesh, India. The session focused on "Nature-Based Solutions for Ground Improvement and Future Opportunities in Geotechnical Engineering." Following this, two technical sessions were organized, chaired by Dr. K. Jagannadha Rao, Professor and Head, of the Department of Civil Engineering at the Chaitanya Bharathi Institute of Technology, Hyderabad, Telangana, India, and Dr. D. Rupesh Kumar, Professor in the Department of Civil Engineering at the University College of Engineering, Osmania University, Hyderabad, Telangana, India. The sessions were moderated by Prof. Krati Sarma and Prof. S. Kesav Kumar from the Vasavi College of Engineering, Hyderabad. In total, 22 papers were presented on the second day of the conference. Later, a keynote talk on "Making Concrete Sustainable and Moving Towards Net Zero" was delivered by Dr. K.V.L. Subramaniam, Professor in the Department of Civil Engineering at the Indian Institute of Technology, Hyderabad, India.

Concluding the proceedings of the second day, the valedictory ceremony welcomed Dr. K.V.L. Subramaniam, Professor and Former Head of the Department of Civil Engineering at the Indian Institute of Technology, as the distinguished Chief Guest. Concurrently, the event also featured Er. Sneha Redla, Vice President of Aarvee Associates, Director of Aarvee Australia & UK, and CEO of Hyve Global Engineering Pvt Ltd in Telangana, India, graced the occasion as an esteemed Chief Guest. The conference report, presented by Dr. S. Vijaykumar, the Organizing Secretary of ICACC 2024, highlighted key themes, notable presentations, and innovative solutions discussed throughout the event. The event culminated as a resounding success, characterized by insightful addresses and sessions delivered by esteemed individuals, wholehearted participation from all our authors, co-authors, and attendees, as well as the dedicated contributions of an expert team of reviewers, coordinators, staff members, and organizing team members. The chief guests and other dignitaries shared their reflections on the conference outcomes and emphasized the importance of continuing the momentum generated by ICACC 2024. At the occasion, tokens of appreciation were presented to the organizing team members, recognizing the achievements of individuals and organizations who demonstrated excellence and leadership in conference organization.

The Vasavi College of Engineering, Hyderabad, Telangana, India and Poornima College of Engineering, Jaipur, Rajasthan, India are leading engineering colleges in India that have the capabilities to organize intranational conferences annually in cooperation with local and international universities and societies. The various committees associated with this conference are as follows

INTERNATIONAL ADVISORY COMMITTEE

- Dr. Indubhushan Patanaikuni, RMIT, Australia
- Dr. Chandrashekhar Putcha, CSU, USA
- Dr. Venkatesh Kodur, MSU, USA
- Dr. U. Jhonson Alengram, University of Malaya, Malaysia
- Dr. Stefano Gabriele, Università Degli Studi Roma Tre, Italy
- Dr. Andrew Pownuk, The University of Texas, USA
- Dr. Amedeo Manuello Bertetto, Politecnico di Torino, Italy
- Dr. Sreevasta Nippani, Maricopa Association of Governments, USA
- Er. Chris Francis, SRF Consulting, USA

NATIONAL ADVISORY COMMITTEE

- Dr. S. Suriya Prakash, IIT Hyderabad, India
- Dr. D. Ramaseshu, NIT, Warangal, India
- Dr. N. Uma Mahesh, NIT, Warangal, India
- Dr. Shamsher Bahadur Singh, BITS- Pilani, India
- Dr. K. Balaji Rao, SERC, Chennai, India
- Dr. K. Srinivasa Raju, BITS-Pilani, Hyderabad, India
- Dr. V. Vinayak Ram, BITS Pilani Hyderabad, India
- Dr. M. Kumar, Osmania University, Hyderabad, India
- Dr. V. Bhikshma, Osmania University, Hyderabad, India
- Dr. P. Rajasekhar, Osmania University, Hyderabad, India
- Dr. B. Dean Kumar, JNTU Hyderabad, India
- Dr. K. M. Laxmana Rao, JNTU, Hyderabad, India
- Dr. K. Jagannadha Rao, CBIT (A), Hyderabad, India
- Dr. S. Bhasker, SERC, Chennai, India

TECHNICAL PROGRAM COMMITTEE

- Dr. Er. Rama Rao Karri, Universiti Teknologi, Brunei
- Dr. Kumar Pallav, CPUT, South Africa
- Dr. Basuraj Bhowmik, IIT, BHU, India
- Dr. Prashanth Vangla, IIT, Delhi, India
- Dr. Prarthita Basu, SRI, New Delhi, India
- Dr. Amol D. Pawar, NICMAR University Pune, India
- Dr. Venkata Dilip Kumar P, Mahendra University, India

- Dr. Sri Kalyana Rama J, Mahendra University, India
- Dr. Ashish Kumar Nayak, PVPSIT, Vijayawada, India

ORGANIZING COMMITTEES

CHIEF PATRONS

- Sri. P. Ramamohan Rao, President, VAE, Hyderabad, India
- Sri. M. Krishna Murthy, Secretary, VAE, Hyderabad, India

PATRONS

- Dr. S.V. Ramana, Principal, VCE, Hyderabad, India
- Dr Mahesh Bundele, Principal & Director, PCE, Jaipur, India

ORGANISING CHAIR

- Dr. B. Sridhar, Professor & Head, Department of Civil Engineering, Vasavi College Engineering, Hyderabad, India
- Dr. Pankaj Dhemla, Professor & Vice Principal, Department of Civil Engineering, Poornima College of Engineering, Jaipur, India
- Dr. Narayan Lal Jain, Professor & Head, Department of Mechanical Engineering, Poornima College of Engineering, Jaipur, India

ORGANISING CO-CHAIR

- Dr. M.V. Rama Rao, Professor, Department of Civil Engineering, Vasavi College Engineering, Hyderabad, India

ORGANIZING SECRETARIES

- Dr. S. Vijaya Kumar, Associate Professor, Department of Civil Engineering, Vasavi College of Engineering, Hyderabad, India
- Dr. M.V.S.S. Sastri, Associate Professor, Department of Civil Engineering, Vasavi College of Engineering, Hyderabad, India
- Dr. Raj Kumar Satankar, Associate Professor, Department of Mechanical Engineering, Poornima College of Engineering, Jaipur, India

LIST OF REVIEWERS

- Dr. B. Narender, Anurag University School of Engineering, Hyderabad, Telangana, India
- Dr. Bharath Kumar Dudam, Chaitanya Bharathi Institute of Technology, Hyderabad, Telangana, India
- Prof. Boddu Jagadeesh, Vasavi College of Engineering, Hyderabad, Telangana, India
- Prof.Dhatri. P, Vasavi College of Engineering, Hyderabad, Telangana, India
- Dr. Harikrishna Damera, Kakatiya Institute of Technology and Science, Warangal, Telangana, India
- Dr. Abhiroop Chowdhury, Jindal School of Environment & Sustainability, O. P. Jindal Global

University

- Dr. Raj Kumar Satankar, Poornima College of Engineering, Jaipur, Rajasthan, India
- Dr. C.S.V.Subrahmanya Kumar, Maturi Venkata Subba Rao Engineering College, Hyderabad, Telangana, India
- Prof. Guntuka Srinivas, Vasavi College of Engineering, Hyderabad, Telangana, India
- Prof. Krati Sharma, Vasavi College of Engineering, Hyderabad, Telangana, India
- Dr. Kuchu Jayasree, Vasavi College of Engineering, Hyderabad, Telangana, India
- Prof. Lavanya Bukke, Sreenidhi Institute of Science and Technology, Hyderabad, Telangana, India
- Dr . Maddhinni Vasantha Laxmi, Vasavi College of Engineering, Hyderabad, Telangana, India
- Dr. Manasa Kotha, Chaitanya Bharathi Institute of Technology, Hyderabad, Telangana, India
- Dr. Mohammed Abdul Kalam, Deccan College of Engineering and Technology, Hyderabad, Telangana, India
- Dr. Mohan Lal Chowdary, Vasavi College of Engineering, Hyderabad, Telangana, India
- Prof. Mulley Preethi, Deccan College of Engineering and Technology, Hyderabad, Telangana, India
- Prof. P. Ashveen Kumar, Matrusri Engineering College, Hyderabad, Telangana, India
- Dr. Rajani Kumar Kommera, Vasavi College of Engineering, Hyderabad, Telangana, India
- Dr. N.R. Dakshina Murthy, Chaitanya Bharathi Institute of Technology, Hyderabad, Telangana, India
- Prof. S Kesav Kumar Arnepalli, Vasavi College of Engineering, Hyderabad, Telangana, India
- Dr. S. Vijaya Kumar, Vasavi College of Engineering, Hyderabad, Telangana, India
- Dr. M.V.S.S. Sastri, Vasavi College of Engineering, Hyderabad, Telangana, India
- Dr. Satish Sajja, Velagapudi Ramakrishna Siddhartha Engineering College, Vijayawada, Andhra Pradesh, India
- Dr. Shiv Sankar Das, Centurion University of Technology and Management, Odisha, India
- Dr. Shravankumar S.M., Sreenidhi Institute of Science and Technology, Hyderabad, Telangana, India
- Dr. Sri Kalyana Rama J, Mahindra University Ecole Centrale School of Engineering, Hyderabad, Telangana, India
- Dr. Srihari Vedartham, National Institute of Construction Management and Research, Hyderabad, Telangana, India
- Dr. T. Muralidhara Rao, CVR College of Engineering. Ibrahimpatan campus, Hyderabad, Telangana, India
- Dr. Yashwanth Pamu, CVR College of Engineering, Ibrahimpatan campus, Hyderabad, Telangana, India

IOP Conference Series: Earth and Environmental Science

PURPOSE-LED PUBLISHING™

OPEN ACCESS

Peer Review Statement

To cite this article: 2024 *IOP Conf. Ser.: Earth Environ. Sci.* **1409** 011002

View the article online for updates and enhancements.

You may also like

- Peer Review Statement
- Peer Review Statement
- Peer Review Statement



This content was downloaded from IP address 47.247.77.11 on 27/11/2024 at 05:27

Peer Review Statement

All papers published in this volume have been reviewed through processes administered by the Editors. Reviews were conducted by expert referees to the professional and scientific standards expected of a proceedings journal published by IOP Publishing.

- **Type of peer review:** Double Anonymous
- **Conference submission management system:** Morressier
- **Number of submissions received:** 102
- **Number of submissions sent for review:** 98
- **Number of submissions accepted:** 63
- **Acceptance Rate (Submissions Accepted / Submissions Received × 100):** 61.8
- **Average number of reviews per paper:** 2.4761904761904763
- **Total number of reviewers involved:** 27
- **Contact person for queries:**
  Name: ICACC 2024
  Email: icacc.vce@gmail.com
  Affiliation: Vasavi Academy of Education - Vasavi College of Engineering

Content from this work may be used under the terms of the Creative Commons Attribution 4.0 licence. Any further distribution of this work must maintain attribution to the author(s) and the title of the work, journal citation and DOI.
Published under licence by IOP Publishing Ltd

IOP Conference Series: Earth and Environmental Science

PURPOSE-LED PUBLISHING™

PAPER • OPEN ACCESS

Unveiling the Potential of Hybrid Deep Learning Algorithm in Streamflow Projection

To cite this article: Rishith Kumar Vogeti *et al* 2024 *IOP Conf. Ser.: Earth Environ. Sci.* **1409** 012001

View the article online for updates and enhancements.

You may also like

- Attenuation characteristics of coda wave in Northern Aceh, Sumatra, Indonesia
T Anggono, S Syuhada, B Pranata et al.
- Grid-connected virtual synchronous generator transient suppression based on proportional differential control and frequency low-pass filtering
Shiyang Fu, Yan Tian, Jian Fang et al.
- Knowledge distillation-based abnormal power consumption pattern detection for edge environment
Yuanliang Fan, Han Wu, Zewen Li et al.



This content was downloaded from IP address 47.247.77.11 on 27/11/2024 at 05:30

Unveiling the Potential of Hybrid Deep Learning Algorithm in Streamflow Projection

Rishith Kumar Vogeti[1*], Rahul Jauhari[2], Bhavesh Rahul Mishra[3] and Pratyush Pandey[1]

[1]Department of Civil Engineering, BITS Pilani Hyderabad Campus, India
[2]Department of Computer Science and Information Systems, BITS Pilani Hyderabad Campus, India
[3]Department of Electrical and Electronics Engineering, BITS Pilani Hyderabad Campus, India

*E-mail: rishith26@gmail.com

Abstract. The present study aims to analyze the potential of a hybrid deep learning algorithm, GRU-RNN-LSTM, for mimicking streamflow and is evaluated using Kling Gupta Efficiency. The case study chosen was the Lower Godavari Basin. Grid search tuning was conducted for the chosen algorithm. GRU-RNN-LSTM has shown a good performance having Kling Gupta Efficiency values of 0.785, and 0.77 in training and testing segments respectively, and is further utilized for streamflow projection by making use of scenario, Shared Socioeconomic Pathway 585 (SSP585). The highest, Lowest, and Average streamflows expected are 2624 m^3/s, 599.03 m^3/s, and 703.36 m^3/s respectively. These projections could assist water resources planners in initiating long-term measures.

Keywords: Streamflow, GRU-RNN-LSTM, Hybrid deep learning algorithm, Grid search

1. Introduction

Modelling is an integral component of water resources planning and is expected to provide multifaceted insights into the behaviour of water systems under diverse climate conditions. Out of the number of approaches employed by various researchers, Deep Learning (DL) techniques are gaining attention in multiple sectors of water resources due to their flexibility and adaptability [1]. Over time, researchers are employing hybridization of DL algorithms to capture complex hydrological processes posed by spatial and temporal variability. They are expected to provide more precise streamflow projections for diverse hydrological situations [2], [3]. A brief literature review is presented to understand the journey of related DL techniques on the studied topic.

Convolutional Neural Networks (CNN) is frequently employed for streamflow projections because of their potential to extract spatial features via the convolution-pooling mechanism [4]. However, they are unsatisfactory in capturing temporal patterns within the data. Recurrent Neural Networks dealt with the challenge of CNN in capturing temporal patterns [5] through their recurring connections [6]. Long Short-Term Memory (LSTM) can tackle vanishing and exploding gradients by utilizing the gating units, one of the lacunae of Recurrent Neural Networks. [7] found LSTM showing dominance in simulating streamflow due to their capability of capturing complex relationships along with peak flows, as also echoed by [8]. However, they fell short in capturing short and mid-term dependencies. In addition, overfitting, random weight initialization, and an

Content from this work may be used under the terms of the Creative Commons Attribution 4.0 licence. Any further distribution of this work must maintain attribution to the author(s) and the title of the work, journal citation and DOI.
Published under licence by IOP Publishing Ltd

exhaustive training process are the difficulties. In this context, Gated Recurrent Unit (GRU) was employed due to its simple architecture, and reduced computational complexity [9] and researchers view it as a viable alternative to LSTM. Furthermore, several researchers suggested of combining two algorithms that would improve the streamflow simulation [2], [3]. In this regard, CNN-LSTM [10], variational mode decomposition-CNN-LSTM [11], CNN-GRU [12], and CNN-RNN [13] have demonstrated greater simulating abilities. In addition, the role of climate change is evident in every sphere of society, especially in the water sector. Many researchers utilized the Global Climate Model-Shared Socioeconomic Pathways (GCM-SSP) framework to analyze the impact of climate change [14]. As evident from the review of literature here and elsewhere, only one study was reported on examining the hybrid DL algorithm CNN-GRU-LSTM specific to streamflow simulation [15]. However, no studies were made using the hybrid algorithm from a climate change viewpoint. Accommodating the salient gap is the basis for formulating the objective of assessing the potential of a GRU-RNN-LSTM, for projecting streamflow in a climate change context using scenario SSP585.

The manuscript covers brief information about the case study, methodology, results, and discussion and conclusions.

2. Case study and data collection

The Lower Godavari Basin is situated between latitude 17° 00' to 19° 00' N and longitude 80° 00' to 83° 04' E. The basin shares boundaries with five states, as shown in Figure 1. Details including data used for modelling are presented in Table 1 [17].

Table 1. Details of the study area and data sources

Characteristic	Information/source
Length of the basin	462 km
Catchment area	39,180 km^2
Annual Rainfall	~1096 mm
Average temperature	26°C to 44°C
Average evaporation loss	~1401 to 2606 mm
Land Use and Land Cover Classes	Forests, Grasslands, Cultivated lands, Shrublands, Artificial surfaces and wetlands
Soil classes	Loam, Clayey loam and Sandy clayey loam
Historic rainfall, maximum, and minimum temperatures for 1982-2020	India Meteorological Department
Streamflow of Polavaram and Perur for 1982-2020	Central Water Commission
Future rainfall, and temperatures based on 13 GCMs in SSP585 for 2021-2095	[16]

The present study uses meteorological information for 52 grid locations covering study area for a time segment of 1982-2020. The observed streamflow is collected for Perur and Polavaram for the same segment for training purposes.

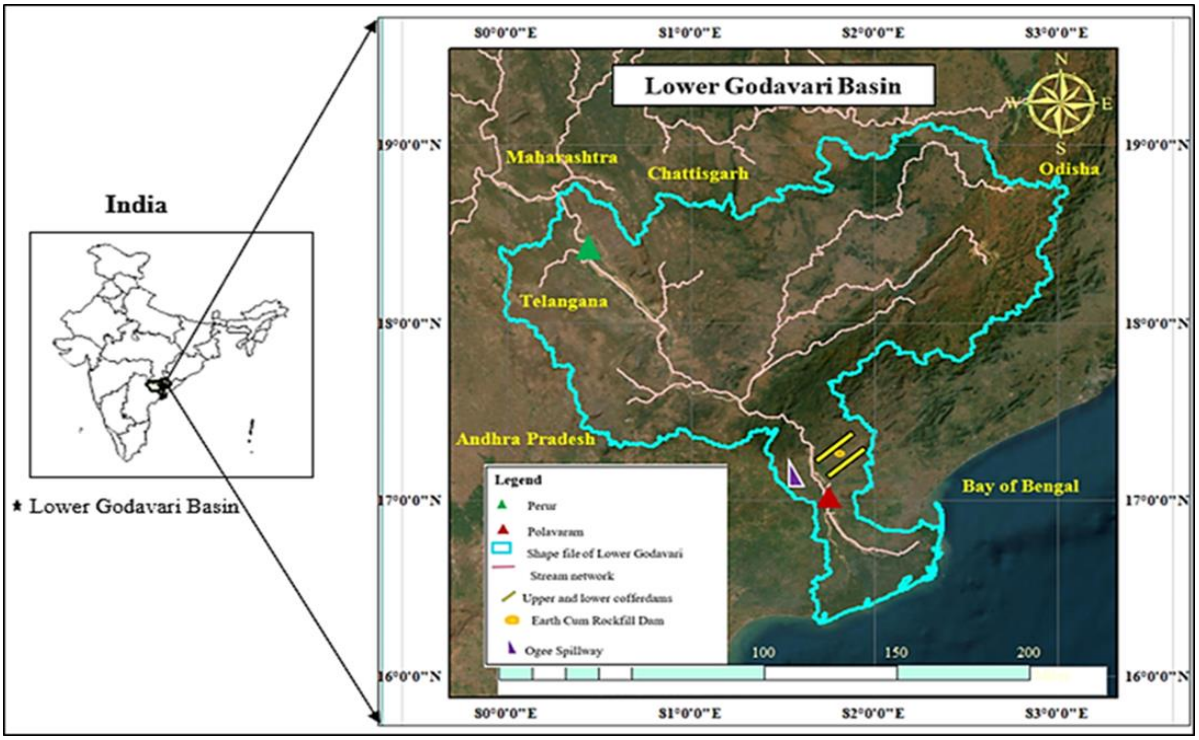


Figure 1. Lower Godavari Basin

3. Methodology

GRU-RNN-LSTM is used for mimicking streamflow and Kling Gupta Efficiency (KGE) is used to diagnose the employed algorithm [18]. Firstly, the input meteorological and observed streamflow are sent to GRU which works using a two-gate mechanism including update and reset gates for generating simulated outcomes. These outcomes are further sent as input to the RNN network. It makes use of recurrent connections to acquire information from one step to subsequent for generating outcomes. These are further transmitted into LSTM which utilizes forget, input, and output gates to generate the final simulated outcomes. The forget gate takes responsibility for controlling the unwanted information, the input gate allows the useful information whereas updated information is retrieved as an outcome in the output gate. Thus, the outcome generated using GRU-RNN-LSTM is expected to be superior as it captivates the strengths of LSTM, GRU, and RNN in capturing long-term, short-term [19] and mid-term temporal dependencies within the data overcoming exploding and vanishing gradients [20]. It is effective in capturing short-term temporal patterns within the data. The flowchart of the methodology is presented in Figure 2.

4. Results

Hyperparameter tuning of GRU-RNN-LSTM in training and testing (374 and 94 records), and streamflow projection in the climate change framework is presented here.

4.1. Hyperparameter Tuning and Evaluation

The grid search approach was employed for hyperparameter tuning, and related information is available in Table 2. The optimal configuration for GRU-RNN-LSTM involves using 128 neurons with a learning rate of 0.001, utilizing the ReLU activation function. In this architecture, the batch

sizes closer to the lower threshold, around 10, are preferred for better performance. A dropout rate of 0.5 is identified. This model demonstrates satisfactory performance, achieving KGE values of 0.785 in training and 0.77 in testing, making it suitable for streamflow projection. The interrelation between the number of neurons, learning rate, and other parameters significantly influences training convergence and overall performance.

Table 2. Information on hyperparameters

Parameters (1)	Range (2)	GRU-RNN-LSTM (3)
Number of neurons	8-256	128
Number of kernels and pooling	NA	NA
Activation function	ReLU, leakyrelu,Tanh	ReLU
Learning rate	0-1	0.001
Batch size	1-256	10
Dropout rate	0-1	0.5
Epochs	10 -1000	100
KGE (Training)	(– ∞ to 1)	0.785
KGE (Testing)	(– ∞ to 1)	0.77

Sieve analysis was conducted for GRU-RNN-LSTM to understand the percentage of frequency match between observed and mimicked streamflow. It was facilitated with four different magnitude bins categorized based on box plot analysis i.e., ≤25%, 25-50%, 50-75%, and ≥75%, which may be difficult to identify from a scatter or line plot. It also provides distributional characteristics, a central tendency similar to a box plot. Colour (red to blue) and hatching (coarser to finer) represent the frequency of the mimicked streamflow records within the corresponding range observed. Red or pale red colour with coarser hatching indicates a poor match. Blue colour with finer hatching suggests a good match. The frequency match is inferred as moderate if the colour of the diagonal bin is pale blue with coarser hatching.

In training, bin-wise observed records are 93, 94, 93, 94, whereas corresponding records mimicked are 60, 46, 52, 77 (refer Figure 3a). In continuation, the first quartile bin (≤79.45 m^3/s) has 64.5% of mimicked values that match the observed, represented by blue colour-moderate hatching. Similarly, the percentage of mimicked values are 48.9, 55.9, and 81.9 for the second quartile bin (79.45 – 143.345 m^3/s) with pale blue-light coarse, third quartile bin (143.345-977.25 m^3/s) with pale blue- light coarse and fourth quartile bin (≥977.25 m^3/s) with dark blue-fine hatching respectively. A higher correlation is observed in the fourth quartile bin, indicating the ability of the algorithm to mimic a higher magnitude.

In testing, mimicked records are 16, 11, 13, and 20 against observed records of 23, 24, 23, and 24 (Figure 3b). The percentage of mimicked values matching with observed streamflow for first quartile bin (≤64.105 m^3/s), second quartile bin (64.105 – 94.445 m^3/s), third quartile bin (94.445 -1062.14 m^3/s), and fourth quartile bin (≥1062.14 m^3/s) are 69.5, 45.83, 56.5, and 83.33, respectively. Similar observations as that of training were noticed.

4.2. Streamflow Projections for 2021-2095

Figure 4 presents the visualization of projected streamflow variations for 2021-2095 in SSP585 in terms of minimum, lower quartile, median, average, upper quartile, upper whisker, and maximum streamflow. The highest, lowest, and average streamflow of SSP585 is observed to be 2624 m^3/s, 599.03 m^3/s and 703.36 m^3/s respectively.

Step-1 Input data
Meteorological information of 52 grid locations for 1982-2020 as input to the architecture

Step-2 GRU Equations
The input data passes through reset gate (R_t) and update gate (z_t) to decide the amount of information (x_t) that needs to be forgotten and retrieved from the input data. The useful information is finally stored with the help of current (h_t) and final hidden states ($\widetilde{h_t}$). The corresponding equations of R_t, z_t,h_t& $\widetilde{h_t}$ are as follows

$$R_t = \sigma(w_r.[h(t-1), x_t])$$
$$z_t = \sigma(w_z.[h(t-1), x_t])$$
$$h_t = tanh\,(w.[(r_t h(t-1), x_t])$$
$$\widetilde{h_t} = (1-z_t)\,h(t-1) + (z_t h_t)$$

Where w_r & w_z presents the weight vectors of reset and update gates information at time t; σ presents the sigmoid activation function; $h(t-1)$is the hidden state information at time $t-1$. Finally, the output obtained from GRU is further sent to RNN architecture.

Step-3 RNN Equations
RNNs process one input at a time, updating their memory (h_t) based on previous inputs (x_t). This allows them to capture relationships and patterns in sequences and generate output (y_t). The corresponding equations of h_t & y_t are as follows

$$h_t = \sigma(W_h \times h_{t-1} + W_x \times x_t + b_h)$$
$$y_t = \sigma(W_y \times h_t + b_y)$$

here, (W_x,W_h,W_y) and (b_x, b_h, b_y) are weight matrices and bias terms of input, hidden and outputs. The output obtained from RNN is further sent to LSTM architecture.

Step-4 LSTM Equations
The output obtained from RNN is further passes through forget, input, update and output gates and the corresponding equations are presented in [25]. The output obtained from the LSTM after grid search hyperparameter tuning is considered as the final output which is evaluated for KGE in training and testing segments benchmarking CWC observed streamflow data.

Step-5 Projecting streamflow for 2021-2095 using SSP585
Future climate data obtained for 2021-2095 for 52 grid locations of SSP585 are imported into architecture and future streamflow are projected using GRU-RNN-LSTM architecture with optimized values obtained from grid search algorithm.

Figure 2. Flowchart of methodology

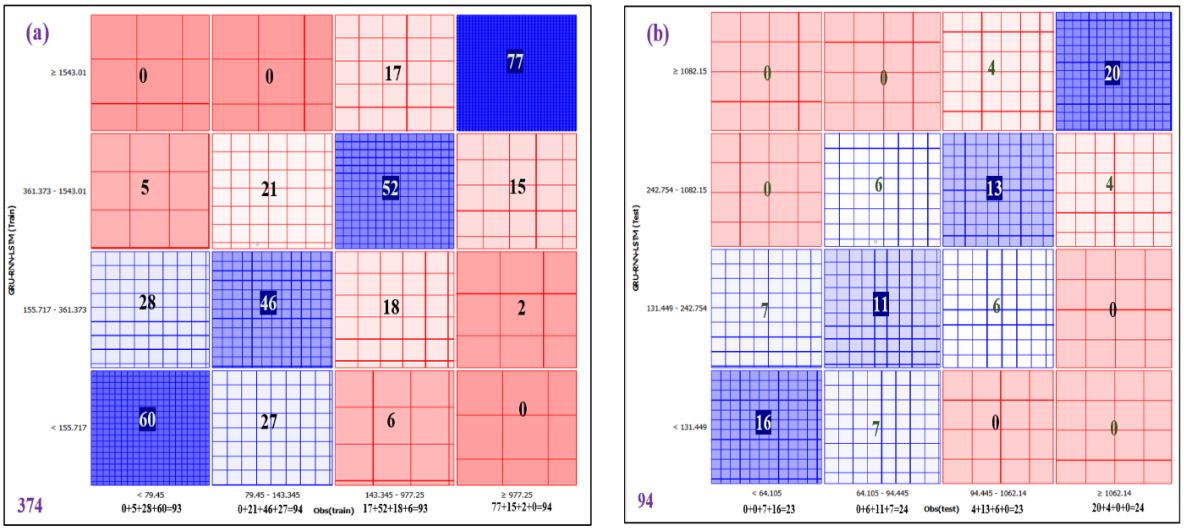


Figure 3. Sieve diagram for GRU-RNN-LSTM in a) Training and b) Testing segments

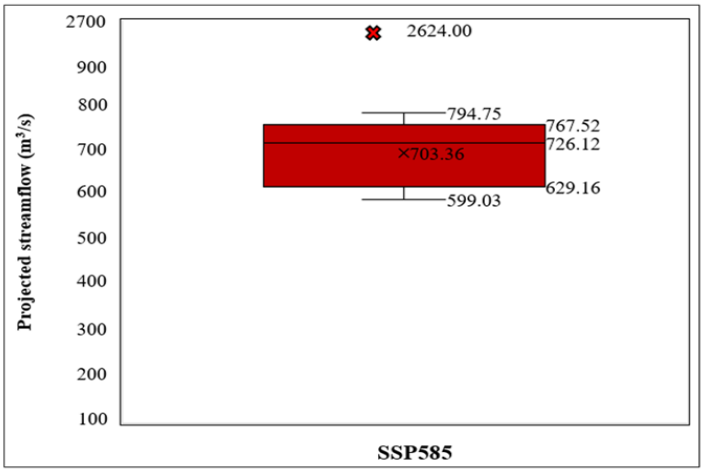


Figure 4. Visualization of variations in streamflow in 2021-2095 for SSP585

5. Discussion and conclusions

It is known that sufficient training size would aid in better streamflow simulation. Previous studies [20]; [21] suggested that a training size of over nine years is sufficient for achieving better efficacy. Further increase in training size improved the performance but was insignificant. [22] noticed that reducing the training size from twenty to ten years significantly impacted algorithm performance in the Sava Dolinka River, whereas it was insignificant for the Yangtze River. They recommended at least twenty years of training for catchments having torrential spatial characteristics. Choosing a performance metric is another critical aspect that draws significant attention in deciding the better algorithm. The present study considers KGE due to its scale-invariant nature and sensitivity to errors in high and low flows than other metrics [23], [24]. The choice of hybridization has a prominent influence on streamflow simulation. In the present study, GRU-RNN-LSTM displayed a satisfactory performance with KGE values of 0.785 and 0.77 in training and testing segments. This finding resonates with previous works stressing the increased performance of hybrid algorithms over the individual in streamflow modelling. [25] employed CNN and LSTM for the Lower Godavari case study. It is noted that KGE training values for CNN and LSTM are 0.76 and 0.75, whereas these values for testing are 0.72 and 0.74. These values are marginally less than the hybridization employed in the present study. Another finding is that CNN-GRU-LSTM didn't display an improvement in simulation efficacy in the study reported by [15]. This infers that every hybrid deep learning algorithm need not necessarily improve the efficacy sometimes for few studies simpler models may dominate the complex architectures depending on the meteorological conditions of the case study. However, one notable observation from the present study is that hybridizing the deep learning algorithms that are dominant in capturing temporal patterns show a better performance for regression problems. Furthermore, there is scope for few improvements from the present study, such as exploration of different combinations of DL and hyperparameter tuning algorithms to further improvise the efficacy.

References

[1] K. P. Wai, M. Y. Chia, C. H. Koo, Y. F. Huang, and W. C. Chong 2022 Applications of deep learning in water quality management: A state-of-the-art review, *Journal of Hydrology*, **613**, 128332

[2] K. W. Ng, Y. F. Huang, C. H. Koo, K. L. Chong, A. El-Shafie, and A. Najah Ahmed 2023 A review of hybrid deep learning applications for streamflow forecasting, *Journal of Hydrology*, **625**, 130141.
[3] I. Abd-Elaty, N. L. Kushwaha, and A. Patel 2023 Novel Hybrid Machine Learning Algorithms for Lakes Evaporation and Power Production using Floating Semi-transparent Polymer Solar Cells," *Water Resources Management*, **37**(12), 4639–4661.
[4] X. Shu, W. Ding, Y. Peng, Z. Wang, J. Wu, and M. Li, 2021 Monthly Streamflow Forecasting Using Convolutional Neural Network, *Water Resources Management*, **35**(15), 5089–5104.
[5] Zhang, J., Chen, X., Khan, A., Zhang, Y.K., Kuang, X., Liang, X., Taccari, M.L. and Nuttall, J., 2021. Daily runoff forecasting by deep recursive neural network. *Journal of Hydrology*, **596**, 126067.
[6] Ren, Y., Zeng, S., Liu, J., Tang, Z., Hua, X., Li, Z., Song, J. and Xia, J., 2022. Mid-to long-term runoff prediction based on deep learning at different time scales in the Upper Yangtze River Basin. *Water*, **14**(11), 1692.
[7] Rahimzad, M., Moghaddam Nia, A., Zolfonoon, H., Soltani, J., Danandeh Mehr, A. and Kwon, H.H., 2021. Performance comparison of an LSTM-based deep learning model versus conventional machine learning algorithms for streamflow forecasting. *Water Resources Management*, **35**(12), 4167-4187.
[8] Li, J., Qian, K., Liu, Y., Yan, W., Yang, X., Luo, G. and Ma, X., 2022. LSTM-based model for predicting inland river runoff in arid region: a case study on Yarkant River, Northwest China. *Water*, **14**(11), 1745.
[9] Wang, Q., Liu, Y., Yue, Q., Zheng, Y., Yao, X. and Yu, J., 2020. Impact of input filtering and architecture selection strategies on GRU runoff forecasting: A case study in the Wei River Basin, Shaanxi, China. *Water*, **12**(12), 3532.
[10] Ghimire, S., Yaseen, Z.M., Farooque, A.A., Deo, R.C., Zhang, J. and Tao, X., 2021. Streamflow prediction using an integrated methodology based on convolutional neural network and long short-term memory networks. *Scientific Reports*, **11**(1), 17497.
[11] Jing, X., Luo, J., Zhang, S. and Wei, N., 2022. Runoff forecasting model based on variational mode decomposition and artificial neural networks. *Mathematical Biosciences and Engineering*, **19**(2), 1633-1648
[12] Wegayehu, E.B. and Muluneh, F.B., 2022. Short-Term Daily Univariate Streamflow Forecasting Using Deep Learning Models. *Advances in Meteorology*, **2022**(1), 1860460.
[13] Shekar, P.R., Mathew, A., Yeswanth, P.V. and Deivalakshmi, S., 2024. A combined deep CNN-RNN network for rainfall-runoff modelling in Bardha Watershed, India. *Artificial Intelligence in Geosciences*, **5**,100073.
[14] M. Elgendy, S. Hassini, and P. Coulibaly, "Review of Climate Change Adaptation Strategies in Water Management," *J. Hydrol. Eng.*, vol. 29, no. 1, p. 03123001, Feb. 2024, doi: 10.1061/JHYEFF.HEENG-6014.
[15] Vatanchi, S.M., Etemadfard, H., Maghrebi, M.F. and Shad, R., 2023. A comparative study on forecasting of long-term daily streamflow using ANN, ANFIS, BiLSTM and CNN-GRU-LSTM. *Water Resources Management*, **37**(12), 4769-4785.
[16] Mishra, V., Bhatia, U. and Tiwari, A.D., 2020. Bias-corrected climate projections for South Asia from coupled model intercomparison project-6. *Scientific data*, **7**(1), 338.
[17] "Polavaram Project Authority Annual Report 2020–21 Ministry of Jal Shakti, Department of Water Resources, River Development & Ganga Rejuvenation, Government of India."
[18] Liu, D., 2020. A rational performance criterion for hydrological model. *Journal of Hydrology*, **590**, 125488.
[19] Nguyen, H.D., 2023. Daily streamflow forecasting by machine learning in Tra Khuc River in Vietnam. *Vietnam Journal of Earth Sciences*, **45**(1), 82-97.
[20] Boulmaiz, T., Guermoui, M. and Boutaghane, H., 2020. Impact of training data size on the LSTM performances for rainfall–runoff modeling. *Modeling Earth Systems and Environment*, **6**(4), 2153-2164.
[21] Fu, M., Fan, T., Ding, Z.A., Salih, S.Q., Al-Ansari, N. and Yaseen, Z.M., 2020. Deep learning data-intelligence model based on adjusted forecasting window scale: application in daily streamflow simulation. **8**, 32632–32651.
[22] Bai, Y., Bezak, N., Sapač, K., Klun, M. and Zhang, J., 2019. Short-term streamflow forecasting using the feature-enhanced regression model. *Water Resources Management*, **33**, 4783-4797.
[23] Aerts, J.P., Hut, R.W., van de Giesen, N.C., Drost, N., van Verseveld, W.J., Weerts, A.H. and Hazenberg, P., 2022. Large-sample assessment of varying spatial resolution on the streamflow estimates of the wflow_sbm hydrological model. *Hydrology and Earth System Sciences*, **26**(16), 4407-4430.
[24] Newman, A.J., Stone, A.G., Saharia, M., Holman, K.D., Addor, N. and Clark, M.P., 2021. Identifying sensitivities in flood frequency analyses using a stochastic hydrologic modeling system. *Hydrology and Earth System Sciences*, **25**(10), 5603-5621.
[25] Vogeti, R.K., Jauhari, R., Mishra, B.R., Raju, K.S. and Nagesh Kumar, D., 2024. Deep learning algorithms and their fuzzy extensions for streamflow prediction in climate change framework. *Journal of Water and Climate Change*, **15**(2), 832-848.

Acknowledgement

The first author acknowledges the funding support provided by the Council of Scientific and Industrial Research-Human Resource Development Group, New Delhi, through Research Associateship grant with File no. 09/1026(18441)/2024-EMR-I dated 01.05.24. Special acknowledgements to Prof. K Srinivasa Raju and Prof. D Nagesh Kumar for their constant guidance and support.

IOP Conference Series: Earth and Environmental Science

PURPOSE-LED PUBLISHING™

PAPER • **OPEN ACCESS**

A review of sugarcane bagasse ash: Characteristics, properties and sustainable applications in concrete

To cite this article: Pratyush Kumar Goyal and Meena Murmu 2024 *IOP Conf. Ser.: Earth Environ. Sci.* **1409** 012002

View the article online for updates and enhancements.

You may also like

- Experimental Investigation on combined effect of eggshell powder and sugarcane bagasse ash as mineral admixture in concrete
G Balaji, R Vetturayasudharsanan, P S Pavan et al.
- Optimization of turning parameters for AlSi$_{10}$Mg/SCBA/SiC hybrid metal matrix composite using response surface methodology
S Shankar, A Balaji and A Pramanik
- Synergic effect of cathodic protection and mineral admixture on the corrosion resistance of reinforcements in concrete
Yogesh Iyer Murthy and Sumit Gandhi



This content was downloaded from IP address 47.247.77.11 on 27/11/2024 at 05:30

A review of sugarcane bagasse ash: Characteristics, properties and sustainable applications in concrete

Pratyush Kumar Goyal[1], Meena Murmu[1]

[1]Department of Civil Engineering, NIT Raipur, India

*E-mail: pkgoyal.phd2022.ce@nitrr.ac.in

Abstract. Concrete is among the most utilized construction materials in the world, with cement as a primary component. Integrating Sugarcane Bagasse Ash (SCBA) into concrete production offers solutions for utilizing this agro-industrial by-product while reducing environmental impacts. This includes minimizing the need for limestone removal in cement production, thereby lowering carbon dioxide emissions and preserving natural deposits for cement manufacturing. To address this challenge, researchers and practitioners are increasingly exploring sustainable alternatives to traditional concrete components. This review focuses on sustainable applications in concrete, with a specific emphasis on environmentally friendly materials and practices that can reduce the carbon footprint of concrete production and improve its long-term sustainability. Sugarcane bagasse ash (SCBA) is a byproduct of the sugar industry used as a sustainable alternative material in concrete production. A comprehensive review provides an overview of the characteristics and properties of SCBA, as well as its sustainable applications in concrete. This paper examines the physical properties and chemical composition of SCBA, emphasizing its potential as a supplementary cementitious material. Various studies on the use of Sugarcane bagasse ash in concrete mixtures are summarized, focusing on its effects on workability by slump test of concrete may increase or decrease with different SCBA concentrations. Additionally, it explores the effects on mechanical properties, durability evaluated via water absorption tests, and microstructural properties of concrete. Generally, concrete containing SCBA exhibits improved mechanical properties with increased SCBA substitution, with an optimal replacement ratio ranging from 5% to 15%.

Keywords: Sugarcane bagasse ash, Sustainable concrete, Microstructure, Fresh and Hardened Properties.

1. Introduction

Concrete is the most widely used manmade construction material globally. Its popularity stems from several factors, including its easy to availability, water resistance, and adaptability to various shapes and dimensions [1]. The rapid global urbanization seen in recent years has led to a significant increase in the consumption of concrete, one of the construction industry's most commonly used materials. Ordinary Portland cement (OPC) serves as the primary cementitious material in concrete. Current projections suggest that cement consumption is expected to rise from its current yearly volume of about 4.2 billion tons to around 5.2 billion tons by the year 2050 [2]. Current methods of cement production release approximately 850 kg of CO_2 into the

Content from this work may be used under the terms of the Creative Commons Attribution 4.0 licence. Any further distribution of this work must maintain attribution to the author(s) and the title of the work, journal citation and DOI.
Published under licence by IOP Publishing Ltd

atmosphere per ton of clinker manufactured [3]. Hence, it is required to discover new materials to replace cement and mitigate the adverse environmental effects of concrete production.

The concept of supplementary cementitious materials is employed to reduce carbon dioxide emissions. Large quantities of agricultural waste, including rice husk ash, sugarcane bagasse ash, wheat straw ash, coconut shell ash, corn cob ash, palm oil fuel ash, along with industrial byproducts like fly ash, ground granulated blast furnace slag, and silica fume, are being effectively utilized to partially substitute of cement in various applications. However, the disposal of these agricultural and industrial and agricultural byproducts on open land poses a significant environmental hazard, resulting in contamination of both air and water bodies [4]. When incorporated as pozzolanic materials in high-performance concrete, these waste products have the potential to enhance both the strength and durability properties of the concrete [5]. Environmentally sustainable materials like pozzolans including rice husk ash, sugarcane bagasse ash, palm oil fuel ash, fly ash, silica fume, and metakaolin exhibit binding properties similar to cement. This makes them highly desirable as substitute raw materials for cement, lowering the production costs of concrete and diminishing environmental impact [6].

Sugarcane bagasse ash (SCBA) is a residual product of the sugar production industry, originating from sugar mills after the extraction of sugar from sugarcane. It is derived from bagasse, the substantial fibrous waste material that constitutes around 30%–34% of the weight of freshly harvested sugarcane [7]. When bagasse is incinerated at a specific temperature in a cogeneration boiler, it produces a significant amount of ash, typically around 2%–3% of the bagasse's mass, known as sugarcane bagasse ash or SCBA [8,9]. Figure 1 displays samples of freshly harvested sugarcane, sugarcane bagasse, and sugarcane bagasse ash, while Figure 2 illustrates the extraction process of originating SCBA from sugarcane.

Fig. 3 illustrates the top producers of sugarcane in 2021 were Brazil and India, collectively representing around 46.3% of global production [13]. It can be seen that India ranks as the second largest producer of sugarcane. The accumulated bagasse waste is often disposed of in landfills in massive quantities, where it is subsequently burned, and converted to ash at a rate of approximately 30%. This sugarcane bagasse ash serves as a significant substitute for cement due to its properties that align with those of cement [14]. Therefore, this study aims to comprehensively review the use of sugarcane bagasse ash as a supplementary cementitious material to produce sustainable concretes. The review covers the properties of SCBA, its Characteristics, and its impact on various properties of concrete including results from slump test, mechanical properties, water absorption tests, and microstructure analysis.



Figure 1. (a) Freshly harvested Sugarcane (b) Sugarcane bagasse [10] (c) Sugarcane bagasse ash [11].

2. Characterisation of Sugarcane bagasse ash

The physical and chemical properties of sugarcane bagasse ash are influenced by several factors, including the combustion temperature, collection method, industrial site location, particle fineness, and cooling process. Sugar mills typically dispose of SCBA in two ways: from the bottom of boilers and through filtration techniques [1]. SCBA obtained from the bottom of the boiler tends to have a coarser grain size compared to ash obtained through filtration [15].

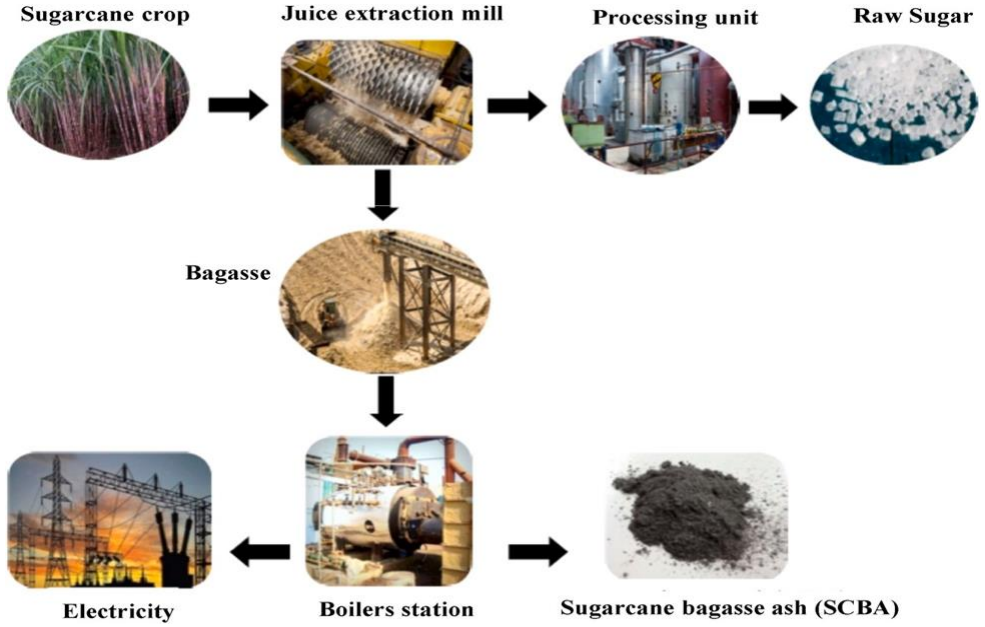


Figure 2. The extraction process of originating SCBA from sugarcane [12].

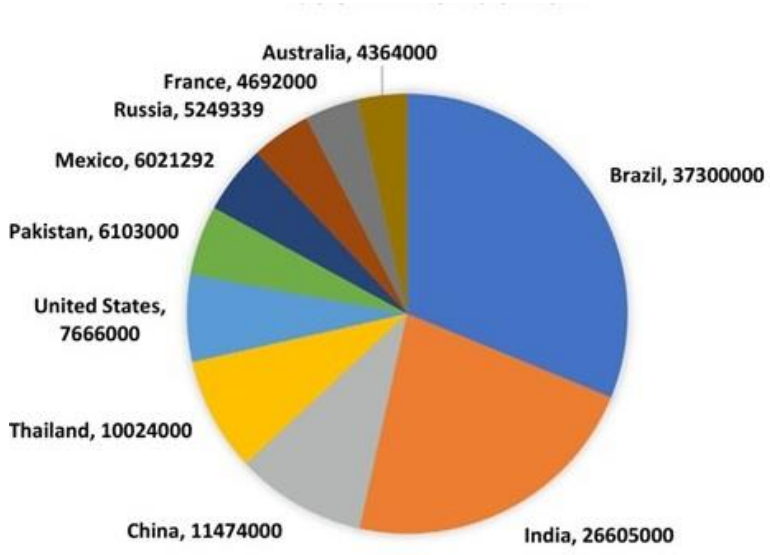


Figure 3. The production of sugarcane bagasse ash in various countries (Thousand metric tons) [13].

2.1. Physical properties of SCBA

The physical properties of Supplementary cementitious materials significantly influence both the fresh and hardened properties of concrete. Figure 4 displays the particle shapes of SCBA, having various morphologies including prismatic, spherical, irregular, and fibrous forms [16,17]. Table 1 compares the physical properties of sugarcane bagasse ash (SCBA) and Ordinary Portland Cement

(OPC), as studied in past research [18,19,20,21–27]. Sugarcane bagasse ash, typically derived from sugar mills, exhibits varying colors such as reddish grey and black attributable to the presence of unburnt carbon [19]. The color variation is impacted by both the combustion process and the structure of silica in the ash. Sugarcane bagasse ash comprises mainly fine particles, with some coarse fibrous particles also present [10, 24]. The specific gravity of sugarcane bagasse ash falls within the range of 1.8 to 2.59, which is lower than the specific gravity of cement (2.9–3.14). Its bulk density varies from 1420 to 2454 kg/m^3, mean particle size ranges from 19.5 to 76.3 µm, and surface area ranges between 145 and 817.1 m^2/kg.

2.2. Chemical properties of SCBA

The pozzolanic reactivity of SCBA as a pozzolanic material primarily depends on its chemical properties, particularly the presence of SiO_2, Al_2O_3, and Fe_2O_3. Table 2 lists the chemical compositions of sugarcane bagasse ash, revealing variations in composition attributed to differences in types of sugarcane, growth conditions, and the methods of calcination and grinding [12]. The pozzolanic oxide content (SiO_2+Al_2O_3+Fe_2O_3) of SCBA ranges from approximately 64.20% to 88.28% of the total composition. Various studies have highlighted SCBA's suitability as a pozzolanic mineral, primarily due to its high SiO_2 content (55%–82.68%) [21, 23, 27–33]. As per ASTM C618-08a [35], natural pozzolans are classified as class C if the total mass of Al_2O_3 +SiO_2+ Fe_2O_3 is greater than 50%, and as class F pozzolans if the total mass exceeds 70%.

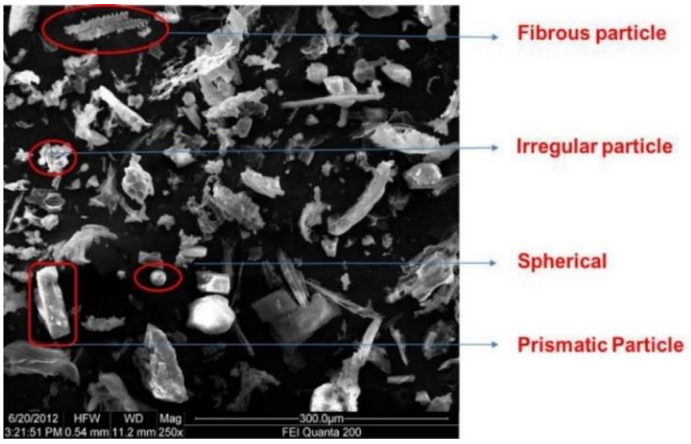


Figure 4. The particle shapes of Sugarcane bagasse ash [16].

Table 1. Physical properties of Sugarcane bagasse ash and Cement [18,19,20,21–27].

Physical properties	Sugarcane bagasse ash	Cement
Colour	Black, grey	Grey
Particle shapes	Spherical, irregular, prismatic, fibrous	–
Specific gravity	1.8–2.59	2.9–3.14
Bulk density (kg/m^3)	1420–2454	1560–3170
Blaine specific surface area (m^2/kg)	145–817.1	308–373
Mean particle size (µm)	19.5–76.3	14.6–28
References	**[20–24]**	**[20,22,25,26]**

Table 2. Chemical properties of SCBA [28-34]

Reference	SiO_2	Al_2O_3	Fe_2O_3	CaO	Na_2O	K_2O	SO_3	MnO	MgO	TiO_2	P_2O_5	Loss of ignition (LOI)	SiO_2+ Al_2O_3 + Fe_2O_3

Bahurudeen et al. [28]	75.67	1.52	2.29	6.62	0.12	9.59	0	0	1.87	0	0	3.0-6.0	79.48
Pereira et al. [29]	78.59	4.47	4.88	1.34	0.22	2.37	0.66	0	1.03	1.16	0	4.4	87.94
Rambabu et al. [30]	64.59	4.38	6.98	11.8	0	3.53	1.48	0	2.51	0	0	4.73	75.95
R. Somna et al. [31]	55	5.1	4.1	11	0.2	1.2	2.2	0	0.9	0	0	19.6	64.2
Ríos-Parada et al. [32]	66.12	15	7.16	2.57	0.54	3.52	0.26	0.22	1.19	1.13	1.14	9	88.28
Yadav et al. [33]	69.7	9.23	4.67	3.85	0.88	3.71	1.67	0	0.07	0.57	2	16.7	83.6
C.K. Gupta et al. [34]	82.68	3.01	1.69	5.58	0.43	0.77	0	0	2.86	1.23	1.56	3.23	87.38

2.3. 2.3 Thermal analysis of SCBA

Sugarcane bagasse ash originates from sugar mills, where the fibrous bagasse ash is burnt at temperatures between 600°C and 1000°C to ensure the presence of silica The silica content is also influenced by the duration of burning at that specific temperature [19]. The color of bagasse ash varies with the rising burning temperature, as depicted in Figure 5. The ash was incinerated at different temperatures in a muffle furnace. The pH value of sugarcane bagasse ash is 12, indicating its alkaline nature [34]. At higher burning temperatures, the ash appears light gray in color [1, 17, 36]

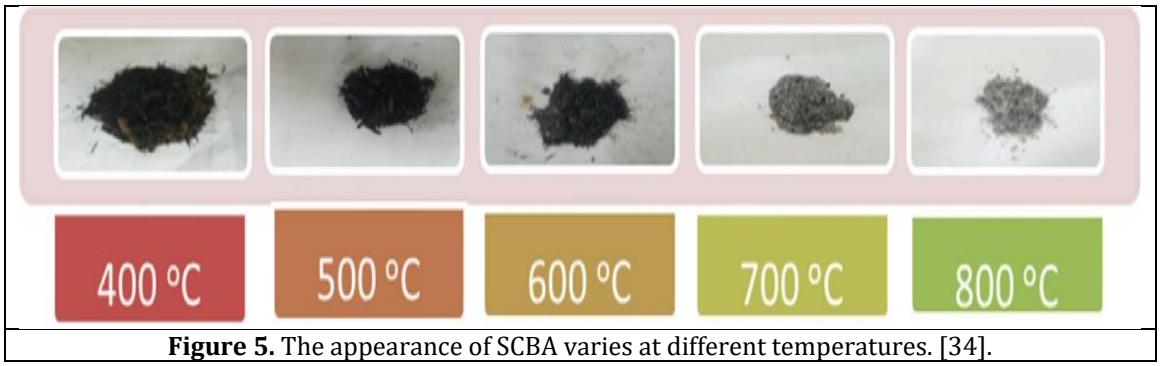


Figure 5. The appearance of SCBA varies at different temperatures. [34].

2.4. Mineral compositions of SCBA

X-ray diffraction tests (XRD) were performed to analyze the mineral composition and identify phases [36]. The majority of minerals were found in the amorphous phase, with some in the crystalline phase [34, 37]. The crystalline phase is mainly composed of quartz and calcite [34]. Peaks in the X-ray diffraction pattern indicate the presence of elements at specific 2θ angles [34, 36]. The mineral compositions are illustrated in Figure 6, which shows the intensity of minerals at those angles.

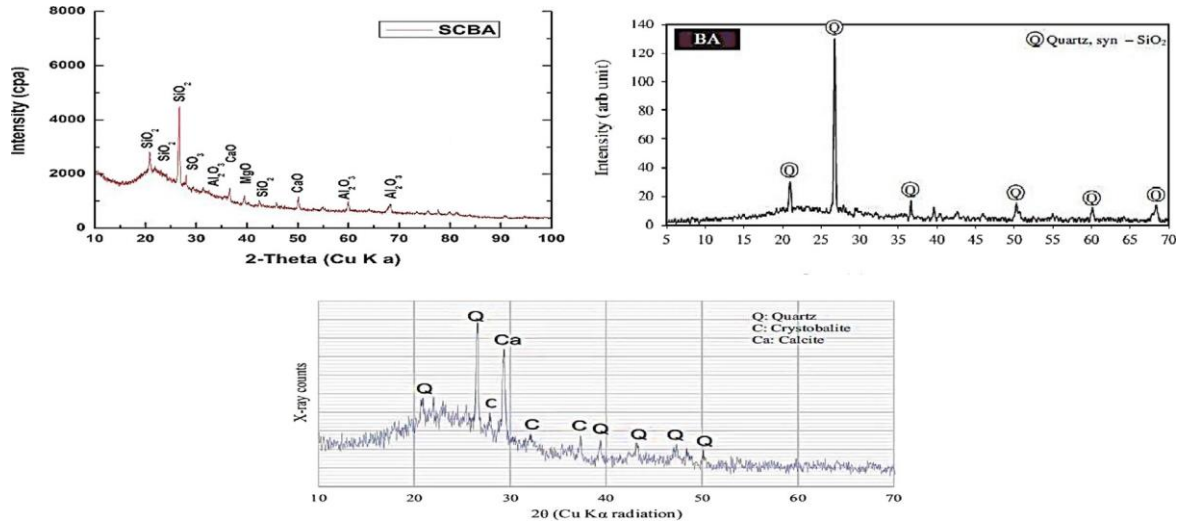


Figure 6. The mineral compositions of SCBA determined by XRD test [33,36,38].

3. Fresh Properties of concrete containing SCBA

3.1. Workability by Slump cone test

The literature suggests that incorporating sugarcane bagasse ash (SCBA) can change concrete's workability, as evidenced by parameters like slump value, water requirement, and the required dosage of superplasticizer. In studies conducted by researchers, the impact of sugarcane bagasse ash as a partial substitute for cement on slump was investigated. It was found that workability generally improves with increasing ratios of SCBA [8, 40, 41]. For example, shown in Fig. 7 from Priya and Ragupathy [41], replacing 0% to 30% of cement with SCBA increased slump values from 70 mm to 160 mm, respectively. This enhancement can be credited to the larger particle size of SCBA.

On the other hand, researchers examined the effect of sugarcane bagasse ash as a partial substitution for cement on slump value and noted a decrease in workability with increasing SCBA percentage [39,42]. For instance, according to Chennakesava and Prabath [39], replacing 0% to 30% of cement with SCBA reduced slump values from 86 mm to 70 mm, respectively. They attributed this reduction in workability to both the surface area and volume fraction of sugarcane bagasse ash content. The decreased workability noticed in mixtures containing SCBA could be attributed to highly irregular shapes, porous nature, and rough surfaces of sugarcane bagasse ash particles. SCBA tends to adsorb water due to its high surface area and higher SCBA replacements require more superplasticizer to achieve the desired slump, likely due to the large number of pores present [44].

Table 3. Impact of sugarcane bagasse ash on the slump of concrete from various references [8, 39-42].

References	Hussein, et al.[8]	Chennakesava and Prabath [39]	Srinivasan and Sathiya [40]	Priya and Ragupathy [41]	Ganesan et al. [42]
SCBA Replacement (%)	Slump value (mm)				
0	160	86	60	70	98
5	170	83	187	85	106
10	175	82	200	90	115
15	180	79	220	100	91

20	190	74	225	125	81
25	200	70	230	160	74
30	215	-	-	-	64
Status	Increases	Decreases	Increases	Increases	Decreases

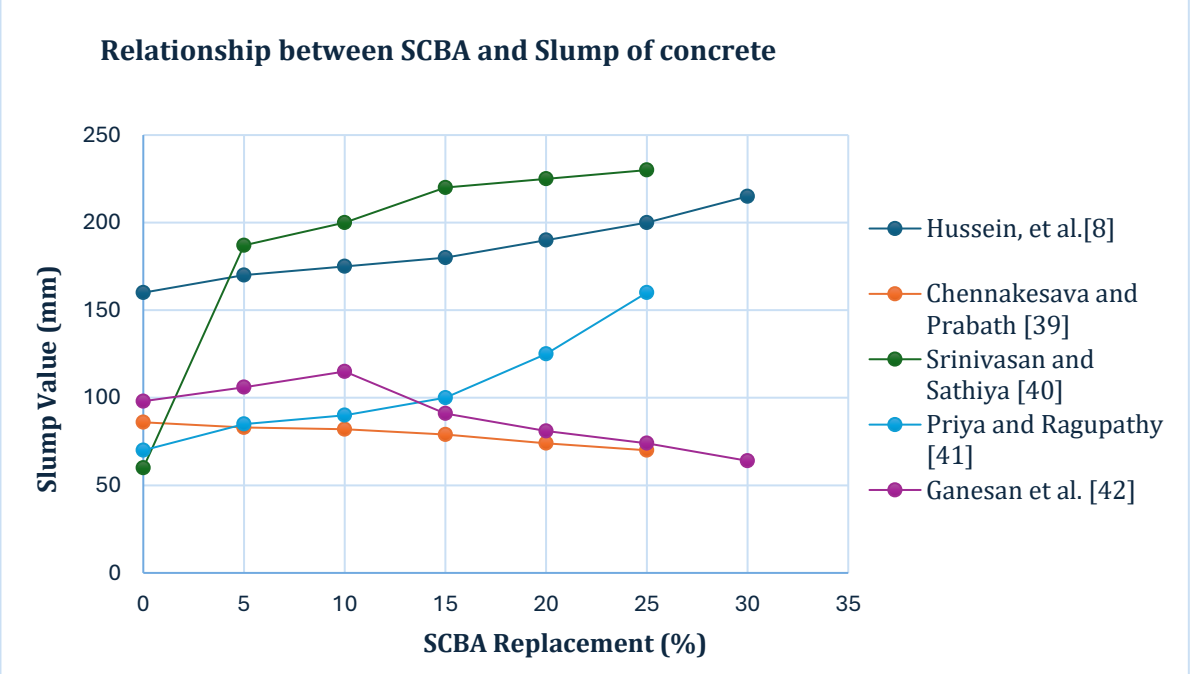


Figure 7. Relationship between SCBA and slump of concrete [8, 39-42].

4. Mechanical properties of concrete containing SCBA

4.1. Compressive strength

Compressive strength development in concrete incorporating sugarcane bagasse ash (SCBA) primarily depends on the substitution ratio, curing period, and the characteristics of sugarcane bagasse ash. Table 4 presents a summary of the compressive strength test results after 28 days, along with the optimal sugarcane bagasse ash replacement ratios from previous studies. In their studies, researchers assessed the hardened properties of M20-grade concrete, employing a water-to-cement ratio of 0.5. They incorporated SCBA, passing through a 75 µm sieve, as a replacement for cement ranging from 5% to 20%. Their test results indicated a significant improvement in the concrete's compressive strength with up to 15% SCBA substitution., after which it began to decrease [9]. According to Chennakesava and Prabath [39] produced M25 concrete by incorporating SCBA as a partial replacement for cement at varying percentages (0 to 25%). Their findings indicated that the concrete blend with a 10% substitution of sugarcane bagasse ash exhibited the maximum compressive strength in comparison to the reference mixture. Another researcher, investigated the impact of SCBA as a substitute for cement in M20 grade concrete, maintaining a water-to-cement ratio of 0.48. They substituted 5% to 25% of the cement weight with SCBA. The study concluded that a 5% substitution was optimal for concrete designated as M20 grade, while the concrete containing 10% sugarcane bagasse ash exhibited a compressive strength higher than that of the reference mixture [40]. Priya and Ragupathy [41] replaced a maximum of 25% of the cement with M25-grade concrete containing SCBA. Concrete specimens were subjected to compressive strength tests in accordance with the IS:516-1959 standards.

Their findings indicated that the most effective replacement level was 10%, while the concrete incorporating 20% SCBA exhibited a compressive strength exceeding that of the reference mixture.

According to the author, cement was replaced with SCBA up to 30% in M25 grade concrete. After collection from the mill, the SCBA was subjected to controlled temperature burning at 650°C for 1 hour, resulting in a reduction of its carbon content ranging from 11.2 to 4.9%. The researchers determined that the optimal replacement level for M25 concrete was 10% based on their findings [42]. In studies conducted by researchers, the mechanical properties of concrete incorporating SCBA were investigated. They examined partial replacements of cement with SCBA, ranging from 5% to 25%. Their research concluded that achieving favorable compressive strength required only a 5% substitution level [45,46]. Figure 8, illustrates the relationship between sugarcane bagasse ash and compressive strength of concrete. The figure indicates that the optimal SCBA content for enhancing compressive strength is between 5% and 15%. According to the authors, the concrete incorporating a 10% SCBA replacement exhibited the highest compressive strength among all other concrete blends The strength reduction was ascribed to the inadequate quantity of $Ca(OH)_2$, which reduces the creation of hydrated calcium silicate (C–S–H) and consequently affects the strength. [18].

Table 4. Impact of sugarcane bagasse ash on Compressive Strength after 28 days from various references [9, 39-42, 45-46].

References	**Manoj kumar et al. [9]**	**Chennakesava and Prabath [39]**	**Srinivasan and Sathiya [40]**	**Priya and Ragupathy [41]**	**Ganesan et al. [42]**	**Ranjith et al. [45]**	**Kiran, and Kishore [46]**
Water/ binder Ratio	0.5	0.42	0.48	0.5	0.53	0.4	0.42
Optimum Ratio	15%	10%	5%	10%	10%	5%	5%
SCBA Replacement (%)	Compressive Strength (MPa)						
0	26.9	36.18	21.5	33.3	37	39.5	39.5
5	26.5	36.89	29.5	37.4	41	40	45.5
10	27.8	37.52	24.7	38.1	42	38	43
15	29.4	33.93	19.3	36.8	41	37.6	39.7
20	26.8	30.07	18.9	35.8	39	37	30.1
25	-	24.85	17.7	30.1	33	36	18.7
30	-	-	-	-	30	-	-

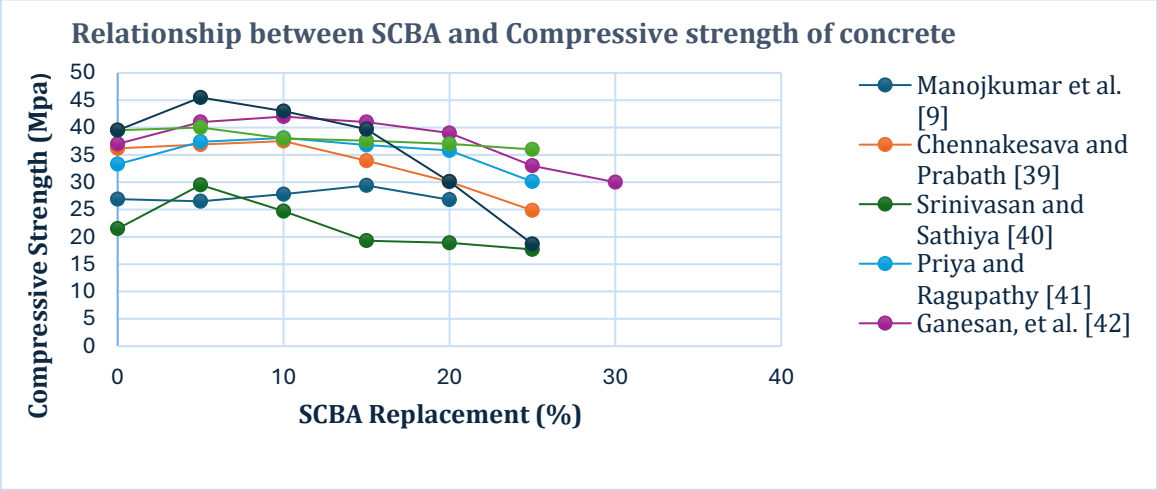


Figure 8. The relationship between SCBA and Compressive Strength of concrete [9, 39-42, 45-46].

4.2. Splitting tensile strength

At the age of 28 days, the splitting tensile strength of concrete, along with the levels of cement substitution with sugarcane bagasse ash and the optimal SCBA ratios identified in prior research, is summarized in table 5. Manojkumar et al. [9] investigated M20 grade concrete in their study, with SCBA replacing 5% to 20% of the cement, sieved through a 75µm sieve size. According to their findings, the maximum splitting tensile strength was attained with a 10% replacement of SCBA. Chennakesava and Prabath [39] investigated the impact of sugarcane bagasse ash as a partial replacement of cement in M25 grade concrete, using 5% to 25% SCBA by weight of cement. They found that only a 10% replacement was optimal for achieving good splitting tensile strength. Srinivasan and Sathiya [40], Kiran and Kishore [46], and Ranjith et al. [45] investigated the impact of SCBA as a substitute for cement, ranging from 5% to 25% sugarcane bagasse ash by weight of cement. Their findings indicated that the highest splitting tensile strength was attained with a 5% SCBA replacement. Figure 9 illustrates the relationship between sugarcane bagasse ash and the splitting tensile strength of concrete. It shows that within the range of 5% to 15% SCBA replacement, there is an enhancement in splitting tensile strength. The highest splitting tensile strength was observed with a 15% replacement, potentially due to the differing levels of reactive silica and aluminum found in sugarcane bagasse ash. Processes such as grinding and burning SCBA may contribute to improving the splitting tensile strength of concrete compared to utilizing raw sugarcane bagasse ash [42,47].

Table 5. Impact of sugarcane bagasse ash on Split Tensile Strength after 28 days from various references [9,39,40,45,46].

References	**Manojkumar et al. [9]**	**Chennakesava and Prabath [39]**	**Srinivasan and Sathiya [40]**	**Ranjith et al. [45]**	**Kiran, and Kishore [46]**
Water/binder Ratio	0.5	0.42	0.48	0.4	0.42
Optimum Ratio	10%	10%	5%	5%	5%
SCBA Replacement (%)	**Split Tensile Strength (MPa)**				
0	1.6	2.55	1.5	2.6	1.3

5	2	2.59	1.9	2.9	1.4
10	2.5	2.75	1.6	2.4	1.3
15	2	2.25	1.5	2.1	1.3
20	1.9	1.92	1.3	1.8	1.1
25	-	1.76	1.2	1.7	0.9

4.3. *Flexural strength*

The flexural strength of Sugarcane bagasse ash after 28 days from earlier studies is summarized in table 6. Figure 10 shows the impact of using SCBA as a replacement for cement on flexural strength. It shows that SCBA replaced 5%–25% of the cement by weight. Chennakesava and Prabath [39] investigated the impact of SCBA as a replacement for cement in M25 grade concrete. They utilized SCBA ranging from 5% to 25% by cement weight and determined that the optimal replacement level was 10%. In their study, Srinivasan and Sathiya [40] investigated the impact of sugarcane bagasse ash as a substitute for cement in M20 concrete. According to their findings, the greatest flexural strength was achieved when 5% of the cement was replaced with SCBA. Kiran and Kishore [46] found that substituting 5% of sugarcane bagasse ash was optimal for M30 grade of concrete. Similarly, Ranjith et al. [45] reported that a 5% SCBA substitution resulted in maximum flexural strength, aligning with the findings of the previous authors.

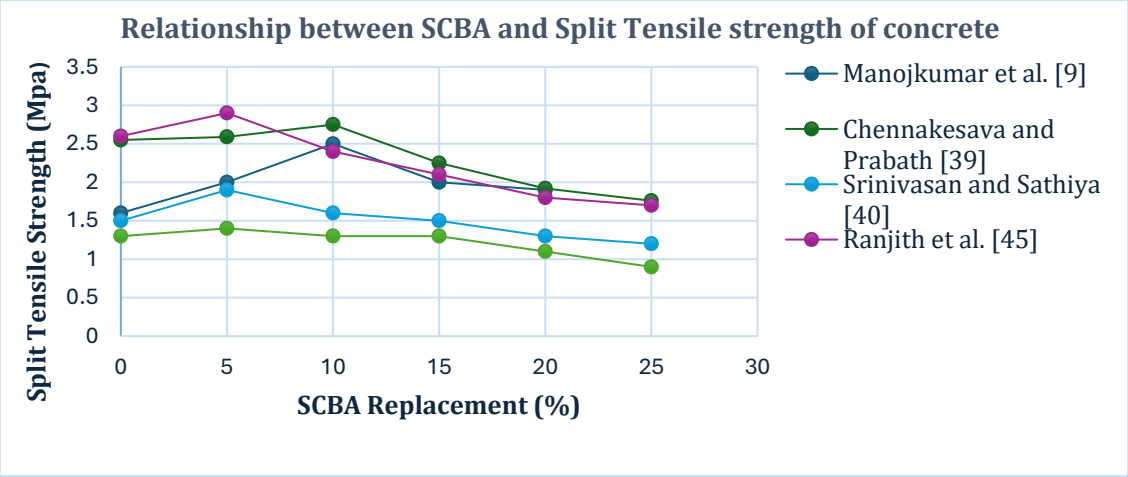


Figure 9. The relationship between SCBA and Split Tensile Strength of Concrete [9,39,40,45,46].

Table 6. Impact of sugarcane bagasse ash on Flexural Strength after 28 days from various references [39,40,45,46].

References	Chennakesava and Prabath [39]	Srinivasan and Sathiya [40]	Ranjith et al. [45]	Kiran, and Kishore [46]
Water/binder Ratio	0.42	0.48	0.4	0.42
Optimum Ratio	10%	5%	5%	5%
SCBA Replacement (%)	Flexural Strength (MPa)			
0	5.9	3.5	4.6	3.9
5	6.1	3.7	4.8	4.4
10	6.45	3.6	4.3	4.1
15	5.8	3.4	4.2	4

20	4.9	3.2	4.1	2.9
25	4.1	3	3.9	2

5. Water absorption Test of concrete containing SCBA

Water absorption refers to the proportion of water contained within the hardened concrete's pores; a factor closely linked with the porosity of concrete. Quedou et al. [48] explored the impact of SCBA as a substitute for cement in concrete on water absorption. Their study involved replacing 0% to 20% of the cement with SCBA. It was noted that water absorption test results increased with higher proportions of SCBA in the mixture and decreased with longer curing periods. The observed trend indicated a rise in water absorption with the incorporation of SCBA. Furthermore, it was observed that test results of the water absorption rate decreased with increasing curing time. The results of water absorption of concrete are illustrated in Figure 11.

For example, Ganesan et al. [42] observed a slight increase in the water absorption test results at 28 days for concrete with SCBA compared to concrete without the addition of SCBA. Similar findings were reported by Le et al. [49] and Zareei et al. [36] in their respective experimental studies. SCBA particles possess inherent porosity and hygroscopic properties, contributing to the elevated water absorption in the mixture. However, it was consistently observed that the water absorption test results of concrete containing sugarcane bagasse ash were reduced with prolonged curing duration [42, 49, 50].

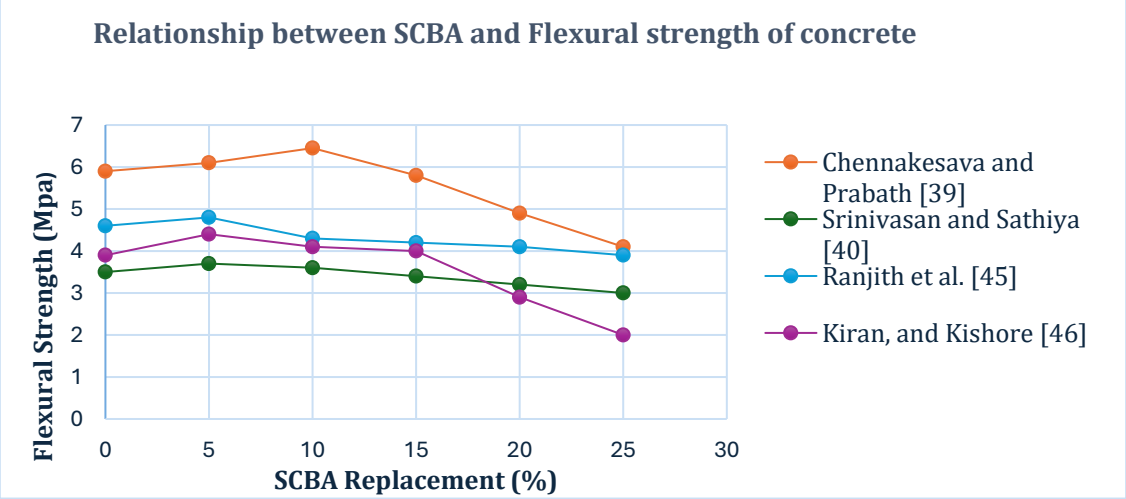


Figure 10. The relationship between SCBA Flexural Strength of concrete [39,40,45,46].

6. Microstructural analysis of concrete containing SCBA

Many researchers have utilized scanning electron microscopy (SEM) to examine the microstructure of Sugarcane bagasse ash concrete due to its capability to illustrate the morphological transformation of raw materials into hydrated forms such as the C-S-H gel. Figure 12 displays the SEM photograph of sample BA2 with 10% bagasse ash. SEM images of specimens with SCBA at 7 and 28 days were examined. It reveals the presence of portlandite (CH) and C–S–H in SCBA incorporated concrete at both 7 and 28 days. Furthermore, at 28 days, SCBA concrete exhibits a highly dense network of C–S–H with minor pores [51].

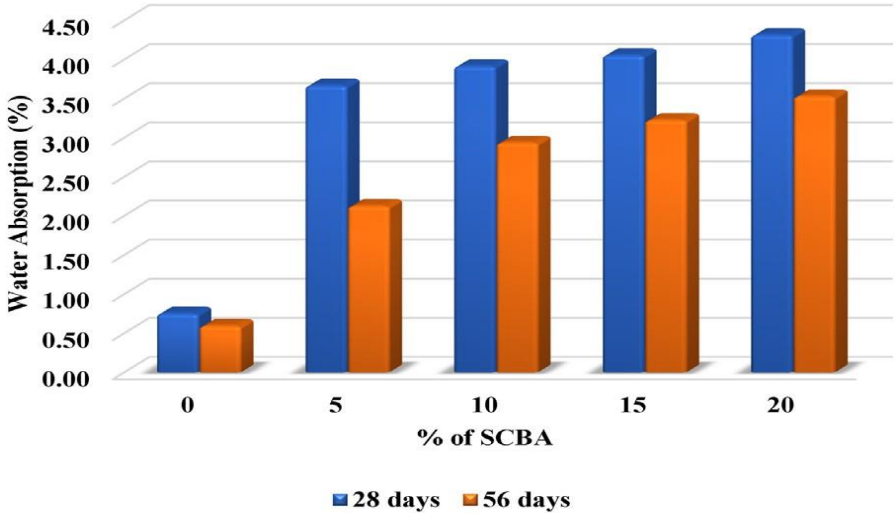
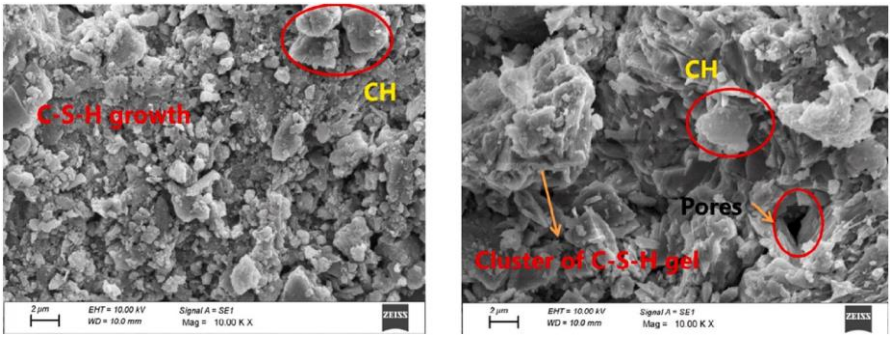


Figure 11. The water absorption test results for concrete with different replacement ratios of SCBA [48].



(a) 7 days (b) 28 days

Figure 12. SEM images depicting SCBA concrete at both 7 days and 28 days [51].

7. Conclusions

- Sugarcane bagasse ash from different sugar processing industries displays varying properties, often characterized by an asymmetrical size, irregular shape, and rough surface.
- Sugarcane bagasse ash (SCBA) typically exhibits a high silica percentage in its chemical properties. Additionally, the chemical properties can be influenced by factors such as the method of incineration, duration, temperature, and grinding process.
- The XRD test of SCBA often indicates a high percentage of silica in its mineral composition. The presence of silica in SCBA is influenced by the incineration temperature and methods used.
- A notable topic of discussion is the effect of SCBA content on concrete slump values. Typically, as the amount of SCBA increases, there is an expectation of higher water demand, which should decrease the slump. However, some research findings suggest the opposite trend, where increasing SCBA content leads to an increase in slump.

- Concrete strength typically increases with up to a 10% SCBA replacement level, but beyond this, there is a decrease in strength due to the complete utilization of free lime. The lack of free lime hinders the formation of calcium silicate hydrate (C-S-H) from SCBA.
- According to the literature, incorporating Portland cement substitutes in the range of 5% to 15% by weight in sugarcane bagasse ash concrete leads to excellent mechanical properties.
- The microstructural analysis indicated that the hydrate formation-induced pore refinement in SCBA blended concrete is responsible for the concrete's denser structure.
- The water absorption test results showed that increasing the amount of SCBA material led to a corresponding increase in water absorption, which then decreased with longer curing times.

References

[1] Khalil, M. J., Aslam, M., & Ahmad, S. (2021). Utilization of sugarcane bagasse ash as cement replacement for the production of sustainable concrete–A review. *Construction and Building Materials*, *270*, 121371. https://doi.org/10.1016/j.conbuildmat.2020.121371.

[2] Jaskulski, R., Jóźwiak-Niedźwiedzka, D., & Yakymechko, Y. (2020). Calcined clay as supplementary cementitious material. *Materials*, *13*(21), 4734. https://doi.org/10.3390/ma13214734.

[3] Antunes, M., Santos, R. L., Horta, R. B., & Colaço, R. (2023). Novel Amorphous-Wollastonitic Low-Calcium Hydraulic Binders: A State-of-the-Art Review. *Materials*, *16*(13), 4874. https://doi.org/10.3390/ma16134874.

[4] Rambabu, PV, K. Dendendra Gupta, and GV Ramarao. (2016). Effect of sodium sulphate (Na2SO4) on concrete incorporating sugarcane bagasse ash as a pozzolanic material. International Journal of Engineering and Applied Sciences, 3(1), 257-749.

[5] Rukzon, S., & Chindaprasirt, P. (2012). Utilization of bagasse ash in high-strength concrete. *Materials & Design*, *34*, 45-50. https://doi.org/10.1016/j.matdes.2011.07.045.

[6] Zerihun, B., Yehualaw, M. D., & Vo, D. H. (2022). Effect of agricultural crop wastes as partial replacement of cement in concrete production. *Advances in Civil Engineering*, *2022*. https://doi.org/10.1155/2022/5648187.

[7] Inbasekar, D. S. M., Hariprasath, P., & Senthilkumar, D. (2016). International journal of engineering sciences & research technology study on potential utilization of sugarcane bagasse ash in steel fiber reinforced concrete. *Int. J. Eng. Sci. Res. Technol*, *5*(4), 43-50.

[8] Hussein, A. A. E., Shafiq, N., Nuruddin, M. F., & Memon, F. A. (2014). Compressive strength and microstructure of sugar cane bagasse ash concrete. *Research Journal of Applied Sciences, Engineering and Technology*, *7*(12), 2569-2577.

[9] Manojkumar, V., Shenbagam, S., & Rekha, M. (2017). Experimental study on the effects of sugarcane bagasse ash in concrete. SSRG Int. J. Civ. Eng, 431-434.

[10] Payá, J., Monzó, J., Borrachero, M. V., Tashima, M. M., & Soriano, L. (2018). Bagasse ash. In Waste and supplementary cementitious materials in concrete (pp. 559-598). Woodhead Publishing. https://doi.org/10.1016/B978-0-08-102156-9.00017-1.

[11] Bahurudeen, A., Marckson, A. V., Kishore, A., & Santhanam, M. (2014). Development of sugarcane bagasse ash based Portland pozzolana cement and evaluation of compatibility with superplasticizers. Construction and Building Materials, 68, 465-475. https://doi.org/10.1016/j.conbuildmat.2014.07.013.

[12] Yadav, A. L., Sairam, V., Muruganandam, L., & Srinivasan, K. (2020). An overview of the influences of mechanical and chemical processing on sugarcane bagasse ash characterisation as a supplementary cementitious material. Journal of Cleaner Production, 245, 118854. https://doi.org/10.1016/j.jclepro.2019.118854.

[13] Agwa, I. S., Zeyad, A. M., Tayeh, B. A., Adesina, A., de Azevedo, A. R., Amin, M., & Hadzima-Nyarko, M. (2022). A comprehensive review on the use of sugarcane bagasse ash as a supplementary cementitious material to produce eco-friendly concretes. Materials today: proceedings, 65, 688-696. https://doi.org/10.1016/j.matpr.2022.03.264.

[14] Yogitha, B., Karthikeyan, M., & Reddy, M. M. (2020). Progress of sugarcane bagasse ash applications in production of Eco-Friendly concrete-Review. Materials Today: Proceedings, 33, 695-699. https://doi.org/10.1016/j.matpr.2020.05.814.

[15] Kumari, A., & Kumar, P. S. (2015). Experimental study on partial replacement of cement by sugaracne bagasse ash. International Journal of Innovative Research in Science, Engineering and Technology, 4(7), 2347-6710.
[16] Bahurudeen, A., & Santhanam, M. (2015). Influence of different processing methods on the pozzolanic performance of sugarcane bagasse ash. Cement and Concrete Composites, 56, 32-45. https://doi.org/10.1016/j.cemconcomp.2014.11.002.
[17] Thomas, B. S., Yang, J., Bahurudeen, A., Abdalla, J. A., Hawileh, R. A., Hamada, H. M., ... & Ashish, D. K. (2021). Sugarcane bagasse ash as supplementary cementitious material in concrete–a review. Materials Today Sustainability, 15, 100086. https://doi.org/10.1016/j.mtsust.2021.100086.
[18] Li, Y., Chai, J., Wang, R., Zhang, X., & Si, Z. (2022). Utilization of sugarcane bagasse ash (SCBA) in construction technology: A state-of-the-art review. Journal of Building Engineering, 56, 104774. https://doi.org/10.1016/j.jobe.2022.104774.
[19] Amin, N. U. (2011). Use of bagasse ash in concrete and its impact on the strength and chloride resistivity. Journal of materials in civil engineering, 23(5), 717-720. https://doi.org/10.1061/(ASCE)MT.1943-5533.0000227.
[20] Embong, R., Shafiq, N., Kusbiantoro, A., & Nuruddin, M. F. (2016). Effectiveness of low-concentration acid and solar drying as pre-treatment features for producing pozzolanic sugarcane bagasse ash. Journal of Cleaner Production, 112, 953-962. https://doi.org/10.1016/j.jclepro.2015.09.066.
[21] Chusilp, N., Jaturapitakkul, C., & Kiattikomol, K. (2009). Effects of LOI of ground bagasse ash on the compressive strength and sulfate resistance of mortars. Construction and Building Materials, 23(12), 3523-3531. https://doi.org/10.1016/j.conbuildmat.2009.06.046.
[22] Cordeiro, G. C., Toledo Filho, R. D., Tavares, L. M., & Fairbairn, E. D. M. R. (2009). Ultrafine grinding of sugar cane bagasse ash for application as pozzolanic admixture in concrete. Cement and concrete research, 39(2), 110-115. https://doi.org/10.1016/j.cemconres.2008.11.005.
[23] Abdalla, T. A., Hussein, A. A. E., Ahmed, Y. H., & Semmana, O. (2024). Strength, durability, and microstructure properties of concrete containing bagasse ash–A review of 15 years of perspectives, progress and future insights. Results in Engineering, 101764. https://doi.org/10.1016/j.rineng.2024.101764.
[24] Bahurudeen, A., & Santhanam, M. (2015). Influence of different processing methods on the pozzolanic performance of sugarcane bagasse ash. Cement and Concrete Composites, 56, 32-45. https://doi.org/10.1016/j.cemconcomp.2014.11.002.
[25] Bahurudeen, A., Marckson, A. V., Kishore, A., & Santhanam, M. (2014). Development of sugarcane bagasse ash based Portland pozzolana cement and evaluation of compatibility with superplasticizers. Construction and Building Materials, 68, 465-475. https://doi.org/10.1016/j.conbuildmat.2014.07.013.
[26] Bahurudeen, A., Marckson, A. V., Kishore, A., & Santhanam, M. (2014). Development of sugarcane bagasse ash based Portland pozzolana cement and evaluation of compatibility with superplasticizers. Construction and Building Materials, 68, 465-475. https://doi.org/10.1016/j.cemconcomp.2012.03.003.
[27] Ganesan, K., Rajagopal, K., & Thangavel, K. (2007). Evaluation of bagasse ash as corrosion resisting admixture for carbon steel in concrete. Anti-Corrosion Methods and Materials, 54(4), 230-236.
[28] Bahurudeen, A., Kanraj, D., Dev, V. G., & Santhanam, M. (2015). Performance evaluation of sugarcane bagasse ash blended cement in concrete. Cement and Concrete Composites, 59, 77-88. https://doi.org/10.1016/j.cemconcomp.2015.03.004.
[29] Pereira, A., Akasaki, J. L., Melges, J. L., Tashima, M. M., Soriano, L., Borrachero, M. V., ... & Payá, J. (2015). Mechanical and durability properties of alkali-activated mortar based on sugarcane bagasse ash and blast furnace slag. Ceramics International, 41(10), 13012-13024. https://doi.org/10.1016/j.ceramint.2015.07.001.
[30] Rambabu, P. V., Gupta, K. D., & Ramarao, G. V. (2016). Effect of sulphates (Na2So4) on concrete with sugarcane bagasse ash as a pozzolana. International Journal of Engineering and Applied Sciences, 3(1), 257749.
[31] Somna, R., Jaturapitakkul, C., Rattanachu, P., & Chalee, W. (2012). Effect of ground bagasse ash on mechanical and durability properties of recycled aggregate concrete. Materials & Design (1980-2015), 36, 597-603. https://doi.org/10.1016/j.matdes.2011.11.065.
[32] V. Ríos-Parada, V.G. Jim´enez-Quero, P.L. Valdez-Tamez, P. Montes-García, Characterization and use of an untreated Mexican sugarcane bagasse ash as supplementary material for the preparation of ternary concretes, Constr. Build. Mater. 157 (2017) 83–95. https://doi.org/10.1016/j.conbuildmat.2017.09.060.
[33] Yadav, A. L., Sairam, V., Srinivasan, K., & Muruganandam, L. (2020). Synthesis and characterization of geopolymer from metakaolin and sugarcane bagasse ash. Construction and Building Materials, 258, 119231. https://doi.org/10.1016/j.conbuildmat.2020.119231.

[34] C.K. Gupta, A.K. Sachan, R. Kumar, Examination of microstructure of sugar cane bagasse ash and sugar cane bagasse ash blended cement mortar, Sugar Tech. 23 (3) (2021) 651–660. https://doi.org/10.1007/s12355-020-00934-8.
[35] Standard, A., C618-08a (2008) ‘’. Standard specification for coal fly ash and raw or calcined natural pozzolan for use in concrete” ASTM International, West Conshohocken, PA, Retrieved August, 2010. 20.
[36] Zareei, S. A., Ameri, F., & Bahrami, N. (2018). Microstructure, strength, and durability of eco-friendly concretes containing sugarcane bagasse ash. Construction and Building Materials, 184, 258-268. https://doi.org/10.1016/j.conbuildmat.2018.06.153.
[37] G. Sua-iam, N. Makul, Use of increasing amounts of bagasse ash waste to produce self-compacting concrete by adding limestone powder waste, J. Clean Prod. 57 (2013) 308–319. https://doi.org/10.1016/j.jclepro.2013.06.009.
[38] Shaik, S. B., Karthikeyan, J., & Jayabalan, P. (2020). Influence of using agro-waste as a partial replacement in cement on the compressive strength of concrete–A statistical approach. Construction and Building Materials, 250, 118746. https://doi.org/10.1016/j.conbuildmat.2020.118746.
[39] Rao, M., & Prabath, N. V. N. (2015). Green concrete using agro industrial waste (sugarcane bagasse ASH). Int. J. Soft Comput. Eng.(IJSCE), 5, 86-92.
[40] Srinivasan, R., & Sathiya, K. (2010). Experimental study on bagasse ash in concrete. International Journal for Service Learning in Engineering, Humanitarian Engineering and Social Entrepreneurship, 5(2), 60-66. https://doi.org/10.24908/ijsle.v5i2.2992.
[41] Priya, K. L., & Ragupathy, R. (2016). Effect of sugarcane bagasse ash on strength properties of concrete. Int. J. Res. Eng. Technol, 5(4), 159-164.
[42] Ganesan, K., Rajagopal, K., & Thangavel, K. (2007). Evaluation of bagasse ash as supplementary cementitious material. Cement and concrete composites, 29(6), 515-524. https://doi.org/10.1016/j.cemconcomp.2007.03.001.
[43] Chi, M. C. (2012). Effects of sugar cane bagasse ash as a cement replacement on properties of mortars. Science and Engineering of Composite Materials, 19(3), 279-285. https://doi.org/10.1515/secm-2012-0014.
[44] Ardalan, R. B., Joshaghani, A., & Hooton, R. D. (2017). Workability retention and compressive strength of self-compacting concrete incorporating pumice powder and silica fume. Construction and Building Materials, 134, 116-122. https://doi.org/10.1016/j.conbuildmat.2016.12.090.
[45] Ranjith, A., Sanjith, J., & Kiran, B. M. (2015). Experimental investigation on performance of sugarcane bagasse ash concrete in acidic environment. Indexed in Scopus Compendex and Geobase Elsevier, Chemical Abstract Services-USA, Geo-Ref Information Services-USA, List B of Scientific Journals, Poland, Directory of Research Journals, 8(02), 471-476.
[46] Kiran, K., & Kishore, I. S. (2017). An experimental study on partial replacement of cement with bagasse ash in concrete mix. International journal of civil engineering and technology, 8(1), 452-455.
[47] Berenguer, R. A., Capraro, A. P. B., de Medeiros, M. H. F., Carneiro, A. M., & De Oliveira, R. A. (2020). Sugar cane bagasse ash as a partial substitute of Portland cement: Effect on mechanical properties and emission of carbon dioxide. Journal of Environmental Chemical Engineering, 8(2), 103655. https://doi.org/10.1016/j.jece.2020.103655.
[48] Quedou, P. G., Wirquin, E., & Bokhoree, C. (2021). Sustainable concrete: Potency of sugarcane bagasse ash as a cementitious material in the construction industry. Case studies in construction materials, 14, e00545. https://doi.org/10.1016/j.cscm.2021.e00545.
[49] Le, D. H., Sheen, Y. N., & Lam, M. N. T. (2018). Fresh and hardened properties of self-compacting concrete with sugarcane bagasse ash–slag blended cement. Construction and Building Materials, 185, 138-147. https://doi.org/10.1016/j.conbuildmat.2018.07.029.
[50] Rukzon, S., & Chindaprasirt, P. (2012). Utilization of bagasse ash in high-strength concrete. Materials & Design, 34, 45-50. https://doi.org/10.1016/j.matdes.2011.07.045.
[51] S. Praveenkumar, G. Sankarasubramanian, S. Sindhu, Strength, permeability and microstructure characterization of pulverized bagasse ash in cement mortars, Construct. Build. Mater. 238 (2020), 117691. https://doi.org/10.1016/j.conbuildmat.2019.117691.

IOP Conference Series: Earth and Environmental Science

PURPOSE-LED PUBLISHING™

PAPER • **OPEN ACCESS**

Development of paver blocks using cupola slag and fly ash

To cite this article: Sangita Meshram *et al* 2024 *IOP Conf. Ser.: Earth Environ. Sci.* **1409** 012003

View the article online for updates and enhancements.

You may also like

- Experimental Analysis of Composite Paver Block Using Bagasse Ash and Crushed Clay Brick
Anant Kumar, Abhigyan Shakar, Mayush Lonhare et al.
- Experimental study on sustainable cement concrete paver blocks incorporating coconut shell aggregate, quarry dust, silica fume and rice husk ash.
Yalangi Vivek, Yeswanth Paluri, P Ganesh et al.
- Laboratory investigation of concrete paver blocks containing RAP aggregates, fly ash and GGBS
Veligatla Ditendra, Yeswanth Paluri, K Rebka et al.



This content was downloaded from IP address 47.247.77.11 on 27/11/2024 at 05:31

Development of paver blocks using cupola slag and fly ash

Sangita Meshram[1*], Siddhi Yerawar[1], Aman Fopare[1], Shruti Nimbarte[1], Ruchira Hadke[1], Prajakta Derkar[1], Riya Rathod[1]

[1]Department of Civil Engineering, Yeshwantrao Chavan College of Engineering, 441110, Nagpur, Maharashtra, India

*E-mail: sangitameshram3@gmail.com

Abstract. The study examines the viability of using fly ash, which is the burned residue of industries and needs to be managed properly where it appears to be an alternative source of building material, in place of some of the cement in paver blocks and cupola slag as a partial replacement of fine aggregate in light of the growing pollution caused by construction materials. The research aims at the possibility of replacing the natural sand and cement with substitutionary in the production of paver blocks. This study is based on several proportions of the replacement of fine aggregate and cement with cupola slag waste, and fly ash. To reduce carbon dioxide emission, the greenhouse effect is caused by due heat of the hydration of cement which creates a bad impact on the environment. The different proportions were made with different percentages such as FA (40%, 45%, 50%, 80%, 85%, 90%) by replacement of cement and CS (50%, 55%, 60%, 100%) by replacing natural soil gives satisfactory results. The compressive strength was satisfactory to normal concrete paver blocks. M3 (60CS:40FA: 50FA: 50Cement) proportion is the optimal proportion out of all of them. The results were noted which determines the use of Paver block in construction materials.

Keywords. cupola slag, fly ash, cement, Paver Blocks, burnt-residue

1. Introduction

Urbanization produced a significant amount of solid garbage, and disposing of this waste became a major problem. Solid waste dumping and landfilling degrade the ecosystem by contaminating soil, and groundwater through leaching, and raising health risks for people. Around the world, paver blocks are a commonly used building material. Because of its remarkable characteristics, which include low cost, great strength, and extended durability, paver blocks are essential to the construction industry [1]. Cupola slag is a waste product produced in cupola furnaces during the ductile iron extraction process. It is primarily derived from coke ash, fluidized refractory lining, and iron and scrap oxidation products. Rapid cooling of the slag promotes vitrification, which leaves the silica in an amorphous state that makes it reactive [2]. One of the potential advancements is the knowledge and application of metallurgical slag, which makes up most of the waste from metallurgical processes. In addition to offering a partial solution to ecological and environmental issues, the use of industrial by-products greatly enhances the microstructure and, as a result, the durability properties of concrete—a feat that has proven challenging to accomplish with the use of pure Portland cement [3]. This paper is about the development of paver blocks, Paver blocks, also known as concrete pavers or interlocking concrete blocks, are prefabricated

Content from this work may be used under the terms of the Creative Commons Attribution 4.0 licence. Any further distribution of this work must maintain attribution to the author(s) and the title of the work, journal citation and DOI.
Published under licence by IOP Publishing Ltd

units used in construction for paving outdoor surfaces like roads, driveways, walkways, and parking lots [4]. They come in various shapes, sizes, and colours and are designed to interlock with each other, creating a durable and stable surface. However, integrating alternative materials such as cupola slag and fly ash offers several advantages in terms of sustainability, cost-effectiveness, and performance. Recently, the civil industry has been growing rapidly, and a lot of construction is taking place, which also increases the demand for cement, which is an important ingredient in construction material [5]. As the use of cement also creates a bad impact on the environment due to the large amount of emulsions of CO_2, and greenhouse gases. It is very important to find a substitute material that can reduce the use of cement, provide good strength with similar engineering properties, and reduce the emulsions of CO_2. Cupola slag which is by product of iron castings, which is later disposed of as a waste is been used as a substitute material for fine aggregate as we find out some similar properties within it. Reusing some amount of fly ash in place of cement shows the oxides present in it. Also, the use of these two products will give some other beneficial qualities to the concrete paste. 6 Different proportions were found to check at which proportion it gives high compressive strength as well as economical [6]. This includes a collection of cupola slag and understanding the material by determining its properties i.e. physical and mechanical properties as the cupola slag available was around 300 microns to 4.75mm in size. In this experiment, it was found first 3 proportions of mixed results that 30-40 % of replacement by volume of cement showed a higher value of compressive strength which was similar to normal concrete paver blocks. But another 3 different proportions result in moderate values of compressive strength and water absorption [7,8].

Also, the use of cement increases the cost of the construction of structures. In overall construction cost about 50% cost is of material only so finding cheap and good quality substitutes is very important to decrease the overall cost of construction [9,10]. The use of waste products such as cupola slag, and fly ash can help to decrease the cost and help to achieve economical concrete. in this summary, it is shown that the partial replacement of fly ash and granulated cupola slag can be used as a partial replacement of cement, showing similar graphical values. This will help to reduce environmental pollution caused by cement and also help to make sustainable economic concrete with good compressive strength.

2. Materials and Test Methodology

2.1. Introduction to raw materials

Cupola Slag is a burnt residue of metals and alloy from a Cupola furnace mainly it is a waste generated from various metals when melted or passed through the furnace, the furnace can melt large metals quickly and efficiently. Cupola slag is a byproduct of cast Iron manufacturing unit, it is produced during the separation of molten steel from impurities in cupola furnace. It is formed in semi-liquid form and after cooling it solidifies. The required composition of cupola slag can be widely turned on the peculiar parameters of the smelting operation. Its design and use became widespread during the Industrial Revolution, particularly in the iron and steel industry. This waste product is being used as an industrial waste product in this study. This sustainable material also helps in helps in reducing the amount of fine aggregate. also, it has various physical and chemical properties which include oxides. In the process of extracting the cupola slag, the oxides separate from the molten iron and float on the surface. The cupola slag was procured from the steel industry Neco Industry, MIDC, Hingna, Nagpur, Maharashtra. It was sieved through 2.36mm as shown in figure 1. The use of cupola slag in the production of paver blocks helps in the reduction of fine aggregates and also increases the strength of paver blocks to ensure this we carried out various

tests and find its physical and chemical properties as shown in (table 4) Fly Ash is a byproduct of burnt crumble coal which undergoes combustion and then collected using electrostatic precipitators and form fly ash which is a very fine powder, fly ash is recycled and used as it contents the cementitious and pozzolanic property which helps us to use as a replacement to cement in this paper. The oxides present in this are mainly silicon dioxide (SiO_2), aluminium oxide ($Al2O_3$), iron oxide (Fe_2O_3), and calcium oxide (CaO) which are also found in cement. Fly ash was collected from the Koradi thermal power plant in Khaperkheda, Nagpur, Maharashtra shown in figure 2. It mainly helps in controlling air pollution which a drastic problem is caused by industry. The utilization of fly ash only helps in reusing the industry waste which also provides the cementitious property, which was observed through various tests conducted on it, the result as shown in (Table 3).

Cement is the main ingredient in the construction material which poses the binding properties that help in binding the materials together also it conducts the hydration properties which release the amount of heat when applied for curing, the use of cement in making the paver block is nothing but to pose a binding property and hydration which is ultimately hard to achieve in any other substitute. As a binding material, OPC grade 53 cement was used.



Figure 1. (a) Cupola Slag before sieving (b) Cupola Slag after sieving



Figure 2. Fly Ash from Koradi Thermal Power Plant

The mixing was done on every trial batch, under each proportion (Table1, Table2) mixing again 12 paver blocks for each proportion was made to do different testing on the sample of Same proportion to get better results. At the time of mixing proper supervision was done so that each material should get mixed properly and proper homogeneous paste should be made. Paver Blocks (Fig 3) were made with the proper molds. The blocks are next cured for 28 days in the curing tank.

Table 1. Mix proportions of raw materials for bricks for M35 grade of Concrete

Mix	No of Specimen	Cupola Slag (%)	Fine Aggregate (%)	Fly Ash (%)	Cement (%)
M1	12	50	50	40	60
M2	12	55	45	45	55
M3	12	60	40	50	50

Table 2. Mix proportions of raw materials for bricks for M35 grade of Concrete

Mix	No of Specimen	Cupola Slag (%)	Fly Ash (%)	Cement (%)
M4	12	100	80	20
M5	12	100	85	15
M6	12	100	90	10

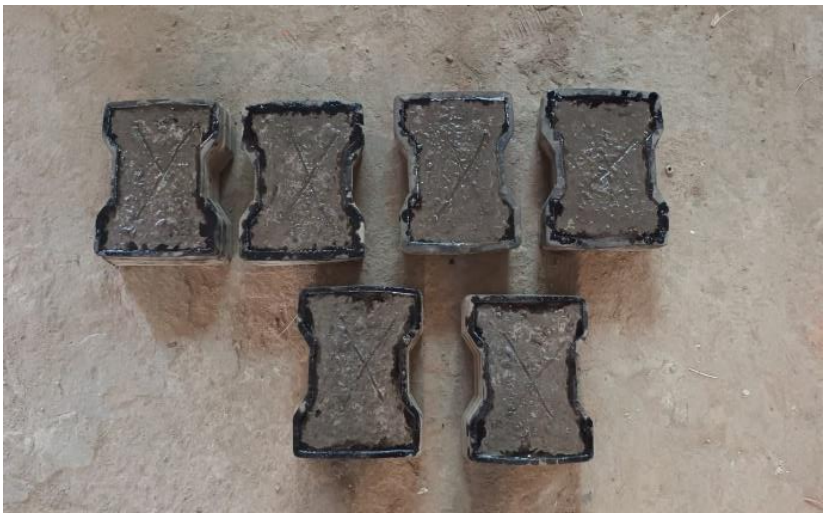


Figure 3. Paver Blocks Specimen

2.2. Test Methodology

The physical and chemical properties of raw materials were analyzed, and the chemical inherits of raw materials were examined by using X-ray fluorescence (XRF). Using an XRF spectrometer, the elemental composition of cupola slag was analyzed (Indian Bureau of Mines, Nagpur). For casting mix was prepared according to the Design of proportion, At the time of mixing proper supervision was done so that each material was mixed properly and a proper homogeneous paste was made, after mixing the mix was then filled in the oil-greased mold (Fig 3). The mix was blended and laid down on the table vibration for a few minutes and the blocks were left to dry for 24 hrs. After 24 hours the blocks were removed from mold and immersed in a curing tank for 7 days, 14 days, and 28 days. The testing on materials was conducted, on every block to know the material behaviour and quality. Tests performed were water absorption, block density, and compressive Strength, which are necessary for paver block. A total of 50 blocks were manufactured on various proportions.

3. Results and Discussion

3.1. Properties of raw material

The chemical composition of raw materials is as shown in (Table 4) cupola slag contains a greater percentage of lime calcium oxide present and then silica which is important for strength and plays a very important role in setting, Aluminium, iron oxide, and magnesium are all some compounds which are present in cupola slag. As the quantity of lime and silica is more in cupola slag it is considerable to replace as a substitute of cement in concreting. In fly ash we can see that silica is present in greater amounts than lime which helps to achieve strength, fly ash can also be used as a substitute in cement in a concreting mix but it will not provide a good binding property as lime is not present in adequate amount, but poses some engineering properties in concrete. Lime acts opposite material and helps to bind the material by creating a bond between two surfaces but to presence of extra lime can cause a delay in the hardening of cement. Aluminium oxide and magnesium oxide are present when cement hydration is produced. Couples like contents more chemicals as compared to fly ash and have more reactivity.

Table 3. Physical proportions of raw materials

Test	Cupola slag	Fly Ash	Cement
Specific gravity	2.88	1.87	3.15
Density (Kg/m^3)	1769	940 kg/m^3	1385
Consistency	-	33%	32%
Fineness	-	20%	15%
Water absorption	0.28%	-	-
Initial setting time	-	-	30min
Final setting time	-	-	10hour

Table 4. Chemical proportions of raw materials

Chemical composition	Cupola Slag (CS)	Fly ash (FA)
Lime, CaO (%)	24.27	1.49
Silica, SiO_2	36.86	58.69
Alumina, AL_2O_3	7.5	25.1
Iron oxide, Fe_2O_3	21.79	5.8
Magnesia, MgO	1.22	2.22
Sulphur trioxide, SO_3	0.11	0.12
Sodium Oxide, Na_2O	0.15	0.59
Potassium oxide, K_2O	0.9	4.04
Titanium Oxide, Tio_2	0.97	--
Pentium Oxide, P_2O_5	0.23	--
Sodium Oxide, NaO	0.15	--
Strontium Oxide, SrO	0.03	--
Barium Oxide, BaO	0.04	--
Magnesium dioxide, MnO_2	1.76	--
Chromium trioxide, CrO3	0.11	--
Zirconium dioxide, ZrO2	0.3	--
Tin oxide, SnO2	0.02	--
Free Cl	--	1.28

3.2. Mechanical Properties

3.2.1. Density of paver blocks

The density of raw materials when the blocks were tested it were noticed that as the proportion of fly ash is increasing and the proportion of cement is decreasing vice versa the proportion of cupola slag is increasing and the proportion of fine aggregate is decreasing. The density of cupola slag is more therefore the density of mix proportions is increasing in kg/m^3 shown in Figure 4. The increase in a density of mixed proportion shows that the compressive strength of blocks is higher, there is a chance of fewer void ports in the blocks which will help to achieve more compressive strength and durability of blocks durability which depends on the density, if it increases the water absorption is less. as shown in (Table 5).

Table 5. Density of Blocks

Mix Proportion	Density (kg/m^3)
M1	1959.6
M2	1968

M3	2141.9
M4	2200.52
M5	2225.26
M6	2355

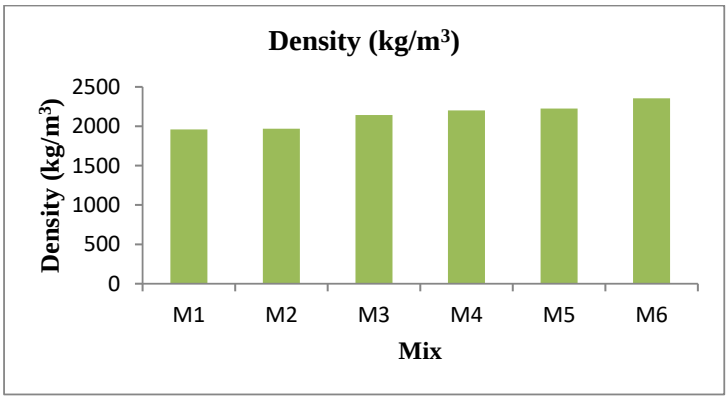


Figure 4. Density of Paver Blocks

3.2.2. Water Absorption

Table 6. Water Absorption of Blocks

Mix Proportions	Water Absorption (%)
M1	9.39
M2	10.79
M3	11.09
M4	3.6
M5	3.01
M6	2.3

Water absorption of blocks resulted in an increasing manner from M1 to M3 mix proportions. There is a major change in water absorption from the M4 mix proportion as the use of cupola slag is 100% replacement of fine aggregate which produces the water absorption in the paver block. The increase in the amount of cupola slag will fill the voids and make it denser, which ultimately leads to a decrease in water absorption. It reduces the porosity of Paver blocks. The blocks were oven-dried for 24 hours, (Figure 5) dry weight is calculated and similarly, wet weight is known through which water absorption for each block is estimated. (Table 6).

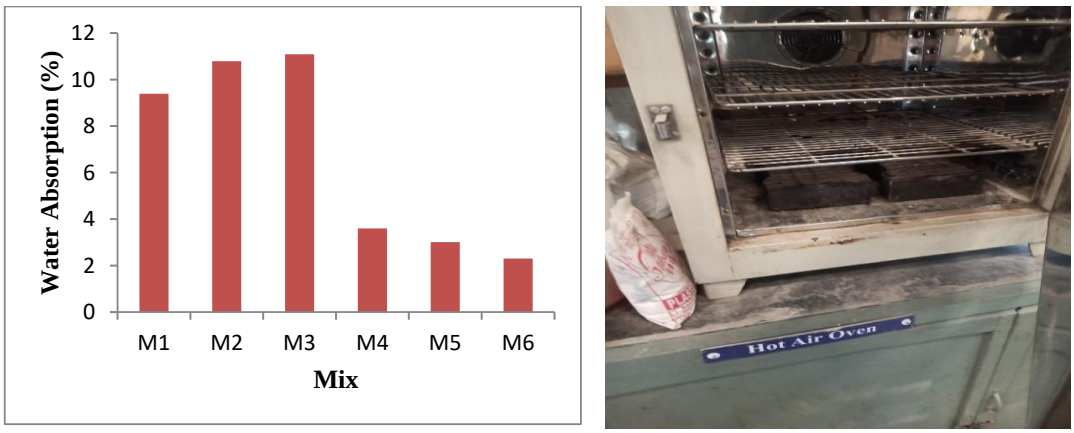


Figure 5. a) Water Absorption of Paver Blocks b) Blocks place in oven

3.2.3. Compressive Strength

The compressive results help in understanding the behaviour of cupola slag when replaced 100% with natural soil, which leads to decreased in compressive strength, hence the combination of cupola slag and fly ash results in increasing compression in M1, M2, and M3, which is useful in making the paver blocks, It was noticed that M3 results are best among all proportions (Table 7) the load of 14 N/mm^2 per min is applied and results were noted (Figure 6).

Table 7. Compressive Test Results for Blocks

Mix Proportions	Compressive strength (N/mm^2)
M1	29.06
M2	30.5
M3	33.96
M4	27.925
M5	25.65
M6	22.26

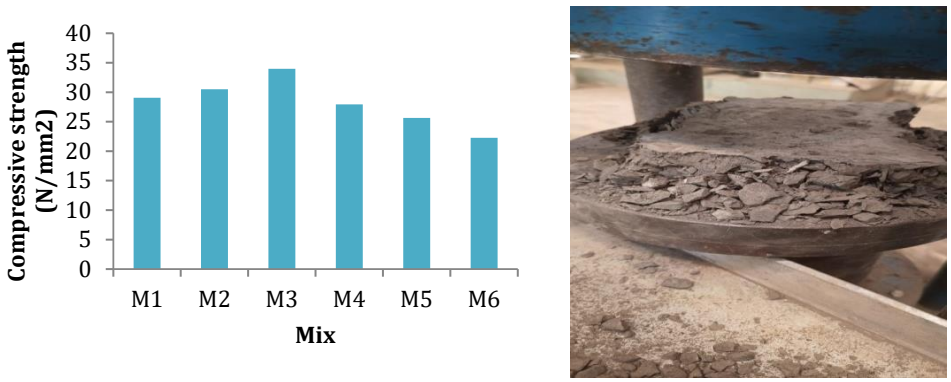


Figure 6. (a) Compressive strength (b) Block specimen in Compressive Strength Machine.

4. Conclusions

Due to the high density of payment blocks, the water absorption is less and the durability and strength of the payment block will be increased. In the water absorption, the conclusion of test results is such that, due to less use of cement in every next trial batch by some percentage the water requirement is less, as cement needs more water for heat of hydration and also the bulk density of cement is more therefore the water absorption is also more if the quantity of cement used in the pavement block is more. From the M1 mix proportion to the M6 mix proportion the quantity of cement used in the proportion is decreasing and therefore the results also show a decreasing graph line from 9.39% to 2.3% there is a huge change in the percentage of water absorption. Fine aggregate also absorbs more water as compared to cupola slag, fine aggregate bulk density is more comparable and creates strong and hard pavement blocks.

The investigation into replacing sand with cupola slag in the development of paver blocks has provided valuable insights into sustainable construction practices. By replacing 100% cupola slag in M35 grade mix designs, the study aimed to reduce environmental impact without compromising structural integrity. Through the meticulous creation of three mix designs and casting six blocks for each, the research explored the viability of this alternative material composition. This iterative approach sought to optimize the mix designs by gradually decreasing cement content while maintaining performance standards. The best of all the proportions M3 has shown acceptable results, however, despite these efforts, the compressive strength achieved at 28 days of curing fell short of the targeted 35 N/mm^2, reaching up to 33 N/mm^2. This outcome highlights the need for continued refinement and optimization in the application of cupola slag in paver block manufacturing.

5. Reference

[1] Meshram, S.S., Raut, S.P. and Madurwar, M.V., 2022. Use of industrial waste burnt residue to develop sustainable brick. Materials Today: Proceedings, 60, pp.732-737.
[2] Sosa, I., Thomas, C., Polanco, J.A., Setién, J., Sainz-Aja, J.A. and Tamayo, P., 2022. Durability of high-performance self-compacted concrete using electric arc furnace slag aggregate and cupola slag powder. Cement and Concrete Composites, 127, p.104399.
[3] BABATUNDE, R.I., ALI, H. and UCHE, O.A., 2022. Investigation On the Potentials Of Cupola Furnace Slag Ash As Partial Replacement For Cement In Concrete Structures.
[4] Chakravarty, S., Haldar, P., Nandi, T. and Sutradhar, G., 2021. Cupola slag reutilization for sustainable waste management: review and economic analysis. International Journal of Environmental Science and Technology, pp.1-16.
[5] Kanawade, B.D. and Nawale, S., 2018. Strength and durability of concrete paver block. NDT test for bridges.
[6] Alabi, S.A. and Afolayan, J.O., 2013. Investigation on the potentials of cupola furnace slag in concrete. International Journal of Integrated Engineering, 5(2).
[7] Raja, R. and Kumar, S., 2023. Cupola slag as a green concrete-making material and its performance characteristics-A review. Renewable and Sustainable Energy Reviews, 185, p.113573.
[8] Meshram, S., Raut, S.P., Ansari, K., Madurwar, M., Daniyal, M., Khan, M.A., Katare, V., Khan, A.H., Khan, N.A. and Hasan, M.A., 2023. Waste slags as sustainable construction materials: a compressive review on physico mechanical properties. Journal of Materials Research and Technology, 23, pp.5821-5845.
[9] Meshram, S.S. and Raut, S.P., 2021. Utilization of cupola slag as a sustainable construction material. Advances in Civil Engineering and Infrastructural Development: Select Proceedings of ICRACEID 2019, pp.43-49.
[10] Meshram, S., Raut, S.P. and Madurwar, M.V., 2023. Utilization of cupola slag blended with coal ash for the development of sustainable brick. In Recent Advances in Material, Manufacturing, and Machine Learning (pp. 1282-1289). CRC Press.

IOP Conference Series: Earth and Environmental Science

PURPOSE-LED PUBLISHING™

PAPER • **OPEN ACCESS**

The influence of land use land cover on the land surface temperature and vegetation index of Pune city, India

To cite this article: Krutika Madkaiker *et al* 2024 *IOP Conf. Ser.: Earth Environ. Sci.* **1409** 012004

View the article online for updates and enhancements.

You may also like

- Examining the effect of urbanization on various land cover classes and environmental quality using remote sensing and GIS methods
Hemant Singh Pokhariya, Khushi Jain and Prashuk Jain
- Spatial-temporal analysis of urban climate dynamics in major Hungarian cities
Attila Buzási, Bettina Szimonetta Beszedics-Jäger and Olivér Hortay
- Modeling spatiotemporal land use/land cover dynamics by coupling multilayer perceptron neural network and cellular automata markov chain algorithms in the Wabe river catchment, Omo Gibe River Basin, Ethiopia
Yonas Mathewos, Brook Abate, Mulugeta Dadi et al.



This content was downloaded from IP address 47.247.77.11 on 27/11/2024 at 05:31

The influence of land use land cover on the land surface temperature and vegetation index of Pune city, India

Krutika Madkaiker[1*], Madhuri Kumari[2], Rommel Mehta[3] and Sudhir Chavan[4]

[1]Amity School of Architecture & Planning, Amity University Uttar Pradesh, Noida, India
[2]Department of Civil Engineering, Amity School of Engineering & Technology, Amity University Uttar Pradesh, Noida, India
[3]Department of Landscape Architecture, School of Planning and Architecture, New Delhi, India
[4]Smt. Kashibai Navale College of Architecture, Sinhagad Technical Education Society, Pune, India

[*]E-mail: krutikamadkaiker@gmail.com

Abstract. The changes in land use land cover (LULC) over time intensifies the land surface temperature (LST). The variation in LST can be extracted from satellite imagery from different spatial resolutions for the summer month. In this study, through remote sensing and GIS techniques, the LST variation is quantified over different LULC classes from 2000 to 2020 using Landsat data in Pune City. The result shows an overall increase in the percentage of the built from 68.43% in 2000 to 85.31% in 2020, displaying a 16.88% rise during the study period. Further, the normalized difference vegetation index (NDVI) is extracted from the satellite imagery at different spatial resolutions for the summer months, and is quantified over the LULC classes for the duration of the study. The extreme variation in the mean NDVI values is seen in the areas with salt pans, semi arid areas, wetland-sparse vegetation and wetland–tree cover, i.e. areas near water bodies and the peripheral areas with less vegetation. The association of NDVI with LST shows a negative correlation that justifies the rise in surface temperature with the intensity of vegetation in the city. The results of this study shall help the planners, architects and policy makers to evaluate the current status of urbanisation, to make informed choices that lead to sustainable cities.

1. Introduction

Urbanisation is a global event notably due to the rapid expansion of the cities, the reasons being increased population, rural to urban migration and industrialisation. This phenomenon exerts consequences on the local climate within urban environments, resulting into the urban heat islands. When city expansion occurs, it changes the surface morphology of the land, resulting in a LULC transition, which impacts the temperature variation, precipitation and air quality.

India exhibits similar signs of escalation in urbanisation, particularly evident in the densely populated metropolitan cities. The implications of rapid urban growth are witnessed in the microclimate of these regions; which include heat stress, air pollution and water scarcity. Urbanization-led transitions magnify the vulnerability of communities to extreme weather events and health hazards, highlighting the necessity of holistic urban planning and management approaches.

Content from this work may be used under the terms of the Creative Commons Attribution 4.0 licence. Any further distribution of this work must maintain attribution to the author(s) and the title of the work, journal citation and DOI.
Published under licence by IOP Publishing Ltd

The impact of urbanization on land composition have a vital role in shaping microclimates. The transformation from natural landscapes into buildings, mobility infrastructure, etc. replaces the vegetation cover with impervious surfaces and aggravates the surface temperature. Additionally, these shifts in land use composition can influence the vegetation dynamics, changing the ecosystem services and biodiversity levels.

In this scenario, the investigations of land use land cover, land surface temperature and vegetation index within urban settings are essential tools to comprehend and curb the effect of urban sprawl on microclimates. The spatio-temporal variations of these attributes, help researchers to analyse the efficacy of urban planning interventions, locate vulnerable areas and suggest policies based on empirical data. This assessment aids the development of targeted approaches to improve urban resilience, mitigate heat distress and risks and facilitate sustainable urban development against the backdrop of rapid urbanisation.

1.1 Urban Heat Island (UHI)

UHI is a concept in which the temperature of a part in a city is warmer than its vicinity. The physical changes in the landscape where infrastructure replaces open land and vegetation and surfaces shift from pervious to impervious, modify the local energy balance in urban areas (especially in dense urban cities) and lead to the formation of UHI. The four significant factors that regulate urban climate proposed by Oke are urban structure, urban cover, urban fabric and urban metabolism (Vujovic, et al., 2021).

Rapid urbanisation could influence the above factors, which leads to transformation in land use and the extension of the built. Increased air temperatures negatively impact urban environments and lifestyles. UHI has a range of effects, which include deterioration of habitats, substantial increase in use and costs of energy consumption for cooling, escalation observed in issues of air quality, influence on human health and comfort, increase in heat stress and degradation of water quality. During the peak summer months, the surface temperature of paving and rooftops is much higher than the present air temperatures (S, et al., 2021).

1.2 Study Area

Pune city in Maharashtra covers an area of approximately 230.84 sqkm. The city is placed at 18°32” N latitude and 73°51” E longitude with an elevation of 560m above the mean sea level (Gohain, et al., 2020). With the rapid expansion of the industrial areas, the climate of Pune has changed in the past thirty years. The average temperature ranges between 19 to 33°C. Summer, monsoon, and winter are the predominant seasons in the city. Pune's summer months extend from March to the 15th of June, with a maximum temperature of about 42°C. The monsoon extends from June through September, with 722mm of annual rainfall and a temperature range between 22 to 28°C. The winters extend from November through January, with daytime temperatures of 26°C and night time temperatures falling below 9°C (Corporation, 2023).

This paper focusses on the land use land cover (LULC) transformation and its influence on the land surface temperature (LST) and the normalized difference vegetation index (NDVI) of the city, particularly in the summer months across the years from 2000 to 2020.

2. Experimental and materials

2.1 Source of Data Collection

The data used in this study employ multi-temporal satellite imagery taken from Landsat 5 TM (2000), Landsat 7 ETM+ (2010), Landsat 8 OLI/TIRS (2020) for Pune city focusing on the summer months of March and April (Table 1).

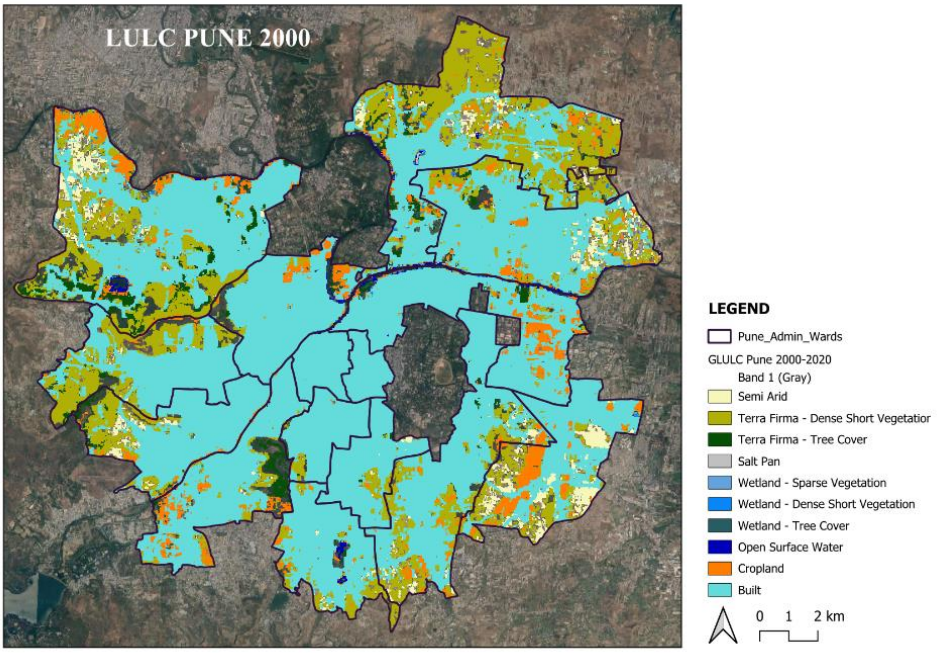


Figure 1. Pune city - LULC of 2000 (Potapov, et al., 2022).

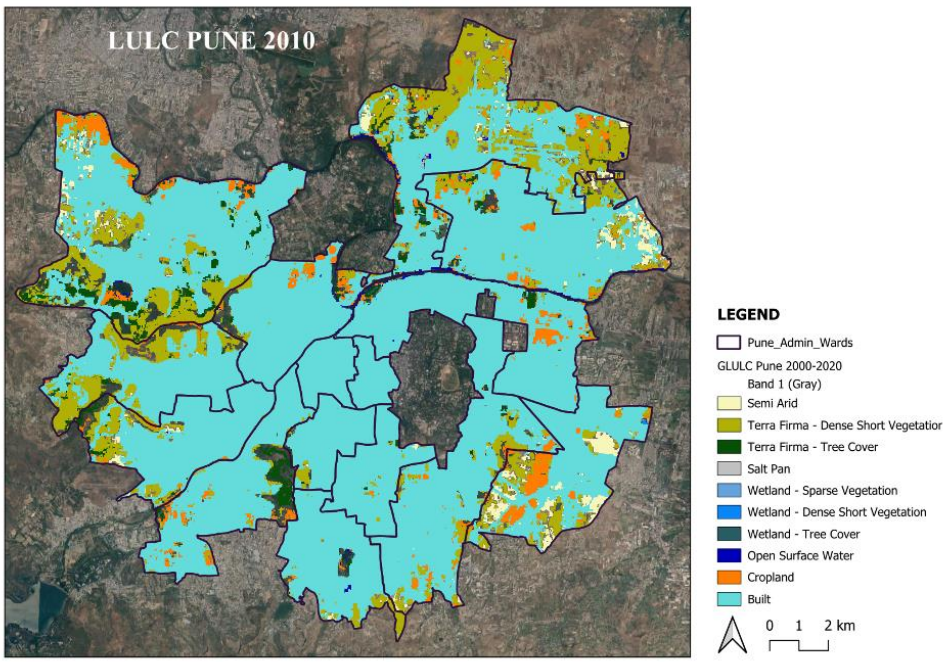


Figure 2. Pune city - LULC of 2010 (Potapov, et al., 2022).

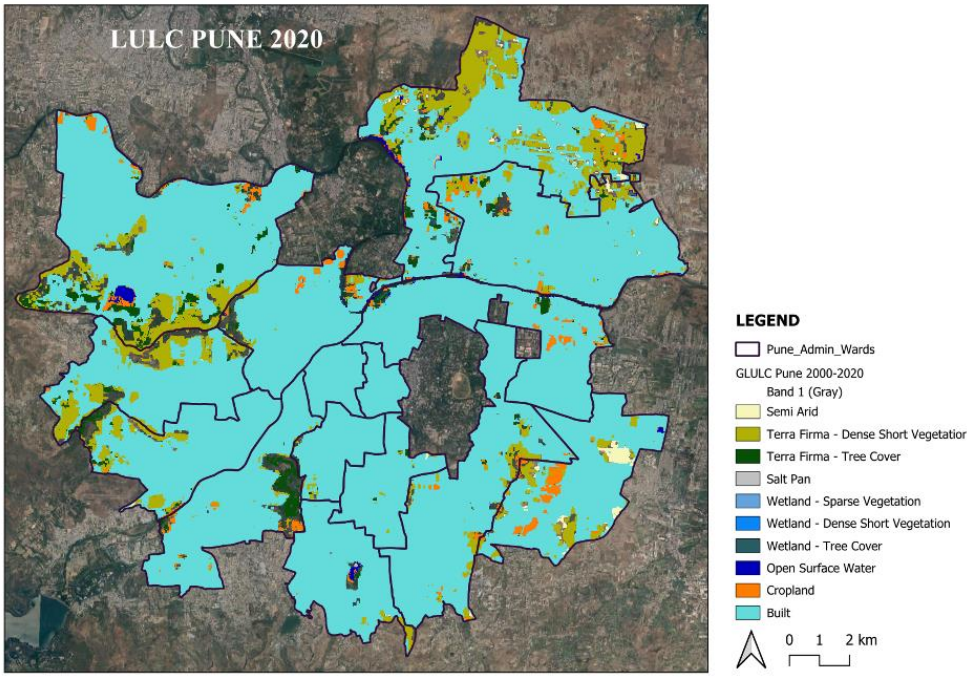


Figure 3. Pune city - LULC of 2020 (Potapov, et al., 2022).

Table 1. Specifics of Landsat satellite imagery

Year	Date & Time	Satellite	Sensor	Source
2020	29-03-2000, 05:02	Landsat 8	OLI/TIRS	USGS Earth Explorer
2010	02-04-2010, 05:20	Landsat 7	ETM+	
2000	05-04-2020, 05:27	Landsat 5	TM	

The LULC maps are referred from Global Land Cover and Land Use 2000 and 2020 (Potapov, et al., 2022) as shown in Figures 1, 2 and 3 and analysed for area computation and its changes.

2.2 Statistical Analysis

The change in LULC data is calculated using MOLUSCE tool in QGIS. The Zonal statistics tool in QGIS was used to collate the values of LST and NDVI over LULC class for the years 2000, 2010, 2020 respectively.

2.3 Retrieval of LST from Landsat data

LST investigates the association between rise in temperature and escalation in urbanisation (Choudhury, et al., 2019). To extract the LST values from Landsat 5 TM (Band 6) for the year 2000, Landsat 7 ETM+ (Band 6 VCID 1) for the year 2010 and Landsat 8 TIRS (Bands 10, 11) for the year 2020 respectively, the spectral radiance method is employed. The LST maps generated for the two decades are shown as Figures 4, 5 and 6. A stepwise method with equations is used to compute the LST (M, et al., 2016), as follows:

For Landsat 8,

(1) *Spectral Radiance (L) = ML x* Q_{cal} *+ AL*

where, ML = Band specific multiplicative recalling factor

AL = Band specific additive rescaling factor

Q_{cal} = Thermal band

(2) Conversion of Spectral Radiance to Surface Temperature (TB) using thermal constants given in the metadata.

$TB = K_2 / \ln (K_1/L + 1) - 273.15$

where, L = Spectral radiance

K_1, K_2 = Band specific thermal conversion constant from the metadata

To obtain the result in Celsius, the temperature is revised by adding absolute zero (approximately -273.15) (Xu & Chen, 2004).

(3) (3) NDVI calculation using bands 4 and 5,

$$NDVI = \frac{(NIR - RED)}{(NIR + RED)}$$

(4) Fraction of vegetation FV of each pixel was computed using the following equation from NDVI (Carlson & Ripley, 1997),

$$FV = \frac{(NDVI - NDVImin)^2}{(NDVImax - NDVImin)^2}$$

where, $NDVi_{min}$= Minimum NDVI value where pixels connote bare soil

$NDVI_{max}$= Maximum NDVI value where pixels connote healthy vegetation (Guha, et al., 2018)

(5) Land Surface Emissivity calculation (E) = 0.004 x FV + 0.986

(6) LST derived using the equation (Weng, et al., 2004),

$$LST = \frac{TB}{1 + \lambda\sigma TB \ln (E)hc}$$

where h = Plank's constant (6.626 x 10 – 34 Js)

c = Velocity of light in a vacuum (2.998 x 10-8 m/sec)

λ = Effective wavelength (10.9 mm for band 10 in Landsat 8, 11.45 mm for band 6 in Landsat 5 & 7)

σ = Boltzmann constant (1.38 x 10 – 23 J/K)

E = Emissivity

For Landsat 5 and 7,

(1) Conversion DN to Spectral Radiance

$$(L) = \frac{(L\max - Lmin)}{(Qcal - Qcal\ min)}(Qcal\ max - Qcal\ min) + Lmin$$

where, L = At sensor spectral radianceQcal = Landsat image [Digital Number (DN)]

Qcal min = Minimum quantized calibrated pixel value corresponding to Lmin (Ebodé, 2023)

Qcal max = Maximum quantized calibrated pixel value corresponding to Lmax

Lmin = Spectral - at sensor radiance that is scaled to Qcal min

Lmax = Spectral - at sensor radiance that is scaled to Qcal max (Nitheshnirmal, et al., 2018)

(2) Conversion of Spectral Radiance to Surface Temperature (TB) using thermal constants given in the metadata.

$$TB = \frac{K_2}{\ln\left(\frac{K_1}{L+1}\right)} - 273.15$$

where, L = Spectral radiance

K_1, K_2 = Band specific thermal conversion constant from the metadata

To obtain the result in Celsius, the temperature is revised by adding absolute zero (approximately -273.15) (Xu & Chen, 2004).igure 1. Pune City- LULC of 2000 (Potapov, et al,. 2022)

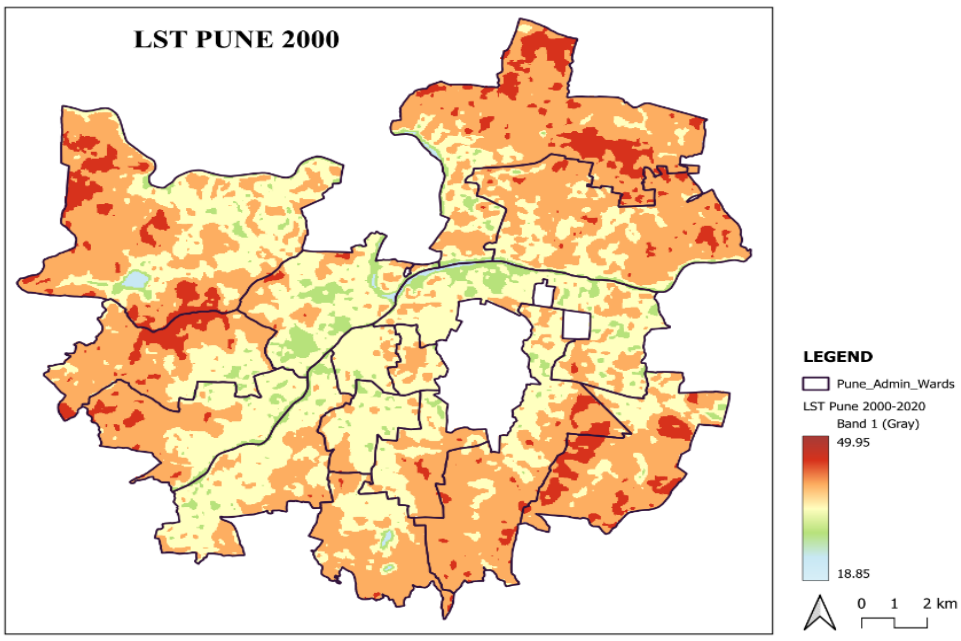


Figure 4. Pune city – LST plot of 2000

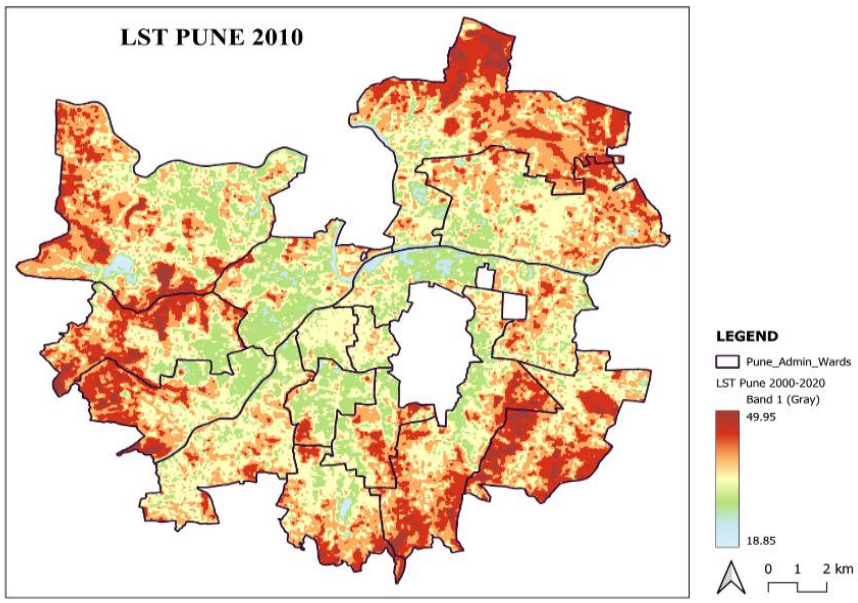


Figure 5. Pune city – LST plot of 2010.

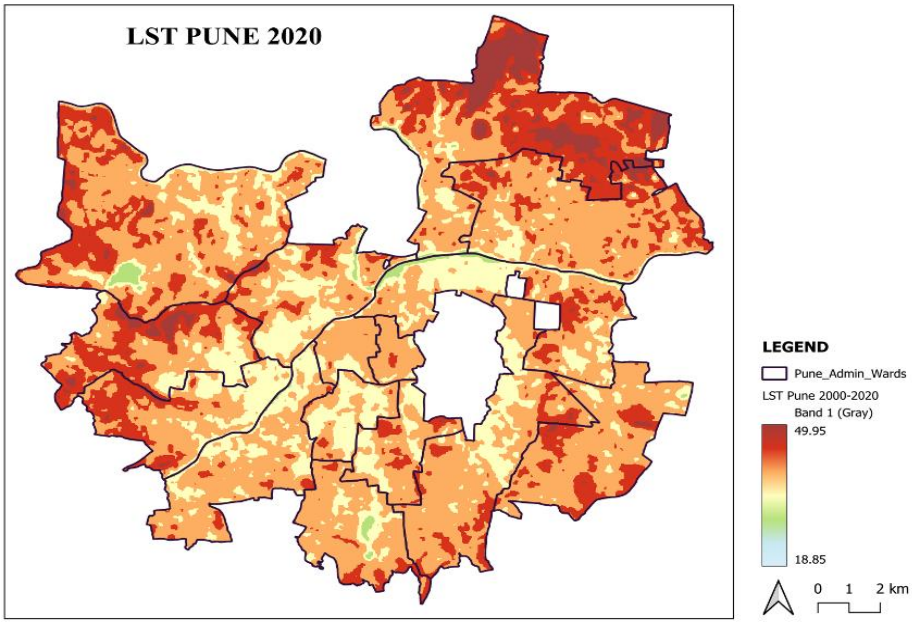


Figure 6. Pune city – LST plot of 2020.

2.4 Retrieval of NDVI from Landsat data

NDVI values are used to decipher the spatial density and distribution of vegetation. They are also an indicator of surface radiant temperature and helps in understanding the plant health, land cover and environmental situation. The NDVI values for the years 2000, 2010 and 2020 were computed from satellite images as the ratio between measured reflectance in the red (R) and near-infrared (NIR) bands using the equation (Xiao & Weng, 2007); as seen in Figures 7, 8 and 9. The Landsat bands used for NDVI calculation for the year 2020 are Bands 4 and 5 and for the year 2010 and 2000 are Bands 3 and 4.

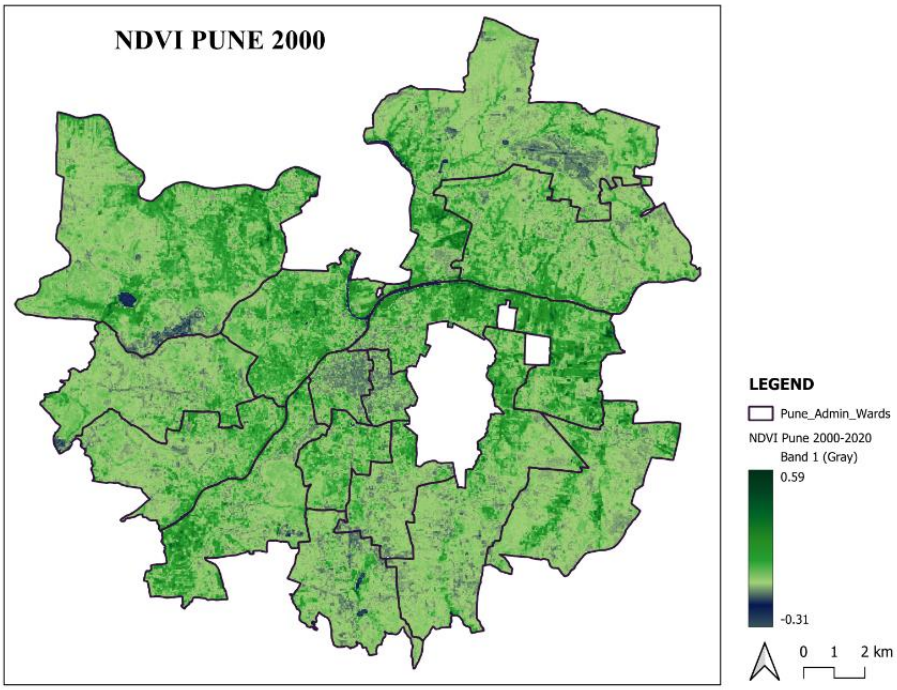


Figure 7. Pune city – NDVI plot of 2000.

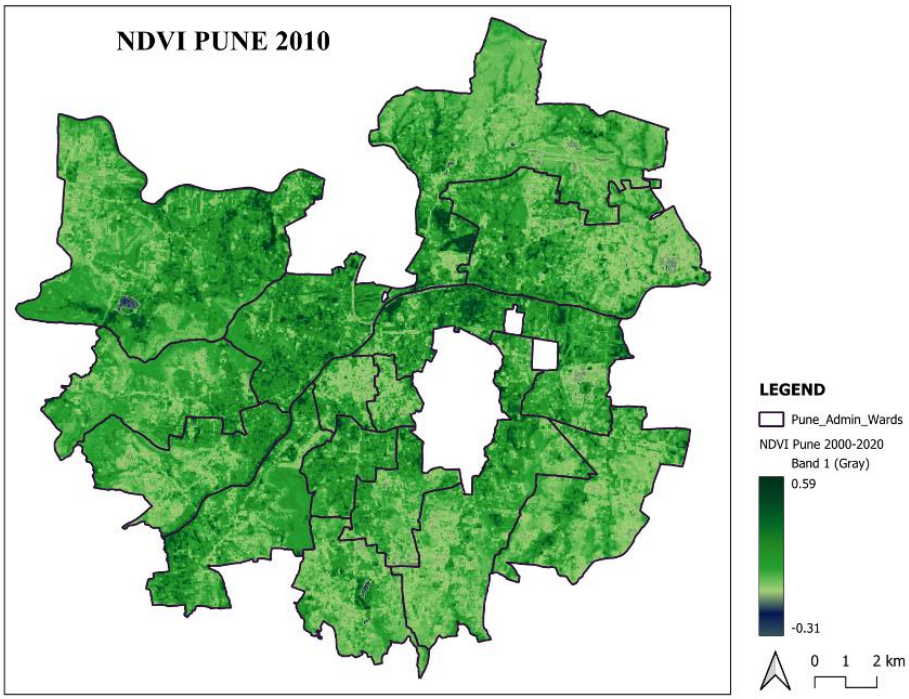


Figure 8. Pune city – NDVI plot of 2010.

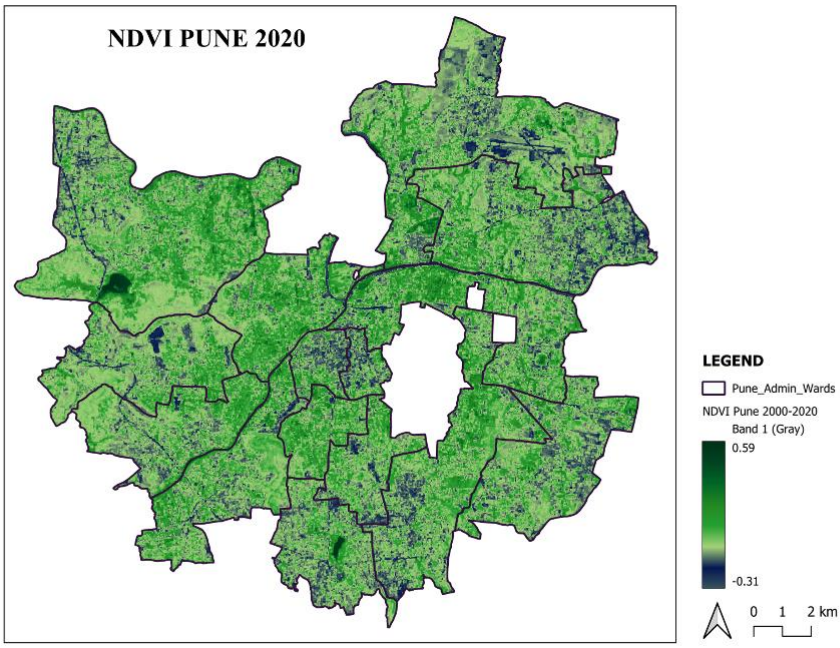


Figure 9. Pune city – NDVI plot of 2020.

3. Results and discussion

3.1 Change in LULC

Table 2. Percentage change in LULC for the years 2000, 2010 and 2020

No	**LULC Classes** (Potapov, et al., 2022)	Area in Percentage			Change in Percentage	
		2000	2010	2020	2000-2010	2010-2020
1	Semi Arid	3.53	1.92	0.52	-1.61	-1.40
2	Terra Firma – Dense Short Vegetation	20.06	14.20	10.15	-5.86	-4.05
3	Terra Firma – Tree Cover	1.97	1.89	1.74	-0.09	-0.15
4	Salt Pan	0.03	0.00	0.00	-0.03	0.00
5	Wetland – Sparse Vegetation	0.03	0.01	0.00	-0.02	-0.01
6	Wetland Dense Short Vegetation	0.20	0.06	0.01	-0.14	-0.05
7	Wetland Tree Cover	0.09	0.09	0.08	-0.01	-0.01
8	Open Surface Water	0.35	0.31	0.26	-0.03	-0.05
9	Cropland	5.31	3.74	1.93	-1.57	-1.82
10	Built	68.43	77.78	85.31	9.35	7.53

In this study, the LULC classes have been distinguished into ten categories; which could be broadly compiled further into Semi-Arid, Terra Firma, Salt Pan, Wetland, Open Surface Water, Cropland and Built for the years 2000, 2010, 2020.

Table 2 presents the percentage change in each LULC class for each of these years. It reveals that over the last twenty years, there has been a substantial rise in the built and a visible decrease

in the other classes. The built area has increased from 68.43% to 77.78% to 85.31%. This change could be a result of the urban extension in the city's peripheral areas.

Table 3. LST values across LULC classes

No	LULC Classes (Potapov, et al., 2022)	LST (°C)								
		2000			2010			2020		
		min	max	mean	min	max	mean	min	max	mean
1	Semi Arid	29.18	38.78	36.69	34.53	47.42	42.09	38.58	47.62	43.23
2	Terra Firma - Dense Short Vegetation	24.97	48.13	35.78	28.33	49.95	41.47	32.56	49.66	41.79
3	Terra Firma - Tree Cover	24.97	40.69	32.49	28.33	43.98	36.00	28.83	45.38	36.12
4	Salt Pan	24.11	30.83	26.78	27.35	31.23	29.60	27.61	30.57	28.63
5	Wetland – Sparse Vegetation	24.55	37.61	29.67	27.35	43.98	33.36	29.62	42.62	38.26
6	Wetland Dense Short Vegetation	25.40	38.39	31.28	27.84	43.11	34.07	32.03	40.56	37.57
7	Wetland Tree Cover	25.40	35.65	29.65	28.33	39.11	32.28	30.67	38.48	33.73
8	Open Surface Water	21.94	34.46	26.98	26.36	40.46	30.30	27.76	42.10	31.73
9	Cropland	23.68	40.69	33.08	25.87	46.14	38.25	28.03	47.38	37.66
10	Built	24.11	42.21	32.82	18.15	47.85	37.14	28.86	47.46	37.63

Table 4. Change in LST values over different LULC classes

No.	LULC Classes (Potapov, et al., 2022)	Change in LST (°C)		
		2000-2010	2010-2020	2000-2020
1	Semi Arid	5.40	1.14	6.54
2	Terra Firma – Dense Short Vegetation	5.69	0.32	6.01
3	Terra Firma – Tree Cover	3.51	0.13	3.64
4	Salt Pan	2.82	-0.97	1.86
5	Wetland – Sparse Vegetation	3.69	4.90	8.59
6	Wetland Dense Short Vegetation	2.79	3.50	6.29
7	Wetland Tree Cover	2.63	1.45	4.08
8	Open Surface Water	3.32	1.43	4.75

9	Cropland	5.17	-0.59	4.58
10	Built	4.32	0.48	4.80

3.2 Change in LST

Satellite images for three years 2000, 2010, and 2020 are studied to configure the LST values for each LULC category. This aided in deriving the impact of LULC change on LST. As shown in Table 3, the spatiotemporal distribution of LST discloses that the semi-arid class exhibits a maximum mean temperature of 36.69°C (2000), 42.09°C (2010) and 43.23°C (2020). This implies that increase in semi arid areas which are devoid of vegetation, elevates the surface temperature in the peripheral areas of the city. The minimum mean temperature is noted in open surface water with 26.98°C (2000), 30.30°C (2010) and 31.73°C (2020). Also, areas with salt pans showed 26.78°C (2000), 31.23°C (2010) and 28.63°C (2020).

Table 4 suggests significant changes in LST across all LULC classes, especially between 2010 and 2020. The study indicates a direct relationship between LST and the built.

3.3 Change in NDVI

NDVI is a system of measurement for assessing vegetation vitality using sensor data. The pixel values of NDVI range within -1 and 1. High negative values depict water; the values near 0 suggest bare soil and the values near 1 signify dense green vegetation. The NDVI values of 2000, 2010 and 2020 have been recorded and compared in Table 5. In the year 2000, the lowest and highest NDVI values ranged from -0.231 and 0.539, later progressively increased to -0.308 and 0.541 in 2010 and further changed from -0.068 to 0.577 in 2020. The lowest mean NDVI values for 2000, 2010 and 2020 are seen in Salt Pan (-0.026), Semi Arid (-0.090) and Wetland-Sparse Vegetation (0.093), respectively. The highest mean NDVI values for 2000, 2010 and 2020 are seen in Wetland Tree Cover (0.189). Wetland Tree Cover (0.277) and Salt Pan (0.542) respectively.

Table 5. NDVI values across LULC classes

No	LULC Classes (Potapov, et al., 2022)	NDVI								
		2000			2010			2020		
		min	max	mean	min	max	mean	min	max	mean
1	Semi Arid	-0.155	0.101	-0.002	-0.171	0.117	-0.090	0.009	0.206	0.101
2	Terra Firma - Dense Short Vegetation	-0.182	0.382	0.022	-0.186	0.407	-0.024	-0.042	0.429	0.142
3	Terra Firma -Tree Cover	-0.101	0.470	0.101	-0.115	0.541	0.127	0.094	0.503	0.225
4	Salt Pan	-0.200	0.391	-0.026	-0.013	0.075	0.029	0.534	0.546	0.542
5	Wetland – Sparse Vegetation	-0.228	0.531	0.031	-0.145	0.368	0.070	0.024	0.162	0.093
6	Wetland Dense Short Vegetation	-0.167	0.489	0.045	-0.219	0.385	0.053	0.060	0.311	0.182
7	Wetland Tree Cover	-0.023	0.421	0.189	-0.034	0.489	0.277	0.126	0.429	0.308

8	Open Surface Water	-0.231	0.539	0.020	-0.308	0.449	0.006	-0.063	0.577	0.297
9	Cropland	-0.167	0.524	0.090	-0.222	0.535	0.061	-0.048	0.573	0.215
10	Built	-0.182	0.527	0.049	-0.242	0.507	0.005	-0.068	0.563	0.161

3.4 Correlation between NDVI and LST

LST and NDVI relationship is assessed by performing Pearson Correlation analysis using PSPP software as shown in Table 6. The correlation coefficients (r) obtained are -.194, -.449, and -.270 for the years 2000, 2010, and 2020 respectively. According to the results, there exists a negative correlation among NDVI and LST values. This validates the point that dense vegetation minimises the proportion of heat stored in the soil and surfaces through evapotranspiration.

Table 6. Correlation analysis between NDVI and LST for 2000, 2010 and 2020

		NDVI 2000	LST 2000
NDVI 2000	Pearson Correlation	1.000	-0.194[a]
	Sig. (2 – tailed)		0.002
	N	250	250
LST 2000	Pearson Correlation	-0.194[a]	1.000
	Sig. (2 – tailed)	0.002	
	N	250	250
		NDVI 2010	LST 2010
NDVI 2010	Pearson Correlation	1.000	-0.291[a]
	Sig. (2 – tailed)		0.000
	N	250	250
LST 2010	Pearson Correlation	-0.291[a]	1.000
	Sig. (2 – tailed)	0.000	
	N	250	250
		NDVI 2020	LST 2020
NDVI 2020	Pearson Correlation	1.000	-0.270[a]
	Sig. (2 – tailed)		0.000
	N	250	250
LST 2020	Pearson Correlation	-0.270[a]	1.000
	Sig. (2 – tailed)	0.000	
	N	250	250

a. Significant at 0.05 level

4. Conclusions

In this study on Pune city between 2000 to 2020, Landsat images have been used to extract and estimate the spatial dispersal of LST and NDVI. LULC maps have been referred from the Global 2000-2020 Land Cover and Land Use Change Dataset Derived from the Landsat Archive (Potapov, et al., 2022) for 2000, 2010 and 2020, respectively. This study discusses the variation within LST and NDVI across the LULC classes. The LULC results reveal a distinct increase in built area over other classes, this can be dedicated to the urban extension in the periphery of the city. The decadal variation observed between 2010-2020 suggest significant changes in the LULC classes. The investigation of LST across LULC categories reveals the highest mean temperature in semi arid

areas; the lowest mean temperatures seen on the open surface waters, followed by areas with salt pans. Again, the decadal variation of LST over LULC is observed significantly between the year 2010 to 2020. The LULC and LST variations may affect the microclimate of the city. NDVI mean values over LULC classes suggest a variation in the salt pan areas from -0.026 in 2000 depicting water, to 0.542 in 2020 suggesting green vegetation. The areas with wetland tree cover reveal high mean values of NDVI from 0.189 in 2000 to 0.277 in 2010 to 0.308 in 2020 informing decadal progression in green vegetation. An indirect relationship among NDVI and LST values suggests that areas with high vegetation show low surface temperature. The growth in built areas and conversion from pervious to impervious surfaces leads to a surge in temperature and creates UHI effect in the city. Usage geographic information systems (GIS) and remote sensing techniques with the aid of satellite sources such as Landsat, provides efficient assessment of urban development patterns and insights into the city's local climate. This research is expected to benefit planners, architects and policymakers to evaluate the urban development through the parameters of land composition and surface temperatures to help enhance their decisions for a better, safer and sustainable city.

References

[1] Carlson, T. N. & Ripley, D. A., 1997. On the relation between NDVI, fractional vegetation cover, and leaf area index. *Remote Sensing of Environment,* Volume 62, pp. 241-252.

[2] Choudhury, D., Das, K. & Das, A., 2019. Assessment of land use land cover changes and its impact on variations of land surface temperature in Asansol-Durgapur Development Region. *The Egyptian Journal of Remote Sensing and Space Sciences,* 22(2), pp. 203-218.

[3] Ebodé, V. B., 2023. Land Surface Temperature Variation in Response to Land Use Modes Changes: The Case of Mefou River Sub-Basin (Southern Cameroon). *Sustainability,* 15(1), p. 864.

[4] Gohain, K. J., Mohammad, P. & Goswami, A., 2020. Assessing the impact of land use land cover changes on land surface temperature over Pune city, India. *Quaternary International,* pp. 1-11.

[5] Guha, S., Govil, H., Dey, A. & Gill, N., 2018. Analytical study of land surface temperature with NDVI and NDBI using Landsat 8 OLI and TIRS data in Florence and Naples city, Italy. *European Journal of Remote Sensing,* 51(1), pp. 667-678.

[6] Mehebub, S., Raihan, A. & Haroon, S., 2016. Analyzing land surface temperature distribution in response to land use/land cover change using split window algorithm and spectral radiance model in Sundarban Biosphere Reserve, India. *Modeling Earth Systems and Environment*, 02 May, Volume 2 (81), pp. 1-11.

[7] Nitheshnirmal, S. et al., 2018. SPATIO-TEMPORAL ANALYSIS OF NATURAL HUMAN HABITABILITY ENVIRONMENT ALONG THE COASTAL TALUKS OF TAMIL NADU, INDIA. *ISPRS Annals of the Photogrammetry Remote Sensing and Spatial Information Sciences,* IV(5), pp. 439-446.

[8] Potapov, P. et al., 2022. The Global 2000-2020 Land Cover and Land Use Change Dataset Derived From the Landsat Archive: First Results. *Frontiers in Remote Sensing,* 13 April, 3(856903), pp. 1-22.

[9] S, V. et al., 2021. Land sy: Causes, Consequences, and Mitigation Measures with Emphasis on Reflective and Permeable Pavements. *Civil Engineering,* pp. 459-484.

[10] Vujovic, S. et al., 2021. Urban Heat Island: Causes, Consequences, and Mitigation Measures with Emphasis on Reflective and Permeable Pavements. *CivilEng,* pp. 459-484.

[11] Weng, Q., Lu, D. & Schubring, J., 2004. Estimation of land surface temperature-vegetation abundance relationship for urban heat island studies. *Remote Sensing of Environment,* 89(4), pp. 467-483.

[12] Xiao, H. & Weng, Q., 2007. The impact of land use and land cover changes on land surface temperature in a karst area of China. *Journal of Environmental Management,* October, 85(1), pp. 245-257.

[13] Xu, H. & Chen, B., 2004. Remote sensing of the urban heat island and its changes in Xiamen City of SE China. *Journal of Environmental Sciences,* 16(2), pp. 276-281.

[14] Corporation, P. M., 2023. *Pune Weather.* [Online] Available at: https://www.pmc.gov.in/en/pune-weather-0 [Accessed 30 03 2024].

IOP Conference Series: Earth and Environmental Science

PURPOSE-LED PUBLISHING™

PAPER • **OPEN ACCESS**

A comprehensive analysis of the water distribution network by using waterGEMS software

To cite this article: Borigarla Brahmamiah *et al* 2024 *IOP Conf. Ser.: Earth Environ. Sci.* **1409** 012005

View the article online for updates and enhancements.

You may also like

- Exploring the Potential of High-Fatty Acid Content Oils for Biodiesel Production: A Catalyst-Free Approach
MD Solikhah, SS Wirawan, AT Sugiarto et al.
- Preparation and application of waste cigarette butts-derived mulch film with excellent mechanical properties and optical transparency
Xianjie Liu, Sijun Huang, Genrong Li et al.
- Development and application of software for designing axial fans in high-temperature environments
Shengli Zhang, Zhichun Zeng, Qianhui Zhu et al.



This content was downloaded from IP address 47.247.77.11 on 27/11/2024 at 05:32

A comprehensive analysis of the water distribution network by using waterGEMS software

Borigarla Brahmamiah[1*], K. Surendra[1] and P. Vani[1]

[1]Department of Civil Engineering, Vignan's Institute of Information Technology (A), Visakhapatnam, Andhra Pradesh, India

[*]E-mail: brahmamg44@gmail.com

Abstract. Water is essential for various human activities, and the water need has dramatically increased with population growth and lifestyle changes. This increased demand underscores the importance of sustainable and efficient water management strategies. This study aimed to create robust, efficient systems to meet growing communities' current and future water needs. WaterGEMS software was used to identify high- and low-pressure zones in junctions and assess water flow velocity in pipes to evaluate hydraulic performance. The results showed considerable differences in water demand, pressure, elevation, and hydraulic grade at various intersections. The minimum and maximum demand of 1.0 L/min and 19.0 L/min were found at J-2 and J-31, respectively. The elevation varied from 33.78 to 67.38 meters, with the lowest at J-20 and the highest at J-31. Hydraulic grade ranged from 39.40 to 110.04 meters, with the weakest at J-30 and the highest at J-41. Furthermore, the multi-linear regression model constructed to forecast head loss in the water distribution network had significant coefficients and an R-squared value of 0.965, indicating an excellent match to the data. All coefficients had significant p-values ($p < 0.05$), indicating the model's reliability.

1. Introduction

Water management is paramount in ensuring the sustainable availability of potable, sanitation, agricultural, and industrial water. Water management involves the strategic organization, expansion, allocation, and preservation of water resources to satisfy current and future needs while preserving the environment. Water distribution networks facilitate the conveyance of water from sources to consumers through complex systems comprising pipelines, pumps, valves, and storage tanks. Water distribution networks constitute a single element within water delivery systems, consisting of storage reservoirs, pipelines, and hydraulic apparatus. As a direct consequence of an increase in water pressure demand, which includes the installation of energy-intensive household pumps, greater emphasis is placed on WDNs. Several studies have looked at different parts of WDN design, such as minimizing costs [1], recovering energy [2], and creating flexible designs using multi-objective optimization [3]. Water companies typically consider several cost-related factors, including the energy required to convey water into the network and costs associated with water network maintenance, leaks, and pipe breaks. According to research into these factors, network pressure significantly impacts the operation of WDNs [4, 5]. Proper adjustment of the pressure variable can result in cost savings for water providers regarding maintenance expenses.

Content from this work may be used under the terms of the Creative Commons Attribution 4.0 licence. Any further distribution of this work must maintain attribution to the author(s) and the title of the work, journal citation and DOI.
Published under licence by IOP Publishing Ltd

Furthermore, recent articles have focused on calibrating leakage in water distribution networks (WDNs) with pressure-driven analysis to eliminate inconsistencies between field measurements and simulation results [6]. Furthermore, there has been an emphasis on a physically based approach to leakage management plans [**7**]. Effective pressure management allows for the simulation, estimation, measurement, and understanding of water loss sites and mechanisms. Proactive leakage management and household background leak repair to reduce the frequency and cost of water leaks [8]. WDNs are challenging to build and operate, and asset owners must invest significantly. According to [9], water distribution systems account for approximately 80% of the entire cost of a water supply project. This demonstrates the significant cost required to construct a water distribution infrastructure for a planned community. The design of a water distribution network (WDN) has been the focus of many researchers over the past three decades. In the WDN design problems, it is usually assumed that the pipe layout, nodal elevations, and demands are known in advance. The task is to find the combination of pipe diameters that can satisfy the required hydraulic head value at the demand nodes with the least cost. As the equations representing the WDN are nonlinear and implicit, the arrival of an exact solution for optimal design by the rigorous algorithm is practically impossible. Linear programming, nonlinear programming, and stochastic optimization algorithms such as the genetic algorithm GA and simulated annealing SA were employed to optimize WDN design. Among these methods, stochastic optimization algorithms successfully discover the optimal solution [10]. The heuristics-based approach is the most economical to find the configuration that satisfies the demand nodes' minimal hydraulic head requirements. The suggested method has successfully developed water distribution networks at the most affordable price [11]. The online hydraulic simulation model showed a Distribution Management Area (DMA) flow event, proving its potential. The investigation revealed the software's capacity to accurately simulate pressures at different nodes inside DMAs, detecting pipe segment concerns early. According to the inventors, AQUIS 7T is a powerful online simulation tool that improves managerial decision-making and consumer awareness [12].

GIS census data will predict future water demand and design transmission and main pipes in Alnavar, Karnataka. GIS was used to integrate and estimate earthwork volume from DEM. The researchers used EPANET 2.0 to model the pipe network system under various demand scenarios. The correctness of the EPANET 2.0 data was validated by comparing it to hydraulic equation calculations [13]. EPANET and ArcGIS will assess the water supply system at Untkhana, Nagpur, India. The study used simulated data to identify continuous and intermittent water supply system leaks. The constant supply system showed higher pressure but was less than 12.0 meters. The researchers found that EPANET accurately reproduced intermittent and continuous water supply systems and that avoiding transmission main tapping and responding quickly to leakage can increase system efficiency [14]. Aquis, WaterGEMS, and WaterCAD are used to construct WDNs and design the water distribution network [15]. Various aspects, including the availability of data, time limitations, financial considerations, resource availability, suitability, and the overall project scope, influence the choice of software. Bentley WaterGEMS will evaluate and improve Sekota water distribution [16]. The hydraulic modeling assumed continuous supply, and the evaluation used an extended-time simulation after calibration. Model performance was criticized by calibrating it with observed pressure levels.

Significant progress has been made in understanding and managing WDNs. However, areas still require further research and development to address challenges and improve the efficiency and sustainability of water distribution systems. This study aimed to analyze the intermediate

and continuous water distribution networks of water GEMS software. Also, we need to develop a head loss model with model results to explore the impact of various parameters on head loss.

2. Methodology

The current study analyzes intermediate and continuous water distribution networks using Water GEMS software. Initially, relevant physical properties of the network, such as pipe sizes, lengths, altitudes, demand nodes, and demographic statistics, are collected. Further, this data is used to create a hydraulic network model using WaterGEMS. Pressure-driven analysis simulates water flow and pressure under different operating situations, revealing insufficient or excessive pressure locations. Leakage analysis is carried out to identify potential leak locations and quantify water loss. Scenario analysis measures the network's performance under various conditions. Optimization is used to increase efficiency and economical water distribution. The methodology for the design of WDNs is shown in Figure 1.

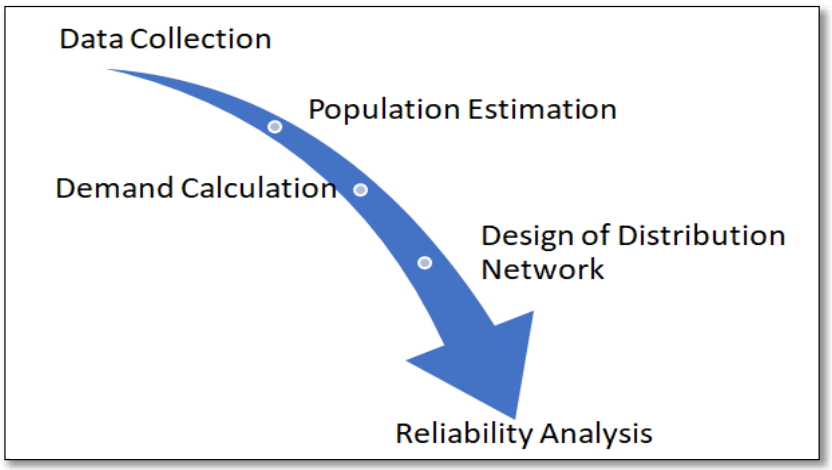


Figure 1. Methodology for design of WDNs

2.1. Study Area

This study was conducted in the Chintalavalasa village of Denkada Mandal in Vizianagaram. It is a small village located in Vizianagaram District's Denkada Mandal. It is located 7.5 kilometers from Vizianagaram's downtown, at 18°04'03 "N and 83°24'34 "E. The settlement's entire area is 3.59 square kilometers. The village's population was around 5900 in 2011. The population of Chintalavalasa has grown fast in recent years and is predicted to continue to rise significantly in the coming years. The water demand is increasing rapidly as the population grows. As a result, this research aims to analyze the water demand and build an extensive intermediate and continuous water distribution network for this hamlet while considering all of the necessary criteria, such as water demand, topography, and others.

2.2. Data Collection

The population data for the study was obtained from the Government of Andhra Pradesh's census report, available on the 2011 Census. The data shows a population of 5921 in 2011, which grew to 7600 by 2021 and is expected to reach 8200 by 2024. This represents a strong population growth rate, projected to increase by 28.35% between 2011 and 2021. The village's significant

population expansion highlights the urgent need to establish a comprehensive water distribution network to satisfy its growing demands.

2.3. Software used for the design of WDS

Google Earth Pro is a widely used software that offers additional features for commercial and expert usage. Along with high-resolution satellite photos and 3D terrain data, it provides several tools for studying, manipulating, and presenting geographic data. Satellite photos are high-quality, and additional features are made possible. Using Google Earth Pro, the developers of this WaterGEMS were able to identify potential pipeline obstructions and residential areas. Global Mapper is used to connect Auto CAD, Google Earth Pro, and WaterGEMS. Global Mapper is also used to convert between different file formats, such as KMZ to DXF or DWG as shown in Figure 2.

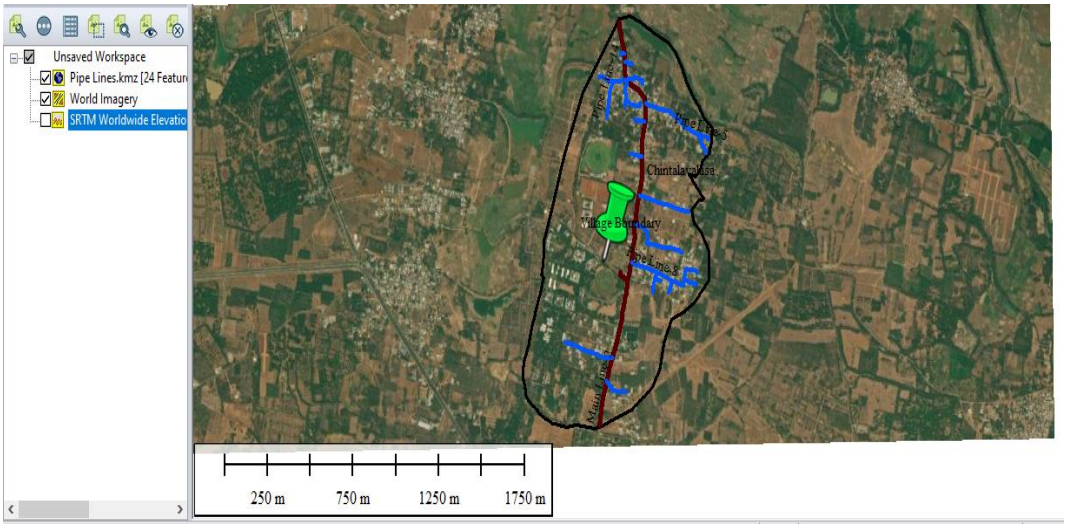


Figure 2. Global Mapper Interface

WaterGEMS software allows you to design and create hydraulic models for water distribution systems, including pipelines, pumps, valves, and storage tanks as shown in figure 3. Hydraulic algorithms are used in the application to simulate and analyze water flow inside the system. This study was used to design optimal WDS and identify potential problems. When combined with geographic information system (GIS) data, WaterGEMS enables users to interact with geographical data, visualize network components, and communicate data more effectively. The program makes optimizing the design and operation of water distribution systems easier, resulting in an excellent economy and efficiency. It can create reports and document modelling techniques, results, and recommendations. It ensures that water supply systems deliver high-quality water by using minimum and maximum head and velocity requirements to calculate the actual supply from each node to each customer. Important variables considered by the software include pipe diameter, altitudes, reservoir capacity, and flow head.

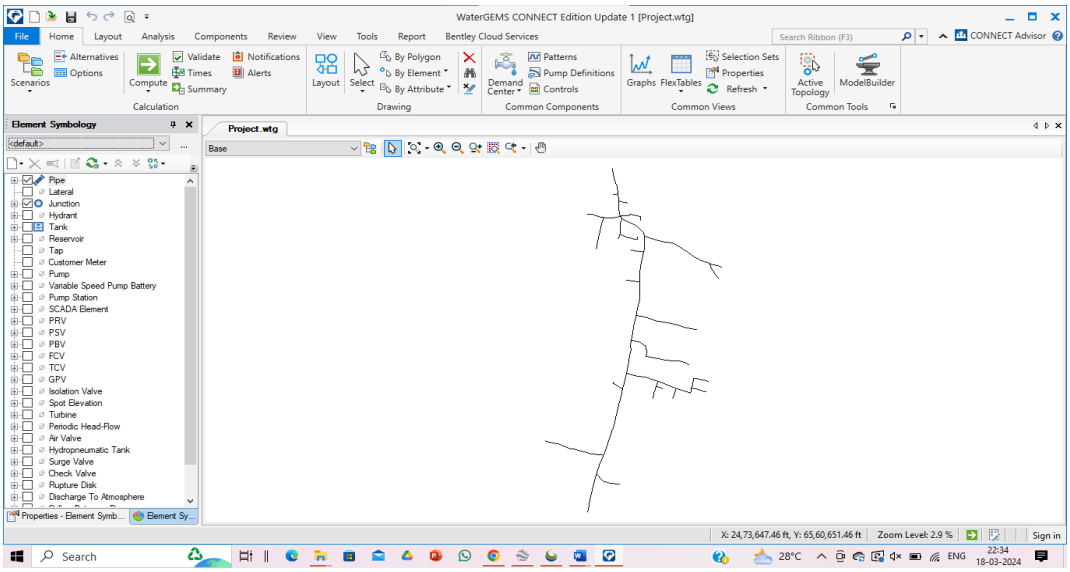


Figure 3. WaterGEMS Software Interface

2.4. Population Estimation

The Geometric Increase Method, one of the four methods used for population estimation, assumes a constant growth rate throughout time. Using the provided statistical data, this technique calculates the population projections for 2034, 2044, and 2054. The process involves calculating the average annual growth rate by examining historical data and then predicting future populations based on this rate. However, it is essential to recognize that the accuracy of these predictions depends on the stability of the growth rate, which can be influenced by various factors such as economic conditions, migration patterns, and policy changes. The area's population has progressively increased from 5921 in 2011 to 12455 in 2054, with an expected increase to 9400 by 2031. The growth rate has been stable, averaging 200-300 persons annually, with a modest acceleration in recent years. This tendency indicates the necessity for careful urban planning to meet the growing population's housing, infrastructure, and services demands.

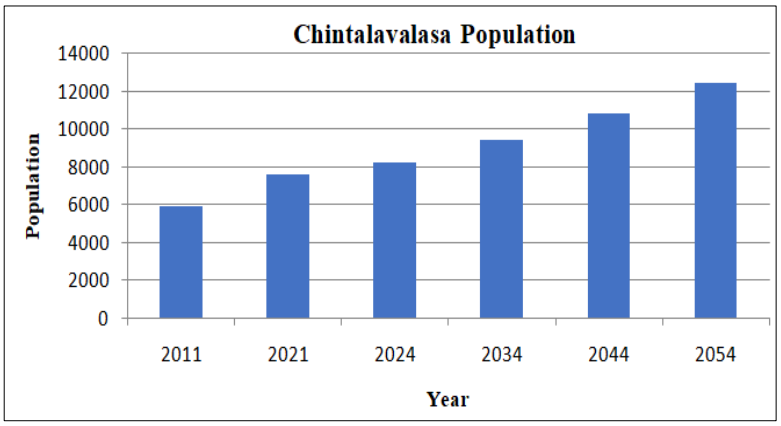


Figure 4: Population of the village (census.co.in)

3. Results and Discussion

Using WaterGEMS, we acquired two distinct reports: the PIPE and JUNCTION reports. The PIPE REPORT contains critical parameters about the pipes, such as pressure, velocity, head loss, and head loss gradient. Conversely, the JUNCTION REPORT presents data on demand, elevation, hydraulic gradient, and pressure at the junction where the pipes are linked. The diameter of the pipe has a direct impact on the velocity of water flowing through it. A more minor diameter results in a higher velocity, while a larger diameter leads to a lower velocity. The link between velocity and pressure in a pipe is directly proportional: higher velocity corresponds to higher pressure, while lower velocity corresponds to lower pressure. Hence, the diameter of the pipe exhibits an inverse relationship with the pressure inside the pipe: smaller diameter pipes correspond to higher pressure, whereas bigger diameter pipes correspond to lower pressure. Table 1 shows the design details of WDNs for Chintalavalasa village.

3.1. Head Loss Model

Head loss in a water distribution network refers to the reduction in pressure that occurs as water flows through pipes, fittings, valves, and other network components. It is a critical parameter that engineers must consider when designing, operating, and maintaining water distribution systems. Darcy-Weisbach equation is widely used and relates head loss to pipe length, diameter, flow rate, and friction factor. This study developed a mathematical model to find the head loss by considering the optimal parameters designed using WaterGEMS software. The designed parameters, pipe length, flow rate, velocity, head loss gradient, pressure at stop, and pressure in atmospheres, show significance with the head loss, as indicated by p values less than 0.05, as shown in Table 2.

Table 2 shows the coefficients, p-values, and R-squared values for a multi-linear regression model to predict head loss in a water distribution network. The coefficient (0.041) for pipe length is positive, showing that increasing pipe length increases head loss. The flow rate (0.092) and head loss gradient (0.421) correlate positively. The negative coefficient of velocity (-10.196) implies that greater velocities cause less head loss. The pressure at a standstill has a negative coefficient of -45.675, while the pressure in atmospheres has a positive value of 472.120. These data show that higher flow rates, steeper gradients, and lower velocities result in more head loss. Higher pressures at stop points can also increase or reduce head loss, depending on the unit of measurement. The model explains 96.5% of the range in head loss, indicating a solid fit for the data.

3.2. Junction Report Analysis

The junction report for Chintalavalasa reveals significant variations in water demand, pressure, elevation, and hydraulic grade across different junctions. Figure 5 shows that higher elevations generally correspond to higher pressures, ranging from 1.00 to 19.00 L/min and from 2.68 to 86.25 m H2O. This suggests a complex hydraulic system with diverse requirements for effective water distribution and highlights the importance of considering factors such as elevation and pressure gradients in optimizing the system's performance and reliability.

Table 1. Designed details of WDNs

S.NO	Label	Start Node	Stop Node	Length (m)	Material	External Diameter (mm)	Internal Diameter (mm)	Flow (Absolute) (L/s)	Velocity (m/s)	Hazen-Williams C	Headloss (Friction) (m)	Minor Loss Coefficient (Local)	Headloss (Minor) (m)	Headloss (m)	Headloss Gradient (m/km)	Pressure (Start) (m H2O)	Pressure (Stop) (m H2O)	Pressure (Start) (atm)	Pressure (Stop) (atm)
1	P-1	T-1	J-45	7	DI	300	300	248	3.51	140	0.22	0.04	0.03	0.24	33.57	47.43	46.71	4.59	4.52
2	P-43	J-45	J-41	51	DI	300	300	248	3.51	140	1.53	0.29	0.18	1.71	33.68	46.71	46.85	4.52	4.53
3	P-41	J-41	J-37	83	DI	200	200	192	6.10	140	11.17	0.59	1.12	12.29	148.02	46.85	36.7	4.53	3.55
4	P-38	J-37	J-35	168	DI	200	200	148	4.72	140	14.1	1.24	1.41	15.51	92.12	36.7	23.1	3.55	2.24
5	P-36	J-35	J-33	129	DI	200	200	123	3.93	140	7.68	0.98	0.77	8.45	65.66	23.1	15.17	2.24	1.47
6	P-34	J-33	J-13	170	DI	200	200	101	3.21	140	6.97	1.33	0.7	7.67	45.06	15.17	11.54	1.47	1.12
7	P-15	J-13	J-9	154	DI	200	200	89	2.84	140	5.02	1.22	0.5	5.52	35.96	11.54	10.59	1.12	1.03
8	P-11	J-9	J-39	79	DI	200	200	80	2.55	140	2.12	0.64	0.21	2.34	29.50	10.59	10.42	1.03	1.01
9	P-40	J-39	J-23	143	DI	200	200	49	1.57	140	1.57	1.25	0.16	1.72	12.03	10.42	16.28	1.01	1.58
10	P-42	J-41	J-31	349	DI	200	200	45	1.45	140	3.27	3.06	0.33	3.6	10.32	46.85	38.99	4.53	3.77
11	P-25	J-23	J-21	16	DI	200	200	35	1.12	140	0.09	0.14	0.01	0.1	6.39	16.28	9.97	1.58	0.97
12	P-37	J-37	J-3	155	DI	150	150	33	1.87	140	3.26	1.83	0.33	3.58	23.12	36.7	34.23	3.55	3.31
13	P-5	J-3	J-7	94	DI	100	100	20	2.58	140	5.82	1.71	0.58	6.4	67.75	34.23	27.77	3.31	2.69
14	P-32	J-31	J-25	99	DI	250	250	19	0.39	140	0.06	0.98	0.01	0.07	0.73	38.99	41.37	3.77	4
15	P-39	J-39	J-19	343	HDPE	75	67.1	16	4.66	145	94.08	10.06	11.14	105.22	306.49	10.42	85.02	1.01	8.23
16	P-23	J-21	J-29	81	HDPE	90	80.75	15	2.84	145	7.16	1.93	0.8	7.96	98.33	9.97	6.54	0.97	0.63
17	P-9	J-7	J-15	96	DI	100	100	13	1.61	140	2.45	1.86	0.24	2.69	28.06	27.77	26.96	2.69	2.61
18	P-26	J-21	J-5	79	DI	200	200	12	0.39	140	0.07	0.91	0.01	0.07	0.91	9.97	9.52	0.97	0.92
19	P-7	J-5	J-1	35	DI	200	200	9	0.28	140	0.02	0.49	0	0.02	0.52	9.52	10.1	0.92	0.98
20	P-35	J-35	J-36	342	HDPE	75	67.1	9	2.45	145	28.48	11.03	3.37	31.85	93.02	23.1	6.93	2.24	0.67
21	P-24	J-23	J-17	79	HDPE	90	80.75	9	1.68	145	2.64	2.05	0.3	2.94	37.13	16.28	9.7	1.58	0.94
22	P-33	J-33	J-34	300	HDPE	75	67.1	8	2.14	145	19.45	9.84	2.3	21.75	72.61	15.17	5.91	1.47	0.57
23	P-31	J-31	J-32	293	HDPE	63	56.45	7	2.96	145	42.35	11.62	5.19	47.53	162.28	38.99	9.97	3.77	0.97
24	P-4	J-3	J-11	26	HDPE	90	80.75	6	0.90	145	0.24	0.72	0.03	0.27	10.43	34.23	32.99	3.31	3.19
25	P-28	J-25	J-42	200	DI	150	150	5	0.29	140	0.13	2.27	0.01	0.14	0.70	41.37	42.49	4	4.11
26	P-29	J-29	J-30	164	HDPE	63	56.45	4	1.66	145	8.09	7.08	0.99	9.08	55.38	6.54	2.68	0.63	0.26
27	P-27	J-25	J-26	133	HDPE	63	56.45	3	1.34	145	4.47	5.93	0.55	5.01	37.66	41.37	39.21	4	3.79
28	P-3	J-1	J-44	133	DI	250	250	3	0.07	140	0	1.72	0	0	0.03	10.1	10.37	0.98	1
29	P-17	J-15	J-38	125	HDPE	100	100	3	0.40	145	0.23	3.72	0.03	0.26	2.10	26.96	23.45	2.61	2.27
30	P-22	J-21	J-22	125	HDPE	63	56.45	3	1.26	145	3.74	5.63	0.46	4.2	33.57	9.97	10.28	0.97	1
31	P-18	J-17	J-18	103	HDPE	63	56.45	3	1.04	145	2.15	4.76	0.26	2.41	23.43	9.7	8.46	0.94	0.82
32	P-20	J-19	J-20	91	HDPE	63	56.45	2	0.92	145	1.51	4.28	0.18	1.69	18.59	85.02	82.25	8.23	7.96
33	P-30	J-29	J-28	84	HDPE	63	56.45	2	0.85	145	1.19	4.01	0.15	1.34	15.95	6.54	6.35	0.63	0.62
34	P-16	J-15	J-16	76	HDPE	75	67.1	2	0.54	145	0.39	3.68	0.06	0.45	5.87	26.96	22.41	2.61	2.17
35	P-14	J-13	J-14	66	HDPE	63	56.45	2	0.67	145	0.62	3.31	0.08	0.69	10.42	11.54	9.96	1.12	0.96
36	P-12	J-11	J-12	66	HDPE	75	67.1	2	0.47	145	0.26	3.27	0.04	0.3	4.50	32.99	30.59	3.19	2.96
37	P-21	J-19	J-40	63	HDPE	63	56.45	2	0.64	145	0.54	3.16	0.07	0.6	9.52	85.02	86.25	8.23	8.35
38	P-10	J-9	J-10	63	HDPE	63	56.45	2	0.63	145	0.52	3.12	0.06	0.59	9.36	10.59	9.64	1.03	0.93
39	P-8	J-7	J-8	57	HDPE	75	67.1	1	0.41	145	0.17	2.87	0.02	0.19	3.40	27.77	27.39	2.69	2.65
40	P-6	J-5	J-6	48	HDPE	63	56.45	1	0.49	145	0.24	2.5	0.03	0.27	5.70	9.52	9.5	0.92	0.92
41	P-13	J-11	J-4	34	HDPE	90	80.75	1	0.17	145	0.02	1.51	0	0.02	0.54	32.99	34.44	3.19	3.33
42	P-19	J-17	J-24	28	HDPE	63	56.45	1	0.28	145	0.05	1.51	0.01	0.06	2.04	9.7	8.72	0.94	0.84
43	P-2	J-1	J-2	26	HDPE	63	56.45	1	0.26	145	0.04	1.41	0.01	0.05	1.84	10.1	9.75	0.98	0.94

Table 2. Model estimates for head loss

Parameters	Coefficients	P-value	R2
Intercept	-0.396	0.288	
Length (m)	0.041	0.000	
Flow (Absolute) (L/s)	0.092	0.000	
Velocity (m/s)	-10.196	0.000	0.965
Head loss Gradient (m/km)	0.421	0.000	
Pressure (Stop) (m H2O)	-45.675	0.021	
Pressure (Stop) (atm)	472.120	0.021	

Table 3 presents detailed information on parameters including demand, elevation, hydraulic grade, pressure in meters of water (m H2O), and pressure in atmospheres for various points in a water distribution network. The minimum demand is 1.00 L/min at point J-2, and the maximum

is 19.00 L/min at point J-31. Elevation ranges from 33.78 to 67.38 meters, with the lowest at J-20 and the highest at J-31. Hydraulic grade varies from 39.40 to 110.04 meters, with the minimum at J-30 and the maximum at J-41. Pressure ranges from 2.68 to 46.85 meters of water and 0.26 to 4.53 atmospheres. This data is crucial for network analysis, design optimization, and ensuring adequate water supply and pressure throughout the system.

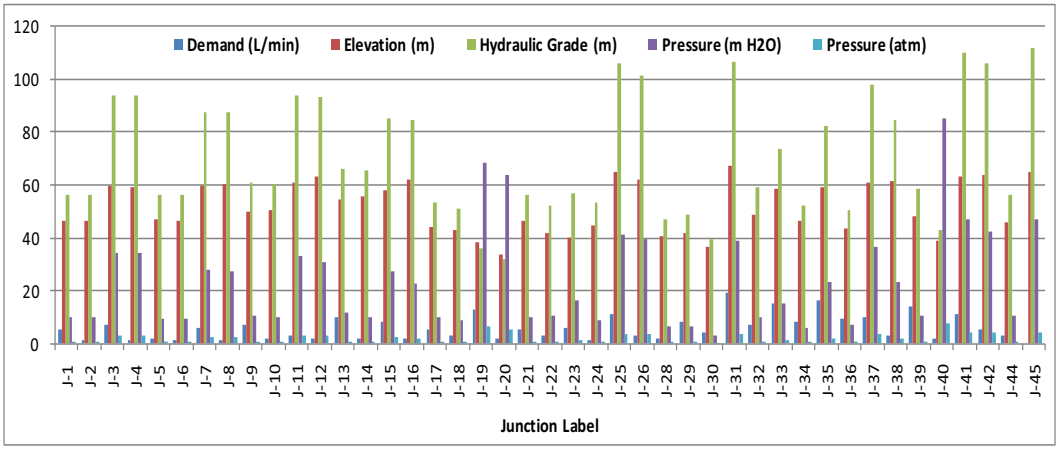


Figure 5. Junction Report

Table 3. Junction Report Obtained from WaterGEMS

S.No	Label	Demand (L/min)	Elevation (m)	Hydraulic Grade (m)	Pressure (m H2O)	Pressure (atm)
1	J-1	5.00	46.23	56.35	10.1	0.98
2	J-2	1.00	46.53	56.3	9.75	0.94
3	J-3	7.00	59.86	94.17	34.23	3.31
4	J-4	1.00	59.37	93.87	34.44	3.33
5	J-5	2.00	46.83	56.37	9.52	0.92
6	J-6	1.00	46.58	56.1	9.5	0.92
7	J-7	6.00	59.94	87.76	27.77	2.69
8	J-8	1.00	60.13	87.57	27.39	2.65
9	J-9	7.00	49.99	60.6	10.59	1.03
10	J-10	2.00	50.36	60.02	9.64	0.93
11	J-11	3.00	60.84	93.89	32.99	3.19
12	J-12	2.00	62.95	93.6	30.59	2.96
13	J-13	10.00	54.56	66.13	11.54	1.12
14	J-14	2.00	55.45	65.43	9.96	0.96
15	J-15	8.00	58.06	85.07	26.96	2.61
16	J-16	2.00	62.17	84.62	22.41	2.17
17	J-17	5.00	43.89	53.61	9.7	0.94
18	J-18	3.00	42.71	51.19	8.46	0.82
19	J-19	13.00	38.24	46.95	85.02	8.23
20	J-20	2.00	33.78	48.64	82.25	7.96
21	J-21	5.00	46.45	56.44	9.97	0.97
22	J-22	3.00	41.94	52.24	10.28	1.00
23	J-23	6.00	40.23	56.54	16.28	1.58
24	J-24	1.00	44.81	53.55	8.72	0.84
25	J-25	11.00	64.92	106.37	41.37	4.00
26	J-26	3.00	62.07	101.36	39.21	3.79
27	J-28	2.00	40.78	47.15	6.35	0.62

28	J-29	8.00	41.93	48.48	6.54	0.63
29	J-30	4.00	36.72	39.4	2.68	0.26
30	J-31	19.00	67.38	106.44	38.99	3.77
31	J-32	7.00	48.92	58.91	9.97	0.97
32	J-33	15.00	58.59	73.79	15.17	1.47
33	J-34	8.00	46.12	52.05	5.91	0.57
34	J-35	16.00	59.1	82.24	23.1	2.24
35	J-36	9.00	43.45	50.39	6.93	0.67
36	J-37	10.00	60.97	97.75	36.7	3.55
37	J-38	3.00	61.31	84.81	23.45	2.27
38	J-39	14.00	47.83	58.27	10.42	1.01
39	J-40	2.00	38.87	47.55	86.25	8.35
40	J-41	11.00	63.1	110.04	46.85	4.53
41	J-42	5.00	63.66	106.23	42.49	4.11
42	J-44	3.00	45.96	56.35	10.37	1.00

4. Conclusion

This Study The water distribution network and water supply are designed with DI (Ductile Iron) and HDPE (High-Density Polyethylene) pipes. The software generates parameters like velocity, pressure, and head loss gradient automatically, eliminating the need for manual calculations. In addition to EPANET we also provide WaterGEMS software to model water distribution networks. When comparing the two, WaterGEMS wins out because of its superior functionality and user-friendly interface. Compared to EPANET, it offers a more complex set of capabilities, a user-friendly interface, and enhanced modelling flexibility. Throughout the network design phase, we faced issues with pressure and velocity within pipes. We observed higher velocity and pressure within the pipelines in areas with steep inclines. As a result, we used pipes with larger diameters to reduce pressure and velocity throughout the pipe system.

The designed network showed considerable differences in water demand, pressure, elevation, and hydraulic grade at various intersections. The minimum demand was 1.00 L/min at J-2, while the greatest was 19.00 L/min at J-31. The elevation varied from 33.78 to 67.38 meters, with the lowest at J-20 and the highest at J-31. Hydraulic grade ranged from 39.40 to 110.04 meters, with the weakest at J-30 and the highest at J-41. The pressure ranged from 2.68 to 46.85 meters of water, or 0.26 to 4.53 atmospheres.

The multi-linear regression model developed to predict head loss in the water distribution network showed significant coefficients and an R-squared value (0.965), indicating a good fit for the data. The p-values for all coefficients were statistically significant ($p < 0.05$), suggesting the model was reliable. The design of water distribution networks is essential in optimizing design parameters to ensure an efficient and sustainable water supply. The findings can inform future planning and management strategies for water distribution systems, aiming to improve performance and reduce costs.

References

[1] Jung, D.; Kim, J.H.Water. (2018),“Distribution System Design to Minimize Costs and Maximize Topological and Hydraulic Reliability”. J. Water Resour. Plan. Manag. 2018, 144, 06018005.

[2] Meirelles Lima, G.; Brentan, B.M.; Luvizotto, E (2018),“Optimal design of water supply networks using an energy recovery approach”. Renew. Energy, 117, 404–413.

[3] Marques, João, Maria Cunha, and Dragan Savić.(2018) "Many-objective optimization model for the flexible design of water distribution networks." Journal of environmental management 226 (2018): 308-319.

[4] Zhang, Chi, Martin F. Lambert, Jinzhe Gong, Aaron C. Zecchin, Angus R. Simpson, and Mark L. Stephens. (2020), "Bayesian inverse transient analysis for pipeline condition assessment: parameter estimation and uncertainty quantification".Water Resources Management 34 (2020): 2807-2820.
[5] Lambert, A. (2001). "Approach to Leakage Control and Water Distribution System Management", Brno, Czech Republic, 16–18 May 2001.
[6] Sousa, J.; Martinho, N.; Muranho, J.; Marques, A.S. (2020)"Leakage Calibration inWater Distribution Networks with Pressure-Driven Analysis: A Real Case Study". Environ. Sci. Proc. 2020, 2, 59.
[7] Berardi, L.; Giustolisi, O. (2021),"Calibration of Design Models for Leakage Management of Water Distribution Networks". Water Resour. Manag.2021, 35, 2537–2551.
[8] Mathye, Risimati Patrick, Miklas Scholz, and Stephen Nyende-Byakika. "Appraisal of socio-technical water loss control strategies using cost-benefit analysis in a water supply network." Water 14, no. 11 (2022): 1789.
[9] Sangroula, U., Han, K. H., Koo, K. M., Gnawali, K., & Yum, K. T. (2022),"Optimization of Water Distribution Networks Using Genetic Algorithm Based SOP–WDN Program". Water (Switzerland), 14(6), 1–24. https://doi.org/10.3390/w14060851.
[10] Keedwell, Edward, and Soon-Thiam Khu. (2006), "Novel cellular automata approach to optimal water distribution network design". Journal of Computing in Civil Engineering 20, no. 1 (2006): 49-56.
[11] S. Mohan and K. S. Jinesh Babu.(2009), "Water Distribution Network Design Using Heuristics-Based Algorithm." J. Comput. Civ. Eng. 2009.23:249-257.
[12] Machell, John, S. R. Mounce, and J. B. Boxall. "Online modelling of water distribution systems: a UK case study." Drinking Water Engineering and Science 3, no. 1 (2010): 21-27.
[13] Ramesh H., Santhosh L.and Jagadeesh C. J. (2012), "Simulation of hydraulic parameters in water distribution network using EPANET and GIS", International Conference on Ecological, Environmental and Biological Sciences (ICEEBS)
[14] Mohapatra S., S. Kamble, A. Sargaonkar& P. K. Labhasetwar (2012), "Efficiency study of a pilot water distribution system using EPANET and ArcGIS10", Conference CSIR-NEERI.
[15] Sonaje, N. P., & Joshi, M. G. (2015). a Review of Modeling and Application of Water Distribution Networks (Wdn) Softwares. International Journal of Technical Research and Applications, 3(5), 174–178.
[16] Kassahun, D.Y.; Dargie, T. (2024), "Performance Evaluation and Optimization of Existing Water Supply Distribution System Using WATERGEMS: Case of Sekota Town". Preprints 2024, 2024020062. https://doi.org/10.20944/preprints202402.0062.v1.
[17] https://cpheeo.gov.in/(Governmentwebsite).

IOP Conference Series: Earth and Environmental Science

PURPOSE-LED PUBLISHING™

PAPER • **OPEN ACCESS**

Laboratory Study on Synthesis of Geopolymer Fly ash sand

To cite this article: K. Renuka *et al* 2024 *IOP Conf. Ser.: Earth Environ. Sci.* **1409** 012006

View the article online for updates and enhancements.

You may also like

- Utilization of River Sand as a Substitution and Addition of Cement to Increase The Shear Strength of Clay Soil
G F Risva, Y Apriyanti and B D A Sandy
- Strength and permeability of concrete containing dimensional stone slurry and crushed sand
Akash Gehlot, Mohd Danish, Pawan Kalla et al.
- Thermal and durability characteristics of optimized green concrete developed using slag powder and pond ash
Jeyaprakash Maheswaran, Maheswaran Chellapandian, Nakarajan Arunachelam et al.



This content was downloaded from IP address 47.247.77.11 on 27/11/2024 at 05:32

Laboratory Study on Synthesis of Geopolymer Fly ash sand

K. Renuka[1], P. Arti Sudam[1]*and K. Srinivas[1]

[1]Department of Civil Engineering, VNR Vignana Jyothi Institute of Engineering & Technology, Hyderabad, Telangana, India

*Email: artisudam_p@vnrvjiet.in

Abstract: Sand is a naturally occurring resource that's often employed in the field of civil engineering. Natural river sand is become harder to come by as a result of increased building activity. This is leading to several environmental issues, including erosion, landslides, tsunamis, river bank scoring, etc. Therefore, the creation of an alternate granular material is required to meet the required demand for natural river sand Geopolymers are utilized as an alternative binder material since they are three-dimensional alumina silicate frameworks with extremely high mechanical strength. Although the direct application of fly is widely recognized in practice, fly ash granule production and its applications are not. This artificial sand is being created utilizing fly ash, industrial waste, and a laboratory-scale disc granulator that uses geopolymerization. byproduct with different NaOH molarities and Na2SiO3 alkaline binders. This study's primary goal is to create fly ash sand (GPS) and evaluate it using an index and engineering properties of river sand that is naturally occurring. These properties include water absorption, specific surface area, optimal and maximum dry density, grain size distribution, angle of shearing resistance, permeability, and more, in addition to geoenvironmental characteristics like pH, EC, and TDS. The findings indicated that GPS can be utilized as a building material in place of NRS since it interprets the same qualities as that of natural river sand.

Keywords: Fly ash; Sodium hydroxide (NaOH); Sodium silicate (Na2SiO3); Fly ash sand (GPS); Natural River sand (NRS).

1. Introduction

There is an enormous increase in infrastructure, primarily due to the requirement of building materials such as river sand [1],[9]. One of the most important ingredients in the production of mortar and concrete [3],[14]. Finding a substitute material is crucial because natural sand is getting harder to acquire owing to the world's rapid growth [6], [19]. GGBS, copper slag, fly ash, foundry sand, washed bottom ash, quarry dust, and waste from construction and demolition are a few of the replacements. This present study emphasizes fly ash geopolymer sand rather than natural river sand for use in mortar and concrete preparation [10],[18].

Among the many industrial wastes, fly ash is one among all other waste that is generated in large quantities and contributes to various problems. But its mineralogical composition is similar to river sand as proved by [8], [16]. So fly ash needs to be converted to granular material and also to accomplish necessary strengths. [5],[13].

Every year, thermal power plants produce around 120 million tons of fly ash, of which only 30 to 40 percent are utilized. The remaining fly ash is dumped in landfills. Certain authors state that fly ash can only be used 100% of the time and substituted up to 40% of other alkaline

Content from this work may be used under the terms of the Creative Commons Attribution 4.0 licence. Any further distribution of this work must maintain attribution to the author(s) and the title of the work, journal citation and DOI.
Published under licence by IOP Publishing Ltd

materials when combined; if fly ash is used 100% of the time, the concrete will not have any compressive strength [8],[20]. The geopolymerization method often requires the use of alkaline materials and involves combining fly ash with sodium hydroxide and sodium silicate in the appropriate ratios [4],[3]. To create geopolymer fly ash sand, the precise chemistry of raw materials like fly ash and geopolymer activators was investigated. This was done with alkali activators that were abundant in silica and alumina [2]. Lightweight aggregate sand was made by using sintered fly ash in place of conventional coarse aggregates. investigated the compressive strengths of manufactured sand mortar, Class-F and Class-C geopolymer fly ash sand, and natural river sand mortar [11],[16]. Geopolymer is an excellent binding material because of its fine sulphate and acidic resistance, little shrinkage, good compressive and flexural strength, and 3D aluminosilicate structure [10],[9]. Geopolymer sand can cut atmospheric CO_2 emissions by 70–80%, mostly from the cement and aggregate industries, and it can potentially mitigate global warming [5]. The strength and workability of the mixture are unaffected by the presence of up to 60% of geopolymer. To assess their comparison, the characteristics of GPS sand such as pH, EC, TDS, particle size distribution, and friction angle—were compared to those of natural river sand. One of the most crucial steps in this process is cost optimization [4],[5]. Since natural river sand is getting more and more expensive every day in the building industry, the cost analysis should also compare GPS sand to natural river sand. The exact process that produces fly ash is uncertain.

Although the industry is aware of the wide range of direct uses for fly ash, fly ash sand synthesis and its applications are restricted to industries. Therefore, to assess the physical, chemical, and environmental properties of geopolymer fly ash sand, large-scale synthesis is necessary [10]. Therefore, the production of geopolymer sand and its characterization for use as a building material are not local processes. Our current investigation's primary goals are to create granular material, or GPS, and determine its strength properties [3],[13]. This work was primarily concerned with creating granular material in the form of geopolymer fly ash sand, which was confirmed using unconfined compressive strength and varied molarities of NaOH (8M, 10M, and 12M) and Na_2SiO_3, also referred to as GPS. Following that, physical characteristics like specific gravity, water absorption, and grain size distribution were examined, as well as chemical characteristics like pH and electrical conductivity, to compare the distinctive features of the synthetic GPS material with those of natural river sand (RS). (EC), total dissolved solids (TDS), and concluded that GPS was a viable substitute for RS mortars [17].

2. Materials and experimental program:

2.1. Materials

Fly ash (Class-F), fly ash polymer solutions, and alkaline activators such as Na_2SiO_3 and NaOH with different concentrations (8M, 10M, and 12M) were used to create GPS [1]. The 90% pure alkaline binders, which are made of sodium hydroxide and sodium silicate, respectively, are depicted in Figures 2 and 3. For these experiments, fly ash was obtained from Hyderabad, Telangana, India's Kondapalli thermal power facility. Alkaline activators were procured from the Hyderabad region of Telangana, India. with the 90% pure alkaline binders, the chemical makeup of the sodium hydroxide and silicate, and the percentage of the constituent elements that were achieved are all listed in Table 1.

The physicochemical and engineering properties of fly ash, such as its specific gravity, water absorption, particle size distribution, angle of shearing resistance, and unconfined compressive strength investigated, and the results were explained below.

Experimental program:

Based on gravimetric weight, several NaOH molarities (8M, 10M, and 12M) were used to synthesize GPS [1],[9]. The fly ash to geopolymer solution ratio was 3:1. Fly and alkaline binders with different molarities of NaOH were used in the unconfined compressive strength test to confirm the strength of fly ash mortar [8],[20]. To reduce human error, machine error, etc., three trials were performed for every molarity in this test. The outcomes were contrasted with the geopolymer fly ash sand's strength [5], [15].

2.2. Synthesis of GPS

Fly ash was heated to 100°C until the granules were totally dry to prepare GPS granules [9],[16]. A 1:1 mixture of sodium hydroxide and sodium silicate with 8M, 10M, and 12M NaOH produced an excellent geopolymer liquid solution [3],[19]. Using a disc granulator, fly ash and alkaline activator (geopolymer liquid solution) were combined in a 3:1 (solid: liquid) ratio for 15 minutes to generate a dry mixture, as shown in Figure 4. The combination was then sieved using a 4.75 mm sieve to produce granules that were not the same size or shape as NRS. To complete the geopolymerization process, the particles were sieved and then heated to 100°C for an hour [7],[18].

The synthesized and oven-dried particles were called GPSS granules as shown in Fig. 1, following a 24-hour storage period at room temperature [20]. Furthermore, measurements and comparisons with the properties of RS were made of the synthesized granules for specific gravity, electrical conductivity, pH, total dissolved solids, grain size distribution, water absorption, compression strength, and angle of shearing resistance [12],[20]. The obtained data were analysed to provide insight into the features of GPS and its usefulness as a substitute [16],[20].



Figure 1. Geopolymer Synthetic sand(8M,10M,12M).



Figure 2. Sodium hydroxide



Figure 3. Sodium silicate

Table 1: Fly ash chemical composition

Elements	% By weight
SiO2	52.36
Al2O3	24.67
Fe2O3	8.93
CaO	4.83
K2O	3.60
TiO2	2.51
SO2	0.48
Others	0.50
LOI	0.12

3. Testing Methodology

The GPS sand is made using fly ash and amorphous solutions such as silica and sodium hydroxide pellets [9,10,11,12]. Fly ash is oven-dried for a full day before being used as a feedstock for geopolymerization. A 4.75 mm IS sieve is used to filter oven-dried fly ash; The molarity of the NaOH pellets (1 Mole = 40 molecular weights of NaOH) determines the ratio of sodium hydroxide to sodium silicate, and the procedure is then repeated with the silicate and sodium hydroxide in various proportions. Fly ash is mixed with the prepared NaOH and Na2SiO3 solution in the granulator.

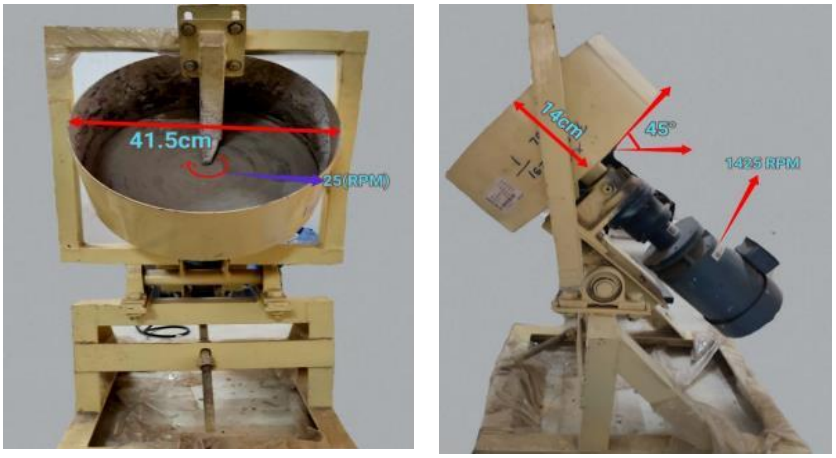


Figure 4. Disc Granulator Front view and side view

The ratios [solid: solution ratio, (3:1)] kept changing the fly ash to the solution was added. Sodium hydroxide in concentrations of 8M, 10M, and 12M is combined with sodium silicate in a ratio to create the granules. liquid-to-liquid ratio of 1:1[1],[9].

4. Results and Discussions

The grain size distribution of the river sand and the GPS (8M, 10M, and 12M) granules are shown in Figure 5. [9,18,20]. According to the IS code, the river sand was categorized as SP based on its coefficient of curvature (Cc=2.35) and uniformity coefficient (Cu= 1.1). The geopolymer fly ash

sand was categorized as poorly graded SP at 8 M GPS (Cc=2.63, Cu=1.08), 10 M GPS (Cc=0.81,2.28), and 12 GPS (1.09,2.79).

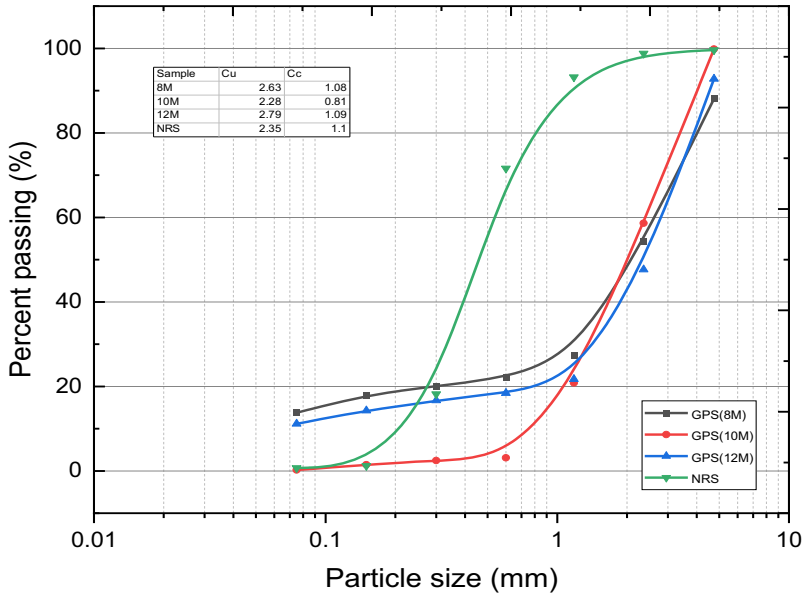


Figure 5. Grain size distribution of GPS sand and NRS.

The symbols D_{60}, D_{30}, and D_{10} represent for the particle size distribution curves for fines of 60, 30, and 10%, respectively. The homogeneity coefficient of curvature of well-graded sand (SW) is more than six and ranges from one to three [7], [14]. Table 1 demonstrates that RS has a specific gravity of 2.78 and that the specific gravities acquired by 8M GPS, 10M GPS, and 12M GPS are 2.05, 2.19, and 1.94, respectively due to voids on the surface of the manufactured granules, so thereby representing lower specific gravity than river sand. The pH values of GPS materials and river sand were found to be 8.35, 11.59, 11.62, and 11.68[11],[19] demonstrating a higher pH for GPS than river sand because fly ash was blended with NaOH to prepare fly ash granules, which may adhere to cement and mortar concrete well without compromising their mechanical properties. River sand and 8M GPS, 10M GPS, and 12M GPS were found to have an electrical conductivity of 0.108 ms/cm, 4.59 ms/cm, 5.20 ms/cm, and 5.53 ms/cm, and TDS of 311 ppm, 3400 ppm, 3200 ppm, and 3400 ppm, respectively. In comparison to river sand, geopolymer fly ash sand is bound with alkaline binders, indicating higher electrical conductivity and TDS [10],[9] due to the usage of alkaline binders for the synthesis of granules.

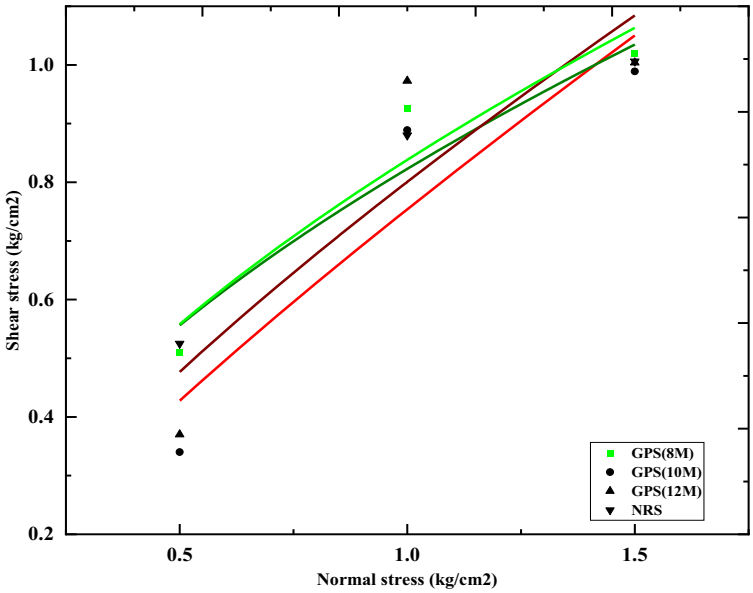


Figure 6. Direct shear test of granular materials

The direct shear test was performed for River sand and 8M GPS, 10M GPS, and 12M GPS as shown in Fig. 6. River sand represents an angle of shearing resistance as 44°, 43°, and 45°. Which is less than river sand (27°), the GPS particles are influenced more by angularity, tightly packed, and have a rough texture compared to river sand, which helped them form strong bonds between individual particles [19].

Table 1: Physical properties of granular materials used in the present study

S. No.	Materials	Specific Gravity (G)	Water absorption (%)	Cu	Cc	Soil classification	pH	TDS (ppm)	EC (ms/cm)	Friction angle (Φ)
1	GPS 8M	2.05	7.78	2.63	1.08	SP	11.59	3400	4.59	44
2	GPS 10M	2.19	7.50	2.28	0.81	SP	11.62	3200	5.20	43
3	GPS 12M	1.94	7.92	2.79	1.09	SP	11.68	3400	5.53	45
4	RS	2.78	1.89	2.35	1.10	SP	8.35	311	0.108	27

To optimize the geopolymer solution for granule synthesis, unconfined compressive strength tests were conducted for fly ash and with the mixing of alkaline binders for changing the molarity of NaOH [2],[7]. The test results demonstrated that 12M GPS gained greater strength and, due to its similar properties to natural river sand, can be utilized as a substitute for river sand in civil engineering applications [19],[20].

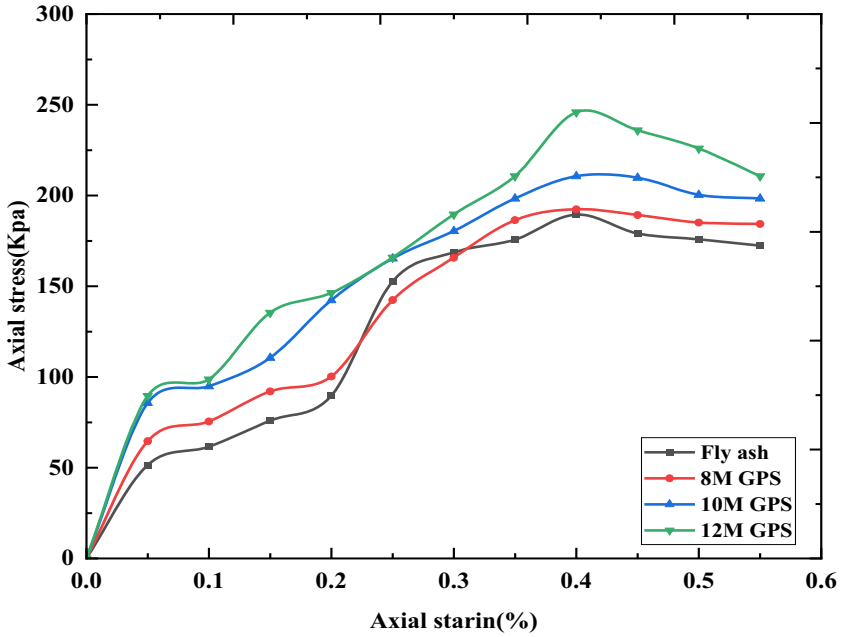


Figure 7. Unconfined compression strength test with and without adding alkaline solution into the fly ash.

Table 2. Unconfined compressive strength values

S. No.	Materials	qu(kPa)
1	Fly ash	189.5
2	8M GPS	192.4
3	10M GPS	210.6
4	12M GPS	245.8

5. Conclusion:

By geopolymerizing fly ash with sodium silicate and 8M, 10M, and 12M NaOH, GPS fine aggregates are produced. The GPS was used to determine the particle size distribution and classify the sand as poorly graded (SP) based on the coefficient of curvature (Cc) and coefficient of uniformity (Cu) values. Its strong bonding and densely packed structure give it a specific gravity of 2.05, 2.19, and 1.94 (8M, 10M, 12M), which is the same as that of natural river sand. The GPS particles had a TDS value of roughly 3400, 3200, and 3400 ppm, which is within permissible limits and can be used as building materials.

Because sodium solution and silicate have a high alkaline composition, GPS particles have a high pH. GPS particles have a high pH because of the significant alkaline content of sodium and silicate fluids. Therefore, using geopolymer sand rather than river sand can be an alternative sustainable material due to its spherical shape, having a high angle of friction of about 45 degrees. The unconfined compressive strength tests proved that 12M produced maximum strength and

can be optimized in comparison with 8M and 10M GPS granules, suggesting an ideal. It can be replaced as a sustainable alternative material for civil engineering purposes.

Nomenclature

GPS	=	Geopolymer sand
NRS	=	Natural river sand
G	=	specific gravity
Cu	=	coefficient of uniformity
Cc	=	coefficient of curvature
EC	=	electrical conductivity
TDS	=	total dissolved solids
pH	=	Hydrogen ion concentration
M	=	molarity
Φ^o	=	Angle of shearing resistance

References

[1] Sharma, A. K., & Anand, K. B. (2019). Comparative study on synthesis and properties of geopolymer fine aggregate from fly ashes. Construction and Building Materials, 198, 359-367.
[2] Rohatgi, P. K., Weiss, D., & Gupta, N. (2006). Applications of fly ash in synthesizing low-cost MMCs for automotive and other applications. Jom, 58, 71-76.
[3] Ojha, P. N., Singh, B., Kaura, P., & Singh, A. (2021). Lightweight geopolymer fly ash sand: an alternative to fine aggregate for concrete production. Res. Eng. Struct. Mater, 7, 375-391.
[4] Son, B. T., Long, N. V., & Hang, N. T. N. (2021). Fly ash-, foundry sand-, clay-, and pumice- based metal oxide nanocomposites as green photocatalysts. RSC advances, 11(49), 30805- 30826.
[5] Gnanadurai, L. T., Renganathan, N. T., & Selvaraj, C. G. (2021). Synthesis and characterization of synthetic sand by geopolymerization of industrial wastes (fly ash and GGBS) replacing the natural river sand. Environmental Science and Pollution Research, 28(40), 56294-56304.
[6] PURGERT, R., BALIŃSKI, A., SOBCZAK, J., DARŁAK, P., SZOLC, M., & SOBCZAK, N.(2006). Fly ash for synthesis of new molding sands (FASAND). Archiwum Technologii Maszyn i Automatyzacji, 26(1), 123-131.
[7] Temuujin, J., van Riessen, A., & MacKenzie, K. J. D. (2010). Preparation and characterization of fly ash-based geopolymer mortars. Construction and Building Materials, 24(10), 1906-1910.
[8] Agrawal, U. S., Wanjari, S. P., & Naresh, D. N. (2019). Impact of replacement of natural river sand with geopolymer fly ash sand on hardened properties of concrete. Construction and Building Materials, 209, 499-507.
[9] Venkatesan, M., Zaib, Q., Shah, I. H., & Park, H. S. (2019). Optimum utilization of waste foundry sand and fly ash for geopolymer concrete synthesis using D-optimal mixture design of experiments. Resources, Conservation and Recycling, 148, 114-123.
[10] Dassekpo, J. B. M., Zha, X., Zhan, J., & Ning, J. (2017). The effects of the sequential addition of synthesis parameters on the performance of alkali-activated fly ash mortar. Results in Physics, 7, 1506-1512.
[11] Ferreira, C., Ribeiro, A., & Ottosen, L. (2003). Possible applications for municipal solid waste fly ash. Journal of hazardous materials, 96(2-3), 201-216.
[12] Al-Qodah, Z., Dweiri, R., Khader, M., Al-Sabbagh, S., Al-Shannag, M., Qasrawi, S., & Al- Halawani, M. (2023). Processing and characterization of magnetic composites of activated carbon, fly ash, and beach sand as adsorbents for Cr (VI) removal. Case Studies in Chemical and Environmental Engineering, 7, 100333.
[13] Lirer, S., Liguori, B., Capasso, I., Flora, A., & Caputo, D. (2017). Mechanical and chemical properties of composite materials made of dredged sediments in a fly-ash-based geopolymer. Journal of Environmental Management, 191, 1-7.
[14] Aygörmez, Y. (2021). Assessment of performance of meta bentonite and metazeolite-based geopolymers with fly ash sand replacement. Construction and Building Materials, 302, 124423.
[15] Hui, T., Sun, H. J., & Peng, T. J. (2021). Preparation and characterization of cordierite-based ceramic foams with permeable properties from asbestos tailings and coal fly ash. Journal of Alloys and Compounds, 885, 160967.

[16] Nemaleu, J. G. D., Kaze, C. R., Metekong, J. V. S., Adesina, A., Alomayri, T., Stuer, M., & Kamseu, E. (2021). Synthesis and characterization of eco-friendly mortars made with RHA- NaOH activated fly ash as binder at room temperature. Cleaner Materials, 1, 100010.
[17] Dong, B., Chen, C., Wei, G., Fang, G., Wu, K., & Wang, Y. (2022). Fly ash-based artificial aggregates synthesized through alkali-activated cold-bonded pelletization technology. Construction and Building Materials, 344, 128268.
[18] Sasui, S., Kim, G., Nam, J., van Riessen, A., Hadzima-Nyarko, M., Choe, G., ... & Jinwuth, W. (2022). Effects of waste glass sand on the thermal behavior and strength of fly ash and GGBS based alkali activated mortar exposed to elevated temperature. Construction and Building Materials, 316, 125864.
[19] Lieberman, R. N., Knop, Y., Palmerola, N. M., Muñoz, C., Cohen, H., Izquiredo, M., ... & Querol,X. (2019). Production of environmentally friendly sand-like products from granitoid waste sludge and coal fly ash for civil engineering. Journal of Cleaner Production, 238, 117880.
[20] Pupalwad Arti Sudam ,M.Heeralal, and Kadali Srinivas,(2023), Strength Characteristics of Geopolymer Synthetic Sand Using Fly Ash.American Society of Civil Engineers.

IOP Conference Series: Earth and Environmental Science

PURPOSE-LED PUBLISHING™

PAPER • OPEN ACCESS

Comparative analysis of environmental footprints: conventional versus high-strength concrete in construction

To cite this article: M.R. Rajagopal *et al* 2024 *IOP Conf. Ser.: Earth Environ. Sci.* **1409** 012007

View the article online for updates and enhancements.

You may also like

- Alternating Current Impedance Electrochemical Modeling of Lithium-Ion Positive Electrodes
Dennis Dees, Evren Gunen, Daniel Abraham et al.
- Ideal Hexagonal Order: Formation of Self-Organized Anodic Oxide Nanotubes and Nanopores on a Ti–35Ta Alloy
Wei Wei, Steffen Berger, Nabeen Shrestha et al.
- A balancing act: the interplay of food supply chain resilience and environmental sustainability in American cities
Michael Gomez and Caitlin Grady



This content was downloaded from IP address 47.247.77.11 on 27/11/2024 at 05:32

Comparative analysis of environmental footprints: conventional versus high-strength concrete in construction

M.R. Rajagopal[1*], Yashwanth Pamu[1] and Indrakanti Anusha[1]

[1]Civil Engineering Department, CVR College of Engineering, Hyderabad, Telangana, India

[*]E-mail: rajagopalmadabushi@gmail.com

Abstract. This paper presents a comparative analysis of the environmental footprints associated with conventional and high-strength concrete in the construction industry. As sustainability becomes increasingly critical in construction practices, understanding the environmental impacts of various concrete types is essential. The study employs a comprehensive methodology to assess key environmental factors, including carbon footprint, energy consumption, water usage, and waste generation, for both conventional and high-strength concrete. Data collection and analysis reveal significant differences between the two concrete types in terms of their environmental impacts. Findings indicate that while high-strength concrete offers enhanced structural performance, it tends to have higher environmental costs compared to conventional concrete. The paper discusses the implications of these findings for sustainable construction practices and emphasizes the importance of informed material selection decisions in reducing the environmental footprint of construction projects.

1. Introduction

In recent years, the construction industry has witnessed a growing emphasis on sustainability, driven by concerns about environmental degradation and the need for resource conservation. The building sector significantly influences energy consumption, accounting for over one-third of global final energy use and contributing to both direct and indirect emissions related to energy. (Chapa, 2019; Globalabc, 2020) [1] [2]. In Europe, the construction industry is estimated to use nearly half of all materials and is responsible for producing more than one-third of all waste (Herczeg, 2014) [3]. Concrete, extensively utilized worldwide for construction and infrastructure projects, is central to these discussions because of its environmental footprint, including substantial carbon emissions, energy use, water consumption, and waste creation. Assessing the environmental impact of concrete production is crucial.

Life Cycle Assessment (LCA) is an established methodology for evaluating the environmental impacts associated with all the stages of a product's life. The application of LCA can lead to enhanced efficiency in the use of resources (Curran, 2017; Sassanelli and Terzi, 2022) [4] [5]. LCA's primary goal is to conduct a comprehensive analysis of resource consumption and environmental impacts across a product's lifecycle. It goes beyond focusing on specific environmental issues, offering a broad perspective on potential environmental effects. The methodology relies on various tools and databases to ensure the transparent and systematic tracking of environmental impacts from the construction phase to the demolition of buildings.

Content from this work may be used under the terms of the Creative Commons Attribution 4.0 licence. Any further distribution of this work must maintain attribution to the author(s) and the title of the work, journal citation and DOI.
Published under licence by IOP Publishing Ltd

LCA enables detailed analysis and quantification of the materials and energy used throughout a product or system's life, aiding in the identification and assessment of environmental impacts. In recent years, the construction industry has increasingly recognized the significance of selecting sustainable building materials to mitigate environmental impacts. This literature review synthesizes key findings from various studies, highlighting the importance of material choice, the application of life cycle assessment (LCA), and the challenges and advancements in sustainable construction practices.

Cole (1999) [6] emphasized the critical role of selecting appropriate building materials in reducing energy consumption and minimizing harmful emissions. He specifically noted the differential environmental impacts of using wood, steel, and concrete, suggesting that strategic material choice is essential for environmental sustainability. Building on Cole's work, Gao et al., (2001); Gustavsson and Sathre (2006) [7] [8] developed a method to compare the environmental performance of buildings constructed from wood and concrete. Their findings support the notion that wood, as a building material, contributes to lower fossil fuel consumption and reduced carbon dioxide emissions, highlighting its potential as a sustainable construction material.

Thormark (2006) [9] further explored the implications of material selection on a building's energy usage and recyclability. He advocated for the use of longer-lasting materials or those that require less energy, pointing out their effectiveness in diminishing environmental impacts.The significance of recycling in the construction sector was detailed by Saghafi and Teshnizi (2011) [10], who proposed a framework to evaluate the recyclability of building materials, considering factors such as material selection, deconstruction practices, and the recycling frequency. Research by Wei et al. (2008) [11] and Wu et al. (2005) [12] examined the material flow, energy across various components, providing insights into how materials influence environmental outcomes throughout their lifecycle.

Haapio and Viitaniemi (2008) [13] underscored the importance of considering a building's expected lifespan in assessing its environmental impacts, suggesting that material longevity plays a critical role in sustainable construction. Innovative materials like hemp-lime walls, studied by Ip and Miller (2012) [14], and kenaf-fiber insulation boards, analyzed by Ardente et al. (2008) [15], emerged as environmentally beneficial alternatives to traditional building materials, offering reduced greenhouse gas emissions and lower environmental impacts. Anastaselos et al. (2009) [16] introduced a tool designed to assist in the selection of thermally insulating materials, emphasizing the need for materials that excel in environmental performance, energy efficiency, and cost-effectiveness. The role of LCA as a tool for assessing the environmental impacts of building materials has been extensively discussed (Ortiz et al., 2009; Bayer et al., 2010) [17] [18]. However, challenges such as the complexity of LCA studies (Keeler and Burke, 2009; John et al, (2005) [19] [20], the reliance on data pertaining to life cycle inventory (Finnveden et al., 2009) [21] and the need for simplified methodologies (Malmqvist et al., 2011; Bribian et al., 2009) [22] [23] have been identified. Additionally, the literature calls for an expanded approach to LCA that incorporates economic and social factors (Esin and Saghafi 2009; Gao et al. 2001) [24] [7] and addresses the limitations related to the recyclability of materials and the closed-loop behavior of construction practices.

In conclusion, the reviewed literature collectively advocates for a more nuanced understanding of sustainable building materials and the adoption of LCA as a comprehensive tool in construction. By addressing the highlighted challenges and leveraging the advancements in material science and assessment methodologies, the construction industry can make significant

strides towards sustainability. The paper aims to compare the environmental footprints of conventional and high-performance concrete i.e. M30 and M70 grade concrete.

2. Materials and Methods

Cement: Ordinary Portland Cement OPC 53 Grade available in the local market was used. The test properties according to IS: 4031-1988 [25] and found to confirming to IS: 12269-1987 was used. Normal Consistency of 32%, Specific Gravity of 3.10, Initial and Final Setting time of 45 min and 580 min respectively, Fineness of 2.37%, and Soundness of 4 mm were measured on Le-Chatlier's apparatus.

Fine aggregate, or sand, is a natural granular substance made up of small, finely fragmented pieces of rock and minerals. Its size is categorized as being smaller than gravel but larger than silt. For this study, the fine aggregate utilized was river sand, which meets the criteria for Zone-II as per IS 383-1970 [26] standards, showing a well-distributed size range and passing through a sieve of 4.75mm with a specific gravity [27] of 2.44 was used.

Coarse Aggregate: In this research, crushed angular granite sourced from local suppliers was employed as the coarse aggregate. The selected aggregate, which passed through a 12mm IS Sieve but was retained on a 10mm IS Sieve, was examined according to IS: 2386-1963 standards [28]. The results confirmed its compliance with the specifications.

Fly Ash: In construction, fly ash is a highly valued by-product that resembles Portland cement in appearance. The fly ash used in this study was classified as Grade I according to IS: 3812-2003, with a Specific Gravity of 2.20 and a Specific Surface Area of 420m^2/kg. Its chemical analysis revealed SiO_2 content of 68%, Al_2O_3 23%, Fe_2O_3 4%, CaO 1.1%, and MgO 0.5%.

Silica Fume: As a by-product of the production of silicon metal or ferrosilicon alloys, silica fume was utilized in this research. Powdered Silica Fume with a Specific Gravity of 2.2 and a bulk density of 220Kg/m^3 was used.

Steel Fibers: The study incorporated hooked-end steel fibers with a diameter of 0.4mm, an aspect ratio of 30, and a length of 12mm. These fibers, hooked at both ends, were added at a rate of 1% by weight of the cementitious material in the M70 concrete mix.

Water: For mixing and curing the concrete specimens, ordinary potable water with a neutral pH of 7 was utilized.

Admixtures: The admixture CONPLAST SP430 was used, meeting the IS: 9103-1979 requirements for high-range water-reducing admixtures. Mix Proportions

The cement: fine aggregate: coarse aggregate ratio for M30 grade concrete [29][30] used was 1: 1.63:2.8, while the water-cement ratio was 0.45. The mix proportion of the M70 grade concrete is shown in Table 1.

Table 1. Mix Proportion M70 Grade Concrete.

Material	Cement	Water	FA	CA	Super-* Plasticizer	Fly Ash	Silica Fume	W/C ratio
M70 Grade Concrete (Kg/m^3)	421	148	725	953	7.578	78.9	26.3	0.28

*CONPLAST-SP430-1.8% by weight of cement

The mixing of M30 grade concrete [31][32], casting of cubes, curing of specimen and testing of the specimen are illustrated in Figures 1-4 respectively. The various tests done for M70 grade

mix proportion are depicted in Figures 5-10. The design mix is fixed based on the experimental results. The paper aims to compare the environmental footprints of conventional and high-performance concrete i.e. M30 and M70 grade concrete.

The Life Cycle Assessment (LCA) process for a product, from material extraction through manufacturing, transportation, utilization, to disposal and reuse, involves examining every stage of a product's life to identify and quantify its environmental impacts. Here's a detailed walkthrough of each phase:

2.1. Material Extraction:

Raw Material Sourcing: This phase involves the extraction of raw materials from the natural environment, which includes mining metals, drilling for oil, harvesting biomass, or extracting minerals.

Environmental Impact: Impacts include energy consumption, habitat destruction, water use, pollution, and biodiversity loss.

Manufacturing:

Processing of Materials: After extraction, materials are processed and transformed into components and products. This may involve chemical processing, refining, and various manufacturing techniques.



Figure 1. Mixing of concrete



Figure 2. Casting of cubes

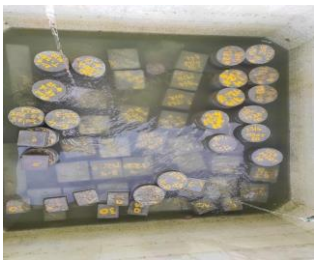


Figure 3. Curing of specimen



Figure 4. Testing of specimen

Environmental Impact: Manufacturing processes often consume significant amounts of energy and water, and can emit a wide range of pollutants including greenhouse gases, particulate matter, and toxic chemicals.

2.2. Transportation

Distribution of Products: Transporting raw materials to manufacturers, finished products to markets, and components between manufacturing stages involves vehicles that may run on fossil fuels or electricity.

Environmental Impact: Transportation contributes to air pollution, greenhouse gas emissions, and noise pollution, depending on the modes of transport (truck, rail, ship, or air) and the efficiency of the vehicles used.

2.3. Utilization:

Usage of the Product: This phase covers the period during which the product is in use by the consumer or in service. It includes the operational life of the product and maintenance.

Environmental Impact: Impacts depend on the product's energy efficiency, the source of electricity (if used), and maintenance practices. Longer product life and lower energy consumption are typically more environmentally favourable.

2.4. Disposal and Reuse:

End of Life: At the end of its useful life, a product is either disposed of or enters a reuse/recycling process.

Disposal: Can involve landfilling, incineration, or composting.

Reuse/Recycling: Products or parts can be reused, refurbished, or recycled into new products.

Environmental Impact: Disposal can lead to methane emissions from landfills, toxic emissions from incineration, and leakage of hazardous materials into the environment. Recycling can reduce the demand for new raw materials and decrease waste, but may also involve significant energy use and emissions.

2.5. Feedback Loops

Continuous Improvement: Information and data gathered from each phase can inform improvements in product design, choice of materials, and manufacturing processes to reduce overall environmental impacts.

Lifecycle Strategies: Strategies such as eco-design, material substitution, and product-as-a-service models aim to extend product life and efficiency, thus minimizing the lifecycle's environmental footprint.



Figure 5. V-funnel test M70



Figure 6. J-ring with flow table



Figure 7. L-box test

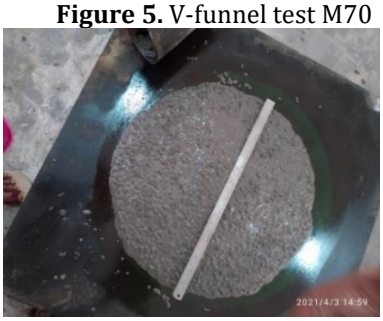


Figure 8. Slump Flow Test



Figure 9. Casting of samples



Figure 10. Curing of samples



Figure 11. Life Cycle Assessment Process.

In summary, a comprehensive LCA helps identify the stages where environmental impacts are most significant, providing insights into where improvements can be made. It also supports companies in making data-driven decisions that can lead to more sustainable practices and products, contributing to a lower environmental footprint across the product's lifecycle. Figure 11 illustrates the process of Life Cycle Assessment (LCA).

3. Results and discussion

The compressive strength of M30 and M70 grade concrete at 28 days obtained was 38 MPa and 75.14 MPa and the material composition used to produce these grades of concrete was utilized for the Life Cycle Assessment.

The environmental impact of producing 100 cubic meters (m^3) of concrete was assessed using the Open-LCA software and the ecoinvent database. Two versions of the ReCiPe 2016 method were used for the Life Cycle Impact Assessment (LCIA): the version 1.03 endpoint (E) and the midpoint (E). These LCIA methods allow for a nuanced evaluation of the environmental impacts, from specific emissions and resource use (midpoint indicators) to broader effects on ecosystem quality, human health, and natural resources (endpoint indicators).

The analysis was conducted for two concrete grades, M30 and M70, to understand the variance in environmental impacts across different strengths of concrete. The results, as detailed in the tables, show a range of impacts across several categories, including ecosystem quality (affecting terrestrial, freshwater, and marine ecosystems), human health (including climate change impacts and toxicity), and the depletion of natural resources (focusing on non-renewable energy sources and materials).

Table 2. Impact values in ReCiPe 2016 v1.03, endpoint (E) LCIA method.

Impact category	M30 Grade	M70 Grade	Reference unit
ecosystem quality - acidification: terrestrial	1.51944E-05	1.72E-05	species.yr
ecosystem quality - climate change: freshwater ecosystems	2.3511E-08	2.68E-08	species.yr
ecosystem quality - ecotoxicity: freshwater	2.61949E-07	2.93E-07	species.yr
ecosystem quality - ecotoxicity: terrestrial	3.36145E-07	3.76E-07	species.yr
ecosystem quality - eutrophication: freshwater	5.25354E-06	5.99E-06	species.yr
ecosystem quality - eutrophication: marine	1.01121E-09	1.15E-09	species.yr
ecosystem quality - land use	1.32106E-05	1.5E-05	species.yr
ecosystem quality - photochemical oxidant formation: terrestrial ecosystems	1.2391E-05	1.41E-05	species.yr
ecosystem quality - water use: aquatic ecosystems	5.9006E-11	5.71E-11	species.yr
ecosystem quality - water use: terrestrial ecosystems	1.31884E-06	1.28E-06	species.yr
ecosystem quality - climate change: terrestrial ecosystems	0.000861829	0.000983	species.yr
ecosystem quality - ecotoxicity: marine	0.000309021	0.000348	species.yr
human health - climate change: human health	0.430919685	0.491492	DALYs
human health - human toxicity: carcinogenic	0.174530312	0.190999	DALYs
human health - human toxicity: non-carcinogenic	0.589143158	0.665552	DALYs
human health - ionising radiation	4.06358E-06	4.52E-06	DALYs
human health - ozone depletion	5.46857E-06	6.15E-06	DALYs
human health - particulate matter formation	0.019444101	0.022081	DALYs
human health - photochemical oxidant formation: human health	8.61403E-05	9.79E-05	DALYs
human health - water use: human health	0.000216876	0.00021	DALYs
natural resources - energy resources: non-renewable, fossil	1012.947674	1148.52	USD 2013
natural resources - material resources: metals/minerals	29.65573026	31.68678	USD 2013

Key findings indicate that the M70 grade concrete has a marginally higher environmental footprint across most categories compared to M30 grade, suggesting that increased strength correlates with increased environmental impact. This trend is evident in categories such as terrestrial acidification, global warming potential, and ecotoxicity, among others.

The midpoint analysis provided specific metrics like terrestrial acidification potential (TAP), global warming potential (GWP1000), and others, quantified in respective units such as kg SO2-Eq for acidification and kg CO2-Eq for climate change, illustrating the concrete's footprint in quantifiable terms. The impact values obtained for the manufacturing of 100m3 of concrete for ReCiPe 2016 v1.03, endpoint (E) LCIA method is mentioned in Table 2.

The impact values obtained for the manufacturing of 100m3 of concrete for ReCiPe 2016 v1.03, midpoint (E) LCIA method are as shown in Table 3.

Table 3. Impact values in ReCiPe 2016 v1.03, midpoint (E) LCIA method.

Impact category	M30	M70	Reference unit in Kg Equivalent
acidification: terrestrial - terrestrial acidification potential (TAP)	71.67508	81.37063	SO2
global warming potential (GWP1000)	34473.56	39319.36	CO2
freshwater ecotoxicity potential (FETP)	378.2859	422.8477	DCB
marine ecotoxicity potential (METP)	2939014	3313454	DCB
terrestrial ecotoxicity potential (TETP)	29510.98	32969.6	DCB
energy: non-renewable, fossil fuel potential (FFP)	4483.548	5097.703	Oil

freshwater eutrophication potential (FEP)	7.844645	8.942505	P
marine eutrophication potential (MEP)	0.594966	0.676597	N
human toxicity potential (HTPc)	52553.35	57512.51	DCB
non-carcinogenic - human toxicity potential (HTPnc)	2583937	2919064	DCB
ionising radiation potential (IRP)	289.969	322.4872	kBq Co-60
agricultural land occupation (LOP)	1488.311	1689.02	m2*a crop-Eq
material resources: metals/minerals - surplus ore potential (SOP)	128.191	136.9706	Cu-Eq
ozone depletion potential (ODPinfinite)	0.004078	0.004584	CFC-Eq
particulate matter formation potential (PMFP)	30.93308	35.1281	PM2.5-Eq
human health - photochemical oxidant formation potential: humans (HOFP)	94.65695	107.5926	NOx-Eq
photochemical oxidant formation: terrestrial ecosystems (EOFP)	96.055	109.1679	NOx-Eq
water consumption potential (WCP)	97.69212	94.5647	m3

4. Conclusions

This study offers a comprehensive evaluation of the environmental impacts due to the production of 100m^3 of concrete, utilizing both the midpoint and endpoint indicators of the ReCiPe 2016 LCIA methodology. The comparison between M30 and M70 grades reveals that higher-strength concrete has a proportionally greater environmental impact, emphasizing the need for sustainable practices and materials in construction to mitigate these effects. Specifically, the increase in global warming potential, ecotoxicity, and resource depletion associated with higher concrete grades underscores the importance of optimizing material use and exploring alternative, less impactful construction materials. This research contributes to the broader understanding of concrete's environmental footprint and highlights the critical balance between structural requirements and environmental sustainability in the construction industry.

References

[1] Chapa, J. (2019). “Bringing embodied carbon upfront,” in Built environment economist: Australia and New Zealand, 38–41.
[2] Globalabc, I. E. A. U. N. E. P. (2020). GlobalABC roadmap for buildings and constructio n 2020-2050, towards a zero-emission, efficient and resilient buildings and construction sector. Paris, France: International Energy Agency.
[3] Herczeg, M. (2014). Resource efficiency in the building sector: Final report to DG environment. Rotterdam: European Commission.
[4] Curran, M. A. (2017).“Overview of goal and scope definition in life cycle assessment,” in Goal and scope definition in life cycle assessment. LCA compendium – the complete world of life cycle assessment. Editor M. A. CURRAN (Netherlands, Dordrecht: Springer), 1–62. 978-94-024-0855-3.
[5] Sassanelli, C., and Terzi, S. (2022). The D-BEST Based digital innovation hub customer journey analysis method: Configuring DIHs unique value proposition. Int. J. Eng. Bus. Manag. 14, 184797902211246. doi:10.1177/18479790221124634.
[6] Cole, R. J. (1999). "Environmental optimization of building materials." Journal of Environmental Management, 55(2), 91-103.
[7] Gao, W., et al. (2001). "Energy impacts of recycling disassembly material in residential buildings." Energy and Buildings, 33(6), 553-562.
[8] Gustavsson, L., and Sathre, R. (2006). "Comparative analysis of the life cycle impact of wood and concrete in construction." Journal of Cleaner Production, 14(15-16), 1259-1270.
[9] Thormark, C. (2006). "The effect of material choice on the total energy need and recycling potential of a building." Building and Environment, 41(8), 1019-1026.

[10] Saghafi, M. R., and Teshnizi, Z. S. H. (2011). "Recycling potential of building materials: A review." Resources, Conservation and Recycling, 55(9-10), 893-910.
[11] Wei, X., et al. (2008). "Environmental impacts of the Swiss residential building sector calculated with a life cycle assessment approach." Journal of Environmental Management, 90(3), 3684-3693.
[12] Wu, P., et al. (2005). "An environmental impact assessment system for construction engineering projects." Construction Management and Economics, 23(3), 295-304.
[13] Haapio, A., and Viitaniemi, P. (2008). "A critical review of building environmental assessment tools." Environmental Impact Assessment Review, 28(7), 469-482.
[14] Ip, K., and Miller, A. (2012). "Life cycle greenhouse gas emissions of hemp-lime wall constructions in the UK." Resources, Conservation and Recycling, 69, 1-9.
[15] Ardente, F., et al. (2008). "Energy and environmental benefits in public buildings as a result of retrofit actions." Renewable and Sustainable Energy Reviews, 12(1), 200-215.
[16] Anastaselos, D., et al. (2009). "Tool for the selection and evaluation of thermal insulation materials for the building envelope." Building and Environment, 44(5), 1025-1035.
[17] Ortiz, O., Castells, F., and Sonnemann, G. (2009). "Sustainability in the construction industry: A review of recent developments based on LCA." Construction and Building Materials, 23(1), 28-39.
[18] Bayer, P., et al. (2010). "AIA guide to building life cycle assessment in practice." Journal of Industrial Ecology, 14(6), 891-904.
[19] Keeler, M., and Burke, B. (2009). Fundamentals of Integrated Design for Sustainable Building. John Wiley & Sons, New York, NY.
[20] John, G., Clements-Croome, D., and Jeronimidis, G. (2005). "Sustainable buildings for healthier environments: Design and analysis." Indoor and Built Environment, 14(5), 411-425.
[21] Finnveden, G., et al. (2009). "Recent developments in Life Cycle Assessment." Journal of Environmental Management, 91(1), 1-21.
[22] Malmqvist, T., et al. (2011). "Life cycle assessment in buildings: The ENSLIC simplified method and guidelines." Energy, 36(4), 1900-1907.
[23] Bribian, I. Z., et al. (2009). "Life cycle assessment of construction materials: comparative analysis of energy and environmental impacts and evaluation of the eco-efficiency improvement potential." Building and Environment, 46(5), 1133-1140.
[24] Esin, T., and Saghafi, M. R. (2007). "Life cycle assessment of residential buildings: A case study in Canada." Journal of Building Physics, 31(1), 1-14.
[25] IS:4031(Part1):1996 Method of Physical Tests for Hydraulic Cement.
[26] IS:383: 1970 Specification for Coarse and Fine Aggregates from Natural Sources for Concrete.
[27] IS:2720 (Part III): 1980 Methods of Test for Soils Part III - Determination of Specific Gravity.
[28] IS:2386 (Part I):1963 Methods of Test for Aggregates for Concrete Part I - Particle Size and Shape.
[29] IS:456: 2000 Plain and Reinforced Concrete - Code of Practice.
[30] IS:10262: 2009 Concrete Mix Proportioning – Guidelines.
[31] IS:1199:1959 Methods of Sampling and Analysis of Concrete.
[32] IS:516:1959 Methods of Tests for Strength of Concrete.

Acknowledgments

The license to carry out the LCA study was granted by Open- LCA and Eco-invent database for which the authors are grateful.

IOP Conference Series: Earth and Environmental Science

PURPOSE-LED PUBLISHING™

PAPER • **OPEN ACCESS**

Potentially toxic elements in fly ash bricks and associated ecological health risk: An opinionated review

To cite this article: Aliya Naz and Abhiroop Chowdhury 2024 *IOP Conf. Ser.: Earth Environ. Sci.* **1409** 012008

View the article online for updates and enhancements.

You may also like

- Breach Forming Scenarios at Concrete Faced Rock-fill Dams
Alina-Ioana Popescu-Busan, Cornel Ilinca, Serban-Vlad Nicoara et al.
- An Analytical Model for Investigations on the Stress Distribution in Planar Solid Oxide Fuel Cells
Vinzenz Guski, Keita Iritsuki, Motohisa Kamijo et al.
- Transmission Electron Microscopic Observation of Both Ionomer and Pt Distribution and Their Effects on Cathode Performance for Polymer Electrolyte Fuel Cells
Masako Kawamoto, Satoru Hommura, Katsuyoshi Kakinuma et al.



This content was downloaded from IP address 47.247.77.11 on 27/11/2024 at 05:33

Potentially toxic elements in fly ash bricks and associated ecological health risk: An opinionated review

Aliya Naz[1]* and Abhiroop Chowdhury[2]

[1]Jindal School of Liberal Arts and Humanities, O.P. Jindal Global University, Sonipat, Haryana, India
[2]Jindal School of Environment and Sustainability, O.P. Jindal Global University, Sonipat, Haryana, India.

*E-mail: naazaliya6@gmail.com

Abstract. Exposure to potentially toxic elements (PTE) from various sources seriously threatens the ecosystem in the modern era. Fly ash produced from coal and solid waste combustion contains a high concentration of PTE. Fly ash is a major by-product of coal-based thermal power plants and municipal solid waste incineration units. Due to the high demand for fly ash reuse due to its unique properties, fly ash is now in demand for manufacturing of various building materials and geo-liner for landfills. Brick is the primary building material used in construction. Fly ash bricks are very popular nowadays due to their low cost and high durability. This study reveals the ecological risk index through the exposure of heavy metals in fly ash reported in various studies. Results indicate extremely high ecological risk mainly due to Cd content in fly ash followed by Hg, As, Cu, and Pb. Fly ash is one of the causative agents for several diseases affecting the nervous system, skin, circulatory system, digestive system, reproductive system, and immune responses in the human body.

1. Introduction

Fly ash is produced while using coal in processes or energy generation. Global energy generation is transitioning from non-renewable to renewable, but 25% of total energy comes from coal-based thermal plants [1]. India's 75% of energy comes from coal-fired thermal power plants [2,3]. As per the report, total fly ash generation in India was about 142.07 million tons during 1st half of 2022-2023, among 111.01 million tons of fly ash utilized for different purposes [4]. Fly ash is also produced as a byproduct of municipal solid waste incineration. However, China produces a lot of fly ash through the incineration process. About 780 million tons of fly ash are produced annually worldwide, but only 17-20% of fly ash is utilized. However, statistics indicate India utilizes 38% of produced fly ash, whereas China utilizes 45%, the USA 65%, Germany and France 85%, Canada 75%, and Denmark, Italy, Netherlands utilize 100% of produced fly ash [5]. Fly ash has excellent binding capacity and originated as a waste material, making them excellent for brickmaking. Fly ash bricks are also lightweight, making them valuable from a design perspective [6]. Thus, the utilization of fly ash as a building material, a promising geo-liner for landfills, has drastically increased in the past few years due to the high demand for sustainability practices, especially the campaigns on ‘waste to resources. Like montmorillonite clay mineral, fly ash also proved an effective liner to prevent the leaching of toxic materials from landfills to water tables [7,8].

With emerging fly ash disposal issues, it is used for building materials, including brickmaking. Although fly ash bricks are the best alternative to clay bricks, which save natural resources like earth clay and water, some health consequences are reported for health and safety purposes. In the modern era, fly ash bricks are often used for buildings, road construction, and liners of landfills

Content from this work may be used under the terms of the Creative Commons Attribution 4.0 licence. Any further distribution of this work must maintain attribution to the author(s) and the title of the work, journal citation and DOI.
Published under licence by IOP Publishing Ltd

and wells [9-10]. In the past few years, the utilisation of fly ash for brick has increased in almost all countries, including India.

It is also reported that fly ash generated from thermal power plants and other processes, such as solid waste incineration, contains a high concentration of potentially toxic elements (PTEs) [11, 12]. Raw coal itself contains various PTEs, once combustion in high temperature and pressure takes place, PTE remains the same in the fly ash and bottom ash [13]. Few studies have also reported that the concentration of PTE in fly-ash sometimes even increases compared to the PTE content in raw coal [14]. This study aims to assess the ecological risk assessment associated with 890anufacturing and storing fly ash bricks in open spaces and the adverse health impacts on humans exposed to PTE-contained fly ash and fly ash bricks. The study also shed light on the management option to reduce the harmful impacts and improve sustainability by achieving the sustainable development goal (SDG) proposed by the United Nations.

2. Material and Method

Secondary data was collected through a random search in the database from 'Google Scholar'. No specific search methods were applied to choose relevant articles for this review article. Major keyword combinations used for this literature review are 'heavy metal in fly ash'; 'potentially toxic elements in fly ash'; 'fly ash generation'; 'fly ash brick'; 'fly ash utilization'; 'fly ash composition'; 'fly ash and waste to resources'; 'heavy metal recovery from fly ash'; 'fly ash management'. A total of 51 relevant articles were included in a compilation of this literature review.

2.1. Ecological risk assessment

Ecological risk assessment was calculated by using the minimum and maximum concentrations of potentially toxic elements in fly ash. The ecological risk assessment is a tool to predict the extent of the ecological effect of harmful elements. Hakanson initially proposed the potential ecological risk index [15]. The method is weighted by multiplying the ratio of the potentially toxic elements to the reference value by the toxicity factor of the same element. It is a set of methods that can well reflect the potential impact of heavy metals on the ecological environment. As fly ash bricks are used and put in open spaces in manufacturing and construction sites for extended periods, exposure to PTEs can be an ecological threat to the flora and fauna. The formulae of ecological risk calculation are as follows-

$$ERI = TR \times Cf$$

$$Cf = \frac{C_{Sample}}{C_{Shale}}$$

$$RI = \sum ERI$$

Where ERI indicates the Ecological risk index, TR denotes the toxicity response coefficient, Cf indicates the contamination. C_{sample} is the potentially toxic element concentration in the sample, and C_{shale} indicates the average shale value of PTEs. The TR for selected potentially toxic elements are following-As=10, Hg=40, Pb=5, Cd=30, Cr=2, Ni=5, Cu=5, and Zn=1. The range of RI indicates the severity of ecological risk. The classification of RI is -RI < 150 represents low ecological risk. 150 ≤ RI < 300 represents moderate ecological risk. 300 ≤ RI < 600 represents a considerable ecological risk, and RI > 600 represents a very high ecological risk.

In the present study, ecological health risk assessment was calculated using the secondary data obtained from the literature. Past studies indicate that the PTE concentration in fly ash was majorly obtained from thermal power plants and that the by-product of municipal solid waste

incineration was considered. We considered only the maximum and minimum (excluding 'not detected' or 'below detection limit' values), to get an overview the maximum and minimum ecological risk of fly ash bricks at manufacturing and construction sites.

3. Result and Discussion

3.1. Fly ash brick composition

Usually, fly ash bricks constitute a high proportion of fly ash with a small amount of binders. Sometimes, a few proportions of cement, lime, and sand are mixed to increase the tensile strength [16] (Table 1). Due to the pozzolanic nature of lime, it acts as a catalyst once mixed with fly ash. After the reaction with lime, the fly ash accelerator ensures the extent of the reaction. This process is followed by compression, curing, and drying.

3.1.1. Pozzolanic reaction

When fly ash is mixed with lime and gypsum or cement, the binding material calcium silicon hydrate forms, which looks and acts like a gel [6]. The involvement of lime and gypsum or cement makes this process costly. Still, it is more eco-friendly than clay-based bricks [6]. Researchers are looking for other binding materials to replace cement and lime, making the process more environmentally friendly and economically viable.

3.1.2. Properties of fly ash brick

Fly ash brick properties depend on its composition. According to Kayali, bricks made with 100% fly ash have a tensile strength about three times higher than normal clay bricks [17]. The compressive strength of fly ash brick was about 43 MPa, and the initial absorption rate was 4.5kg/m^2/min with a 10% absorption capacity [17].

3.1.3. Leaching of PTE from fly ash

The major environmental concern of fly ash usage in brick formation is the high concentration of potentially toxic elements in it. The study also suggested the PTE concentration differs with the type of coal combustion or the type of waste gets incinerated. Lignite and bituminous coal produce comparatively higher contaminated fly -ash, while anthracite coal combustion produces less PTE concentrated fly ash. In India, the majority of coal used in thermal power plants is lignite and bituminous; thus, the PTE concentration in fly ash is found to be higher than that in countries that are highly dependent on anthracite coal-based power plants.

Table 1. Composition of fly ash bricks.

Material	Proportion
Fly ash	57-65%
Sand/stone dust	18-27%
Gypsum	5%
Sludge Lime	15% to 22%
Cement	8-12%

3.2. Concentration of PTEs in fly ash

Table 2 indicates the PTEs concentration in fly ash obtained from different thermal power plants and solid waste incineration units across the globe. The PTE content in the fly ash can pose ecological hazards, particularly when stored outside (Fig.1). PTEs are known to cause environmental and health toxicity. Very high arsenic concentration was reported in the bottom ash and fly ash obtained from the combustion of lignite [18]. Another study by Gopinathan et al.,

2022 suggested extremely high concentrations of Co, Pb, Cu, Cr, Ni, and Zn were in the fly ash of the coal mine area in India [19]. Thus, the PTE concentration varies with the type of parent material that gets combusted. Basically, fly ash is generated in countries like India, where over 86.35% of Megawatt of energy is generated from coal-based thermal power plants [3,20,21]. Indian thermal power plants are based on the bituminous and lignite coal, which comparatively contains high PTEs. Pb, particularly in the Pb^{2+} form, can cause impairment in the neurological system and impact the brain. Long-term or chronic exposure can lead to memory loss, fatigue, dementia, and learning disabilities in children. Hg, though not that toxic in elemental form, but its organic derivative, methyl mercury, can cause bioaccumulation in the fat-rich portion of the human body. Brain cells are nerves with high concentrations of lipids, which form an insulating lining of the neurons, also known as the myelin sheath. Methyl mercury accumulates in these sections of the body, causing neuron toxicity. Over-exposure to hg can lead to memory loss and uncoordinated movement as the metal impacts the brain's motor cortex and tremors. Positively charged metal ions impart cellular toxicity by disrupting the enzymatic functioning of the cells. Chromium, particularly in the hexavalent form, can also cause genotoxicity, resulting in carcinogenesis. Similarly, Cd, being in the same periodic group as Zn, can replace the metal in cells, resulting in higher bioaccumulation into the cells [22].



Figure 1. Outdoor storage of Fly ash bricks meant for building construction

Table 2. Potentially toxic elements (mg/kg) in fly ash, where ND indicates 'not detected', and NR indicates 'not reported'

References	Remarks	As	Co	Cu	Hg	Pb	Cd	Cr	Mn	Ni	Zn
[13]	Fly ash samples were analyzed from Four thermal power plants in China	4.59-15.0	NR	NR	0.064-0.977	ND-41.6	ND-0.98	6.2-88.6	NR	3-53	NR
[50]	Fly-ash samples	NR	8-18	56-83	NR	20-56	NR	87-103	47-139	28-63	60-124

	from three power plants in North India										
[19]	A total of 20 fly ash samples were collected from various mining areas of Talcher Coalfield, India.	NR	69.6-113	168.9-248.4	NR	151.2-309	ND-3.6	260.4-387.9	NR	86.9-162.2	116.9-418.7
[51]	PTE content in Fly ash produced by Municipal solid waste incineration in China	3.8-42	NR	43-913	1.5-2.9	65-312	0.80-17.4	25-303	NR	6.0-115	282-2630
[52]	PTE content in the fly-ash generated from coal-fired thermal power plant, Parichha, Jhansi, India	NR	NR	NR	NR	34.809	NR	64.772	286.205	51.609	NR
[14]	Potentially toxic elements in fly ash obtained from bituminous coal burning	ND	31-43	65-95	NR	20-70	ND	139-254	325-393	100-135	49-85
[18]	PTE content in bottom ash and fly ash of Lignite/hard rock	7.6–135	0.03–2.0	4.4–66	NR	NR	0.2–74	4.0–92	NR	16–79	19–155

3.3. Ecological risk assessment

The ecological health risk obtained through maximum and minimum concentrations of PTE is tabulated in Table 3. *It indicates* that the maximum ecological risk is exceptionally high as it is more than 2.5 times higher than the maximum ecological risk index category (> 600 ERI). Higher ecological risk indicates a threat to the ecosystem, which could be contaminated with PTEs. Which directly and indirectly affects the human population and all flora and fauna in nearby areas. A very high ecological risk index can be seen through Cd, followed by Hg, As, Cu, and Pb in fly ash (Table 3). Wang et al. also reported that the maximum ecological risk posed by Cd exposure to PTE by fly ash [13]. While not a direct health impact on humans, the environmental consequences of fly ash pollution can indirectly affect human health through contaminated water sources, soil, and food chains. Storage and disposal of fly ash brick can have a negative impact on plants and affect soil fertility [23].

Table 3. Ecological Risk Index (ERI) calculated through maximum and minimum PTE concentrations of various fly ash

	As	Cd	Cr	Cu	Ni	Pb	Zn	Hg	Mn	Co	ERI
ERI max	69	1160	6	68	8	52	18	193	0.3	8	1582
ERI Min	2	13	0.1	0.3	0.1	3.3	0.1	4.3	0.04	0.00	24

3.4. Major health issues from Fly ash

3.4.1. Respiratory Issues

Fly ash particles are extremely fine, often smaller than 2.5 micrometres ($PM_{2.5}$), which allows them to penetrate deep into the respiratory system [24, 25]. Inhalation of fly ash can lead to respiratory problems such as asthma, bronchitis, and aggravated symptoms in individuals with pre-existing respiratory conditions [26]. Sometimes, PTE present in fly ash is also exposed to humans through ingestion and causes potential health issues such as tumours and pulmonary cancers [29, 30].

3.4.2. Neurological Effects

Potentially toxic elements such as Pb, Cd, As, and Hg, found in fly ash, can have neurotoxic effects and brain cancer [31,32]. Prolonged exposure to these substances may impair cognitive function and contribute to neurological disorders. Once metallic ion enters living cells, they interfere with cellular metabolic activities to produce ROS, which ultimately affects cell cycling progression [33]. Sometimes, these free radicals (ROS) can be the reason for a few major neurological disorders, such as Parkinson's [34-36].

3.4.3. Skin Irritation

Direct contact with fly ash can cause skin irritation and dermatitis in sensitive individuals. It is reported that heavy metal exposure through fly ash generated through municipal solid waste incineration poses human health risks, especially through inhalation and dermal contact [35]. A review study indicated that skin disorder is a major health issue among workers and those near cement industries [24,38,39]. Fly ash usage in brick and cement production is very common nowadays, which indicates its alarming health hazard if fly ash is not characterized earlier for PTE concentration.

3.4.4. Reproductive Health

Exposure to certain components of fly ash, such as heavy metals, has been linked to reproductive issues, including reduced fertility and developmental abnormalities in fetuses. It is proven that

the reproductive health of fish is negatively impacted by exposure to PTE from coal ash [38]. Studies also suggested that exposure to fly ash can cause birth defects and abnormalities in fetuses due to chronic exposure to PTEs through ash particles [39]. Another study also suggested that the endocrine system gets impacted through exposure to fly ash, which ultimately creates imbalances in reproductive hormones [40].

3.4.5. Immune System Impairment

Chronic exposure to fly ash may weaken the immune system, making individuals more susceptible to infections and illnesses. Fine particles of fly ash through manufacturing and disposal processes have proven hazardous for the immune health of children [41]. PTEs such as Pb, Cd and Hg exposure through fly ash bricks can cause immune system impairment, mostly in infants, children, and elderly age groups. Sometimes chronic exposure of these PTE is responsible for cancer progression [42-45].

Potentially toxic elements in fly ash can have adverse effects on human health. The fly ash brick containing PTEs can pose different health hazards to humans exposed to it from the manufacturing unit to the disposal units. PTEs, mainly Cr, Mn, Ba, Rb, Be, Co, Cu, Ni, As, Cd, Pb, Zn, Se, and Hg, are major PTEs reported in the fly ash [44]. Recovery and removal of PTE from the fly ash before reusing it for brick-making can be a management recommendation for reducing health impacts [47]. Recent studies suggested that recovery of PTEs is possible through the adsorption and leaching processes [48,49]. An enclosed environment for manufacturing and storage can also increase the scope of reutilization of fly ash for a better future to achieve a sustainable environment. Thus, the UN sustainable development goals (SDG) can be achieved. SDG 3 -Good health and well-being, SDG 11-Sustainable cities and communities, and SDG 12- responsible consumption and production.

4. Conclusion and recommendation

This study concludes that untreated fly ash can pose ecological and human health hazards if used for any building and construction work. It is suggested that manufacturing and storing fly ash-based building materials, primarily fly ash bricks, must be kept in an enclosed environment instead of in an open space for extended periods. Putting fly ash in the open can lead to the leaching of heavy metal eighter due to areolar erosion or water. Fly ash can cause respiratory, neurological, reproductive, and other toxic responses in humans, and heavy metals can bioaccumulate in the food chain, causing ecotoxicity.

5. References

[1] Our world data 2024 https://ourworldindata.org/energy-mix (Retrieved on 6 March 2024)
[2] MOC, Ministry of Coal, India 2024 Ministry of Coal, Government of India (Retrieved on 6th March 2024)
[3] Dahiya S, Lolla A, Gupta P, Sivalingam N. 2023 India's Coal and Coal-Fired Electricity Needs by 2030: Clearing Vision beyond Black Coal and Hazy Skies. *In The Role of Coal in a Sustainable Energy Mix for India* (pp. 13-27). Routledge India.
[4] CEA, Central electricity Authority Delhi, 2024, Report On Fly Ash Generation At Coal / Lignite Based Thermal Power Stations And It's Utilization In The Country For The 1st Half Of The Year 2022 – 2023 (April 2022 to September 2022) https://cea.nic.in/wp-content/uploads/tcd/2023/05/Half_Yearly_Ash_Report_2022_23.pdf
[5] Shrivastava U, Khan M. Z and Mishra V 2020 A study on components of fly ash of different locations and its utilization for production of improved quality materials: A Review *IOP Conf. Ser. Mater. Sci. Eng* **798**, 012004 IOP Publishing.
[6] Balasubramaniam T, Karthik P. S. Sureshkumar S, Bharath M and Arun M. 2021 Effectiveness of industrial waste materials used as ingredients in fly ash brick manufacturing *Mater. Today: Proc.* **45** 7850-7858.

[7] Naz A, Chowdhury A. 2022 Pollutant extraction from water and soil using Montmorillonite clay-polymer composite: a rapid review *Mater. Today: Proc.* **60** 1-7.
[8] Chowdhury A, Naz A and Chowdhury A. 2022 Waste to resource: Applicability of fly ash as landfill geoliner to control ground water pollution *Mater. Today: Proc.* **60** 8-13.
[9] Kelechi S E, Adamu M, Uche O A U, Okokpujie I P, Ibrahim Y E and Obianyo I I 2022 A comprehensive review on coal fly ash and its application in the construction industry *Cogent Eng.* **9** 2114201.
[10] Dan A K, Bhattacharjee D, Ghosh S, Behera S S, Bindhani B K Das D and Parhi P K 2021 Prospective utilization of coal fly ash for making advanced materials. *In Clean Coal Technologies: Beneficiation, Utilization, Transport Phenomena and Prospective* 511-531. Cham: Springer International Publishing.
[11] Smołka-Danielowska D. 2006 Heavy metals in fly ash from a coal-fired power station in Poland *Pol. J. Environ. Stud* **15**.
[12] Paswan D, Shabiimam M A, Shaikh M, Nadar A and Maniyar S D 2017 Heavy metals in fly ash; Its impact on human health and environment. *In NICMAR 2nd International Conference on Construction, Real Estate, Infrastructure and Project (CRIP) Management* 10-11.
[13] Wang C Q, Liu K, Huang D M, Chen Q, Tu M J, Wu K and Shui Z H 2022 Utilization of fly ash as building material admixture: Basic properties and heavy metal leaching. *Case Stud. Constr. Mater* **17** e01422.
[14] Koukouzas N, Ketikidis C, Itskos G 2011 Heavy metal characterization of CFB-derived coal fly ash *Fuel Process. Technol* **92** 441-446.
[15] Hakanson L. 1980 An ecological risk index for aquatic pollution control. A sedimentological approach. *Water res* **14** 975-1001.
[16] Mainuddin M, Ruhul Amin M, Sarkhel S, Bhowmick P and Ahmed A 2019 Stresses in Fly Ash Brick using different proportion of Lime, Cement, Gypsum, Sand and Stone Dust. *Int. J. Innov. Technol. Explor. Eng* **9** 4288-4292.
[17] Kayali O 2005 High performance bricks from fly ash. In Proceedings of the World of Coal Ash Conference, Lexinton, Kentucky **11**.
[18] Lecuyer I, Gueraud S and Bursi J M Different uses of CF Bash-EDF investigations, 42ndIEA-FBCMeeting,Sydney, NovaScotia, Canada, May 10-112001.
[19] Gopinathan P, Santosh M S, Dileepkumar V G, Subramani T, Reddy R, Masto R E and Maity S 2022 Geochemical, mineralogical and toxicological characteristics of coal fly ash and its environmental impacts *Chemosphere* **307** 135710.
[20] Guttikunda S K and Jawahar P 2014 Atmospheric emissions and pollution from the coal-fired thermal power plants in India *Atmospheric Environment* **92** 449-460.
[21] Vig N, Ravindra K and Mor S 2023 Environmental impacts of Indian coal thermal power plants and associated human health risk to the nearby residential communities: A potential review *Chemosphere* 140103.
[22] Chowdhury A, Naz A and Maiti S K 2023 Distribution, speciation, and bioaccumulation of potentially toxic elements in the grey mangroves at Indian Sundarbans, in relation to vessel movements *Mar. Environ. Res* **189** 106042.
[23] Sonwani S, Gupta A, Saxena P and Rani A 2023 Fly ash toxicity, concerned issues and possible impacts on plant health and production. *Plants and Their Interaction to Environmental Pollution* 109-123.
[24] Tumane R, Pingle S, Jawade A and Randive K 2022 Toxicity and occupational health hazards of coal fly ash. *In Medical Geology in Mining: Health Hazards Due to Metal Toxicity* 349-359. Cham: Springer International Publishing.
[25] Whiteside M, Herndon J M 2018 Aerosolized coal fly ash: Risk factor for COPD and respiratory disease *Journal of Advances in Medicine and Medical Research* **26** 1-13.
[26] Lahiri S S 2021 Fly ash: Safety and health issues 4. *Handbook of Fly Ash* **77.**
[27] Bourliva A, Papadopoulou L, da Silva E F and Patinha C 2020 In vitro assessment of oral and respiratory bioaccesibility of trace elements of environmental concern in Greek fly ashes: Assessing health risk via ingestion and inhalation *Sci. Total Env.* **704** 135324.
[28] Wu J, Tou F, Yang Y, Liu C, Hower J C, Baalousha M., ... Hochella Jr M F 2021 Metal-containing nanoparticles in low-rank coal-derived fly ash from China: characterization and implications toward human lung toxicity *Environ. Sci. Technol*. **55** 6644-6654.
[29] Agnihotri S K and Kesari K K 2019 Mechanistic effect of heavy metals in neurological disorder and brain cancer *Networking of Mutagens in Environmental Toxicology* 25-47.
[30] Woimant F and Trocello J M 2014 Disorders of heavy metals *Handbook of clinical neurology* **120** 851-864.
[31] Guo W, Xing Y, Luo X, Li F, Ren M and Liang Y 2023 Reactive oxygen species: A crosslink between plant and human eukaryotic cell systems *Int. J. Mol. Sci.* **24** 13052.
[32] Montgomery Jr, E B 1995 Heavy metals and the etiology of Parkinson's disease and other movement disorders *Toxicology* **97** 3-9.

[33] Sankhla M S, Sharma K and Kumar R 2017 Heavy metal causing neurotoxicity in human health. International Journal of Innovative Research in Science *Eng. Technol.* **6**.
[34] Rehman Q, Rehman K and Akash M S H 2021 Heavy metals and neurological disorders: from exposure to preventive interventions. In Environmental contaminants and neurological disorders (pp. 69-87). Cham: Springer International Publishing.
[35] Zhou J, Wu S, Pan Y, Zhang L, Cao Z Zhang, X. ... Qian G 2015 Enrichment of heavy metals in fine particles of municipal solid waste incinerator (MSWI) fly ash and associated health risk *Waste Manage*. **43** 239-246.
[36] Helepciuc, C. M., Barbuta M, Ciocan V, Serbanoium A and Gradinaru A C 2017 Health and environmental effects of heavy metals resulted from fly ash and cement obtaining and trials to reduce their pollutant concentration by a process of combining-exclusion. *International Multidisciplinary Scientific GeoConference: SGEM* **17** 441-447.
[37] Rauf A U, Mallongi A, Astuti R D P 2020 Heavy metal contributions on human skin disease near cement plant: a systematic review *OAMJMS* **8** 117-122.
[38] Pracheil B M, Marshall Adams S, Bevelhimer M S, Fortner A M, Greeley M S, Murphy C A ... Peterson M J 2016 Relating fish health and reproductive metrics to contaminant bioaccumulation at the Tennessee Valley Authority Kingston coal ash spill site *Ecotoxicology* **25** 1136-1149.
[39] Kravchenko J and Lyerly H K 2018 The impact of coal-powered electrical plants and coal ash impoundments on the health of residential communities *N. C. Med. J.* **79** 289-300.
[40] Liu, G. 2017 Adverse thyroid health effects of coal ash exposure (Doctoral dissertation, University of Pittsburgh).
[41] Zheng K, Zeng Z, Tian Q, Huang J, Zhong Q and Huo X 2023 Epidemiological evidence for the effect of environmental heavy metal exposure on the immune system in children *Sci. Total Env.* **868** 161691.
[42] Ebrahimi M, Khalili N, Razi S, Keshavarz-Fathi M, Khalili N and Rezaei N 2020 Effects of lead and cadmium on the immune system and cancer progression *Journal of Environmental Health Science and Engineering* **18** 335-343.
[43] Koller L. D. 1980 Immunotoxicology of heavy metals. *Int. Immunopharmacol* **2** 269-279.
[44] Mishra K P 2009 Lead exposure and its impact on immune system: a review *Toxicology in Vitro* **23** 969-972.
[45] Bhargava P, Gupta N, Vats S and Goel R. 2017 Health issues and heavy metals. *Austin J Environ Toxicol* **3**(1), 3018.
[46] Zierold K M and Odoh C 2020 A review on fly ash from coal-fired power plants: chemical composition, regulations, and health evidence *Rev. Environ. Health* **35** 401-418.
[47] Sahoo P K, Kim K and Powell M A Equeenuddin S M 2016 Recovery of metals and other beneficial products from coal fly ash: A sustainable approach for fly ash management *Int. J. Coal Sci. Technol.* **3** 267-283.
[48] Tang J, Su M, Wu Q, Wei L, Wang N, Xiao E. ... Xiao T 2019 Highly efficient recovery and clean-up of four heavy metals from MSWI fly ash by integrating leaching, selective extraction and adsorption *J. Clean. Prod* **234** 139-149.
[49] Kuboňová L, Langová Š, Nowak B and Winter F 2013 Thermal and hydrometallurgical recovery methods of heavy metals from municipal solid waste fly ash *Waste Manag.* **33** 2322-2327.
[50] Sushil S and Batra V S 2006 Analysis of fly ash heavy metal content and disposal in three thermal power plants in India. *Fuel* **85** 2676-2679.
[51] Wang P, Hu Y and Cheng H 2019 Municipal solid waste (MSW) incineration fly ash as an important source of heavy metal pollution in China *Environ. Pollut.* **252** 461-475.
[52] Verma C, Madan S and Hussain A 2016 Heavy metal contamination of groundwater due to fly ash disposal of coal-fired thermal power plant, Parichha, Jhansi, India *Cogent Eng.* **3** 1179243.

IOP Conference Series: Earth and Environmental Science

PURPOSE-LED PUBLISHING™

PAPER • **OPEN ACCESS**

Exploring the role of green intrinsic motivation in predicting ecological automobile use: the mediating role of green self-efficacy within the framework of theory of planned behaviour

To cite this article: Suyesha Singh and Vaishnavi Nambiar 2024 *IOP Conf. Ser.: Earth Environ. Sci.* **1409** 012009

View the article online for updates and enhancements.

You may also like

- Environmental Concerns, Communal Orientation, and Environmental Self-Efficacy as Predictors of Ecologically Conscious Consumer Behaviour Among Young Adults
Suyesha Singh and Geeta Khanwani
- Energy conservation behavioural intention: attitudes, subjective norm and self-efficacy
J W C Lee and A Tanusia
- The relationship between gender and academic performance in undergraduate physics students: the role of physics identity, perceived recognition, and self-efficacy
Ewan Bottomley, Antje Kohnle, Kenneth I Mavor et al.



This content was downloaded from IP address 47.247.77.11 on 27/11/2024 at 05:34

Exploring the role of green intrinsic motivation in predicting ecological automobile use: the mediating role of green self-efficacy within the framework of theory of planned behaviour

Suyesha Singh[1]* and Vaishnavi Nambiar[1]

[1]Department of Psychology, Manipal University Jaipur, Jaipur, Rajasthan, India

*Email: suyeshasingh@gmail.com

Abstract. The increasing rate of climate change and the exhaustion of natural resources have caused sustainability to be of paramount importance across the globe. The transportation industry is one of the most important sectors that impacts the environment through greenhouse gas emissions and other pollutants produced by traditional vehicles. In response to these environmental problems, there has been an increased effort to promote green transportation alternatives such as electric vehicles and carpooling, which can help mitigate the adverse effects of commuting and travel. Previous literature has demonstrated that the intention of individuals to engage in green behaviors is affected by various factors, such as their personal motivation to create a positive change in their environment. However, the green behavior of different segments of the population needs to be further scrutinized to comprehend its prevalence and the resulting consequences. This paper aimed to understand the effect of green intrinsic motivation on ecological automobile use and the mediating role of green self-efficacy among middle-aged individuals using the theory of planned behavior. Findings show that green intrinsic motivation has a positive relationship with and predicts ecological automobile use among middle-aged individuals. Green self-efficacy mediates the relationship between green intrinsic motivation and ecological automobile use. Through discovering the psychological dynamics of establishing eco-friendly transport habits among this group, this study aims to provide effective solutions to design interventions and policies that would encourage green travel behavior. This understanding has significance for policymakers, who can use the findings of the study to frame interventions and policies promoting eco-friendly transportation alternatives.

Keywords. Green Intrinsic Motivation, Green Self-Efficacy, Ecological Automobile Use

1. Introduction

The need for sustainable practices has been on the rise in the face of increasing environmental problems [1, 2] that call for a re-evaluation of individual behaviors and societal norms among different demographic groups. One of the many sources of human activity that harms the environment is transportation, which, due to its high emissions and ecological footprint, is the most significant sector [3]. Environmentally responsible transportation options like electric cars have been regarded as a solution to environmental effects and a path towards sustainability. Elucidation of the factors contributing to the choice of eco-automobile mode, along with the development of targeted interventions and policies for a green transport culture, is of great importance.

Content from this work may be used under the terms of the Creative Commons Attribution 4.0 licence. Any further distribution of this work must maintain attribution to the author(s) and the title of the work, journal citation and DOI.
Published under licence by IOP Publishing Ltd

Ecological automobile use (EAU) is the use of vehicles by individuals abiding by environmental norms and concerns. It involves the use of electric vehicles, carpooling, or other eco-friendly transport alternatives. Green intrinsic motivation (GIM) reflects the internal drive and interest of individuals in performing environmental behaviours [4], while green self-efficacy (GSE) reflects the beliefs of the individuals in their ability to successfully execute positive actions in the environment [5].

Psychological theories offer valuable frameworks for understanding the underlying motivations and beliefs that specify the behaviour of people, including their responses to ecological maintenance. For instance, the Self-Determination Theory (SDT) [6] and the Social Cognitive Theory [7] offer insight into psychological mechanisms that stimulate pro-environmental behaviour. Although the theoretical importance of these features has been taken into consideration, there has been scarce empirical research that highlights the role of green intrinsic motivation and green self-efficacy as determinants of ecological car usage among middle-aged individuals.

By measuring these psychological constructs empirically, the present study aims to enrich the existing corpus of knowledge on sustainable mobility behaviours and to support the formulation and implementation of specifically focused programmes to promote environmental responsibility, predominantly in middle-aged adults and in the general population.

1.1. Significance of sustainable transportation

Sustainable transportation plays a major role in transforming and addressing issues related to climate change. By embracing different alternatives such as electric vehicles, cycling, and walking that help reduce the incidence of hazards in the environment, communities can greatly contribute to establishing a sustainable future. It leads to a reduction in greenhouse gas emissions, better physiological wellness, and increased wellbeing in the community. Moreover, allowing equilibrium in the availability of sustainable transportation alternatives to individuals, especially those from the unaffordable sections of society, can enhance the quality of the environment as it permits social inclusion in the contribution towards creating a sustainable environment.

1.2. Theory of Planned Behaviour and Sustainable Automobile Use

The Theory of Planned Behaviour (TPB) was developed by Ajzen (1991) [8]. The theory explains three constructs or dimensions that shape an individual's behaviour: attitude towards behaviour, perceived behaviour control, and subjective norms. Earlier literature has integrated and evolved the theory to understand the impact of the green behaviour of consumers on their purchasing behaviour from a psychological perspective [9, 10,11].

'Attitude towards behaviour' entails the positive or negative evaluation of the individual towards a stimulus [8]. 'Perceived behavioural control' is the perceived complexity of that behaviour or action and is influenced by the individual's assessment of the opportunities and available resources [12]. While the third construct, 'subjective norms' imply the societal pressure experienced by the individual to either participate in or refrain from an activity [8].

The variables of the study may be explained as follows based on the constructs of TPB:

Green intrinsic motivation: This variable may be related to the construct of attitude towards behaviour. If the individual values an action or behaviour, they will be internally motivated or driven to engage in the same, as they aspire to create change in their surroundings. In the realm of the study, it may be understood that individuals can be intrinsically motivated to pursue green automobiles that contribute to establishing a sustainable environment.

Green self-efficacy: This variable may be associated with the construct of perceived behavioural control, wherein an individual is aware of the impact of their own behaviour or actions on the environment. If the individual has high self-efficacy, it means that they are capable of producing more sustainable behaviours. They are self-conscious of the role they play in the creation or destruction of the environment and take the necessary steps for the same.

Ecological Automobile Use: Lastly, this construct is related to the construct of subjective norms. The individual subscribes to the environmental regimes and abides by the expected norms of the community in building a sustainable environment together through the use of ecological vehicles.

2. Review of Literature

2.1. Green Intrinsic Motivation and Ecological Automobile Use

Bagga et al., (2024) [13] assessed the impact of intrinsic motivation on consumers' intentions towards electronic vehicles. It was found that the intrinsic motivation of consumers was a significant predictor of their intention to purchase electric vehicles. Kautish et al., (2024) [14] examined the enablers and inhibitors of consumers during the purchase of electronic vehicles. It was found that the personal motives of consumers played a significant role in their intention to purchase electronic vehicles. He et al., (2021) [15] used the new energy vehicles to examine the effect of the behavioural motivation of individuals on green purchasing behaviour through behaviour intention. Founded on grounded theory, the findings show that the behavioural motivation of individuals indirectly influences green purchasing behaviour through their behavioural intention.

A similar study by Abbasi et al., in 2021 [16] investigated consumer motivation and knowledge of the environment on use of electronic vehicles. It was found that the motivation of consumers significantly influences their intention to purchase electronic vehicles, as their knowledge and awareness of the environmental issues predominate their purchasing behaviour.

Earlier studies have investigated the pro-environmental behaviour of individuals. However, with the rising trend of eco-friendly transportation alternatives such as electric vehicles, there is an increasing need to understand how individuals perceive and hold beliefs towards such changes. Middle-aged individuals, rigid about their attitude and belief system, may find it challenging to adopt changes in their lifestyle. Hence, it is necessary to understand the attitude and motivation of middle-aged individuals towards the adoption of ecological automobiles in daily life so that suitable interventions may be framed targeting the attainment of environmental sustainability using eco-friendly transportation alternatives. Therefore, the following hypotheses have been deduced:

H1: GIM will have a positive relationship with EAU among middle-aged individuals.

H1.1: GIM will significantly predict EAU among middle-aged individuals.

2.2. Green Self-efficacy and Ecological Automobile Use

Chou et al., (2024) [17] investigated the travel-related self-efficacy of individuals in China in reducing the use of private vehicles and promoting the use of community-based electric sharing. It was found that self-efficacy improved eudaimonic and normative values to enable sustainable behaviour intention among individuals. Anwar et al., (2022) [18] examined the impact of an individual's self-efficacy on the consumer's switching intention from conventional to green vehicles. Findings show that individuals with higher decision self-efficacy have a greater intention to purchase environmentally friendly vehicles.

Al Mamun et al., (2019) [19] studied the factors that predicted green purchasing behaviour towards the adoption of ecological vehicles among individuals from Malaysia. Results show that self-efficacy was an important contributor to building intention among individuals towards green purchasing behaviour and the adoption of green vehicles. Ng et al., (2018) [20] assessed the green purchasing intentions of individuals in Hong Kong with relation to electric vehicles. It was found that personal values, beliefs, and self-efficacy significantly influence an individual's intent to purchase electric vehicles.

Previous literature has examined the role of GSE in instigating EAU among individuals in different settings. However, there is still scope for understanding the mediating role of GSE in promoting healthy and eco-friendly transportation options among individuals. The second hypothesis of the study is:

H2: GSE will mediate the relationship between GIM and EAU among middle-aged individuals. Figure 1 represents the conceptual model of the study.

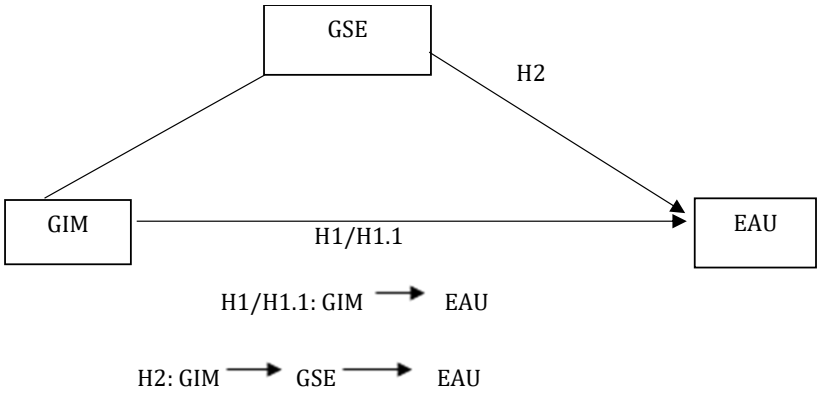


Figure. 1. Conceptual model of the association between GSE and EAU among middle aged individuals

3. Methodology

3.1. Participants and procedure

Purposive sampling was used to collect the data. The sample comprised 208 individuals belonging to the age group of 45-60 years. Individuals undergoing treatment for mental health were not considered to not aggravate their negative emotions. Informed consent was obtained from the participants before the study, and they were assured of the confidentiality of the data.

The questionnaire was distributed through Google Forms. The statistical analyses were performed through SPSS 26. The relationships shared among the GIM, GSE, and EAU were measured using correlation, regression, and mediation analysis.

3.2. Measures:

3.2.1. Green Intrinsic Motivation Scale

The scale was developed by Li et al., (2020) [4] and consists of six questions. The scale is used to measure the intrinsic motivation of individuals to engage in pro-environmental behaviours. The scale consisted of a 7-point Likert scale, ranging from 1 (strongly disagree) to 7 (strongly agree). The scale had a Cronbach's alpha of 0.96.

3.2.2. Green Self-efficacy Scale

The scale was developed by Chen et al., (2014) [21] and consisted of six items. This scale is used to measure the perception of the individual regarding their capacity to produce positive change in the environment. The Cronbach's alpha of the scale is 0.90.

3.2.3. Ecological Automobile Use

A subscale of the Green Ecological Behaviour Scale, developed by Kaiser (1998) [22], is used to measure individuals' sustainable use of green vehicles. The subscale contains four items. The scale had a reliability of 0.70 and an internal consistency of 0.74.

4. Results and findings

The average age of the participants was 50.22 years (SD = 4.52). The ratio of women to men was 94:143. The minimum score of participants on the GIM scale was 9, and the maximum score was 42 (mean = 25.20, SD = 13.29). The minimum score on the GSE scale was 9, and the maximum score was 30 (mean = 20.79, SD = 8.79). Similarly, on the EAU scale, participants scored a minimum score of 1, and a maximum score of 5 (mean = 3.46, SD = 0.98). Descriptive statistics are shown in Table 1.

Table 1. Descriptive statistics

	Age	GIM	GSE	EAU
Valid	208	208	208	208
Mean	50.226	25.202	20.798	3.462
Std. Deviation	4.529	13.297	8.795	0.987
Minimum	44.000	9.000	9.000	1.000
Maximum	60.000	42.000	30.000	5.000

GIM=Green Intrinsic Motivation, GSE=Green Self-Efficacy, EAU= Ecological Automobile Use

Pearson correlation analysis reflects the relationship between GIM and EAU. The result of the analysis is shown in Table 2.

Table 2. Pearson correlation of GIM, EAU

Variable		GIM	EAU
1. GIM	Pearson's r	—	
	p-value	—	
2. EAU	Pearson's r	0.598*	—
	p-value	< .001	—

*Significant at 0.001 level, GIM=Green Intrinsic Motivation, EAU= Ecological Automobile Use

Table 2 shows that GIM and EAU ($r=0.598$, $p<0.001$) shared a significant positive relationship. Hence, H1 was accepted.
The results of the regression analysis show that GIM contributed to about 85.9% of the variance in EAU among middle-aged individuals.

Table 3. Linear regression analysis of GIM and EAU

Model	R	R^2	Adjusted R^2	RMSE
H_1	0.927	0.860	0.859	1.350

GIM=Green Intrinsic Motivation, EAU= Ecological Automobile Use, Dependent variable: EAU Independent variable: GIM

Table 4. Unstandardized and standardized coefficients of GIM and EAU

Model		Unstandardized	Standard Error	Standardized	t	p
H_1	GIM	0.117	0.003	1.579	35.652	< .001

Fit for model $R^2=0.860$, Adjusted $R^2=0.859$, $p<0.001$, GIM=Green Intrinsic Motivation, EAU= Ecological Automobile Use

Tables 3 and 4 show that GIM significantly predicts EAU among middle-aged individuals ($R=0.927$, $R^2=0.860$, Adjusted $R^2=0.859$, $p<0.001$).

Table 5. Mediation analysis of GIM, GSE and EAU

					95% Bca Confidence Interval	
	Estimate	Std. Error	z-value	p	Lower	Upper
GIM → GSE → EAU	0.050	0.013	3.938	< .001	0.025	0.074

Note: Delta method standard errors, normal theory confidence intervals, ML estimator, Bca=Bias correlated accelerated percentile bootstrap, CL=class interval, GIM=Green Intrinsic Motivation, GSE=Green Self-Efficacy, EAU= Ecological Automobile Use

Table 6. Path coefficients of GIM, GSE and EAU

						95% Confidence Interval	
		Estimate	Std. Error	z-value	p	Lower	Upper
GSE	→ EAU	0.079	0.02	3.952	< .001	0.04	0.118
GIM	→ EAU	-0.005	0.013	-0.404	0.686	-0.031	0.021
GIM	→ GSE	0.631	0.014	45.591	< .001	0.604	0.658

Note. Delta method standard errors, normal theory confidence intervals, ML estimator

Tables 5 and 6 show that GSE significantly mediated the association between GIM and EAU among middle-aged individuals, hence accepting H2.

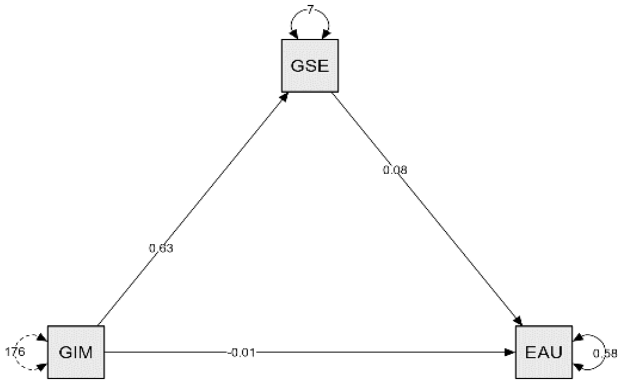


Figure. 2. Path plot of the relationship between GIM and EAU and GSE as mediator.

Figure 2 shows that GIM has a direct relationship with EAU and GSE has an indirect relationship with EAU among middle-aged individuals and Table 7 shows that the hypotheses of the study were accepted.

Table 7. Findings of the study

Hypotheses	**Results**
H1: GIM will have a significant positive relationship with EAU among middle aged individuals	Accepted
H1.1: GIM will significantly predict EAU among middle-aged individuals	Accepted
H2: GSE will mediate the relationship between GIM and EAU among middle-aged individuals	Accepted

GIM=Green Intrinsic Motivation, GSE=Green Self-Efficacy, EAU= Ecological Automobile Use

5. Implications of the study

The study's findings have implications at the individual and policy levels.

5.1. Individual level

Environmental education campaigns, skill development, and empowerment initiatives, that ~~are~~ suit the personal values and beliefs of individuals may help foster eco-friendly behaviour, so as to decrease the carbon footprint and preserve the environment. This can further lead to tangible advantages such as a reduction in greenhouse gas emissions, an upgraded quality of air, and reduced dependence on fossil fuels.

5.2. Policy level

Policymakers can utilise the knowledge of the psychological mechanisms that drive middle-aged individuals to use ecological automobiles to frame policies, including subsidies for electric automobiles, designing infrastructure that supports alternative transportation options, and instrumenting educational campaigns to promote environmental sustainability. Such policies can help middle-aged individuals create an environment that is conducive to future generations, promote the use of sustainable transportation alternatives among youth, and mitigate issues related to climate change.

6. Discussion

The paper aimed to examine the relationship between GIM and EAU among middle-aged individuals, and GSE as a mediating variable. The results of the study portray a significant positive relationship between GIM and EAU. Findings also show that GIM contributes to about 85.9% of the variance in EAU. Moreover, GSE significantly mediated the relationship between GIM and EAU.

H1, which states that GIM will have a positive relationship with EAU among middle-aged individuals, was accepted ($r=0.598$, $p<0.001$). The findings closely resonate with the study of De Groot and Steg (2010) (23). The association between GIM and EAU is multifaceted and dynamic. GIM is rooted in an individual's intrinsic drive to adhere to environmental norms and adopt eco-friendly actions, such as using electric vehicles. H1.1, which states that GIM will predict EAU, was accepted. The middle-aged individuals are conscious of their higher carbon footprint, as compared to those belonging to the present generation (24). Hence, middle-aged individuals are prone to engaging in eco-friendly actions, as they are highly motivated to create positive change in their environment. Middle-aged individuals may channel their GIM in many ways, such as using electric vehicles, carpooling, or using public transport. These individuals may possess a higher purchasing power due to their greater financial status, which may be used to reinforce their GIM to utilise ecological automobile alternatives. Support from the community in the form of awareness of climate change and incentives for pursuing eco-friendly activities can improve the incidence of ecological behaviour among middle-aged individuals (25).

H2, which states that GSE will mediate the relationship between GIM and EAU among middle-aged individuals, was accepted. The findings are similar to those of the study conducted by Ng et al., (2018) (20). GSE acts as a personal power an individual possesses to direct intrinsic motivation towards environmental stewardship, such as purchasing eco-friendly vehicles. This mediating role played by GSE is characterised by factors such as awareness of transport alternatives and participation in activities that promote pro-environmental behaviour. Middle-aged individuals who are shaped by their past experiences and feelings of competence and self-assurance can influence their choice to use ecological automobiles (26). With appropriate awareness of green self-efficacy, suitable interventions may be designed to promote the use of eco-friendly vehicles among middle-aged individuals and enhance the scope for environmental sustainability.

Both GIM and GSE play a significant role in encouraging middle-aged individuals to use environmentally friendly vehicles in their daily lives. Hence, suitable strategies must be adopted at individual and community levels to promote eco-friendly behaviours and actions.

7. Conclusion

The paper aimed to study the association between GIM and EAU and the mediating role of GSE. The findings reflect that GIM has a positive relationship with EAU and contributes to 85.9% of the variance in EAU among middle-aged individuals. Moreover, GSE mediates the relationship significantly, thereby promoting the use of eco-friendly vehicles among middle-aged individuals.

Through the findings of the study, insights into the psychological mechanisms promoting the use of ecological automobiles may be uncovered. Examining the pivotal role of GIM in the light of environmental sustainability and the desire to imbibe ecological values in individuals can encourage researchers to delve further into the area. Leveraging the findings of the study, middle-aged individuals and policymakers can work together to create an environmentally sustainable future.

Abbreviations:

GIM: Green Intrinsic Motivation
GSE: Green Self-Efficacy
EAU: Ecological Automobile Use
TPB: Theory of Planned Behaviour

References

[1] Wang X and Xu, X 2024 Sustainable resource management and green economic growth: A global prospective *Resources Policy* 89 104634.
[2] Rashid, A, Baloch, N, Rasheed, R and Ngah, A H 2024 Big data analytics-artificial intelligence and sustainable performance through green supply chain practices in manufacturing firms of a developing country *Journal of Science and Technology Policy Management* ahead of print.
[3] Satrovic, E, Cetindas, A, Akben, I, and Damrah, S 2024 Do natural resource dependence, economic growth and transport energy consumption accelerate ecological footprint in the most innovative countries? The moderating role of technological innovation *Gondwana Research* 127 116-130.
[4] Li, W, Bhutto, T A, Xuhui, W, Maitlo, Q, Zafar, A U and Bhutto, N A 2020 Unlocking employees' green creativity: The effects of green transformational leadership, green intrinsic, and extrinsic motivation *Journal of cleaner production* 255 120229.
[5] Chen, Y S, Chang, C H, Yeh, S L and Cheng, H I 2015 Green shared vision and green creativity: The mediation roles of green mindfulness and green self-efficacy *Quality & Quantity* 49 1169-1184.
[6] Ryan, R M and Deci, E L 2020 Intrinsic and extrinsic motivation from a self-determination theory perspective: Definitions, theory, practices, and future directions *Contemporary educational psychology* 61 101860.
[7] Bandura, A 2001 Social cognitive theory: An agentic perspective *Annual review of psychology* 52(1) 1-26.
[8] Ajzen, I 1991 The theory of planned Behaviour. *Organizational Behaviour and human decision processes* 50(2), 179-211.
[9] Paul, J, Modi, A and Patel, J 2016 Predicting green product consumption using theory of planned Behaviour and reasoned action *Journal of retailing and consumer services* 29 123-134.
[10] Yadav, R and Pathak, G S 2017 Determinants of consumers' green purchase Behaviour in a developing nation: Applying and extending the theory of planned Behaviour *Ecological economics* 134 114-122.
[11] Yarimoglu, E and Gunay, T 2020 The extended theory of planned Behaviour in Turkish customers' intentions to visit green hotels *Business Strategy and the Environment* 29(3) 1097-1108.
[12] Ajzen, I and Madden, T J 1986 Prediction of goal-directed Behaviour: Attitudes, intentions, and perceived Behavioural control *Journal of experimental social psychology* 22(5) 453-474.
[13] Bagga, T, Ansari, A H, Shahid Akhter, D A M and Mittal, A 2024 Environmentally Sustainable Transportation *International Journal of Environmental Sciences* 10(1).
[14] Kautish, P, Lavuri, R, Roubaud, D and Grebinevych, O 2024 Electric vehicles' choice behaviour: An emerging market scenario *Journal of Environmental Management* 354 120250.
[15] He, Z, Zhou, Y, Wang, J, Li, C, Wang, M and Li, W 2021 The impact of motivation, intention, and contextual factors on green purchasing Behaviour: New energy vehicles as an example *Business Strategy and the Environment* 30(2) 1249-1269.

[16] Abbasi, H A, Johl, S K, Shaari, Z B H, Moughal, W, Mazhar, M, Musarat, M and Borovkov, A 2021 Consumer motivation by using unified theory of acceptance and use of technology towards electric vehicles *Sustainability* 13(21) 12177.
[17] Chou, C C, Iamtrakul, P, Yoh, K, Miyata, M and Doi, K 2024 Determining the role of self-efficacy in sustained Behaviour change: An empirical study on intention to use community-based electric ride-sharing *Transportation Research Part A: Policy and Practice* 179, 103921.
[18] Anwar, S, Hussain, B, Usman, M, Naqvi, S A A and Shah, A A 2022 Consumers' switching intentions from conventional to green vehicles in the context of smog risk in Pakistan *Case Studies on Transport Policy* 10(3) 1695-1705.
[19] Al Mamun, A, Masud, M M, Fazal, S A and Muniady R 2019 Green vehicle adoption Behaviour among low-income households: Evidence from coastal Malaysia *Environmental Science and Pollution Research* 26 27305-27318.
[20] Ng, M, Law, M and Zhang, S 2018 Predicting purchase intention of electric vehicles in Hong Kong. *Australasian Marketing Journal* 26(3) 272-280.
[21] Chen, Y S, Chang, C H and Lin, Y H 2014 Green transformational leadership and green performance: The mediation effects of green mindfulness and green self-efficacy *Sustainability 6*(10) 6604-6621.
[22] Kaiser, F 1998 A General Measure of Ecological Behaviour *Journal of Applied Social Psychology* 28 395 -422
[23] De Groot, J I and Steg, L 2010 Relationships between value orientations, self-determined motivational types and pro-environmental behavioural intentions *Journal of Environmental Psychology* 30(4) 368-378.
[24] Skeirytė A, Krikštolaitis, R and Liobikienė, G 2022 The differences of climate change perception, responsibility and climate-friendly Behaviour among generations and the main determinants of youth's climate-friendly actions in the EU *Journal of environmental management* 323 116277.
[25] Davidescu, A A, Apostu, S A and Paul, A 2020 Exploring citizens' actions in mitigating climate change and moving toward urban circular economy. a multilevel approach *Energies* 13(18) 4752.
[26] Wang, S, Zhang, R, Guo, X, Ma, H, Wu, J, Wang, Y and Fan, S 2023 Does the Pro-Environmental Behaviour of Household PV Installation Contribute to the Shaping of Users' Green Purchasing Behaviour? Evidence from China *Behavioural Sciences* 13(7) 612.

IOP Conference Series: Earth and Environmental Science

PURPOSE-LED PUBLISHING™

PAPER • **OPEN ACCESS**

Emission of carbon footprint from building construction materials: A review

To cite this article: Rajendra Dighade *et al* 2024 *IOP Conf. Ser.: Earth Environ. Sci.* **1409** 012010

View the article online for updates and enhancements.

You may also like

- Analysis on the Quality Problems and Preventive Measures of Prefabricated Building Construction
Yadi Duan and Guanlei Li
- The carbon footprint of future engineered wood construction in Montreal
Felicity Meyer, Thomas Elliot, Salmaan Craig et al.
- Application of the theory of planned behaviour to assess the impact of the intention of architects, designers, and engineers regarding the usage of sustainable construction materials (SCM) in India
R Joshi, K Vashishtha, S Tripathi et al.



This content was downloaded from IP address 47.247.77.11 on 27/11/2024 at 05:34

Emission of carbon footprint from building construction materials: A review

Rajendra Dighade[1], Virendra Gomase[1]*, Radha Peshattiwar[1], Anchal Selokar[1], Nilay Sangidwar[1], Savi Peshattiwar[1] and Sameer Malve[1]

[1]Department of Civil Engineering, Yeshwantrao Chavan College of Engineering, Nagpur-441110, Maharashtra, India

*E-mail: virendragomase143@gmail.com

Abstract. The construction industry, a cornerstone of global development, is also a notable contributor to environmental degradation. A staggering 39% of the total carbon footprint stems from the production and construction processes, emphasizing the urgency to address this issue. This review narrows its focus on residential building construction, a critical segment of the construction sector. Examining the carbon emissions within residential construction unveils the pivotal role played by various construction materials. Concrete, steel, and traditional bricks, while indispensable, contribute significantly to the sector's carbon footprint. This necessitates a thorough investigation into alternative materials that can mitigate this impact. In this context, the study delves into innovative solutions and alternative materials that hold the potential to substantially reduce carbon emissions. This review emphasizes the importance of recognizing the carbon emissions stemming from construction materials used in residential buildings. It underscores the pressing need to shift towards more sustainable approaches. Identifying and embracing alternative materials is a pivotal measure in addressing the environmental risks linked to building construction. Ultimately, this research adds to the ongoing conversation about sustainable construction methods, to lead the path towards an eco-friendlier and environmentally aware future in residential building construction.

Keywords: carbon emissions, carbon footprint, construction materials, residential buildings, environment.

1. Introduction

An important contributing factor to both global warming as well as climate change is the rise in emissions of carbon [1]. The construction industry is one of the primary producers of greenhouse gases that fuel global warming. The construction sector accounts for 39% of the world's energy usage and 25% of global CO_2 emissions [2]. We are approaching a crucial moment in the global effort to tackle the pressing issue of the climate crisis. Two natural consequences have been an increase in the Earth's temperature and essential energy. Global greenhouse gas emissions are rising along with the number of nations promising to attain net zero emissions (NZE) by the middle of the century or soon after. To limit global warming up to 1.5 °C, carbon dioxide (CO_2) emission must be reduced to net zero by 2050. The countries that have committed to achieving

Content from this work may be used under the terms of the Creative Commons Attribution 4.0 licence. Any further distribution of this work must maintain attribution to the author(s) and the title of the work, journal citation and DOI.
Published under licence by IOP Publishing Ltd

net-zero emissions have grown significantly over the past year, and they currently produce about 70% of the world's CO2 emissions [39]. However, even if these targets are successfully met, there will still be approximately 22 billion tons of CO_2 emissions globally in 2050 [3].

Analyzing the life cycle of products, carbon emissions from connected activities, and the building's maintenance and demolition phases are all necessary for calculating the CFP. Assessing a construction's lifetime ecological impact requires evaluating all of its components and life cycle stages, which makes it a challenging process to accomplish (Yalcintas, 2005) [4]. Present studies focus on carbon emissions of manufacturing of materials and energy utilization of buildings. Globally, each person's carbon footprint amounts to around 4.7 tons of CO_2. India's carbon emissions grew in the last few decades, rising from 0.39 metric tons to 1.91 metric tons between 1970 and 2022. India has a 5.5 percent increase in carbon emissions compared to 2021. It is a truth that global warming originates from a single scientific issue and spreads to encompass a wide variety of global concerns pertaining to politics, business, society, technology, environment, and ecology [5].

2. Literature Review

Concept of carbon footprint: The "ecological footprint" idea was originally referred to as "carbon footprint" in 1996. The total number of hectares of water and biologically productive land required to maintain a specific human population is referred to as the "ecological footprint". According to this theory, a person's "carbon footprint" is the amount of land needed to absorb all of the CO2 that people have produced throughout their lives. Eventually, the phrase "carbon footprint" became commonly used on its own, albeit in a modified form, as global warming acquired prominence on the global environmental agenda (East 2008) [9].

Materials Life Cycle Assessment: The best method for determining the environmental impact of building materials is life cycle assessment or L.C.A. Numerous software tools are available to calculate CO2 emissions [10]. Researchers computed embodied materials' carbon emissions. in India to be 748.759 kg of CO2 equivalent [11] and the carbon emission of electricity to be 4266.150 kg of CO2 equivalent [12]. So, let's say someone wants to lower carbon emissions on a global scale. In that circumstance, it is vital to use embodied materials that are less carbon-emitting or sustainable [13]. By producing less carbon footprint throughout the building life, the electricity demand for operating operations will be decreased [14].

Carbon emissions are calculated to perform life cycle assessment using a mix of manual life cycle assessment theory and BIM-LCA technology. The ICE, GaBi, and ecoinvent databases are used in conjunction with BIM technologies to generate 3D models, which in turn are used to calculate the building's carbon emissions [15,34]. Emphasized that determining the carbon footprint is possible by measuring the CO2 equivalent emissions generated by the environment, waste generation and disposal, building sites, and several other sources [16]. carbon footprint as a technique used to estimate the entirety or full amount of the emission of GHG from a specific product running through the aforesaid life-cycle, starting from the initial stage of using unprocessed raw materials in the production process to the actual production of the finished good. Further argued that it is a technique used to recognize and quantify each GHG emissions activity discovered in a chain process [17,38].

Throughout the lifespan of a product or activity, the term "carbon footprint" has become synonymous with a comprehensive analysis of greenhouse gas emissions. The cornerstone of low-carbon research lies in conducting carbon footprint assessments [40]. Nowadays, businesses are employing carbon footprint assessments to gauge both their own emissions and those associated

with their products. This enables them to respond to the growing consumer demand for eco-friendly products. [25,26] Consequently, there is a significant potential for businesses to enhance their production efficiency, reduce resource usage and waste, stimulate innovation and technological progress, and explore new avenues for business growth. [18,24]. The study analyzed the entire construction process of Building B1, starting from its inception to its completion, to compare the carbon emissions associated with two different construction approaches. The findings indicated that employing prefabrication, which involves a high degree of assembly, substantially lowered carbon emissions.[28,29] The decreases in carbon emissions are mostly attributable to the benefits of steel, proficiently utilizing BIM design technology can lead to a notable decrease in material wastage, along with the efficiency of the prefabrication system.[35,36] Furthermore, the decrease in carbon emissions will be ascribed to the streamlined on-site assembly process, as preconstructed assemblies have the potential to expedite construction schedules while enhancing overall construction quality and productivity. This, in turn, results in a substantial reduction in the overall consumption of resources such as water, electricity, fuel, and labor [19][27].

Most scholars argue that the focus of research on carbon emissions from buildings should shift toward the phases of regular usage and material selection. The emissions generated during the construction process, on the other hand, are considered minimal and often overlooked, if not entirely disregarded. [20]. Construction industry studies have concentrated on building construction and industrial relevance [21, 22]. There has been a limited number of articles addressing the overall factors influencing carbon emissions and making predictions for the construction industry at a large scale. This is a critical aspect in ascertaining the direct carbon footprint of the sector and in forecasting when the region will reach its peak carbon emissions. This involves integrating metrics such as economic output and population size, which serve as indicators of the sector's broader energy usage and composition. [30,31].

Table 1. Carbon Emission with respect to different Sources

S. No.	Materials	Sources			Alternate material to reduce CO emission
		ICE	GaBi	Eco-invent	
1.	Cement	66.6%	69.3%	52.5%	Brick dust and Marble dust
2.	Masonry block	9.4%	8.4%	4.3%	Fiberglass-Reinforced Plastic
3.	Ceramic tiles	8.1%	6.4%	3.8%	Terracotta Tiles
4.	Bricks	15.7%	15.9%	39.45%	Lime, Geopolymer-Bricks

In the ICE database, it is recorded that during the construction phase of a reinforced concrete (RCC) structure, the total carbon emissions amount to about 98.65 metric tons of CO2 equivalent. Among these emissions, cement production is responsible for roughly 66.6%, concrete masonry blocks contribute around 9.4%, and ceramic tiles & bricks make up about 8.1%. Together, these components account for 15.7% of the overall emissions. From cradle to gate impacts, cement accounts for about 89 tCO2e, or 52.5%, followed by concrete blocks at 4.3%, bricks at 39.4%, and ceramic tiles at 3.8% in the eco-invent database [37]. Comparably, the GaBi database shows that 6.4% of the emissions are from ceramic tiles, 15.9% are from bricks, 64 tCO_2e from cement, and 8.4% are from concrete blocks. Furthermore, Figure 7 makes it clear that out of all the datasets, cement contributes the most to carbon emissions [15,33].

Fly ash, or waste from the burned coal industry, is added to the cement mix to create fly ash cement bricks. Fly ash is crucial for lowering carbon emissions in addition to aiding with trash

management. After cement and lime, geopolymer is a third-generation binder that has several advantages for sustainable development. Using industrial byproducts like fly ash, slag, and other building waste items, geopolymer bricks provide an alternative.

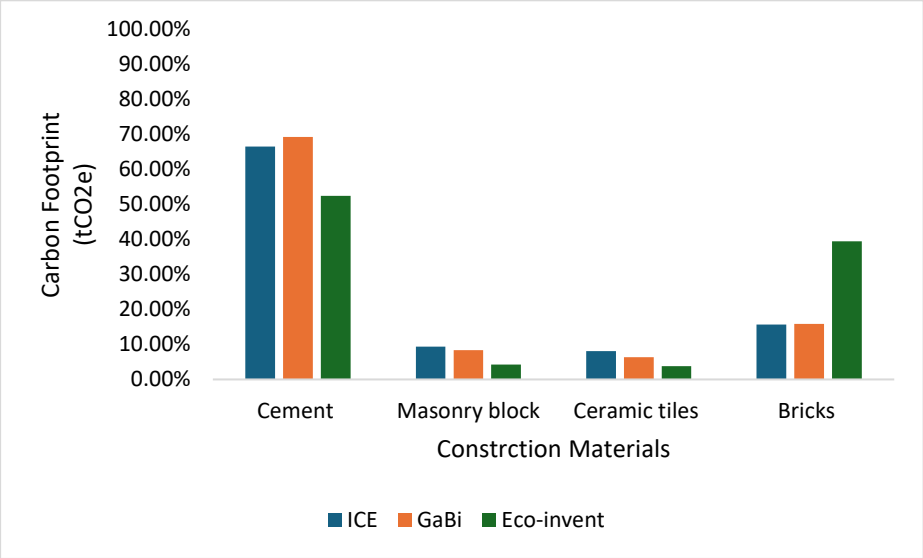


Figure 1. Carbon footprints of building materials for different databases.

It also provides an overview of the latest research on methods for reducing carbon footprints at every stage of construction, such as the use of substitute additives in building materials, better design, recycling waste during construction, encouraging the use of alternative water resources, and boosting the effectiveness of water technologies and other building systems. Reports state that at different stages of building construction and operation, the use of alternative systems, materials, methods, and additions can reduce CO2 emissions by up to 90% [23,32].

3. Carbon footprint and alternative materials

Comparing the entire quantity of greenhouse gases released by a product, company, activity, or nation is made feasible via the carbon footprint. The standard way to report carbon footprint is in tons of emissions per unit of comparison. These units include kilometers travelled, years, people, and kilograms of protein.

According to some assessments, the carbon footprint of six structures accounted for 1800 kg of CO2 emissions per square meter, with just six materials accounting for 70% of the emissions that were embodied. Unexpectedly, concrete made up the largest percentage of all materials roughly 80%. And mortar ranks second highest.

Table 2. Alternate material to reduce Carbon Emission

S. No.	Name of the material	Percentage of Carbon Emission	Partial replacement of materials/ alternative material	Reduction of CO2e
1.	Cement	4-8%	Fly Ash	30-40% reduction by addition of fly ash
2.	Sand	0.76%	Washed copper slag	0.5-0.6% reduction in carbon footprint

3.	Aggregate	0.81%	Algae grown alternative material	Less than 0.762%, absorb 50% of CO2 from atmosphere
4.	Concrete	82%	Adding fly ash Porous asphalt	40% of fly ash reduces CO2 emission Produces 75% of less CO2 emission
5.	Reinforcement	8%	No Alternative for steel	--
6.	Mortar	65%	Biomass fly ash	By adding this 40% of carbon footprint can be reduced.
7.	Bricks	9%	Fly ash bricks	It can reduce up to 85% of carbon emission
8.	Tiles	10%	Terra cotta Tiles	negligible/ no CO2 emission

Table 2 shows the various major construction materials which have the biggest impact on carbon footprint and their alternative construction to reduce the carbon emission produced.

4. Result

By using alternative materials and construction techniques, the carbon emissions linked to different building materials may be greatly decreased. By substituting fly ash for some of the cement, which is a significant source of carbon emissions, the carbon footprint of cement may be reduced by 4-8% and by 30–40%. Similarly, using washed copper slag can help reduce the carbon footprint of sand (which emits 0.76% less carbon dioxide) by 0.5–0.6%. Algae-grown substitutes can partially replace aggregate, which contributes 0.81% of carbon emissions. These substitutes absorb 50% of CO2 from the atmosphere and produce less than 0.762% carbon.

With a high 82% carbon footprint, concrete may be significantly reduced by using fly ash and porous asphalt, which can reduce CO2 emissions by 40% when 40% of the asphalt is made of fly ash. In addition, it emits 75% less CO2 than conventional concrete. There are presently no practical substitutes for reinforcement materials, which are mostly steel with an 8% carbon emission. Adding fly ash from biomass can reduce carbon emissions from mortar, which accounts for 65% of emissions, by 40%. Fly ash bricks may substitute bricks, which contribute 9% of carbon emissions, and achieve an amazing 85% decrease in carbon emissions.

Terra cotta tiles can be used in place of tiles, which account for 10% of carbon emissions and produce little to no emissions of CO2. These results demonstrate how careful material selection and creative substitutes may significantly reduce carbon footprints throughout the building sector. When utilized in partly of the primary building materials, fly ash is a significant factor in reducing carbon footprints.

5. Conclusion

The important aspect of energy consumption is to reduce the operation of energy and to decrease the requirement. Carbon footprint has been increasing rapidly over the years and 40% of global energy consumption is by the manufacturing of materials, transportation, and equipment usage. Also, 70% of carbon emissions have been generated by construction materials itself. Alternatives were found to lower emissions during the building and construction activities once the entire quantity of emissions was calculated. This paper has shown the various construction materials used in building construction with their carbon emission and also has suggested alternative materials to reduce the carbon emission. Usage of alternative materials may be the next step toward the reduction of carbon footprint in the construction sector. Using alternative materials

minimizes waste, cuts down on energy and time spent moving resources, decreases building costs, and lessens carbon impact. These resources may be used to build structures that are resilient to the climate in the area. India needs sustainable long-term solutions, not just short-term fixes. At different phases of the construction industry, energy consumption and greenhouse gas emissions may be reduced by up to 90% by switching to efficient HVAC systems and utilizing various building operations/systems.

References

[1] Wu, H.J., Yuan, Z.W., Bi. J. and Zhang, L., 2012. Life cycle energy consumption and CO 2 emission of an office building in China. The international journal of life cycle assessment, 17, pp.105-118.
[2] Tan, X. and Wang, C.C., 2012, October. Estimating Carbon Footprint in the Construction Process of a Green Educational Building. In Proceedings of the 2012 International Conference on Construction and Real Estate Management, Kansas City, MO, USA (pp. 1-2).
[3] IEA., P., 2021. Net zero by 2050-a roadmap for the global energy sector. Int. Energ. Agency, 224.
[4] Adalberth, Karin, Anders Almgren, and Ebbe Holleris Petersen. "Life cycle assessment of four multi-family buildings." International Journal of Low Energy and Sustainable Buildings 2 (2001)..
[5] Knappenberger, & Michaels, P. J., P. C. (1996). The United Nations intergovernmental panel on climate change and the scientific “consensus” on global warming. Energy & Environment, 7(4), 333-348.
[6] Lenzen, M., Wiedmann, T., & Wood, R. (2010). Uncertainty analysis for multi-region input–output models–a case study of the UK's carbon footprint. Economic Systems Research, 22(1), 43-63.
[7] Larsen, H. N., & Hertwich, E. G. (2009). The case for consumption-based accounting of greenhouse gas emissions to promote local climate action. Environmental Science & Policy, 12(7), 791-798.
[8] Hertwich, Edgar G., and Glen P. Peters. "Carbon footprint of nations: a global, trade-linked analysis." Environmental science & technology 43, no. 16 (2009): 6414-6420.
[9] Pandey, Divya, Madhoolika Agrawal, and Jai Shanker Pandey. "Carbon footprint: current methods of estimation." Environmental monitoring and assessment 178 (2011): 135-160.
[10] Chukka, Naga Dheeraj Kumar Reddy, and Muthumani Krishnamurthy. "Seismic performance assessment of structure with hybrid passive energy dissipation device." In Structures, vol. 27, pp. 1246-1259. Elsevier, 2020.
[11] Ahmed, Noha, Mahmoud M. Abd El-Razik, Mohamed Abdel-Hamid, and Karim M. El-Dash. Impact of sustainable design in the construction sector on climate change. Ain Shams Engineering Journal 12, no. 2 (2021): 1375-1383.
[12] Tirth, Vineet, S. Algarni, N. Agarwal, and A. Saxena. "Greenhouse gas emissions due to the construction of residential buildings in Moradabad, India." Applied Ecology & Environmental Research 17, no. 5 (2019).
[13] Suzuki, Michiya, Tatsuo Oka, and Kiyoshi Okada. The estimation of energy consumption and CO2 emission due to housing construction in Japan. Energy and buildings 22, no. 2 (1995): 165-169.
[14] Wong, Peter SP, Sarah Holdsworth, Lachlan Crameri, and Aiden Lindsay. "Does carbon accounting have an impact on decision-making in building design?" International Journal of Construction Management 19, no. 2 (2019): 149-161.
[15] Kishor Sitaram Kulkarni, Rosaliya, Kurian, Prasanna Venkatesan Ramani, Raffaello Cozzolino, Ashok Kumar, and Chandan Swaroop Meena. "Estimation of carbon footprint of residential building in warm humid climate of India through BIM." Energies 14, no. 14 (2021): 4237.
[16] Patel, J. "Green sky thinking." Environment Business 122 (2006): 32.
[17] Pandey, Divya, and Madhoolika Agrawal. "Carbon footprint estimation in the agriculture sector." Assessment of Carbon Footprint in Different Industrial Sectors, Volume 1 (2014): 25-47.
[18] Gao, Tao, Qing Liu, and Jianping Wang. "A comparative study of carbon footprint and assessment standards." International Journal of Low-Carbon Technologies 9, no. 3 (2014): 237-243.
[19] Mo, Zhoujin, Tianyu Gao, Wen Jiang, Zhenyu Cao, and Jie Qu, Gangwei Cai. "An Empirical Study of Carbon Emission Calculation in the Production and Construction Phase of a Prefabricated Office Building from Zhejiang, China." Buildings 13, no. 1 (2022): 53.
[20] Xikai, Mao, Wang Lixiong, Li Jiwei, Quan Xiaoli, and Wu Tongyao. "Comparison of regression models for estimation of carbon emissions during building's lifecycle using designing factors: a case study of residential buildings in Tianjin, China." Energy and Buildings 204 (2019): 109519.

[21] Yuxin Xia, and Qi, Yuan. "Research on Accounting and Transfer Pathways of Embodied Carbon Emissions from Construction Industry in China." Sustainability 14, no. 22 (2022): 15165.
[22] Luo, Lei, and Yiyu Chen. "Carbon emission energy management analysis of LCA-Based fabricated building construction." Sustainable Computing: Informatics and Systems 27 (2020): 100405.
[23] Sizirici, B., Y. Fseha, C. S. Cho, I. Yildiz, and Y. J. Byon. "A review of carbon footprint reduction in construction industry, from design to operation. Materials 2021, 14, 6094." Sustainable Construction Materials (2021): 125.
[24] Larsen, Hogne N., and Edgar G. Hertwich. "The case for consumption-based accounting of greenhouse gas emissions to promote local climate action." Environmental Science & Policy 12, no. 7 (2009): 791-798.
[25] Hertwich, Edgar G., and Glen P. Peters. "Carbon footprint of nations: a global, trade-linked analysis." Environmental science & technology 43, no. 16 (2009): 6414-6420.
[26] Wiedmann, Thomas, and Jan Minx. "A definition of 'carbon footprint'." Ecological economics research trends 1, no. 2008 (2008): 1-11.
[27] Change, IPCC Climate. "The physical science basis." (No Title) (2013).
[28] Hu, Shan, Yi Jiang, and Da Yan. "China Building Energy Use and Carbon Emission Yearbook 2021." China Architecture & Building Press: Beijing, China (2021).
[29] Mao, Chao, Qiping Shen, Liyin Shen, and Liyaning Tang. "Comparative study of greenhouse gas emissions between off-site prefabrication and conventional construction methods: Two case studies of residential projects." Energy and Buildings 66 (2013): 165-176.
[30] Dara, Caroline Hachem-Vermette and Chinyere. "Evaluation of low-impact modular housing using energy optimization and life cycle analysis." Energy, Ecology and Environment 4 (2019): 286-299.
[31] J. J. McArthur, and Gelowitz, M. D. C. "Comparison of type III environmental product declarations for construction products: Material sourcing and harmonization evaluation." Journal of Cleaner Production 157 (2017): 125-133.
[32] Databases. Available online: https://gabi.sphera.com/databases (accessed on 4 July 2021).
[33] Asif, Mohammad, T. Muneer, and R. Kelley. "Life cycle assessment: A case study of a dwelling home in Scotland." Building and environment 42, no. 3 (2007): 1391-1394.
[34] Kania, Gabriela, Klaudia Kwiecień, Mateusz Malinowski, and Maciej Gliniak. "Analyses of the Life Cycles and Social Costs of CO2 Emissions of Single-Family Residential Buildings: A Case Study in Poland." Sustainability 13, no. 11 (2021): 6164.
[35] Kania, Gabriela, Klaudia Kwiecień, Mateusz Malinowski, and Maciej Gliniak. "Analyses of the Life Cycles and Social Costs of CO2 Emissions of Single-Family Residential Buildings: A Case Study in Poland." Sustainability 13, no. 11 (2021): 6164.
[36] Xu, X.; Mumford, T.; Zou, P.X.W. Life-cycle building information modelling (BIM) engaged framework for improving building energy performance. Energy Build. 2021, 231, 110496.
[37] Bernhard Wohner, Erik, Pauer, and Manfred Tacker. "The influence of database selection on environmental impact results. Life cycle assessment of packaging using gabi, ecoinvent 3.6, and the environmental footprint database." Sustainability 12, no. 23 (2020): 9948.
[38] Pathak, H., N. Jain, A. Bhatia, S. Mohanty, and Navindu Gupta. "Global warming mitigation potential of biogas plants in India." Environmental monitoring and assessment 157 (2009): 407-418.
[39] Peters, Glen P. "Carbon footprints and embodied carbon at multiple scales." Current Opinion in Environmental Sustainability 2, no. 4 (2010): 245-250.
[40] Wbcsd, W. R. I. "The greenhouse gas protocol." A corporate accounting and reporting standard, Rev. ed. Washington, DC, Conches-Geneva (2004).

Acknowledgments

The authors thank our beloved Principal, Dr. U. P. Waghe, for providing this wonderful opportunity to work on a project with the topic Emission of carbon footprint from building construction materials.

IOP Conference Series: Earth and Environmental Science

PURPOSE-LED PUBLISHING™

PAPER • **OPEN ACCESS**

Application of the theory of planned behaviour to assess the impact of the intention of architects, designers, and engineers regarding the usage of sustainable construction materials (SCM) in India

To cite this article: R Joshi *et al* 2024 *IOP Conf. Ser.: Earth Environ. Sci.* **1409** 012011

View the article online for updates and enhancements.

You may also like

- A review on wastes as sustainable construction materials
M. Besma Fahad, A. Mais Abdulkarem and T. Huda Hamed
- Exploring bundle bamboo split technique in bending *dendrocalamus asper* for landscape structure
Meor Abdullah Zaidi Meor Razali, Sapura Mohamad, L. Y. Lee et al.
- The sustainable materials roadmap
Magda Titirici, Sterling G Baird, Taylor D Sparks et al.



This content was downloaded from IP address 47.247.77.11 on 27/11/2024 at 05:34

Application of the theory of planned behaviour to assess the impact of the intention of architects, designers, and engineers regarding the usage of sustainable construction materials (SCM) in India

R Joshi[1], K Vashishtha[1*], S Tripathi[1], S Roy[2], and C Dhankar[1]

[1]Department of Psychology, Manipal University Jaipur, Jaipur, India
[2] Department of Architecture, National Institute of Technology, Hamirpur, India

[*]E-mail: kriti.vashishtha@jaipur.manipal.edu

Abstract. The present interdisciplinary (psychology and architecture) study was conducted to assess the impact of intention on the behaviour of architects, designers, and engineers related to the recommendation and usage of sustainable construction materials (SCM). The authors employed the theoretical framework of planned behaviour (TPB) on sustainable construction materials usage by different stakeholders and developed a questionnaire based on the same. Fifty-nine architects/designers and engineers filled out the developed questionnaire after giving their written informed consent. The survey was followed by semi semi-structured interview schedule, developed by the researchers. The results demonstrated that the intention to use SCM was present, but it was not reflected much in the actual behaviour. The semi-structured interview schedules findings like attitude, social norms, perceived effectiveness, and value proved to have influenced intention, which in turn influenced actual behaviour. The results of the study were substantiated by themes generated by semi-structured interviews that were conducted with architects, interior designers, and civil engineers which were lack of adequate research on the development of sustainable construction materials, economic constraints, and lack of skilled labourers for construction with vernacular or traditional construction materials. The findings of the study can be used for comprehension and implications for sustainable construction materials usage. In the present scenario, the findings of the study are important as sustainable construction materials are the need of the hour owing to severe climate damage and for resolving unmet challenges of urbanization.

Keywords. Theory of planned behaviour, Interdisciplinary study, Architecture, Psychology, Sustainable construction materials.

1. Introduction

Climate change, deforestation, effects of unplanned urbanization are some of the prime challenges of the present era. All the stakeholders of society have an important role to play in the preservation of the environment, reducing the impact of air, water, and noise pollution, trying for the attainment of

Content from this work may be used under the terms of the Creative Commons Attribution 4.0 licence. Any further distribution of this work must maintain attribution to the author(s) and the title of the work, journal citation and DOI.
Published under licence by IOP Publishing Ltd

sustainable development goals, etc. Built spaces, their architecture, their designs, and construction materials play a significant role in resident and environmental well-being. Buildings built with sustainable construction materials and pro-environmental practices are an emerging trend of present times.

In recent times the environmental concerns related to the construction industry have been glaring at both developers and consumers. The construction industry accounts for a high rate of greenhouse gas emissions and carbon footprints apart from high energy and resource consumption. Complicating the problem further, there is a constant pressure of housing the rising population across the world. Not only is the population rising at a rapid speed, but it is also moving towards rapid urbanization (Ritchie, et al., 2024)

In a scenario like this the producers, engineers, architects, and designers are confronted with dual problems of not just building and designing comfortable and aesthetic living spaces for residents but also simultaneously addressing environmental concerns.

On the same line of thought, the present study intends to identify the factors that are responsible for architects, designers, and engineers' intentions; that eventually lead to actual behaviour in recommending and using sustainable construction materials. Some of the sustainable construction materials include bamboo, hempcrete, recycled steel and glass, reclaimed wood earth blocks, etc.

There are several studies and research that have been conducted across the globe that stress on importance of sustainable construction materials. In a review study conducted by Maraveas (Chrysanthos, 2020) on the use of agricultural waste ranging from rice husk ash (RHA), and sugarcane bagasse ash (SCBA) were found to have adhered to qualities of durable modern building materials and possess the ability to replace the current materials in use but with more economic and environmental efficiency. In one of the research projects on a case study of the foundation reuse of Mahatma Gandhi Setu highlighted the importance of sustainable (Basarkar, et al., 2024) construction. Nilima (2023) reviewed and emphasized the use of green concrete and supplementary cementitious materials (SCM) to encourage sustainability in the construction (Nlimaa, 2023).

That sustainable construction materials are beneficial for the environment is an undisputed face however, the possibility of their usage is dependent on a variety of factors, in most important criterion is the intention of architects, designers, and engineers. It is therefore important to know what the barriers between intentions and actual execution are. To provide a viable explanation for this gap a theoretical framework is being used in the present study by the authors.

The succeeding section of the research highlights the theoretical background of the study, the third section describes the methodology, the fourth section illustrates results and discussion, and fifth section focuses conclusion, and the sixth is limitations and future directions.

Theoretical underpinnings

Numerous theories explain intentions and behaviours related to different aspects like fitness, healthy lifestyles, food choices sustainability, etc. The authors seek to apply the theory of planned behaviour (Lau & Hashim, 2020) to the current problem. The TPB model can provide explanations and predictions for myriad behaviours. The theory is deeply embedded in social cognitive psychology and is based on assumptions that an individual's actual behaviour can be predicted if their intentions

can be known. Intentions are nothing but motivations of an individual to engage in a particular behaviour. Personal attitudes, social norms, and perceived behaviour control play a significant role in establishing and identifying intention which in turn leads to actual behaviour. As mentioned above, among the various theories that predict intentions and the actual behaviour of different aspects, the authors decided to apply TPB to predict the intentions and practicing behaviour of architects, designers, and engineers for using SCM. Lau and Hashim (2020) (Lau & Hashim, 2020) conducted a study to assess the developer's intention to adopt green concept in housing projects in Malaysia. The results demonstrated that PBT was a significant mediator between environmental concerns and intention and actual behaviour. Similarly. Many studies established that attitudes, subjective norms, and perceived behaviour control have a significant role in the green development behaviour of construction enterprises. (Jack, 2017) (Vasić, et al., 2023). A thorough review of the literature established that multiple studies have been conducted on TPB and sustainable construction materials. There is however little or no research conducted on the same variables within the Indian Context. The researchers intend to conduct a study on the application of TPB to assess the intentions and actual behaviour of Indian architects, designers, and engineers related to recommendations and usage of SCM.

2. Research Model

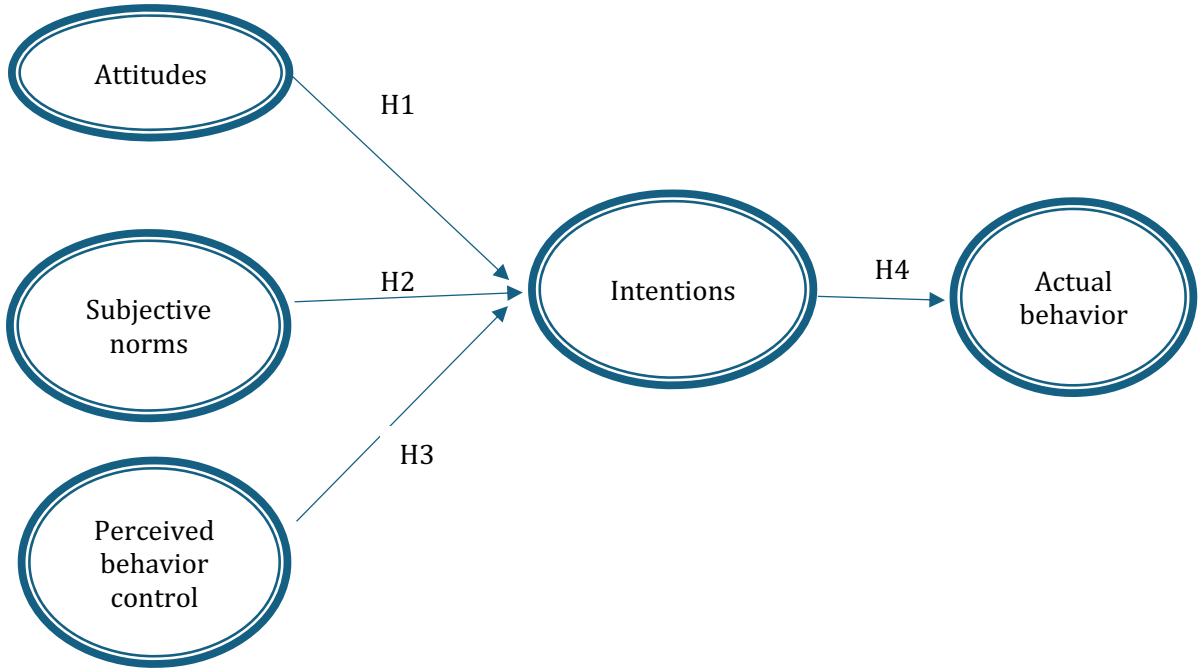


Figure 1. Theory of planned behaviour model by Ajzen (2005)

3. Methodology

The present study is aimed at assessing the impact of intentions, which are affected by attitudes, subjective norms, and perceived behaviour control, on the actual behaviour of architects, interior designers, and civil engineers regarding the usage of SCM. TPB has been known to identify factors affecting a variety of behaviour s as already mentioned above. Based on the review of observations from a review of the literature, the following hypotheses were formulated.

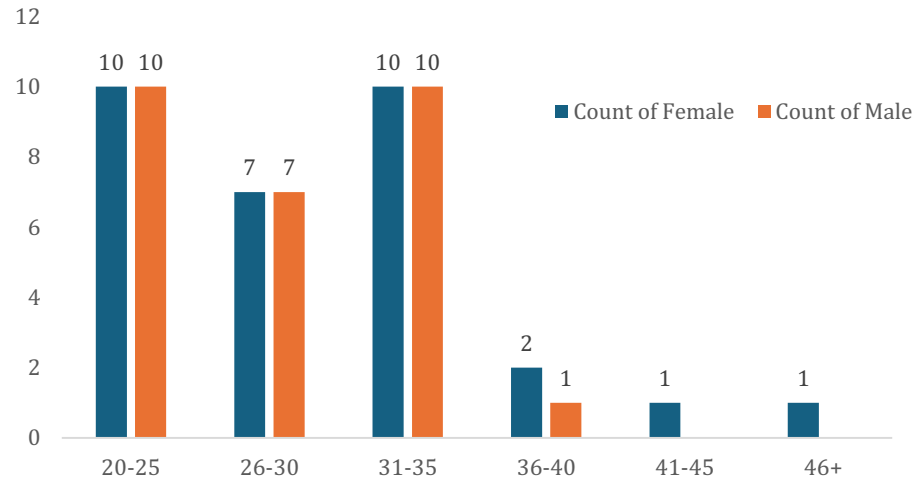
- H1: Attitudes of architects, interior designers, and civil engineers will influence intention regarding usage of SCM.
- H2: Subjective norms of architects, interior designers, and civil engineers will influence the intention regarding usage of SCM.
- H3: Perceived behaviour control (perceived availability, cost, and effectiveness) will influence the intention of architects, interior designers, and civil engineers regarding the usage of SCM.
- H4: The intention will influence the actual behaviour of architects, interior designers, and civil engineers regarding the usage of SCM.

4. Research Design

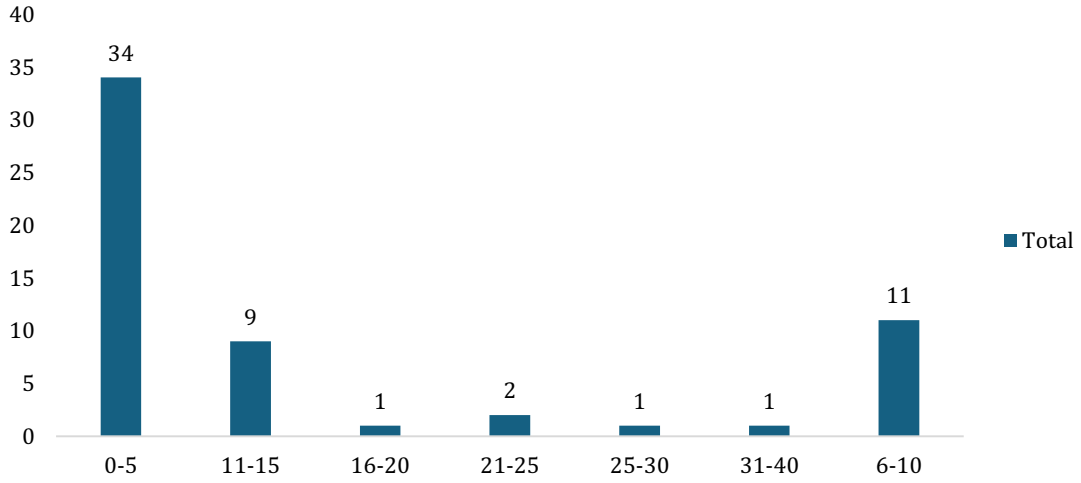
The present study employed a mixed method approach to conduct the study that included both quantitative and qualitative methods to analyze the survey method to collect responses from 50 architects, designers, and engineers after obtaining written informed consent. The questionnaire was developed by researchers on the theoretical framework of TPB and measured the components of attitudes, subjective norms, and perceived behaviour control through 18 items. The component of perceived behaviour control was further divided into sub-components of perceived value, perceived effectiveness, and perceived value and items were generated and calculated accordingly. The survey was conducted in both online and offline mode.

5. Participants and procedure

The sample consisted of 31 females and 28 males between the age range of 22 -61 years old (Mean age=30) recruited with the non-probability method of snowballing technique. The participants participated in the study after providing their written informed consent for the same. The years of experience ranged from 0 months to 41 years.



Graph 1. Graphical representation of the distribution of age of participants



Graph 2. Graphical representation of the distribution of years of experience of participants

6. Instruments

The study was conducted with the help of a questionnaire designed by researchers based on the theoretical framework of the theory of planned behaviour. It consisted of 18 items. Items were divided into seven sections, covering attitude, social norms, perceived behaviour control (including perceived value, effectiveness, and availability), intention, and actual behaviour.

7. Results and Discussions

7.1. Demographic details

Predictor variables: Attitude, social norms, perceived availability, perceived effectiveness, intention, and Dependent variable: Actual behaviour related to the usage of SCM.

SPSS 21 was employed for the analysis of data. Ensuring that outlines and missing data were checked, regression analysis was performed. Actual behaviour regarding usage of SCM was dependent behaviour and attitude, social norms and perceived behaviour control (perceived value, availability, and effectiveness) were independent behaviour. The method used was analyzing stepwise regression. The usage of SCM depended on variables that were regressed onto predictor behaviour. The results of the regression analysis demonstrate that Attitude, social norms, perceived availability, perceived effectiveness accounted for 36.3 % for influencing intention and when intention was added in step two it accounted for almost one and a half increase that resulted in 37.6 %. It indicates the intention of architects, interior designers, and civil engineers is present however, they are unable to realize this intention into actual behaviour, thus proving all the hypotheses.

Table 1. Gender

Gender	Total number	Percentage
Male	28	47%
Female	31	52%

Table 2. Regression analysis

Step	Predictor	R^2	Adjusted R^2	F Change	Step	
					1	2
1	Attitude				0.032	0.045
2	Social norms				0.232	0.214
3	Perceived availability				0.145	0.137
4	Perceived effectiveness	0.418	0.363	7.604	0.187	0.121
5	Perceived value				0.256	0.222
6	Intention				0.032	0.178
7	Actual Behaviour	0.440	0.376	2.092		0.045

The results were further supported by findings from semi-structured interviews conducted with 10 participants. The interviews were limited to 8 participants due to saturation of data in terms of similar responses.

The major themes that came up after the interviews were as follows:

7.1.1. Lack of proper research in the development, storage, and procurement of SCM.

The architects, designers, and engineers shared their views and experiences that largely influenced intentions, social norms, and perceived behavior control. Most of the practitioners in the

field maintained that they were ecologically aware and wanted to use SCM or in the words of one of the architects" created from nature and going back to nature" but were unable to do so. All the participants expressed their concerns related to the lack of proper research on efficient materials. Reinforced cement concrete (RCC), for instance, is preferred by most of builders and clients owing to its durability and easy accessibility. However, the use of RCC certainly damages the environment in many ways, for example, it leaves a land barren once a living space with RCC usage is being demolished. Despite knowing about the ill-effects of using RCC for construction many architects, designers, and engineers still use it due to its durability and cost-effectiveness. In the words of one of the architects from Himachal Pradesh*" Not just urban, but clients from rural background also prefer latest construction materials as traditional construction materials like timber, s late require a lot of maintenance, apart from cost-effectiveness. So many times, reptiles like snakes, rat mongoose, etc. dig holes in houses constructed with conventional materials like mud and slate, etc. something that does not happen very often in spaces created by contemporary materials"*

"RCC building would not require maintenance in terms of whitewash at least for 4 to 5 years, whereas the conventional materials like walls built of mud would require whitewash within one year" quips another architect from Bihar.

There is no research on eco-friendly alternatives of RCC, in the absence of which it is being used continuously despite knowing its damaging effects on nature. So is the case with other construction materials that lack effective research.

The lack of research conducted in the field of effective SCM is one of the major concerns that negatively influence the intention. Owing to the problems mentioned above, most of the practitioners in the field recommend and use contemporary construction materials thereby affecting social norms and availability concerns that impact control over behavior. – All the above-mentioned factors then influence the intention of suing SCM which in turn affects actual behaviour.

7.1.2. Economic Concerns

One of the major concerns related to the usage of SCM is cost-effectiveness. The technologically sustainable materials are very expensive and add on to cost massively.

In the words of another architect from Rajasthan,*" It becomes very difficult for us to convince the clients as to why they must pay double and sometimes triple the amount for something whose cheap and more endurable alternatives are easily available."*

Economic concerns are one of the most significant barriers to the implementation of SCM usage by all stakeholders, developers, and residents (Arya & Chaturvedi, 2022). Cost-effective SCM availability is one of the major factors that influence intention and subsequently actual behavior towards SCM usage.

7.1.3. Lack of availability of skilled labours

There is a severe dearth of availability of skilled labours in the field of traditional construction materials. Even if there is a serious intent to use SCM while building, skilled labours are not available for construction with traditional materials like mud, slate, bamboo, limestone, etc. Most skilled and semi-skilled labours are working with contemporary building materials like RCC and cannot work with traditional materials.

"One of the wealthy retired couples from Rajasthan wanted to build a house with some traditional mud structures. But I could not find one labour who could build that." One of the architects from Rajasthan recalls.

With the advent of contemporary building materials, the ease and convenience of building came along which the traditional materials were unable to provide. Therefore, the majority of the workforce is now inclined towards using the latest materials.

Apart from the above-mentioned themes the architects, designers, and engineers talked about difficulties with clients where they preferred aesthetics over sustainability. One of the architects from Karnataka mentioned that being prone to high rainfall, the houses there need to have slanted roofs, however, that pattern will not support high-rise and multiple-storied buildings. Likewise, the local architecture of Meghalaya (north-east India) mostly employs bamboo which cannot support multi-storied buildings.

The findings highlighted that even though the architects, designers, and engineers had low to moderate intentions to use SCM, however, the factors like availability, research, and availability of SCM were some of the factors that influenced actual behaviour s where they were not able to use SCM even if they wanted to employ pro-environmental materials.

TPB is one of the widely used theories that predict specific behaviour s and causes behind the same. If the causes can be understood and addressed, a particular behaviour can be explained and encouraged. Here we found that proper research into the subject is paradoxically both a promising and lacking area in the field that influences environmentally friendly practices. Some of the architects who were also academicians expressed concerns that the architecture syllabus was very generic throughout the country and the vernacular architecture elements were missing largely.

8. Conclusion & Summary

The present study was interdisciplinary in nature and employed tenants of both psychology and architectural disciplines. The authors intended to assess the role of intention on the actual behaviour of architects, designers, and engineers regarding recommendations and usage of SCM. Through survey and semi-structured interviews of architects, designers, and engineers it was found that the intention to sustainable construction materials was present, however, there were barriers to realizing this intent. The factors like availability of cost-effective SCM easily, thorough and latest research, availability of skilled labour, etc. were a few of the prime factors that prevented actual behaviour for using SCM. Psychology is one of the all-pervasive disciplines. It percolates to every aspect of human life be making choices, arriving at decisions, or reviewing those decisions The TPB framework is often used to assess the intention that influences actual behaviour. There is a significant increase in research related to employing TPB in different walks of life, including climate change, awareness related to environmental issues like eco-anxiety, sustainable transport, etc. (Arya & Chaturvedi, 2022) (Arya & Kumar, 2023)

Climate change, environmental concerns, and rapid urbanization are two daunting challenges of present times that need to be tackled speedily and efficiently. One of the ways to do so is by using SCM. However, the usage of SCM is dependent on many factors, intention, social norms, and behaviour al controls are one of them. These factors in turn affect actual behaviour. It is therefore necessary to address the concerns that are mentioned in the themes generated from semi-structured interviews.

9. Limitations and future directions

The present- study was conducted to assess the impact of impact on recommendations and usage of SCM by architects, designers, and engineers by employing the theoretical framework of TPB. 59 architects, designers and engineers were contacted to participate in a survey based on items framed based on TPB. The survey was followed by semi semi-structured interview schedule with 8 architects, designers, and engineers.

The study gave direction in terms of the importance of proper research for SCM which would make it cost effective and easily accessible. The construction industry seriously needs to take the environmental concerns into account. One of the implications of the study is that as the architects, designers, and engineers increasingly push for SCM, the producers will be forced to think and work in that direction. This will set into action a chain reaction that will only stop at sustainable solutions.

Social norms are another factor that influences intention and actual behaviour. If the majority of architects, designers, and engineers begin to use SCM, it will inspire others to do the same. The seniors are required to set up benchmarks related to sustainability and the concept of group dynamics may inspire all architects, interior designers, and civil engineers to insist on the usage of SCM.

Further, it was revealed that lack of skilled labours for working with traditional and vernacular architecture was also one of the huge challenges. If architects, designers, engineers, builders, researchers, and developers join hands to use SCM, not only will it generate employment for traditional skills person but also preserve and promote local and vernacular traditions of culture and architecture. This will balance the ecological and environmental concerns that are usually at loggerheads.

The study however was conducted on a small sample of 59 participants from India. In the future, the number of participants can be increased and working professionals from wider geographical locations can be recruited.

10. References

[1] Arya, B. & Chaturvedi, S., 2022. Psychological Predictors of Sustainable Transportation Behaviour: Implications for Low Carbon Economy and Society. I. s.l., IOP Publishing., p. 012045.
[2] Arya, B. & Kumar, H., 2023. An Investigation of Climate Change, Eco-Anxiety and Risk Perception in The Context of Theory of Planned Behaviour.. s.l., IOP Publishing, p. 012020.
[3] Basarkar, ,. S. S., Dasgupta, ,. T. & Khatavkar, A., 2024. A Case Study of Foundation Reuse for Sustainable Construction. Indian Geotech Journal.
[4] Chrysanthos, M., 2020. Production of Sustainable Construction Materials Using Agro-Wastes.. Materials., 13(2), p. 262..
[5] Jack, K. B., 2017. Environmental economics in developing countries: An introduction to the special issue. Journal of Environmental Economics and Management, 86(C), pp. 1-7.
[6] Lau, J. L. & Hashim, A. H., 2020. Mediation analysis of the relationship between environmental concern and intention to adopt green concepts. Smart and Sustainable Built Environment, 9(4), 539-556., 9(4), pp. 539-556.
[7] Nlimaa, J., 2023. Smart materials and technologies for sustainable concrete construction. Developments in the Built Environment, p. 100177.
[8] Ritchie, H., Samborska, V. & Roser, M., 2024. Urbanization. [Online] Available at: https://ourworldindata.org/urbanization [Online Resource]
[9] Vasić, M. V. et al., 2023. Socio-Economic Analysis of the Construction and Building Materials' Usage—Ecological Awareness in the Case of Serbia.. Sustainability, 15(5), p. 4080.

11. Supplementary data- Appendix

Questionnaire for applying the theory of planned behavior to sustainable construction materials.

Behavior	Questionnaire
Attitude	I would prefer to use sustainable construction materials since they support nature.
	My preference is to use sustainable construction materials because the environment is being badly damaged by human beings.
Social norms	Those who can influence my thought process would think that I must recommend and use sustainable construction materials.
	People who hold importance in my life would think I should use and recommend my client's sustainable construction materials.
Perceived availability	I can buy sustainable building materials.
	It would be easy for me to procure sustainable construction materials from my neighborhood.
	I believe sustainable construction materials are available quite easily.
Perceived effectiveness	Individual engineers/architects/designers doing something about the environment is a fruitful enterprise.
	When I buy construction materials, I weigh how my attitudes and practices can affect the environment and other builders/ engineers/ architects/ designers.
	Pro-environmental practices and recommendations of engineers/ architects /designers can have a positive effect if they buy from socially responsible suppliers.
Perceived value	The quality of sustainable construction materials is mostly reliable.
	Sustainable construction materials offer good value to both buyers and sellers in terms of money and quality.
Intention	Recommending and using sustainable construction materials will give a good feeling to builders/ engineers/architects/designers for doing something good about environmental sustainability.
	I would like to recommend and use sustainable construction materials.
	I would actively seek out sustainable construction materials from suppliers to purchase and use it.
Actual Behaviour	I frequently recommend and use sustainable construction materials.
	I prefer sustainable construction materials over non-sustainable construction materials if the quality and cost are similar to one another.
	I recommend and use sustainable construction materials even if it cost more than non-sustainable construction materials.

Semi-structured interview Schedule

- What are your views on SCM?

- Do you intend to use SCM?
- Do you use SCM?
- What are the barriers to using SCM?
- How do actions of other architects, designers, and engineers using SCM influence you and your material recommendations?
- Can you share an anecdote related to SCM usage?

Acknowledgments

We acknowledge and appreciate the support extended to us by Ar. Harshita Sharma and Ar. Ishani Gogoi for this study.

IOP Conference Series: Earth and Environmental Science

PURPOSE-LED PUBLISHING™

PAPER • **OPEN ACCESS**

Biomass recovery and wastewater treatment in shrimp aquaculture: A comparative study on the performance of HRAPS and PMBR

To cite this article: Doan Thi Thu Hang *et al* 2024 *IOP Conf. Ser.: Earth Environ. Sci.* **1409** 012012

View the article online for updates and enhancements.

You may also like

- Research on the Mechanism of Simultaneous and Efficient Removal of Ammonia, NO_3-N and TN in the Coking Wastewater
Chunjuan Dong, Pan Qingye and Sun Yaquan
- The treatment of wastewater from pangasius catfish ponds using peat-derived adsorbent materials
Ho Sy Thang, Nguyen Minh Thao, Vo Thang Nguyen et al.
- Electric field determination in air plasmas from intensity ratio of nitrogen spectral bands: I. Sensitivity analysis and uncertainty quantification of dominant processes
Adam Obrusník, Petr Bílek, Tomáš Hoder et al.



This content was downloaded from IP address 47.247.77.11 on 27/11/2024 at 05:34

Biomass recovery and wastewater treatment in shrimp aquaculture: A comparative study on the performance of HRAPS and PMBR

Doan Thi Thu Hang[1], Truong Tan Dat[2], Duong Ngoc Nghi[2], Nham Hai Nhu[2], Le Hoai Nam[3], Tran Thi Bich Phuong[3], Le Duc Trung[4] and Thanh Tran[1,4,*]

[1]Research and Development Institutes Advanced Agrobilogy, Nguyen Tat Thanh University, Ho Chi Minh City, 700000, Vietnam.
[2] Faculty of Chemical Engineering and Food Technology, Nong Lam University, Ho Chi Minh City, 700000, Viet Nam.
[3] Faculty of Environmental, Ho Chi Minh City University of Natural Resources and Environment, Ho Chi Minh City, 700000, Vietnam.
[4] Institute for Environment and Resources, Vietnam National University Ho Chi Minh City (VNU-HCMC), Ho Chi Minh City, 70000, Vietnam.

*E-mail: thanhtran2710@gmail.com

Abstract. In this study, the utilization of Chlorella vulgaris microalgae for shrimp aquaculture wastewater treatment was explored through two photosynthetic systems: High-Rate Algae Ponds (HRAPs) and Membrane Photobioreactors (PMBR). The application of microalgae and bacteria in shrimp wastewater treatment in both systems exhibited good treatment efficiency, with effective removal rates of COD, N-NO_3^-, N-NO_2^-, N-NH_4^+, TN, and P-PO_4^{3-} reaching 27.4%, 58.7%, -35%, 92.2%, 77%, and 93.5% respectively in the HRAPs model, and 29.7%, 24.5%, 26%, 83.9%, 75%, and 93.4% respectively in the PMBR model. Both models demonstrated similar capabilities in COD and P-PO_4^{3-} removal. However, HRAPs showed higher efficiency in N-NO_3^- removal compared to PMBR, whereas PMBR was more effective in N-NO_2^- removal. Regarding daily biomass recovery, HRAPs achieved 5474 mg/day compared to PMBR, which reached 7265 mg/day, indicating a higher biomass recovery capability of PMBR over HRAPs. These results unveil the potential application of microalgae in shrimp aquaculture wastewater treatment, providing a comprehensive insight into the performance and advantages of each system in wastewater treatment and biomass recovery.

Keywords: *Chlorella vulgaris*; High-Rate Algae Ponds (HRAPs); Membrane Photobioreactors (PMBR); Shrimp farming wastewater.

1. Introduction

In the context of sustainable development and the increasing emphasis on green technology applications, *Chlorella Vulgaris*, a microalgae, has been recognized for its significant role in wastewater treatment [1]. This particular interest in the microalgae arises not only from its rapid growth rate and ease of cultivation but also due to its extraordinary adaptability and development potential in wastewater conditions. Studies have demonstrated that *Chlorella Vulgaris* can significantly reduce the salinity levels in saline wastewater [2], bringing it to a safe level for the growth of other plant species, a critical advancement for the restoration of ecosystems affected by wastewater [3]. Furthermore, the potential of *Chlorella Vulgaris* to absorb up to 74% of carbon

Content from this work may be used under the terms of the Creative Commons Attribution 4.0 licence. Any further distribution of this work must maintain attribution to the author(s) and the title of the work, journal citation and DOI.
Published under licence by IOP Publishing Ltd

dioxide when cultivated in photosynthetic reaction conditions has been emphasized by researchers [4], which not only improves water quality but also contributes to mitigating climate change. Within the context of wastewater from aquaculture, especially shrimp farming, which contains a large number of organic pollutants and antibiotics, the direct discharge of untreated wastewater into the environment is a serious issue. The shift towards using biological technology for wastewater treatment not only reflects a commitment to environmental protection but also offers a cost-effective and efficient solution, promising to open new avenues in wastewater management and recycling, while enhancing sustainability in aquaculture production.

In the quest for appropriate wastewater treatment systems that are both efficient and suitable for rural applications, a critical assessment emerges between open systems like high-rate algae ponds (HRAPs) [5] and closed systems such as Membrane Photobioreactors (MPBRs) [6]. This delineation is paramount as each system presents distinct advantages and limitations that merit careful consideration. HRAPs, characterized by their open-channel pond system utilizing natural light, have been acknowledged for their lower operating and capital costs in comparison to conventional treatment ponds. A notable study by Soka University, Japan, demonstrated HRAPs' capability to eliminate 100% of nutrients—specifically ammonia, nitrate, and phosphate—and over 80% of organic matter from aquaculture wastewater [7]. These findings underscore HRAPs' efficacy in aquaculture wastewater treatment and the potential valuation of the produced algal biomass.

Conversely, Membrane Photobioreactors (MPBRs) represent a closed-loop biological treatment approach. Despite higher operating costs, their efficiency in water treatment and the quality of the treated water for reuse is unparalleled. However, the significant investment required for MPBR systems poses a challenge to their adoption in rural settings [7]. The functionality and nutrient removal efficiency of MPBRs has been scrutinized in relation to key operating parameters. Research by Solmaz and Işık, employing a mixed culture of *Chaetophora* sp. and *Navicula* sp. in synthetic secondary treated wastewater, explored the influence of hydraulic retention time (HRT) on nutrient removal, maintaining a solids retention time (SRT) of 3 days [8]. This investigation contributes to the understanding of operational dynamics critical to optimizing MPBR performance.

This comparative analysis not only aids in selecting the most suitable model for specific farm conditions but also heralds new biotechnological applications aimed at minimizing the environmental impacts of shrimp farming. The ability of both technologies to facilitate water reuse underscores their significance in offering sustainable solutions to the aquaculture industry. Beyond addressing wastewater pollution, PMBR and HRAP systems yield added value through water recycling and the production of valuable bio-products [9], an aspect increasingly vital amid dwindling water resources and the demand for effective, sustainable wastewater treatment methods.

Hence, the primary objective of this investigation is to rigorously evaluate and juxtapose the wastewater treatment efficacies of two distinct models, whilst embarking on exploratory research aimed at refining the treatment methodologies. This endeavor seeks to diminish operational expenditures and augment the efficiency of water reuse, particularly in the face of escalating water resource scarcity. This study endeavors to not only illuminate the comparative advantages of these systems within the shrimp farming context but also to pioneer advancements in optimizing their operational efficiencies. By delving into the potential for cost reduction and enhanced water reuse capabilities, this research aspires to extend the horizons of sustainable aquaculture practices. Moreover, it aims to contribute substantially to the development of eco-friendly wastewater

treatment technologies, underscoring the urgent need for innovative solutions in the sustainable management of aquaculture effluents. Through this research, we aim to provide pivotal insights into the practical applicability of these models, thereby facilitating informed decision-making for the aquaculture industry. This, in turn, will not only serve the immediate needs of shrimp farming sustainability but also contribute to the broader discourse on environmental conservation and resource management, marking a significant step forward in the quest for sustainable and environmentally benign aquaculture practices

2. Materials and research methods

2.1. Research Materials and Chemicals

The salt-tolerant *Chlorella vulgaris* algae source from the algae farming and treatment model at the Institute of Applied Technology and Sustainable Development - Nguyen Tat Thanh University [10]. The algae were cultivated to a biomass concentration of 10^6 in the laboratory before being tested for wastewater treatment [11]. The shrimp farming wastewater, with a salinity level of approximately 7 ppt, was evaluated in experimental trials using two closed photobioreactor systems and an open pond system (as depicted in Figure 1) over a treatment period of 30 days. The wastewater from shrimp farming exhibited characteristic properties with COD ranging from 65-180 mg/l, BOD_5 approximately 20 - 60 mg/l, total nitrogen around 5 to 20 mg/l, $P\text{-}PO_4^{3-}$ about 0.1 to 10 mg/l, $N\text{-}NH_4^+$ ranging from 1 to 10 mg/l, $N\text{-}NO_2^-$ around 0.1 - 5 mg/l, and $N\text{-}NO_3^-$ between 0.4 - 3 mg/l.

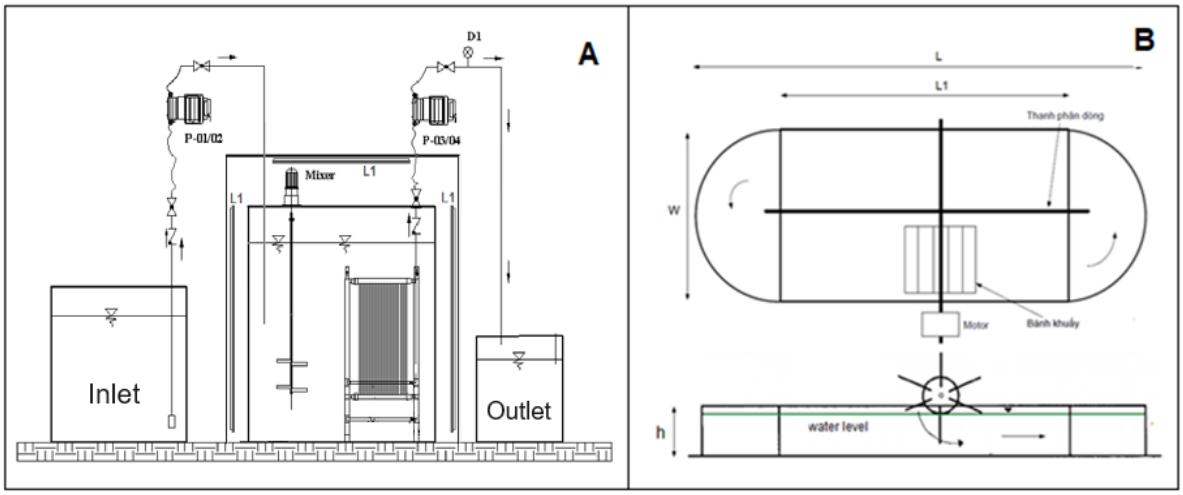


Figure 1. The photobioreactor closed system (A) and the open pond system (B).

The High-Rate Algal Pond (HRAP) system operates with a useful volume of 20 liters, encapsulated within a tank that boasts a total volume of 87 liters. This model is characterized by a Nutrient Loading Rate (NLR) of 0.07 kg nitrogen per cubic meter per day, indicating the system's capacity to accommodate and process a specified amount of nutrients within a given time frame. The hydraulic retention time (HRT) and biomass retention time (BRT) are remarkably similar, recorded at 9.6 and 9.59 days, respectively. These metrics signify the duration during which water and biomass are held within the system, essential for adequate treatment and biomass cultivation. The daily biomass discharge is measured at 9.07 liters per day, facilitating the removal of biomass from the system. Furthermore, the HRAP model adheres to a natural light: dark mode of 12:12 hours, mirroring the diurnal cycle and ensuring that the algal biomass receives a balanced exposure to light for optimal photosynthetic activity.

Conversely, the Photobioreactor (PMBR) system also maintains a useful volume of 20 liters but with a tank volume of 70 liters. This model introduces a membrane suction/rest time of 8:2 minutes, optimizing the filtration process while maintaining membrane integrity and function. The design flux is established at 10 liters per cubic meter per hour, with a daily membrane flux (Q) of 20 liters per day, indicating the system's efficiency in filtrating and recirculating water through the membrane. The Nutrient Loading Rate (NLR) mirrors that of the HRAP system at 0.07 kg nitrogen per cubic meter per day. However, the PMBR system exhibits a longer hydraulic retention time (HRT) of 84 hours and a biomass retention time (BRT) of 14 days, suggesting a more extended period for water and biomass treatment within the system. The daily biomass discharge varies, recorded at 5 and 7 liters per day, which allows for flexibility in managing the biomass output. Similar to the HRAP model, the PMBR system operates under a natural light:dark regime of 12:12 hours, facilitating a conducive environment for algal growth and photosynthesis.

2.2. Analytical method

To assess the efficacy of the treatment process, both the influent and effluent water will be subjected to analytical scrutiny, focusing on specific environmental parameters. The analysis of Chemical Oxygen Demand (COD) will be conducted in accordance with the TCVN 6186:1996-ISO 8467:1993 (E) methodology, a standard that ensures the comparability and reliability of the results. The concentration of phosphorus, specified as P-PO_4^{3-}, will be determined utilizing the method outlined in the Standard Methods for the Examination of Water and Wastewater (SMEWW) 4500-P B&E:2012, which provides a comprehensive framework for accurate phosphorus quantification. Furthermore, the analysis of ammonia nitrogen (N-NH_4^+) and total nitrogen (TN) will be performed employing the Kjeldahl method, as specified in TCVN 8125:2015. This method is renowned for its precision in nitrogen determination, thereby ensuring the accuracy of the analytical results [12, 13].

To ensure the robustness and reliability of the evaluation, samples will be collected and analyzed thrice weekly. The overall duration designated for the effective evaluation of the treatment system's performance is set at 40 days of continuous operation.

3. Results and Discussion

3.1. Efficiency of removing organic compounds in two closed-loop photobioreactor systems PMBR and open-channel HRAPs

The microalga *Chlorella vulgaris*, when incorporated into wastewater treatment systems, harnesses photosynthesis to degrade organic pollutants, thereby reducing COD levels in the aquatic environment. This process is akin to the absorption of CO_2 during photosynthesis, with the alga utilizing available organic compounds such as glucose, fructose, amino acids, and fatty acids as substrates. The consumption of these organics by Chlorella vulgaris results in a concomitant decline in COD, enhancing the treatment efficacy of photobiological systems like HRAPs and PMBRs [14].

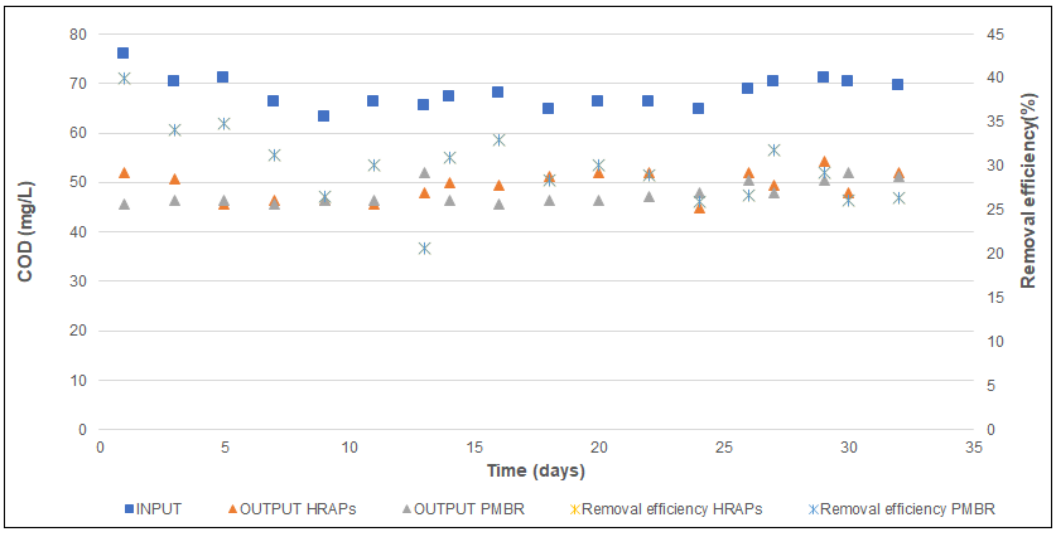


Figure 2. The efficiency of organic matter treatment in shrimp farming wastewater between two phototrophic biological model systems HRAPs and PMBR.

In Figure 2, we observe the representation of organic matter concentration (COD) in wastewater treated by both HRAP and PMBR systems, manifesting average removal efficiencies of 27.4% and 29.7%, respectively. Statistical analysis via One Way ANOVA yields a P-value of 0.101, which surpasses the 0.05 threshold, indicating that the variance in COD removal between HRAPs and PMBR systems does not reach statistical significance at a 95% confidence level. The recorded post-treatment COD minima stand at 44.8 mg/L for HRAPs and 45.6 mg/L for PMBRs, underscoring a negligible difference in the purifying performance of the two systems. Such results imply that both HRAPs and PMBRs exhibit a robust capacity for COD elimination.

In an algal-bacterial synergistic system, the algae provide oxygen through photosynthetic activity, which in turn aids bacterial degradation of organic compounds. This cooperative interaction enhances the overall efficiency of COD removal. The analysis of the provided data suggests that both systems achieve commendable COD reduction, aligning with the QCVN 08-MT:2015/BTNMT national technical regulations on surface water quality, meeting the B2 standard for environmental discharge (<50 mg/L). It is imperative to note that while the efficiency of both systems is relatively close, continuous optimization could yield further improvements in COD reduction, resource recovery, and cost-effectiveness, critical factors in the scalability and practical application of these treatment technologies.

3.2. Analytical method: The effectiveness of eliminating Ammonia and total Nitrogen in two phototrophic biofilm systems, HRAPs and PMBRs.

In examining Figure 3A, the efficacy of Ammonium N-NH_4^+ removal within the wastewater treatment paradigms is presented. The HRAPs system boasts an impressive average removal rate of 92.2%, surpassing the PMBR system, which achieves an average efficiency of 83.9%. Such differential performance, as corroborated by One Way ANOVA, reveals a P-value of 0.013, substantiating the superior effectiveness of HRAPs over PMBR systems at a 95% confidence interval. The mean difference value further accentuates the HRAPs system's proficiency in Ammonium N-NH_4^+ mitigation. These outcomes are consistent with the reported benchmarks, suggesting that N-NH_4^+ treatment efficiencies typically range within 80-90% [15].

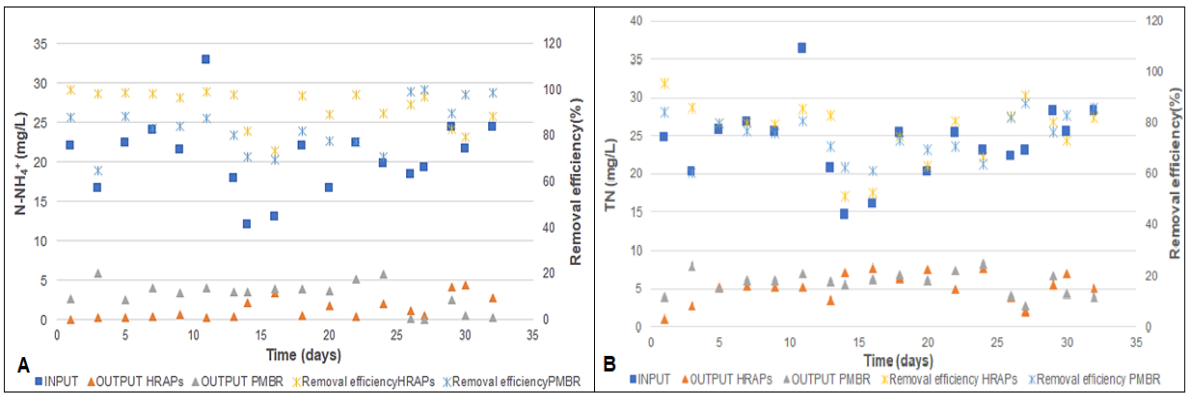


Figure 3. Comparison of the efficiency of removing (A) Ammonium N-NH_4^+ and (B) Total Nitrogen by the microalgae *Chlorella vulgaris* in treating shrimp aquaculture wastewater.

Delving into Figure 3B, it depicts the comparative results of Total Nitrogen (TN) removal. The HRAPs model exhibits an average efficiency of 77%, while the PMBR model records an average efficiency marginally lower at 75%. Such findings are in harmony with prior research indicating that the synergistic use of Chlorella vulgaris algae and TN removal bacteria can attain removal rates upwards of 75% [16]. According to the One-Way ANOVA test, the P-value stands at 0.527, exceeding the 0.05 mark, thereby denoting no statistically significant difference between the HRAPs and PMBR systems in terms of TN removal at a 95% confidence level. Despite this statistical parity, it's important to recognize that both systems demonstrate robust TN removal efficiencies.

The observed disparities in performance between the HRAPs and PMBR systems underscore the complexity of biotic interactions within each system. In HRAPs, the open structure may facilitate better gas exchange and light penetration, potentially enhancing the photosynthetic activity of Chlorella vulgaris and the associated nitrification-denitrification processes. Conversely, the PMBR system, through its closed configuration, could be expected to provide more controlled environmental conditions, which might favour the Chlorella-bacteria consortium in different ways. Nevertheless, both systems exhibit a high competency in the treatment of nitrogenous compounds, underscoring their viability as sustainable options for shrimp aquaculture wastewater treatment. This performance is particularly significant, given the need for effective nitrogen removal processes to mitigate the environmental impact of aquaculture effluents and to maintain aquatic ecosystem health.

3.3. Removal Efficiency of Total P-PO43- in Two Photobiological Model Systems HRAPs and PMBR

Figure 4 delineates the proficiency of both HRAPs and PMBR systems in treating P-PO_4^{3-} within wastewater. A symbiotic relationship between *Chlorella vulgaris* and bacteria underlies this process, wherein bacteria facilitate the transformation of phosphorus compounds into less soluble forms, thus mitigating their availability for reabsorption and lessening the risk of eutrophication upon environmental discharge [17].

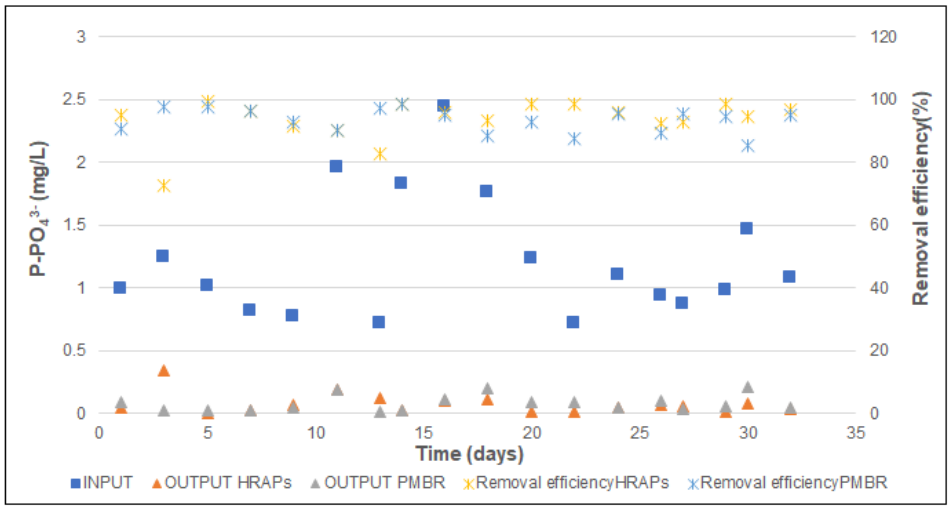


Figure 4. The efficiency of total phosphorus removal in shrimp aquaculture wastewater between the two photobiological models HRAPs and PMBR.

In the HRAPs system, a commendable average phosphorus removal efficiency of 93.5% is observed, closely matched by the PMBR system with an efficiency of 93.4%. This high level of removal efficiency exemplifies the systems' capability to significantly reduce phosphorus concentrations, surpassing the efficiency reported by E Amini et al. in 2020, which was 84% [18]. The negligible difference between the removal efficiencies of the two systems, which is statistically supported by a One-Way ANOVA P-value of 0.924, exceeding the 0.05 threshold, confirms that there is no significant difference at the 95% confidence level between the performances of the HRAPs and PMBR models.

Both HRAPs and PMBRs demonstrate almost equivalent effectiveness in phosphorus reduction, indicating that each model is well-suited for phosphorus-laden wastewater treatment in aquaculture systems. The striking similarity in phosphorus removal efficiency also suggests that both models can be applied interchangeably in this context without compromising treatment results. This is particularly pertinent in settings where environmental conservation is paramount and phosphorus discharge limits are strictly regulated. The efficacy of these systems in phosphorus removal not only aligns with sustainable wastewater management practices but also demonstrates the potential of photobiological treatment methods in achieving high treatment standards for shrimp aquaculture wastewater.

3.4. The biomass content in the two photosynthetic model systems HRAPs and PMBRs

Evaluating Figures 5 and 6 reveals intriguing aspects of biomass recovery in the context of photobiological wastewater treatment systems using Chlorella vulgaris.

Figure 5 demonstrates the ratio of mixed liquor volatile suspended solids (MLVSS) to biomass, providing an indicator of the efficiency with which each system converts volatile solids into useful biomass. The HRAPs model exhibits an average MLVSS to biomass ratio of 1.011 mg/L, indicative of a robust conversion process within this open system. In comparison, the PMBR model, with its lower ratio of 0.316 mg/L, suggests a less efficient solid-to-biomass conversion. Notably, a higher ratio is preferable, signifying a more effective system in terms of volatile solid assimilation per unit biomass. Statistically significant differences between the two systems are confirmed by a One Way ANOVA, with a P-value of 0.002, asserting greater efficiency within the HRAPs system at a 95% confidence level. Figure 6 focuses on the actual biomass recovery capabilities of the HRAPs and PMBR systems. Here, the HRAPs system manages a daily biomass recovery rate of 5474 ± 3061 mg/day, while the PMBR system surpasses this, achieving a rate of 7265.3 ± 2330 mg/day. The

superior biomass recovery rate of the PMBR model underpins its potential for higher yields of algal biomass, which can be repurposed for applications such as aquaculture feed or converted into bioenergy sources like biodiesel.

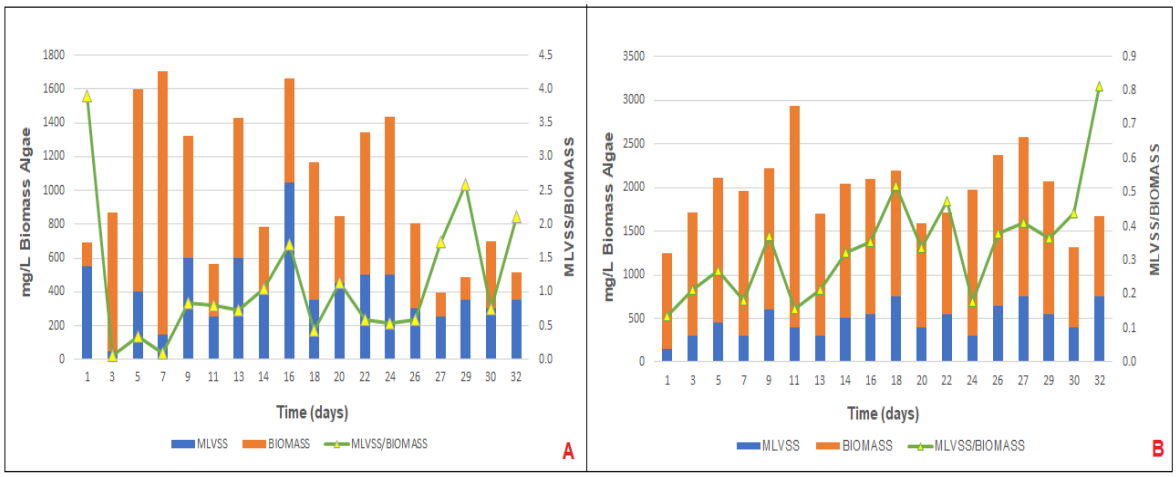


Figure 5. The ratio of algal biomass content to volatile suspended solids (MLVSS) in two photosynthetic model systems A (HRAPs) and B (PMBR).

The contrast between the two systems is stark. While PMBRs demonstrate better efficiency in biomass recovery, this comes at the expense of higher operational costs, potentially rendering them less feasible for widespread application, especially in resource-constrained settings. Conversely, the HRAPs, despite a lower recovery efficiency, offer a more cost-effective and practical solution, aligning more closely with the economic and logistical realities of many aquaculture operations.

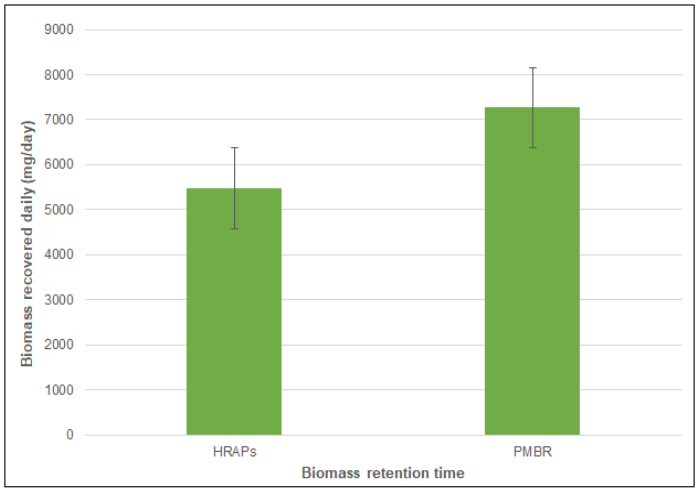


Figure 6. The daily biomass recovery levels of the HRAPs and PMBR models

Both the HRAPs and PMBR models have their merits in the context of sustainable aquaculture, each playing a role in the development of closed-loop systems that leverage wastewater to produce valuable biomass. This biomass serves not only as feed within the aquaculture cycle but also harbors the potential for bioenergy production, illustrating a multi-faceted approach to waste minimization and resource maximization in shrimp farming operations.

4. Conclusion

This study has explored and demonstrated the potential of the microalga Chlorella vulgaris in treating shrimp aquaculture wastewater, particularly through the utilization of two closed-loop photosynthetic systems: Photobioreactor (PMBR) and High-Rate Algae Pond (HRAPs). With its ability to thrive in conditions of salinity and nutrient sources such as nitrogen and phosphorus, this microalga not only aids in water remediation but also produces valuable biomass. Through effective treatment assessments, the HRAPs model has shown better efficiency in removing nitrogen and ammonia levels compared to PMBR, whereas PMBR, conversely, exhibits superior organic matter removal than HRAPs. This opens up a new approach to addressing pollution issues from shrimp aquaculture wastewater while enhancing value addition through biomass production. Proposed further research includes optimizing environmental conditions and treatment processes to enhance efficiency as well as exploring the wide-ranging applications of both models in aquaculture towards sustainable development goals.

References

[1] Kusuma HS, Illiyanasafa N, Jaya DEC, Darmokoesoemo H, Putra NR. Utilization of the microalga Chlorella vulgaris for mercury bioremediation from wastewater and biomass production. *Sustainable Chemistry and Pharmacy*. 2024;**37**:101346.

[2] Tran T, Le TD, Vo T-K-Q, Bui X-T. Exploring the combined effects of bicarbonate, NPK fertilizers, and salinity on Chlorella vulgaris growth. *Systems Microbiology and Biomanufacturing*. 2024;**4**(2):766-82.

[3] Bhuyar P, Hong D, Mandia E, Rahim M, Maniam G, Govindan NJJBMOA. Salinity reduction from poly-chem-industrial wastewater by using microalgae (Chlorella sp.) collected from coastal region of peninsular Malaysia. 2020;**1**(1):105.

[4] Keffer J, Kleinheinz GJJoIM, Biotechnology. Use of Chlorella vulgaris for CO 2 mitigation in a photobioreactor. 2002;**29**:275-80.

[5] Butterworth S, Fallowfield H. Comparison of the wastewater treatment performance of continuously and discontinuously mixed high-rate algal ponds at Kingston on Murray. *Water Science & Technology*. 2024;**89**(3):505-12.

[6] Thanigaivel S, Saranya V, Gnanasekaran L, Rajendran S, Soto-Moscoso M. Harnessing algal power: Algal membrane photobioreactors revolutionizing toxic wastewater matter separation and treatment–A comprehensive review. *Journal of the Taiwan Institute of Chemical Engineers*. 2024:105506.

[7] Kishi M, Takee H, Kawai M, Nagao N, Toda TJJoEB. Sequential high rate algal ponds operation for enhanced treatment of organic wastewater. 2018;**39**(5):835-42.

[8] Solmaz A, Işık MJB, Bioenergy. Optimization of membrane photobioreactor; the effect of hydraulic retention time on biomass production and nutrient removal by mixed microalgae culture. 2020;**142**:105809.

[9] Flores-Salgado G, Thalasso F, Buitrón G, Vital-Jácome M, Quijano G. Kinetic characterization of microalgal-bacterial systems: Contributions of microalgae and heterotrophic bacteria to the oxygen balance in wastewater treatment. *Biochemical Engineering Journal*. 2021;**165**:107819.

[10] Tran T, Le TD, Vo T-K-Q, Bui X-T. Exploring the combined effects of bicarbonate, NPK fertilizers, and salinity on Chlorella vulgaris growth. *Systems Microbiology and Biomanufacturing*. 2023:1-17.

[11] Minh T, Tien N, Giang L, Loc H, Hien V, Tran T, editors. Green technologies for air pollution treatment by microalgae in tubular photobioreactor. IOP Conference Series: Earth and Environmental Science; 2021: IOP Publishing.

[12] Nguyen BD, Van Le TT, Doan TTH, Le TH, Tuong LQ, Vi PTT, Tran TVT, Le TD, Thanh T, editors. Application of a membrane photobioreactor combined with microalgae for shrimp culture wastewater treatment. E3S Web of Conferences; 2023: EDP Sciences.

[13] Anh LD, Loc HH, Irvine KN, Thanh T, Tuong LQ. The waterscape of groundwater exploitation for domestic uses in District 12, Ho Chi Minh City, Vietnam. *Environment, Development and Sustainability*. 2021;**23**:7652-69.

[14] Mujtaba G, Rizwan M, Lee KJJoI, Chemistry E. Removal of nutrients and COD from wastewater using symbiotic co-culture of bacterium Pseudomonas putida and immobilized microalga Chlorella vulgaris. 2017;**49**:145-51.

[15] Gera GS, Salunkhe V, Kharul U, Jadhav SY, Mulay P, Bhattacharjee T, Kamble SJCEE. Treatment of Sewage Water Using Microalgae in Combination with Membrane Bioreactor: An Eco-Friendly Approach. 2018;**5**(1):35-46.
[16] Sun L, Tian Y, Zhang J, Cui H, Zuo W, Li JJCEJ. A novel symbiotic system combining algae and sludge membrane bioreactor technology for wastewater treatment and membrane fouling mitigation: performance and mechanism. 2018;**344**:246-53.
[17] Dhir B. *Phytoremediation: role of aquatic plants in environmental clean-up*: Springer; 2013.
[18] Amini E, Babaei A, Mehrnia MR, Shayegan J, Safdari M-SJJoWPE. Municipal wastewater treatment by semi-continuous and membrane algal-bacterial photo-bioreactors. 2020;**36**:101274.

Acknowledgements

This research is funded by Nguyen Tat Thanh University, Ho Chi Minh city, Vietnam, under the grant code 2023.01.181. Additionally, Thanh Tran was funded by the Master, PhD Scholarship Programme of Vingroup Innovation Foundation (VINIF), code VINIF. 2023.TS.113.

IOP Conference Series: Earth and Environmental Science

PURPOSE-LED PUBLISHING™

PAPER • **OPEN ACCESS**

Strategic Optimization of PFC Coagulation for Saline Water Pre-treatment: Enhancing RO Filtration Efficiency in the Mekong Delta

To cite this article: Do Vinh Duong *et al* 2024 *IOP Conf. Ser.: Earth Environ. Sci.* **1409** 012013

View the article online for updates and enhancements.

You may also like

- Efficacy of nanochitosan impregnated polyurethane foam in removing phosphate from aqueous solutions
P Sasidharan Anjali, V Meera and P Raphael Vinod
- A hybrid photocatalytic fuel cell integrated electro-Fenton system for Amaranth dye degradation and electricity generation
Shen-Hui Thor, Li-Ngee Ho, Soon-An Ong et al.
- PFC Performance Evaluation Based on Modeling and Identification of Unit's Main Parameters
Jun Li, WenXiao Qian, XiangRong Meng et al.



This content was downloaded from IP address 47.247.77.11 on 27/11/2024 at 05:35

Strategic Optimization of PFC Coagulation for Saline Water Pre-treatment: Enhancing RO Filtration Efficiency in the Mekong Delta

Do Vinh Duong[1,2], Phung Chi Sy[3], Nguyen Hoang Thai[4], Le Duc Trung[1], Ngoc-Han T. Huynh[4] and Thanh Tran[1,2,*]

[1]Institute for Environment and Resources, Vietnam National University Ho Chi Minh City (VNU-HCMC), Ho Chi Minh City, 70000, Vietnam.
[2]Research and Development Institutes Advanced Agrobilogy, Nguyen Tat Thanh University, Ho Chi Minh City, 700000, Vietnam.
[3]Institute of Applied Technology and Sustainable Development, Nguyen Tat Thanh University, Ho Chi Minh City, 700000, Vietnam.
[4]Faculty of Environmental, Ho Chi Minh City University of Natural Resources and Environment, Ho Chi Minh City, 700000, Vietnam.

*Email: tthanh@ntt.edu.vn

Abstract. This study critically evaluates the application of Poly Ferric Chloride (PFC) as a pre-treatment coagulant in desalination, particularly for enhancing Reverse Osmosis (RO) filtration in the saline-affected Mekong Delta region. The research focuses on the optimization of PFC dosages and pH levels to maximize coagulation efficiency in varying salinity conditions. Through an extensive series of experiments, an optimal coagulation efficiency of 93.7% for Total Suspended Solids (TSS) removal was achieved with a PFC dosage of 0.7 ml at a pH of 11 in a 5 ppt saline solution. However, increasing salinity levels were found to complicate this relationship, revealing a nuanced interplay between PFC dosage, pH, and salinity. A particularly critical observation was the decreasing effectiveness of PFC as salinity levels rose, indicating a need for escalating PFC dosages in higher saline waters to sustain coagulation effectiveness. The study significantly contributes to the understanding of PFC pre-treatment in water desalination processes, highlighting the compound's role in improving the input quality for RO systems and extending membrane longevity. These findings are pivotal for designing adaptive water treatment strategies, ensuring the sustainability and effectiveness of water purification in salinity-vulnerable contexts.

Keywords. Poly Ferric Chloride, coagulation efficiency, water treatment strategies.

1. Introduction

In Ben Tre, a coastal province of Vietnam, fresh water is becoming extremely scarce, largely due to the increased saltwater intrusion linked to climate change [1, 2], has necessitated innovative solutions for sustainable water supply. Among these, Reverse Osmosis (RO) filtration emerges as a pivotal technology for desalination, offering a beacon of hope for securing fresh water for domestic and agricultural purposes [3-5]. Nonetheless, the efficacy of RO systems is significantly hampered by the accumulation of sediments and suspended particles, which not only degrade the performance but also shorten the lifespan of the RO membranes [6]. This predicament

Content from this work may be used under the terms of the Creative Commons Attribution 4.0 licence. Any further distribution of this work must maintain attribution to the author(s) and the title of the work, journal citation and DOI.
Published under licence by IOP Publishing Ltd

underscores the critical need for effective pre-treatment measures to ensure the longevity and efficiency of RO systems.

Addressing this imperative, our research introduces a novel pre-treatment strategy employing Poly Ferric Chloride (PFC) as a coagulant to mitigate the burden of particulates on RO membranes. PFC stands out for its proficiency in coagulating suspended particles, facilitating the formation of flocs that are easily separable from water, thereby enhancing the quality of water introduced into the RO system [7-9]. This pre-treatment significantly reduces the risk of membrane clogging, promising an uplift in the system's operational performance and durability.

To refine the pre-treatment process and optimize its parameters, this study leverages the Response Surface Methodology - Central Composite Design (RSM-CCD). This advanced statistical approach enables the meticulous determination of optimal conditions, including the appropriate dosage of PFC, pH levels, and settling times, tailored to accommodate varying salinity concentrations [10, 11]. The employment of RSM-CCD has yielded precise, scientifically grounded insights into the pre-treatment process, offering a robust foundation for enhancing RO system efficiency in the face of salinity challenges.

The novelty of this research lies in its integrated approach, combining the strengths of RO desalination with an innovative PFC pre-treatment, underpinned by the strategic application of RSM-CCD for parameter optimization. This holistic methodology not only addresses the immediate technical challenges associated with RO filtration but also contributes significantly to the scientific and practical realms of water treatment. By ensuring the quality and efficiency of RO systems, this research marks a pivotal advancement in combating water scarcity, particularly within the saline-affected regions of the Mekong Delta, thereby underscoring its scientific merit and practical significance in the context of climate change-induced challenges [12].

2. Materials and research methods

2.1. Research Materials

Poly Ferric Chloride (PFC), with its chemical structure $[Fe_2(OH)_nCl_{6-n}]_m$, was selected for its superior coagulation efficiency, capable of releasing polymer particles that effectively remove water contaminants by forming flocs. This attribute allows PFC to swiftly combine with and precipitate suspended solids and pollutants into larger, easily separable flocs [9, 13]. Water samples for this research were sourced from the Luong Quoi River and subjected to coagulation-flocculation testing using PFC to evaluate treatment effectiveness. The study focused on optimizing the coagulant's dosage and the pH conditions to maximize treatment efficiency.

2.2. Research Methodology and Analysis

The experiment was designed to identify the pH, dosage, and settling time for the coagulation-flocculation process. It was conducted using the Jar test model to assess the effectiveness of the coagulation-flocculation process.

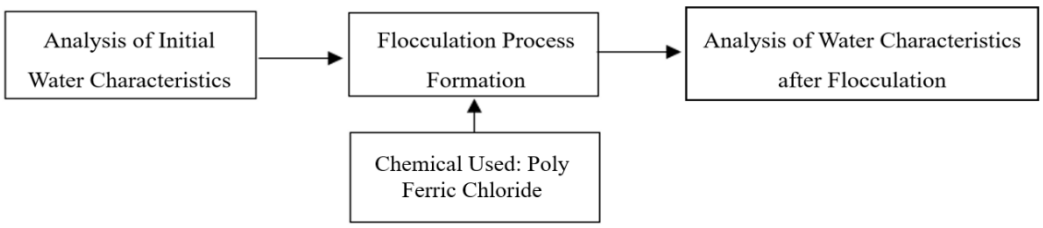


Figure 1. Process Flow Diagram for Experimental Research.

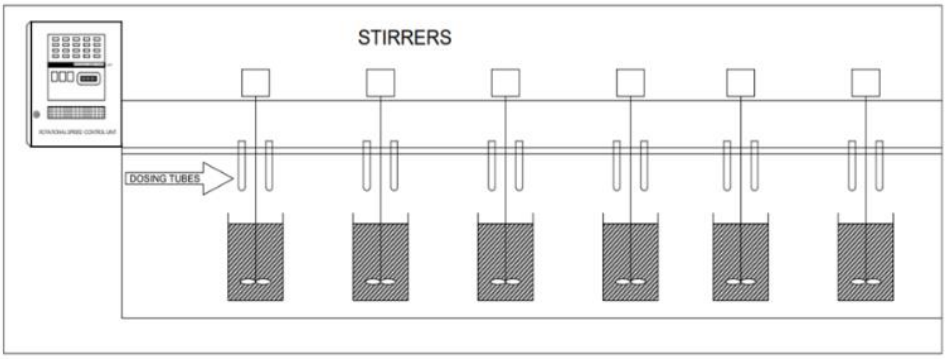


Figure 2. Jar test Model.

2.3. Determining the Influence of pH, Dosage, and Settling Time on the PFC Flocculation Process.
This investigation utilized the Response Surface Methodology – Central Composite Design (RSM-CCD) to assess the influence of pH, dosage, and settling time on coagulation-flocculation efficiency [14, 15]. Through RSM-CCD, an experimental design was established, varying these parameters across three levels to systematically explore their effects. The optimization process, particularly for PFC dosage and settling time, was rigorously executed via CCD, which structured the evaluation across two key levels: a lower level (−1) and an upper level (+1). Data analysis was performed using Design-Expert software, leveraging RSM-CCD to identify optimal conditions that significantly elevate treatment efficacy. This method efficiently streamlined the experimental process, allowing for the discernment of each variable's specific impact while reducing the number of necessary trials, thereby enhancing the study's overall precision and reliability.

Table 1. The values of pH, dosage, and settling time used in the RSM-CCD method with PFC as the coagulant material.

Surface Response	Factor Name	Research Scope	Level		
			-1	0	1
R	pH	5 – 11	5	8	11
	Dosage (mg)	100 – 1.000	100	550	1.000
	Settling Time (minutes)	2 – 30	2	16	30

The experimental design was meticulously structured to evaluate the efficacy of water treatment across various quality indicators, including Total Suspended Solids (TSS), turbidity, color, and hardness. These parameters were rigorously analyzed employing recognized standard methods: TSS as per TCVN 6625:2000 - ISO 11923:1997, turbidity according to TCVN 6184 - 1996 – ISO 7027 - 1990 and SMEWW 2130 B, color in line with ISO 7887 - 1985 or SMEWW 2120, and hardness following TCVN 6224 - 1996 or SMEWW 2340 C [16-19].

The core objective of this experiment is to investigate the effects of incremental salinity concentrations, ranging from 0 ppt to 15 ppt, on the aforementioned water quality indicators. These concentrations were systematically increased in 2.5 ppt increments. At each specified concentration level, measurements of TSS, turbidity, color, and hardness were conducted. This approach is designed to elucidate the correlation between varying salinity levels and the alterations in water quality metrics, thereby facilitating the identification of threshold values. Such insights are instrumental for delineating the response of water quality under varied conditions, significantly contributing to the advancement of environmental water quality management strategies.

3. Results and Discussion

3.1. Efficiency of pretreatment with PFC flocculation at different salinities

The provided data and accompanying graphical analyses delineate the nuanced effects of Poly Ferric Chloride (PFC) coagulation under varying salinity conditions, crucial for the pretreatment phase prior to Reverse Osmosis (RO) filtration. The studies, represented across multiple figures, demonstrate the efficacy of PFC in aggregating and precipitating algae, with a particular focus on indicators such as Total Suspended Solids (TSS), turbidity, colour, and hardness.

Starting from a zero-salinity level, as depicted in Figure 3, the data underscore the prominence of pH and PFC dosage in the coagulation process. Optimal removal of TSS was noted at an alkaline pH with higher PFC concentrations. In contrast, a reduction in PFC dosage highlighted a significant decrease in coagulation efficiency, indicating the critical interplay between these factors. A notable balance was achieved under central conditions, suggesting a potential zone of operation for effective water treatment.

The collective analysis of Figures 3 through 9 illuminates the detailed behaviour of PFC as a coagulant across a spectrum of salinity levels. It is evident that PFC's efficiency in treating water is intricately linked to the harmonized management of pH levels, coagulant dosages, and the settling time against the backdrop of salinity changes.

Figure 3 elucidates the scenario at 0 ppt salinity, serving as the baseline for subsequent comparisons. At this salinity, a high pH of 11 paired with a PFC dosage of 0.7 ml catalyzed an impressive TSS removal efficiency of 91.2%. This efficiency underscores the favourable conditions for coagulation at higher pH levels and PFC concentrations in the absence of salinity.

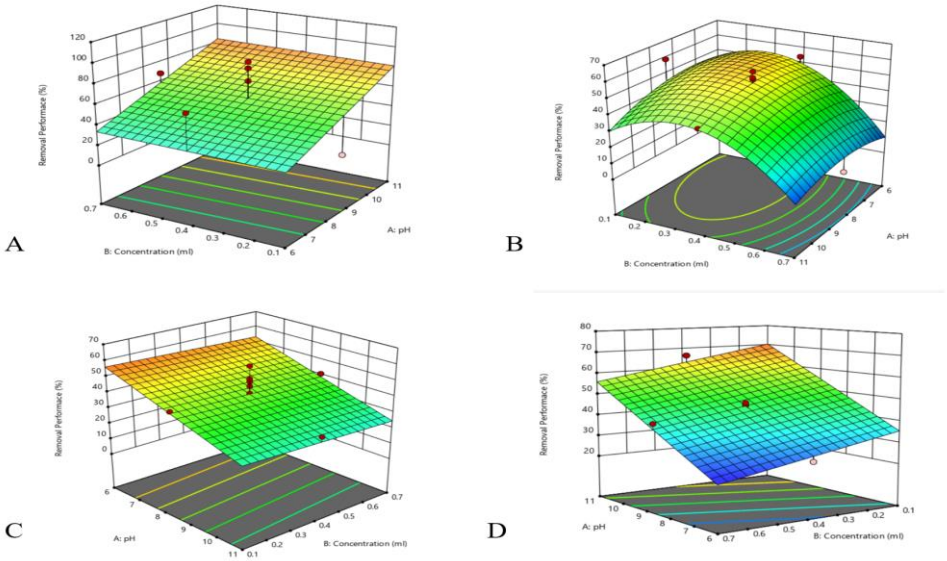


Figure 3. Efficiency of the flocculation process using PFC material at a salinity level of 0 ppt with respect to indicators (A) TSS (B) Turbidity (C) Colour (D) Hardness.

Moving to Figure 4, representing a salinity level of 2.5 ppt, a slight shift in the trend becomes discernible. The peak efficiency for TSS removal remained high at 93.7% under similar conditions of high pH and PFC dosage, hinting at PFC's robust coagulation capabilities even as salinity begins to increase. This figure also reveals that moderate pH and PFC dosages provide substantial removal efficiencies, indicating PFC's versatility as a coagulant.

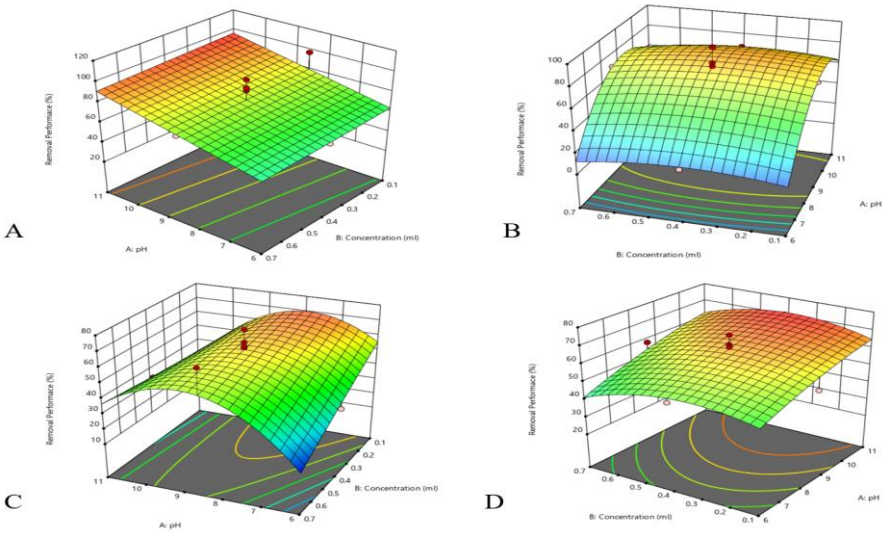


Figure 4. Efficiency of the flocculation process using PFC material at a salinity level of 2.5 ppt with respect to indicators (A) TSS (B) Turbidity (C) Colour (D) Hardness.

As we progress to Figure 5 with a salinity of 5 ppt, the TSS removal efficiency exhibits a minor decline to 86.8% at the same optimal pH and PFC dosage, suggesting the onset of salinity's impact on the coagulation process. Yet, even at reduced efficiencies, the process remains highly effective under optimized conditions.

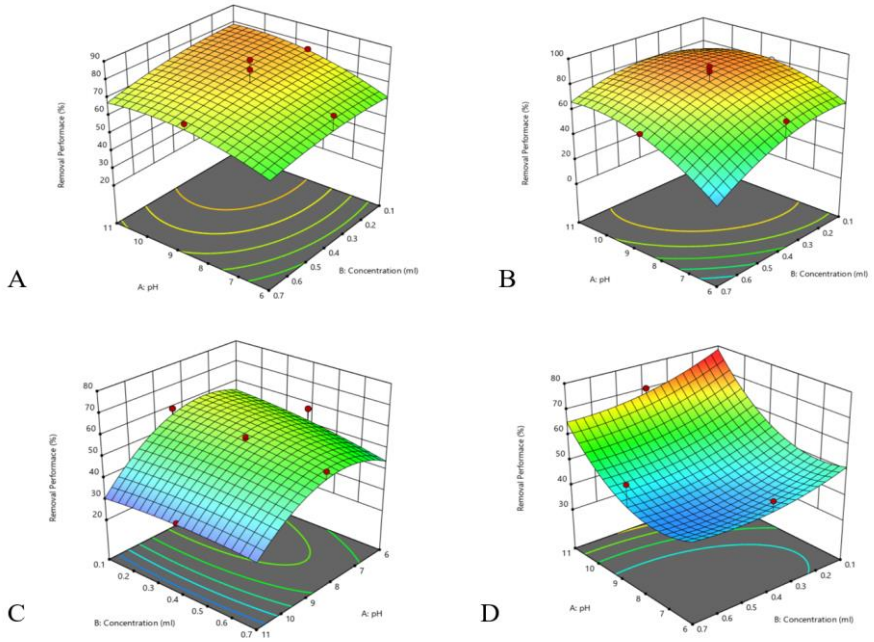


Figure 5. Efficiency of the flocculation process using PFC material at a salinity level of 5 ppt with respect to indicators (A) TSS; (B) Turbidity; (C) Colour (D) Hardness.

Figure 6 shows the treatment efficiency at 7.5 ppt salinity, where the highest TSS removal is observed at an efficiency of 89.4%, achieved at a slightly acidic pH of 8. At this juncture, the data point to the increasing need for careful adjustment of the treatment parameters to maintain high efficiency as salinity imposes more significant influence.

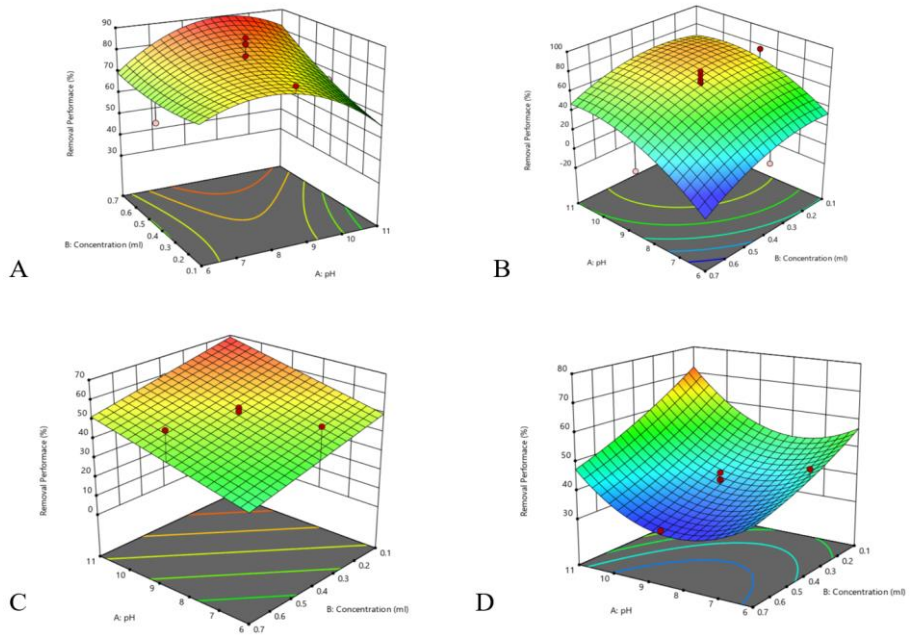


Figure 6. Efficiency of the flocculation process using PFC material at a salinity level of 7.5 ppt with respect to indicators (A) TSS (B) Turbidity (C) Colour (D) Hardness.

As depicted in Figure 7 at a salinity of 10 ppt, the maximum TSS removal efficiency at an acidic pH indicates a shift in the optimal pH for coagulation. The highest TSS removal rate drops to 80.4%, signifying the tangible effects of elevated salinity levels on the coagulation process and the potential need for increased dosages of PFC.

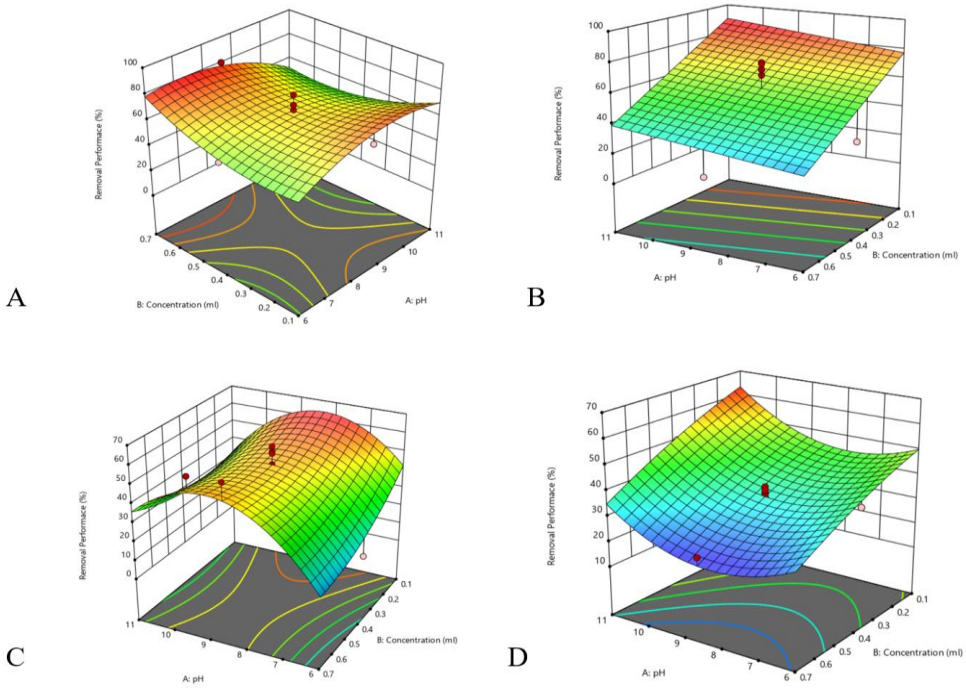


Figure 7. Efficiency of the flocculation process using PFC material at a salinity level of 10 ppt with respect to indicators (A) TSS (B) Turbidity (C) Colour (D) Hardness.

At the salinity level of 12.5 ppt in Figure 8, the efficiency for TSS removal peaks at 81.4%, suggesting that while the treatment process is still effective, the coagulation capacity of PFC is beginning to wane, necessitating closer attention to optimizing pH and PFC dosages to counteract the inhibitory effects of increased salinity.

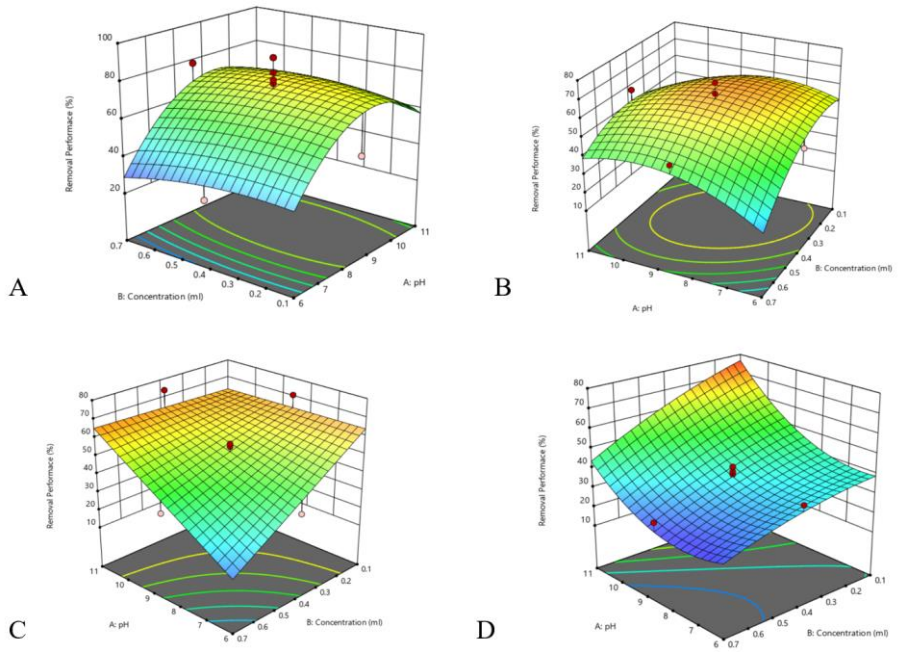


Figure 8. Efficiency of the flocculation process using PFC material at a salinity level of 12.5 ppt with respect to indicators (A) TSS (B) Turbidity (C) Colour (D) Hardness.

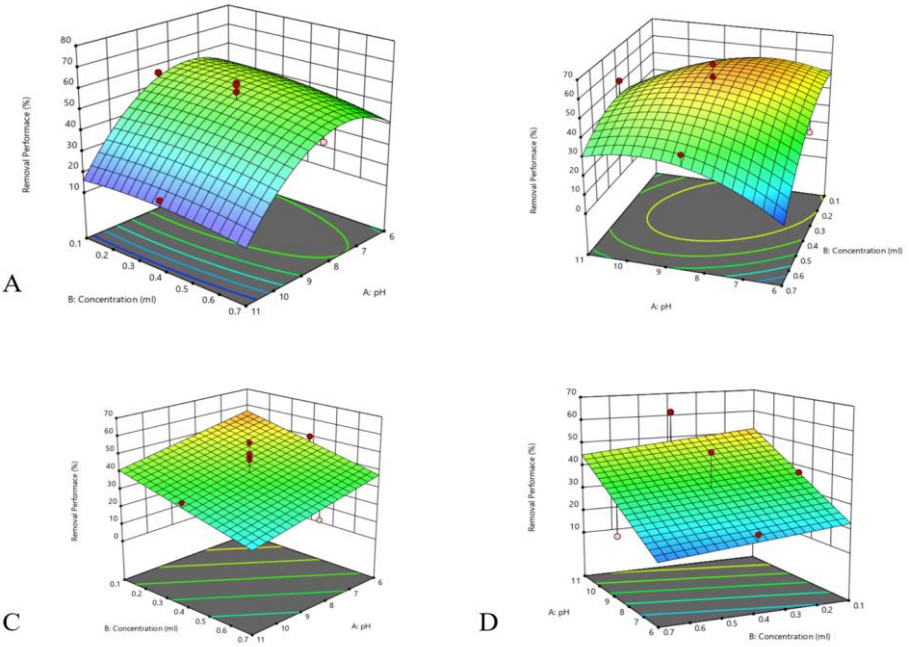


Figure 9. Efficiency of the flocculation process using PFC material at a salinity level of 15 ppt with respect to indicators (A) TSS (B) Turbidity (C) Colour (D) Hardness.

Finally, Figure 9 presents the scenario at 15 ppt salinity. Here, the highest TSS removal efficiency is considerably reduced to 57.6%, indicating the upper threshold of PFC's effectiveness

in the face of high salinity. This figure starkly demonstrates the challenges at extreme salinity levels, where the coagulation process may require significant adaptation to maintain efficacy.
In summary, these figures collectively establish a comprehensive understanding of PFC's role in the pretreatment phase for RO systems. They highlight the criticality of strategic pH management, precise PFC dosing, and the necessity of adapting to changing salinity conditions. The transition from high efficiency in non-saline conditions to reduced efficacy at high salinity levels necessitates a dynamic, adaptable approach to coagulation treatment processes, ensuring optimal preparation of water for subsequent RO filtration.

3.2. Dosage trend of PFC use as salinity increases and the application in pretreatment desalination.
As salinity levels increased incrementally, a consistent pattern emerged: PFC coagulation maintained high efficiency at elevated pH levels and higher PFC dosages. However, the efficacy of the coagulation process began to exhibit sensitivity to salinity changes, hinting at a threshold beyond which PFC efficiency could be compromised.

In the initial phase, as seen in Figures 3 to 5, the effectiveness of PFC in water with low to moderate salinity levels remains relatively high without substantial increases in dosage. This suggests that PFC's coagulating action is not significantly impeded by salinity at these levels. The observed removal efficiencies for TSS, turbidity, and colour are robust across a range of pH levels with the PFC dosages applied, implying that PFC is an efficient coagulant under these conditions without necessitating higher dosages.

However, as salinity continues to rise, depicted from Figures 6 to 9, the trend indicates a need for higher PFC dosages to achieve similar coagulation efficiencies. This change signifies a shift in the coagulation dynamics due to the interaction between dissolved salts and the coagulation process. Salts in the water can affect the charge balance and the zeta potential of the particles, which in turn can influence the aggregation and settling of flocs formed by PFC. At higher salinities, more PFC may be required to overcome the competition between salts and the coagulant for binding sites on the suspended particles, and to neutralize the increased ionic strength that can hinder floc formation. Towards the upper end of the salinity spectrum, the trend indicated a diminishing return on PFC efficiency, particularly for TSS removal. While pH and PFC dosage remained influential, the interrelationship between these factors and increased salinity levels necessitated a recalibration of treatment protocols.

The distilled essence of this research pivots on the interplay between three pivotal variables in the coagulation process utilizing Poly Ferric Chloride (PFC): the pH value, the PFC dosage, and the salinity of the water. The investigation reveals a nuanced understanding of PFC's coagulation behaviour, establishing its efficacy at low salinity levels and the need for careful dosage recalibration as salinity increases. This manifests as a distinctive dosage trend, where PFC's dosage maintains consistency up to a threshold of salinity. Beyond this critical juncture, there is a discernible requirement for incrementally increased dosages to maintain the effectiveness of the coagulation.

This nuanced trend speaks to the innovative core of the research, highlighting the need for a dynamic, informed approach to water treatment strategies, especially in saline conditions that present a complex, variable water chemistry. Mapping out the dosage trend is vital not only for ensuring the coagulation process's efficiency but also for safeguarding the longevity and functionality of subsequent RO systems. This foresight enables proactive adjustments in treatment protocols to preserve water quality without overburdening the system with excessive coagulant, which could potentially complicate the RO phase. The study provides an academic and practical blueprint for optimizing the pre-RO coagulation procedure. It underscores a methodical approach

to managing pH, PFC dosage, and salinity interdependencies. Environmental engineers and water treatment professionals are thus armed with empirical evidence to adeptly manage water purification processes under variable salinity levels, ensuring the integrity and efficacy of RO systems.

Specifically, for the commonly encountered salinity range of 3 - 5 ppt in the Ben Tre region, the proposed PFC dosage and conditions should be fine-tuned to this salinity window. Based on the findings, a recommended PFC dosage would be at the midpoint of the effective range identified for 0 ppt and 2.5 ppt salinities, acknowledging the necessity to offset the initial impacts of salinity. The pH should be adjusted to the optimal range determined for this salinity level, potentially around 8.5, where the coagulation efficiency remained high during trials. Settling time and PFC concentration would then be calibrated to this pH level, ensuring that the coagulation process is efficient, economical, and environmentally sustainable, ultimately contributing to the robustness and success of the RO water treatment infrastructure in Ben Tre.

4. Conclusion

This research has successfully demonstrated the potential of Poly Ferric Chloride (PFC) as an effective coagulant in saline water pre-treatment for Reverse Osmosis (RO) systems. It was found that PFC maintains coagulation efficiency in low to moderate saline waters without significant increases in dosage, making it a valuable asset in areas like Ben Tre, where salinity from intrusion is an ongoing concern. The broader implications of this study are substantial, providing a robust scientific foundation for refining pre-treatment strategies and facilitating the development of future coagulation treatments. These findings could significantly impact the design of water treatment protocols worldwide, particularly in salinity-affected regions. In essence, this study enhances the scientific understanding of water treatment under salinity stress and provides actionable guidance for environmental engineers and water treatment practitioners. It underscores the importance of adaptive, economically viable strategies for water purification, offering a methodological benchmark for future research in the field.

References

[1] L. V. Tan, T. Tran, and H. H. J. A. Loc, "Soil and water quality indicators of diversified farming systems in a saline region of the Mekong Delta, Vietnam," vol. **10,** no. 2, p. 38, 2020.

[2] N. T. H. Diep, H. H. Loc, C. T. Nguyen, E. Park, T. J. E. M. Tran, and Assessment, "Spatial-social evaluations of ecosystem services of adaptive aquaculture models using SAR and multivariate analyses: a case in the Vietnamese Mekong Delta," vol. **194,** no. Suppl 2, p. 778, 2022.

[3] P. Mackay, M. Russell, and S. J. T. A. C. s. R. Merz, "Socialist republic of Vietnam: climate change impact and adaptation study in the Mekong Delta," vol. **60,** 2011.

[4] G. B. Gholikandi, M. Delnavaz, R. J. E. E. Riahi, and M. Journal, "Use of Artificial Neural Network for prediction of coagulation/flocculation process by PAC in water treatment plant," vol. **10,** no. 11, 2011.

[5] X. Huang, Y. Wan, B. Shi, and J. J. C. Shi, "Effects of powdered activated carbon on the coagulation-flocculation process in humic acid and humic acid-kaolin water treatment," vol. **238,** p. 124637, 2020.

[6] T. Tran, T. T. B. Phuong, and L. V. Giang, "Study on application of cationic modified starch in combination with poly aluminium chloride for treatment of flocculation of aquatic wastewater," in *AIP Conference Proceedings*, 2022, vol. 2610, no. 1: AIP Publishing.

[7] M. Mohamed Noor, S. Wong, N. Ngadi, I. Mohammed Inuwa, L. J. I. J. o. E. S. Opotu, and Technology, "Assessing the effectiveness of magnetic nanoparticles coagulation/flocculation in water treatment: a systematic literature review," vol. **19,** no. 7, pp. 6935-6956, 2022.

[8] H. Rong, B. Gao, R. Li, Y. Wang, Q. Yue, and Q. J. C. E. J. Li, "Effect of dose methods of a synthetic organic polymer and PFC on floc properties in dyeing wastewater coagulation process," vol. **243,** pp. 169-175, 2014.

[9] Y. Wang, B. Gao, Q. Yue, J. Wei, and Q. J. C. E. J. Li, "The characterization and flocculation efficiency of composite flocculant iron salts–polydimethyldiallylammonium chloride," vol. **142,** no. 2, pp. 175-181, 2008.
[10] L. V. Tan and T. Thanh, "The effects of salinity on changes in characteristics of soils collected in a saline region of the Mekong Delta, Vietnam," 2021.
[11] H. Pashaei, A. Ghaemi, M. Nasiri, and B. J. A. o. Karami, "Experimental modeling and optimization of CO2 absorption into piperazine solutions using RSM-CCD methodology," vol. **5,** no. 15, pp. 8432-8448, 2020.
[12] F. Katrivesis, A. Karela, V. Papadakis, and C. J. J. o. W. P. E. Paraskeva, "Revisiting of coagulation-flocculation processes in the production of potable water," vol. **27,** pp. 193-204, 2019.
[13] T. Tran, D. A. Le, N. H. Hai, T. P. Hung, N. C. Danh, L. Van Tan, V. T. D. Hien, and X.-T. J. M. T. P. Bui, "Study on optimal conditions of poly ferric chloride (PFC) dosage treating tannery wastewater," vol. **38,** pp. 2981-2987, 2021.
[14] M. Moradnia, K. Dindarlo, H. J. E. H. E. Ali Jamali, and M. Journal, "Optimizing potassium ferrate for textile wastewater treatment by RSM," vol. **3,** no. 3, pp. 137-142, 2016.
[15] D. N. Nguyen, H. N. Bui, K.-Y. A. Lin, Y.-S. Perng, T. Tran, L. T. K. Nguyen, H. T. Nguyen, H. M. J. S. E. T. Bui, and Assessments, "Efficient removal of reactive red 24 from aqueous solution through electron beam and aeration tank using response surface methodology," vol. **53,** p. 102452, 2022.
[16] B. D. Nguyen, T. T. Van Le, T. T. H. Doan, T. H. Le, L. Q. Tuong, P. T. T. Vi, T. V. T. Tran, T. D. Le, and T. Thanh, "Application of a membrane photobioreactor combined with microalgae for shrimp culture wastewater treatment," in *E3S Web of Conferences*, 2023, vol. 405: EDP Sciences, p. 01003.
[17] L. Giang, D. Duong, D. Hang, L. Tuyet, L. Hai, and T. Tran, "Terminalia catappa leaf solution: an eco-friendly approach to managing color, algae, and microbial activity in aquaculture systems," in *IOP Conference Series: Earth and Environmental Science*, 2023, vol. 1267, no. 1: IOP Publishing, p. 012072.
[18] T. Tran, T. B. Nguyen, H. L. Ho, D. A. Le, T. D. Lam, D. C. Nguyen, A. T. Hoang, T. S. Do, L. Hoang, and T. D. Nguyen, "Integration of membrane bioreactor and nanofiltration for the treatment process of real hospital wastewater in Ho Chi Minh City, Vietnam," *Processes,* vol. **7,** no. 3, p. 123, 2019.
[19] L. D. Anh, H. H. Loc, K. N. Irvine, T. Thanh, and L. Q. Tuong, "The waterscape of groundwater exploitation for domestic uses in District 12, Ho Chi Minh City, Vietnam," *Environment, Development and Sustainability,* vol. **23,** pp. 7652-7669, 2021.

IOP Conference Series: Earth and Environmental Science

PURPOSE-LED PUBLISHING™

PAPER • OPEN ACCESS

Optimizing roofing efficiency: utilizing GGBS and coir fibre in cement tile production

To cite this article: K. Jagannadha Rao *et al* 2024 *IOP Conf. Ser.: Earth Environ. Sci.* **1409** 012014

View the article online for updates and enhancements.

You may also like

- Effect of manufactured sand, micro silica, and GGBS on properties of high-performance concrete
Jaydeep B Chougale and A A Bage
- Fluidized solidified soil using construction slurry improved by fly ash and slag: preparation, mechanical property, and microstructure
Tianhong Feng, Kaihao Lin, De Zhang et al.
- Thermal and durability characteristics of optimized green concrete developed using slag powder and pond ash
Jeyaprakash Maheswaran, Maheswaran Chellapandian, Nakarajan Arunachelam et al.



This content was downloaded from IP address 47.247.77.11 on 27/11/2024 at 05:35

Optimizing roofing efficiency: utilizing GGBS and coir fibre in cement tile production

K. Jagannadha Rao[1], Sastri, M.V.S.S.[2*], T. Swetha[1] and Ch. Poojita[1]

[1]Department of Civil Engineering, Chaitanya Bharathi Institute of Technology (A), Hyderabad, Telangana, India
[2]Department of Civil Engineering, Vasavi College of Engineering (A), Hyderabad, Telangana, India.

[*]Email: mvss.sastri@staff.vce.ac.in

ABSTRACT: The roof of a dwelling is the most significant and expensive. Low-cost heavy roofing construction frequently resulted in higher costs. The potential usage for coir, an eco-friendly building material, is as a raw material for corrugated roofing sheets and tiles. This study deals with the effects of using Ground Granulated Blast Furnace Slag (GGBS) as a partial replacement in cement roof tile production. The work is based on an experimental study of roofing tiles produced with Ordinary Portland Cement (OPC) and 10%, 20%, 30%, 40%, and 50% (OPC) replaced by GGBS (Ground Granulated Blast furnace slag). The optimum combination of fibre of 0.8% and replacement of GGBS of 40% in tiles was found optimum.

Keywords: Roofing Tiles, Coir Fibre, GGBS, mechanical properties, water absorption

1. Introduction

The roof is one of the most essential parts of a house. Having a durable roof that can withstand any weather condition can help ensure people's safety. Almost all developing countries need more roofing materials. Local resources such as soil, stone, grass, and palm leaves are commonly used for roofs, but they require significant maintenance and have little resistance to heavy rain. To make the concrete roofs lighter, natural fibre can be incorporated. Fibre composites offer benefits such as high strength, lightweight, water, chemical, electrical, fire, and corrosion resistance. They can also be engineered according to requirements, making them cost-effective in most usage. Incorporating natural fibre into composites can make roofs more cost-effective and environmentally friendly. Natural fibres have found desirable applications in construction with the advent of lightweight concrete technology. Organic fibre composites are crucial for constructing low-cost structures in developing nations. Contrarily, manufacturing fibre-reinforced cementitious composites using synthetic fibres leads to higher costs and more energy usage [1]. The organic-fibre-reinforced composites can substantially contribute to the infrastructure in developing nations when used as flat sheets, roofing tiles, and pre-cast components [2]. The pre-treatment of coconut fibres enhances the resistance to a highly alkaline environment, thereby making the fibre cost-effective and environmentally friendly otherwise, it is reported that untreated fibre has more water absorption [3]. GGBS, a by-product, is cost-effective and suitable for ready-mixed concrete, cast-in-situ and precast product manufacturing in large quantities [4]. GGBS produces lower heat during hydration and enhances resistance from chloride and acid

Content from this work may be used under the terms of the Creative Commons Attribution 4.0 licence. Any further distribution of this work must maintain attribution to the author(s) and the title of the work, journal citation and DOI.
Published under licence by IOP Publishing Ltd

attacks compared with OPC. Lower production costs may also result from the raw material's inexpensive availability. As a result, the cost of housing for roofing—which is often the most expensive aspect of building construction—can be significantly reduced.

1.1. Aim and Objectives

This research aimed to explore the possibility of using GGBS and coir fibre to reduce the cost of production of concrete roof tiles by partially replacing Ordinary Portland cement (OPC) with GGBS. The objectives are:

- To determine the physical properties of GGBS. These include specific gravity, particle size distribution, setting time with cement paste, and particle size distribution of the fine aggregate.
- To produce concrete roof tile using GGBS with replacement of cement (5, 10, 15, 20 and 25 %) and adding coir at 0.2, 0.5, 0.8 and 1%
- Testing the produced sample for physical variations from the control sample.
- (Compressive strength, flexure test and water absorption)
- To compare the obtained results with those of conventional cement tiles.

1.2. Scope and Limitations

This study focuses on using GGBS as a partial replacement for cement in the production of concrete roofing tiles. It uses the growing of GGBS and coir by varying its proportions of GGBS (10, 20, 30, 40 and 50 %) in partial cement replacement and adding coir (0.2,0.5,0.8 and 1%) used for concrete roof tiles.

2. Literature review

Darsana et. Al. [5] used a 1:4 mix proportion with 10% coir fibre replacement and a 0.6 water-cement ratio to produce lightweight concrete roofing tiles. Tile specimens with dimensions of 320mmx280mmx15mm are produced for tile processing. Coir fibre tiles have a lower self-weight and cost when compared to plain tiles. Mechanical properties like cracking load and ductility have been enhanced. According to Sudheer et al, the compressive and flexural tensile strength are at maximum with a 5% addition of coconut fibre with a water-cement ratio of 0.5. Beyond this amount, a decrease in strength was reported [6]. The mechanical properties of roofing tiles, replacing 15% of the cement with fibres derived from coconut coir, banana, and sugarcane. Compared to banana and sugarcane fibres, coir fibre tiles had shown enhanced mechanical qualities such as flexural strength and ductility while decreasing self-weight and cost [7]. The fibre length, fibre volumes and casting pressure were studied [8] for randomly distributed coir fibre-reinforced cement composites as low-cost materials for roofing sheets. The study found that the most cost-effective composite is 3.75 cm long with a 7.5% fibre volume fraction and 1.67 MPa with casting pressure, outperforming locally available roofing materials in terms of cost. The characteristics of panels strengthened with treated coir fibres were studied and the treatment in cold and hot water improved the coir's ability to strengthen compounds by enhancing the interfacial adhesion between the coir and the matrix [9]. When coconut fibres up to 38 mm and a volume percentage of 4% were utilised, [10] the mechanical properties of cement paste composites improved in terms of tensile strength and modulus of rupture when reinforced with 38mm long coconut fibre and volume fractions of 2%, 3%, 4%, 5%, and 6%, respectively. A further increase in length or volume fraction could reduce the strength of the composite. The study [11] found that natural fibres like coir and sugarcane bagasse enhance mechanical properties like compressive strength, split tensile strength, modulus of rupture, and flexural performance.

However, at earlier curing ages, natural fibres improve strength qualities, but at later curing, the rate of increments is slower than in standard concrete elements.
Coconut fibres have a high potential to be used in composites for non-structural components since they are ductile, energy-absorbing, and beneficial as a construction material in civil engineering [12]. Comparing costs had shown that this composite was significantly less expensive than the readily available roofing materials. Abdulla et al. [13] examined the effect of natural fibre content on the physical, mechanical, and fracture behaviour of composite cement reinforced with coconut fibre and found that the composite with nine weight per cent of coconut fibre had the highest compressive strength and modulus of rupture. The Indian Plywood Industries Research & Training Institute and Coir Board (IPIRTI), Bengaluru, clearly explained the steps in purchasing the coir felt, dimensioning the fibres, compression, bonding, and preservative resins, stabilising and drying the coir mats, hot pressing them to create rigid sheets, and finishing the sheets. When roofing tiles were exposed to the atmosphere, water absorption was seen to cause a loss in bulk density and an increase in the void volume, with less adsorption than was observed in the laboratory [14] and when tiles are exposed to a tropical climate, has caused a severe reduction in mechanical properties. This behaviour can be attributed to the alkaline attack, the natural fibre's petrifaction, and the cement matrix's progressive micro-cracking [15]. Also, Uzoegbo et al. [16] have concluded the same. In addition, the strength of roofing tiles generally depends on the admixture rather than the type of natural fibre, as the shape is an essential parameter while testing under flexure. Otunyo et al. stated [17] that up to 6% of coconut fibre can be included in roofing tiles without significantly affecting their mechanical characteristics, but more than that can have a detrimental impact on all of the qualities of the tiles. However, it can increase the resistance to crack propagation. Santosh et al, [18] reported that 20% fly ash and 0.3% fibres by volume are optimum for all studied mechanical properties.

3. Materials and experiments conducted

Cement (Ordinary Portland cement - (OPC) of 53 grade confirming to IS: 12269 [19] was used.

Table 1. Properties of GGBS

A.	Physical Properties	GGBFS
1	Specific Gravity	2.92
2	Fineness (cm^2/gm)	4000
3	Glass Content (%)	85
4	Loss of Ignition %)	2.1
B.	Chemical Properties	GGBFS
1	Cao	40.3
2	SiO_2	43.4
3	$Al_2 O_3$	12.5
4	Na_2O	0.9
5	K_2O	0.6
6	MgO	1.5
7	LOI	2.1

GGBS (Ground Granulated Blast Furnace Slag) properties were listed in Table 1. Portable water available in the concrete technology laboratory was used. The fine aggregate was procured locally and conformed to Indian standard Specifications [20] and the properties were listed in Table 2. The brown coir fibre used in the experiment is shown in Fig 1 and properties were shown in Table 3.

Table 2. Properties of fine aggregate

Property	Description
Particle size	75 microns to 4.75 mm
Fineness modulus	2.8
Specific gravity	2.60
Water absorption	1.2%

Table 3. Properties of brown coir fibre

Property	Description
Fibre length	Typically ranges from 15 to 20 cm.
Fibre diameter	Ranges from 100 to 200 microns
Tensile Strength	High
Moisture content	Absorbs and retains moisture well
Density	1.4 g/cc
Swelling in water (diameter)	5%
Moisture at 65% RH	10.50%
Breaking elongation%	30%
Place of procurement	Locally available in Hyderabad



Figure 1. Coir Fibre



Figure 2. Wooden Mould

3.1. Fabrication of mould

A 250 x 150 x 15 mm wood mould was fabricated to cast the specimen. Commercially available corrugated AC Sheets were used to corrugate the specimen (Figure 2)

3.2. Mortar Mixing

Composites were made by a manual mix of coir fibre, cement, water, and GGBS of different proportions, and the selected water-to-cement ratio was 0.5.

3.3. Casting of tiles

Initially, a homogenous dry mix was prepared by mixing cement with GGBFS and sand; later, water was added, and after three minutes of mixing, brown coir fibre was added to the slurry. Three sets of samples, each comprising the combination of mix proportions of dimension 250x150x15 mm, were cast to conduct compression, water absorption and flexure tests.

3.4. Curing

After demolding, Curing was done by placing the tiles in a water pond, and the specimens were kept for curing for seven days and 28 days. The average compressive strength, three-point flexure strength and water absorption are calculated according to IS: 516 [21].

3.5. Water Absorption Test

The water absorption test measures the moisture quantity that roofing tile may absorb. Water absorption is expressed as a per cent by weight of water against the dry weight of the individual tiles after 24 hours of soaking in water.

3.6. Flexure Test

To perform the flexure test, the tile is placed apart by a distance of L, and a load is applied at the centre of the tile until it breaks. The maximum load at the point of failure, P, is recorded and used in the calculation formula to determine the flexure strength. A hydraulic jack was utilized to apply the load at the centre of the tiles.

4. Results and Discussion

Table 4: Test results of the various mechanical properties

% OF GGBFS	% of Fibre	water absorption		Compressive Strength (MPa)		flexural strength (MPa)	
		7D	28D	7D	28D	7D	28D
0	0.0	8.5	7.2	11.47	21.55	3.10	4.3
10		8.1	7.19	10.67	21.33	2.66	4.34
20		8.15	7.16	10.88	22.83	2.75	4.35
30		8.35	7.14	11.07	23.87	2.79	4.37
40		8.5	7.25	11.44	23.33	2.83	4.41
50		8.6	7.3	11.68	23.25	2.88	4.43
10	0.2	8	7.2	10.80	21.60	2.83	4.52
20		8.1	7.35	10.93	22.85	2.83	4.61
30		8.25	7.48	11.01	23.97	2.79	4.78
40		8.3	7.6	11.17	23.23	2.76	4.83
50		8.4	7.65	11.12	23.15	2.75	4.87
10	0.5	8.02	7.3	10.93	21.68	2.66	4.52
20		8.15	7.5	11.07	22.91	2.68	4.56
30		8.28	7.65	11.28	24.00	2.69	4.61
40		8.35	7.7	11.39	23.87	2.73	4.68
50		8.48	7.72	11.33	23.65	2.70	4.70
10	0.8	8.2	7.29	11.07	21.76	2.83	4.77
20		8.27	7.52	11.17	22.99	2.88	4.78
30		8.35	7.67	11.28	24.13	2.86	4.83
40		8.4	7.78	11.41	24.40	2.84	4.86
50		8.5	7.8	11.36	23.33	2.79	4.85
10	1.0	8.26	7.3	11.01	21.68	2.88	4.74
20		8.34	7.54	11.07	21.73	2.84	4.78

30	8.5	7.7	11.23	22.00	2.82	4.78
40	8.52	7.8	11.28	22.37	2.79	4.81
50	8.59	7.9	11.20	22.32	2.75	4.79

5. Discussion on Water absorption results

The depiction of water absorption with different percentages of cement replacement with GGBS and coir is shown in Table 4.

5.1. Water absorption test results in % for tiles with GGBS

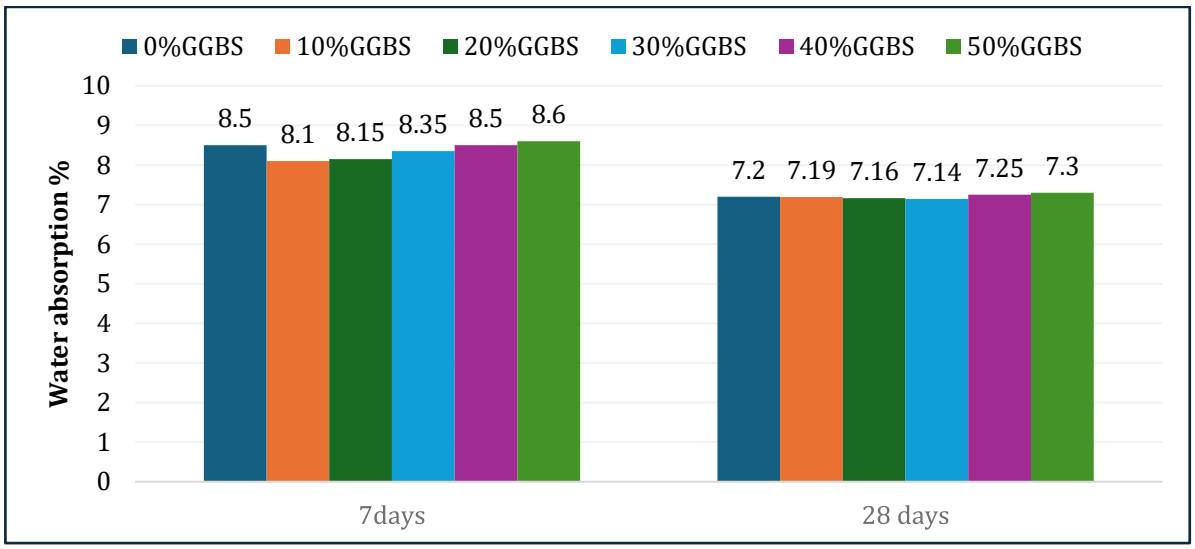


Figure 3. Water Absorption of Tiles with GGBS

Table 4 and Figure 3 show that in the case of conventional cement tiles, the water absorption is 8.5% for seven days and 7.2% for 28 days. The regression in the water absorption is observed by 1.3% within 28 days of casting. It is observed that there is no significant change in water absorption if GGBS replaces the cement. However, it is to be noted that as we increase the GGBS percentage up to 30%, a small decrease in water absorption and an increase when cement is replaced with GGBS to the extent of 40% to 50% due to porous tiles.

5.2. Water absorption results in a percentage for tiles, including coir, with partial replacement of cement with GGBS.

From Fig 4 and 5, the percentage of water absorption increased with the increase in the coir addition percentage. The reason is that coir fibre absorbs more water, increasing water absorption. However, the change is insignificant in affecting the overall performance of resulting tiles as the percentage of water absorption is less than 10%.

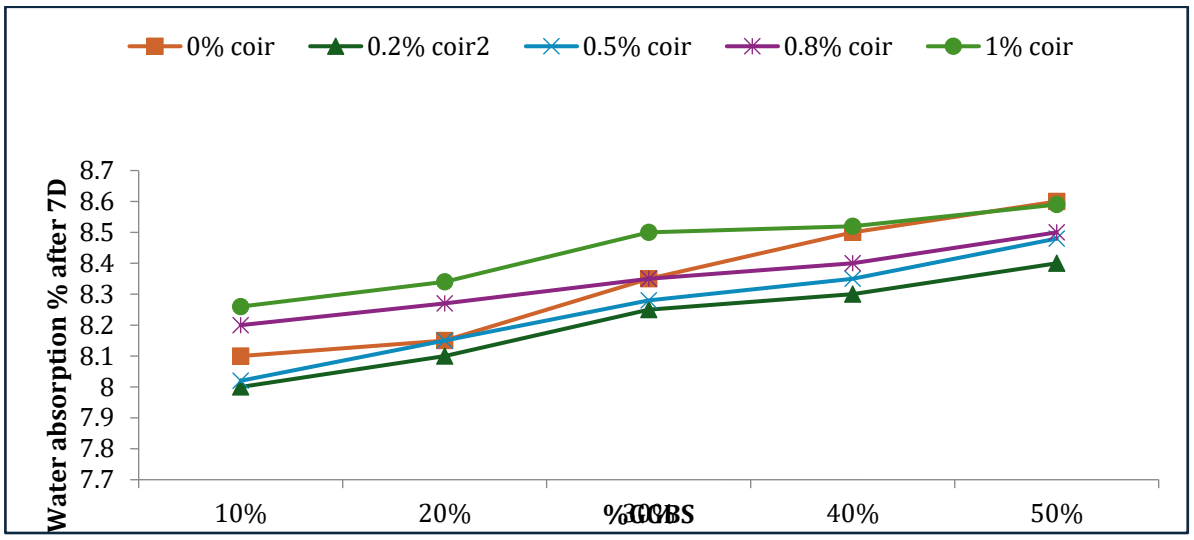


Figure 4. Water Absorption Graph of Tiles with GGBS at seven days of water curing (10%, 20%, 30%, 40% and 50%) and coir 0.2%, 0.5%, 0.8% and 1%)

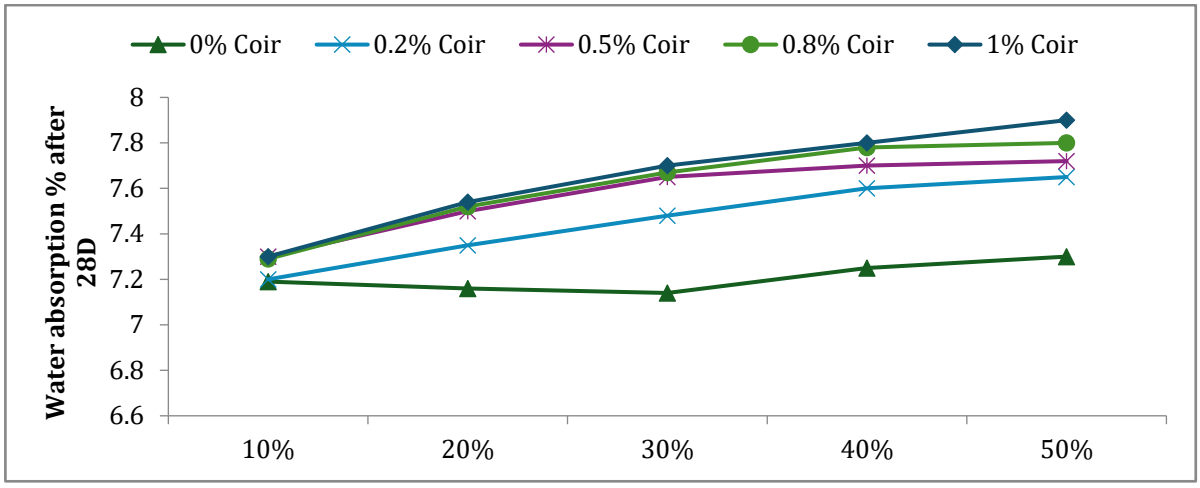


Figure 5. Water Absorption Graph of Tiles with GGBS at 28days of water curing (10%, 20%, 30%, 40% and 50%) and coir (0.2%, 0.5%, 0.8% and 1%)

6. Compression test results

6.1. Discussion on Results of compression test of tiles of various proportion replacements of GGBS

The Table 4 and Figure 6, the 7 and 28 days, the strength of plain mortar was 11.4 N/mm^2 and 21.54 N/mm^{2,} respectively. It is also observed that for various proportions of cement and GGBS without coir, an increase in the compressive strength (at 28 days) of tiles up to 30% replacement of GGBS, indicating 30% replacement gives optimum results compared to conventional plain tiles.

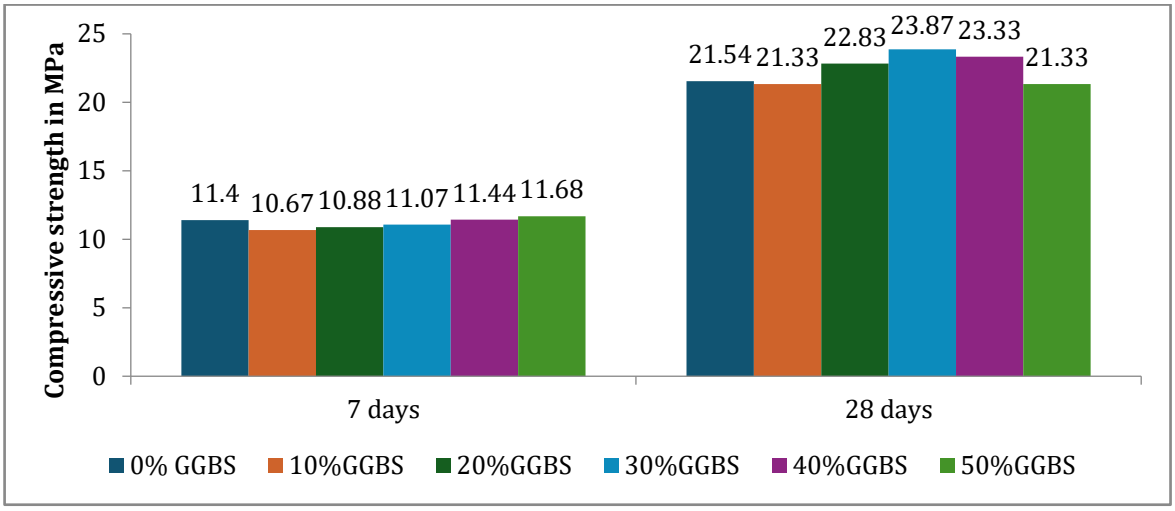


Figure 6. Compressive Strength of tiles with GGBS (10%,20%,30%,40% and 50%)

6.2. Results of compression test of tiles (% of GGBS + 0.2% of coir)

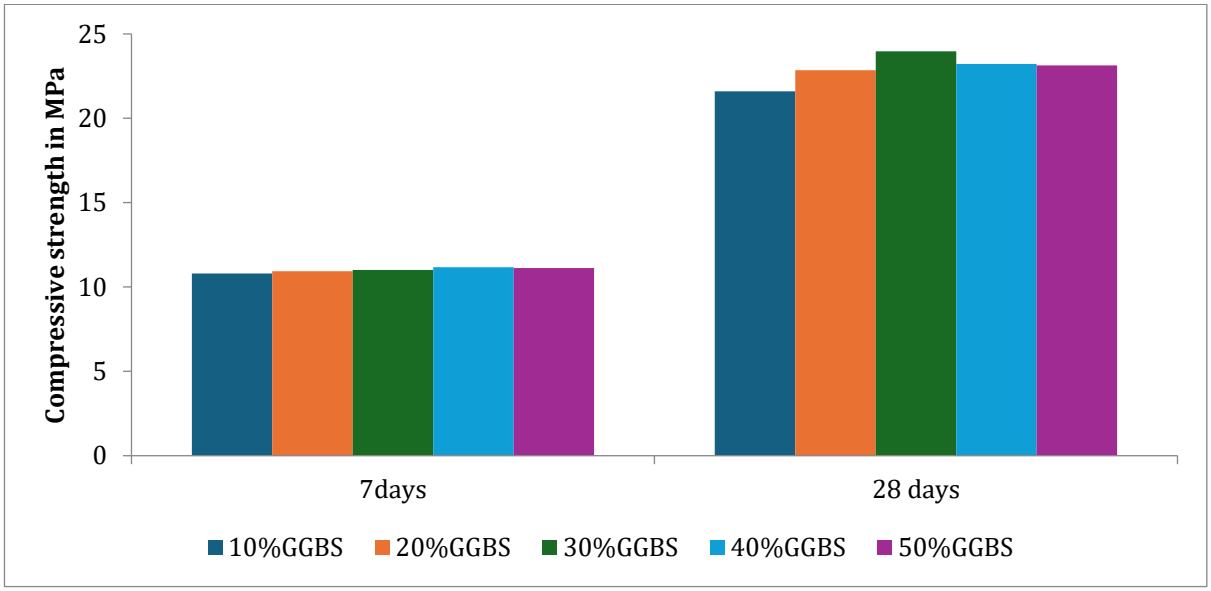


Figure 7. Compressive Strength of tiles (0.2% of coir + GGBS (10%,20%,30%,40% and 50%)

Referring to Figure 7, there was a slight variation in the compressive strength by adding 0.2% of coir fibre. It is observed that 30% of GGBS with the addition of 0.2% of coir fibre has shown similar strength when compared to tiles with only 30% replacement with GGBS; therefore, adding coir doesn't diminish the strength of tiles.

6.3. Results of compression test of tiles (% of GGBS + 0.5% of coir)

From Figure 8, the compressive strength of roofing tiles with the various proportions of GGBS and 0.5% of coir fibre was a marginal increase in the compressive strength. Maximum Compressive strength was observed at 30% of GGBS replacement with the addition of 0.5% of coir fibre, 11% more than the control.

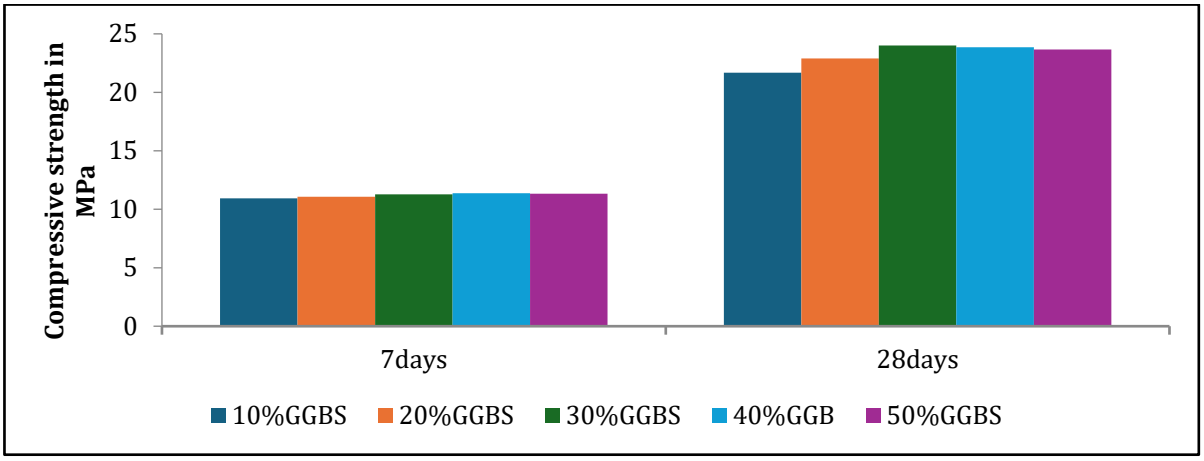


Figure 8. Compressive Strength of tiles (0.5% of coir + GGBS (10%,20%,30%,40% and 50%)

6.4. Results of compression test of tiles (% of GGBS + 0.8% of coir)

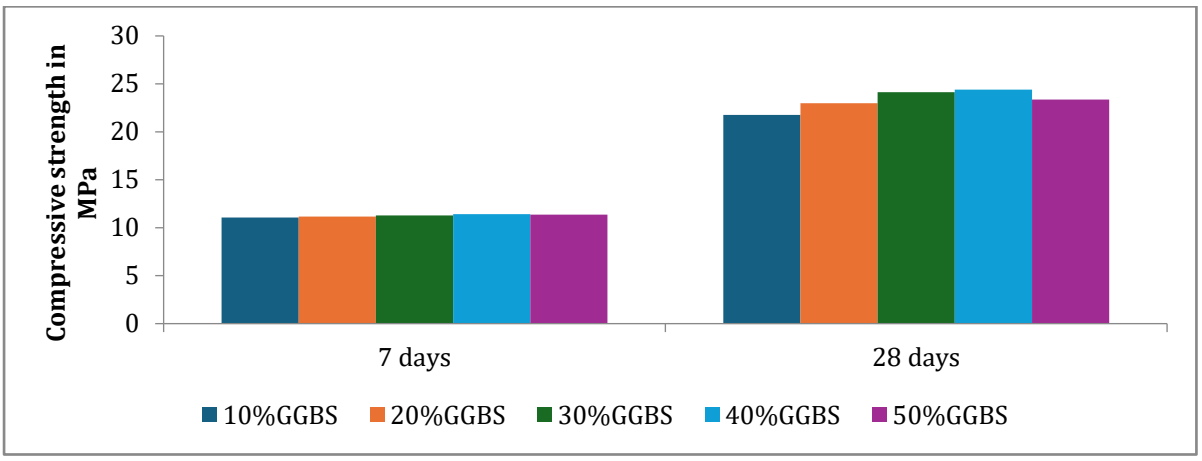


Figure 9. Compressive Strength of tiles (0.8% of coir + GGBS (10%,20%,30%,40% and 50%)

From Figure 9, it was observed that for various proportions of GGBS and 0.8% of coir fibre, the compressive strength was increased up to 40% replacement of GGBS by 13% with the addition of 0.8% of coir fibre.

6.5. Results of compression test of tiles (% of GGBS + 1% of coir)

From Figure 10, the compressive strength of roofing tiles with various proportions of GGBS and 1% of coir fibre, a marginal decrease in the strength is observed as compared to the other mix proportions of the coir fibre, and the decrement is due to overdosage of fibre in the matrix.

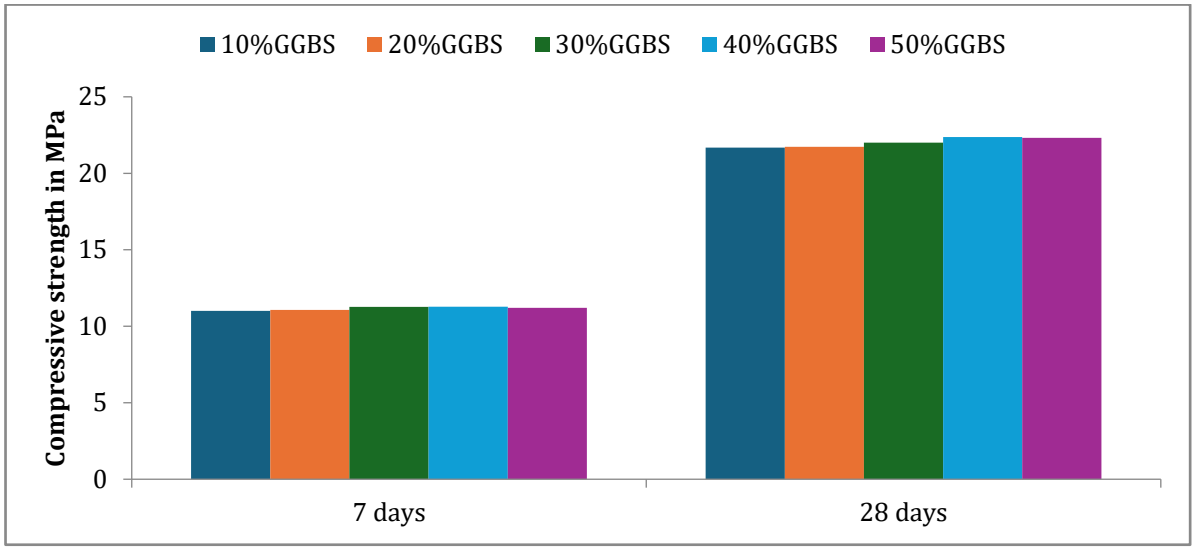


Figure 10. Compressive Strength of tiles (1% of coir + GGBS (10%,20%,30%,40% and 50%))

6.6. Comparison of different fibre contents on 28D Compressive strength

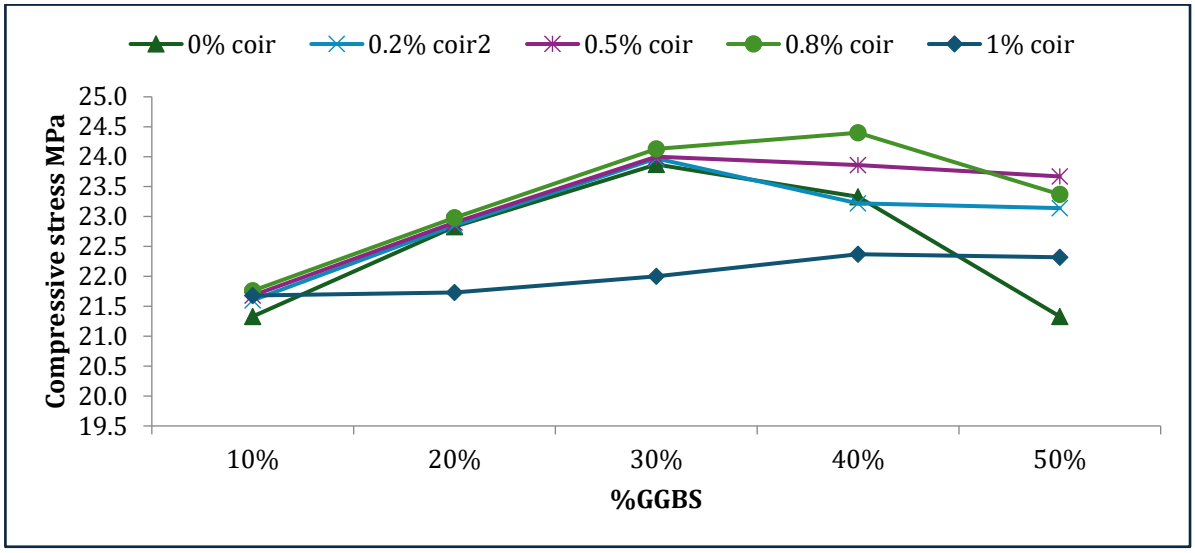


Figure 11. 28-day Compressive Strength of tiles with different coir contents

From Figure 11 it is observed that 0.8% coir fibre along with 40% GGBS results in maximum compressive strength.

7. Flexure Test

Table 4 it shows the flexure test results of tiles with various proportions replacement of GGBS in cement and addition of coir fibre.

7.1. Discussion on Results of Flexure test of tiles of various proportion replacements of GGBS

The Table 4 and Figure 12, for the 7 and 28 days, the flexural strength of plain mortar was found to be 3.1N/mm^2 and 4.34 N/mm^{2,} respectively. It is also observed that replacement of cement with GGBS up to 50% has shown improved flexural strength.

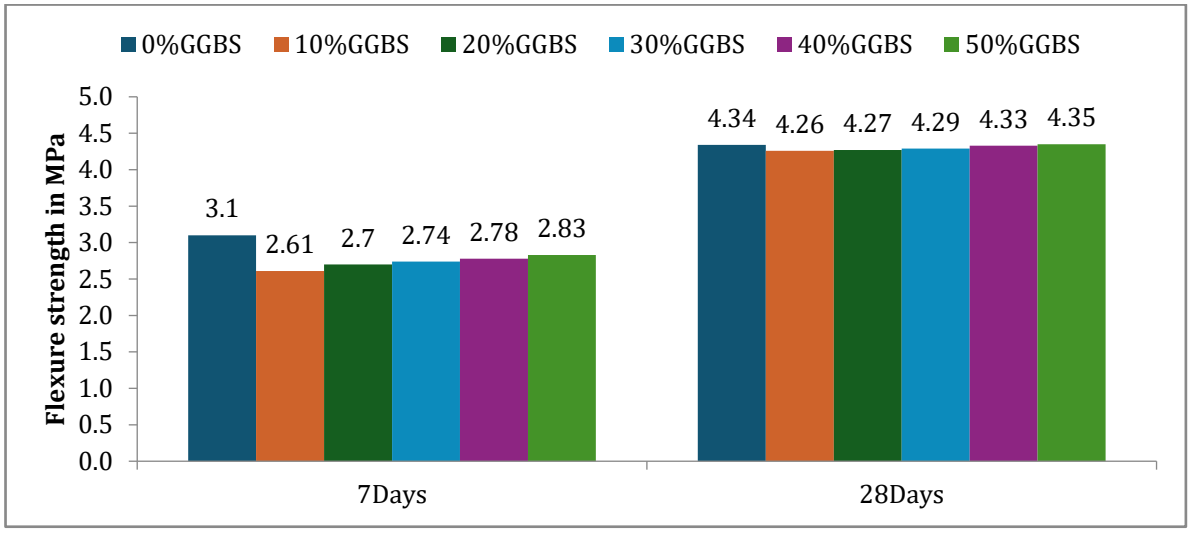


Figure 12. Flexural Strength of tiles with GGBS (10%, 20%,30%,40% and 50%)

7.2. Comparison of different fibre contents on 7D Flexural strength

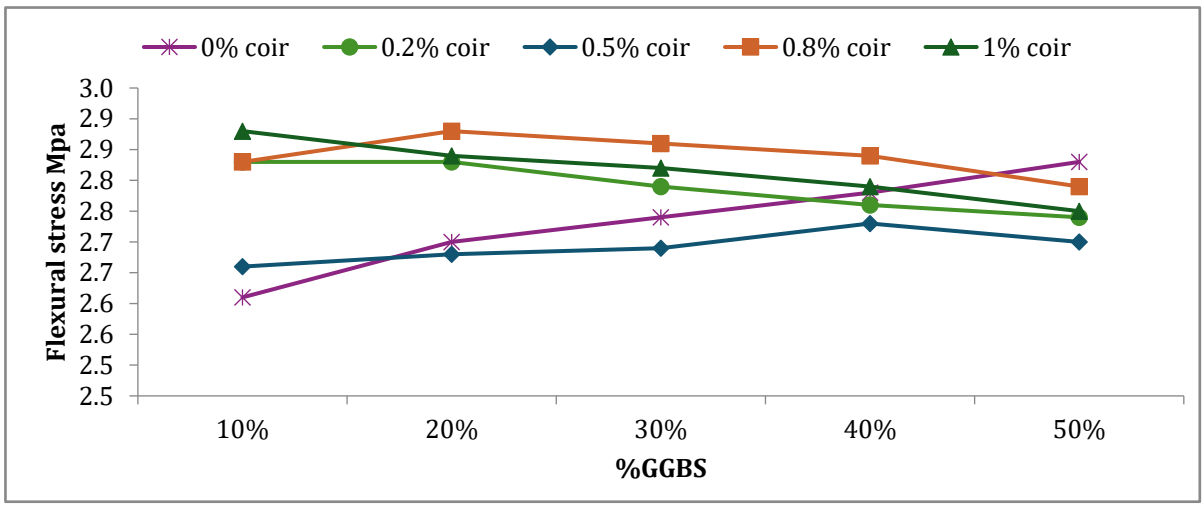


Figure 13. 7-Day Flexural Strength of tiles with different fibre contents

Referring to Figure 13, the 7-day flexural strength was high with 0.8% coir fibre with 20% of GGBs, whereas the plain mortar without coir has shown an improved strength with increments in GGBS.

7.3. Comparison of different fibre contents on 28D Flexural strength

Referring to Figure 14, the 28-day flexural strength was high with 0.8% coir fibre with 40% GGBS, whereas the plain mortar without coir had less strength as compared to all the fibres included. The presence of fibre in tiles has improved their strength as per the earlier literature. The addition of 0.8% coir fibre has shown an improved strength of 14% compared to plain tiles.

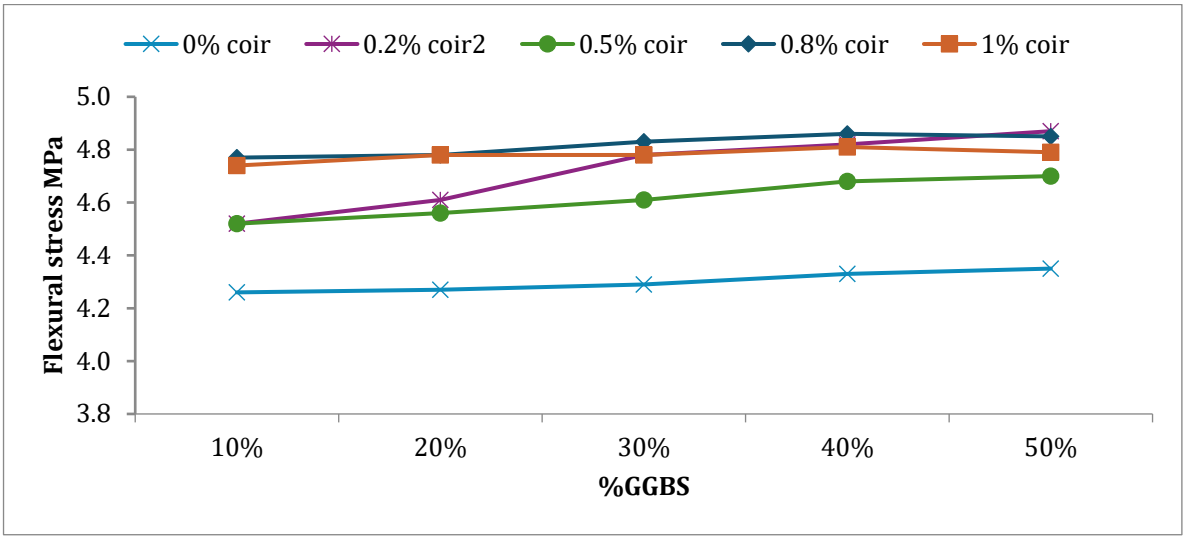


Figure 14. 28-Day Flexural Strength of tiles with different fibre contents

8. Relation between compressive, Flexural strength and percentage water absorption of roofing tiles

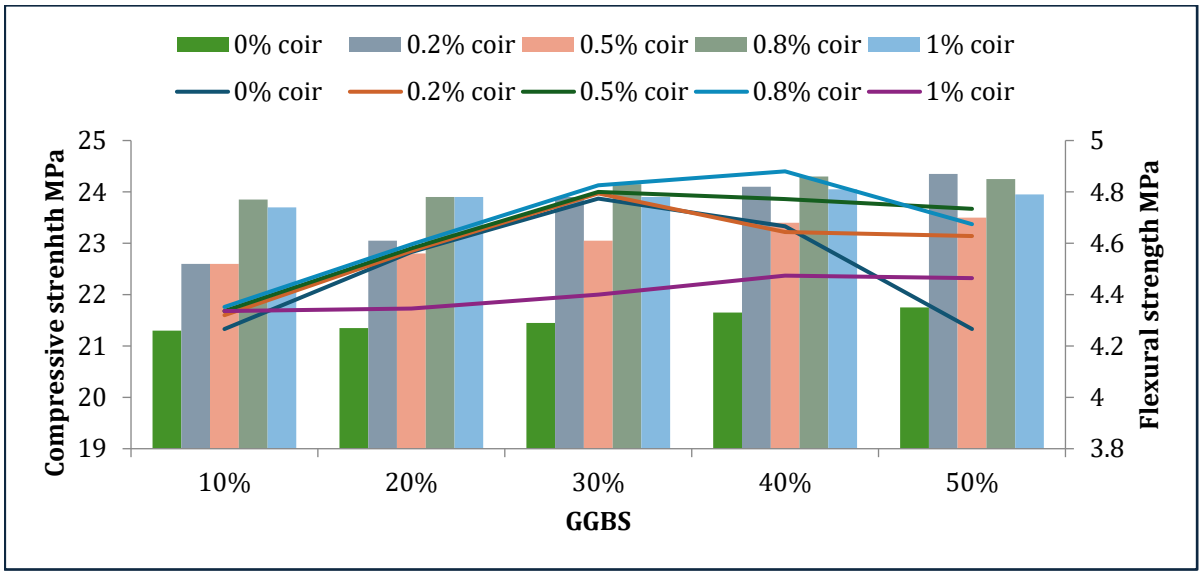


Figure 15. 28-Day comparison of Flexural Strength and compressive strength of tiles with different fibre contents and percentage of GGBS

From Figure 15 it is observed that 0.8% Coir has the highest flexural strength of 4.86MPa and has a compressive strength of more than 0.2 and 0.5% fibres volume, in addition, if the quantity is more than 0.8% volume it causes balling of fibres, hence from the practical point of view 0.8% volume fraction of fibre is workable.

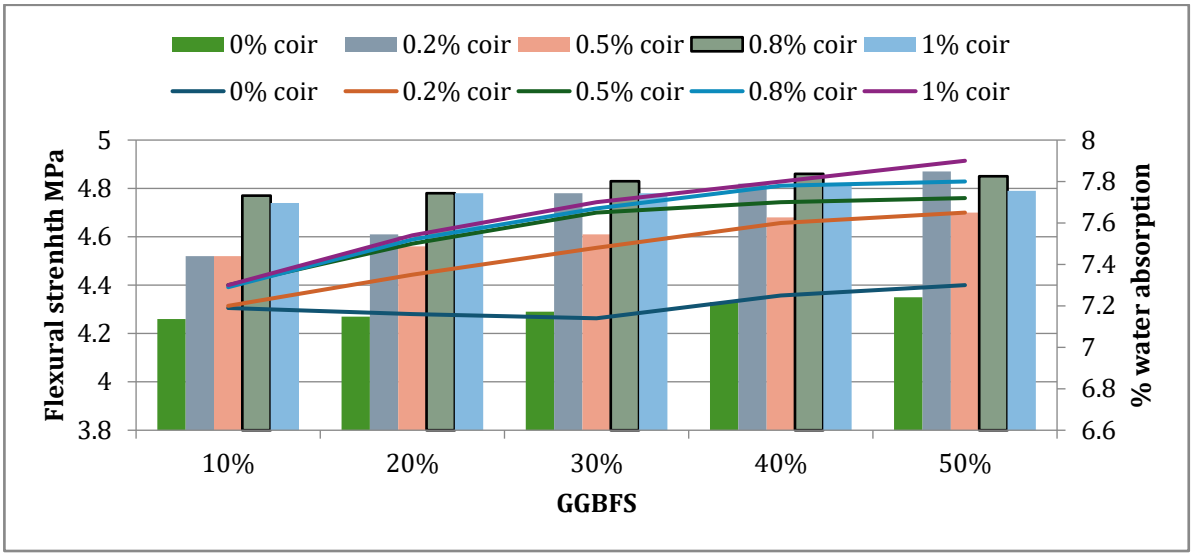


Figure 16. 28-Day comparison of Flexural Strength and percentage water absorption of tiles with different fibre contents and percentage of GGBS

Referring to Figure 16 the 0.8% coir fibre with 50% of GGBS has the highest flexural strength and also has water absorption lower than 1% of coir volume, hence it is recommended to use 0.8% coir along with 40% GGBS replacement in the tile making.

9. Results of Ductility of Roofing Tiles

9.1. Results of ductility on tiles of various proportion replacement of GGBS

Flexural cracks in tiles randomly occurred at the bottom, spreading towards the compressed concrete zone as the load increased. Coir fibre-incorporated tiles changed failure mode from mortar-crushing to ductile, with fewer cracks and width. Fig. 17, the replacement of cement with 40% GGBS has shown an improved ductility.

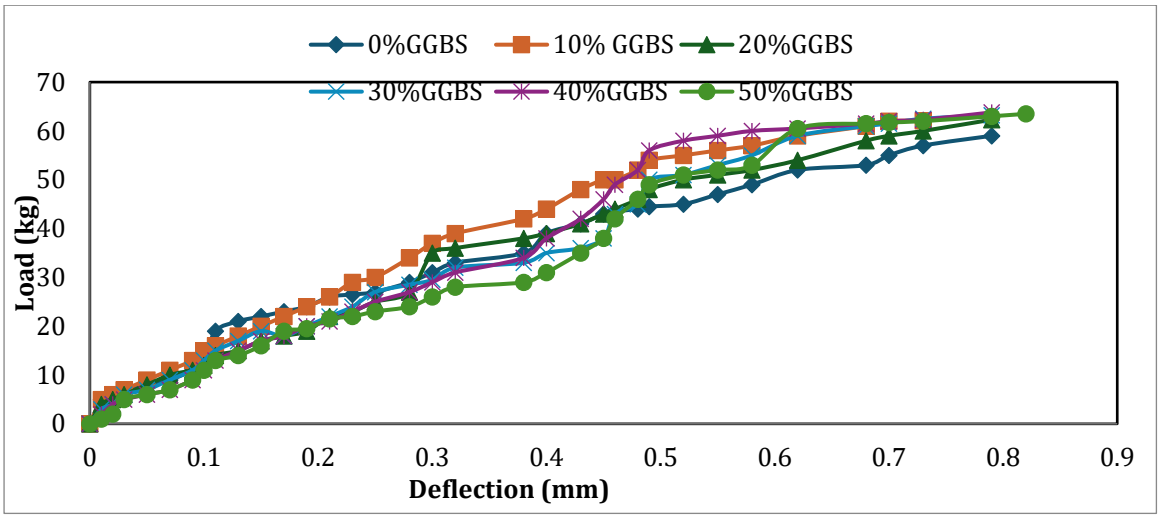


Figure 17. Load v/s Deflection for replacement of GGBS at 28 days

9.2. Result of flexure test on tiles of (various proportions of GGBS +0.2% of coir fibre)

Figure 18 shows improved ductility with the addition of coir fibres. It was observed that there were small variations in flexure strength. For 40% replacement of GGBS and coir fibre at 0.2% the deflections were less compared to other replacements.

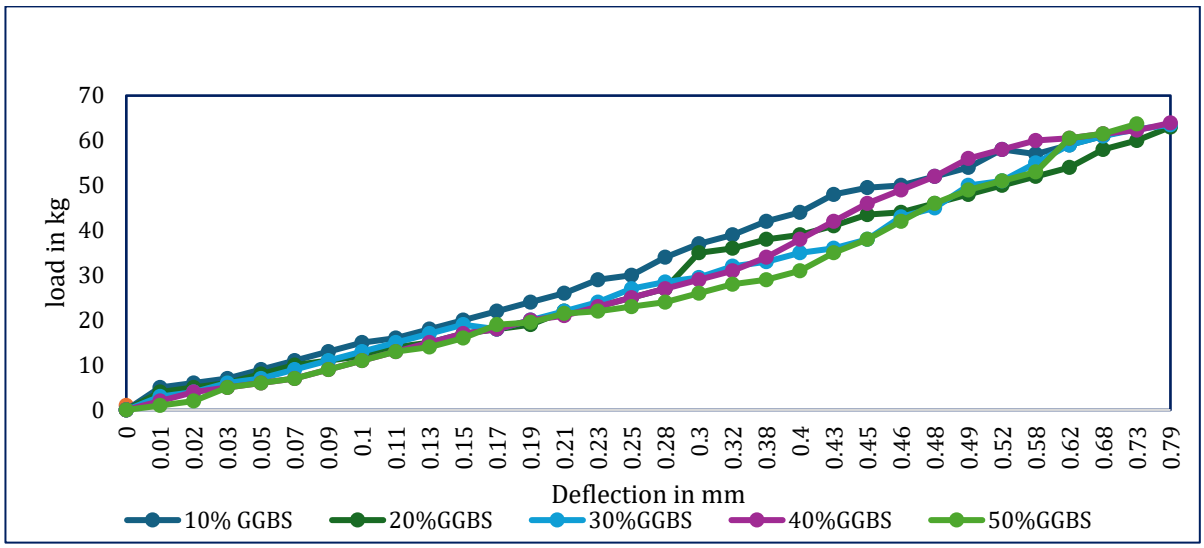


Figure 18. Load v/s Deflection for replacement of GGBS and 0.2%coir for 28days

9.3. Result of flexure test on tiles of (various proportions of GGBS +0.5%of coir)

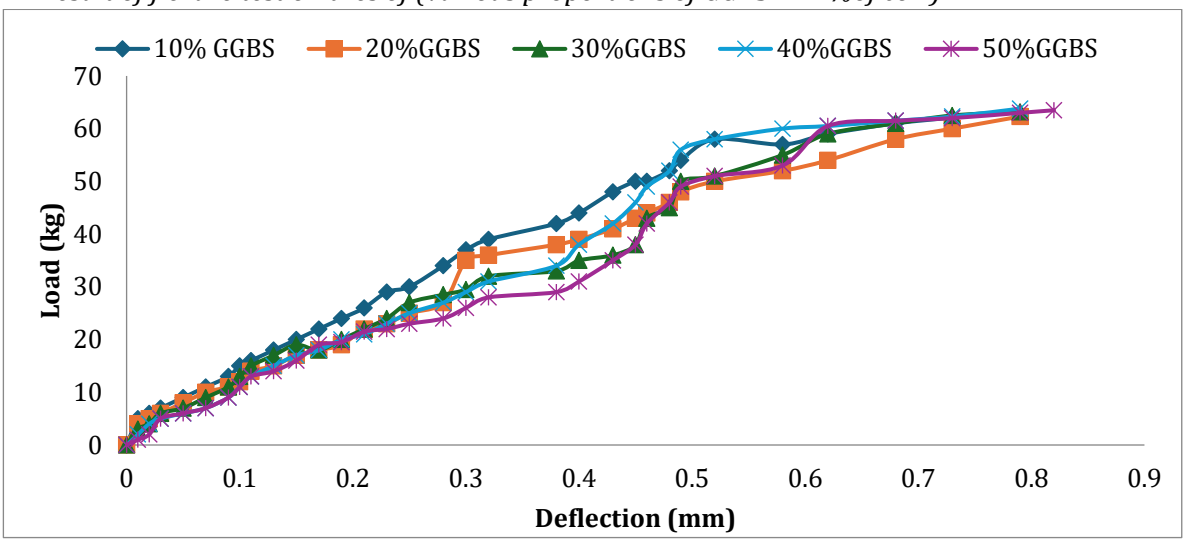


Figure 19. Load v/s Deflection for replacement of GGBS and 0.5%coir for 28days

From the Figure 19 the stiffness of 50% replacement of cement with 0.5% Coir is more than other combinations.

9.4. Result of flexure test on tiles of (various proportions of GGBS +0.8%of coir)

From the Figure 20 the stiffness of 50% replacement of cement with 0.8% Coir is more than other combinations but at ultimate loads 40% GGBS is reporting the maximum load carrying capacity.

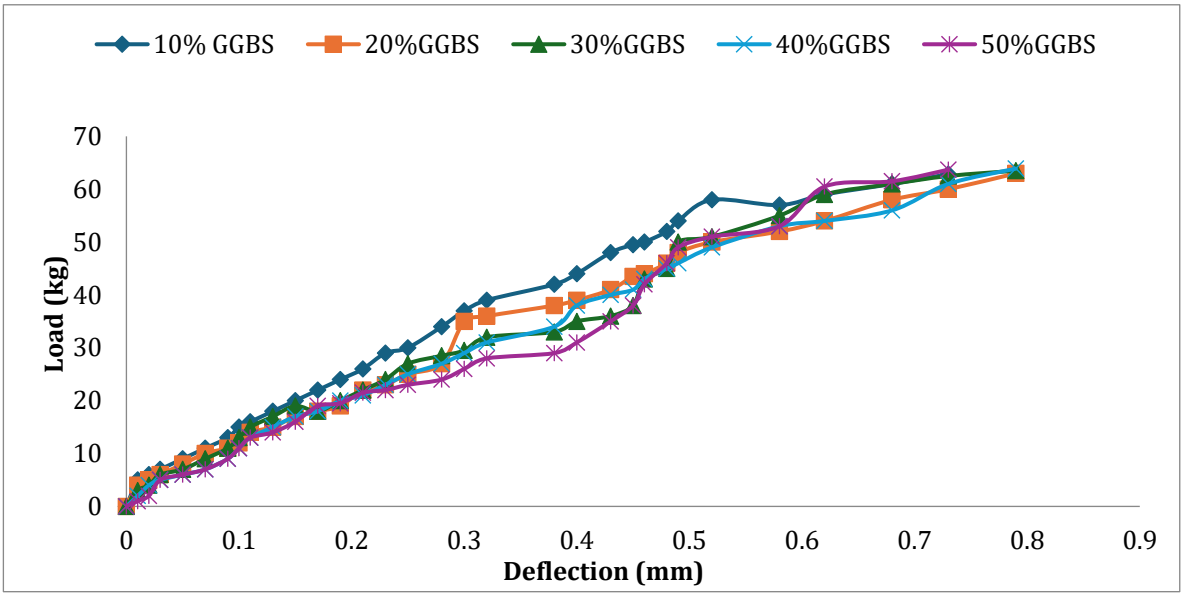


Figure 20. Load v/s Deflection for replacement of GGBS and 0.8%coir for 28days

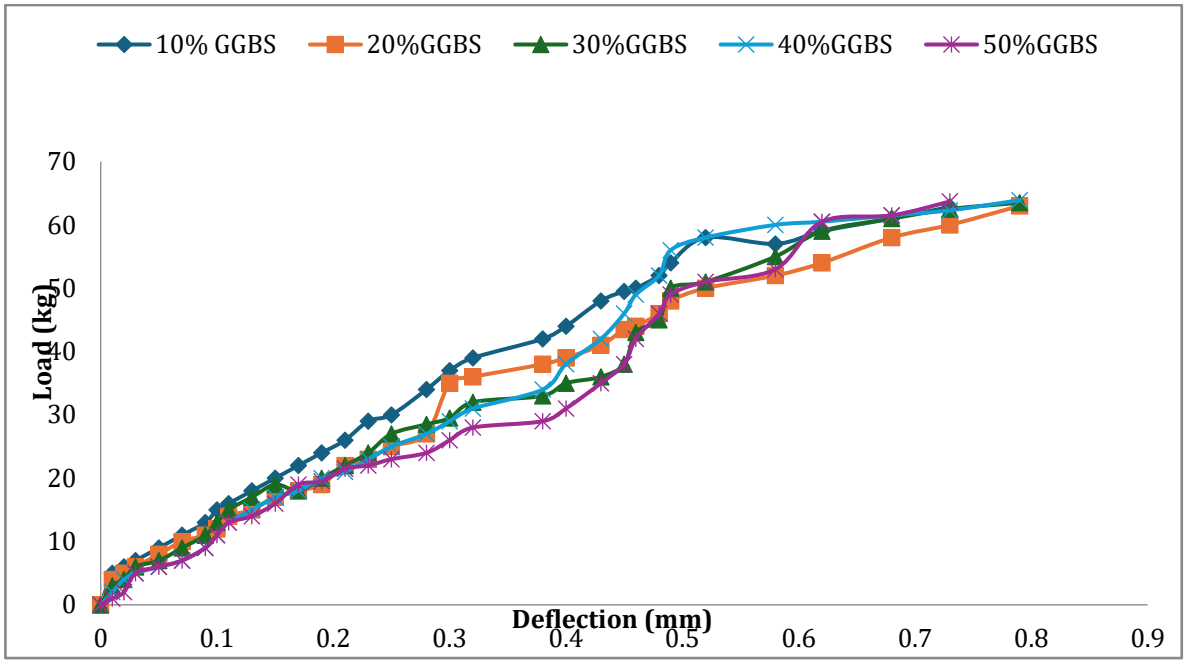


Figure 21. Load v/s Deflection for replacement of GGBS and 1%coir for 28days

From Figure 21 the stiffness of 40% replacement of cement with 1.0% Coir is more than other combinations.

10. Conclusions

10.1. Water absorption

The water absorption for plain tiles was 7.2%, and by the addition of GGBS (10%, 20%, 30%, 40% and 50%) this has been decreased up to 30% and by the addition of the coir fibre, there is an increase in the water absorption.

10.2. Compressive strength

The compressive strength for the plain tiles was 21.54N/mm^2 and it was increased up to 30% replacement of cement with GGBS and thereafter there was a decrease in the compressive strength. With the addition of coir fibre for 0.2% there was an increase in strength up to 30% and then it decreased.

Using 0.5% of coir fibre there was an increase in compressive strength of up to 30% and for the 0.8% addition of coir fibre, it was observed that there was an increase in compressive strength of up to 40%. For the addition of 1% of coir fibre, the strength was decreased compared to 0.8% of coir fibre.

For the tiles with coir fibres, there is a difference in cracking pattern. It is observed that the cracks are sharper for the tiles without coir fibre. This can be justified because the presence of coir fibre in roofing tile arrests the crack propagation. Maximum compressive strength of 24.4N/mm^2 was achieved at an optimum combination of fibre 0.8% and replacement of GGBS of 40%.

10.3. Flexure strength

Flexure strength for tiles with 0.8% coir fibre had the highest strength and the specimens with 30% GGBS replacement were better than other replacements of GGBS.

Compared to plain tiles, an increase in compression and flexure strength for tiles with 0.8% coir fibre and 40% GGBS.

Conclusion: The optimum combination of fibre of 0.8% and replacement of GGBS of 40% in tiles is optimum.

11. References

[1] R. S. P. Coutts, "A review of Australian research into natural fibre cement composites," Cement and Concrete Composites, vol. **27,** no. 5, pp. 518-526, 2005, DOI: 10.1016/j.cemconcomp.2004.09.003.

[2] R. N. Swamy, "Influence of slow crack growth on the fracture resistance of fibre cement composites," nternational Journal of Cement Composites vol. **2,** 1, pp. 43-53, 1980, DOI: 10.1016/0010-4361(80)90435-8.

[3] K. M. F. Hasan, P. G. Horváth, M. Bak, and T. Alpár, "A state-of-the-art review on coir fiber-reinforced biocomposites," RSC Advances, vol. **11,** no. 18, pp. 10548-10571, 2021, DOI: 10.1039/D1RA00231G.

[4] R. Siddique, "Utilization (recycling) of iron and steel industry by-product (GGBS) in concrete: strength and durability properties," Journal of Material Cycles and Waste Management, vol. **16,** no. 3, pp. 460-467, 2014, DOI: 10.1007/s10163-013-0206-x.

[5] P. Darsana, R. Abraham, A. Joseph, A. Jasheela, P. R. Binuraj, and J. Sarma, "Development of Coir-fibre Cement Composite Roofing Tiles," Procedia Technology, vol. **24,** pp. 169-178, 2016, DOI: 10.1016/j.protcy.2016.05.024.

[6] S. Sudheer and J. Omprakash, "Coir Fiber used as Composite Material in Roofing Tiles and Concrete Structures," International Journal of Advanced and Innovative Research, vol. **6,** no. 5, pp. 18-21, 2017.

[7] P. Chakravarthi, A. Karthikeyan, P. Kumar, R. Prakash, and G. Karthik, "Analysis of Reinforced Natural Fibre Cement Composite Roofing Tiles," International Journal of Engineering Science and Computing, pp. 221-229, 2019.

[8] D. J. Cook, R. P. Pama, and H. L. S. D. Weerasingle, "Coir fibre reinforced cement as a low cost roofing material," Building and Environment, vol. **13,** no. 3, pp. 193-198, 1978, DOI: 10.1016/0360-1323(78)90043-4.

[9] C. Asasutjarit, J. Hirunlabh, J. Khedari, S. Charoenvai, B. Zeghmati, and U. C. Shin, "Development of coconut coir-based lightweight cement board," Construction and Building Materials, vol. **21,** no. 2, pp. 277-288, 2007, DOI: 10.1016/j.conbuildmat.2005.08.028.

[10] A. Aziz, P. Paramasivam, and S. L. Lee, Concrete reinforced with natural fibres (Concrete Technology and Design). Surrey University Press, 1984, pp. 106-140.

[11] M. Sivaraja, Kandasamy, N. Velmani, and M. S. Pillai, "Study on durability of natural fibre concrete composites using mechanical strength and microstructural properties," Bulletin of Materials Science, vol. **33,** no. 6, pp. 719-729, 2010, DOI: 10.1007/s12034-011-0149-6.

[12] M. Ali, "Coconut fibre: A versatile material and its applications in engineering," Journal of Civil engineering and construction Technology, vol. **2,** no. 9, pp. 189-197, 2011.

[13] A. Abdullah, "Composite Cement Reinforced Coconut Fiber: Physical and Mechanical Properties and Fracture Behavior," Australian Journal of Basic and Applied Sciences, vol. **5,** pp. 1228-1240, 2011.
[14] G. H. D. Tonoli, S. F. Santos, H. Savastano, S. Delvasto, R. Mejía de Gutiérrez, and M. d. M. Lopez de Murphy, "Effects of natural weathering on microstructure and mineral composition of cementitious roofing tiles reinforced with fique fibre," Cement and Concrete Composites, vol. **33,** no. 2, pp. 225-232, 2011, DOI: 10.1016/j.cemconcomp.2010.10.013.
[15] L. C. Roma, L. S. Martello, and H. Savastano, "Evaluation of mechanical, physical and thermal performance of cement-based tiles reinforced with vegetable fibers," Construction and Building Materials, vol. **22,** no. 4, pp. 668-674, 2008, DOI: 10.1016/j.conbuildmat.2006.10.001.
[16] H. C. Uzoegbo, "Development of test methods for fibre reinforced roofing tiles," International Journal of Advanced Technology in Civil Engineering, vol. **1,** no. 2, pp. 76-81, 2017, DOI: 10.47893/IJATCE.2012.1011
[17] A. W. Otunyo and N. D. Nyechieo, "Mechanical Properties and Fracture Behaviour of Coconut Fibre Reinforced Concrete (CFRC)," American Journal of Civil Engineering and Architecture, vol. **5,** no. 5, pp. 208-216, 2017, DOI: 10.12691/ajcea-5-5-5.
[18] B. Santhosh, N. Ragharendra, J. Deepesh, S. Vishal, and P. Ayush, "Strength of corrugated roofing element reinforced with coir," International Research Journal of Engineering and Technology (IRJET), vol. **4,** pp. 2371-2374, 2017.
[19] IS:12269-2013 "Specification for ordinary Portland cement, 53 grade (first revision)," Bureau of Indian Standards, New Delhi, India.
[20] IS:383-2016 "Coarse and fine aggregate for Concrete - Specification (Third Revision)," Bureau of Indian Standards, New Delhi, India.
[21] IS:516-1959 "Methods of Tests for Strength of Concrete," New Delhi, India.

Acknowledgements

The authors acknowledge the laboratory support by Chaitanya Bharathi Institute of Technology for carrying out the experimentation and financial support by Vasavi College of Engineering, Hyderabad.

IOP Conference Series: Earth and Environmental Science

PURPOSE-LED PUBLISHING™

PAPER • OPEN ACCESS

Investigating alkali-activated concrete with recycled aggregate substitution in experimental research

To cite this article: B. Sridhar and M.V.S.S. Sastri 2024 *IOP Conf. Ser.: Earth Environ. Sci.* **1409** 012015

View the article online for updates and enhancements.

You may also like

- Deformation mechanism of the dual thermo-sensitive hydrogel bilayer structure
Huilong Jiang, Jincheng Lei and Zishun Liu
- Sulfate resistance of alkali-activated flyash-slag-lime concrete: comparative study of drying-wetting cycles and conventional exposure
H M Jagadisha, Shreelaxmi Prashant, Poornachandra Pandit et al.
- Acetylammonium chloride as an additive for crystallization control and defect passivation in $MAPbI_3$ based perovskite solar cells
Akhil Alexander, Varun Srivastava, Poovannan Ravichandran et al.



This content was downloaded from IP address 47.247.77.11 on 27/11/2024 at 05:36

Investigating alkali-activated concrete with recycled aggregate substitution in experimental research

Sridhar, B.[1*] and Sastri, M.V.S.S.[1]

[1]Department of Civil Engineering, Vasavi College of Engineering (A), Hyderabad, Telangana, India.

[*]Email: b.sridhar@staff.vce.ac.in

Abstract. In the present experimental investigation, a constant (optimum) percentage of GGBFS and fly ash in Alkali activated concrete (AAC) of M40 grade equivalent concrete. The natural aggregates are incorporated at percentages of 0.5 and 1.0 in the AAC composition. The studies indicate that Fly ash AAC demonstrates lower strength due to the necessity of heat curing for proper development, while the inclusion of Recycled Concrete Aggregate (RCA) leads to decreased compressive, split tensile, and flexural strengths, indicating a detrimental effect on mechanical properties. Despite slightly improved performance with 100% RCA content, it remains inferior to natural aggregates, attributed to adhered cement mortar potentially enhancing strength properties, which shows the need for further research to optimize mix designs and fully exploit the benefits of these alternative materials in AAC production.

Keywords: Alkali activated concrete, compressive strength, split tensile strength, recycled concrete aggregate

1. Introduction

Traditional Portland cement-based concrete, although widely used, contributes significantly to carbon emissions and resource depletion. In response to these challenges, alternative materials and technologies are being explored to develop more sustainable construction practices. The construction industry is exploring alternative materials like alkali-activated concrete to reduce its environmental impact and meet infrastructure demands. Geopolymers, synthesized from aluminosilicate precursors, can be produced at ambient temperatures, reducing carbon emissions compared to traditional Portland cement-based concrete. Recycling building and demolition debris is an important choice as a way to reduce the pressure on landfills and conserve resources, especially when it comes to aggregates. In addition to having properties similar to those of natural aggregates, recycled aggregates made from demolished concrete buildings offer a sustainable way to solve the problems of waste management and a shortage of raw materials in the building industry. By combining these two ecologically friendly strategies, research on alkali-activated concrete that substitutes recycled aggregate offers a robust chance to advance green building techniques [1]. The alkali-activated system consists of alumino-silicate sources combined with one or more alkaline activators.

The adoption of readily available commercial by-products such as fly ash and blast furnace slag in construction serves multiple purposes. First and foremost, it addresses the growing demand for construction materials in a sustainable manner. Utilizing these by-products, which

Content from this work may be used under the terms of the Creative Commons Attribution 4.0 licence. Any further distribution of this work must maintain attribution to the author(s) and the title of the work, journal citation and DOI.
Published under licence by IOP Publishing Ltd

would otherwise require disposal, in construction, not only reduces the burden on waste management but also cuts down on the need for raw materials extraction [2].

1.1. Aim and Objectives

This report aimed to analyze various methodologies for Geopolymer production and evaluate their suitability as construction materials for industrial applications. Specific topics covered include:

- To determine the workability of recycled concrete aggregates geopolymer concrete using Fly ash and GGBFS for 6M and 8M.
- To investigate the mechanical properties of geopolymer concrete made with recycled concrete aggregates, utilizing fly ash and GGBFS, under ambient temperature conditions.

2. Literature review

A thorough assessment of the state of knowledge on the AAC was provided by Amer *et al.*[3]. According to the study, AASC outperforms PCC in terms of bond performance and mechanical attributes. Adding up to 500 kg/m^3 of GGBFS to AASC enhances compressive strength. Mishra *et al.* [4] reviewed the combination of GGBFS with other mineral admixtures and concluded that blending GGBFS with aluminosilicate wastes in appropriate proportions offers a sustainable alternative for construction applications, reducing reliance on conventional cement. These alkali-activated concrete demonstrated minimal permeability to chloride ions and reduced water absorption. Pavithra *et al.* [5] developed a mix design methodology for RCA concrete using a two-stage mixing, incorporating natural and recycled aggregates for strength relation. Abhishek et al. [6] investigated the potential of incorporating industrial and agro-based by-products as additives to enhance the performance of slag and fly ash-based materials, thereby influencing their setting time and flow properties. The molarity of NaOH and the ratio of Na_2SiO_3 to NaOH were found to be significantly affected due to the dissolution of aluminosilicates in the alkaline solution, the flow, viscosity and setting time of the AAB paste were alternated.

The study by Tran [7] on recycled fine and coarse aggregates' impact on geopolymer concrete compressive strength also reported that fine aggregates negatively affected strength, while coarse aggregate replacement up to 100% had no significant effect. Zhang *et al.* [8] stated that when it comes to compressive strength, NAGPC outperforms RCAGPC, with RCA quality being a major factor in strength. The increased viscosity of GPC components improves workability [9]. Kathirvel et al.[10] and Ren et al. [11] also concluded the same as natural aggregates can be completely replaced to prepare high-strength geopolymer concrete.

Xie et al. [12] investigated the workability, mechanical strength, and hydration mechanism of alkali-activated geopolymer RCA containing GGBFS and fly ash. The study evaluated various levels of natural aggregate replacement with recycled aggregate (RA). The authors noted that the incorporation of fly ash and GGBFS in geopolymer, along with the use of RA, led to significant improvement in compression resistance in concrete. Ding *et al.* [13] studied the fracture properties of geopolymer concrete (GPC) containing fly ash and slag and found that GPC cured at ambient temperature, has higher ductility than plain concrete. Jayarajan et al. [14] observed improved geopolymer concrete's mechanical properties with the addition of steel fibres with a higher increment in split tensile strength than compressive strength. Shi *et al.* [15] found that RCA-used geopolymer has improved ITZ compared to PCC with RCA, but a decrease in elastic modulus and compressive strength compared to natural aggregates.

In summary, investigating the synergistic benefits of alkali-activated concrete and recycled aggregate use presents a step towards encouraging sustainable construction methods as the global construction industry moves towards more resource-efficient and sustainable methods.

3. Materials used

3.1. Fine Aggregate

Clean river sand, sourced locally and devoid of organic content, was utilized as the fine aggregate passing through a 4.75 mm sieve. The sand exhibits a specific gravity of 2.52 and conforms to grading zone II specifications.

3.2. Coarse Aggregate

Crushed granite aggregate with a nominal size of 20mm was used consistently in the project. The specific gravity of the coarse aggregate is 2.87.

3.3. Fly Ash

The fly ash utilized in the study was obtained from RMC ready-mix and collected via an electrostatic precipitator. Only the portion of fly ash passing through a 90-micron sieve was utilized in the experiment. Refer to Table 1 for the details of the fly ash.

3.4. GGBFS

Table 1. Properties of Fly Ash and GGBFS

A.	Physical Properties	Fly Ash	GGBFS
1	Specific Gravity	2.38	2.92
2	Fineness (cm2/gm)	373	4000
3	Glass Content (%)	75	85
4	Loss of Ignition (%)	2.1	2.1
B.	Chemical Properties		
1	CaO	40.3	40.3
2	SiO_2	59.7	43.4
3	$Al_2 O_3$	95.80	12.5
4	Na_2O	0.9	0.9
5	K_2O	0.6	0.6
6	MgO	1.04	1.5
7	LOI	0.37	2.1

The GGBFS is procured from TATA steel and the chemical and physical properties are available in Table 1. Laboratory-available Fresh potable water was used.

Table 2. Properties of Sodium Hydroxide

A)	Physical Properties: -	
1	Specific Gravity	1.52
2	Molecular Weight	39.997 g/mol
3	Boiling Point	13880 C
4	Appearance	Liquid (gel)
B)	Chemical Properties: -	
1	Carbonate ($Na2CO_3$)	97%
2	Chloride (Cl)	2.2%
3	Sulphate (SO_2)	0.05%

3.5. Sodium Hydroxide (NaOH)

NaOH is also commonly used as an alkaline activator in geo-polymer production. The properties are listed in Table 2.

3.6. Sodium meta-silicate (Na_2SO_3)

The sodium meta-silicate solution (Na_2SiO_3) used is available locally. The composition of the solution is Na_2O=12.65%, SiO_2=29.93% and H_2O=56.42% by mass.

4. Experimental procedure

4.1. Mixing

The experiments were planned to determine the mechanical properties of AAC due to the mixture of RCA and combination of fly ash and GGBFS and compared to a 100% fly ash AAC mix.

The study variables included fly ash/GGBFS with consistent proportions of fine and coarse aggregate, maintaining a water-cement ratio of 0.45 and a mix ratio of 1:1.31:2.18. Following the mix design guidelines proposed by Hardjito et al. [16], the combination of fly ash and GGBFS was determined based on previous optimization studies of the binder. The sodium hydroxide molarity was either 6M or 8 M. The alkaline activator to binder (fly ash + GGBFS) ratio remained constant at 0.5, and the ratio of sodium silicate to sodium hydroxide solution was set at 2.5.

As per the design specifications, NaOH pellets were dissolved in one litre of water to achieve the desired NaOH concentration, one day before usage. Before mixing the constituent materials, an alkaline activator comprising NaOH and Na_2SiO_3 was prepared in a ratio of one-part NaOH to 2.5 parts Na_2SiO_3.

Table 3. AAC mix proportions per Cum.

Materials	Mass (kg/m^3)	
Sample	FA100-GGBFS0	
Coarse aggregate 20mm	776	
Coarse aggregate 10 mm	517	
Fine aggregate	554	
Fly ash (Class F)+GGBFS	480	
Extra water	55	
Alkaline solution/ (FA+GGBFS) (by weight)	0.5%	
Mass of super plasticizer	1.5% of binder	
Molar weight	8 M	16 M
Sodium silicate solution (kg/m3)	171	
Sodium Hydroxide pellets (kg/m3)	21.94	21.94
Cost	6M Cost in Rs.	8M Cost in Rs.
Sodium silicate solution (kg/m3)	5486	5486
Sodium Hydroxide pellets (kg/m3)	1086	1448
Total cost in Rs.	6572	6934

Initially, GGBFS, FA, and aggregate were dry-mixed in the mixer for three minutes. To produce fresh AAC, the alkaline solution was then added to the dry mix and mixed for an additional five minutes. Gradually, 1.5% of Superplasticizer was introduced into the AAC mix and mixed for a further five minutes to compensate for workability losses in the fresh state and to enhance the flowability of the fresh concrete.

Table 4. Mix proportions

Sample	Recycled Aggregates (%)	Molarity	Fly Ash (%)	GGBFS (%)
P1	0	8%	50	50
P2	50	8%	50	50
P3	100	8%	50	50
P10	0	8%	100	0
S1	0	6%	50	50
S2	50	6%	50	50
S3	100	6%	50	50
S10	0	6%	100	0

4.2. Casting

The cubes were cast in moulds of size 150 x 150 x 150mm (internal) cylinders 150 x 300mm (internal) and prisms of 100x100x500mm. (Figure 1)



Figure 1. Casting of the standard specimens

4.3. Curing

The specimens were demoulded 24 hours after casting and subsequently placed in a shaded area to dry. Testing was conducted after 28 days of curing under ambient conditions. The room temperature during this period ranged from 30 to 35°C.

4.4. Testing

The cube samples were used for a compressive strength test using a 2000kN compression-testing machine. Prisms measuring 500x100x100 mm were cast and tested under two-point loading for flexural strength. Similarly, the cylinders were cast, cured, and tested under split tensile strength testing using compression in the same testing machine.

The investigation was designed for two concrete mixes, denoted as 6M and 8M. The percentages of fly ash and GGBFS that replaced cement in the mixes were as follows: 0% fly ash and 100% GGBFS, and a blend of 50% fly ash and 50% GGBFS.

5. Discussion of test results

To examine the impact of replacing RCA on the properties of Alkali activated Concrete (AAC), different proportions of RCA were combined with fixed amounts of GGBFS and fly ash at 50%. Using natural sand and varying the coarse aggregate content from 0% to 100% in 50% increments, along with fly ash, GGBFS, sodium silicate, and sodium hydroxide as the primary materials, a series of cubes, cylinders, and prisms were cast and tested following 28 days of ambient curing.

5.1. Effect of RCA on fly ash + GGBFS on Compressive Strength of AAC

Observations reveal that the 28-day compressive strength of 8M AAC surpasses that of 6M concrete when employing 50% GGBFS and natural aggregates, with strengths recorded at 56.47 MPa and 66.74 MPa, respectively. Notably, the influence of GGBFS appears to be predominant in AAC concrete, as evidenced by the fact that concrete with 100% fly ash achieved a strength of less than 50%. Introducing Recycled Concrete Aggregate (RCA) appears to yield lower strength, although 100% replacement of natural aggregates attains comparable strength to 50% RCA usage. Economic analysis, as depicted in Figure 2, suggests that cement can be replaced by fly ash + GGBFS up to 50%, given their eco-friendly attributes compared to cement.

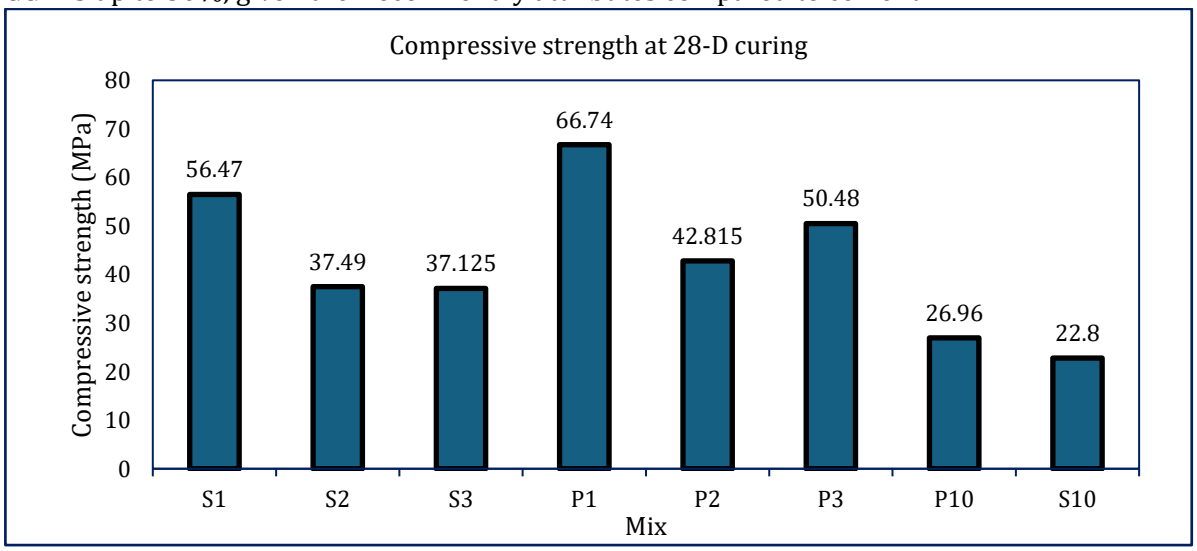


Figure 2. Compressive Strength

5.2. Effect of Fly ash +GGBFS on Split Tensile Strength

Figure 3 shows the results of the 28-day split-tensile strength of cylinders. Comparing 6M and 8M mixes:

- For both 6M and 8M mixes, increasing the RCA content seems to result in a decrease in split tensile strength. This can be observed by comparing S1 and S3 in 6M and P1 and P3 in 8M.
- Within each mix (6M and 8M), the split tensile strength generally decreases as the RCA content increases. For example, within the 6M mix, S1 has the highest split tensile strength (1.90 MPa) while S3 has the lowest (1.31 MPa).
- Comparing equivalent RCA content (e.g., S1 and P1, S2 and P2, S3 and P3), the 8M mix tends to exhibit higher split tensile strength compared to the 6M mix.

Comparing mixes with the same RCA content:

- Comparing mixes with the same RCA content (e.g., S1, S2, and S3 in 6M or P1, P2, and P3 in 8M), the addition of GGBFS has a varied effect on split tensile strength. Referring to 6M, the split tensile strength decreases as GGBFS content increases, while in 8M, the tensile strength decreases from P1 to P2 but then increases slightly from P2 to P3.

In general, the split tensile strength of the AAC concrete samples appears to be affected by the mix composition, notably the inclusion of GGBFS and RCA. Additionally, the effect of GGBFS on split tensile strength appears to vary depending on the specific mix and RCA content.

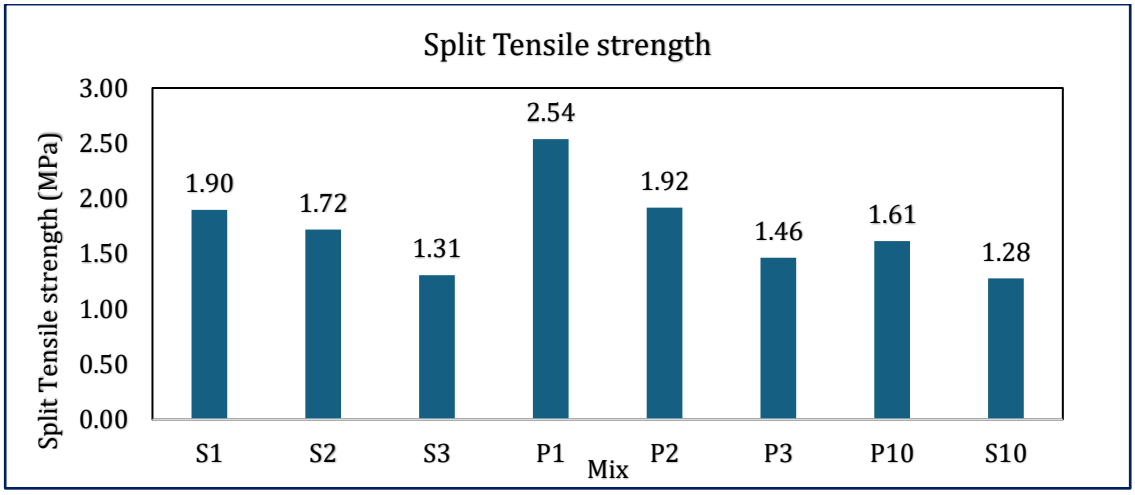


Figure 3. Split tensile strength test values

5.3. Effect of Fly ash+ GGBFS on Flexural Strength

Figure 4 reports the results of 28 days of Flexural strength of the prisms.

Comparing mixes within the same molarity (6M or 8M), we observe variations in flexural strength as GGBFS and RCA content changes.

- Generally, for both molarities, an increase in RCA content has a mixed effect on flexural strength it results in higher flexural strength (e.g., S3, P3) for 100% RCA, while in 50% RCA, it leads to a decrease (e.g., S2, P2).
- The influence of GGBFS on flexural strength appears to vary depending on the specific mix and RCA content. For instance, in 6M mixes, the presence of GGBFS leads to a decrease in flexural strength from S1 to S2, but then a slight increase from S2 to S3. However, in 8M mixes, the flexural strength decreases consistently with the addition of GGBFS (e.g., from P1 to P3).

Comparison between 6M and 8M mixes:

- It is observed that 6M mixes exhibit higher flexural strength compared to 8M mixes, except for some specific cases (e.g., P3 in 8M).

Effect of RCA alone:

- Comparing P10 (8M, no RCA) with S10 (6M, no RCA) and only Fly ash content results in lesser strength values under ambience curing.

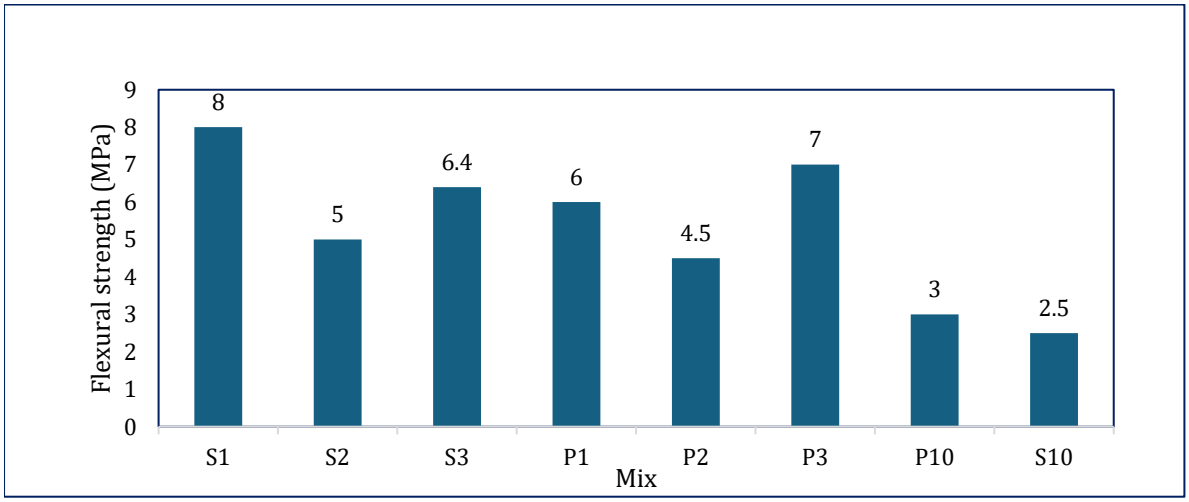


Figure. 4. Flexural test

6. Conclusions

Based on the present investigation and detailed results presented in tabular and graphical forms on AAC concrete using GGBFS and Fly Ash. The conclusions of the project are as follows:

- Fly ash AAC (Alkali Activated Concrete) exhibits the lowest strength among the tested specimens. This could be attributed to the requirement of heat curing, as indicated by the literature. Heat curing is crucial for the proper development of strength in materials containing fly ash.
- The inclusion of Recycled Concrete Aggregate (RCA) in the concrete mixes results in a decrease in compressive strength, split tensile strength, and flexural strength. This suggests that the presence of RCA has a detrimental effect on the overall mechanical properties of the AA concrete.
- Comparing the performance of concrete mixes with different proportions of RCA, it is evident that 100% RCA content shows slightly improved performance compared to mixes with 50% RCA. However, all strengths measured for these RCA-containing mixes are lower than those of the control AAC with natural aggregates. This indicates that while higher RCA content may offer some enhancement, it still falls short of achieving the strengths attained with natural aggregates.
- The observed improvement in strengths with 100% RCA content may be attributed to the presence of adhered cement mortar on the recycled aggregates. This adhered mortar can potentially react with alkalis present in the concrete mix, contributing to enhanced strength properties. However, despite this improvement, the strengths achieved are still inferior to those of the control mix with natural aggregates.
- In summary, the findings highlight the complexities involved in incorporating fly ash and RCA into AAC mixes. While RCA inclusion may offer some benefits, such as potential chemical reactions with alkalis, it also poses challenges in maintaining satisfactory mechanical properties. Further research and optimization of mix designs are warranted to fully leverage the advantages of these alternative materials while addressing their limitations.

References

[1] M. Bassani, L. Tefa, A. Russo, and P. Palmero, "Alkali-activation of recycled construction and demolition waste aggregate with no added binder," Construction and Building Materials, vol. 205, pp. 398-413, 2019, DOI: 10.1016/j.conbuildmat.2019.02.031.

[2] N. E. Maameri, H. Bensaci, and S. Kenai, "The effect of treated recycled steel fibers and slag on the properties of recycled self-compacting concrete," MRS Advances, vol. 8, no. 10, pp. 613-617, 2023, DOI: 10.1557/s43580-023-00616-z.

[3] I. Amer, M. Kohail, M. S. El-Feky, A. Rashad, and M. A. Khalaf, "A review on alkali-activated slag concrete," Ain Shams Engineering Journal, vol. 12, no. 2, pp. 1475-1499, 2021, DOI: 10.1016/j.asej.2020.12.003.

[4] J. Mishra, B. Nanda, S. K. Patro, and R. S. Krishna, "A comprehensive review on compressive strength and microstructure properties of GGBS-based geopolymer binder systems," Construction and Building Materials, vol. 417, p. 135242, 2024, DOI: 10.1016/j.conbuildmat.2024.135242.

[5] P. Pavithra, M. Srinivasula Reddy, P. Dinakar, B. Hanumantha Rao, B. K. Satpathy, and A. N. Mohanty, "A mix design procedure for geopolymer concrete with fly ash," Journal of Cleaner Production, vol. 133, pp. 117-125, 2016/10/01/ 2016, DOI: 10.1016/j.jclepro.2016.05.041.

[6] H. S. Abhishek, S. Prashant, M. V. Kamath, and M. Kumar, "Fresh mechanical and durability properties of alkali-activated fly ash-slag concrete: a review," Innovative Infrastructure Solutions, vol. 7, no. 1, p. 116, 2021, DOI: 10.1007/s41062-021-00711-w.

[7] N. T. Tran, "Experimental Study of Geopolymer Concrete Using Re-cycled Aggregates Under Various Curing Conditions," in Computational Intelligence Methods for Green Technology and Sustainable Development, Cham, Y.-P. Huang, W.-J. Wang, H. A. Quoc, L. H. Giang, and N.-L. Hung, Eds., 2021: Springer International Publishing, pp. 469-478.

[8] P. Zhang, X. Sun, F. Wang, and J. Wang, "Mechanical Properties and Durability of Geopolymer Recycled Aggregate Concrete: A Review," Polymers, vol. 15, no. 3, doi: 10.3390/polym15030615.

[9] K. H. Younis, K. A. Salihi, and T. K. Ibrahim, "An overview of geo-polymer concrete including recycled aggregate," Int. J. Sci. Technol. Res, vol. 9, pp. 6239-6245, 2020.

[10] P. Kathirvel and S. R. M. Kaliyaperumal, "Influence of recycled concrete aggregates on the flexural properties of reinforced alkali activated slag concrete," Construction and Building Materials, vol. 102, pp. 51-58, 2016, DOI: 10.1016/j.conbuildmat.2015.10.148.

[11] X. Ren and L. Zhang, "Experimental Study of Geopolymer Concrete Produced from Waste Concrete," Journal of Materials in Civil Engineering, vol. 31, no. 7, p. 04019114, 2019, DOI: 10.1061/(ASCE)MT.1943-5533.0002750.

[12] J. Xie, J. Wang, B. Zhang, C. Fang, and L. Li, "Physicochemical properties of alkali activated GGBS and fly ash geopolymeric recycled concrete," Construction and Building Materials, vol. 204, pp. 384-398, 2019, DOI: 10.1016/j.conbuildmat.2019.01.191.

[13] Y. Ding, C.-J. Shi, and N. Li, "Fracture properties of slag/fly ash-based geopolymer concrete cured in ambient temperature," Construction and Building Materials, vol. 190, pp. 787-795, 2018, DOI: 10.1016/j.conbuildmat.2018.09.138.

[14] G. Jayarajan and S. Arivalagan, "An experimental studies of geopolymer concrete incorporated with fly-ash & GGBS," Materials Today: Proceedings, vol. 45, pp. 6915-6920, 2021, DOI: 10.1016/j.matpr.2021.01.285.

[15] X. S. Shi, Q. Wang, X. L. Zhao, and F. Collins, "Discussion on Properties and Microstructure of Geopolymer Concrete Containing Fly Ash and Recycled Aggregate," Advanced Materials Research, vol. 450-451, pp. 1577-1583, 2012, DOI: 10.4028/www.scientific.net/AMR.450-451.1577.

[16] D. Hardjito and B. V. Rangan, "Development and properties of low-calcium fly ash-based geopolymer concrete," Research report GC 1, Curtin University of technology Perth, Australia., 2005.

Acknowledgements

The authors express gratitude towards our undergraduate students for the experimental works carried out also like to thank the principal and management Vasavi College of Engineering (A), Hyderabad, for providing the necessary help in executing this project.

IOP Conference Series: Earth and Environmental Science

PURPOSE-LED PUBLISHING™

PAPER • **OPEN ACCESS**

Imparting concepts of sustainability and green buildings via a case study on an educational building

To cite this article: Mahesh Kona *et al* 2024 *IOP Conf. Ser.: Earth Environ. Sci.* **1409** 012016

View the article online for updates and enhancements.

You may also like

- A review of carbon footprint reduction of green building technologies in China
Xi Wang, Yiqun Pan, Yumin Liang et al.
- Research on the Whole Life Cycle Management of Environmental Protection and Energy Saving for New Green Buildings
Qiyan Lin
- Research on Green Building Energy Saving and Environmental Protection Design Based on BIM Technology
Qiyan Lin



This content was downloaded from IP address 47.247.77.11 on 27/11/2024 at 05:36

Imparting concepts of sustainability and green buildings via a case study on an educational building

Mahesh Kona[1], Yashwanth Pamu[1], Jagadeesh Bommisetty[1], and Praveen Samarthi[1]

[1]Department of Civil Engineering, CVR College of Engineering, Hyderabad, Telangana, India

*Email: yashwanthpamu@gmail.com

Abstract: Sustainable building construction is the need of the hour for any developing nation. Sustainable or Green buildings mainly focus on the conservation of energy, water, and other scarce resources. Indian Green Buildings Council (IGBC) and Green Rating for Integrated Habitat Assessment (GRIHA) are two organizations in India which certifies buildings of various categories based on the sustainable practices adopted in the buildings. Certification is given for existing as well as new buildings. This paper attempts to evaluate the sustainable features of an existing school as per IGBC standards. The study revealed that the school under consideration has few sustainable features. Very few points were scored in the most important criteria i.e., water efficiency and energy efficiency, which contributes to more than 50% of the total points. The existing school building can be converted into a green building with certain modifications to the existing school infrastructure. This detailed study on various existing features of the building will help the school authorities to improve the building for a sustainable environment to the school students.

Keywords: Sustainable building, school building, students, Energy efficiency, Water efficiency, IGBC, GRIHA.

1. Introduction

The requirements of society are met, quality of life is improved, and a nation's economy grows pursuant in large part to the building sector. However, because to its extensive use of natural resources and energy consumption, it has come under harsh criticism for being a significant cause of carbon emissions, environmental deterioration, and global warming. Construction activities can generate a significant amount of dust, particulate matter, and other pollutants, which can have harmful effects on human health, particularly for workers who are exposed to these pollutants daily. Several studies have shown that construction workers experience eminent risk of growing respiratory diseases, such as asthma and chronic obstructive pulmonary disease (COPD), due to exposure to these pollutants [1][2]. Construction sites can generate high levels of noise, which can be a source of stress and irritation for people living or working nearby. Numerous studies have demonstrated that prolonged exposure to loud noise can cause cardiovascular illness, hearing loss, and sleep difficulties [3][4]. Construction activities can cause soil erosion, sedimentation, and pollution, harming aquatic ecosystems and human health. Studies indicate construction sites significantly contribute to urban water pollution [5][6]. Additionally, construction often destroys natural habitats, negatively impacting local ecosystems and wildlife, leading to biodiversity

Content from this work may be used under the terms of the Creative Commons Attribution 4.0 licence. Any further distribution of this work must maintain attribution to the author(s) and the title of the work, journal citation and DOI.
Published under licence by IOP Publishing Ltd

declines [7] [8]. The construction sector is a major greenhouse gas emitter due to energy-intensive materials like cement and steel [9][10]. However, strategies such as green building design and renewable energy can mitigate these impacts.

Green building education is essential for reducing environmental impact in the construction industry. University curricula often include green building courses, though interdisciplinary programs are lacking [11][12]. Experiential learning, including real-life projects, effectively enhances understanding of sustainable design [13]. Green building education also benefits professionals and younger students, promoting sustainable practices and environmental awareness [14][15]. Effective teaching strategies include experiential learning, interdisciplinary approaches, and real-world examples [16][17] [18].

This article explores the application of green building concepts in educational facilities, showcasing sustainable strategies and technologies in design, construction, and operation. It aims to raise awareness among researchers, architects, engineers, and educators about the benefits of green building principles. The case study highlights energy-efficient systems, renewable energy, water conservation, eco-friendly materials, and indoor environmental quality. The article also addresses implementation challenges and evaluates performance outcomes, serving as a resource for promoting sustainable practices in future building projects. This research emphasizes interdisciplinary programs, experiential learning, standardized education programs, and stakeholder collaboration to advance green building knowledge and practice.

2. Methodology

This paper tries to quantify the points obtained by a non-green school building. This is done based on the sustainable features of this existing school building. The building considered for the study is an engineering college building located in the outskirts of the Hyderabad city, India. The allocation of points is done based on Green Existing Buildings Operations & Maintenance Rating System for schools prescribed by IGBC. There are five criteria and the total points for which the building will be ratified is 100. Each criterion may have a number of sub-criteria. Figure 1 illustrates the names of each criterion and points allotted to each criterion. If the cumulative points scored in all criteria is 50-59, best practices rating will be awarded. Similarly for 60-69 points outstanding performance, 70-79 points national excellence and for 80-100 points, global leadership rating will be awarded.

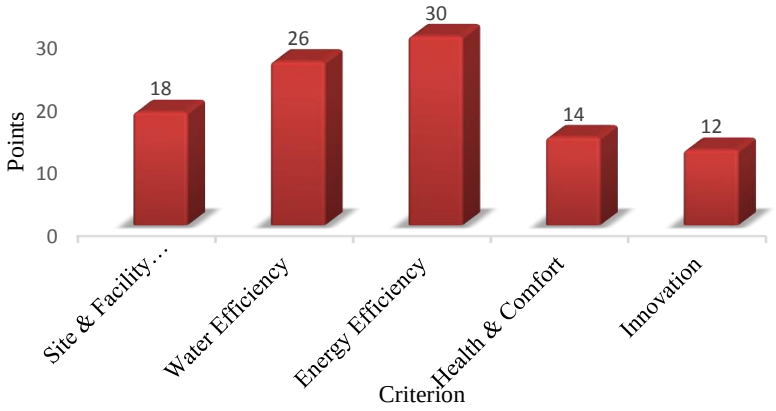


Figure 1. Points for various criterion as per IGBC manual

2.1. Criterion - 1 Management of Site and Facility at Institution

2.1.1. Environmental - friendly Commuting Practices

The main objective of this sub-criterion is to lower the usage of natural resources like petrol, diesel, oil, and natural gas. Bus pooling also reduces the CO_2 emissions and promotes equality among students. Carpooling by teachers may generate new and innovative ideas across various disciplines by discussions during their travel to school. To park all the vehicles safely, a parking facility should be provided. The school considered in the case study has ample parking place as shown in Figure 2.



Figure 2. Parking space



Figure 3. Plantations around the building

Table 1. Points for sustainable travelling practices

S. No	Proportion of inhabitants using school bus or pooling service	Points
1	25%	2
2	50%	4 (max.)

Table 1. shows points allotted for different percentages of occupants using bus/pool service. Four points can be granted to this sub-criterion as there are 60 buses. Each bus can accommodate 50 students which makes 3000 students using bus/poll service. Total strength of the school is 5000, which implies that more than 50% of the occupants use pool service.

2.2. Eco-friendly landscaping practices

The maximum points in this sub-criterion are two (2). The purpose of this sub-criterion is to plant locally adaptive species and to use only organic fertilizers. It saves water and doesn't deteriorate the soil health. The maintenance of these plants is simple thus reducing the expenses on the maintenance of landscape.

Table 2. Points for encouraging native plants.

Proportion of native plants	Credits / Points
50%	1
75%	2 (max.)

Table 2. indicates credits / points for various proportions of locally adaptive (native) plants. Plantations in the school are native plants which require minimum or zero water. Two (2) points can be awarded for this sub-criterion as per table 3. Figure 3. represents landscape pictures surrounding the building.

2.3. Eco-friendly landscaping practices

Heat island refers to the built-up areas that experience relatively higher temperatures than the surrounding areas. Increase in heat island results in elevated day-time temperature causing the building occupants to use air-conditioners for longer durations. This increases the peak demand of electricity.

Table 3. Points for non-roof heat island reduction

Proportion of non-roof shaded areas	Credits / Points
50%	2
75%	4 (max.)

Table 3. shows points for different percentages of shaded non-roof hardscape areas. There are no shaded non roof hardscape areas in the school. Therefore, zero points will be given in this sub-criterion.

2.4. Roof Heat Island Reduction

The maximum points in this sub-criterion are four (4). Heat island reduction aims to mitigate the negative effects of urban heat islands (UHIs), which are areas in cities that experience significantly higher temperatures than surrounding rural areas due to human activities such as energy use, transportation, and building materials. These higher temperatures can lead to a range of negative consequences, including increased energy consumption, heat-related illnesses, reduced air quality, and damage to infrastructure.

Table 4. Points for roof heat island reduction

S.No	Reflective materials on roof area	Points
1	50%	2
2	75%	4

The main purpose of heat island reduction is to improve the overall quality of life in urban areas by reducing the impacts of UHIs. This may be accomplished through a variation in strategies such as improvement of vegetation cover, using reflective surfaces, improving building design and materials, and reducing energy consumption. By implementing these strategies, cities can create more comfortable and healthier environments for their residents, while also reducing their carbon footprint and promoting sustainability. Heat island reduction is therefore an important aspect of urban planning and design and can contribute to the creation of more liveable and resilient cities.



Figure 4. Roof covered with solar panels



Figure 5. Sewage Treatment Plant

Table 4 displays points for the proportion of roof area covered with materials which are highly reflective. 2 points can be awarded in this condition as greater than fifty percent of the institution building roofs are facilitated with highly reflective solar panels represented in Figure 4.

2.4.1. Reduction in Pollution related to Outdoor Light (Max. 2 points)
Outdoor light pollution refers to the excessive and intrusive artificial light that is emitted into the outdoor environment, typically from outdoor lighting sources such as streetlights, buildings, and illuminated signs. This type of pollution can have a range of undesirable influence on the human habitat and natural environment. Two points can be obtained in this sub-criterion as the school closing time is 4.00 PM.

2.4.2. Building Operation & Maintenance (Max. 2 points)
The purpose of building operation and maintenance is to ensure that buildings and their associated systems and equipment are running efficiently and effectively. This includes tasks such as regular cleaning and maintenance of building components, monitoring and adjusting temperature and humidity levels, and ensuring proper functioning of HVAC systems, lighting, and other building systems. By maintaining buildings properly, building owners can prolong the life of the building, reduce energy consumption and costs, and ensure the safety and comfort of occupants. This educational institution can secure two points in this particular sub-criterion as the building operation and maintenance is done periodically.

2.5. Criterion - 2 Water Resources Efficiency

2.5.1. Efficiency of water fixtures (Max. 6 points)
The intent of using water-efficient fixtures is to reduce water consumption and waste, conserve natural resources, lower water bills, and promote sustainable living. By installing such fixtures, we can help protect our planet's water resources and ensure their availability for future generations. Owing to the usage of conventional water fixtures, zero points will be given.

2.5.2. Rainwater Harvesting (Max. 6 points)
The intent of using water-efficient fixtures is to reduce water consumption and waste, conserve natural resources, lower water bills, and promote sustainable living. By installing such fixtures, we can help protect our planet's water resources and ensure their availability for future generations.

Table 5. Points for Efficiency of Water Fixtures

S.No	Percentage of rainwater harvested from both non-roof and roof areas	Points
1	25%	2
2	50%	4

Table 5 indicates points for percentage of rainwater harvested on building site from both non-roof and roof areas. Due to the absence of rainwater harvesting facilities, no points can be scored in this sub-criterion.

2.5.3. Wastewater Treatment (Max. 4 points)
The intent of wastewater treatment is to remove harmful pollutants and contaminants from wastewater before it is released back into the environment. This helps protect public health and the environment by preventing the spread of disease, reducing water pollution, and conserving water resources. All the wastewater produced in the school is treated on campus in a sewage

treatment plant as shown in figure 5 and disposed of safely. So, 4 points can be granted in this sub-criterion.

2.5.4. Wastewater Reuse (Max. 4 points)

The intent of wastewater reuse is to reduce the strain on freshwater resources and provide a sustainable alternative for non-potable water demands. By treating wastewater to a suitable quality, it can be used for irrigation, industrial processes, and even replenishing groundwater. This reduces the amount of freshwater needed for these activities, conserves resources, and helps protect against water scarcity in areas where it is a concern.

As per IGBC manual, two points can be achieved if 75% of treated water is reused. Four points can be secured if 100% of treated water is reused. The wastewater that is treated in the sewage treatment plant in disposed without reusing. So, no points can be given in this sub-criterion.

2.5.5. Water Metering (Max. 4 points)

Water metering promotes responsible water use, accurate billing, leak detection, and data for water management. It encourages conservation and sustainability, identifies high usage areas, and supports targeted initiatives and infrastructure investments. Water metering ensures fair distribution of water resources and is crucial for managing demand during shortages. It fosters accountability, transparency, and innovation in water management. The college has water meters on all major pipelines, highlighting their importance in efficient water usage. Four points can be given in this sub-criterion as the college has water meters placed on all important pipelines.



Figure 6. Water meter



Figure 7. Renewable energy on-site

2.5.6. Turf Area

Due to high turf area present in the school, no points can be given in this sub-criterion.

2.6. Criterion - 3 Energy Efficiency (30 points)

2.6.1. Enhanced Energy Performance (Max. 14 points)

This sub-criterion aims to verify practices implemented by school to be energy efficient. Reduction in energy consumption leads to reduction in environmental impacts. On the basis od Energy Performance Index (EPI), points are awarded as 2, 4, 6, 8, 10, 12 and 14 for different climates. Unfortunately, the educational building studied in this case does not maintain the limits as specified in the IGBC manual. Therefore, zero points will be given to the building in this criterion.

2.6.2. Renewable Energy facility On-site (Max. 6 points)

On-site energy generation produces electricity or energy at the location where it is consumed, offering several benefits like cost savings, energy independence, environmental benefits, reliability and increased control.

Overall, on-site energy generation provides a sustainable, cost-effective, and reliable energy source, benefiting both users and the environment. Two, four and six points can be scored if 2.5%, 5% and 7.5% of total energy consumed is in the form of renewable energy. of total energy consumed of renewable energy. Approximately 20% of the total energy consumption is generated at site using solar panels. Therefore, six points for this sub-criterion can be awarded.

2.6.3. Off-Site Renewable Energy (Max. 6 points)

Off-site renewable energy generates energy at a separate location from its consumption, helping organizations offset their carbon footprint and reduce fossil fuel dependence. Using off-site renewable energy reduces environmental impact and supports renewable energy growth. To score points in this sub-criterion, at least 25% of the annual energy consumption should be utilized from offsite renewable sources. Two, four and six points will be awarded for 25%, 50% and 75% respectively. The educational building under study can score zero points in this sub-criterion.

2.6.4. Energy Metering

The purpose of energy metering is to measure and monitor energy consumption over a specific period of time, enabling users and providers to manage energy usage efficiently. This helps reduce energy costs, identify energy wastage, improve energy efficiency, and promote sustainable energy practices. The school should have renewable energy generation, backup systems for power failure situations and consumption related to interior lighting. As per the IGBC manual instructions, 4 points can be scored in this particular sub-criterion as the building fulfills all the requirements.

2.7. Criterion – 4 Comfort and Health (14 points)

2.7.1. CO_2 Monitoring & Control (2 points)

The green feature deals with continuous monitoring and regulation of CO_2 levels. This is a very essential precautionary measure for occupants. As there are no such provisions, no points can be awarded in this sub-criterion.

2.7.2. Pollution related Equipment & Systems Isolation (2 points)

Primary intent of this is to decrease contact of structure's occupants to hazardous indoor pollutants that have negative effects on interior quality of air and health of inhabitants.

No points can be secured in this sub-criterion.

2.7.3. Eco-friendly housekeeping chemicals (2 points)

The purpose is to reassure the administration to use only certified housekeeping chemicals which are safe to well-being of the students and staff in the school.

Two points can be awarded in this section as the school administration only uses certified housekeeping chemicals.

2.7.4. Indoor room temperature and Thermal comfort (2 points)

The building of the school is surrounded by trees in all directions as shown in figure 8, providing a comfortable learning environment to the students at the school.

Two points are scored in this sub-criterion.



Figure 8. Building surrounded by trees



Figure 9. Wheelchair ramp

2.7.5. Facilities for physically challenged people (4 points)
Ramps are provided for differently abled people in the building entrance and lifts are provided for easy transit among floors is shown in Figure 9. Four points can be awarded for this sub-criterion.

2.7.6. Facilities for occupant's well-being (Max. points 2)
Figure 10 and Figure 11 shows the cricket ground and basketball court facilites in the school respectively. They are provided to strike a balancé between academics, physical and mental fitness of the students. Full points (2) can be awarded in this sub-criterion.



Figure 10. Cricket ground



Figure 11. Basketball court



Figure 12. Biogas plant in the school campus

2.8. Criterion - 5 Innovation Category (Maximum 12 points)
Apart from the standards mentioned in the manual, school can adopt any innovative sustainable practices. One such practice is generation of gas from food waste of the cafeteria which is shown in figure 12. Two points can be scored in this sub-criterion.

3. Results and Discussions

Sustainable or green buildings have a lower environmental impact compared to conventional buildings due to efficient energy and water use. Green building rating systems suggest ways to use these resources efficiently and ratify buildings based on their sustainable features. Evaluating a school for its sustainable features shows that conventional buildings can also incorporate green elements. With 40 out of 100 points, the school wasn't initially designed as a green building but has potential. By following IGBC specifications and simple measures, it can be transformed into a green building.

In site and facility management, the school scored 55% of the points. For water efficiency, it secured only 30%, which can be improved. Six sub-criteria include replacing water fixtures with

efficient ones, fitting sensors for automatic taps, and adding aerators to save water. Figures 13 and 14 illustrate aerators and efficient fixtures, respectively.



Figure 13. Aerator



Figure 14. Water efficient fixture



Figure 15. Carbon-di-oxide sensor

In the second sub-criterion, no points were scored due to the lack of rainwater harvesting. Rainwater harvesting increases groundwater, conserves water and energy, and improves water quality at a low cost. Reusing treated water from the STP for plants is another improvement. For energy efficiency, only 33% of points were secured. Enhancing energy performance and utilizing at least 25% offsite renewable energy can improve the score. For health and comfort, 2 points can be gained by placing CO2 sensors. Encouraging innovative ideas from students and staff can also boost points in the innovation category.

By implementing the measures stated in this section, the number of points in each sub-criterion can be increased. Figure 16 depicts the comparative graph between the total number of points attained by the school, the total number of points that can be achieved by following the suggestions mentioned in this section and total number of points in each criterion.

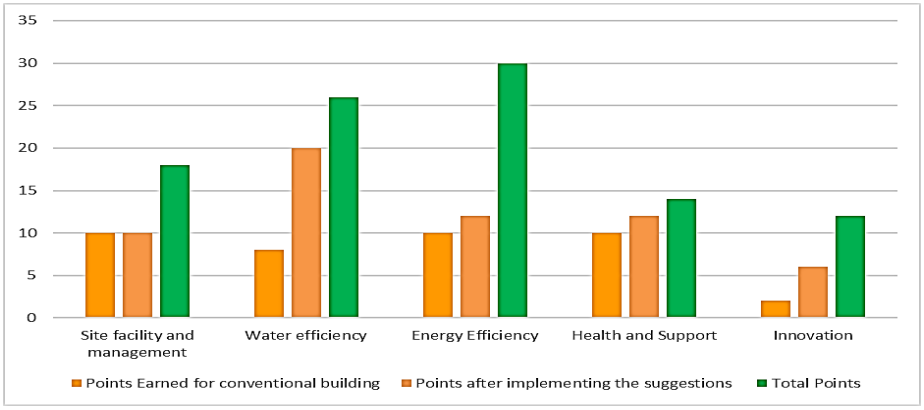


Figure 16. Graph indicating points earned for a conventional building, points earned after implementing the suggestions and total points

4. Conclusions

This study provides strong evidence supporting the notion that every existing building possesses inherent sustainable features. Through effective rehabilitation measures, these buildings can be transformed into green or sustainable buildings. However, prior to embarking on any modifications, it is crucial for school authorities to make a well-informed decision regarding the certification organization, such as IGBC or GRIHA, that will oversee the ratification process. While

the ultimate goal of all green building certification agencies remains the same, it is important to note that the implementation procedures may vary.

Based on the findings of the study conducted by Pamu et al (2019)., it can be conclusively stated that the IGBC certification system stands out as the most accessible and feasible option among various certification agencies. Furthermore, the results and discussions indicate that a conventional building typically scores only 40 points on a scale of 100 in terms of sustainability. However, by implementing the simple procedures outlined in this study, significant improvements can be achieved. For instance, the water efficiency criterion can be increased by 12 points, energy efficiency by 2 points, health, and comfort by 2 points, and innovation by 4 points. Consequently, the total points obtained can reach a maximum of 60, thereby elevating the conventional building to the status of a green building with exceptional performance, as illustrated in Table 1.

References

[1] Nieuwenhuijsen, M., Basagaña, X., Dadvand, P., Martinez, D., Cirach, M., Beelen, R., ... & Brunekreef, B. (2017). Air pollution and human fertility rates. Environment international, 98, 209-214.
[2] Saini, R., Mani, K., & Deodhar, S. D. (2019). Respiratory morbidity among construction workers in India. International Journal of Medical Science and Public Health, 8(2), 104-107.
[3] Basner, M., Babisch, W., Davis, A., Brink, M., Clark, C., Janssen, S., ... & Stansfeld, S. (2014). Auditory and non-auditory effects of noise on health. The Lancet, 383(9925), 1325-1332.
[4] World Health Organization. (2011). Burden of disease from environmental noise: Quantification of healthy life years lost in Europe. Copenhagen, Denmark: World Health Organization Regional Office for Europe.
[5] McMillan, S. K., Keefe, D. M., & Roy, A. H. (2019). Stormwater management at construction sites: A review of best management practices and pre-treatment options for improved off-site water quality. Environmental Science: Water Research & Technology, 5(12), 2055-2074.
[6] Singh, A. K., & Kumar, M. (2014). Urbanisation and storm water quality: A review of environmental policies and management practices to control sustainable urban storm water discharge. Journal of Environmental Management, 132, 358-372.
[7] Haddad, N. M., Brudvig, L. A., Clobert, J., Davies, K. F., Gonzalez, A., Holt, R. D., ... & Tewksbury, J. J. (2015). Habitat fragmentation and its lasting impact on Earth's ecosystems. Science Advances, 1(2), e1500052.
[8] Raudsepp-Hearne, C., Peterson, G. D., & Bennett, E. M. (2010). Ecosystem service bundles for analyzing trade offs in diverse landscapes. Proceedings of the National Academy of Sciences, 107(11), 5242-5247.
[9] Creutzig, F., Fernandez, B., Haberl, H., Khosla, R., Mulugetta, Y., & Seto, K. C. (2015). Beyond technology: demand-side solutions for climate change mitigation. Annual Review of Environment and Resources, 40, 193-218.
[10] International Energy Agency. (2019). Global CO2 emissions from energy sector flattening, but far from a decline. Retrieved from https://www.iea.org/news/global-co2-emissions-from-energy-sector-flattening-but-far-from-a-decline.
[11] Paquette, J., & Gravel, M. (2018). Teaching green building in Canadian universities: A review of curricula. Journal of Cleaner Production, 185, 326-335.
[12] Thomas, V. M., & Jin, X. (2018). A review of green building curricula in higher education. Journal of Cleaner Production, 174, 1417-1428.
[13] Boudia, S., & Van Den Bossche, P. (2018). Learning through experience: A review of experiential learning methods in green building education. Journal of Cleaner Production, 174, 1410-1416.
[14] Kostovska, O., Drakalska, E., & Filipovska, L. (2020). The Impact of Green Building Education on Building Professionals: Evidence from Macedonia. Journal of Cleaner Production, 269, 122271.
[15] Lu, Y., Zhang, X., Wang, Y., & Sun, Y. (2021). Effectiveness Evaluation of Green Building Education for Elementary School Students in China. Journal of Cleaner Production, 295, 126263.
[16] Ahn, Y., Hwang, K., & Lee, S. (2019). Overview of Green Building Education: Curriculum, Pedagogy, and Assessment. Sustainability, 11(22), 6448.
[17] Meza, V. G., & Martínez, R. A. (2018). Green Building Education: A Systematic Literature Review for Architects and Engineers. Journal of Cleaner Production, 196, 296-313.
[18] Reddy, K. S., & Chen, Y. (2019). A Review of Green Building Education Initiatives in Asia-Pacific. Journal of Cleaner Production, 209, 952-964.

IOP Conference Series: Earth and Environmental Science

PURPOSE-LED PUBLISHING™

PAPER • **OPEN ACCESS**

Determining the issues associated with the urban centre: A case of Jalandhar city

To cite this article: Rajat Nainwal *et al* 2024 *IOP Conf. Ser.: Earth Environ. Sci.* **1409** 012017

View the article online for updates and enhancements.

You may also like

- Influence of Recycled Coarse Aggregates in the Application of Prestressed Concrete Members-A Review
M Tharun Bhargav and K Senthil
- A Systematic Review on Utilization of Rice Husk Ash in Manufacturing of Concrete
Omkar Abhay Phatak and Roop Kishor
- Prediction of Ground Response Spectrum of Jalandhar City of Punjab using Non-Linear Ground Response Analysis
Anjali G Krishna and Senthil Kasilingam



This content was downloaded from IP address 47.247.77.11 on 27/11/2024 at 05:36

Determining the issues associated with the urban centre: A case of Jalandhar city

Rajat Nainwal*[1], Rahul Bharmoria[1]and Himani Belwal[2]

[1]Lovely School of Architecture and Design, Lovely Professional University, Phagwara, Punjab, India-144411.
[2]Division of Research and Development, Lovely Professional University, Phagwara, Punjab, India-144411.

*Email: rajat.30469@lpu.co.in

Abstract. Urban centers often serve as the centers of economic, social, and cultural activity within a region, playing a pivotal role in its development and growth. However, with this centralization comes a myriad of challenges, ranging from infrastructure strains to socio-economic disparities. Jalandhar city, situated in the Indian state of Punjab, exemplifies this complexity as it grapples with various issues associated with its centre. Rapid urbanization and population growth have resulted in increased pressure on transportation networks, utilities, and public services. This paper aims to delve into the multifaceted challenges facing Jalandhar's city centre, shedding light on the intricacies of urban management and development in the context of a rapidly evolving urban landscape. Traffic congestion, inadequate parking facilities, and overburdened utilities contribute to the deteriorating quality of life for residents and commuters alike. The major problems identified in the study area includes inadequate parking; poor road maintenance; noise and safety issues; unavailability of street lighting, pathways, and proper seating space. Addressing these issues requires comprehensive planning, infrastructure improvements, and community engagement to enhance the overall liveability and functionality of the study area.

1. Introduction

Urban centres play a pivotal role in the vitality and appeal of city centres, impacting local economies, urban planning strategies, and community well-being which aligns with the Goal 11 of the Sustainable Development Goals, formulated by United Nations in 2015 [1]. The perceived attractiveness of city centres and shopping malls significantly influences consumer preferences and shopping behaviours [2]. Understanding how the appeal of shopping destinations affects consumer choices between city centre shopping and e-shopping is crucial for urban planners and retailers aiming to enhance the shopping experience. The proliferation of shopping malls has reshaped retail landscapes and consumer habits [3]. Investigating the utilization and appeal of shopping malls offers insights into the evolving shopping patterns within urban environments, shedding light on the changing dynamics of city centers and suburban areas. The competition among various retail formats, such as shopping malls and traditional shopping streets, is a fundamental aspect of urban retailing [4]. Analysing the adaptive resilience of retail agglomeration formats provides valuable perspectives for town centre and mall managers, retailers, and developers striving to navigate the competitive retail landscape. The impact of shopping centers on urban regeneration and sustainability is a topic of interest [5]. City centre revitalization through residential development can contribute to the sustainability of local economies and enhance the vibrancy of urban spaces, underscoring the interconnectedness between residential communities and commercial activities.

Content from this work may be used under the terms of the Creative Commons Attribution 4.0 licence. Any further distribution of this work must maintain attribution to the author(s) and the title of the work, journal citation and DOI.
Published under licence by IOP Publishing Ltd

However, with this centralization comes a myriad of challenges, ranging from infrastructure strains to socio-economic disparities. Urban sprawl and population density play a significant role in shaping the epicentre of a city. Cities have become the epicentre of various phenomena, including the spread of diseases like COVID-19 [6]. The concentration of population and activities in urban areas can amplify the impact of any issue originating from the epicentre [6], [7]. Moreover, issues related to urban decline, as discussed by, can further complicate the management of infrastructure and resources in the epicentre of a city [8]. Infrastructure challenges, such as water and wastewater management, are critical issues that can affect the epicentre of a city, emphasize the importance of retooling alternatives to addressed challenges arising from urban decline, which can have a direct impact on the epicentre of a city [8]. Additionally, the financialization of property markets can influence urban development and planning decisions in the epicentre, particularly regarding the role of city governments in shaping urban landscapes [9]. Public health concerns, especially in the context of disease outbreaks like COVID-19, are paramount when analysing the issues associated with a city's epicentre. Studies by and underscore the importance of factors such as temperature, transmissibility, and proximity to the original epicentre of a pandemic in understanding disease dynamics within cities [10], [11]. The effectiveness of prevention and control measures in major cities is crucial for managing health crises originating from the epicentre [12].

The same issue is being faced by the one of the most crowded and renowned cities of the Northern state of Punjab in India, i.e. Jalandhar. The city of Jalandhar is historically renowned for its industrial prowess and cultural heritage, stands as one of Punjab's prominent urban hubs. Its city centre, characterized by bustling markets, historical landmarks, and administrative institutions, serves as the nucleus of economic and social activities. However, beneath the surface of vibrancy lie deep-seated issues that demand attention and resolution.

One of the foremost challenges confronting Jalandhar's city centre is the strain on its infrastructure. Rapid urbanization and population growth have resulted in increased pressure on transportation networks, utilities, and public services [13]. Traffic congestion, inadequate parking facilities, and overburdened utilities contribute to the deteriorating quality of life for residents and commuters alike. The socio-economic disparities exacerbate the issues faced by the city's epicentre. While the central district flourishes with commercial activity and modern amenities, peripheral areas often languish in neglect, grappling with inadequate infrastructure and limited access to essential services. This spatial divide perpetuates socio-economic inequalities, hindering the city's overall progress and cohesion. The environmental concerns add another layer of complexity to the challenges confronting Jalandhar's city centre. Pollution, waste management issues, and diminishing green spaces pose significant threats to public health and ecological sustainability. Addressing these environmental woes requires a holistic approach that integrates urban planning, resource management, and community engagement.

Considering these challenges, it becomes imperative to analyse and understand the issues associated with Jalandhar's city centre comprehensively. This paper aims to delve into the multifaceted challenges facing Jalandhar's city centre, shedding light on the intricacies of urban management and development in the context of a rapidly evolving urban landscape.

The structure of this paper includes a detailed methodology in section 2; the results are discussed in section 3; section 4 discusses the interventions of issues identified in section 3; followed by the conclusion in section 5.

2. Methodology

The stretch along the PPR mall in Jalandhar which is acting as an urban centre of Jalandhar city, is taken for the data collection and further analysis in this study. It offers economic boost, convenience cultural hub, and improved infrastructure contributing to the local economy,

attracting businesses, and fostering the unity of community [14]. The unique blend of commercial and residential spaces in this area leads to the harmonious coexistence of urban amenities and community living, which makes it appropriate for the consideration in this study. The data was collected using questionnaire and the issues were identified in the study area.

The information such as ownership status of the building, types of shops and the visiting frequency in shops, average per day operating hours and number of weekly working days, frequency of vehicular movement, traffic congestion, parking availability, satisfaction levels of services in the study area, were collected using the survey questionnaire. The questionnaire used in the survey is shown in annexure and the location of the study area is shown in Figure 1.

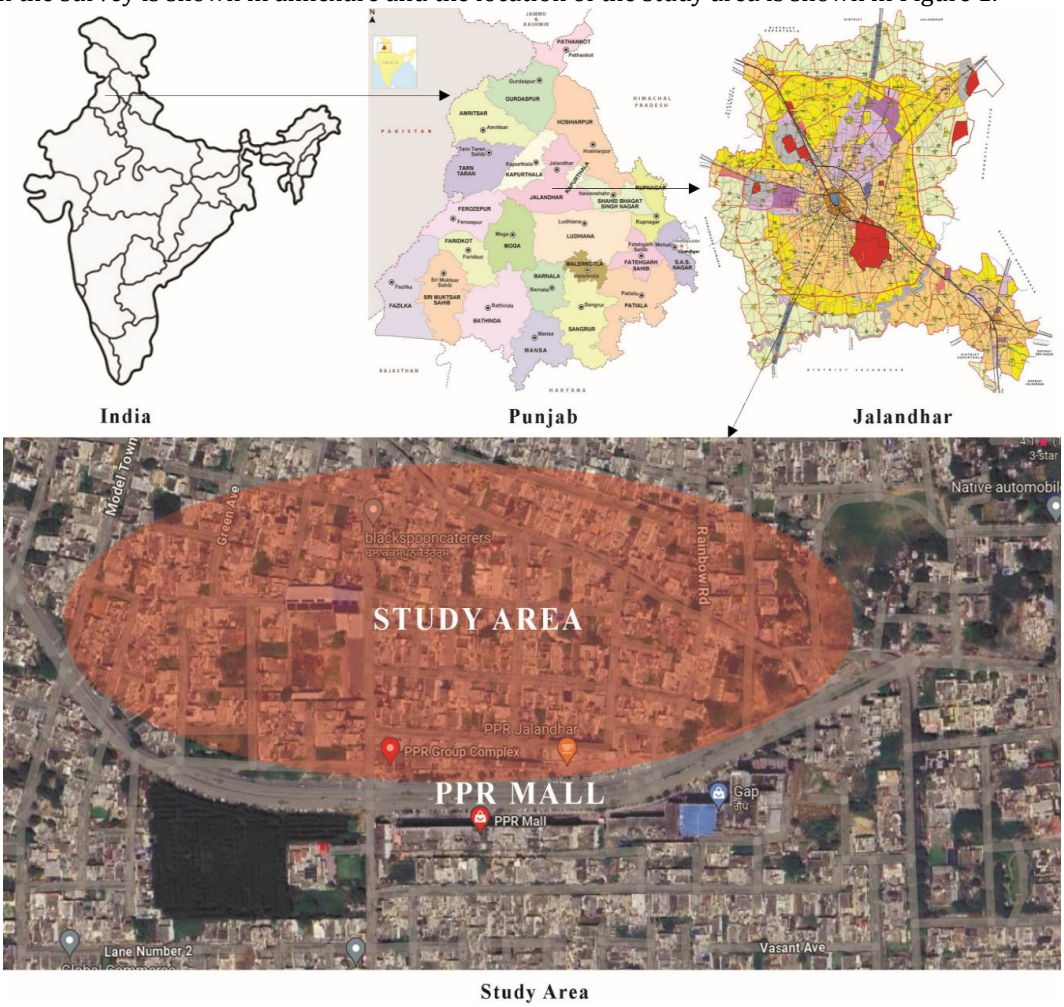


Figure 1. Location of Study Area

3. Results and Discussion

Using the questionnaire, the survey was conducted in the study area with a total sample size of 400 persons. This includes the residents, shop owners, and visitors; and the ratio of division of these categories was 50:30:20. The respondents of different age and income groups were considered in this study to include the varying requirements of different age and income levels, as shown in figure 2 and 3. Various other factors such as transportation, parking, and other services including water supply, drainage, and waste management were studied.

3.1. Demographics of the respondents

It is seen in Figure 2 that the highest percentage of respondents is from the age group of 30-40 years, i.e., 60.0%, suggesting that the survey sample is predominantly composed of individuals in their thirties and early forties. Further, the share is followed by the age group of 20-30 years comprising of 26.0%, indicating a significant presence of younger adults. The respondents above 40 years of age are in a smaller proportion, comprising 14.0% of the overall respondents. Figure 3 shows that most of the respondents are from an income level of more than 20 Lacs per Annum (LPA) i.e., 60.0%, which indicates that a significant portion of the surveyed population earns a relatively high income. The income levels of respondents are followed by the income bracket of 10-20 LPA i.e., 16.0%, less than 5 LPA i.e., 14.0%, and the income level of 5-10 LPA i.e., 6.0%.

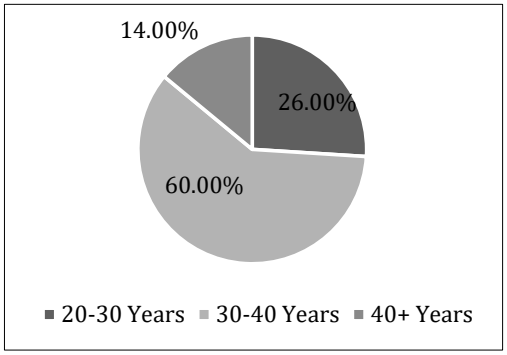


Figure 2. The age groups of the respondents

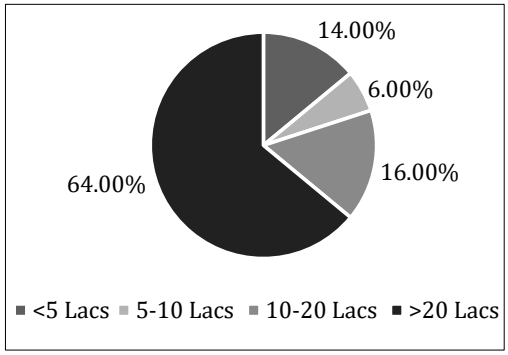


Figure 3. The income status of the respondents

3.2. Transportation in the study area

Following the demographics of the respondents, the data related to transportation was surveyed and the issues related to the same were identified. In this, various determinants such as mode of transportation used to access the study area, availability of public transportation in the study area, frequency and time of traffic congestion faced by the respondents, and the main cause of traffic congestion were determined with respect to the residents, shop owners, & visitors; and presented in Figure 4-8.

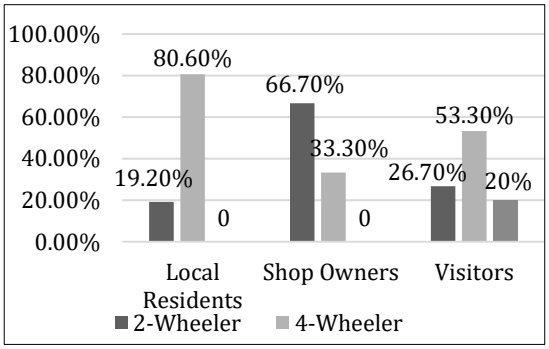


Figure 4. Mode of transportation used by the residents, shop owners, and visitors to reach the study area.

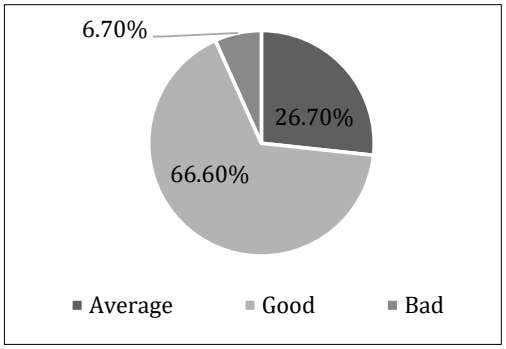


Figure 5. Availability of Public Transportation in the study area.

It is seen in Figure 4 that 80.6% of the residents prefer 4-wheelers to access the study area, whereas only 33.3% of the shop owners and 53.3% of the visitors prefer 4-wheelers to access the study area, indicating a strong reliance on cars or similar vehicles for commuting. When it comes

to the access of study area by 2-wheelers, 19.2% of the residents, 66.7% of the shop owners, and 26.7% of the visitors, uses 2-wheelers to access the study area. This indicates a preference for 2-wheelers among shop owners and a relatively higher usage among visitors, as compared to residents. A notable finding is that 20.0% of visitors use public transport to access the study area, suggesting that a portion of the population relies on public transportation such as buses and shared autos for commuting. This highlights the importance of public transit options in catering to the needs of visitors to the study area. When the availability of public transportation was studied, a significant majority of respondents (66.0%) perceive the availability of public transportation as good, as shown in figure 5. This positive perception suggests that a substantial portion of the population believes that public transport services are readily accessible and meet their needs effectively.

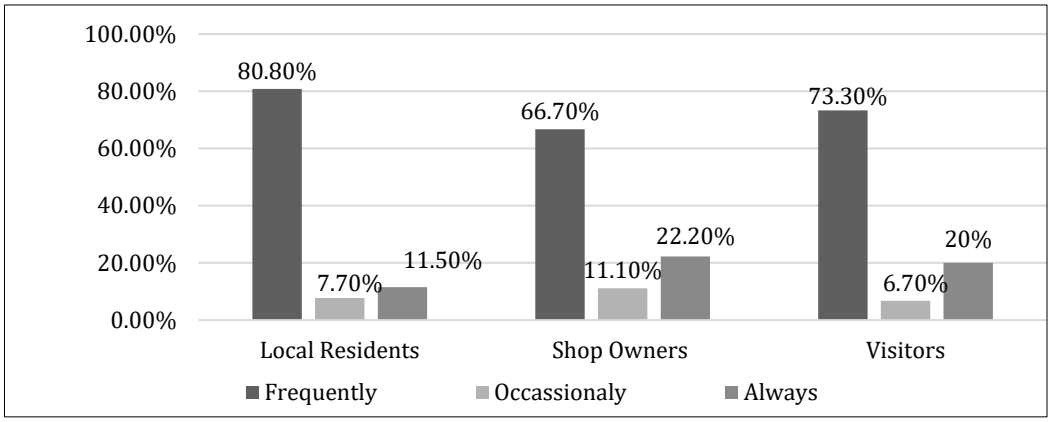


Figure 6. Frequency of traffic congestion faced by the residents, shop owners, and visitors in the study area.

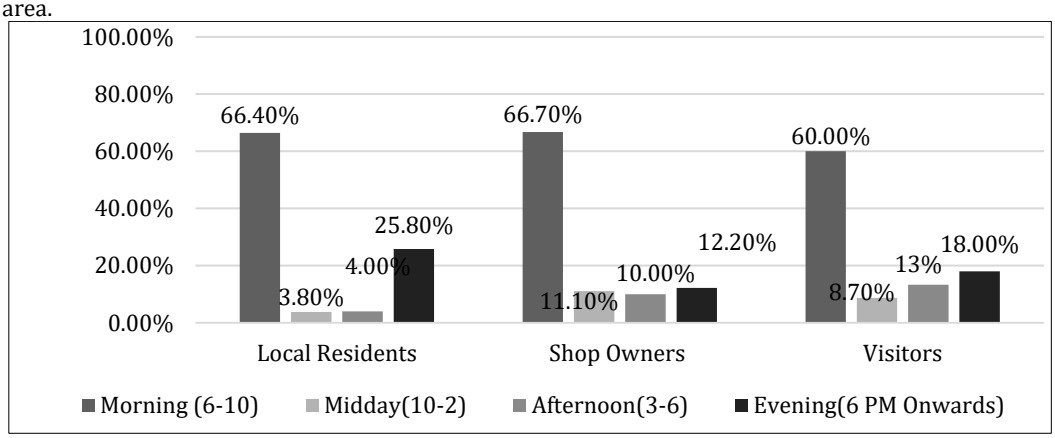


Figure 7. Time at which most traffic congestion is faced by the residents, shop owners, and visitors in the study area.

It is seen in Figure 6 that the frequent traffic congestions were faced by all the respondent groups and a significant number of respondents feel that the traffic congestion was always faced by them in the study area. This indicates that traffic congestion is a prevalent issue that affects residents, shop owners, and visitors alike, regardless of their demographic or occupational status. Also, it is not just an occasional inconvenience but rather a persistent problem that impacts the daily lives of individuals navigating through the area. Most of the respondents feel that traffic congestion is primarily faced during the morning time, as shown in Figure 7. This suggests that peak traffic congestion occurs during rush hours, likely coinciding with the morning commute as

people travel to work or school. Additionally, a significant number of respondents also feel that congestion is experienced during the evening time.

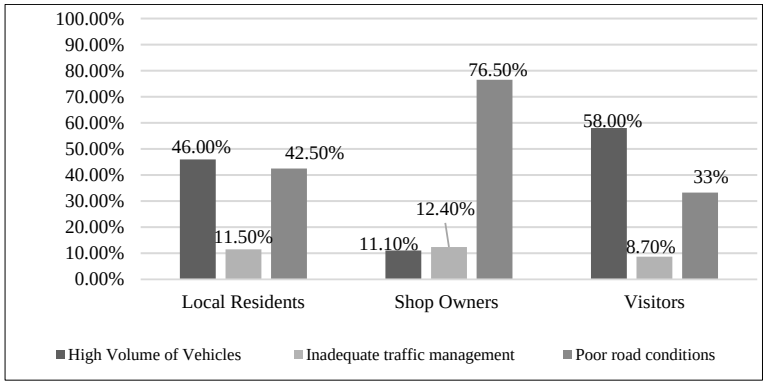


Figure 8. Main cause of traffic congestion according to the residents, shop owners, and visitors in the study area.

It is seen in Figure 8 that a significant number of respondents identified the high volume of vehicles as a primary cause of traffic congestion. This suggests that the sheer number of vehicles on the roads exceeds the capacity of the infrastructure, leading to congestion. High volumes of vehicles can result from factors such as population growth, urbanization, economic activity, and inadequate public transportation options. Another key cause of traffic congestion identified by respondents is inadequate traffic management. This indicates that issues related to traffic flow, signal coordination, lane management, and enforcement of traffic rules contribute to congestion. Inefficient traffic management can exacerbate congestion by causing bottlenecks, gridlock, and delays in traffic movement. Also, the poor road conditions were found to be a significant factor contributing to traffic congestion. This includes factors such as potholes, uneven surfaces, lack of maintenance, and insufficient road capacity. Poor road conditions can slow down traffic, increase travel times, and create hazards for vehicles.

3.3. Parking in the study area

Upon studying the space availability for parking in the study area, as shown in figure 9, it was observed that a relatively small proportion of residents (23.2%) and visitors (26.0%) have dedicated parking spaces in the study area. This suggests that a significant portion of the population does not have access to dedicated parking facilities, potentially leading to competition for limited parking spaces. Also, a significant percentage of local residents (11.5%), shop owners (22.2%), and visitors (40.7%) utilize surface parking indicating that the individuals are resorting to alternative parking options due to the limited availability of dedicated parking spaces. The majority of residents (65.3%), shop owners (77.6%), and a significant proportion of visitors (33%) perceive a lack of space availability for parking in the study area, reflecting the challenges faced by individuals in finding adequate parking spaces, which can contribute to congestion, inconvenience, and frustration among motorists. Further, as determined from figure 10, parking in the study area is not well-maintained. The lack of maintenance implies that parking facilities are suffering from issues such as litter, potholes, inadequate lighting, and lack of signage, which is detracting from the overall user experience and safety of parking areas.

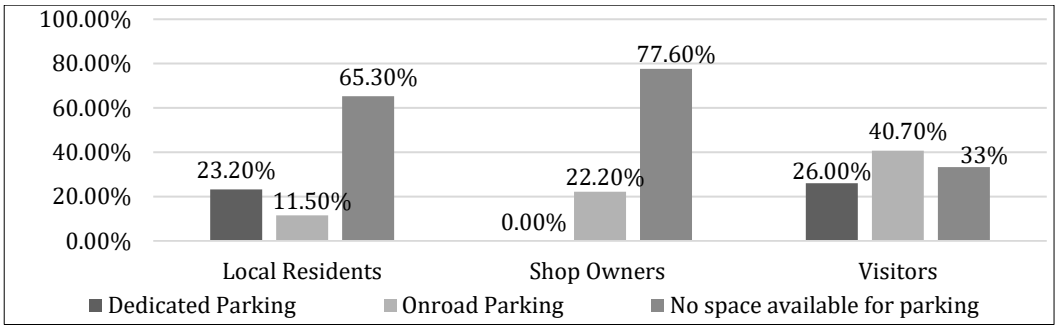


Figure 9. Space availability for parking with respect to the residents, shop owners, and visitors in the study area.

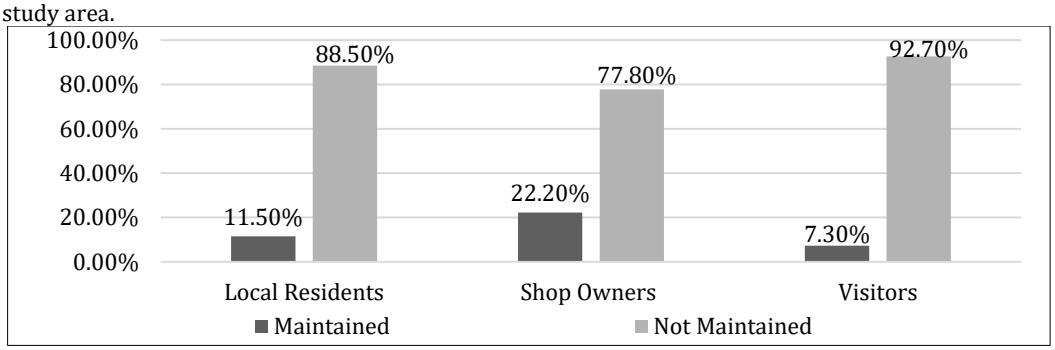


Figure 10. Condition of parking area.

It is seen in Figure 11 that during morning and mid-day times, a significant number of respondents find it easy to park indicating that the parking availability is relatively better during these periods, likely due to lower demand or fewer activities taking place in the study area at those times. Whereas it is very difficult to find parking space during the evening time which indicates that the parking availability is severely constrained during the evening hours due to peak activity periods, such as after-work hours and leisure outings, leading to heightened competition for parking spaces. Also, the chaotic conditions created by the presence of the PPR mall and food kiosks in the study area indicates that commercial establishments and entertainment venues in the vicinity contribute to increased vehicular traffic and parking demand, resulting in congestion and chaotic parking situations during peak hours.

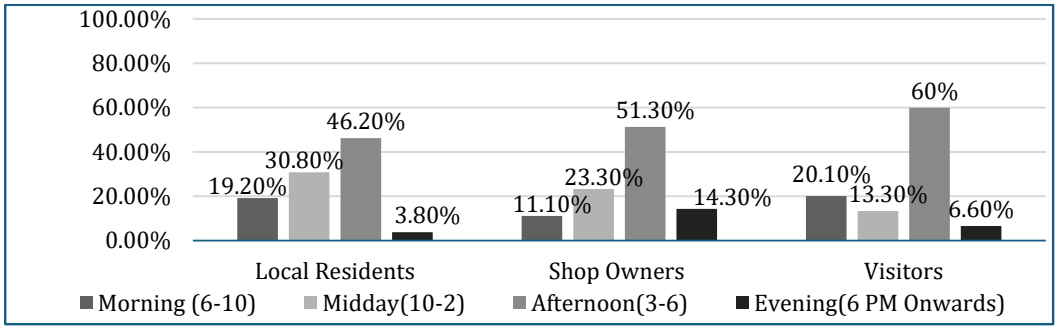


Figure 11. Easy availability of parking for the residents, shop owners, and visitors in the study area.

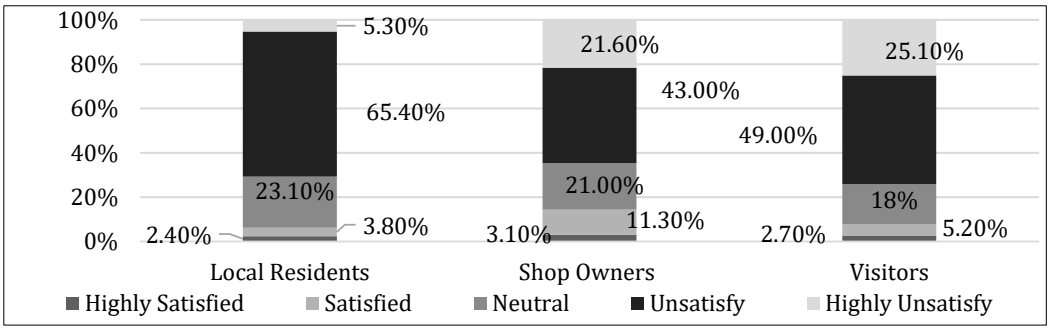


Figure 12. Satisfaction of residents, shop owners, and visitors with parking infrastructure in the study area.

While investigating the satisfaction levels for parking infrastructure, as shown in figure 12, it was observed that most of the residents (70.7%), shop owners (64.6%), and visitors (74.1%) express dissatisfaction with the parking infrastructure indicating a widespread discontent among all respondent groups regarding the current state of parking facilities in the study area. However, only a small percentage of residents (6.2%), shop owners (14.4%), and visitors (7.9%) report being satisfied with the parking infrastructure indicating a markedly low satisfaction levels across all the respondent groups. The patterns of satisfaction and dissatisfaction levels with parking infrastructure are emphasizing the inadequacy of existing parking facilities to meet the needs and expectations of users.

3.4. Services in the study area

After evaluating the current conditions of transportation and parking conditions and discussing the issues associated with them, this sub-section discusses the current conditions of water supply, power cuts, waste management, and drainage, in the study area.

3.4.1. Water Supply

Upon investigation, it was observed that the water is supplied in two shifts, i.e., 5-9 AM and 5-9 PM, in the residential area by the municipal corporation of Jalandhar. The provision of water in shifts may be a strategy employed by the municipal corporation to manage water distribution efficiently and ensure equitable access among residents. However, there is no water supply by the municipal corporation in the commercial area, indicating that businesses and commercial establishments in the area do not receive water supply from the municipal corporation and may need to rely on alternative sources for their water needs. This highlights the high usage of motorable and groundwater in the commercial area. The reliance on alternative water sources may be due to the absence of municipal water supply or insufficient supply to meet the demands of commercial activities.

3.4.2. Power Cuts

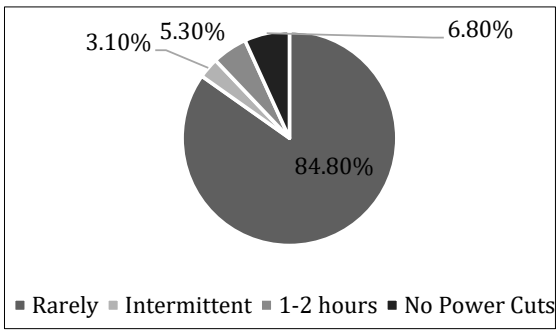


Figure 13. Frequency of power cuts in the study area.

It is seen in figure 13 that most of the respondents, accounting for 84.8%, feel that power cuts rarely occur in the study area implying that the power supply is generally reliable, with interruptions in electricity supply being infrequent occurrences for most residents and commercial units. Additionally, a small percentage of respondents, 6.8%, report that they have not observed any power cuts in the study area. Generally, the power cuts were occurred during some faults in the electricity supply lines. This indicates that the interruptions in power supply are primarily due to technical issues such as equipment malfunctions, infrastructure failures, or maintenance activities rather than systematic deficiencies in the electricity grid.

3.4.3. Waste Management

Upon investigating the condition of waste management in the study area, shown in figure 14-16, it was observed that majority of the respondents (93.3%) report that door-to-door waste collection takes place in the study area which shows that there is a systematic process in place for collecting waste. Further, the remaining waste is collected through dhalaos, which are community dustbins indicating a dual waste collection system aimed at ensuring comprehensive waste removal from the study area. However, the frequency of waste collection appears to be - insufficient, as only 19.2% of respondents indicate that waste is collected every day. While most of the respondents (68.3%) agree to segregate waste at the source, a significant proportion may not be actively participating in waste segregation practices. So, it can be concluded that there exists a gap between awareness and implementation of waste segregation practices among the respondents. Proper waste segregation is essential for efficient waste management and recycling initiatives, and efforts may be needed to increase compliance and participation in waste segregation activities.

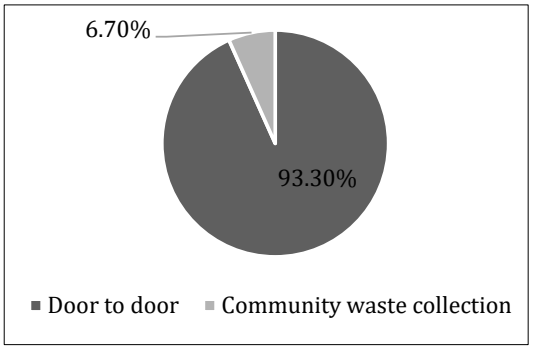


Figure 14. Method of waste collection in the study area

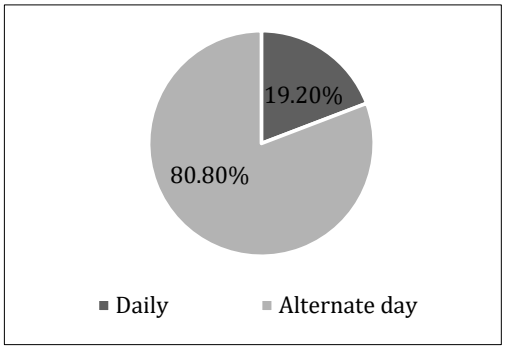


Figure 15. Frequency of waste collection in the study area

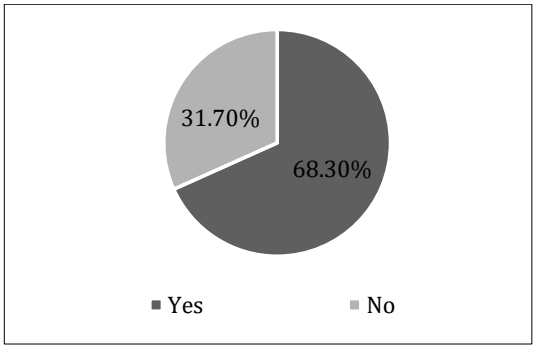


Figure 16. Segregation of waste at source in the study area

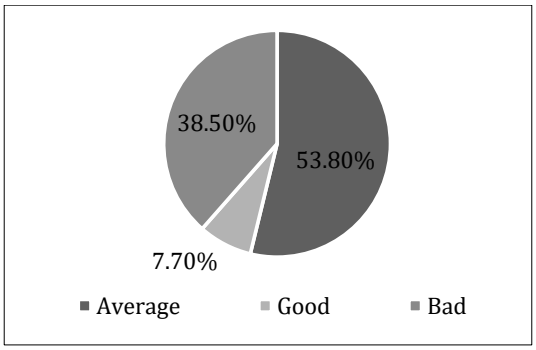


Figure 14. Condition of Storm Water Drainage in the study area.

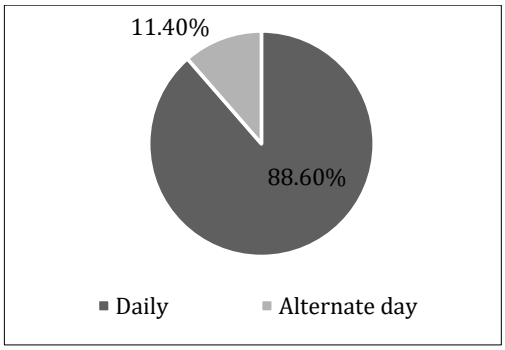


Figure 18. Frequency of roads cleaning in the study area.

3.4.4. Drainage

Although rain was not observed in the past 60 days in the study area, while enquiring about the condition of stormwater drainage, as shown in Figure 17, it was observed that 53.80% of the respondents felt that the conditions of stormwater drainage were average, whereas, a significant number of respondents, i.e., 38.5%, reported the poor drainage of stormwater during heavy rainfalls. Upon investigating the frequency of cleaning of roads, as shown in figure 18, 88.6% of the respondents reported the daily cleaning of roads, while the rest reported that the cleaning is done on alternate days.

3.5. Section Inference

The results of the survey were discussed in subsections 3.1 to 3.4. In this sub-section, the inferences of the above-discussed survey are discussed.

The findings in the study area with respect to the demographics of the respondents indicate a predominance of individuals in their thirties and forties with relatively high-income levels.

The findings with respect to transportation in the study area provide insights into the transportation preferences and perceptions of public transport availability among residents, shop owners, and visitors to the study area, highlighting the diversity of transportation modes utilized and the importance of public transit infrastructure. The findings also highlighted the widespread and persistent nature of traffic congestion in the study area, underscoring the need for effective solutions to alleviate congestion and improve mobility for all stakeholders. Further, these findings implied the multifaceted nature of traffic congestion, with causes ranging from factors related to vehicle volume and traffic management to issues pertaining to road infrastructure and conditions. These issues require comprehensive strategies that focus on improving transportation systems, enhancing infrastructure, and implementing effective traffic management practices.

The findings with respect to the parking in the study area highlighted the inadequate availability and maintenance of parking facilities in the study area, contributing to challenges such as parking shortages, congestion, and dissatisfaction among residents, shop owners, and visitors. These issues require strategies to improve parking infrastructure, increase availability, and enhance maintenance efforts to meet the needs of the growing urban population. Also, the temporal variability in parking conditions was highlighted in the study area, with ease of parking observed during off-peak times and significant challenges encountered during peak hours, particularly in the evening. The presence of commercial and recreational attractions increases parking demand during peak hours, implying the need for effective parking management strategies to alleviate congestion and improve the parking experience for users. Further, widespread dissatisfaction with parking infrastructure in the study area was observed, indicating the urgent need for improvements and enhancements to address the parking challenges faced by residents, shop owners, and visitors. These concerns can contribute to alleviating congestion, enhancing convenience, and improving the overall urban experience in the study area.

The findings with respect to the water supply in the study area highlighted the differences in water supply infrastructure and usage patterns between residential and commercial areas in the study area. While residents receive water supply in shifts from the municipal corporation, businesses in the commercial area rely on motorable and groundwater sources to fulfill their water needs. The disparities in water supply and ensuring adequate access to safe and reliable water sources is crucial for promoting the well-being and sustainability of both residential and commercial communities in the area.

The findings with respect to the power cuts in the study area suggested that power cuts are relatively rare occurrences and are typically associated with specific technical issues rather than widespread infrastructure deficiencies. The overall reliability of electricity supply in the area contributes to the functioning and productivity of residents and commercial, minimizing disruptions and ensuring uninterrupted access to essential services powered by electricity.

The findings with respect to waste management in the study area highlighted the challenges related to the frequency of collection and the adoption of waste segregation practices. These challenges require improvements in waste collection scheduling, public awareness campaigns promoting waste segregation, and community engagement initiatives to encourage active participation in waste management practices.

The findings with respect to the drainage in the study area highlighted the importance of effective stormwater drainage infrastructure and regular road cleaning practices for maintaining cleanliness, preventing flooding, and ensuring the overall well-being of residents. Addressing any deficiencies in stormwater drainage and maintaining consistent road cleaning practices can contribute to improved infrastructure resilience and enhanced quality of life for residents.

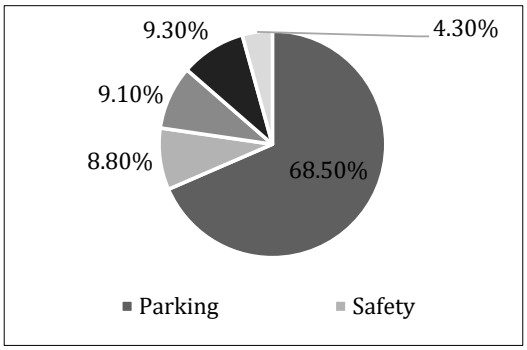


Figure 15. Issues identified in the study area with respect to the residents.

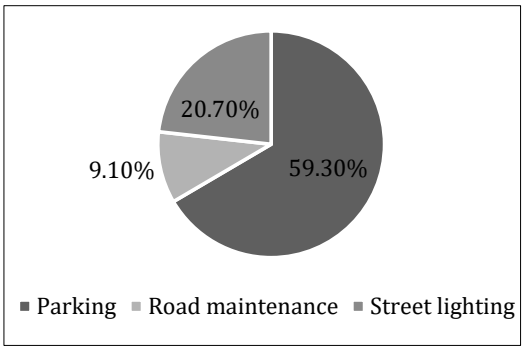


Figure 16. Issues identified in the study area with respect to the shop owners.

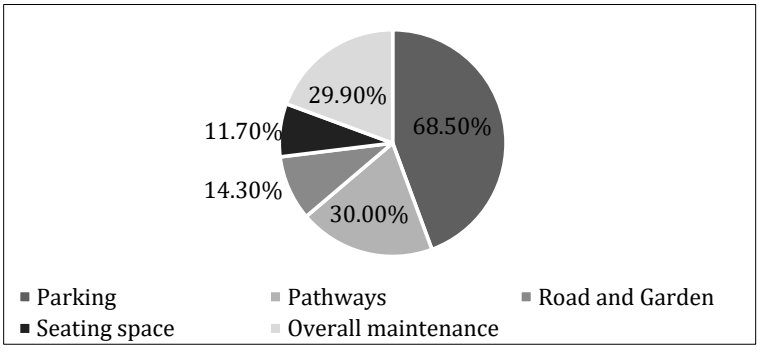


Figure 17. Issues identified in the study area with respect to the visitors.

The overall issues faced by the respondents highlight a range of concerns and priorities, as shown in Figure 19-21, identified by residents, shop owners, and visitors in the study area, including parking facilities, safety, road maintenance, noise, street lighting, and amenities such as seating and green spaces. It was observed that most of the respondents from all groups - residents (68.5%), shop owners (59.3%), and visitors (68.5%) - feel that parking facilities in the study area need improvement suggesting the concerns about the availability, accessibility, or quality of parking infrastructure, indicating a need for enhancements to address parking-related challenges. A small percentage of residents (8.8%) also feel that the safety in the study area needs improvement highlighting the concerns related to crime, lighting, pedestrian safety, or other safety-related issues that need to be addressed to enhance the overall safety and security of residents and visitors. Some residents (9.1%) and shop owners (9.1%) feel that roads need maintenance and gardens need to be improvised. This highlights the concerns about the condition of roads and green spaces in the study area, indicating a need for maintenance, repair, or beautification efforts to improve the aesthetic appeal and functionality of these areas. Also, a small percentage of residents (9.3%) identify noise as a disturbing factor in the study area from sources such as traffic, construction, or commercial activities that affect the quality of life for residents. Some shop owners (20.7%) feel that street lighting needs to be improved, while a smaller percentage of visitors (11.7%) feel that seating along the area needs to be increased, which highlights the concerns about lighting levels for safety and visibility, as well as the availability of comfortable seating for residents and visitors to enjoy public spaces.

4. Conclusion

Rapid urbanization and population growth have resulted in increased pressure on transportation networks, utilities, and public services. Traffic congestion, inadequate parking facilities, and overburdened utilities contribute to the deteriorating quality of life for residents and commuters alike. The major problems identified in the study area include inadequate parking; poor road maintenance; noise and safety issues; and unavailability of street lighting, pathways, and proper seating space. Addressing these issues requires comprehensive planning, infrastructure improvements, and community engagement to enhance the overall liveability and functionality of the study area.

- Three main factors contributing to the traffic congestion in the study area were identified, namely high volume of traffic, inefficient traffic management, and poor road conditions. These issues require comprehensive strategies that focus on improving transportation systems, enhancing infrastructure, and implementing effective traffic management practices.
- The mobility in the study area needs to be improved so that the traffic congestion can be alleviated.
- Due to the inadequate availability and maintenance of parking facilities in the study area, various challenges such as parking shortages, congestion, and dissatisfaction among residents, shop owners, and visitors, were identified. These issues require strategies to improve parking infrastructure, increase availability, and enhance maintenance efforts to meet the needs of the growing urban population.
- The disparities in water supply need to be taken care and adequate access to safe & reliable water sources is crucial and needs to be ensured for promoting the well-being & sustainability of both residential and commercial communities in the area.
- The challenges related to the frequency of waste collection and the adoption of waste segregation practices require improvements in waste collection scheduling, public awareness campaigns promoting waste segregation, and community engagement initiatives to encourage active participation in waste management practices.

References

[1] R. Bharmoria and V. Sharma, "Analyzing the urban sustainable development impact of degraded visual quality on streetscape causing visual variation: A case of Dharamshsla, himachal Pradesh," *Environ. Dev. Sustain.*, 2024, doi: 10.1007/s10668-024-04606-5.

[2] J. W. J. Weltevreden and T. Van Rietbergen, "e-Shopping versus City Centre Shopping: The role of perceived city centre attaractiveness.," *Tijdschr. voor Econ. en Soc. Geogr.*, vol. 98, no. 1, pp. 68–85, 2007, doi: https://doi.org/10.1111/j.1467-9663.2007.00377.x.

[3] F. Erkip, "The rise of the shopping mall in Turkey: the use and appeal of a mall in Ankara," *Cities*, vol. 22, no. 2, pp. 89–108, 2005, doi: https://doi.org/10.1016/j.cities.2004.10.001.

[4] C. Teller, S. Wood, and A. Floh, "Adaptive resilience and the competition between retail and service agglomeration formats: an international perspective," *J. Mark. Manag.*, vol. 32, no. 17, pp. 1537–1561, 2016, doi: https://doi.org/10.1080/0267257x.2016.1240705.

[5] R. Bromley, A. Tallon, and C. Thomas, "City centre regeneration through residential development: contributing to sustainability," *Urban Stud.*, vol. 42, no. 13, pp. 2407–2429, 2005, doi: https://doi.org/10.1080/00420980500379537.

[6] K. Lata, K. Thapa, and A. Rajput, "Liveability of indian cities and spread of covid-19-- case of tier-1 cities.," *Indian J. Public Adm.*, vol. 67, no. 3, pp. 365–382, 2021, doi: https://doi.org/10.1177/00195561211038063.

[7] R. Nainwal and A. Sharma, "Energy efficiency initiatives and regulations for commercial buildings in India: a review," *Environ. Dev. Sustain.*, 2023, doi: https://doi.org/10.1007/s10668-023-03884-9.

[8] K. Faust, D. Abraham, and S. McElmurry, "Water and wastewater infrastructure management in shrinking cities.," *Public Work. Manag. Policy*, vol. 21, no. 2, pp. 128–156, 2015, doi: https://doi.org/10.1177/1087724x15606737.

[9] A. Guironnet, K. Attuyer, and L. Halbert, "Building cities on financial assets: the financialization of property markets and its implications for city governments in the Paris city-region.," *Urban Stud.*, vol. 53, no. 7, pp. 1442–1464, 2015, doi: https://doi.org/10.1177/0042098015576474.

[10] S. Chen *et al.*, "Revisiting the association between temperature and covid-19 transmissibility across 117 countries.," *Erj Open Res.*, vol. 6, no. 4, 2020, doi: https://doi.org/10.1183/23120541.00550-2020.

[11] A. Ghosh, S. Nundy, S. Ghosh, and T. Mallick, "Study of covid-19 pandemic in london (uk) from urban context.," *Cities*, vol. 106, 2020, doi: https://doi.org/10.1016/j.cities.2020.102928.

[12] Q. Cheng, Z. Liu, G. Cheng, and J. Huang, "Heterogeneity and effectiveness analysis of covid-19 prevention and control in major cities in China through time-varying reproduction number estimation.," *Sci. Rep.*, vol. 10, no. 1, 2020, doi: https://doi.org/10.1038/s41598-020-79063-x.

[13] R. Nainwal and A. Sharma, "Comparison of multi linear regression and artificial neural network to predict the energy consumption of residential buildings," *IOP Conf. Ser. Earth Environ. Sci.*, vol. 1084, p. 012005, 2022, [Online]. Available: 10.1088/1755-1315/1084/1/012005

[14] R. Nainwal and A. Sharma, "Development of an energy prediction model for residential buildings using Artificial Neural Network," *IOP Conf. Ser. Earth Environ. Sci.*, vol. 1279, no. 1, p. 012006, 2023, doi: 10.1088/1755-1315/1279/1/012006.

ANNEXURE

SURVEY QUESTIONNAIRE

Demographics				
Name:				
Age Group:	20-30 Years	30-40 Years	40+ Years	
Income Level:	5-10 LPA	10-20 LPA	>20LPA	
Category of Respondents:	Resident	Shop Owner	Visitor	
		Traffic and Transportation		
Travel Mode:	2-Wheeler	4-Wheeler	Public Transport	
Frequency of Traffic Congestion:	Frequently	Occasionally	Always	
Time of Traffic Congestion:	Morning (6-10AM)	Midday (10-2PM)	Afternoon (3-6 PM)	Evening (6PM onwards)
Cause of Traffic Congestion:	High Volume of Vehicles	Inadequate Traffic	Management Poor Road conditions	
Availability of Public Transportation:	Average	Good	Bad	
		Parking		
Location of Parking:	Dedicated	On road/outside	No space available	
Parking Condition:	Maintained	Not maintained		
Easy availability of Parking:	Morning (6-10AM)	Midday (10-2PM)	Afternoon (3-6 PM)	Evening (6 PM onwards)
Satisfaction with Parking Infrastructure:	Highly Satisfied	Satisfied	Neutral	Unsatisfactory	Highly unsatisfactory
Mode of transportation:	Pedestrian	2-Wheeler	4-Wheeler	
Frequency to visit PPR:	Daily	Weekly	Monthly	
		Services		
Water Supply:	No. of Shifts:	Duration of Supply:		
Power Cuts:	Rarely	Intermittent	1-2 Hours	No power cuts
Waste Management:	*Method*:	Door to Door	Community	
	Frequency:	Daily	Alternate Day	
	Segregation of waste at source:	Yes	No	
Drainage *Condition:*	Good	Average	Bad	
Maintenance:	Good	Average	Bad	
Cleaning of Roads:	Daily	Alternate		

IOP Conference Series: Earth and Environmental Science

PURPOSE-LED PUBLISHING™

PAPER • **OPEN ACCESS**

Sustainable utilisation of sugar cane molasses as a partial replacement to bitumen in bituminous pavements

To cite this article: Jayasree Kuchu 2024 *IOP Conf. Ser.: Earth Environ. Sci.* **1409** 012018

View the article online for updates and enhancements.

You may also like

- Sub-Doppler laser cooling of fermionic ^{40}K atoms in three-dimensional gray optical molasses
D. Rio Fernandes, F. Sievers, N. Kretzschmar et al.
- Effect of Different Levels of Brewer's Yeast *Schizosaccharomyces pombe* and Molasses on some Growth Parameters of Common Carp *Cyprinus carpio* L.
Mariam Jassim Mohammed, Haider Kadhum Abd and Jassim Kassim Al-Gharawi
- The effect of molasses addition on physicochemical and sensory characteristics of tempeh-based soy sauce
F Widodo and D Lo



This content was downloaded from IP address 47.247.77.11 on 27/11/2024 at 05:37

Sustainable utilisation of sugar cane molasses as a partial replacement to bitumen in bituminous pavements

Jayasree Kuchu[1*]

[1]Department of Civil Engineering, Vasavi college of Engineering, Hyderabad, India

*Email: kuchu.jayasree@staff.vce.ac.in

Abstract. Energy consumption in manufacturing bitumen is high and limited availability of non-renewable energy resources in the production of bitumen lead to explore alternatives to bitumen in road construction. The alternatives included exploration of sugar molasses that is sustainable, nontoxic, economical and environment friendly option and obtained from industrial wastes. There are more than 700 sugar factories in India and they produce Molasses as by product. The objective of this study is to determine the effect of sugarcane waste molasses in bituminous mix design. Comparison of conventional bitumen and molasses bitumen is done using laboratory tests. Bitumen has been replaced with molasses from 0% to 11% and Marshall stability test has been performed. It was observed that 10% replacement of Molasses has shown optimal results in improving the performance of the mix.

Keywords: sustainable, ecofriendly, molasses

1. Introduction

Bitumen is the conventional binder used in flexible pavement construction throughout the world. The properties of the bitumen play a very important role in the performance of the pavement. All the natural resources used in the manufacturing process are depleting due to globalisation and there is always a challenge to the present generation to explore and investigate new alternatives for construction. Out of the alternatives available, use of waste materials is gearing up in construction industry to promote sustainability. The use of various alternatives for bitumen and aggregates in bituminous mixtures is currently considered as one of the main challenges in pavement industry for reducing bitumen and aggregate consumption to achieve sustainable transportation that promotes environmental, economic, and health benefits. Some of the alternatives for aggregates include slag aggregates, recycled aggregates, demolition waste, crumb rubber, synthetic aggregates and so on. The alternatives for bitumen include sugar cane molasses, beet molasses, swine manure, waste cooking oil and wood waste. One of these replacement alternatives that are sustainable, nontoxic and environmentally friendly material is sugar cane by-product called molasses. During the preparation of sugar, molasses is the final effluent obtained by repeated crystallization. It consists of 3-4% of cane juice. It is a dark black liquid of varying viscosity based on the purity. Molasses is environment friendly and also reduces the cost of construction. The purpose of this study is to determine molasses as an alternative partial replacer for bituminous binder to create a low-cost, less polluting and locally available paving material for road construction.

Content from this work may be used under the terms of the Creative Commons Attribution 4.0 licence. Any further distribution of this work must maintain attribution to the author(s) and the title of the work, journal citation and DOI.
Published under licence by IOP Publishing Ltd

The conceptual framework for this study is centered around addressing the challenges of high energy consumption and the limited availability of non-renewable resources in the production of bitumen. As the construction industry seeks more sustainable practices, the exploration of alternative materials becomes crucial. Sugar molasses, a byproduct of the sugar industry, emerges as a viable option due to its sustainability, non-toxicity, and cost-effectiveness. With over 700 sugar factories in India producing molasses, this byproduct offers significant potential for reuse in road construction. The study aims to investigate the impact of incorporating sugarcane waste molasses into bituminous mixtures, focusing on how it affects the material properties and overall performance of the pavement. The research involves replacing conventional bitumen with varying percentages of molasses, ranging from 0% to 11%, and conducting laboratory tests, including the Marshall stability test, to assess the performance of these modified mixtures. This approach is designed to identify the feasibility and optimal conditions for using molasses as a partial substitute for bitumen in pavement construction, contributing to more sustainable infrastructure development.

Utilizing sugar cane molasses as a partial replacement for bitumen in pavements offers several social benefits. It supports agricultural communities by providing farmers with additional income from molasses, a byproduct, while promoting sustainable practices in farming. This substitution reduces reliance on fossil fuels, contributing to lower greenhouse gas emissions and improved air quality, which benefits public health. Moreover, if cost-effective, molasses-based pavements could lower infrastructure costs, making road development more accessible, particularly in underserved regions. Engaging local communities in this initiative can also foster social equity and ensure that the benefits of sustainable infrastructure are widely shared.

Rangaraj and Srinivasan (2020) have done experimental investigation by using molasses and quarry dust with 15% and 21 % respectively in the mix by replacing bitumen and fine aggregates [1]. Vaishali et al (2015) have replaced bitumen with 0 to 3 % sugarcane molasses and found that the penetration and softening point have increased with addition of the binder [2]. The rutting resistance of the bituminous binder is found to decrease with increase in the percentage of modifiers after it is subjected to short term ageing. Jayanthi et al (2014), Prakash et al (2014) have done an experimental study on molasses and have observed the change in behaviour of bitumen with improved characteristics of penetration, ductility and Marshall stability values [3,4]. Werku and Tewordros (2020) have replaced bitumen ranging from 0 -20% and analyzed properties of molasses modified binders in the bitumen mix [5]. It was observed that low moisture in the molasses can be used as a partial replacement to bitumen to improve the rheological characteristics of the bitumen [5]. Ujjawal and Deepak (2019) have evaluated the mix by replacing bitumen with molasses from 0-15% and found that 11% replacement was ideal in terms of improvement of strength if bitumen mix. Meanwhile, another researcher evaluated the mix. [6]. Mose and Ponnurangam (2018) have investigated the effect of cane molasses on bitumen. They have conducted the experiments with three types of molasses, Molasses –A, B and C. As per their study, bitumen can be replaced to 20% in case of Molasses A to improve the performance of the road [7]. Padmapriya et al (2019) have investigated the effect of cane molasses on bitumen mix performance and have found improvement in the performance characteristics [8].

1.1. Objectives of the study

- Design of bitumen mix by partially replacing sugar cane molasses with bitumen in the mix.
- To determine the impact of using sugar cane molasses on the performance of bitumen mix.

- To check the feasibility of use of molasses as an alternate to bitumen with partial replacement in bituminous mix

2. Material properties

Materials that are used for this study are Aggregates, Bitumen and Molasses.

2.1. Aggregate

Both Fine aggregates and coarse aggregates obtained from the stone quarries located nearby are obtained for the conduct of experiments. The material passing through 20mm sieve and retained in 4.75mm sieve for coarse aggregates and material passing through 4.75mm sieve for fine aggregates are taken for the study. The nominal size of the aggregate taken for the study is 37.5 mm corresponding to Dense grade bituminous macadam grade I whose minimum BT content is 4%. Dense graded mix is a closely graded mix used in road construction in base or a binder course to cater to the heavy wheel load traffic. DBM provides good quality riding surface that is smooth in texture.

Variety of aggregate tests were conducted to ensure better quality control. The characteristics of aggregate obtained from the lab tests are shown in the table 1. The grading requirements of DBM as per IRC MORTH specifications is given in table 2 [9]. Job mix formula has been developed using Rothfuch method with three aggregate sizes and the obtained particle size distribution is shown in fig 1.

Table 1. Characteristics of aggregates

S.No.	Property	Result	Specification	Test method
1	Bulk specific gravity	2.62 g/cm3	2.5 – 3.0 g/cm3	IS: 2386 part III
2	Apparent specific gravity	2.63 g/cm^3	2.5 – 3.0 g/cm^3	IS: 2386 part III
3	Water absorption	0.2%	0.1 – 2 %	IS: 2386 part III
4	Soundness	5.2%	12%	IS: 2386-part V
5	Flakiness Index	8.3%	15%	IS: 2386 part I
6	Combined flakiness and elongation index	16.8%	35%	IS: 2386 part I
7	Impact value	12.5%	<30%	IS: 2386 part IV
8	Crushing value	15.5%	<35%	IS: 2386 part IV
9	Los Angeles Abrasion value	19.2%	<35%	IS: 2386 part IV

Table 2. Grading Requirement for Dense Bituminous Macadam (DBM)

IS Sieve (mm)	Cumulative % by weight of total aggregate passing
45	100
37.5	95-100
26.5	63-93
13.2	55-75
4.75	38-54
2.36	28-42
0.3	7-21
0.075	2-8

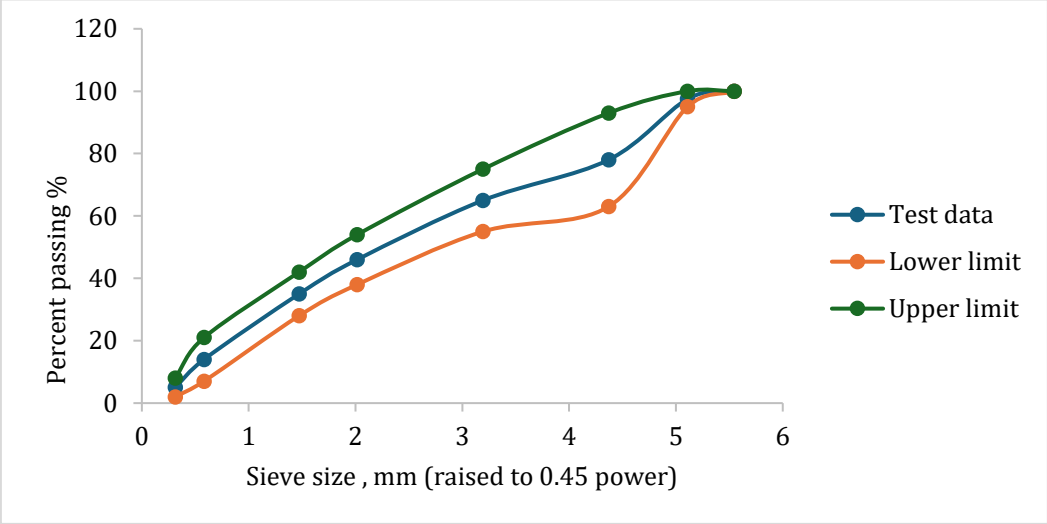


Figure 1. Particle size distribution curve

2.2. Bitumen

VG 30 grade bitumen was used in the study. To find the properties of the bitumen following tests given in table 3have been performed.

Table 3. Characteristics of bitumen

S.No.	Property	Result	Specification	Test method
1	Penetration at 25°C, 100 g, 5 s, 0.1 mm	60	45 Min	IS 1203 1978
2	Softening point °C	52.5	35 deg C-70 deg C	IS 1205 1978
3	Ductility at 250C, cm	101	100 Min	IS 1208 1978
4	Specific Gravity Test	0.99	0.97 -1.02	IS 1202 1978
5	Flash point (Cleveland open cup), °C	250	220	IS 1448
6	Absolute viscosity at 60°C, Poises	2600	2400 – 3500	IS 1206 Part 2
7	Kinematic viscosity at 135°C, cSt	367	350	IS 1206 Part 3
8	Solubility in trichloroethylene, percent	99.8	99	IS 1216

2.3. Molasses

Sugars are extracted from sugarcane and sugar beets. During the extraction process of sugars from these natural products, a byproduct called Molasses is obtained. It is dark, sweet and a viscous the colour of Molasses may vary depending on the variety or how much sugar has been extracted. Even the other characteristics like sweetness and viscosity vary. Cane molasses obtained from sugar cane industries in Telangana has been used for the study. Molasses with a sugar purity of about 95% has been used for the study. The molasses was used as a partial replacement for bitumen to prepare a molasses-modified binder.

3. Methodology

Following were the methodological steps adopted in the study

Step1: Determination of the material properties used in the study and comparison with the relevant specification. This step includes aggregate material characterisation tests as given in table 1 and bitumen material characterisation tests as given in table 3.

Step 2: Development of job mix formula for the local materials available using Rothfuch method

Step 3: Determination of optimum binder content without any replacement using Marshall stability test
Step 4: Partial replacement of bitumen with molasses and determination of optimum binder content using Marshall stability test.

3.1. Determination of optimum binder content without any replacement using Marshall stability test
The mix requirements as per MORTH specifications are given in Table 4. The stability of the test determines the worst condition of the test sample at a loading rate of 5.08 cm/minute. During loading, a dial gauge is used to measure the flow value along with the corresponding deformation. Optimum bitumen content is the binder content where the sample attains highest stability value. In order to find the optimum bitumen content marshal stability test is done and the result has been presented in table 5. For the proposed design mix gradation, four specimens are prepared for each bitumen content within the range of 4.0–5.5% at increments of 0.5 percent, in accordance with ASTMD1559 using 50 blows. The optimum bitumen content (OBC) for the DBM mixture is determined and is found to be 5 % (by wt. of total mix). This mixture without additives is considered as the control mixture for the subsequent studies.

Table 4: Requirements of DBM mix as per MORTH specifications

Test	Specification
Marshall Stability	Min 9.0 KN or 900 kg
Marshall Flow	2-4 mm
Marshall Quotient (Stability / Flow)	2-5
% Air Voids	3-5 %
% Void filled with Bitumen	65-75 %
Tensile Strength Ratio	Min 80%
% Voids in mineral Aggregate	Less than 18 %
Fines to Bitumen Ratio	0.6-1.2
Optimum Bitumen Content	OBC±0.3%

Table 5. Optimum bitumen content from Marshall stability test without any replacement

Bitumen %	Stability KN	Flow value mm	VMA %	VFB%	Air voids %
4	701.17	7.23	18.05	71.95	9.19
4.5	994.8	3	17.27	72.73	7.23
5	1006.19	1.6	15.59	72.41	4.33
5.5	950.22	2.5	17.15	72.85	4.89

3.2. Partial replacement of bitumen with molasses and determination of optimum binder content using Marshall stability test
In this study, bitumen is replaced with waste material i.e. sugar cane molasses by its weight. Bitumen replacement with molasses is attempted from 1% - 11% in the increments of 1% and Marshall Stability test is performed. Bitumen is partially replaced with molasses before preparation of the mix. A homogeneous blend of molasses and bitumen is made by mixing them at 150 degrees centigrade in a mixer for about 10 minutes. This modified binder is used in the bitumen mix and the Marshall Stability test is conducted for varying percentage of these modified binders. The results are enclosed in table 6 below.

Table 6. Stability and flow values after replacement with molasses

Molasses (%)	Stability (KN)	Flow value mm	Air voids (Vv%)	Voids in mineral aggregate (VMA %)	Voids filled with bitumen (VFB %)

1	1007.46	4.9	5.29	17.12	69.10
2	1012.12	4.3	4.99	16.87	70.42
3	1021.38	4.1	4.842	16.752	71.10
4	1032.77	3.6	4.8	16.72	71.29
5	1045.43	3.1	4.75	16.68	71.52
6	1059.35	2.9	4.63	16.564	72.05
7	1073.27	2.8	4.49	16.46	72.72
8	1141.62	2.8	4.32	15.43	72.00
9	1183.38	2.7	4.4	15.1	70.86
10	1208.7	2.6	3.9	14.9	73.83
11	1191.27	2.5	3.8	15.2	75.00

The sample in the Marshall stability apparatus is shown in Figure 2.



Figure 2. Sample prepared and Marshall stability testing in progress

The variation of data for all percentages of replacement is presented in the graphs from figures 3 to 7.

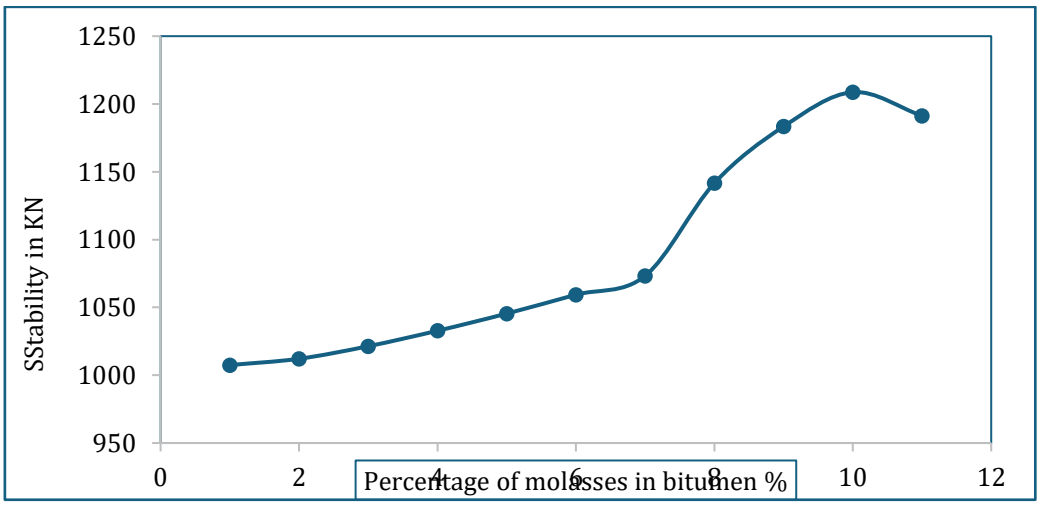


Figure 3. The effect of molasses content on stability

In the above figure 3, as the percentage of bitumen increases, the stability also increases till 10% molasses in bitumen. After 10% replacement, it is found that Stability decreases. Hence it is optimal to replace 10% bitumen with the sugar molasses. Stability is the maximum load that can be taken by the bitumen mix. With the increase of stability of the bituminous mix, the strength of the road increases which improves the performance of the road in the design life. The point where the stability value reaches a peak in the graph is taken as optimum and is taken as the design molasses content.

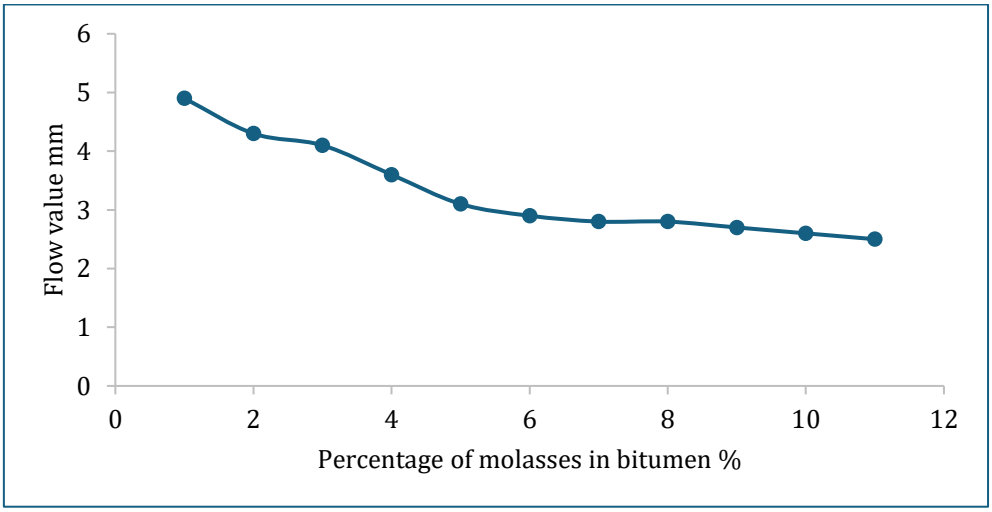


Figure 4. The effect of molasses content on flow value

It is found from the Figure 4 that highest flow value occurred at 1% partial replacement and minimum flow value occurred at 10% partial replacement of bitumen. The findings show that as percent replacement of bitumen with molasses increase, the flow value decrease. However, the ideal flow value recommended for the mix should lie between 2- 4% which is satisfied with 3% - 11% replacement of bitumen with sugar molasses. Considering this criterion of flow value, partial replacement of bitumen with 10% molasses is optimum.

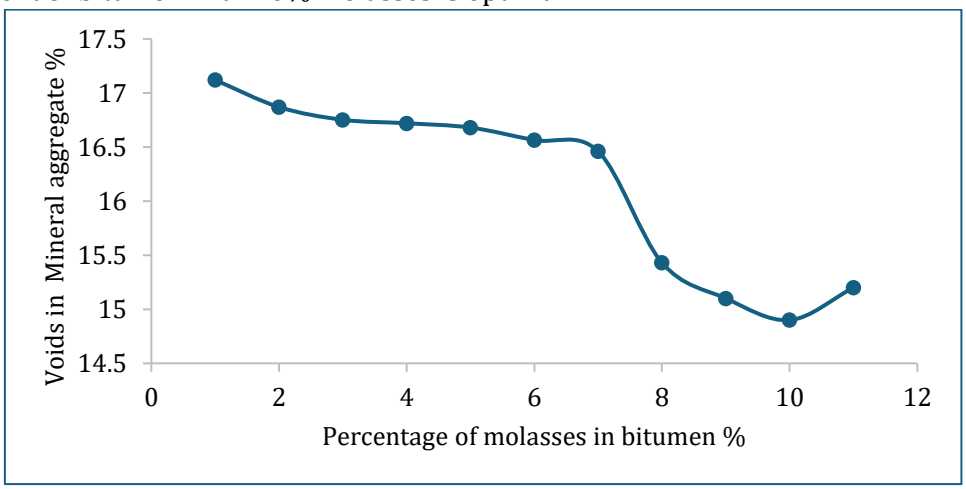


Figure 5. The effect of molasses content on VMA

As the percent of molasses in bitumen increases, voids in mineral aggregate decreases. Up to 10% replacement this trend has been observed but beyond 10% partial replacement, VMA

increased. The ideal requirement of VMA satisfying less than 18% is maintained for all stages of partial replacement.

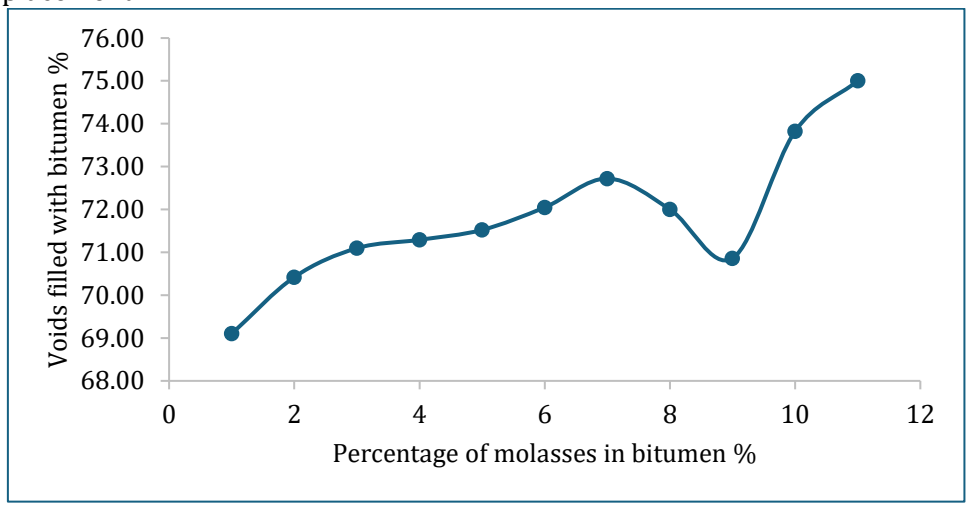


Figure 6. The effect of molasses content on VFB%

The change of voids filled with bitumen with respect to percentage of molasses in bitumen is not following the same trend as observed from figure 6. The VFB has increased with increase in replacement of molasses in bitumen up to7% and then decreased till 10% and then again increased from 10%. However, all the percentages of replacements exhibited VFB in the ideal conditions i.e. values in the range of 65%-75%. This enables to maintain a densely close graded mix that will ensure higher strength of the bitumen mix.

The ideal air voids in the bitumen mix is recommended as 3-5%. As seen in the Figure 7, as the replacement of molasses with bitumen in the mix is increasing, the percentage of the air voids is decreasing. All the samples above 2% replacement are found to fall in ideal category. 10% partial replacement of bitumen with molasses satisfies the condition for air voids in the mix.

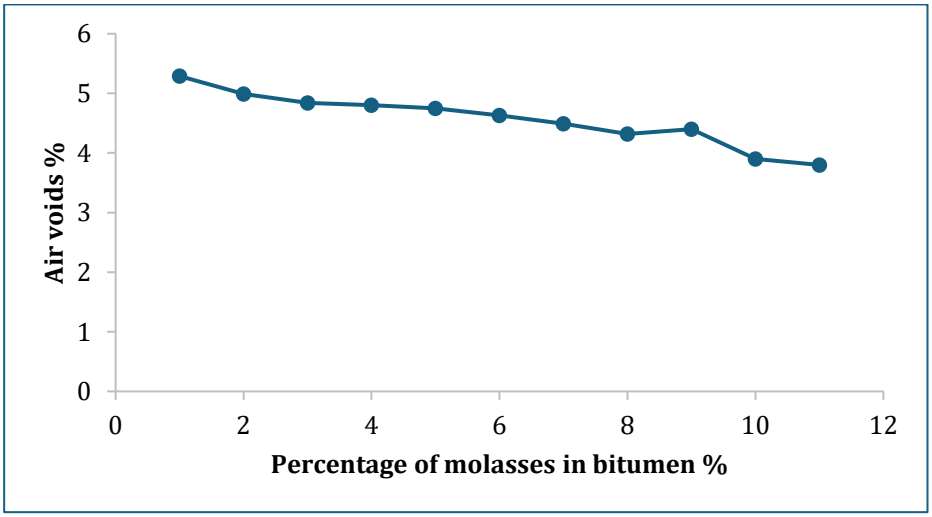


Figure 7. The effect of molasses content on Air voids

4. Conclusion

Addition of sugarcane waste molasses has increased certain properties like Marshall stability, bulk unit weight etc, and decreased the void percent in the mix. The addition of molasses prevents the moisture absorption in the mix. It also helps in preventing the oxidation of bitumen entrapped air. From this study, the behaviour of molasses modified bituminous mix has been analysed and it was found that the partial replacement of bitumen with molasses has given improved marshal characteristics. Partial replacement of 10% bitumen with molasses has resulted in satisfying all the mix conditions related to Marshall stability value, Flow value, VFB, VMA and air voids. A more stable and sustainable solution for alternative materials is achieved through this study that can use waste effectively. This eco-friendly solution can improve the pavement load bearing characteristics in the design life and also evolve as a solution to the pavement engineers in designing long lasting pavements.

References

[1] A.Rangaraj, N.P.Srinivasan, Experimental investigation on partial replacement of bitumen with sugarcane molasses and quarry dust, Adalya Journal (2020) , Volume 9, Issue 1, 298-305

[2] V.S. Vaishali, Hitesh Dave, Harpalsinh J Raol, Dhara D. Kalasareeya, A study on changes in rheological behaviour of paving grade bitumen using admixtures, International Journal of Advanced Scientific Research Development (2015), 3, 2024-2028

[3] Jayanthi, M Mahalaksmi, Meiyarasu,Abhirami, and K Shankar, Experimental study on eco-friendly tar, IJIAREC(2014), 5, 895-898.

[4] K. SPrakash,M Phanindra, S. R Surya,andJ.Naresh, Percentage replacement of bitumen with sugarcane Waste molasses, IJCIET(2014), 5, 188-197.

[5] H. Werku, G. Tewodros, Rheological properties and application of molasses modified bitumen in hot mix asphalt, Applied Science Journal (2020), 10, 1-22

[6] G. Ujjwal, J. Deepak, Partial replacement of bitumen with the sugarcane waste molasses, International Journal of Innovative Technology and Exploring Engineering (2019),8, 330-334

[7] GemechuYilikalMose and Palani Ponnurangam, Investigating the Effect of Cane Molasses on the Performance of Base Bitumen, International Journal of Research and Innovation in Applied Science (2018),3, 54-58

[8] K M Padma Priya, M. Goutham Kumar, M.Hariharan, R Shanmugam , Experimental investigation on bitumen with partial replacement of sugarcane waste molasses, IRJET, 6, 7390 – 7394

[9] MORTH specifications Hand book by Indian Roads congress, Fifth edition

Acknowledgements

The author acknowledge the laboratory and financial support given by Vasavi College of Engineering, Hyderabad, India.

IOP Conference Series: Earth and Environmental Science

PURPOSE-LED PUBLISHING™

PAPER • **OPEN ACCESS**

Influence of the basalt fibre and fly ash on the structural properties of sustainable high-strength concrete

To cite this article: S. Pallavi Charitha and S. Vijaya Kumar 2024 *IOP Conf. Ser.: Earth Environ. Sci.* **1409** 012019

View the article online for updates and enhancements.

You may also like

- Mechanical properties of high strength concrete incorporating chopped basalt fibers: experimental and analytical study
Mohit Gupta, Ritu Raj and Anil Kumar Sahu
- Effect of fiber synergy on strength & durability of high-performance concrete
Mohit Gupta, Ritu Raj, Anil Kumar Sahu et al.
- An Experimental Investigation on Concrete with Basalt Rock Fibers
Seena Simon, Arun Prathap, Sharanya Balki et al.



This content was downloaded from IP address 47.247.77.11 on 27/11/2024 at 05:37

Influence of the basalt fibre and fly ash on the structural properties of sustainable high-strength concrete

S. Pallavi Charitha[1], S. Vijaya Kumar[2*]

[1]Department of Civil Engineering, National Institute of Technology, Warangal, Telangana, India
[2]Department of Civil Engineering, Vasavi College of Engineering, Hyderabad, Telangana, India

[*]Email: s.vijayakumar@staff.vce.ac.in

Abstract The present article describes the experimental research carried out to investigate the properties of concrete containing basalt fibre reinforcement and concrete containing basalt fibres and fly ash additives. Each test was done as per Indian standards (IS-516). The experiments sought to establish both fresh and hardened concrete properties. In respect of new concrete, slump, setting time, bleeding, temperature, and density were estimated to check its quality. Compressive, flexural and split tensile strength are the three main parameters for assessing those qualities in a solidified state. It was determined that the utilization of fly ash with 20%, 30% or 40% proportions of cement involved resulted in a stronger concrete mixture. To these samples, different contents of basalt fibres 0.25%, 0.5%, and 0.75% by volume were added respectively. Standard samples were cast, cured and tested accordingly. Thus, the studies show that it is possible to mix concrete with basalt fibres without any segregation or balling effect on it or even sticking together during the mixing processes. Modestly increased splitting tensile and bending strengths have been obtained due to the introduction of basalt fibres on this composite material using which improved workability can be achieved more rapidly than conventional hydration reactions based solely upon Portland Cement chemistry, moreover, thermal stability has also been considerably enhanced, besides that even basic physical-chemical properties should be very much similar to those of ordinary Portland cement. Based materials thus ensuring better compatibility during processing from raw constituents towards final composites up-to-date with known technological aspects related specifically towards production practices carried out in developing countries like India. Such situations usually result primarily due to poor engineering control exercised over construction activities. Resulting problems areas namely joint locations limited access space between steel reinforcement bars inside walls. So often appearing weak points in overall design yield inadequate structural performance compared to intended specifications. Another reason why sustainable building methods cannot be fully adopted has been found that they lack proper skilled manpower despite having all necessary resources that are easily renewable. By compared with traditional ones made up of non-renewable sources such as fossil fuels. However, fly ash used in place of concrete only makes it harder without improving workability and strength at the optimum percentage.

Content from this work may be used under the terms of the Creative Commons Attribution 4.0 licence. Any further distribution of this work must maintain attribution to the author(s) and the title of the work, journal citation and DOI.
Published under licence by IOP Publishing Ltd

Keywords: Admixtures, fly ash, basalt fibres, mix design, regression analysis, and sustainable concrete

1. Introduction

The concrete is brittle, less crack-resistant, and has low tensile strength. It contains built-in micro cracks that grow as a result which causes concrete to crack and make it brittle. As a result of poor tensile strength, Conventional plain concrete displays no ductility. However, it has been shown that the addition of small fibres spaced regularly throughout the mix can significantly enhance its static and dynamic properties while contributing towards arresting crack growth and getting sustainable concrete. This is what is referred to as fibre-reinforced concrete. In terms of flexibility, ease of manufacture and use, and understanding of purpose, cement concrete has become the most popular building material for dwellings offices or commercial outlets plus public infrastructure. However, three things are starting to take centre stage. First is the durability of concrete which affects how well a structure performs over time. Second, is achieving economy through better design and reduced costs in construction materials used for buildings. Third is to protect economy and environment. Fly ash can be added thus to address these three problems correctly.

2. Literature review

V. Ramakrishnan [1] posits that FRC is a sustainable material for use in construction in the development of novel synthetic structural FRC (SSFRC) and its testing in different areas of structural applications. This composite has given an increase to the durability of concrete and it surpasses fibrous polypropylene concrete in relation to crack arresting and some other properties. In 2012, Pande, A.M.[2] covered the categorization of fly ash specifications, their incorporation into code provisions and the interrelations among various parameters. The author discussed several fly ash samples obtained from different thermal power plants. He looked at physical and chemical characteristics, lime reactivity, water requirement, and permeability, as well as other pertinent ratios in them. The author came to the conclusion that there are various qualities of fly ash concrete depending on where this fly ash is sourced from. Mechanical characteristics of High Strength Concrete (HSC) were studied by A Siva Kumar, Manu Santhanam and Ravichandran et al [3] , [4] using metallic and non-metallic fibres. It was established that non-metallic fibres increase ductility while reducing micro-cracks in concrete while metallic ones enhance strength. In 2014, Adel Kaikea et al [5] examined “High Performance Fibre Reinforced Concrete: The Effect of Mineral Admixtures and Steel Fibre Volume Fractions”. In 2015, Dipti Ranjan Saho [6] did experimental work with a collaborator titled “Effect of steel and polypropylene fibres on flexural behaviour of RC beams” in 2007, Baruah, P. and Talukdar [7] carried out the study “A Comparative study on Compressive flexural, tensile and shear strength of Concrete with fibres of different origins”. There are years 2022 and 2023 when S Vijaya Kumar et al., researched the impact of metakaolin on concrete as well as the bond strengths in fibrous concrete [8-10]. In the ACI manual published in 1973 called “Recommended Practice for Selected Proportions for normal weight concrete” [11] and [12] written by “Measurement of Properties of Fibre Reinforced Concrete” [13]. IR-82 "State-of-the-Art on Fibre Reinforced Concrete" was a report published by ACI in May 1982 under its journal Concrete International Design and Construction.

3. Materials Used

3.1. Cement

In this experimentation, ordinary Portland cement (OPC) 53 grade conforming to IS-269 [14] standards is used.

3.2. Fly ash

Fly ash is pozzolana material, it is a byproduct of industry. Several thermal power plants located all around the world produce a lot of fly ash. When utilized in conjunction with concrete as a mineral additive, this substance was once viewed as a byproduct that was difficult to dispose of the material of enormous value.

Massive amounts of fly ash are endangering the natural equilibrium and the environment surrounding human habitat. A lot of research is being done on fly ash to use it as an alternative building material in construction due to the significant problems mentioned above. Globally conducted studies have established the viability of using fly ash as a beneficial building ingredient as one of the sustainable.

3.3. Basalt fibres

Basalt fibres can be used to meet strong fire resistance requirements and mild strengthening needs for civil buildings, while FRP strengthening can be taken into consideration for pure strengthening. The mechanical properties of basalt fibres have been investigated for their suitability as a reinforcing agent for concrete structural materials. In hydraulic engineering and construction, unidirectional rods and basalt filaments are used to hold concrete slabs in seismically susceptible places.

The usage of basalt fibre in concrete is very significant from this angle. The igneous rock known as basalt is created when lava quickly cools down close to the earth's surface. The Indian Deccan region has an abundance of basalt rocks. It is made up of the majority of crustal rocks. Basalt and glass fibres are produced in comparable methods and in the construction field basalt fibres are more environmentally sustainable.

Table 1 lists the general characteristics of basalt fibres. It is a continuous fibre made by pulling the melted basalt rock into the appropriate shape after it has melted to a temperature of roughly 1500°C. A more recent addition to structural composites and fibre-reinforced polymers (FRP) is basalt fibre. Its chemical composition is akin to that of glass fibre, and it exhibits great resistance to both salt and conditions that are either acidic or alkaline. Basalt fibre is typically recommended for use in coastal construction and on bridges because it provides superior corrosion resistance when incorporated into concrete.

Table 1. Basalt fibres properties

Properties	Value Range
Strength of the fibre	3100-4850 MPa
Young's Modulus(E)	80-94 GPa
Percentage of elongation	2.90 per cent
diameter of the fibre	21 x 10^{-5} cm
Density	60-65 kg/m^3
Temperature	-260 to +700

3.4. Fine Aggregate

The river sand that is easily accessible in the area is adopted as fine aggregate in this experiment. The sand is free of biological contaminants, clay, and salt. The sand is tested for multiple

characteristics, such as bulk density and specific gravity, in accordance with IS 2386-1963 [15]. Zone II of IS 383-2016 is revealed by the grain size distribution of sand [16].

3.5. Coarse Aggregate

As a coarse aggregate, machine-crushed granite material a nearby source is used. There are no pollutants present, such as muck, dust, biological debris, etc. Additionally, the various characteristics of the coarse aggregate are looked at. The specific gravity of the coarse aggregate is 2.64, and its fineness modulus is 7.14. Coarse aggregate has a bulk density of 1700 kg/m3. Water having a pH less than 6 is used in this experiment.

3.6. Superplasticizer

A high-range water reduction chemical admixture from M/s. Fosroc (India) Ltd., was used sparingly to preserve the workability level (Conplast-430D).

4. Experimental Details

4.1. Concrete Mix Design for M60

The DOE technique and the IS Code [17] were used to create the M60 concrete mix]. The mix proportions meeting the design requirements were determined after tests. Tables 2 and 3 display the mix specifications.

Table 2. Concrete mix proportions (M 60 grade)

Cement (OPC)	Fine Aggregate (FA)	Coarse aggregate (CA)	Water to cement ratio
1	1.02	1.74	0.42

Table 3. For 1 cubic meter of concrete, the quantities of materials required

Cement in kg in kg	FA in kg in kg	CA in kg in kg	Water in litres
590	598	1018	238

(Note: Superplasticizer was added @ 0.5% for getting good workability)

Ballast fibres were used in the M60 concrete that was created using the aforementioned specifications at percentages of 0, 0.25, 0.50, and 0.75 by volume of concrete. Figure 1 shows the ballast fibres used in this experiment.



Figure 1. Basalt Fibres

4.2. Mixing, casting and curing

After mixing all of the concrete's ingredients with the ballast fibre, the compacting factor equipment was used to determine the workability. For casting, standard cube, cylinder, and beam moulds were utilized. The table vibrator established enough vibration to lead to compaction. Following a 24-hour air drying period, the specimens underwent demoulding, and curing periods of 7, 28, and 60 days, and they were assessed. Enough examples have been cast and cured. All operations were performed following the approved protocols. Every sample was examined by IS 516 guidelines [18].

The failure pattern of the standard specimens for compression, split tensile and flexural was shown in Figure 2.

Table 4. M-60 grade Concrete fly ash for various strengths

S. No.	% of fly ash	Compressive strength (MPa)			Split Tensile Strength (MPa)			Flexural strength (MPa)		
		7days	28days	60days	7days	28days	60days	7days	28days	60days
1	0.0	43.92	75.16	77.22	2.64	3.22	3.80	7.02	7.92	8.22
2	20.0	56.48	79.00	81.92	3.72	4.89	5.22	7.55	8.62	9.12
3	30.0	57.90	79.65	82.66	5.42	6.02	6.18	8.12	9.22	9.42
4	40.0	55.48	76.42	79.42	5.14	5.30	5.38	7.75	9.15	9.33



Compression failure



Split tensile failure



Flexural failure

Figure 2. The failure pattern of the standard specimens

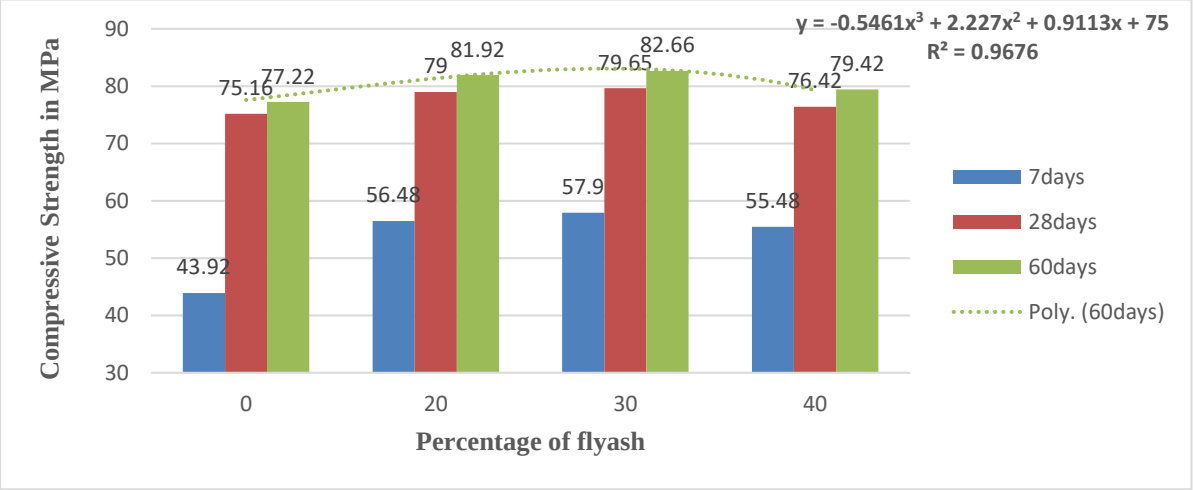


Figure 3. The compressive strength correlates to the concrete's age and fly ash

The regression equation for the best-fit curve for the compressive strength at 60 days of cured concrete is a third-degree polynomial equation,

$$s = -0.5461p^3 + 2.227p^2 + 0.9113p + 75 \text{ and } R^2 = 0.9676 \quad (1)$$

Where s= compressive strength in MPa, p is the percentage of fly ash

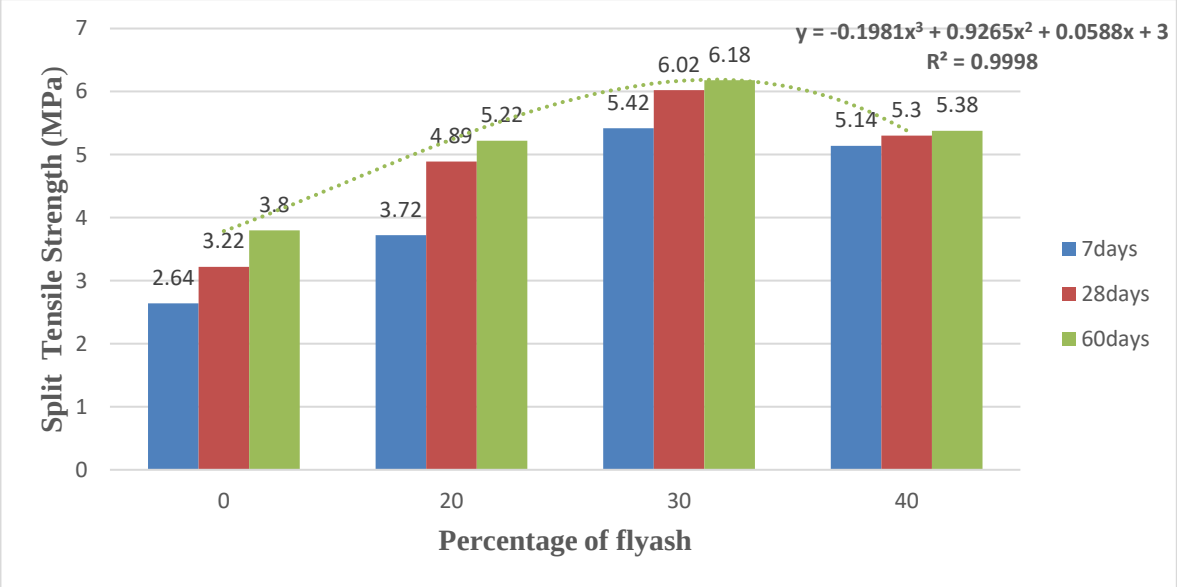


Figure 4. The split tensile strength correlates to the concrete's age and fly ash percentage

The regression equation for the best-fit curve for the split tensile strength at 60 days cured concrete is third-degree polynomial equation,

$$t = -0.1981\,x^3 + 0.9265\,x^2 + 0.0588\,x + 3 \text{ and } R^2 = 0.9998 \quad (2)$$

Where t= Split tensile strength in MPa, p is the percentage of fly ash

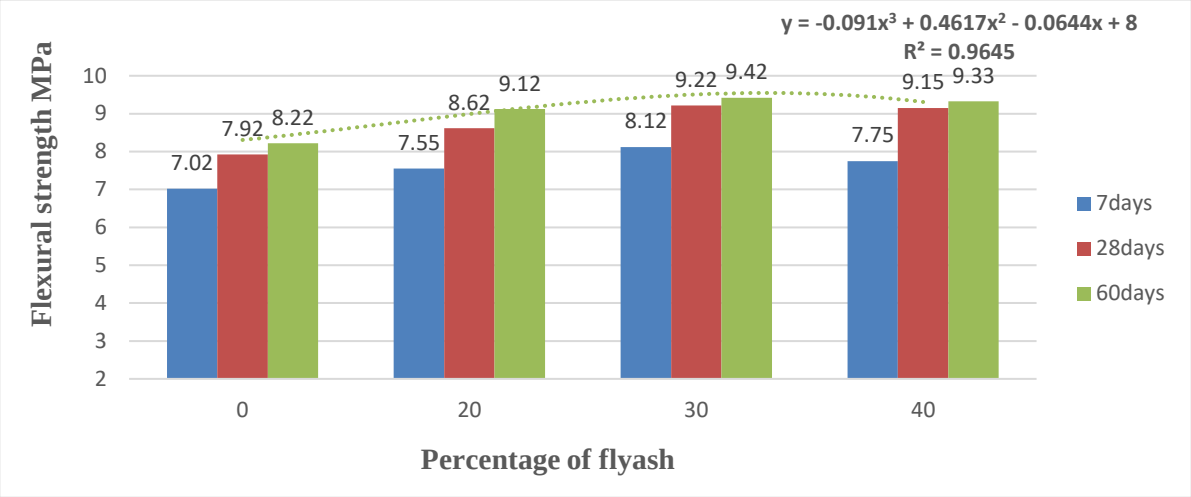


Figure 5. The flexural strength correlates to the concrete's age and fly ash percentage

The best-fit curve for the flexural strength of the concrete at 60days water cured is a polynomial equation is

$$f = -0.091\,p^3 + 0.4617\,p^2 - 0.0644\,p + 8 \text{ and } R^2 = 0.9645 \quad (3)$$

Where f= flexural strength in MPa, p is the percentage of fly ash

Table-5. M60 concrete strengths at 28 days with various percentages of Basalt fibres and fly ash percentages

S.No	% fly ash	% of Basalt fibres	Compressive Strength (MPa)	Split tensile Strength (MPa)	Flexural Strength (MPa)
1	0.0	0.00	75.14	3.20	7.90
		0.25	77.23	3.71	8.00
		0.50	78.15	4.25	8.27
		0.75	78.80	4.72	8.58
2	20	0.00	79.02	4.88	8.80
		0.25	80.12	5.22	8.89
		0.50	80.75	5.62	8.94
		0.75	81.50	5.82	9.40
3	30	0.00	79.67	6.01	9.20.
		0.25	81.50	6.25	9.42
		0.50	82.17	6.68	9.80
		0.75	84.96	6.15	9.95
4	40	0.00	76.40	5.28	9.10
		0.25	78.35	5.41	9.20
		0.50	80.75	5.62	9.42
		0.75	82.15	5.75	9.50

5. Discussion on the Results

5.1. Fly ash as an admixture

In the current experimental work, fly ash was used in place of OPC in variable amounts, up to a maximum of 40%. 36 standard cubes measuring 150 mm each were used to evaluate compressive strength; 36 cylinders measuring 150 mm in diameter and 300 mm in height were used to evaluate split tensile strength; and 36 more specimens measuring 100 mm by 100 mm by 500 mm were ready for flexural strength testing. The findings indicate that strength levels have

slightly improved at 28 days, reaching up to 30% replacement. 30% is the ideal point after which 40% of the strengths are lost.

The strengths develop as the curing period is extended beyond 28 days up to 60 days because fly ash is pozzolanic and continues to acquire strength beyond 28 days. Therefore, it is preferable to use fly ash in concrete as a partial replacement for OPC because it is more cost-effective and offers additional benefits, as well as increasing strength over time. Figures 3, 4, and 5 depicted the change of the different strengths with the percentage of fly ash as a partial replacement. They are seven days, twenty-eight days, and sixty days together with a cure period.

The mathematical equation from the regression analysis for the compressive strength of the concrete in terms of the percentage of basalt fibres is given by

$$S_1 = 0.2413\,x + 9 \; and \; R^2 = 0.9672 \quad (4)$$

Where S1 is the compressive strength of the basalt fibre concrete with optimum fly ash as a replacement to cement, x is the percentage of basalt fibres

A mathematical equation from the regression analysis based on the experimental investigation for the split tensile strength of the basalt fibre concrete is given

$$t_1 = 0.2413\,x + 9 \; and \; R^2 = 0.9672 \quad (5)$$

where t1 is the split tensile strength of the basalt fibre concrete with optimum fly ash as a replacement to cement, x is the percentage of basalt fibres

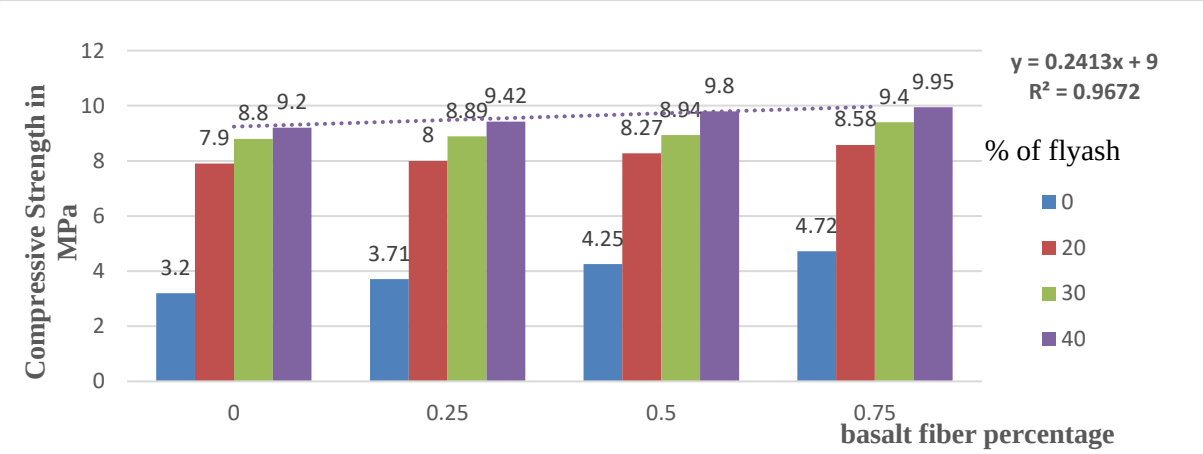


Figure 6. The compressive strength correlates with the percentage of fly ash and basalt fibre

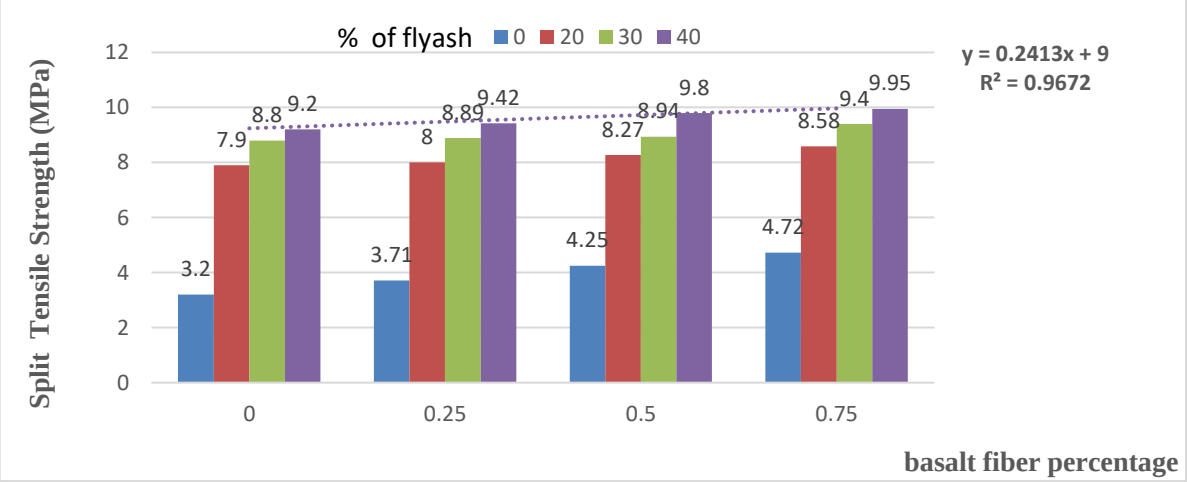


Figure 7. The split tensile strength correlates with the percentage of fly ash and basalt fibre

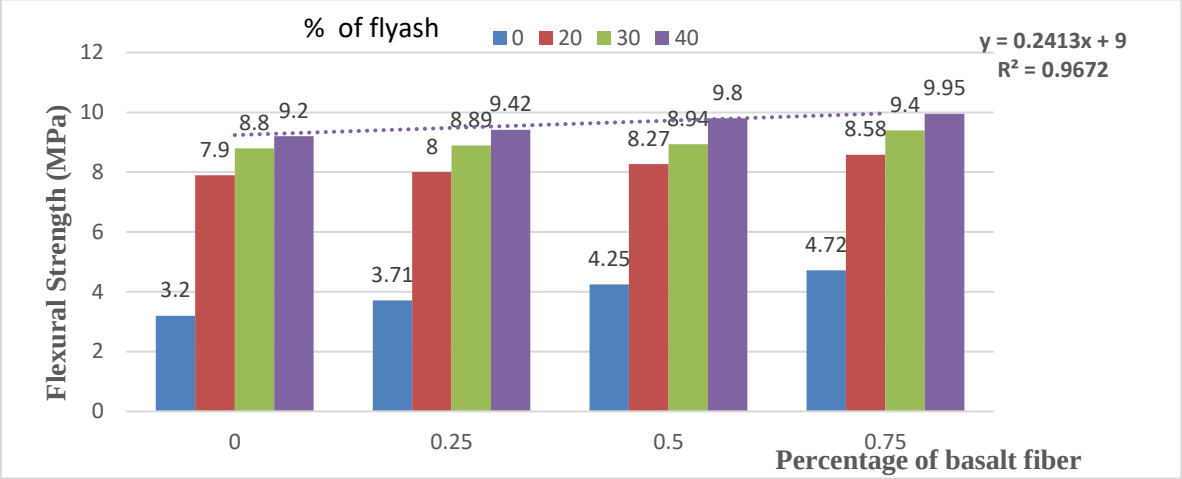


Figure 8. The flexural strength correlates with the percentage of fly ash and basalt fibre

A mathematical equation from the regression analysis based on the experimental investigation for the flexural strength of the basalt fibre concrete is given

$$f_1 = 0.2413\,x + 9 \; and \; R^2 = 0.9672 \quad (6)$$

where f1 is the flexural strength of the basalt fibre concrete with optimum fly ash as a replacement to cement, x is percentage of basalt fibres.

5.2. Contribution of Basalt Fibres

For every 4% of basalt fibres, 48 standard cubes were cast and their compressive strength was evaluated. Afterwards, 48 standard prims were cast to assess the flexural strength, and 48 more cylindrical samples were produced to test the split tensile strength. Figures 6 to 8 and Table 5 demonstrate how the strengths of the concrete increase with the percentage of basalt fibre. The gains in compressive, split tensile, and flexural strengths without fly ash are 5%, 48%, and 9%, respectively, with a maximum proportion of 0.75% of basalt fibres. The benefits grow more noticeable as the fly ash percentage rises. The addition of 30% fly ash and 0.75% fibre causes the strengths to increase at the quickest rates. For the compressive, split tensile, and flexural strengths, the corresponding increases above the reference concrete are 13%, 110%, and 26%, respectively. It is evident from this that basalt fibre strengthens, especially under stress and flexure.

5.3. Other Advantages of using basalt fibres

In addition to improving concrete's ability to bend, basalt fibres have also been shown to increase ductility. The flexure test specimens are seen to eventually fail after forming cracks. The crack propagation and pattern were more uniform. The beam specimens' ability to rotate was improved.

5.4. Limitations on the Use of Basalt Fibres

The Basalt fibres were used in the current experimental inquiry up to a maximum proportion of 0.75 of the volume of concrete. When the dosage is higher, there is a minor tendency for the fibres to ball up. Hence, for a smooth dispersion of fibres in concrete, basalt fibre usage should be kept between 0.5 and 0.75.

6. Conclusions

The following inferences are made in light of the experimental inquiry that was carried out.

- Fly ash can partially substitute cement (OPC), which not only makes concrete easier to work with but also somewhat boosts its mechanical properties.
- A 30 per cent fly ash replacement rate is determined to be the ideal level. The strengths decline beyond 30 per cent.
- The strength of fly ash concrete is further increased as the drying time (age) is extended past 28 days.
- The strengths of ballast fibre grow with the percentage of fibre used. The flexural strength and split tensile strength have both considerably improved. The combination of 30% fly ash and 0.75% basalt fibre yields the optimum strength values.
- The current analysis discovered a tendency for fibre balling when the utilisation of ballast fibre exceeded 0.75 per cent.
- Because ballast fibre is corrosion-resistant, it is advised to use high-strength concrete containing 30% fly ash and 0.75% ballast fibre when building buildings, particularly bridges, in coastal locations.

References

[1] R. Ramakrishnan, "A new look at Fiber Reinforced Concrete," in Proc of the International Conference on sustainability challenges and Advances in connote technology (SCACT) organized by P.S.G College of Technology, Coimbatore (T.N), India, May 2-4 2012, pp. 129-141.

[2] A. M. Pandey, "Flyash from characterisation to sustainable utilisation – some studies," in Proc of the International Conference on sustainability challenges and Advances in connote technology (SCACT) organized by P.S.G College of Technology, Coimbatore (T.N), India, May 2-4 2012, pp. 675-684.

[3] A. Sivakumar and M. Santhanam, "Mechanical properties of high strength concrete reinforced with metallic and non-metallic fibres," Cement and Concrete Composites, vol. 29, no. 8, pp. 603-608, 2007, DOI: 10.1016/j.cemconcomp.2007.03.006

[4] A. Ravichandran, K. Suguna, and P. N. Ragunath, "Strength modeling of high-strength concrete with hybrid fibre reinforcement," American Journal of Applied Sciences, vol. 6, no. 2, p. 219, 2009.

[5] A. Kaïkea, D. Achoura, F. Duplan, and L. Rizzuti, "Effect of mineral admixtures and steel fiber volume contents on the behavior of high performance fiber reinforced concrete," Materials & Design, vol. 63, pp. 493-499, 2014, DOI: 10.1016/j.matdes.2014.06.066.

[6] R. Sahoo Dipti, A. Solanki, and A. Kumar, "Influence of Steel and Polypropylene Fibers on Flexural Behavior of RC Beams," Journal of Materials in Civil Engineering, vol. 27, no. 8, p. 04014232, 2015, DOI: 10.1061/(ASCE)MT.1943-5533.0001193.

[7] P. Baruah and S. Talukdar, "A comparative study of compressive, flexural, tensile and shear strength of concrete with fibres of different origins," Indian concrete journal, vol. 81, no. 7, pp. 17-24, 2007.

[8] S. Vijaya Kumar, B. Dean Kumar, and B. L. P. Swami, "Regression Analysis for the Bond Strength of Steel Fibre Self-compacting Concrete Based on the Experimental Studies," Civil Engineering and Architecture, vol. 11, no. 1, pp. 175-181, 2023, DOI: 10.13189/cea.2023.110115.

[9] S. Vijaya Kumar, B. Dean Kumar, and B. L. P. Swami, "Effect of metakaolin and condensed silica fume on the rheological and structural properties of self-compacting concrete," Civil Engineering and Architecture, vol. **8,** pp. 1057-1062, 2020, DOI: 10.13189/cea.2020.080532.

[10] V. K. Urooj Masood, S. and B. L. P. Swami, "Mixed Fiber Reinforced Concrete (MFRC) - Study on Strength and Behaviour," in Proc of First International Conference on Recent Innovations in Engineering and Technology (ICRIEAT-2016), Aurora Scientific Technological and Research Academy, Hyderabad, (India), May 2-4 2016, pp. 675-684.

[11] ACI211.1-1973 "Recommended Practice for selecting proportions for normal weight concrete," American Concrete Institute, Farmington Hills, MI, USA.

[12] ACI:544.1R-1996 "State of the art report on fibre Reinforced Concrete," American Concrete Institute Farmington Hills, MI, USA.

[13] ACI:541.2R-78-1982 "Measurement of Properties of Fiber Reinforced Concrete," American Concrete Institute, Farmington Hills, MI, USA.
[14] IS:269-2015 "Ordinary Portland Cement- Specifications (Sixth Revision)," Bureau of Indian Standards, New Delhi, India.
[15] IS:2386-1963 "(Part III): Methods of Test for Aggregates for Concrete: Specific Gravity, Density, Absorption and Bulking.," Bureau of Indian Standards, New Delhi, India.
[16] IS:383-2016 "Coarse and fine aggregate for Concrete - Specification (Third Revision)," Bureau of Indian Standards, New Delhi, India.
[17] IS:10262-2019 "Concrete Mix Proportioning -Guidelines (First Revision)," Bureau of Indian Standards, New Delhi, India.
[18] IS:516-1959 "Methods of Tests for Strength of Concrete," Bureau of Indian Standards, New Delhi, India.

Acknowledgements

The authors express sincere thanks to the management of Vasavi College of Engineering, Hyderabad, for enabling them to use the Concrete lab facilities for carrying out the research investigation.

IOP Conference Series: Earth and Environmental Science

PURPOSE-LED PUBLISHING™

PAPER • **OPEN ACCESS**

Assessment of self-compacting lightweight concrete: preparation of eco-friendly fiber content on mechanical and durable characteristics

To cite this article: K. Chandrasekhar Reddy *et al* 2024 *IOP Conf. Ser.: Earth Environ. Sci.* **1409** 012020

View the article online for updates and enhancements.

You may also like

- A comprehensive study on physico-mechanical properties of non-metallic fibre reinforced SCC blended with metakaolin and alcofine
S S Vivek, B Karthikeyan, Senthil Kumaran Selvaraj et al.
- Impact and hardness optimisation of composite materials inspired by the babassu nut (*Orbignya speciosa*)
Gerrit Staufenberg, Nina Graupner and Jörg Müssig
- Composite design bioinspired by the mesocarp of Brazil nut (*Bertholletia excelsa*)
M Sonego, V F Sciuti, R Vargas et al.



This content was downloaded from IP address 47.247.77.11 on 27/11/2024 at 05:37

Assessment of self-compacting lightweight concrete: preparation of eco-friendly fiber content on mechanical and durable characteristics

K. Chandrasekhar Reddy[1*], Marri Rohini Kumar[2] and B. Vinod[3]

[1]Department of Civil Engineering, Siddharth Institute of Engineering & Technology, Puttur, Chittoor District, Andhra Pradesh, India – 517583
[2]Department of Mechanical Engineering, Siddharth Institute of Engineering & Technology, Puttur, Chittoor District, Andhra Pradesh, India – 517583

[*]E-mail: kamasani.kcr@gmail.com

Abstract. In recent years, a growing focus has been on creating eco-friendly concrete alternatives, garnering increased attention and support. Using natural fibers in the construction industry will minimize the exploitation of natural raw materials and promote sustainability in the construction industry. This work aims to investigate the influence of palmyra fruit mesocarp fiber (PFMF), Polyolefin fiber (PF), and glass fiber (GF) on the production of self-compacting concrete (SCC). The fiber content was used in three ratios, 1, 1.5, and 2%, as an alternative to fine aggregate. This research was conducted in two phases. In the first phase, a preliminary investigation was carried out to find the maximum adding percentage of fiber content in the successful production of SCC. The mechanical characteristics (compressive, split tensile, and flexural strength) and durability (water absorption, Acid attack, and ultrasonic pulse velocity) were evaluated. The second phase incorporates the fresh characteristics (T500 and slump flow). Adding 1.5%(PFMF/PF/GF) with 10% SF in SCC significantly enhanced the mechanical and durability properties. The compressive, splitting tensile strength, and flexural strength at 28 days increase to 4.30 MPa, 120 MPa, and 4.3 MPa compared to SCC. Scanning electronic microscopic (SEM) and X-ray diffraction (XRD) analysis was performed to evaluate the microstructure of concrete samples. Overall, the incorporation of up to 1.5% as a replacement of fine aggregate in manufacturing fiber-blended SCC mixtures can be recommended.

Keywords: Palmyra fruit mesocarp fiber, self-compacting concrete, mechanical characteristics, durability

1. Introduction

Cement-based products, such as mortar, normally compacted concrete (NCC), and self-compacting concrete, are essential for developing structural applications. Moreover, the use of SCC in the construction field in place of NCC has been progressively intensifying due to the superior flowability, passing ability, and stability characteristics of SCC [1]. This technology has improved the economy, productivity, and effectiveness of construction. A successful SCC mixture must have better filling ability, passing ability, and segregation resistance. Apart from the above attributes, separating paste from the mixture attribute is also evenly requisite for a successful SCC mixture. Naturally mined materials, such as cement, fine aggregate (i.e., river sand), and coarse aggregate,

Content from this work may be used under the terms of the Creative Commons Attribution 4.0 licence. Any further distribution of this work must maintain attribution to the author(s) and the title of the work, journal citation and DOI.
Published under licence by IOP Publishing Ltd

are the noteworthy constituents of cement-based products [2]. Due to the endless construction of infrastructure, there is a requirement for a continuous supply of these naturally mined materials, which ultimately causes an enormous impact on the ecosystem and living beings. Using natural waste in the construction industry as an alternative to natural sources reduces the congregation of waste products and saves non-renewable natural sources [3]. Moreover, the idea of sustainable development, fulfilling the present craves without altering the ability of the forthcoming generation, could be attained by incorporating fiber wastes in the construction industry. Waste fiber materials are defined as by-products for which no economic demand and disposal is required. Disposal of fiber waste is a big challenge as these are biodegradable and non-biodegradable materials [4].

This leads to a waste disposal crisis and adverse impacts on the environment. Recycling is one of the solutions to effectively utilize the waste generated from natural plants to save energy and resources while also protecting the environment. The effective utilization of fiber waste materials generated will depend on several factors, including the purpose of the application, the nature of end use, economic factors involved in handling waste, and existing environmental regulations. Ganta et al. [5] have studied polypropylene with glass fiber content replaced with fine aggregates that are inversely proportional to the size of the aggregates. The properties of fibers are favourably affected by the SCC mixture, adversely impacting the density, absorption, and mechanical properties. Jen et al. [6] investigated SCC durability and mechanical performance by incorporating fiber in a percentage of 0.5% to 1.5% by weight of cement.

Concrete properties like mechanical, durability, and drying shrinkage were analyzed. SCC prepared with the addition of fiber improved the resistance against CO2 attack. It was due to the dense and packed structure achieved in filling voids by fiber ratio. Drying shrinkage reduced up to 38% with increased fiber content in SCC. The outcome of this experimental study revealed that glass fiber enhanced overall properties due to improved compacted mortar density. Bhagwat et al. [7] found that PVA and GF fibres were used in concrete as a fine aggregate substitute. The replacement percentage was 1.0%, 2.0%, and 3.0% by weight of river sand. The mechanical strength increased to 32.7% using a 2% fiber ratio. The reason was compactness and proper grading of fine aggregate. From the literature reviews, it is found that waste fibers can be preferred as an alternative to cement and sand. Limited studies of fiber waste with SCC are available in the literature. The addition of fibers has the potential to be an essential filler alternative for the development of inexpensive self-compacting concrete (SCC) [8]. Therefore, this research intends to explore the efficiency of hybrid concrete in producing SCC with combined fibers as a substitute for fine aggregate. This was accomplished by performing tests and evaluating the mechanical, durability, and workability properties. Furthermore, the microstructure of the concrete examples was evaluated using SEM and XRD. The following are the objectives of the current study:

- To evaluate the maximum percentage of PFMF, PF, and GF, which can replace natural fine aggregate and cement in SCC, respectively.
- To assess the fiber-blended SCC's fresh, mechanical, and durability qualities to substitute natural fine aggregate.
- To evaluate the microstructure properties of fiber blended SCC mixture.
- Trial mixes were prepared for varying weight fractions with a superplasticizer dosage to arrive at a workable mix. Potable water was used to arrive at all mix proportions. Strength tests were conducted for the trial mix proportions.

2. Experimental and materials

2.1. Cement

Cement is the traditional material used for construction. It is a binding material that binds fine and coarse aggregate after adding water. Ordinary Portland Cement 53 was used in this work. All properties of cement were determined by referring to IS 12269-1987 standards [9]. The physical properties of OPC are listed in Table 1.

Table 1. Physical properties of OPC

Properties of Cement	Results Obtained
Grade of Cement	53
Specific gravity	3.15
Initial setting of time	28 min
Fineness of cement	7.45%
Final setting of time	600 min
Normal Consistency	33%

2.2. Natural Fibers

Figure *1*a shows the palmyra fruit mesocarp fiber procured from S.V.J. Palm Fibre Exports, Mumbai, India. Polyolefin fibre is a superior replacement for infrastructure components or systems. The Polyolefin fiber is supplied from Vasanth Enterprises, Chennai, India, and the raw material image is shown in Fig*ure 1*b. Glass fibres are being investigated as a potential replacement compared to other fibers due to its lightweight, noncorrosive, and exhibiting high specific strength minimizing crack resistivity, and low environmental impact, as suggested by Clark et al. [10]. The glass fiber is obtained from P K Fiber Glass, Hyderabad, India, shown in Fig*ure 1*c.

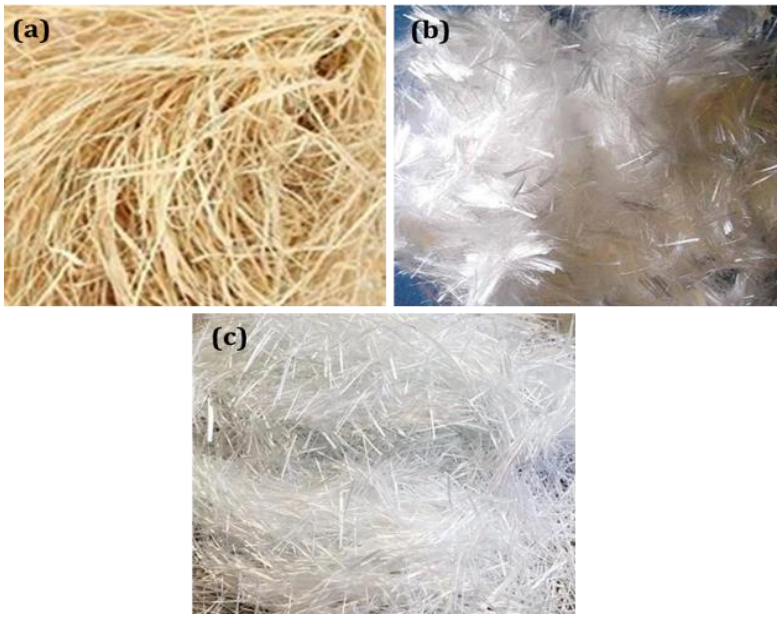


Figure 1. Raw material of (a) Palmyra fruit mesocarp fiber, (b) Polyolefin fiber, and (c) Glass fiber

2.3. Coarse and Fine Aggregates

The Engineering properties of particles were tested, confirming IS 383-1993 (Part 3) [11], and river sand is used as a fine aggregate. The recycled aggregates were screened and segregated to arrive at 20mm and 12.5mm downsize aggregates, and waste in the form of adhered mortar

content was eliminated, respectively. The coarse and fine aggregate particles are shown in Fig*ure 2*. The properties of coarse aggregate are represented in Table 2.

Table 2. Coarse Aggregate Properties

Properties	Values
Specific gravity	2.74
Bulk density	1462 Kg/m^3
Fineness modulus	6.74



Figure 2. Manufacturing and Casting of Specimens.

2.4. Water and Chemical Admixture

In the current study, ordinary water was used for casting and curing. A x` to arrive at a workable high-strength mixture to achieve the required workability. The superplasticizer used meets the requirements listed in IS 9103-1999 (R2004) [12].

2.5. Concrete mixture details

Three series of SCC mixes were made during the preparation phase. A control SCC mixture (i.e., 0%) was included in Mix-I. A fibre mixture made using SCC was included in Mixes II, III, and IV, with the percentages varying from 1.5% to 2%. Table 3 lists the specifics of SCC combinations (for initial research). A constant binder content of 546.79 kg/m^3 and an effective water-to-binder ratio of 0.37 were maintained throughout the creation of all the SCC mixes. The dosage of SP was modified to attain a slump flow within the range of 700 ± 30 mm. Table 3.3 provides the mix ID for each SCC blend.

Table 3. Mixed portions of SSC and Fiber content

Mixtures	Mixed portions							
	Cement	Water	Crushed Stones	Sand	Fibers content, %			
					PFMF	PF	GF	Super plasticizer (SF), %
SCC	420	210	1200	650	0	0	0	0
$FRHC_1$	390	210	1100	650	1	1	1	10
$FRHC_2$	382	210	1100	650	1.5	1.5	1.5	10
$FRHC_3$	375	210	1100	650	2	2	2	10

2.6. Manufacturing and Casting of Specimens

Every component of the SCC mixes was mixed using a rotating drum-style mixer. The mixer was filled with the necessary weighed amounts of coarse aggregate, fine aggregate, fibres, cement, and SP. The mixture was then mixed for a minute. After that, stirring took two minutes, and three-quarters of the water was added slowly. After that, the mixture was given another three minutes of mixing after the admixture and the remaining water were added. After the admixture was activated, the mixer was maintained in a stable state for two minutes, and mixing continued for an extra two to three minutes, as shown in Fig*ure 2*. Fresh properties testing of SCC mixtures before pouring them into testing molds. All cast specimens were allowed to sit in room temperature moulds for a day before being demolded and submerged in water the next day to cure until the testing age. Under IS 10262-2019 and SP 23 [13], a concrete mix was developed for the control concrete. A 0.40 water-to-cement ratio was attained. After the specimens have been fully demolded, they can be placed in water tanks or curing tanks to cure for testing for a while, such as seven, fourteen, and twenty-eight days.

2.7. Testing Procedure

The flexural test is carried out according to IS 456 (2000) standards by inserting a material sample into a testing apparatus and applying a load whose magnitude gradually increases. After 24 hours, the specimens are removed from the cubes and cured in water for 7 to 28 days. The splitting tensile test was evaluated using a Universal Testing Machine (IS 516-1959 norms) [14]. The material's split tensile strength was tested using 150 x 300 mm concrete cubes.

The compression tests were conducted at 7, 14, and 28 days of age using UTM relevant to IS: 516 (1959) [15]. The 15 x 15 x 15 cm mould was utilized to cast cube specimens by compacting each layer of concrete to a thickness of 5 cm. The samples are averaged, and the final value is obtained. Cylindrical specimens are split tensile tested as soon as possible following removal from the curing tank. Place the specimen's axis perpendicular to the force in the center of the compression testing machine's location markers. This will ensure the load is applied frequently and shock-free around the cylinder's curved surface area.

3. Results and discussion

3.1. Fresh SCC blended test results

3.1.1. Slump flow

The average of the most extensive spread concrete diameter and the diameter perpendicular to the slump flow is taken to determine the slump flow. The slump flow test assesses efficiently the concrete flows and deforms. As mentioned, the slump flow diameter was maintained within 700 ± 30 mm. The EFNARC criteria (EFNARC, 2005) determined the slump flow diameter values for all the mixtures. These values are appropriate for everyday application tasks like columns and walls.

The SCC, $FRHC_1$, and $FRHC_3$ slump values were 66, 67, and 69 mm, respectively. The maximum slump value was achieved as $FRHC_2$, which was 71 mm (Table 4). Less water absorption of glass particles compared to cement is due to increased slump. Rao et al. [17] conducted the slump ranging from around 40 mm for the 0% fly ash and fiber reference mix to 160 mm at 1.5% glass fiber. They reported that adding a glass-fiber ratio improves the slump compared to the SCC mix. Li et al. [18] concluded that the increase in slump results was carried out due to less water absorption of glass, and improvement in slump values has been observed. Similarly, the compaction factor value increases from 0.79 to 0.81 for adding $FRHC_1$ to $FRHC_3$, as listed in Table

4. A low compaction factor is identified for SCC (0.72), and adding 1.5% hybrid fiber content ($FRHC_2$) exhibits a high compaction factor of 0.84, which is 2.47% higher than the SCC sample.

Table 4. Workability of SCC and hybrid fiber mixture

Mixture ID	Slump (mm)	Compaction factor
SCC	66	0.72
$FRHC_1$	68	0.79
$FRHC_2$	74	0.84
$FRHC_3$	70	0.81

3.1.2. T_{500} slump flow rate

T500 time was noted when the concrete mixture reached the 500 mm diameter of spread concrete during the slump flow test. As per European Guidelines (2005) [18], T_{500} time values in this experimental work vary from 1 sec to 5 sec for the different mixes. According to EFNARC, all mixes indicate the measured T500 time is within the SCC acceptability range. T_{500} time for fiber blended SCC mixture containing PFMF up to 1.5% was less than 1.98 sec, according to EFNARC standard (EFNARC, 2005), whereas the same parameter for SCC, the flow rate time is maximum for the mix proportions $FRHC_1$ and $FRHC_3$ specimens, which is 2.54 sec and 2.36 sec. Hence, the flow rate is quick for these mix proportions, and including SP increases the time required for flow. The $FRHC_2$ mixtures (1.98 sec) have strong filling ability and can be used for structures with dense reinforcement, much like the slump flow type, but SCC mixtures generally exhibit segregation. Iman et al. [19] also noticed an enhancement in the ability of SCC to flow when fibers were added as a mineral additive. However, in contrast to the SCC mixture, the hybrid fiber blended SCC mixtures with up to 1.5% fine aggregate replaced by GF showed a decrease in T_{500}. This decrease in time resulted from the smooth and spherical shape of the fiber particles, which helped counteract the negative impact on workability. The time required to flow increases with increased fiber content. The combined use of SP and fiber content also increases the time needed to flow. The increased value of T500 time indicates the increase in viscosity. As shown in Figure 3, all the flow rate values are between 3.47 and 5.81 seconds. When fiber increases from 1% to 1.5%, the viscosity of the mix increases correspondingly. While comparing the SCC, 1.5% hybrid fiber-replaced mixtures have taken a long time to achieve a slump flow of 500 mm. However, 2% fiber-replaced mixtures show less time to accomplish a slump flow of 500 mm.

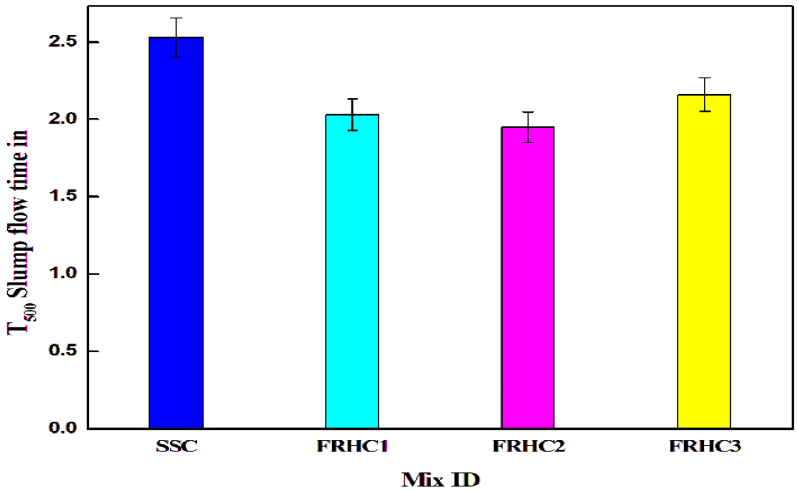


Figure 3. Slump flow rate at T_{500}.

3.2. Mechanical blended test results

3.2.1. Split Tensile Strength

The test was determined in cylinder specimens of 150mm diameter and 300mm length. It is calculated using indirect methods because the direct method is too complicated. It should be emphasized that these approaches produce findings superior to those of the uniaxial tensile test. These indirect methods include, for instance, the split cylinder test and the flexural test. As shown in Figure 4, when hybrid mixes are added to FRHC2, the strength increases by 38% after 28 days. At 7, 14, and 21 days after replacing fiber with 1.5% compared to SSC, the splitting tensile strength increases from 2.37 to 3.42 MPa, 2.98 to 4.07 MPa, and 3.06 to 4.19 MPa, respectively. The $FRHC_2$ is the optimal blend for maximum efficiency (4.52 MPa) at 28 days. Hence, the use of pozzolanic admixtures or decreasing the cement content led to enhancing the tensile strength. Guler et al. [20] identified that the strength of concrete made using glass and basalt fiber reinforcing particles increased faster than that of regular concrete by 26%. However, adding 2% hybrid fiber particles, the tensile strength dropped dramatically to 14%, causing a decreased tensile strength of 4.37 MPa at 28 days.

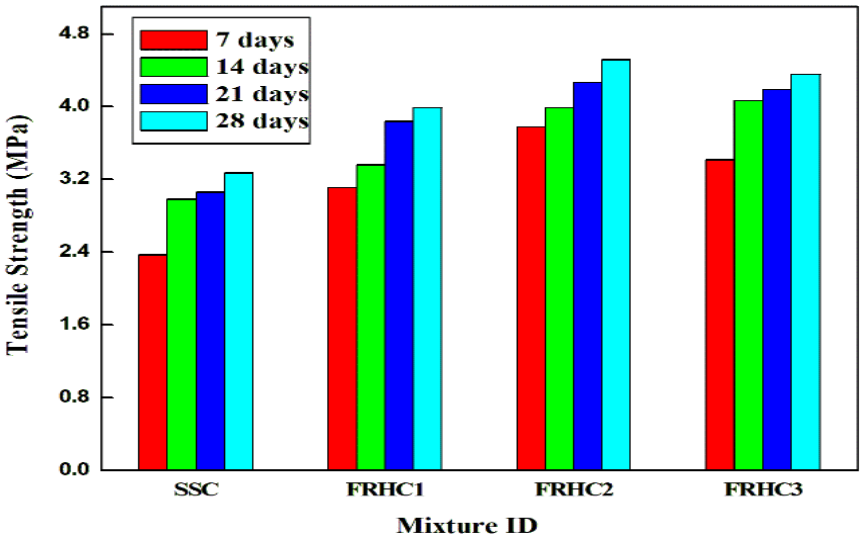


Figure 4. Split Tensile Strength of FRHC Mix.

3.2.2. Compressive strength

Figure 5 illustrates the variation in compressive strength for all mixtures from 7 to 28 days. Compressive strength can improve by adding 1.5% fiber separation before declining again. At 7 days after 1.5% (PFMF/PF/GF) with SCC replacement, the compressive strength improves from 25.13 to 32.69 MPa, for 14 days from 27.48 to 33.18 MPa, and for 28 days from 30.21 to 38.09 MPa, respectively. Kavya et al. [21] reported that replacing glass and PF fiber with FA particles may enhance the mechanical properties of concrete. Maximum compressive strength is achieved at optimal additive amounts, significantly improving over traditional concrete. The results suggested that 1.5% $FRHC_2$ was ideal for maximizing compressive strength. After adding a further 2% (PFMF/PF/GF) with SCC replacement, there is no reaction, and the material essentially performs as an inert, resulting in a decrease in compressive strength.

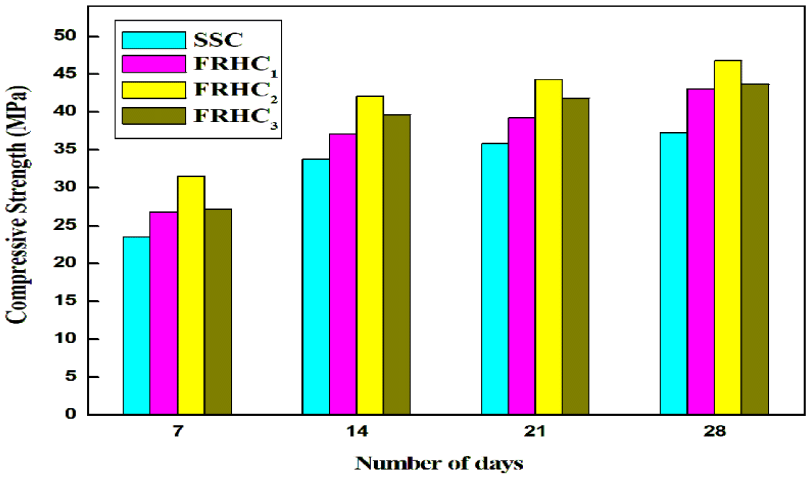


Figure 5. Compressive Strength of FRHC Mix.

3.2.3. Flexural strength

Mixing SCC with hybrid particles results in a significant increase in flexural strength at 28 days. Figure 6 shows the results of the flexural test. The flexural strength of regular concrete is increased by an average of 3.12 MPa to 4.07 MPa when using the fiber content. At 28 days, the measured flexural strength of $FRHC_2$ is 5.73 MPa, which is much higher than that of $FRHC_1$ (4.53 MPa). Adding superplasticizers with fiber content substitution is more prominent in increasing flexural strength than in regular concrete. The formation of a pozzolanic gel in copper slag is attributed to this occurrence. According to studies by Dhadiwal et al. [22], the amount of glass fibre in ternary mixed concrete increased from 1.0% to 2.0% in flexural strength. The GF and SH-reinforced concrete's flexural strength is significantly higher than SCC concrete once cured. $FRHC_2$, which has a very wide surface area, helps reduce the pores in concrete, increasing the material's strength. The hybrid waste particles in the concrete mix work as split arresters, stopping cracks from starting in the plastic state and spreading in the hardened state. Adding 1.5% (PFMF/PF/GF) weight fraction resulted in a 33% increase in flexural toughness. The strength decreases to 5.11 MPa when adding a further 2% ($FRHC_3$), as shown in Figure 6. The flexural strength of a material could be affected by flaws in the material. The material may not hold up well under pressure if it has holes or cracks.

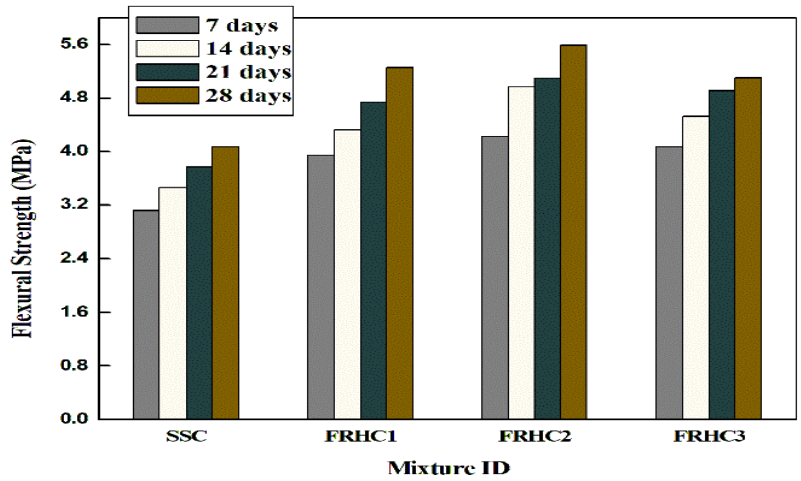


Figure 6. Flexural Strength of FRHC Mix.

3.3. Durability blended test results

3.3.1. Saturated water absorption

A saturated water absorption test was conducted on 7 to 28 days cured samples of 100 × 100 × 100 mm cubes as per ASTM: C642 (2013). The samples were maintained in an oven at 105 ± 5°C until a steady dry weight was achieved. Specimens were then immersed in water, and an increase in weight was determined at a difference of 24 hours until a constant weight (final absorption) was obtained. Initial surface absorption at 30 minutes was also measured to compare the quality of concrete as per Moradikhou et al. [23]. An increase in weight for initial and final absorption was reported as a percentage of dry weight.

The water absorption results for control and blended mixes are represented in Table 5. Initially, at 7 days, the water absorption of all samples is very high, varying from 5.8% to 3.6%, as represented in Table 5. It is reduced as the number of days is treated, and the average water absorption value is reduced by incorporating an optimum percentage of fiber content. At 28 days, the SWA is minimized from 3.8% to 2.3%, respectively. While adding 1.5% fiber content achieves low SWA (1.6%) compared to other compositions. Reducing water absorption was due to the reduced porosity of blended mixes. The SEM images of blended mixes indicated compact and denser packing with GF and PF incorporated mix. Lalinde et al. [24] reported reduced water absorption due to less porosity and compact packing of void spaces by granite fines. The reasons for decreased water absorption were less voids and compactness, leaving no space for the water to penetrate. Higher incorporation of glass and granite fines with 2% fiber increased the average water absorption (2.9%). The reason is that the higher SWA is fine to present in unbalanced mixes w/b the ratio.

3.3.2. Ultrasonic pulse velocity (UPV)

The interior temperature was measured using a K-type thermocouple in a gas-regulated furnace to ascertain the precise fire attack. The dimensions of the furnace chamber were 520 520 1050 mm. Using 100 mm cubes, ultrasonic pulse velocity (UPV) measurements were used to assess the firing performance. According to BIS: 516 (1959), the compressive strength and UPV tests were carried out. The samples underwent a day of cooling at room temperature (27 ± 2 °C) after being subjected to varying high temperatures of 200 ± 10 °C, 400 ± 10 °C, and 600 ± 10 °C. After the specimens' exposure to the intended high temperature, their weight, compressive strength, and UPV values were measured. Subsequently, the average of three specimens was presented [25]. We compared these recorded values to their initial measurements made at room temperature. This test is used to determine the concrete's overall quality and longevity. Superior-grade concrete will have UPV values larger than 3.0 km/s, whereas medium- and good-grade concrete will have UPV values between 2.9 and 4.7 km/s and 1.7-3.7 km/s, respectively. Higher UPV values indicate better concrete quality. Figure *7* displays the UPV values for different mixtures when subjected to different temperatures. All types of concrete fiber mixtures exhibited an increase in UPV at a temperature of 200°C. However, as the temperature exceeded 200°C, there was a decrease in UPV. Nonetheless, even at temperatures up to 600°C, the concrete quality of all mixtures (except the SCC mixture) was rated higher than medium concrete quality. The fiber-blended SCC mixtures exhibited higher UPV at every temperature than the SCC mixture. The blended SCC with 1.5% (PFMF/PF/GF) has minimized microcracks, indicating higher UPV values. As a result, the 1.5% PF and PFMF blended SCC with GF combinations had higher UPV values at 200^{o}C (5.8 km/s) and 600^{o}C (3.78) than the standard mixture, indicating higher quality. However, this improves the fibre blended SCC with GF's compressive strength. Nematzadeh et al. [26] additionally observed improved UPV values during glass fiber-based SCC fire exposure, including superplasticizer aggregate as coarse aggregate.

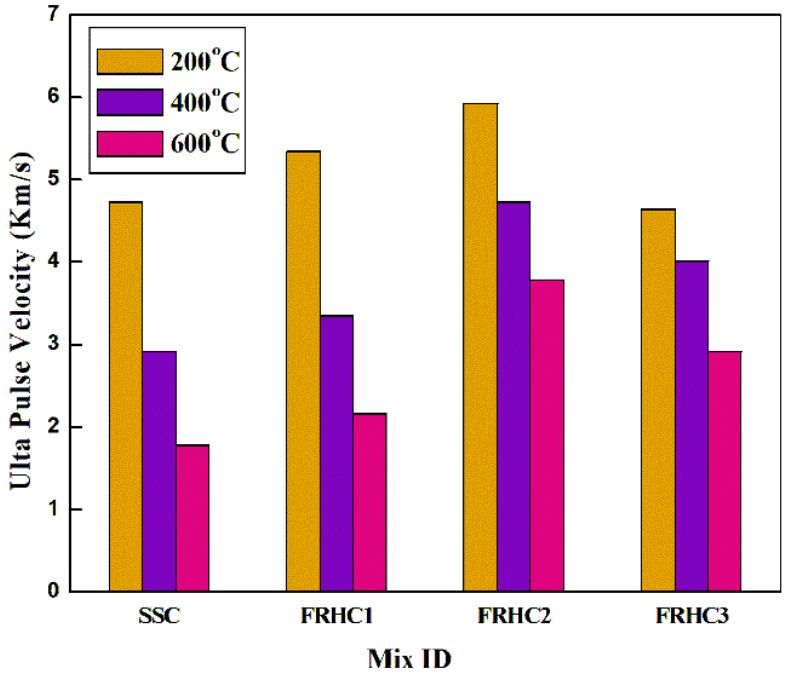


Figure 7. Graphical representation of UPV.

3.3.3. Change in weight

The chloride resistance test was conducted on SCC-quality concrete after the concrete was soaked in the chemical water solution containing 5% H_2SO_4 for 90 days. In addition to a slight mix, several combinations of style mix proportions are obtained. Concrete weight decreases when sulphate attack decreases with the replacement of support content. The sample's weight loss drops from 7.28% to 2.87% when treated for 90 days in chemical water at a 1.5% replacement of PF and PF with GF particles, compared to SCC concrete. Because of this, the $FRHC_2$ mix (2.69%) is regarded as the best combination for significantly enhanced performance after 90 days, as represented in Table 6. The $FRHC_1$ and $FRHC_3$ mixture achieved more toughness than the SCC mix of immersion in a 5% H_2SO_4 solution. According to a study by Patil et al. [27], using BF fiber in conjunction with filler goods like GF and SF helps compress the microstructure and create capillary pore networks with smaller diameters far more resilient to acid impacts. The loan consolidation of significant amounts of pozzolanic filler exposes the SCC to varying degrees of sulphate hit. Consequently, both grade and the influence of sulphate strike are impacted by the $FRHC_2$ mix content.

Table 6. Loss of weight of concrete curing chemical solution

Mixture ID	Weight of the sample before curing chemical solution (w_1) for 90 days, (Kg)	Weight of the sample after curing chemical solution (w_2) for 90 days, (Kg)	% loss in the weight of the sample for 90 days
SCC	7.284	7.033	2.83
$FRHC_1$	7.213	7.109	2.76
$FRHC_2$	6.981	6.541	2.69
$FRHC_3$	6.527	6.310	2.87

3.3.4. Change in compressive strength

In this test, the performance of SCC, FRHC added concrete in 5% sulphuric acid was evaluated at 90 days and is listed in Table 7. Concrete exposed to seawater, for instance, needs to be tested for its ability to withstand sulphate. In contrast, concrete set in acidic soils must be evaluated for its ability to resist chloride. Concrete makes for an excellent construction material in most circumstances. Its adaptability may require challenging circumstances like those in sewage and wastewater treatment plants. Deterioration and eventual collapse of structures can occur well before the end of their expected lifespan. Depending on the concentration and form, hydrogen chloride solution is a non-detrimental acid commonly used in concrete that reduces the degradation rate and no damage to the material. Table 7 illustrates that compressive strength significantly decreased for specimens exposed to sodium chloride solution over 90 days. Increasing the GF/CR replacement percentage also improves the concrete's endurance to acid. After 90 days in contact with sulfuric acid, Li et al. [28] found that the concrete's strength had decreased by 13% compared to untreated concrete. After 90 days, the strength of $FRHC_2$ has degraded by only 7.81%, compared to 8.93% for no mixer replacement.

Table 7. Change in compressive strength after 90 days of curing chemical solution

Mixture ID	Compressive strength before curing water solution (N/mm^2)	Compressive strength after curing water solution (N/mm^2)	% loss in compressive strength
SCC	25.7	21.8	8.93
$FRHC_1$	29.3	23.5	8.22
$FRHC_2$	32.1	27.3	7.81
$FRHC_3$	30.6	25.4	8.53

3.4. Microstructural Analysis

The characteristics of concrete, such as its strength and durability, are affected by its behaviour on a microscopic scale. A scanning electron microscope (SEM) is used after conducting tests on samples subjected to compression to examine the microscopic structure of concrete. SEM images of SCC for magnifications 50 μm are represented in Fig*ure 8* (a-d), respectively. The SEM images of SCC and FRHC show that a complete hydration process has been carried out, and the formation of hydration products, i.e., CSH bonds, is visible. From the SEM image of SCC, it can be observed that the cracks on a surface are the formation of ettringite, which is porous. The compressive strength for SCC has attained 12.64% less than $FRHC_1$, as observed. The SEM image of Fig*ure 8*b shows the reduced cracks and pores due to the presence of fiber content. In specimen $FRHC_2$, the fiber content was higher than that of specimen $FRHC_1$. The presence of fiber orientation led to increased material strength in the concrete. As a result, as Fig*ure 8*c illustrates, the specimen with the flat surface has a high compressive strength. In the SEM photos, the color of the CSH-gel appears stronger. Further addition of 2% hybrid fiber content (Fig*ure 8*d) possesses an initial fracture surface, which reduces the strength of a material. Glass fiber is a mineral fiber that has a better bonding capacity with cement paste and enhances the mechanical properties of foam concrete up to a certain limit. Wani et al. [29] made similar findings. Therefore, adding fiber particles influences the strength of SCC concrete. $FRHC_2$ mix is a more rigid and durable blended mix than the other mixes.

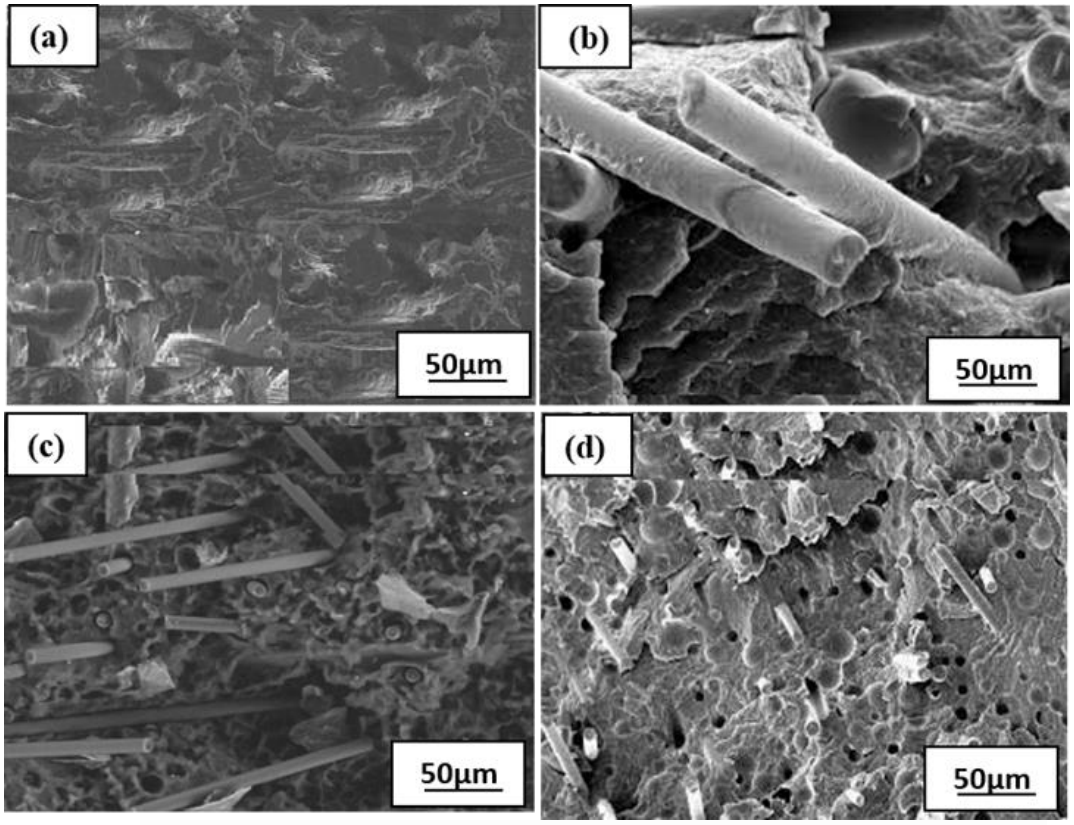


Figure 8. SEM analysis of (a) SCC, (b) $FRHC_1$, (c) $FRHC_2$, and (d) $FRHC_3$ mixture at 28 days

3.5. XRD analysis

The analysis of SCC concrete specimens was carried out by subjecting the samples collected from SCC specimens to X-ray beams, where the XRD received and processed by the detector are represented by a graph with the x-axis representing the angle of diffraction (2θ values) and the y-axis representing the number of counts in the energy levels. Adding fiber content exhibits silicon dioxide, which can be present as quartz and glass, as shown in Figure 9(b-d). It was observed that they all occur in different phases, but each has a unique diffraction pattern. The final graph for each mix combines the diffraction patterns of all such phases for an element. The dominant peaks can be distinguished clearly from the graph. Figure 9c shows the graph plotted from the XRD analysis carried out for $FRHC_2$. The ionization energy ranges of almost all elements are 0-3.6Kev, and the angle of 2θ ranges between 33º-42º. From analysis carried out for R-0, it was observed that four major peaks exist and indicate the presence of carbon and quartz in the form of SiO_2, Brownmillerite, iron oxide, and carbon. From Figure 9d, it was observed that the counts of iron oxide were increased by 300 counts, and the carbon count and silicon count were reduced by 60 and 166 counts, with all other elements being similar to SCC. The higher number of peaks represents the amorphous nature of the material. However, as the replacement 2% fiber ratio, the formation of a peak minimizes the crystalline form of the material. The major components present in concrete are reducing silica and carbon content at 2θ angle of 27º-28º. The broad parts of the elements indicate that the elements are amorphous when the diffraction of particles takes place. However, the 1.5% hybrid ratio presence of carbon, aluminium oxide, calcium oxide, and silicon dioxide in different percentages indicates that SCC has attained strength. A similar observation by Saribiyi et al. [30], adding more fibre particles to the SCC may result in the formation of an

important phase during annealing at the smooth interface, strengthening the material's resistance to cracking.

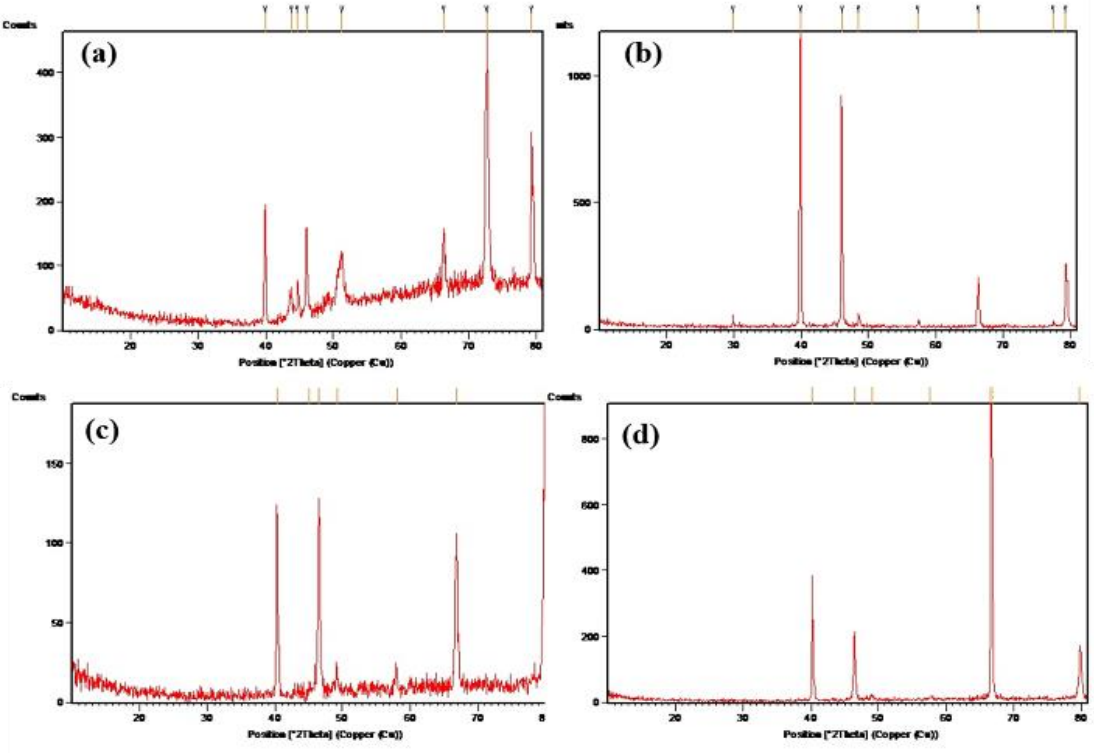


Figure 9. XRD analysis of (a) SSC, (b) $FRHC_1$, (c) $FRHC_2$, and (d) $FRHC_3$ mix at 28 days.

4. Conclusions

The research examines concrete mixes' mechanical, durable, and fresh qualities with various replacement material ratios. The following are the conclusions as follows:

- A modified trial mix was used to achieve high strength and durability. The optimum mix ratios with appropriate workability levels ensure an efficient casting process and increased strength.
- The slump value decreased from 3.7% to 2.5% ($FRHC_2$) with a minor reduction in air voids as the dosage of fibre in the mix increased. Slump decreases as fibre content rises above 2% because of the fibres' resistance to compaction.
- At 28 days, the $HRWC_3$ mixture has an increased compressive strength (32.7 MPa) than SCC concrete (26.1 MPa). Because the PFMF-GF/PF substance fills the pores of the concrete, the desirable $FRHC_2$ combination increases its strength. While adding the $FRHC_3$ mix reduces that strength substantially.
- At 28 days, the tensile strength of 1.5% (PFMF/PF/GF) blended SCC hybridization particles is greater than that of SS from 3.34 MPa to 3.98 MPa. When more $FRHC_3$ mixture is added, the porosity level rises, which impacts mechanical characteristics and leads to premature breaking of the material.
- Mechanical strength was increased by 10% superplasticizer with 1.5% added. The ideal mix is fine GF and PF, which fill pores and enhance the concrete's strength. In addition, the mechanical strength decreases, and it can become distorted by adding a 2% mixture due to excessive clustering.

- Workability decreases in mono and hybrid fiber forms at higher fiber dosages. Considering the workability criteria, the maximum volume fraction of steel fiber recommended for a hybrid combination should not exceed 0.5%.
- At 90 days, $FRHC_2$-mixed concrete has a minimum weight loss of 0.50% less than SCC concrete. Compared to regular concrete and other compositions, the UPV value (22.3%) of the 1.5% hybrid fiber particles reinforced concrete was significantly higher. $FRHC_2$ mix concrete exhibits a less in compressive strength from acid attack than SCC.
- When compared to concrete without admixtures, water absorption is high. At 28 days, a mixture of $FRHC_2$ reduced SWA by a maximum of 31.24% compared to SCC. After 28 days, the water saturation level dropped from 3.1% to 1.5%.
- The microscopic analysis reveals that the fibre particles are uniformly dispersed throughout the SCC. A smooth surface and 1.5% of hybrid fiber concrete are identified.

References

[1] Ahmad J, Aslam F, Zaid O, Alyousef R, Alabduljabbar H, Manan A 2021 Self-fibers compacting concrete properties reinforced with propylene fibers *Sci. and Eng. of Comp. Mater.* **28** 64-72.
[2] Kumari G J, Mousavi S S, Bhojaraju C 2023 Influence of thermal cycles and high-temperature exposures on the residual strength of hybrid steel/glass fiber-reinforced self-consolidating concrete. *InStructures*. **55** 1532-1541.
[3] Anuradha V, Madhavi T C 2022 Behaviour of self compacting concrete hybrid fiber reinforced hollow beams. *InStructures*. **35**, 990-1001.
[4] Ahmad J, Zhou Z, Deifalla A F 2023 Structural properties of concrete reinforced with bamboo fibers: a review. *J. Mater. Res. and Tech.* **24**, 844-865.
[5] Ganta J K, Rao M S, Mousavi S S, Reddy V S, Bhojaraju C 2022 Hybrid steel/glass fiber-reinforced self-consolidating concrete considering packing factor: Mechanical and durability characteristics. *InStructures*, 2020, **28**, 956-972.
[6] Jen G, Trono W, Ostertag C P 2016 Self-consolidating hybrid fiber reinforced concrete: Development, properties and composite behavior. *Const. & Building Mater.* **104** 63-71.
[7] Bhagwat Y, Nayak G, Pandit P, Lakshmi A 2023 Effect of polypropylene fibres on strength and durability performance of M-sand self compacting concrete. *Cogent Eng.* **10** 2233783.
[8] Ahmad J, Zhou Z, Deifalla A F 2023 Steel Fiber Reinforced Self-Compacting Concrete: A Comprehensive Review. *Inter. J. Concrete Struct. and Mater.* **17** 51.
[9] Chandrasekhar Reddy K, Giribabu B 2023 Assessment of recycled waste fiber and BC soil on the performance of hybrid concrete: reaction and subsequent sulfuric acid exposure. *Innov. Infrast. Sol.* **8** 114.
[10] Clark E, Bleszynski M, Valdez F, Kumosa M 2020 Recycling carbon and glass fiber polymer matrix composite waste into cementitious materials. *Resources. Cons and Recycling* **155** 104659.
[11] Mastali M, Abdollahnejad Z, Dalvand A, Sattarifard A, Illikainen M 2020 Comparative effects of using recycled CFRP and GFRP fibers on fresh-and hardened-state properties of self-compacting concretes: a review. *New Mater in Civil Eng.* 643-55.
[12] Pan Z, Zhu Y, Zhang D, Chen N, Yang Y, Cai X 2020 Effect of expansive agents on the workability, crack resistance and durability of shrinkage-compensating concrete with low contents of fibers. *Constr. & Building Mater.* ***259*** 119768.
[13] Reddy K C 2022 Experimental investigation on mechanical, durable and stress–strain behaviour of hybrid reinforced concrete admixed BC soil: a novel use of waste fibers to reduce disposal challenges. *J. Building Pathology and Rehab.* **7** 14.
[14] Hasan R, Sobuz M H, Akid A S, Awall M R, Houda M, Saha A, Meraz M M, Islam M S, Sutan N M 2023 Eco-friendly self-consolidating concrete production with reinforcing jute fiber. *J. Building Eng.* **63** 105519.
[15] Zhang H, Sarker P K, Wang Q, He B, Kuri J C, Jiang Z 2023 Comparison of compressive, flexural, and temperature-induced ductility behaviours of steel-PVA hybrid fibre reinforced OPC and geopolymer concretes after high temperatures exposure. *Const. & Building Mat.* **399** 132560.
[16] Vivek S S, Karthikeyan B, Bahrami A, Selvaraj S K, Rajasakthivel R, Azab M 2023 Impact and durability properties of alccofine-based hybrid fibre-reinforced self-compacting concrete. *Case Studies in Const. Mater.* **19** e02275.
[17] Rao M D, Dey S, Rao B P 2023 Characterization of fiber reinforced self-compacting concrete by fly ash and cement. *Chemistry of Inorganic Mat.* **1** 100010.

[18] Tang W, Khavarian M, Yousefi A, Chan R W, Cui H 2019 Influence of surface treatment of recycled aggregates on mechanical properties and bond strength of self-compacting concrete. *Sustainability.* **11** 4182.
[19] Iman A, Mohamad N, Raain F, Sofia A, Mydin A, Samad A A 2020 Properties and Flexural Behavior of Self-Compacting Concrete with Added Coir Fiber And POFA. InIOP Conference Series: *Mater. Sci. and Eng.* **713** 012011
[20] Guler S, Akbulut Z F 2022 Effect of high-temperature on the behavior of single and hybrid glass and basalt fiber added geopolymer cement mortars. *J. Building Eng.* **57** 104809.
[21] Kavya B R, Sureshchandra H S, Prashantha S J, Shrikanth A S 2022 Prediction of mechanical properties of glass and basalt fiber reinforced concrete using ANN. *Asian J. Civil Eng.* **23** 877-86.
[22] Dhadiwal A J, Rajak T K 2023 Near surface mounting technology with glass fibre reinforced polymer and sisal rope fibre for flexural strengthening of reinforced concrete beams. *Mater. Today: Proceed.* **74** 836-42.
[23] Moradikhou A B, Esparham A, Avanaki M J 2019 Effect of hybrid fibers on water absorption and mechanical strengths of geopolymer concrete based on blast furnace slag. *J. civil Eng. and Mater. App.* **3** 195-211.
[24] Lalinde L F, Mellado A, Borrachero M V, Monzó J, Payá J 2022 Durability of Glass Fiber Reinforced Cement (GRC) Containing a High Proportion of Pozzolans. *Applied Sci.* **12** 3696.
[25] Zulkifli N I, Alisibramulisi A, Saari N, Hassan R, Shaffie E, Bhkari N M, Sidek M N 2021 Experimental Investigation of Ultrasonic Pulse Velocity (UPV) Test Specimen in Assessing the Strength of Steel Fiber Reinforced Concrete Structure. *J. Advanced Industrial Tech. and App.* **2** 34-41.
[26] Nematzadeh M, Tayebi M, Samadvand H 2021 Prediction of ultrasonic pulse velocity in steel fiber-reinforced concrete containing nylon granule and natural zeolite after exposure to elevated temperatures", *Const. & Building Mater.* **273** 121958.
[27] Patil S, Rao H S, Ghorpade V G 2023 The influence of metakaolin, silica fume, glass fiber, and polypropylene fiber on the strength characteristics of high performance concrete. *Mater. Today: Proceed.* **80** 577-86.
[28] Li W, Shumuye E D, Shiying T, Wang Z, Zerfu K 2022 Eco-friendly fibre reinforced geopolymer concrete: A critical review on the microstructure and long-term durability properties. *Case Studies in Const. Mater.* **16** e00894.
[29] Wani T A, Ganesh S 2022 Study on fresh properties, mechanical properties and microstructure behavior of fiber reinforced self compacting concrete: A review. *Mater. Today: Proceed.* **62** 6663-70.
[30] Saribiyi A, Gurbuz G 2021 Effects of glass fiber reinforced polymer pipe waste powder usage on concrete properties. *Revista. de la const.* **20** 463-78.

Acknowledgment

The authors thank S.V. University, Tirupathi, Andhra Pradesh, India for providing lab facilities and the Siddharth Institute of Engineering and Technology, Puttur, Andhra Pradesh, India, for their research support.

IOP Conference Series: Earth and Environmental Science

PURPOSE-LED PUBLISHING™

PAPER • **OPEN ACCESS**

Municipal solid waste management practices vs public opinion study of Telangana State during and after the COVID-19 pandemic

To cite this article: Vasantha LaxmiMaddhinni and Jyothi Mushti 2024 *IOP Conf. Ser.: Earth Environ. Sci.* **1409** 012021

View the article online for updates and enhancements.

You may also like

- Overview of Municipal Solid Waste Generation and Energy Utilization Potential in Major Cities of Indonesia
Fatimah Dinan Qonitan, I Wayan Koko Suryawan and Ari Rahman
- Prediction of municipal solid waste treatment and disposal in high cold and high altitude area based on system dynamics: a case study of Lhasa
Ziyun Liu, Qinxiao Zhang and Hongbo Liu
- Indonesia municiple solid waste life cycle and environmental monitoring: current situation, before and future challenges
Susmono



This content was downloaded from IP address 47.247.77.11 on 27/11/2024 at 05:37

Municipal solid waste management practices vs public opinion study of Telangana State during and after the COVID-19 pandemic

Vasantha LaxmiMaddhinni[1*] and Jyothi Mushti[2]

[1]Department of Chemistry, Vasavi College of Engineering, Hyderabad, Telangana 500031, India.
[2]Department of Humanities and Social Sciences, Vasavi College of Engineering, Hyderabad, Telangana 500031, India.

[*]E-mail:vasumadineni@vce.ac.in

ABSTRACT. Municipal solid waste management is an important environmental concern of the new era. The fast-evolvinglifestyles of the people, rapid population growth and industrialization, and a certain amount of unawareness and negligence on the part of the public add to the MSW management issues. Many studies indicated that a greater amount of municipal solid waste is not effectively managed. An efficient management of municipal solid waste is therefore called for to protect the public and environment from waste hazards. The current paper proposes to offer a holistic view of efficient practices for municipal solid waste management in Telangana. An online survey has been conducted with the help of Google Formsusing social media platforms like WhatsApp, Facebook, and Snapchat to understand the concerns of the society about proper methods of Municipal Solid Waste Management in Telangana. The number of responses received is 219 in a total of 32 districts in Telangana state. Statistical analysis has been carried out with the help of the Chi-square test at a 5% level of significance to identify the existence of a significant relation between Municipal Solid Waste management aspects and the demographic variables namely gender and place of residence.

Keywords. Waste, Municipal solid waste, Urban, Environment, Landfills.

1. Introduction

The term "waste" implies that it is of no value to anyone because the intrinsic value of the material as a resource of further utility has not been fully recognized. The waste generated by the general public comprises Municipal Solid Waste, the management of which envelops generation, storage, collection, transfer and transportation, treatment, and disposal of municipal solid waste.The management of MSW is becoming complicated due to the generation of higher MSW with the advent of software companies, pharmaceutical industries, continental food franchises, online buying, disposable items usage, party culture for all occasions, and urbanization.The densityof the population and flats culture coupled with commercial and industrial activities impacted the environment adversely withsolids, gaseous, and liquid discharges.

MSW management practices and techniques involve huge expenditures but did not receive considerable attention from the administrators in terms of funds allocation. Insufficient funds,

Content from this work may be used under the terms of the Creative Commons Attribution 4.0 licence. Any further distribution of this work must maintain attribution to the author(s) and the title of the work, journal citation and DOI.
Published under licence by IOP Publishing Ltd

scanty attention towards municipal solid waste management, public negligence, and die-hardhabits resulted in improper MSW practices. In an attempt to manage MSW efficiently, the state of Telangana must consider management techniques implemented by developed nations with proper modifications to suit the state requirements. Replicating the developed nations, the state of Telangana adopted door to door collection system, the waste stored in standardized containers in each premises is collected through a varied process using different modes of transport. Direct and storage discharge techniques are adopted at some transfer stations where multipurpose facilities are made available to serve a wide range of users.

2. WORLD SCENARIO

The extent of the problem of waste generation and its management is fast becoming a global problem. According to a recent United Nations report, the observations are:

- Per capita waste generation in the developed nations has increased three-fold over the past 20 years.
- Waste generation in the developed nations is now approximately five to six times higher than in the developing world.
- In developing nations, waste production is estimated to double during the next decade.
- By 2025, it is estimated that there will be a five-fold increase in global waste generation.
- Roughly 30to 40 percent of the allocated funds are consumed for waste management services in the cities of developing nations. Despite this enormous financial sanction, most cities are unable to keep pace with the growing demand.
- vi)Municipal Solid waste management is a complicated processthatrequires close cooperation between the users, the private sector, and governmental and non-governmental organizations.

3. Review ofliterature

Stephen Oppong Kwakye et.al. (2024) uncovered a positive tendency toward payment for improved waste collection services in a significant number of households. This paper emphasized the necessity of educational campaigns about well-organized waste management practices [1].Addis Taye et.al 2024 examined the relationship between MSW management, demographics, and socioeconomic factors. The results established a relationship with gender, age group, and education with regard to MSW disposal methods [2]. Huifang Li et.al 2023 consider remote sensing as a promising tool to realize the detection and monitor MSW. In their research, they constructed a dataset (DSWD) by using 3192 Google Earth images and proposed a deep learning network for MSW detection and its fast extraction. The LKN-ME technique uses spot pool and essential convolution to capture the key points of an object [3].Noman et.al (2023), expressed in their paper that there is a relation between the income of the family and the quantity of waste generation and time of collection and source segregation rate [4].Xiaoning Shen et.al,(2023) used five state-of-the-art algorithms to compare, find the best solution, and constructthe best model for Energy efficient vehicle routing for multiple trips and efficient collection by using full potential vehicle resource use[5].

M.D.Meena et.al (2023) in their review concluded that time-to-time amendments should be made in waste management rules to enhance effectiveness atthe end-user level as a bottom-up approach. The paper also stressed the importance of the involvement of all stakeholders [6].Kiran D.A et.al 2023 observed the inefficiency of MSW management in many cities due to a

lack of enough infrastructure and funds for waste processing but by continuous monitoring an improvement is observed in the existing system. According to him, Resource recoveries and integration of the informal sector in MSW management are the key aspects for better MSW management in Indian cities [7].In this study (Yash Pujara et.al 2023) the author quantified the environmental impact related to MSW management in Rajkot City, India using the life cycle assessment. Output of this research work was decentralized Material Recovery facility and Source Segregation which eases the MSW management in Indian cities and will also be able to achieve sustainable development goals [8].

Oshan Mudannayake et.al (2022) concluded in their paper that machine learning models are better when compared to deep learning models for forecasting municipal solid waste generation trends in selected areas [9].According to Navarro et.al 2021 MSW management parameters variation is high in developing cities due to the non-availability of primary data. The author also discussed the environmental benefits of recycling [10]. The available review of literature on MSW is attempted here. Hari Bhakta Sharma opines that sufficient data collection and regular monitoring are desirable for designing an efficient MSWM system. Sharma also recommends the usage of technological solutions such as remote sensing, GIS, and mathematics optimization for efficient MSWM [11].Rajkumar Joshi and Sirajuddin Ahmed argued that public unawareness, insufficient fund allocation, inefficient legislation, and lack of technically competent personnel resulted in inefficient MSW management. Som Dutta Banerjee highlighted addressing infrastructure deficiency and private participation issues to remedy the public coffers problems [13,18] .Chavan and Zambare observed inadequacies in municipal solid waste treatment techniques. Annepu suggested suitable practices for MSW reduction and open burning of municipal solid waste. He recommended the transformation of the informal recycling process into a formal system through training the personnel for efficient waste collection and recyclables sales. Gopal Krishna favors addressing the institutional and financial issues for effective MSW management. Krishna emphasizes the provision for NIMBY syndrome and Extended Producer Responsibility (EPR) for reuse and recycling of products [11,21].

In another study in 2017, the emphasis was on local resource creation, local code implementation and central government commitment tothe effective implementation of existing polices. A Chinese study reveals that municipal solid waste separation at source, energy generation from waste, proper landfill management and leachate treatment, waste recycling, and appropriate taxation systems are highly desirable for MSW management [16]. The study results show the effect of land filling on all analyzed impact categories leaving ozone layer depletion and human toxicity. On the other hand, the low impact on all analyzed damage categories excluding global warming and human toxicity by incineration is considered. [17]. In another study, the inefficiency of the state in addressingmunicipal solid waste problems was highlighted while emphasizingthe creation of local resources, execution of local codes, and commitment from the central government for the free exercise of existing policies [14]. Erfani, et al suggested an integrated model for proper storage and collection systems through modelling, location-allocation problem-solving, and vehicle routing problems through Geographic Information Systems (GIS) [15].

4. Municipal solidwaste management (MSWM)

Municipal solid waste management envelops generation, segregation, transfer, sorting, treatment, recovery, and disposal.In Telangana state, an average of about 2687 TPD (Excluding Greater Hyderabad Municipality Area) MSW is generated while per capita of waste generation in

the ULBs ranges from 0.2-0.4kg/capita/day.The MSWis expected to increase at the rate of 5% perannum while the collection efficiency is expected to be 80-90%.

5. Methods of data collection

This study administered a questionnaire to collect quantitative data from the people of Telangana to collect information about MSW awareness, the generation of MSW and characteristics of MSW, importance of segregation, collection, and disposal systems.

6. Municipal solid waste management in Telangana- results and discussion:

6.1. Age

As per the survey results 18-29 age group participated actively with 73.1% participation, followed by the 30-39 age group with 20.5% participation. The response from 60-65 age groups is nominal with one person responding contributing 0.5% participation. (Figure 1)

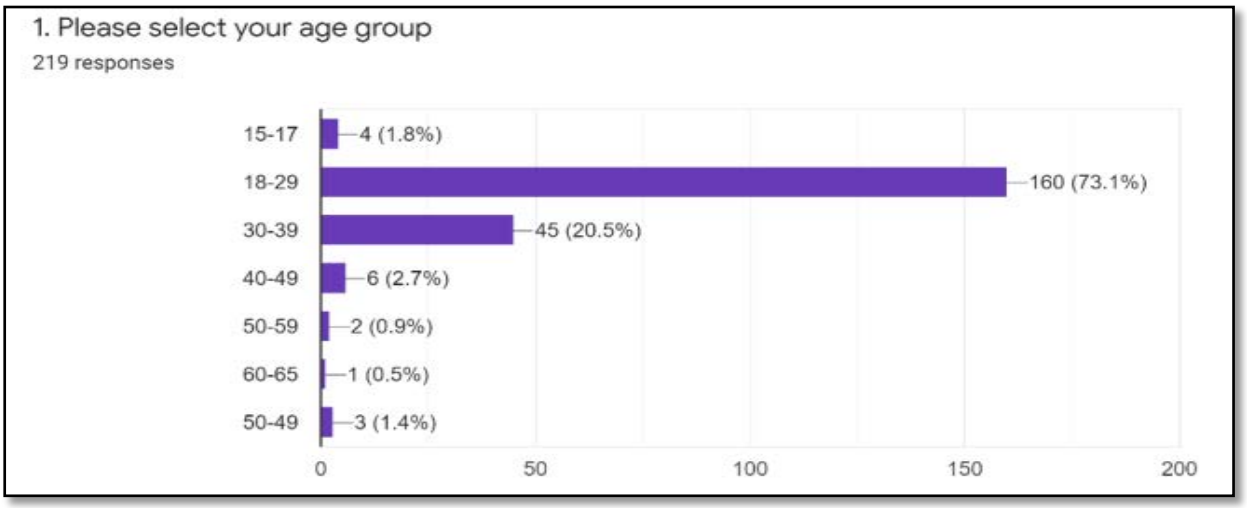


Figure.1. Age group of respondents (Source: Google survey form)

6.2. Districts

We have identified that out of 219 responses, 214 people have selected their districts. The majority of respondents are from Hyderabad city with 78 people (36.4%) participating in the survey. The response is poor in Ranga Reddy district with two persons (12%) participation followed by 9.7% participation from Suryapet district 0.5% participation from Bhoongir, Kamareddy, and Warangal with one person responding from each district.

6.3. Gender:

The composition of responses across gender indicates higher participation from males as against females. 141 men (64.4%) and 78 women (35.6%) participated in the survey. The results indicated active participation of men as compared to women.

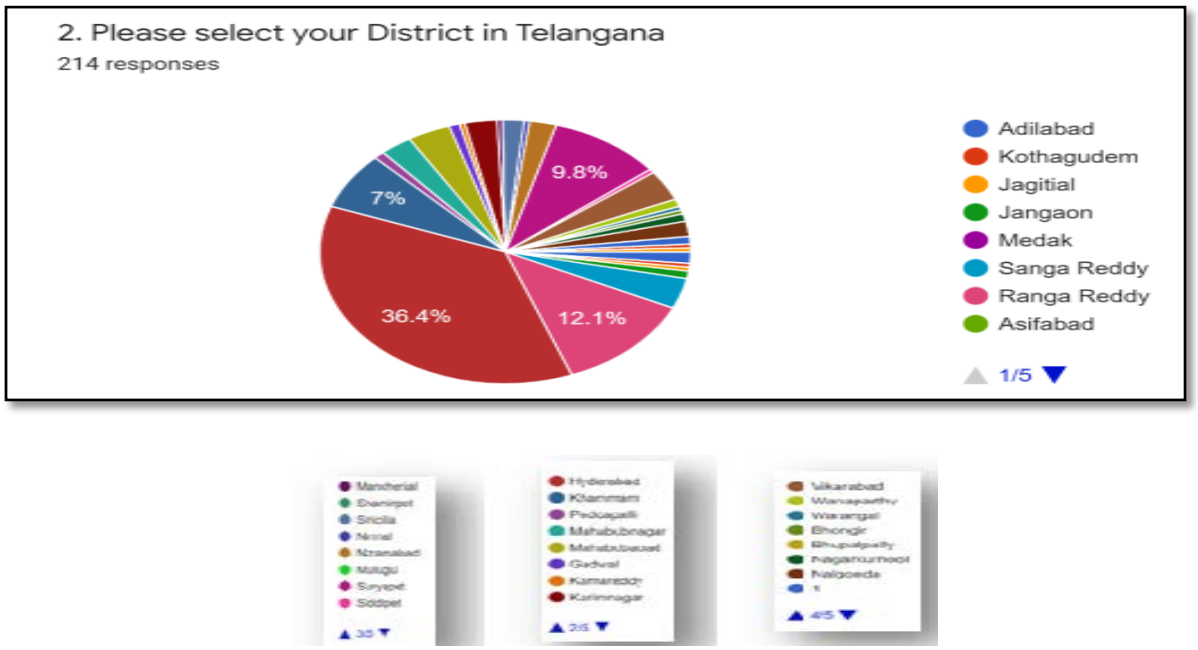


Figure-2. District wise responses(Source: Google survey form)

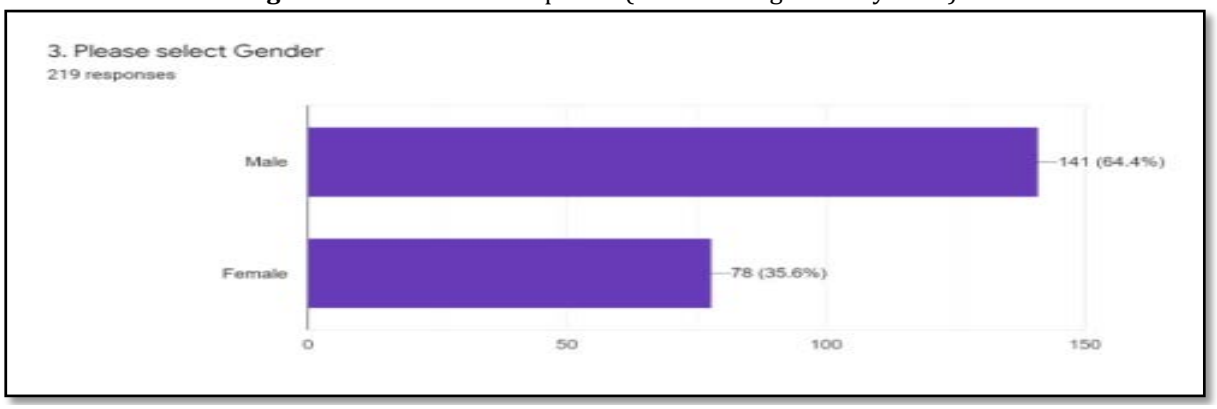


Figure-3. Gender wise responses(Source: Google survey form)

6.4. Occupation:

The respondents belong to various occupations with varied participation. 6.5% respondents from govenament sector, 9.7% respondents are enterprenours, 9.7% are from farming sectors, 21.65% from private employment and 56.2% from student community.The participation student community is higher as compared to other occupations.

6.5. Number of people per house

It is observed that 96 people (44%) gave responses with 4 people from each household. It follows that on an average, 1.6 kg waste generation from each family presuming that the family constituted with four members.

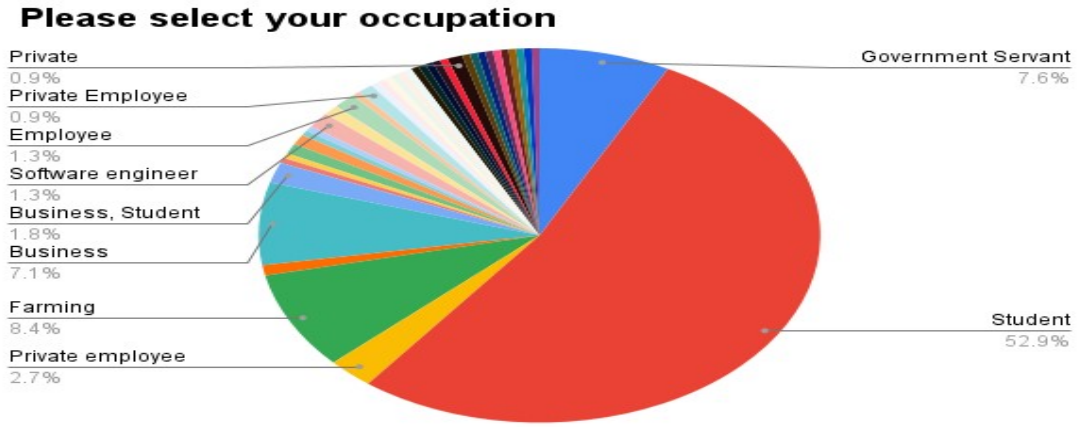


Figure-4. Occupation wise responses (Source: Google survey form)

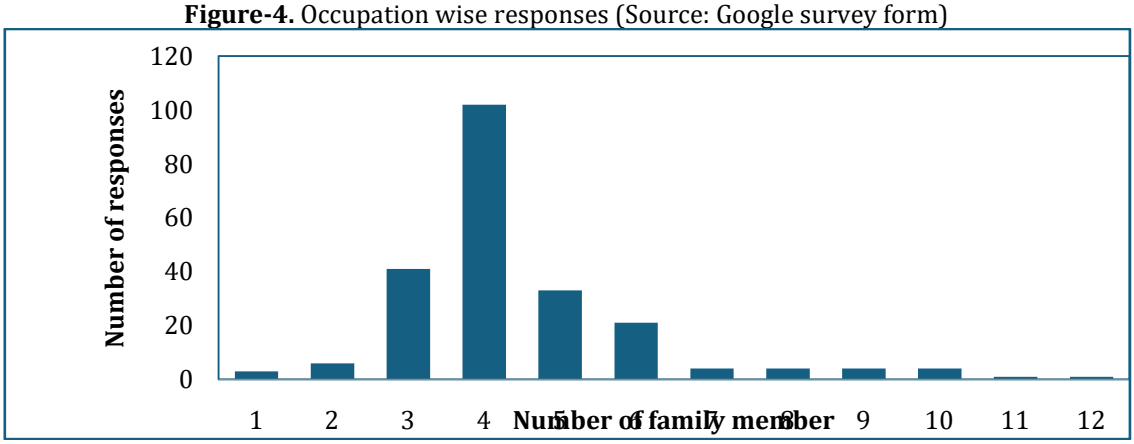


Figure-5. No of Persons in a household of Telangana state(Source: Google survey form)

6.6. Awareness about municipal solid waste management

A pre-requisite to the efficient Municipal Solid Waste Management is public awareness about MSW. According to Figure 6, out of 219 responses, 75.8% of people in Telangana district are aware of the term Municipal Solid Waste Management and are concerned about MSWM and its practices. A comparative analysis reveals that the awareness rate is relatively higher in city (84.33 percent) as expected. Interestingly, awareness in village (76.19 percent) is more as compared to towns (69.67 percent).

Place	**YES**	**%**	**NO**	**%**
City(Hyderabad)	70.00	84.33	13.00	15.67
Towns(24 district head quarters of Telangana)	85.00	69.67	37.00	30.32
Village (Ramdas Thanda)	16.00	76.19	5.00	23.81
Total	**171.00**	**75.66**	**55.00**	**24.33**

Table 1 Public awareness about MSW

- H0 There is no association between gender and place of residence and awareness about MSW

- H1 There is a significant relation between MSW awareness and gender and place of residence.

Gender association with MSW awareness is absent (p value is greater than 0.05) but Place of residence shows a significant relation with MSW awareness. (P value is less than 0.05)

6.7. Wet and dry waste segregation

69.1% of respondents separate dry and wet waste before clearing the trash can at their residences. 28.6% of respondents do not separate wet and dry waste before clearing the trash can. Around 2.3% of respondents practice wet and dry waste segregation occasionally. A comparative analysis shows that the respondents living in towns appear to be more conscious about segregation at source as against village and city. The segregation at source is relatively low in Hyderabad city with 66.27 respondents segregating waste at source preceded by 66.67 percent in Ramdas Thanda village and 77.87 percent of the sample population living in towns.

	YES	**%**	**NO**	**%**	**TOTAL**	**%**
City(Hyderabad)	55.00	66.27	28.00	33.73	83.00	36.73
Towns(24 district head quarters of Telangana)	95.00	77.87	27.00	22.13	122.00	53.98
Village (Ramdas Thanda)	14.00	66.67	7.00	33.33	21.00	9.29
Total	164.00	72.57	62.00	27.43	226.00	100.00

Table 2 Waste segregation at source

H0 There is no association between waste segregation and gender and place of residence.

H1 There is a significant relationship between waste segregation and gender and place of residence.

As p-value is greater than 0.05 (0.99) both gender-wise and place of residence-wise, the null hypothesis is accepted showing no relation between waste segregation and gender and place of residence.



Figure-6. Municipal Solid Waste Management Awarenessin the Telangana state (Source: Google survey form)

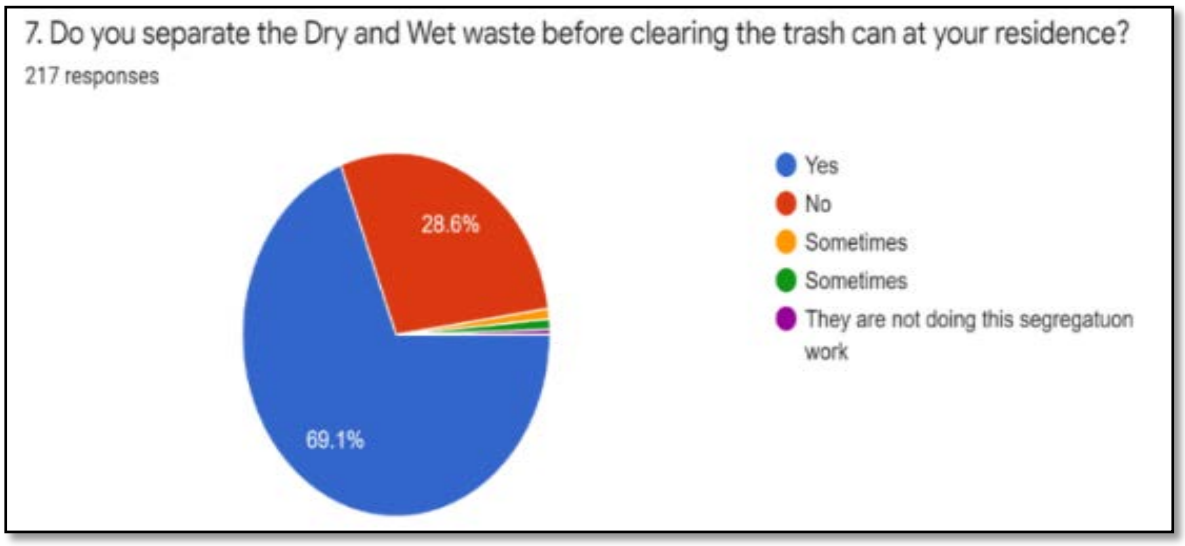


Figure-7. Separation of Dry and Wet Waste ratio in Telangana state (Source: Google survey form)

6.8. Types of solid waste generated from house.

From the survey, it is observed that 169 out of 219 people i.e., 77.2% of respondents have reported that plastic is the major municipal solid waste generated from their household.Food Waste takes second place with 161 people i.e., 73.5% generating food waste followed by 107 people (48.9%) generating paper waste. Glass waste is also part of household waste generated by 49 people (22.4%).

In the wake excess plastic waste generation, recycling facilities for plastic in Telangana must be improved, otherwise the plastic waste will pollute environment, decreases soil quality and effects ground water level, blocks drainage system and flood flow channel during rainy season. Another major problem with plastic waste is that it releases dioxins when burnt. The dioxins enter the food chain and get stored in animal fat and human body for 7-11 years causing cancer.

6.9. Garbage disposal

It is found that 101 respondents put the collected waste in garbage truck while 81 respondents put it in the trash cans. 16 respondents throw it in open areas, 19 respondents use public bins and 2 respondents reported that they burn the household waste in open areas.

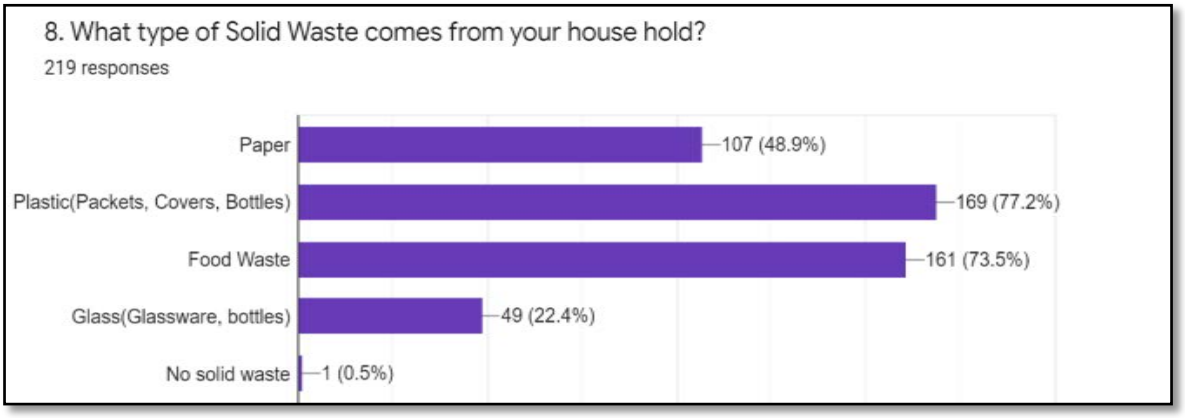


Figure-8. Types of Solid Waste generated by household in Telangana state (Source: Google surveyform)

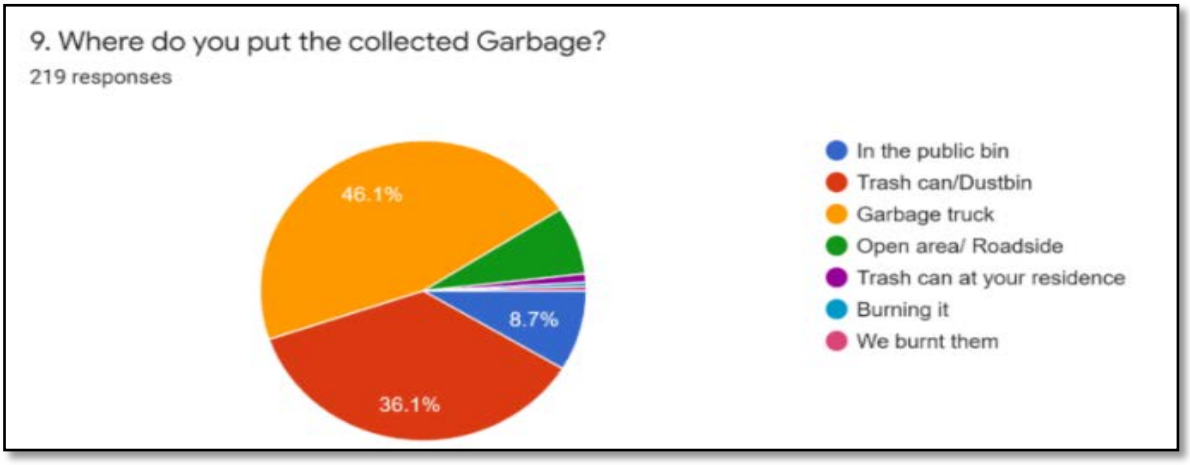


Figure 9. Garbage disposal ways by respondents in Telangana state(Source: Google survey form)

6.10. Precautions taken by garbage collectors.

As per the survey results, only55% respondents found the garbage collectorswearing a mask or gloves during waste collection process. 45% respondents observed that the garbage collectors do not use mask or gloves. This practice results in disease spreading by transferring the bacteria from their hands to the residents of the households when they knock the door or press the calling bell or while returning the emptied bins. Hence all the garbage collectors should be instructed to wear mask and gloves.

H0 There is no association between precautions taken by garbage collectors and gender and place of residence.

H1 There is significant relation between precautions taken by garbage collectors and gender and place of residence.

As p value is greater than 0.05 both gender wise and place of residence wise, the null hypothesis is accepted showing no relation between precautions taken by garbage collectors and gender and place of residence.

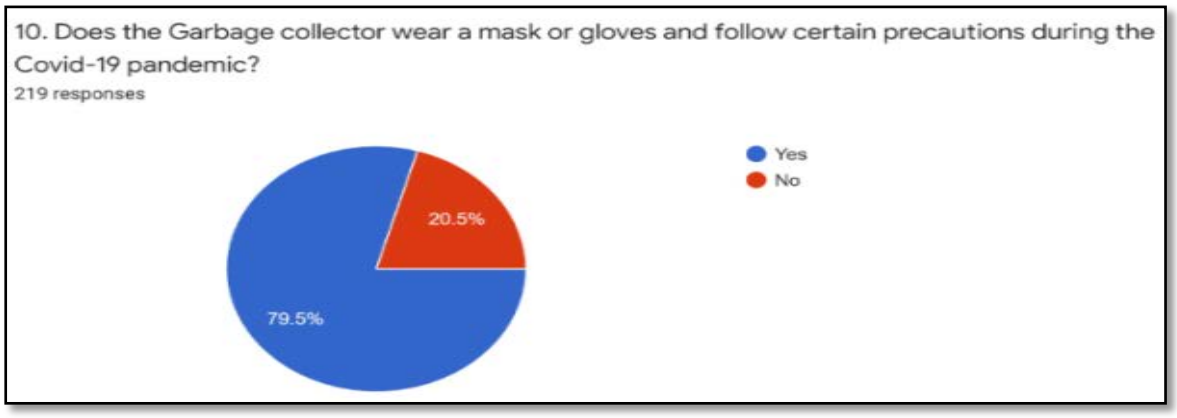


Figure-10. Awareness in garbage collectors about precautions during garbage collection in Telangana state (Source: Google survey form)

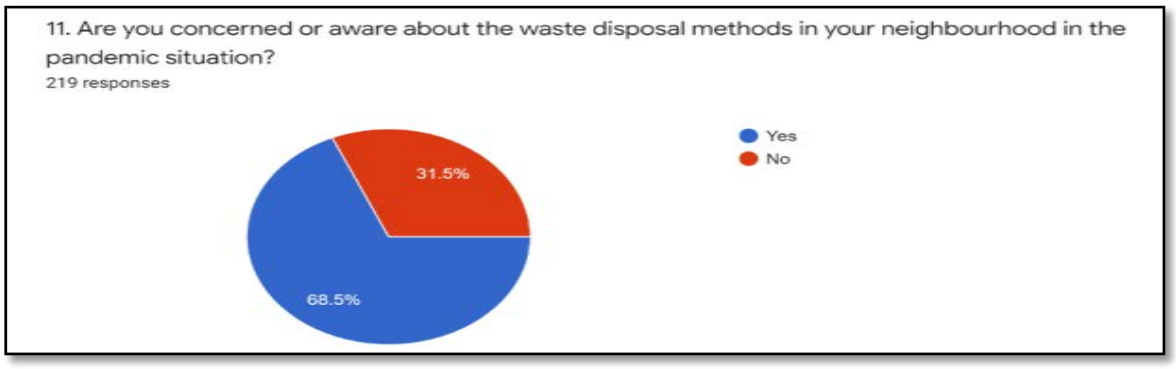


Figure-11. Respondents' awareness about MSW disposal methods (Source: Google survey form)

6.11. Awareness about waste disposal methods.

It is observed that only 68.5% ofrespondents are concerned about the waste disposal methods in their neighbourhood. The remaining 31.5% of respondents in Telangana districts are not aware about the waste disposal methods.

H0 – There is no association between awareness about waste disposal methods and gender and place of residence.

H1 - There is significant association between awareness about waste disposal methods and gender and place of residence.

The p value being less than 0.05 for both the demographic variables, the null hypothesis is rejected indicating that there is a significant relationship with gender and place of residence about waste disposal methods used in their neighbourhood.

6.12. Municipal solid waste volume growth

It is concluded that out of 219 responses, 117 people have noticed an increase ofmunicipal solid waste in their household and 102 people i.e., nearly half the respondents did not notice any change in the generation of municipal solid waste even during the pandemic time.But according to GHMC higher officials, 39% waste decrease is observed during covid 2019.

H0 – There is no association between waste increase and gender and place of residence.

H1 - There is significant association between waste increase and gender and place of residence.

The p value (0.55) is greater than the level of significance (0.05) and hence the null hypothesis is accepted indicating the absence of relation between gender and place of residence and increase in the municipal solid waste growth.

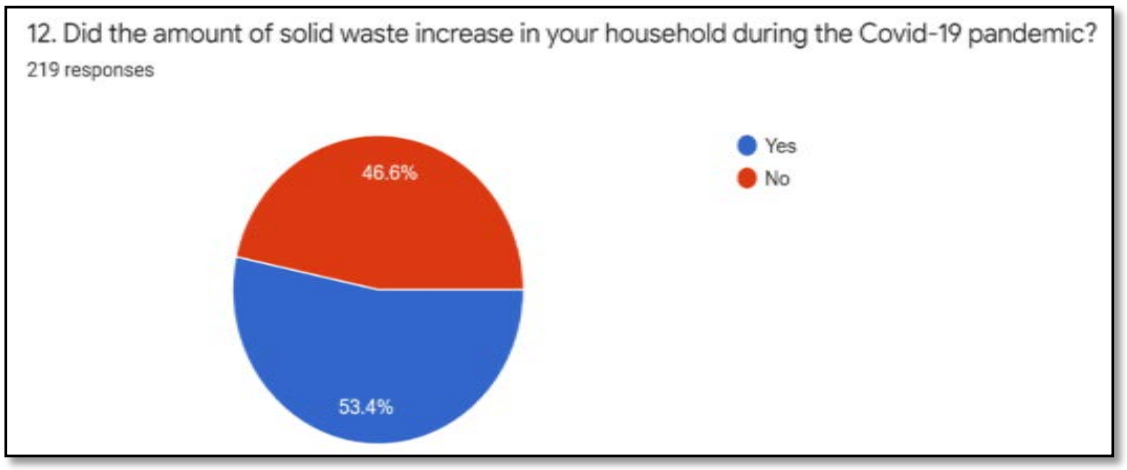


Figure-12. Increase in Municipal Solid Waste year by year in Telangana state (Source: Google survey form)

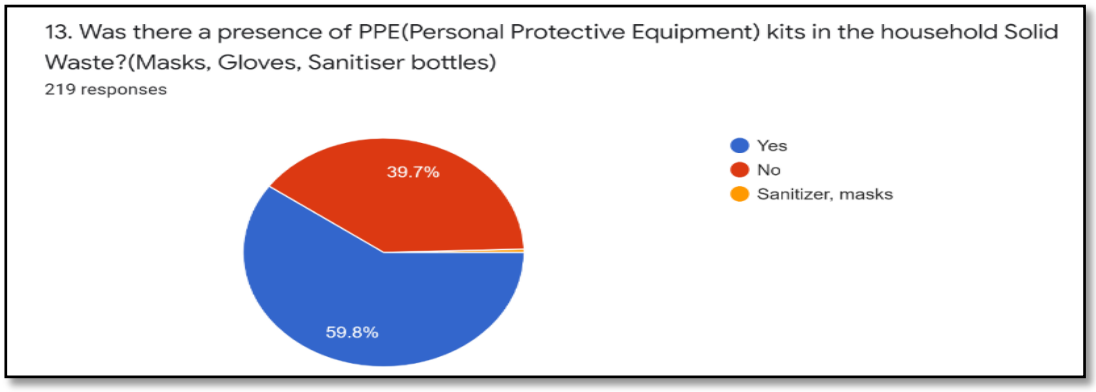


Figure-13. Presence of PPE in Household Waste mentioned by the respondents during the covid-19 pandemic (Source: Google survey form)

6.13. Medical waste types

The survey results indicate that only 131 in 219 people have noticed the presence of PPE kits, gloves, masks, sanitizer bottles in the household solid waste whereas, the remaining 81 have not noticed any presence of used PPE kits in the household Solid Waste.

H0 – There is no association between presence of medical waste and gender and place of residence.

H1 - There is significant association between presence of medical waste and gender and place of residence.

The p values (0.99) for both the demographic variables are greater than the level of significance (0.05) the null hypothesis is acceptable. This means there is no significant association between region wise group, gender and kind of medical waste is generated in the house.

6.14. Presence of garbage in open areas, landfills

The results show that out of 219 responses, 150 people i.e., 68.5% have noticed the presence of Heavy Garbage dumped in open areas and Landfills whereas 33.8% of the people did not notice any Garbage in open areas or anywhere near their surroundings.In order to combat dumping thegarbage in open areas penalty collection should be strictly implemented.

H0 – There is no association between garbage observed in open areas and gender and place of residence.
H1 - There is significant association between garbage found in open areas and gender and place of residence.
p values are greater than 0.05 and hence the null hypothesis is accepted

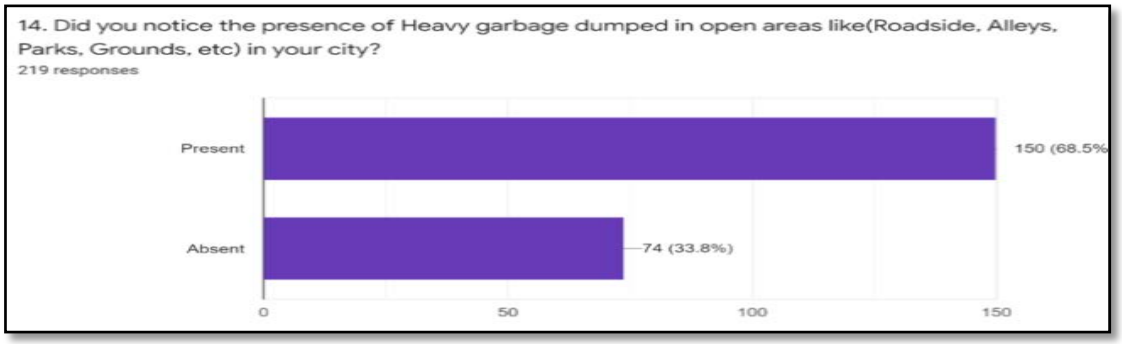


Figure-14. Presence of Garbage on Open roads, Landfills observed (Source: Google survey form)

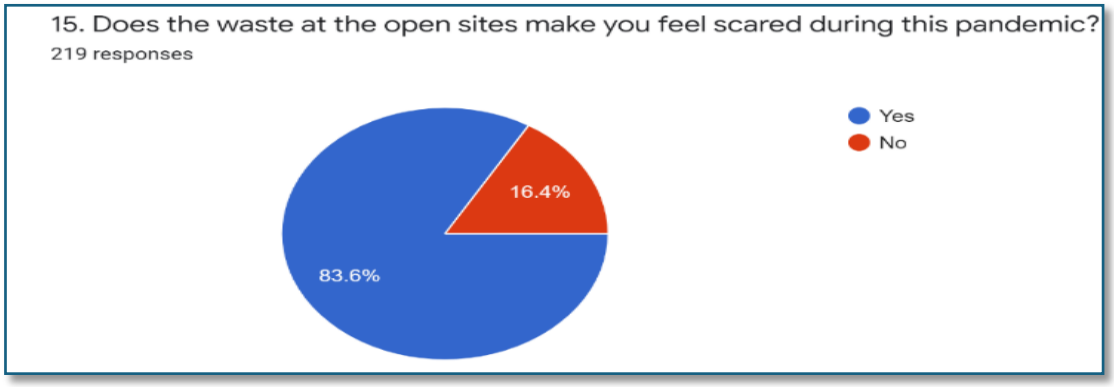


Figure-15. Respondents' opinion on open dumping in Telangana state (Source: Google survey form)

6.15. Respondents'opinion on open dumping

Survey reveals that during the pandemic situation, 183 of 219 people i.e., 83.6% were concerned about the heavy dumping of waste at open sites and landfills.36 people i.e., 16.4% are not concerned about the wrong practices of Garbage disposal and presence of waste at open sites during the pandemic period.
H0 – There is no association between concern about open dumping of waste especially during pandemic and gender and place of residence.
H1 - There is significant association between concern about open dumping especially during covid and gender and place of residence.
P values are greater than the level of significance indicating the absence of association between concern about open dumping of waste and gender and place of residence.

6.16. Livestock presence at open areas andlandfills

It has been observed that 79.9% of dogs, 37.9% of waste pickers, 37.4% of cows and buffaloes are the livestock that are noticed at open dumping areas and landfills. Majority of People in Telangana district is concerned about the transmission of viruses due to the presence of livestock at the dumping yards and open landfills. Many toxic chemicals enter the food chain

causes serious health problems in human body through consumption of milk and other meat products.

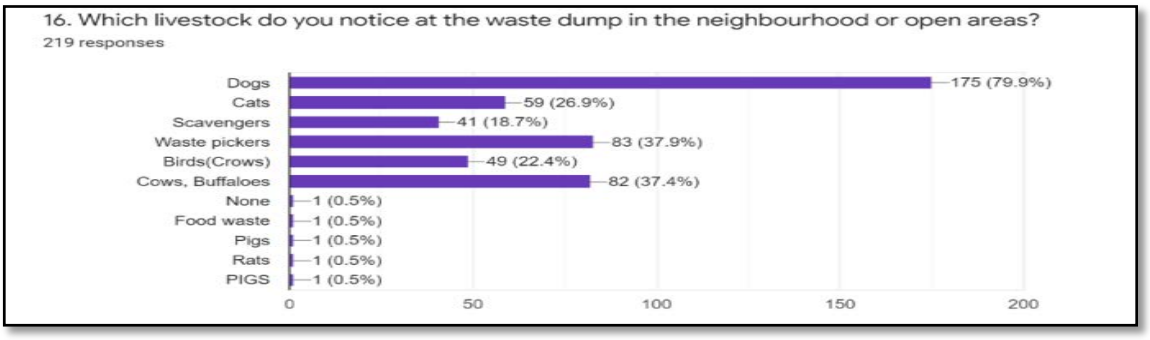


Figure-16. Livestock near garbage observed by the respondents in the Telangana state (Source: Google survey form)

6.17. Solid waste generation due to excessive online shopping

It has been observed that 197 respondents (90%) have seen an increase in the frequency of online shopping during the Covid-19 pandemic. Only 10% haven't noticed any change in the rate of online shopping. The increase in online shopping leads to increase in municipal solid waste in the form of packingmaterial such as paper carton, plastic cover, plastering material, air bags inside the carton to protect the product for their safe transportation.

H0 – There is no association between excessive online shopping and gender and place of residence.

H1 - There is significant association between excessive online shopping and gender and place of residence.

Chi-square analysis reveals that there is no relation between excessive online shopping and gender and place of residence even during pandemic.



Figure-17. Increase in online shopping in the Telangana State (Source: Google survey form)

6.18. Food preference during pandemic time

During pandemic, 94.06% respondents in Telangana district opted for fresh, home prepared food, while 44 respondents (20.1%) have opted for packaged or online ordered food, 6.4% respondents only resorted to readymade foods during the pandemic time. During the pandemic time, most of the restaurants and hotels were closed and hence packing materials decreased. Food waste also decreased because the person who prepares the food had the estimation about the quantity of food to be cooked.

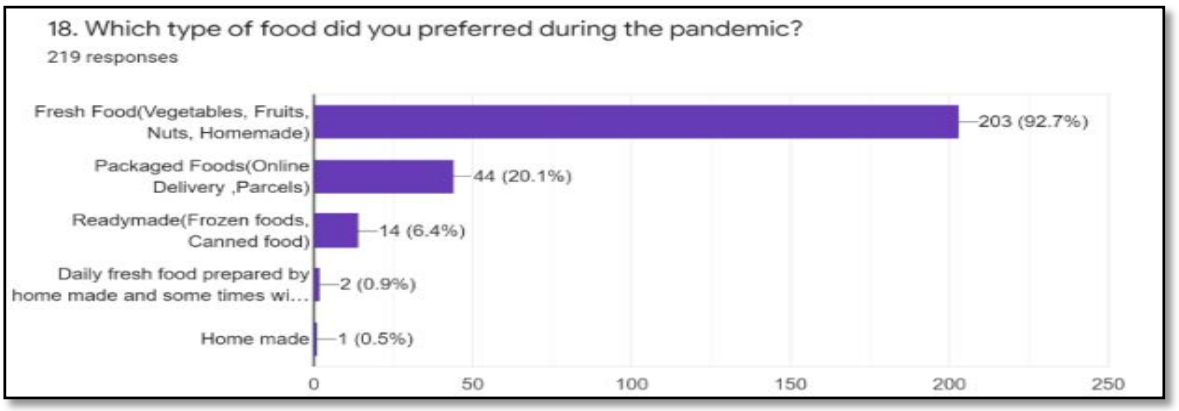


Figure-18. Type of Food Preferred by the respondents in Telangana (Source: Google survey form)

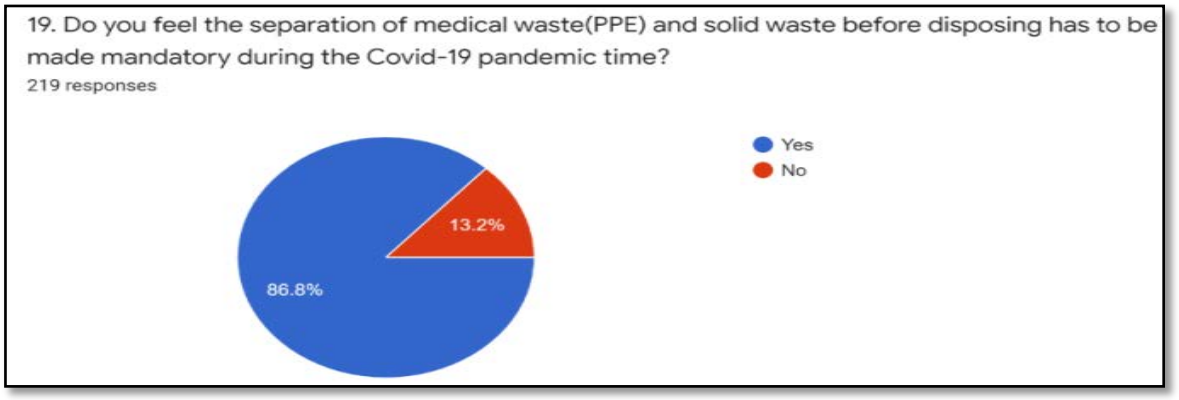


Figure-19. Separation of Medical and Municipal Solid Waste in household (Source: Google survey form)

6.19. Separation of medical waste and municipal solid waste

According to survey, we have noticed that out of 219 respondents from Telangana, 86.8% people feel that the separation of medical waste and municipal solid waste is necessary during the Covid-19 pandemic time while 13.2% people feel that this practice is not happening properly in the state.

H0 – There is no association between medical waste and MSW separation and gender and place of residence.

H1 - There is significant association between separation of medical and MSW and gender and place of residence.

Gender has shown significant relation between the need to separate medical waste and MSW as the p value (0.03) is less than 0.05 but place of residence has no significant impact on the opinion of medical and MSW segregation.

6.20. Awareness amongst waste collectors

It has been observed that nearly half of the respondents in Telangana i.e., 54.4% strongly feel that the waste collectors are not well trained to guide people on how to deal with medical waste and control the spread of pandemic and other diseases. The remaininghalf of the respondents i.e., 45.6% feel that garbage collectors are well trained about how to deal with medical waste. Generally medical waste is rarely present barring the houses with chronic patients. But during the pandemic, most of the asymptomatic covid patients were at home contributing to higher medical waste.

H0 – There is no association between waste collectors' efficiency in guiding people in the process of medical waste and MSW segregation and gender and place of residence.
H1 - There is a significant association between waste collectors' role in guiding people to segregate medical and MSW and gender and place of residence.
Place of residence and gender are independent of the assistance provided by waste pickers as p-value is higher than 0.05.

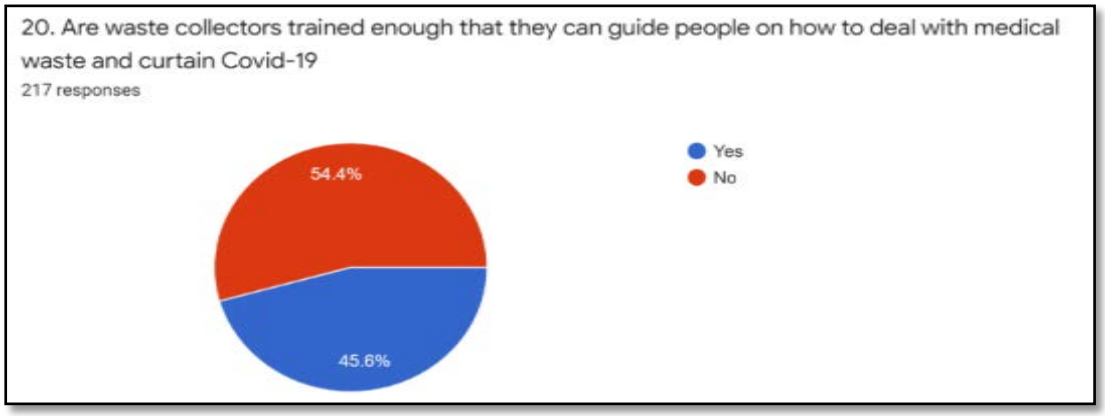


Figure-20. Awareness and Training needed for Waste collectors (Source: Google survey form)

6.21. Suggestions given by respondents
The varioussuggestions offered by the respondents are shown in the graphical representation below in Figure21, where the majority suggested 3Rs and Waste segregation.



Figure-21. Suggestions given by respondents for better MSW management in Telangana state(Source: Google survey form)

7. Conclusion

- In the journey of understanding the MSW awareness, generation, collection, transportation, and disposal methods, gender has no impact on the various parameters tested except for expressing the need to separate MSW and medical waste. Place of

residence has an influence on the awareness about MSW and its disposal methods leaving other parameters which are considered to be independent of the demographic variables used.

- Most of the villages in Telangana have municipal solid waste management sites.
- The number of recycling facilities for plastic has to increase in Telangana state.
- Garbage collectors are aware of the procedures but they are not practicing which calls for strict implementation policies.
- Penalties for breaking the rules exist but are not strictly enforced, which is the cause of present scenario in Telangana.
- Transportation safety measures are taken for online-shopped products, so they are packed using paper cartons, plastic covers, airbags, and plastering materials, resulting in an increase in the amount of municipal solid waste for every product.
- The recovery and recycling of material facilities reduces the burden on the landfill extending its life. Composting also facilitates extension of landfill life, diversion of organic matter to the composting pitreduces gas and leachate risks at the landfill.
- MSWM is a major problem that remains in the whole world. This is our small research to understand MSWM after and duringthe COVID-19 pandemic time and to improve it. We conducted a survey in which the people of Telangana were asked to give their responses.
- It is surprising tonote that 25%of respondents are unaware of municipal management and out of the remaining 75%, 60% of respondents undertake waste segregation at source. One of the advantages of separating dry waste and wet waste is that one can earn money by selling dry goods in scrap, which can further be recycled or used for other purposes.
- During the pandemic, many people did their job in MSWM work keeping an eye on all the Guidelines of Covid-19 and the municipal solid waste collectors also maintained Covid precautions. Eventually, successful MSWM will be effective with proper funding, legislation, and institutional policy.

Data availability statement: Data will be made available on request.

References

[1] Stephen Oppong Kwakye , Ebenezer Ebo Yahans Amuah , Kingsford Agyapong Ankoma, Emmanuella Boateng Agyemang, Boadi-George Owusu January 2024Understanding the performance and challenges of solid waste management in an emerging megacity: Insights from the developing world. *Environmental Challenges*, Volume **14**, 100805

[2] Addis Taye, Engdawork Assefa , Belay Simane2024Analysis of practices and factors of solid waste management among urban households of Addis Ababa city, Ethiopia Challenges, Volume, 100811.

[3] Huifang Li, Chao Hu, Xinrun Zhong , Chao Zeng , and Huanfeng Shen 2023Solid Waste Detection in Cities Using Remote Sensing Imagery Based on a Location-Guided Key Point Network With Multiple Enhancements, IEEE Journal *Applied Earth Observations and Remote sensing*, vol.16,Page no 191-201.

[4] A Noman, Islam M. Rafizul, S.M. Moniruzzaman, E. Kraft , S Berner 2023Assessment of municipal solid waste from households in Khulna city of Bangladesh. *Heliyon*, Volume **9**, Issue 12, e22446.

[5] Xiaoning Shen, Hongli Pan, Zhongpei Ge, Wenyan Chen, Liyan Song, and Shuo Wang 2023 Energy-Efficient Multi-Trip Routing for Municipal Solid Waste Collection by Contribution-Based Adaptive Particle Swarm Optimization. *Complex System Modeling and Simulation* ISSN 2096-9929 03/06 pp 202−219 Volume 3, Issue 3, DOI: 10.23919/CSMS.2023.0008

[6] M D Meena, M L Dotaniya, B L Meenaa , P.K. Raia, R S Antil , H S Meena, L K Meena , C K Dotaniya , Vijay Singh Meena, Avijit Ghosh, K N Meena, Amit K Singh, V D Meena, P C Moharana, Sunita Kumari Meena, Ch

Srinivasarao, A L Meena, Sumanta Chatterjee, D K Meena, M Prajapat, R B Meena 2023 Municipal solid waste: Opportunities, challenges and management policies in India: A review *Waste Management Bulletin*, Volume **1**, Issue 1, , Pages 4-18.

[7] Kiran D A , Pushkara S V , Jitvan R , Darshan S. 2023 Characterization, quantification and management of municipal solid waste in Shivamogga city, Karnataka, India. *Waste Management Bulletin*, Volume **1**, Issue 3, Pages 18-26.

[8] Yash Pujara , Janki Govani, Harshit T Patel , Pankaj Pathak, Deepak Mashru , P Sankar Ganesh. 2023 Quantification of environmental impacts associated with municipal solid waste management in Rajkot city, India using Life Cycle Assessment. *Environmental Advances*, Volume **12**, 100364.

[9] Oshan Mudannayake, Disni Rathnayake, Jerome Dinal Herath, Dinuni k. Fernando , and Mgnas Fernando, 2022 Exploring Machine Learning and Deep Learning Approaches for Multi-Step Forecasting in Municipal Solid Waste Generation *Applied Research*. Volume: **10** , Journal Article, Publisher: IEEE.

[10] Navarro Ferronato, Luca Moresco, Gabriela Edith Guisbert Lizarazu, Marcelo Antonio Gorritty Portillo, Fabio Conti, Vincenzo Torretta, 2021 Sensitivity analysis and improvements of the recycling rate in municipal solid waste life cycle assessment: Focus on a Latin American developing context *Waste Management*, Volume **128**, Pages 1-15.

[11] Praveen Kumar Gopala krishnan, John Hall, Sara Behdad2021 Cost analysis and optimization of Block chain-based solid waste management traceability system. *Waste Management.* Volume 120, 1, Pages 594-607

[12] Hari Bhakta Sharma, Kumar Raja Vanapalli , V R Shankar , Cheela Ved Prakash Ranjan, AmitKumar Jaglan , Brajesh Dubey , Sudha Goel , Jayanta Bhattacharya 2020 Challenges, opportunities, and innovations for effective solid waste management during and post COVID-19 pandemic *Resources, Conservation and Recycling*Volume **162**, 105052.

[13] Somdutta Banerjee & Prasenjit Sarkhe2020Municipal solid waste management, household and local government participation: a cross-country analysis *Journal of Environmental planning and Management* Volume 63, -Issue 2.

[14] Mohan B Dangi , Erica Schoenberger, and John J Boland. 2017 Assessment of environmental policy implementation in solid waste management in Kathmandu, Nepal *Waste Management &Research: The Journal for a Sustainable circular Economy*Volume 35, Issue 6; https://doi.org/10.1177/0734242X17699683.

[15] Seyed Mohammad Hassan Erfani, Shahnaz Danesh , and Rouzbeh Shad,2017 A novel approach to find and optimize bin locations and collection routes using a geographic information system Waste Management & Research: *The Journal for a Sustainable circular Economy*Volume 35, Issue 7 ;https://doi.org/10.1177/0734242X17706.

[16] Md Manik Mian, Xiaolan Zeng, Allama al Naim Bin Nasry & Sulala M Z F Al-Hamadani 2017 Municipal Solid Waste management in China:a comparative analysis-review*Journal of Material Cycles and Waste Management* published ;13 volume 19,pages1127-1135.

[17] Avinash Rajcoomar and Toolseeram Ramjeawon 2016 Life cycle assessment of municipal solid waste management scenarios on the small island of Mauritius Waste Management & Research *The Journal for a Sustainable circular Economy*Volume 35 Issue 3https://doi.org/10.1177/0734242X16679883.

[18] Rajkumar Joshi ,Sirajuddin Ahmed 2016, Status and challenges of municipal solid waste management in India: A review*Cogent Environmental Science* Volume 2, 2016 - Issue 1https://doi.org/10.1080/23311843.2016.1139434.

[19] Dr Karthikeyan V ,Dr Sathyamoorthy G L 2016 Municipal Solid Waste Management in Salem City, India *Asian Journal of Research in Social Sciences and Humanities* Volume 6 Issue 6 page 2189-2208 Online ISSN : 2249-7315.Article DOI : 10.5958/2249-7315.2016.00355.5.

[20] Elbert Dijkgraaf and Raymond Gradus 2014 Chapter 11: *Waste management in the Netherlands* Category: Handbook Chapter Published: 30 Page Range: 287–315 Collection: EconomicsDOI: https://doi.org/10.4337/9780857936868.00019.

[21] B L Chavan, N S Zambare 2013 A Case Study on Municipal Solid Waste Management in Solapur City, Maharashtra, India *International Journal of Research in Civil Engineering, Architecture & Design* Volume 1 Issue 2 October-December pp. 46-53, © IASTER 2013 www.iaster.com, ISSN Online: 2347-2855, Print: 2347-8284.

Acknowledgments

The authors acknowledge thefinancial support for publication was provided by the Vasavi College of Engineering, Hyderabad, Indiaand data collection was aided by MD. Muqtar Patel, B. Raju, G.V. Abhigyan, and P. Deepa Sree.

IOP Conference Series: Earth and Environmental Science

PURPOSE-LED PUBLISHING™

PAPER • **OPEN ACCESS**

Seismic isolation of liquefied natural gas storage tanks using quintuple friction pendulum system (QTFP)

To cite this article: Vipul H. Vyas *et al* 2024 *IOP Conf. Ser.: Earth Environ. Sci.* **1409** 012022

View the article online for updates and enhancements.

You may also like

- Natural gas fuel and greenhouse gas emissions in trucks and ships
Jamie Speirs, Paul Balcombe, Paul Blomerus et al.
- Global liquefied natural gas expansion exceeds demand for coal-to-gas switching in paris compliant pathways
Shuting Yang, Sara Hastings-Simon and Arvind P Ravikumar
- Policy approaches to mitigate in-use methane emissions from natural gas use as a marine fuel
Imranul I Laskar and Amanda Giang



This content was downloaded from IP address 47.247.77.11 on 27/11/2024 at 05:38

Seismic isolation of liquefied natural gas storage tanks using quintuple friction pendulum system (QTFP)

Vipul H. Vyas[1], V. R. Panchal[2] and D. P. Soni[2]

[1]M. S. Patel Department of Civil Engineering, Chandubhai S. Patel Institute of Technology (CSPIT), Faculty of Technology & Engineering (FTE), Charotar University of Science and Technology (CHARUSAT), CHARUSAT campus, Changa 388421, Gujarat, India.
[2]Department of Civil Engineering, Sardar Vallabhbhai Patel Institute of Technology, Vasad, Gujarat, India

*e-mail: vipulvyas.cv@charusat.ac.in

Abstract: The current study explores the dynamic behaviour of a compressed (liquefied) natural gas tanks (LNG) that is separated utilizing a Quintuple Friction pendulum (QTFP) device. This is done by evaluating different earth-quake motions happening along fault lines. The main objective of this investigation is to enhance the dynamic adaption of isolated Liquefied Natural Gas Tanks by the application of QTFP. A numerical model has been developed using the equations of motion to simulate the reaction of the LNG tanks to seismic excitations. A non-linear dynamic study using the Newmark-Beta approach has been conducted to compare the results of isolated and uncontrolled LNG Tanks. The simulation modelling technique has been carried through utilizing MATLAB Simulink to analyze the efficacy of the LNG Storage tanks. The investigation evaluated the tank's displacement, acceleration, velocity, frequency characteristics, and base shear of the LNG tank. The findings reveal that the separation of Liquefied Natural Gas (LNG) through QTFP is successful when exposed to different seismic excitations, in contrast to uncontrolled LNG tanks. Seismic isolation improves LNG storage tank sustainability. These solutions limit seismic structural damage and leakage, decreasing risks to nearby ecosystems and populations. Thus, LNG storage facilities with seismic isolation technologies provide energy infrastructure sustainability, safety, and resilience.

Keywords. Seismic isolation, LNG storage tanks, Quintuple Friction Pendulum Isolator, Seismic analysis

1. Introduction

The industrialized world's lifeline projects are LNG storage tanks. More and bigger LNG storage tanks will be needed to cater for growing need for energy. Liquefied natural gas (LNG) tanks for storage are becoming more frequent and extremely large tanks are built for storing LNG. With a volume of nearly 160,000 m^3, these storage structures are immense [3]. There are actually three layers within these tanks: a steel inner tank, a concrete outer tank, and an insulating layer lies in between (Fig. 1). The inner tank holds the LNG, while the outside tank protects it.

Content from this work may be used under the terms of the Creative Commons Attribution 4.0 licence. Any further distribution of this work must maintain attribution to the author(s) and the title of the work, journal citation and DOI.
Published under licence by IOP Publishing Ltd

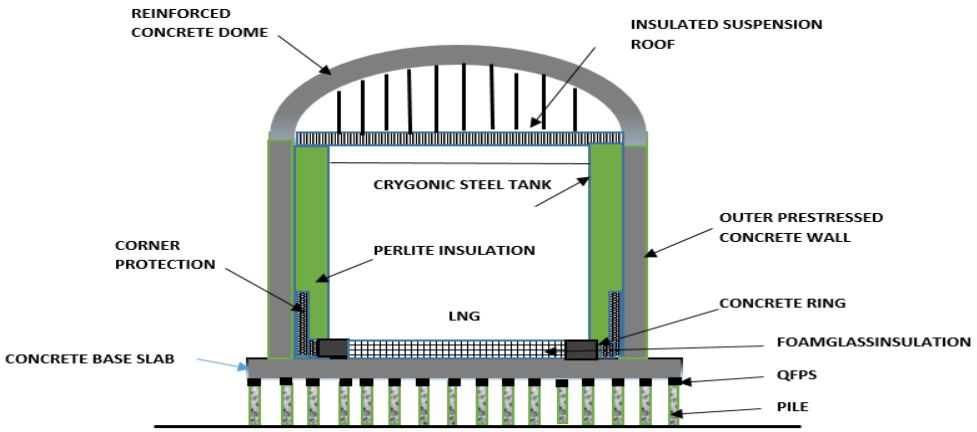


Figure 1. Schematic view of LNG tank with QTFP [3]

The fundamental frequency of most ultra-large LNG tanks stands within the 2 to 10 Hz range, which coincides to the resonance seen in virtually all of earthquake motions on earth [9]. The burst of extremely large LNG storage tanks during a seismic event would represent a considerable issue. Many real occurrences illustrate that conventional tanks are subject to destruction during earthquake. Breaking down at the intersection of the bottom surfaces and compressing buckled of the structure's outermost wall (elephant foot buckle) triggered by lift up, sliding of the bottom, a collapse of the anchorage structure, slosh destruction surrounding the roof, failures in the supply mechanisms, and a structural deformation of the bottom surface seemed common forms of tank damage during earlier earthquakes like the year 1989, Loma Prieta, in the year 1994, North Ridge, Chi-Chi Taiwan, and the year 1999, Kocaeli [1]; Chalhoub and Kelly, 1990). There are analytical and experimental evaluations of the seismic sensitivity of tanks that hold liquid because of the damage they encountered during previous earthquakes.

Base isolation approach is one of the effective and successful, passive control consider to protect the storage tanks from the damages induced by earthquakes. The effectiveness of this technique has improved due to the emergence of new base isolation technologies. Moreover, the base-isolated structures might suffer serious damage when triggered by various forms of earthquakes. Thus, earthquakes set a crucial amount of energy into the structures with long-period pulse enabling fewer cycles of resilient inelastic deformations to emit the energy. They also transmit noteworthy isolator displacement in base-isolated structure, which could lead to full collapse of the isolation system. Hence it becomes vital to evaluate the efficiency of the isolation devices and structure itself under various excitations [3].

The friction pendulum mechanism, which is a kind of verified resistance sliding technology, may substitute a lead-rubber bearing that is not durable at very low temperatures, particularly for use in extremely cold places (Zayas et al., 1987). thereafter, a revised isolation designated as the multiple frictional pendulum device was presented to deal with the considerable shift created by earthquakes with longer dominant periods by Tsai, Chiang et al [10]. Various advantages connected with FPS in tanks for liquids have been emphasized (Wang, Teng, and Chung 2001).In its further investigation, [7] at first carried out predictive assessments to measure the earthquake resistance of tanks separated through different bearing systems and damping characteristics. In the past few years, Panchal and Jangid [5] looked into the ability to adapt of the variable friction pendulum technique (VFPS) isolated tanks to nearfield earthquakes and discovered that response to transient ground shaking and corresponding movements generates identical results at isolation periods over 3 s. Abalı and Uçkan [1] looked into the earthquake stability of both wide and narrow tank base separation

using Friction pendulum system and then evaluated the influence of overturn moment and upward acceleration on the direction of axial load variability at their bearing surfaces.

There are more combined parts within exceptionally big LNG tank as compared to conventional tanks, resulting in stronger obstacles for isolator displacement over ground movements. The liquid content of the tanks in typical usage fluctuates often hence substantially impacts the isolated technique's vibration duration. Furthermore, the low temperature, soft land in addition to other factors of nature linked to the LNG tank lead to extra requirements for safeguarding the effectiveness and long-term reliability of bearing. The workings of extremely large LNG tank safeguarded through QTFP are addressed in this paper. A modified finite element approach created by Praveen K. Malhotra and Wieland [6]. Malhotra and Dunkerley is employed to analyze the effectiveness of the isolated mechanisms. Data supplied and analytically analyzed comprises of pile shear, isolated displacement, impulse acceleration and convective acceleration. The advantages or limitations of adopting QTFP are examined.

The relatively recently constructed Quintuple Friction Pendulum System [4] bearing is an upgraded variant of the TFPS comprised out of six elliptic surfaces that slide. It generates a more complex range of capability than the TFPS isolation, that may be employed to customize the response.

The fundamental purpose of the study is to explore the usefulness of QTFP in aseismic design for an LNG tank. The QTFP have been intended for obtaining particular time periods and shifting displacement capacity. Liquid storage tank had been seismically examined for distinct near-fault earthquakes. The seismic demand parameters looked into are base shear, isolator displacement, convective displacement and impulsive displacement.

2. Concept of quintuple friction pendulum system (QTFP)

The QTFP [7] may be classified as a number of models comprised of a total of five separate spherical Frictional pendulum elements coupled in a sequence as indicated in Figure 1(a) and Figure 1(b). Each individual cylindrical FP sliding part with an alternating arrangement of (1) a linear elastic spring with rigidity, $1/\bar{R}_{eff}$, which represents a force that recovers produced by a surface that is moving, (2) a friction component, $\bar{\mu}_i$, which symbolizes the friction of the surface, and (3) gap part, $\bar{d}_i$, which is representing the particular displacement capacity of each of the surface that slides.

The frictional coefficients, the efficient curvature radius of the surfaces that slides, the displacements capacity of each of the five FP sections of the sequential design are specified as

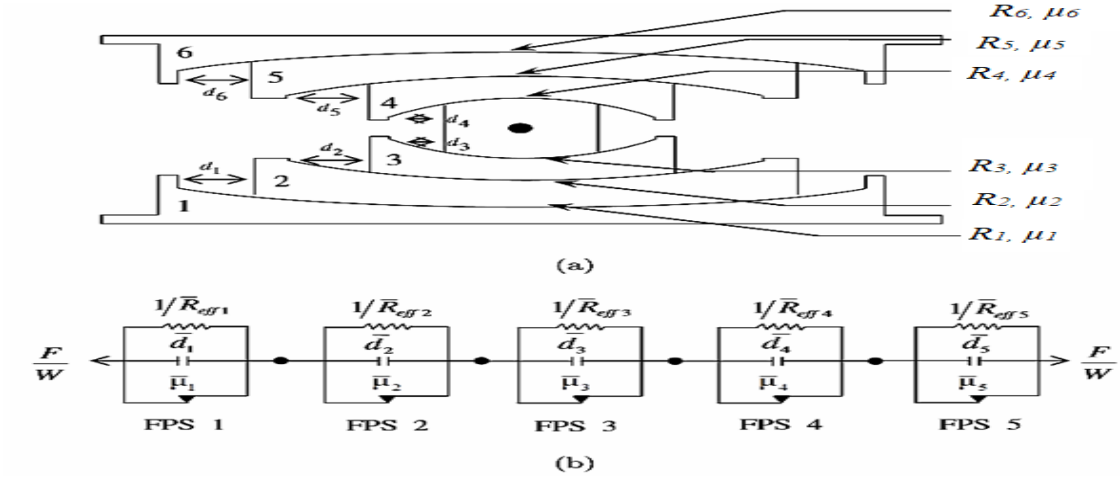


Figure 2. (a) Simplified representation of QTFP (b) The series prototype of the QTFP [4]

$$\bar{R}_{eff1} = R_{eff3} + R_{eff4} \quad (1)$$
$$\bar{R}_{eff2} = R_{eff5} - R_{eff4} \quad (2)$$
$$\bar{R}_{eff3} = R_{eff2} - R_{eff3} \quad (3)$$
$$\bar{R}_{eff4} = R_{eff6} - R_{eff5} \quad (4)$$
$$\bar{R}_{eff5} = R_{eff1} - R_{eff5} \quad (5)$$

When Reff, i = Ri - hi, Ri is the curvature radius of the ith layer surface of the isolator and hi is the radial distance from the pivoting point of its articulated sliders and ith layer.

$$\bar{\mu}_1 = \mu_3 = \mu_4 \quad (6)$$
$$\bar{\mu}_2 = \mu_5 \quad (7)$$
$$\bar{\mu}_3 = \mu_2 \quad (8)$$
$$\bar{\mu}_4 = \mu_6 \quad (9)$$
$$\bar{\mu}_5 = \mu_1 \quad (10)$$
$$\bar{d}_1 = d^*_{total} - (\bar{d}_2 + \bar{d}_3 + \bar{d}_4 + \bar{d}_5 + \bar{d}_6) \quad (11)$$
$$\bar{d}_2 = \left(\frac{d_5^*}{R_{eff5}} + \frac{d_6^*}{R_{eff6}}\right)(R_{eff5} - R_{eff4}) \quad (12)$$
$$\bar{d}_3 = \left(\frac{d_1^*}{R_{eff1}} + \frac{d_2^*}{R_{eff2}}\right)(R_{eff2} - R_{eff3}) \quad (13)$$
$$\bar{d}_4 = d_6^* \left(1 - \frac{R_{eff5}}{R_{eff6}}\right) \quad (14)$$
$$\bar{d}_5 = d_6^* \left(1 - \frac{R_{eff5}}{R_{eff6}}\right) \quad (15)$$

where

$d^*_{total} = d_1^* + d_2^* + d_3^* + d_4^* + d_5^* + d_6^*$ is the displacement capacity of isolator.

$d_i^* = d_i \, (R_{eff,i} / R_i)$ is the actual displacement capacity of isolator.

where d_i is the displacement capacity of isolator slider.

3. Numerical study

The present research evaluates isolated Liquefied Natural Gas (LNG) tanks equipped with QTFP and compares them with conventional LNG tanks. The equation of motion is investigated using New-Mark's linear acceleration procedure, and mathematical representations of the LNG tank separated employing QTFP are provided in Figures 3 and 4. Six different near-fault movements on the ground served as input grounds motions, and Table 1 and Table 2 show the characteristics of isolated LNG Tanks and the six near fault ground movements that were used in the investigation, accordingly. All ground motions have a particular peak acceleration (PGA).

The fundamental design of LNG tank shown in Fig.1 involves of an internal tank made up of metal (9% nickel steel especially for cryogenic operating temperatures) and an outer tank of post tensioned concrete construction. The ambient temperature of LNG held in the innermost tank is going to be around -168 ºC. For numerical research an LNG tank of 150,000 m3 (150 million liters) size is considered investigated by Christovasilis and Whittaker [2]. The thickness of the inner tank wall gradually ranges from 8 mm and at top to 34 mm at the lowest point of tank (average thickness = 21 mm) while the average thickness of outside tank is 900 mm. The overall height of inner tank is 40.6 m with designed elevation of LNG being 37.4 m. The outermost tank is 45 m high and the rise of the roof is 1.86 m. The inside and outside tank has radius 37m and 38m appropriately.

The typical dimensions for the LNG tank looked at in the current investigation are provided within Table II. The mass density ρ, is 480 kg/m3; the Elastic Modulus of concrete, Ec, and steel, Es, is 3 x

10^{10} N/mm^2 and 2 x 10^{11} N/ mm^2 each, while the Poisson's ratio for concrete material exists, μc , is 0.3.

Table 1. Dimension of External Tank, Internal tank and Enclosed Liquid [2]

Tank Measure	External Tank	Internal Tank
Height Wall (m)	45	40.6
Radius (m)	38	37
Typical thickness of wall (mm)	900	21
Maximum height of compressed LNG (m)	--	37.4

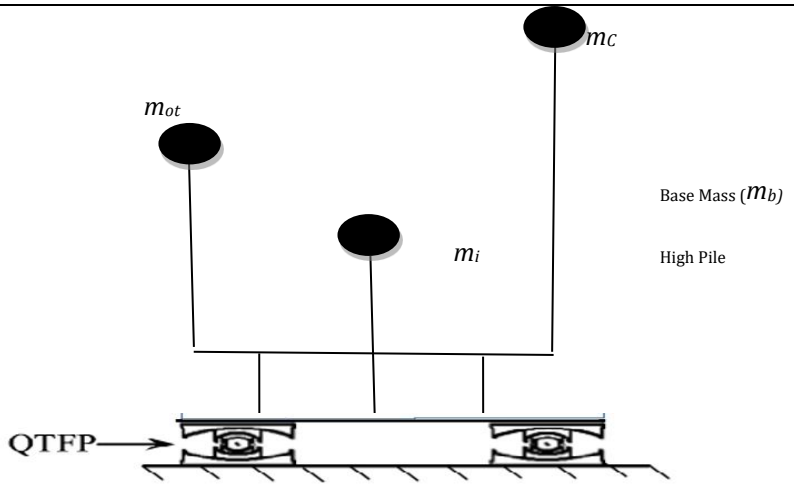


Figure 3. Schematic illustration of Modified representation of an LNG tank separated using QTFP

Table 2. Characteristics of near-fault earthquakes

Earthquake	Year	Record Station	Time (sec)	PGA (g)
Imperial Valley, California	October 15,1979	El Centro Array #5 (EQ11)	39.420	0.37
Imperial Valley, California	October 15, 1979	El Centro Array #7 (EQ21)	36.900	0.46
Northridge, California	January 17, 1994	Newhall (EQ31)	60.000	0.72
Landers, California	June 28, 1992	Lucerne Valley (EQ41)	49.284	0.71
Northridge, California	January 17, 1994	Rinaldi (EQ51)	14.950	0.89
Northridge, California	January 17, 1994	Sylmar (EQ61)	60.000	0.73

Table 3. Characteristics of Serial model for QTFP isolator (refer to Fig.1(b))

	D(m)	$\bar{R}_{eff1}$	$\bar{R}_{eff2}$	$\bar{R}_{eff3}$	$\bar{R}_{eff4}$	$\bar{R}_{eff5}$	$\bar{\mu}1$	$\bar{\mu}2$	$\bar{\mu}3$	$\bar{\mu}4$	$\bar{\mu}5$
QTFP	1.0	1.014	0.372	0.372	6.980	22.318	0.01	0.03	0.06	0.007	0.1

4. Result and discussion

Result of peak response of numerous variables like outer tank displacement, convective displacement, impulsive displacement of conventional tank and isolated displacement of separated tank employing QTFP.

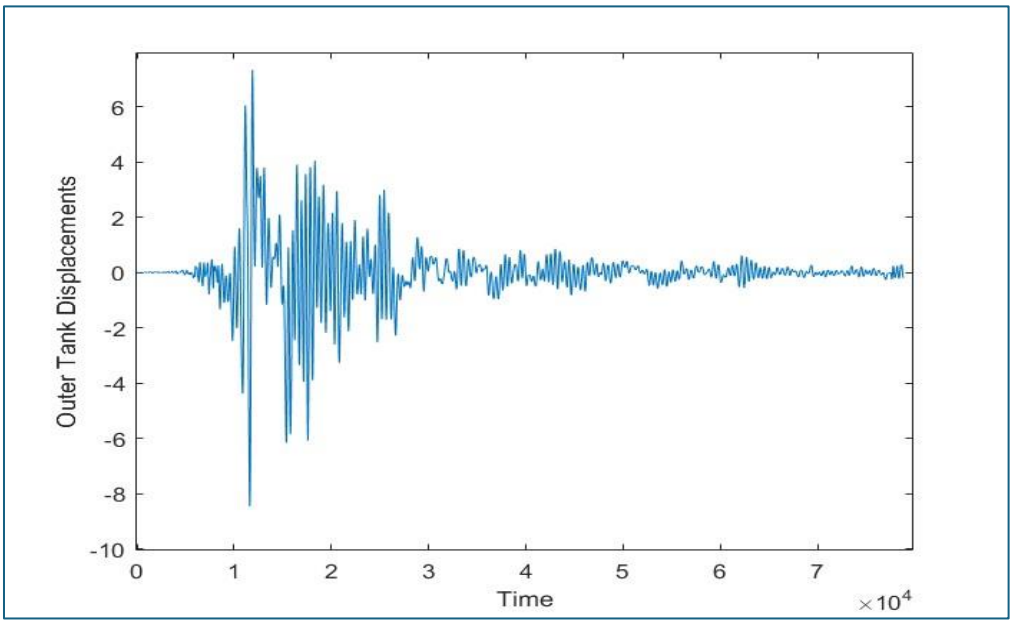


Figure 4. Time vs Outer tank Displacement (cm) for uncontrolled tank under 1979, Imperial Valley, California ground motion

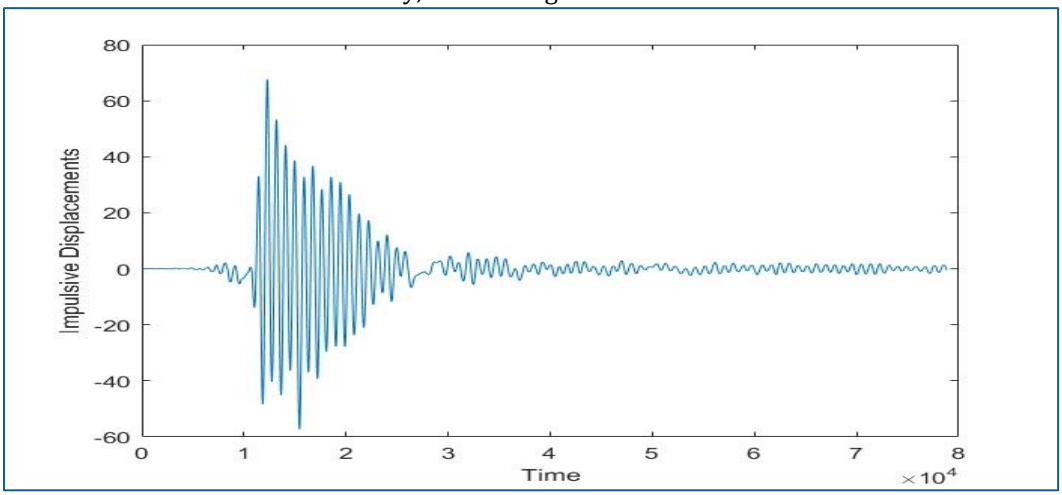


Figure 5. Time vs Impulsive Displacement (cm) for uncontrolled tank under 1979, Imperial Valley, California. ground motion

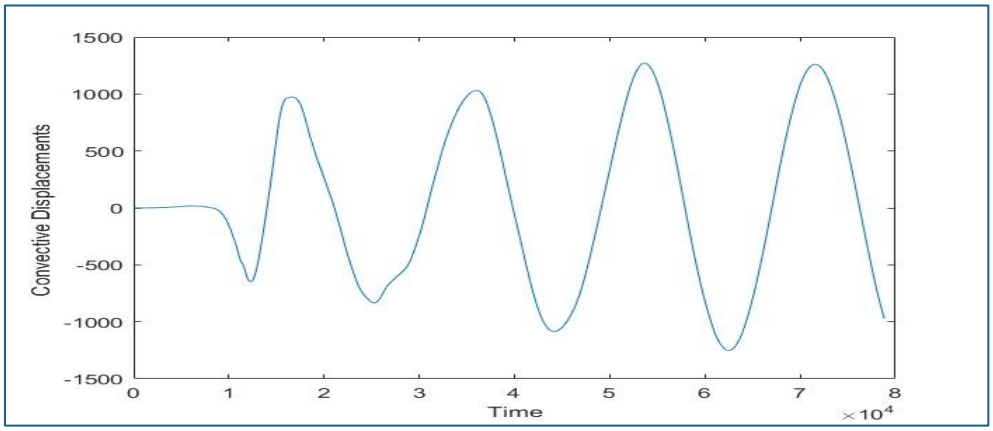


Figure 6. Time vs Convective Displacement (cm) for uncontrolled tank under 1979, Imperial Valley, California. ground motion

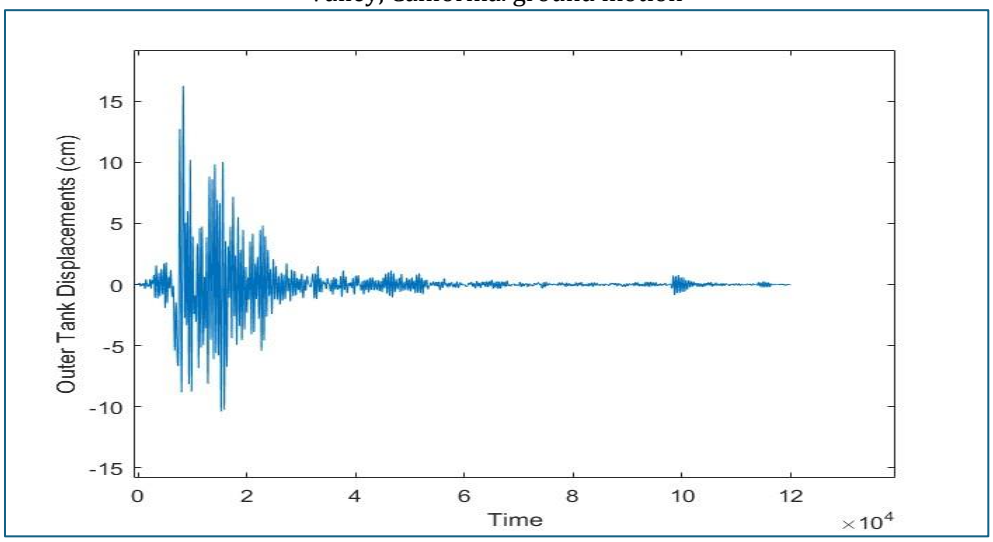


Figure 7. Time vs Outer tank Displacement (cm) for uncontrolled tank under 1994 Northridge, California. ground motion

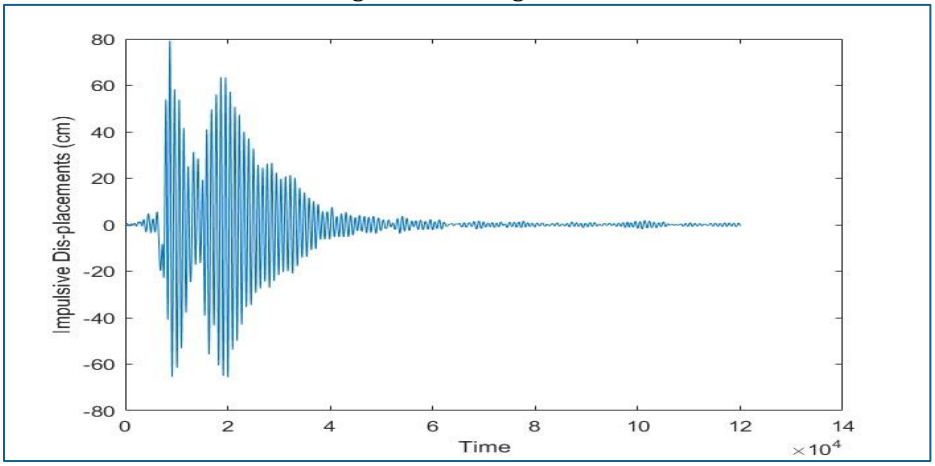


Figure 8. Time vs Impulsive Displacement (cm) for uncontrolled tank under 1994 Northridge, California. ground motion

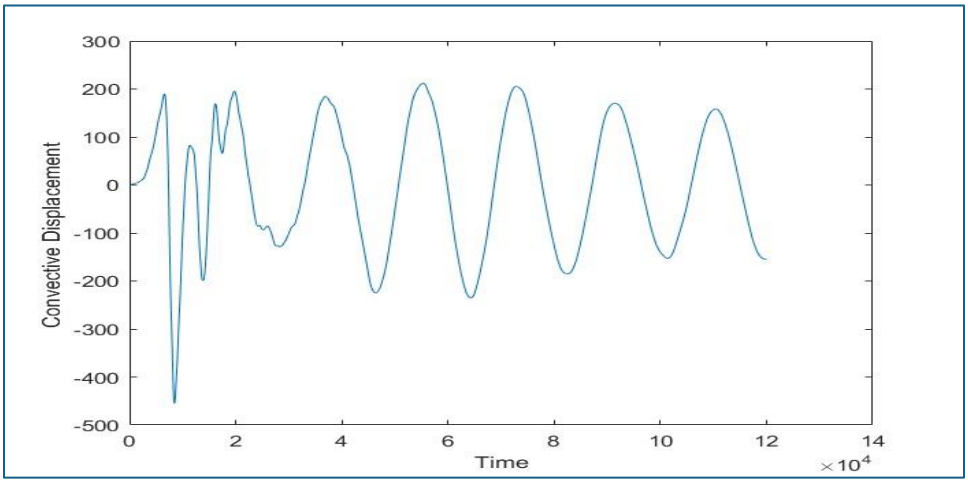


Figure 9. Time vs Convective Displacement (cm) for uncontrolled tank under 1994 Northridge, California. ground motion

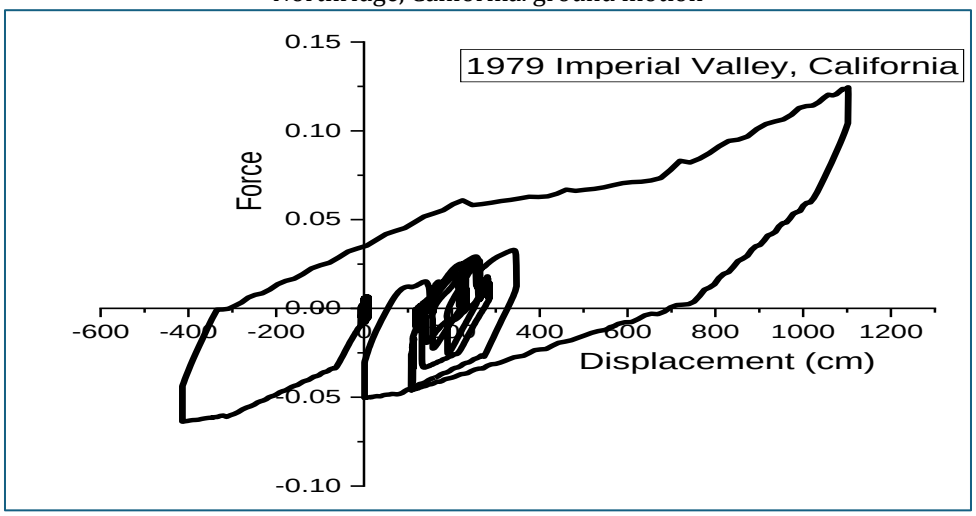


Figure 10. Hysteresis loop for LNG Controlled tank with QTFP under 1979 Imperial Valley, California ground motion

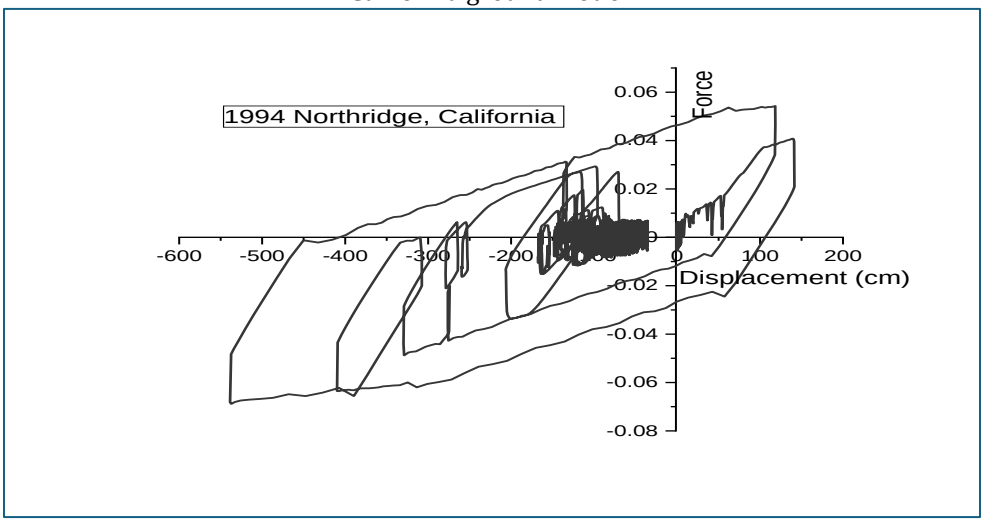


Figure 11. Hysteresis loop for LNG Controlled tank with QTFP under 1994, Northridge, California ground motion

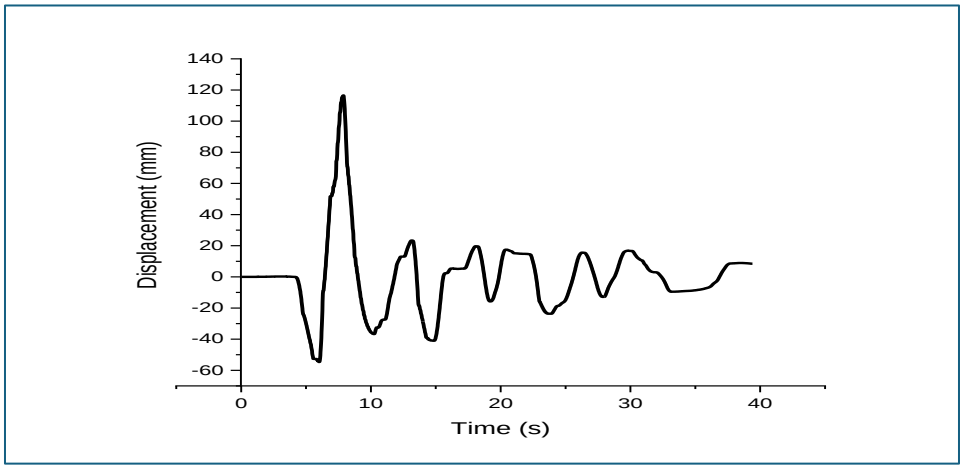


Figure 12. Time vs Displacement, for LNG tank with QTFP under 1979, Imperial Valley, California. ground motion

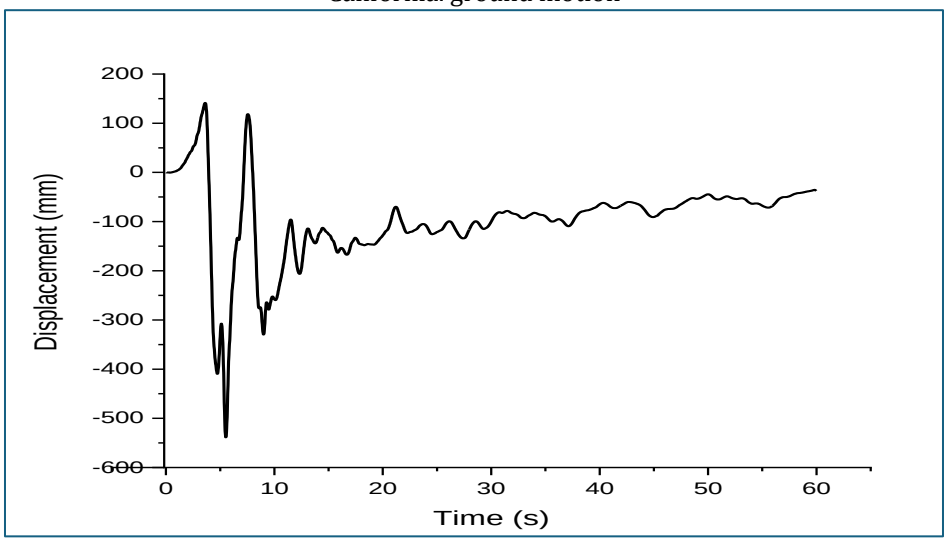


Figure 13. Time vs Displacement, for LNG tank with QTFP under 1994, Northridge, California. ground motion

Table 4. Comparison of LNG Tank Performance: Fixed Base vs. QTFP Isolation Across Varied Ground Motions

Near-Fault Ground Motion	LNG Tank: Uncontrolled Tank			LNG Tank with QTFP		
	Outer Tank Displacements uc(mm)	*Impulsive Displacements* X_i *(mm)*	*Convective Displacements* X_c *(mm)*	*Outer Tank Displacements uc(mm)*	*Impulsive Displacements* X_i *(mm)*	*Convective Displacements* X_c *(mm)*
Imperial Valley 1979 (Array # 5)	8.4471	67.6646	1271.1	1.0857	4.2779	1300.9
Imperial Valley 1979 (Array # 7)	9.37	66.33	796.6	0.88792	3.4187	706.85

Northridge 1994, (Newhall)	26.53	111.26	499.86	0.81429	3.3638	508.79
Landers (Lucerne-Valley)	17.19	41.43	2063.91	1.3017	5.2904	2545.5
Northridge 1994, (Rinaldi)	18.85	98.5	461.29	0.72875	3.7369	380.03
Northridge 1994, (Sylmar)	16.25	79.13	455.12	0.63858	2.6992	191.58

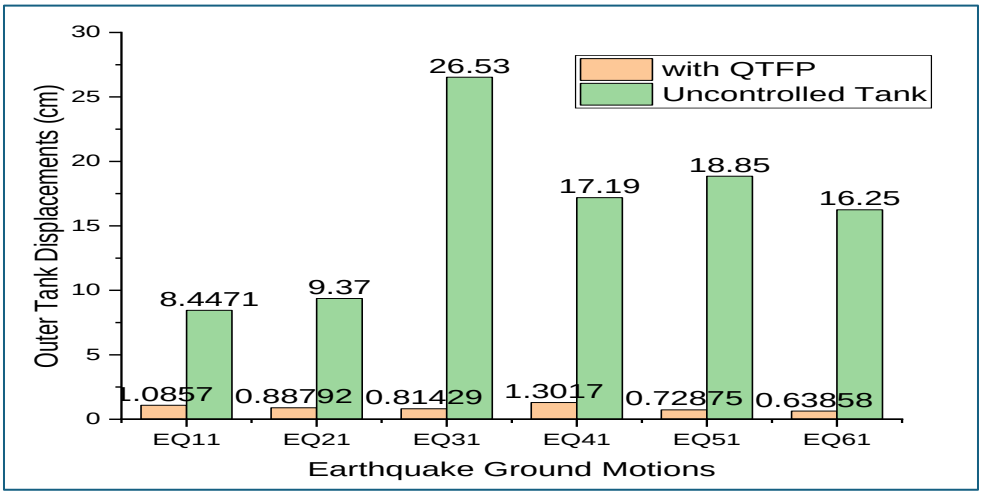


Figure 14. EQ Ground motion vs Outer tank Displacement (cm), for LNG tank with QTFP

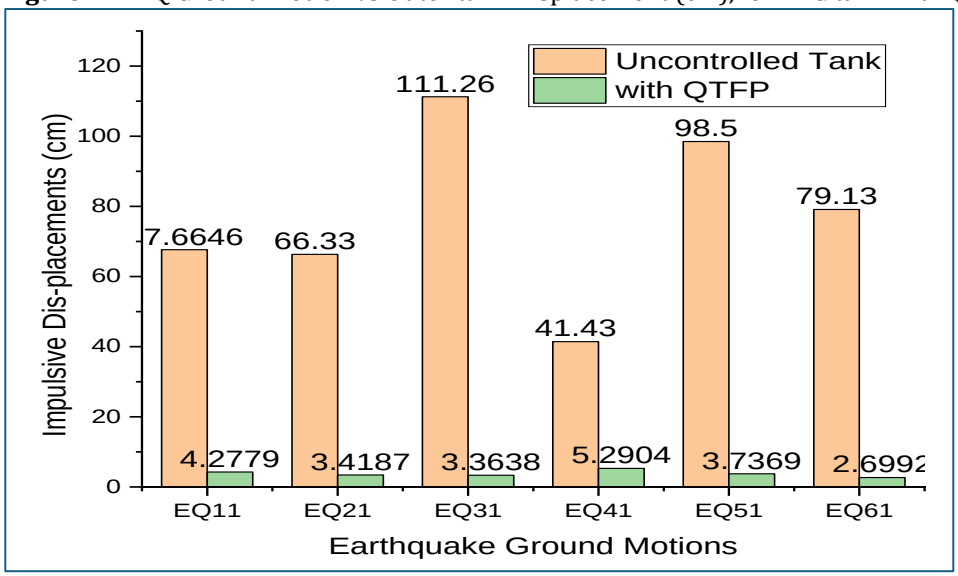


Figure 15. EQ. Ground motion vs Impulsive Displacement (m), for LNG tank with QTFP

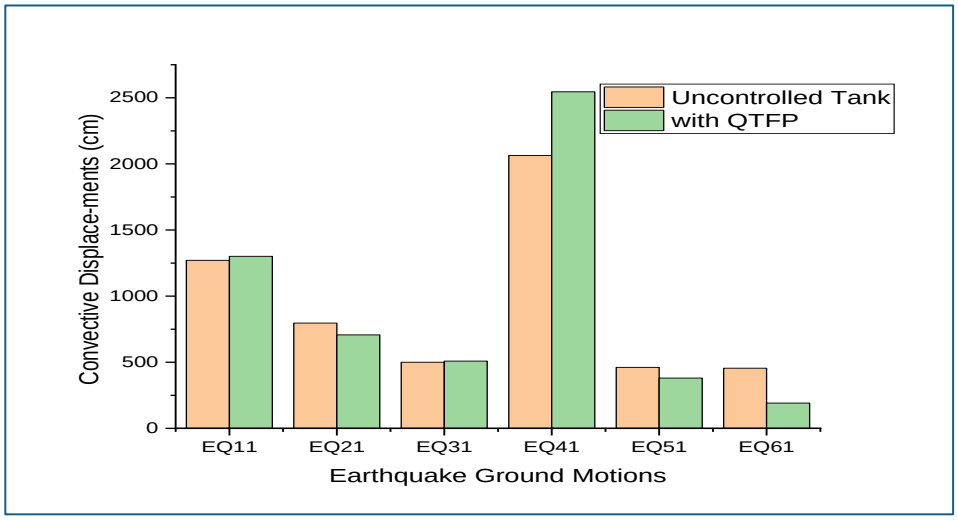


Figure 16. EQ. Ground motion vs Convective Displacement (m), for LNG tank with QTFP

5. Conclusions

The responses to earthquakes of big LNG storage tanks built with QTFP devices reduces according to this study. The effectiveness of LNG storage tanks in conjunction with and without QTFP device has been examined using multiple variables, such exterior tank displacement, convective displacement, impulsive displacement, etc. The efficacy confirmed during numerous near-fault, earthquake ground movements.

We are able to derive the subsequent outcomes based on this current investigation.

- According to the analytical results, LNG tanks with QTFP are more suitable in earthquake-prone locations because of their effectiveness in reducing seismic behaviours.
- The present investigation demonstrates that QTFP displays outstanding flexibility to a range of ground motions; in particular, LNG tanks fitted with QTFP efficiently minimize impulsive displacement. Additionally, as the periods of the isolated and convective modes were properly separated, it was shown that the presence of QTFP had no significant influence on the sloshing mode (convective) responses.
- When compared to LNG tanks without an isolation device, LNG tanks with QTFP efficiently reduces the outer tank displacement under different ground motions.
- Among all the ground motion data, it was observed that the LNG tank's base displacement employing QTFP diminishes with time, giving a more efficient manner of managing the tank's responses.

The reduction in seismic behaviours and outer tank displacement resulting from QTFP not only provides safer operations but also prevents the need for expensive repairs and maintenance, therefore boosting economic sustainability. it is crucial that we concentrate on solutions that not only deal with immediate safety issues but furthermore suitable with larger sustainability objectives, ensuring the resilience and longevity of crucial infrastructure in the face of seismic hazards.

References

[1] Abalı, E. and Uçkan, E. (2010) 'Parametric analysis of liquid storage tanks base isolated by curved surface sliding bearings', *Soil Dynamics and Earthquake Engineering*, 30(1), pp. 21–31. Available at: https://doi.org/https://doi.org/10.1016/j.soildyn.2009.08.001.

[2] Christovasilis, I.P. and Whittaker, A.S. (2008) 'Seismic analysis of conventional and isolated LNG tanks using mechanical analogs', *Earthquake Spectra*, 24(3), pp. 599–616. Available at: https://doi.org/10.1193/1.2945293.
[3] Kharde, S.H. and Soni, D.P. (2022) 'Seismic Response Mitigation of Extra-Large LNG Storage Tanks', *Journal of Earthquake and Tsunami*, 16(5). Available at: https://doi.org/10.1142/S1793431122500142.
[4] Lee, D. and Constantinou, M.C. (2016) 'Quintuple Friction Pendulum Isolator: Behaviour, Modeling, and Validation', *Earthquake Spectra*, 32(3), pp. 1607–1626. Available at: https://doi.org/10.1193/040615EQS053M.
[5] Panchal, V.R. and Jangid, R.S. (2008) 'Variable friction pendulum system for seismic isolation of liquid storage tanks', *Nuclear Engineering and Design*, 238(6), pp. 1304–1315. Available at: https://doi.org/https://doi.org/10.1016/j.nucengdes.2007.10.011.
[6] Praveen K. Malhotra, T.W. and Wieland, M. (2000) 'Simple Procedure for Seismic Analysis of Liquid-Storage Tanks', *Structural Engineering International*, 10(3), pp. 197–201. Available at: https://doi.org/10.2749/101686600780481509.
[7] Shrimali, M.K. and Jangid, R.S. (2002) 'Non-linear seismic response of base-isolated liquid storage tanks to bi-directional excitation', *Nuclear Engineering and Design*, 217(1), pp. 1–20. Available at: https://doi.org/https://doi.org/10.1016/S0029-5493(02)00134-6.
[8] Sodha, A.H. *et al.* (2017) 'Behaviour of Quintuple Friction Pendulum System Under Near-Fault Earthquakes', *Journal of Earthquake and Tsunami*, 11(05), p. 1750017. Available at: https://doi.org/10.1142/S1793431117500178.
[9] Tajirian, F.F. and Engineering, S.I. (1998) 'Base Isolation Design for Civil Components and Civil Structures', *Proceedings, Structural Engineers World Congress, San Francisco, California, July (1998)*, p. 11.
[10] Tsai, C.S., Chiang, T.-C. and Chen, B.-J. (2003) 'Seismic Behaviour of MFPS Isolated Structure Under Near-Fault Sources and Strong Ground Motions With Long Predominant Periods', in. (Pressure Vessels and Piping Conference), pp. 73–79. Available at: https://doi.org/10.1115/PVP2003-2104.

IOP Conference Series: Earth and Environmental Science

PURPOSE-LED PUBLISHING™

PAPER • **OPEN ACCESS**

Assessing the impact and response to the disaster in Mananthavady Town: A Case Study

To cite this article: V.B. Bigith *et al* 2024 *IOP Conf. Ser.: Earth Environ. Sci.* **1409** 012023

View the article online for updates and enhancements.

You may also like

- Preface
- Basic Framework of Regional Model for Disaster Waste Estimation and Distribution by Using Spatial Approach in Central Java-Indonesia
M Maryono, K Seruningtyas, A D Roynaldi et al.
- Study on hidden danger investigation and impact assessment method for earthquake-induced secondary disasters in coal mines
Qingjie Qi, Wengang Liu, Anhu Wang et al.



This content was downloaded from IP address 47.247.77.11 on 27/11/2024 at 05:38

Assessing the impact and response to the disaster in Mananthavady Town: A Case Study

Bigith, V.B.[1], Sooraj, G.[1], Rajat Nainwal[1*] and H.S. Kumara[2]

[1]Lovely School of Architecture and Design, Lovely Professional University, Punjab, India-144411.
[2]School of Planning and Architecture, University of Mysore, Mysuru, Karnataka, India-570006.

*Email: rajat.30469@lpu.co.in

Abstract. The study aims to assess the impact of a disaster on Mananthavady town, Kerala, and the response taken by the authorities to mitigate the effects of the disaster. The disaster in occurred in Wayanad was a severe flood that occurred in May 2018, which affected several regions of Kerala. The study uses a case study approach to examine the disaster's impact on Mananthavady town, including the damage to infrastructure, loss of life and livelihoods, and the community's resilience. Additionally, the study helps the government and local organizations to support the affected community and promote their recovery. The findings of the study contribute to the understanding of disaster management practices and their effectiveness in addressing the challenges posed by natural disasters.

1. Introduction

Disaster is a devastating event that can have far-reaching and long-lasting consequences for communities and societies. These events can take many different forms, including natural disasters like hurricanes, earthquakes, and floods, or human-made disasters like industrial accidents or acts of terrorism. Regardless of their cause, disasters can result in significant losses of life, property, and infrastructure, and can have a profound impact on the economic and social fabric of affected communities [1] and its alleviation is one of the targets of the Sustainable Development Goals. In some cases, disasters can even lead to the displacement of entire populations, as people are forced to flee their homes in search of safety. One of the key factors that can influence the severity of a disaster is the vulnerability of the human settlement or community in question. This vulnerability can be influenced by a range of factors, including the physical characteristics of the built environment, the socio-economic status of the inhabitants, and the quality of governance and institutions in the affected area [2]. Given the ongoing process of urbanization around the world, understanding the linkages between disasters and human settlements has become increasingly important. Cities and other densely populated areas are particularly vulnerable to the impacts of disasters, as they often have large populations living near one another and to infrastructure and other critical resources. To address these challenges, disaster risk reduction strategies focus on a range of preventive measures aimed at reducing people's and infrastructure's exposure to natural hazards. These can include measures like improving building codes and standards, developing early warning systems, and investing in disaster response and recovery efforts. At the same time, it is important to recognize that disasters are often deeply intertwined with broader social, economic, and environmental factors. To develop truly effective strategies for disaster risk reduction, it is therefore critical to take a holistic and

Content from this work may be used under the terms of the Creative Commons Attribution 4.0 licence. Any further distribution of this work must maintain attribution to the author(s) and the title of the work, journal citation and DOI.
Published under licence by IOP Publishing Ltd

integrated approach that addresses the underlying drivers of vulnerability and builds resilience at all levels of society [3].

The district of Wayanad, situated entirely within the ecologically sensitive Western Ghats, is one of the most ecologically delicate regions in the country having a population of 8.17 lakhs with a growth rate of 4.71% during 2001-2011 [4]. A significant number of settlements in Wayanad District are situated in highly vulnerable areas, either due to their proximity to flood-prone regions or areas susceptible to landslides [5]. According to a study conducted by Kerala University, Mananthavady, which is part of the Wayanad region, is the most susceptible to landslides. The study also found that Wayanad is the second most landslide-prone area after Idukki. Moreover, the neighbouring districts of Wayanad, namely Malappuram, and Kozhikode, have been classified under zone III in the multiple zonation map created by NCESS in 2015. As a result, these districts experience landslides of varying sizes every year [6].

In Wayanad district, the floods that occurred in 2018 caused significant damage and loss. They were particularly devastating because of their widespread geographic reach, severity of destruction, and impact on the local population. The floods and landslides caused extensive harm to public and private infrastructure, such as homes, roads, bridges, schools, and healthcare facilities, as well as other essential services. The floods also had a significant impact on the production sectors in the area [7].

2. Background of Hazards in Wayanad district and Mananthavady Town

In the past, Wayanad has faced various issues due to landslides. The National Centre for Earth Science Studies (NCESS) has identified the Wayanad-Kozhikode border as a highly prone area for landslides within the state [8]. Notable instances include the Mundakkai, Kappikkalam, and Valamthode landslides/debris flows. The Mundakkai debris flow, which occurred in 1984, resulted in the loss of valuable agricultural land and claimed the lives of 14 individuals. Similarly, the Kappikkalam Urulpottal near Padinjarathara in 1992 caused the death of 11 individuals. In addition, a severe landslide took place in Valamthode on 23rd February 2007, resulting in the loss of 4 lives. Apart from these incidents, numerous other landslides of varying magnitudes have occurred in Wayanad in the past [8].

According to the 2015 Multiple Hazard Zonation Map created by the NCESS, areas of Wayanad that are susceptible to floods and landslides are indicated in Fig 1displays a similar map for Mananthavady, which has no recorded instances of droughts, cyclones, or earthquakes, and is not expected to experience such disasters due to its geographic location and geological and topographical features. Mananthavady's terrain is characterized by undulating hills, some of which have steep slopes exceeding 45°, making these areas prone to landslides according to the NCESS hazard zonation map. Because these areas are part of a Reserve Forest, human activities are limited, and the dense vegetation helps reduce the risk of landslides [9].

A multiple hazard zonation map of Mananthavady is a map that identifies and highlights areas within the region that are susceptible to various natural hazards. The map would typically include several layers depicting different types of hazards such as landslides, floods, earthquakes, forest fires, and so on. Used various indicators such as topography, soil types, precipitation levels, vegetation cover, and geological features to determine the areas of potential hazard. Each hazard type would be given a different colour or shading to help distinguish the different hazard zones.

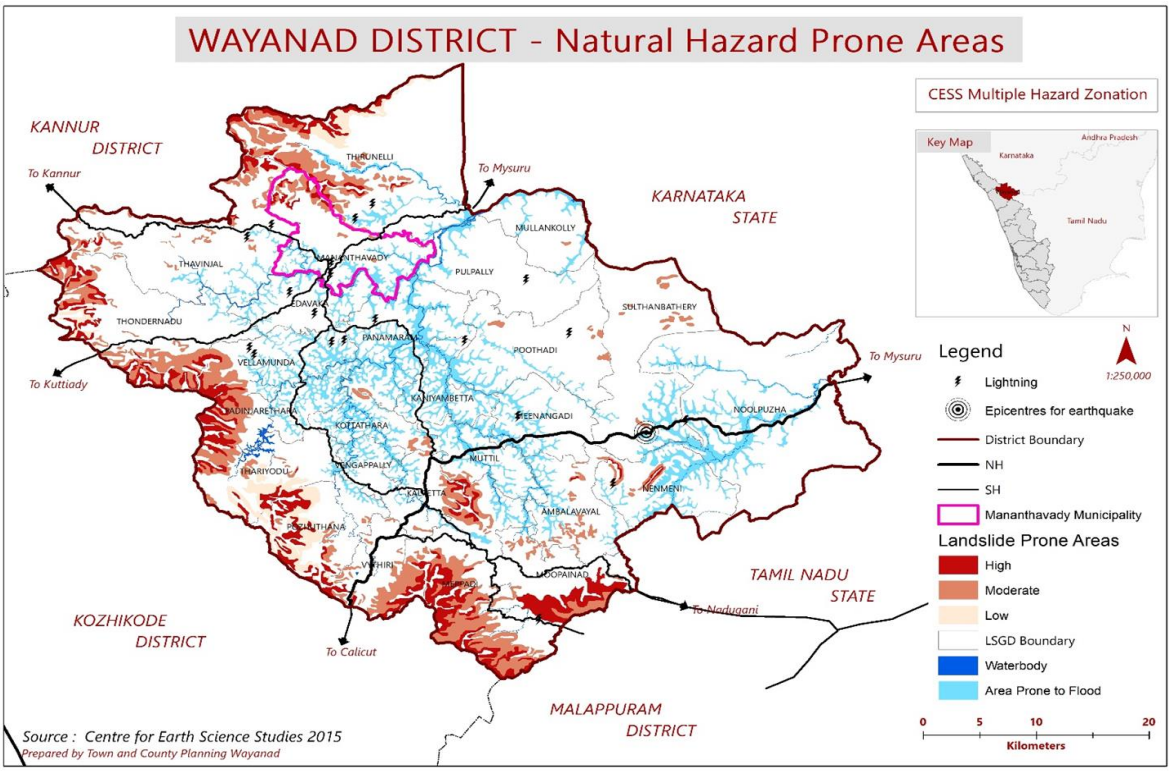


Figure 1. Multiple hazard Zonation map of Wayanad District [6]

3. Background of Floods and Landslides of 2018

On May 29th, the southwest monsoon began, and its impact on the district can be divided into three phases: June 1st to August 14th, July 7th to July 25th, and August 8th to August 17th. Wayanad experienced unprecedented heavy rainfall during June, July, and August, with the district receiving 3068 mm of rainfall from July 1st to September 30th, compared to the normal rainfall of 2631 mm over four months. The rainfall in 2018 was significantly higher than usual, as shown in Figure 2, which was the primary cause of the hazard in the district. The highest rainfall, as indicated in Figure 2, was recorded on August 9th, 2018, at 245.37 mm [10].

4. Flood and Landslide occurred areas in Mananthavady Town

In Mananthavady, 12.29 sq.km out of a total area of 80.1 sq.km has been affected by flooding. Of the flooded area, 0.54 sq.km is experiencing depths beyond 6 feet, 1.52 sq.km is experiencing depths between 4-6 feet, 2.32 sq.km is experiencing depths between 3-4 feet, and 2.82 sq.km is experiencing depths between 2-3 feet. The remaining 5.08 sq.km of the flooded area has inundation depths less than 2 feet. Two areas within the municipality, Pilakkavu and Pancharakolli, were most affected by landslides, with a total area of 0.12 sq.km.

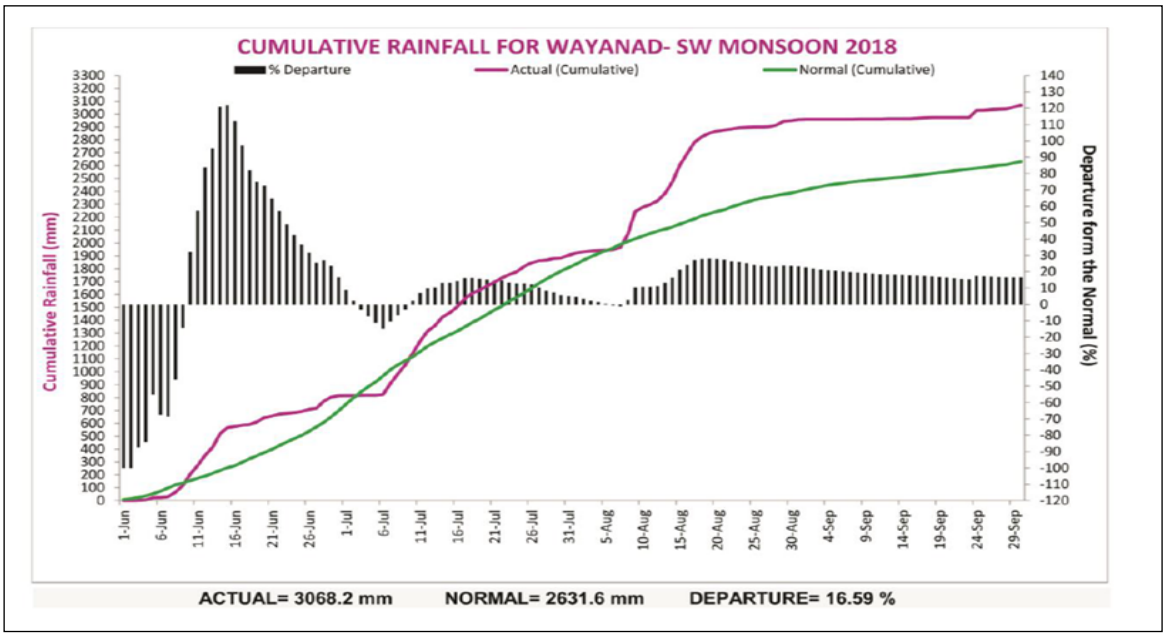


Figure 2. Details of Monsoon in Wayanad between 1st June - 30th Sept 2018 [11]

5. The effects of the significant flood that occurred in 2018 on Mananthavady Town

The 2018 floods that occurred in Kerala were a rare occurrence with an estimated interval of 100-120 years. Wayanad district, located in Kerala, was severely affected by floods during that year. From the beginning of the South-West Monsoon on May 29, 2018, the district faced 47 landslides, 155 landslips, and 45 incidents of land subsidence or cave-ins. These natural disasters had a direct or indirect impact on a significant portion of the district's population. Kabani River floods resulted in the displacement of over 900 households from their homes for several weeks. The map of flood and landslide occurrences in Mananthavady Town in 2018, created as part of the Rebuild Wayanad project, is displayed [13].

The data sources used for this analysis were primarily the Mananthavady master plan, as well as a primary survey conducted in the affected areas. The Mananthavady master plan provided valuable insights into the areas most affected by the floods and landslides. The data collected showed that the hilly regions were the most vulnerable, with landslides causing severe damage to roads, bridges, and buildings. The towns of Mananthavady, Kalpetta, and Sulthan Bathery were among the worst affected, with many houses and shops suffering extensive damage. The agricultural sector was also hit hard, with crops destroyed and farmlands rendered unusable. To gain a more in-depth understanding of the situation, a primary survey was conducted in the affected areas. The survey revealed that many households had suffered significant losses, with many people losing their homes and possessions. The floods had caused extensive damage to infrastructure, with roads and bridges severely affected. The landslides had also destroyed many buildings, including schools and hospitals. The data collected from both the Mananthavady master plan, and the primary survey were analysed to identify the key areas of concern. It was found that the most pressing issues were the rehabilitation of affected households, the restoration of damaged infrastructure, and the recovery of the agricultural sector.

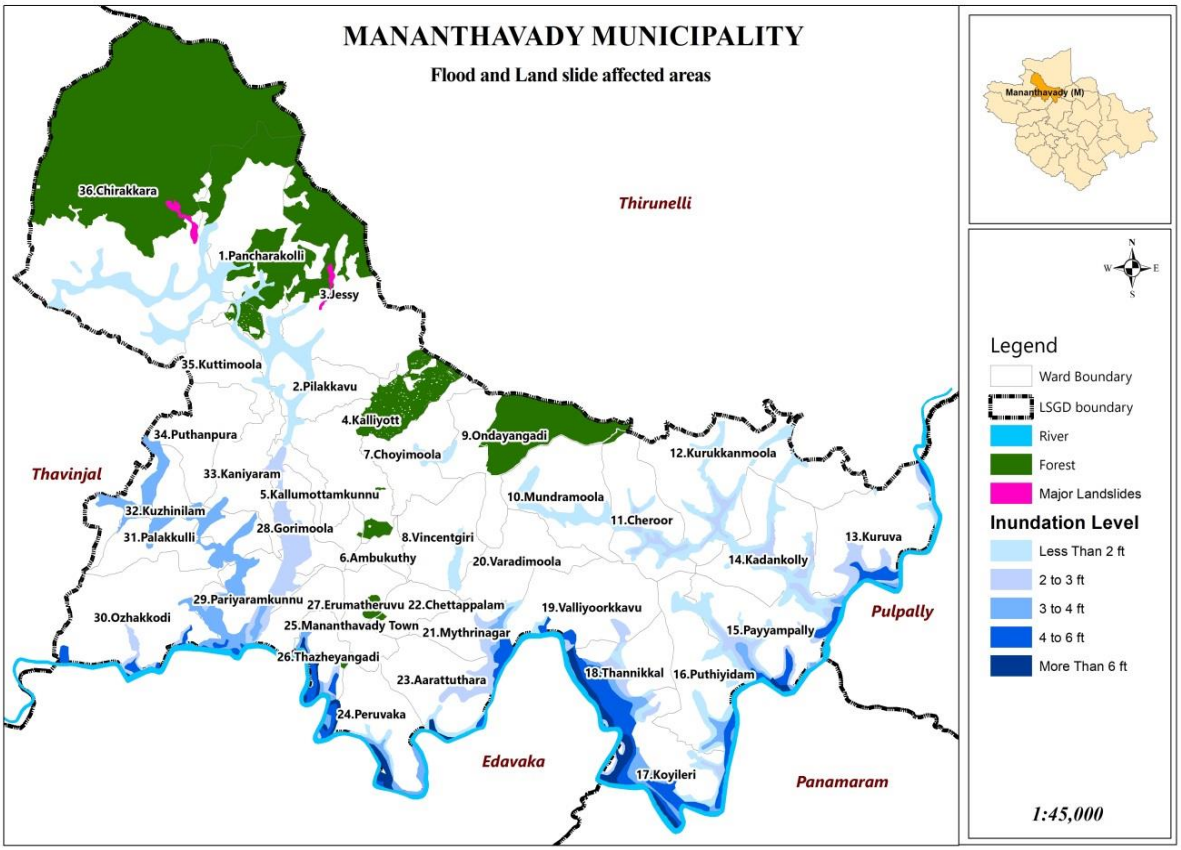


Figure 3. Flood and Landslide affected areas of Mananthavady Town [12]

The government and local authorities have been working tirelessly to address these issues and provide support to those affected by the floods and landslides. In the areas affected by floods and landslides, a total of 749 buildings were assessed. The assessment classified the damages to houses and settlements into three categories: completely collapsed, partially damaged, and no damage. The categorization of buildings in Mananthavady Town reveals that a significant majority, approximately 82%, are constructed using durable materials like brick and tile, or block and slab. However, the presence of a substantial number of Kucha houses in the flood-prone areas raises concerns, particularly for the more vulnerable groups who are at a higher risk of being affected by natural disasters. The materials used are tents, thatch, brick tile, and block slab. Most of the wards use brick tile and block slab as their primary housing materials, with 63.16% and 26.32% respectively in ward 1 and 40% and 58.06% respectively in ward 3. In general, the area has an average of 13.04% of tents, 5.66% of thatch, 43.17% of brick tile, and 38.13% of block slab. The collapse of electric towers, transformers, and poles due to the erosion of their foundations resulted in damages within the transmission subsector. To prevent further hazards, electricity was shut down in various locations. The distribution subsector also experienced damages and losses, primarily due to faults, collapsed poles, and power outages in flooded areas. However, the KSEB authorities promptly responded to the situation by restoring systems and reconnecting consumers to the grid. The majority of households were reconnected within a day, and the longest service interruption lasted for only two days.

The management of public water supply schemes in Mananthavady Town is the responsibility of both KWA and the Municipality. Flooding caused some damage to the water supply systems, but

there were no significant disruptions to the services provided. While regular customers were unable to access the services due to the floods, alternative arrangements were made, and no major gaps in access to services were reported. Most of the damages reported were to the water intakes situated along the rivers and streams. Landslides caused a heavy load of mud and silt, which blocked and damaged the intakes of water systems in the surrounding areas, resulting in temporary shutoffs and the need for extensive cleaning. Moreover, the floods caused instability in the distribution networks of several systems, with pump houses and critical structures being inundated. The heavy rainfall led to increased levels of dissolved solids and microbial pollutants in all surface water sources, which prompted KWA to allocate more resources to turbidity removal and disinfection in their conventional treatment plants.

The productive sector encompasses various industries, including agriculture, livestock, fisheries, industry and commerce, tourism, as well as banking and finance. The agriculture, soil, fisheries, and livestock sectors suffered significant losses during the flood, with crops such as tea, paddy, banana, pepper, and coffee being particularly affected. It is worth noting that although the loss of crops is a visible outcome of the flooding, there are also broader challenges related to the loss of topsoil, degradation of fertile land, and silt accumulation in paddy fields, which make the restoration of agricultural activities a complex undertaking.

The assets of different commerce and industries, including wood, oil mills, textiles, clay, tires, and furniture, have been lost. The Mananthavady to Calicut road was submerged at Kayilery, and the area around Valliyoorkavu was flooded for approximately three days, resulting in a complete disconnection to the administrative center in Kalpetta. Similarly, the Koodalkadavu-Chaligadha road along the river was destroyed due to the flood. More information about the roads affected by the flood in Mananthavady Town is provided in the following details.

The harm to the environment includes erosion of riverbanks (in Mananthavady and Panamaram River), destruction of wetlands, soil erosion, and accumulation of silt in low and agricultural lands, as well as loss of forest and agricultural lands. Landslides negatively impact the landscape by causing offsite harm like silt buildup on agricultural lands and in water bodies. Floods also contribute to land degradation by causing severe soil erosion and depositing silt in low-lying areas, wetlands, and agricultural lands. The disposal of waste generated during emergency and early recovery also adds to the costs of the damage. The forested areas in Mananthavady municipality were also impacted by landslides and land slips, which is uncommon since these areas are typically less prone to landslide risks. However, during the heavy floods in 2018, the Pancharakolly and Maniyankunnu areas of Mananthavady municipality were significantly affected by landslides.

6. Approach for identifying Vulnerable Clusters

In the report on flood disaster impact and responses in Nepal Tarai's marginalized basins, Dixit created a list of vulnerability indicators that were adapted and refined for the district of Mananthavady. The selected indicators were grouped into five categories: Physical, social, economic, access to drinking water, and psychological. Table 1 displays these categories.

To identify areas of vulnerability within the municipality, survey data from affected households were plotted on a map, revealing 15 major clusters. Using the 12 selected indicators and their corresponding data, each cluster was ranked on a scale of 1-5 and converted to a weighted scale. The total score for each cluster was then calculated based on the 12 indicators, and clusters were categorized according to their level of vulnerability.

Table 1. Parameters of Vulnerability

Parameters	Indicators
Physical	Occurrence of Flood and Landslide
	Severely Damaged Houses
	Severely Damaged Plots
	Isolated Areas
	Houses near High Slope area
	Houses near the Riverbanks
Social	SC/ST HHs Affected
	Livelihood Affected
	Dependent Population
Economical	Livelihood affected HHs
Access to Drinking Water	Affected Drinking Water Sources
Psychological	Psychological stress

Parameters of Vulnerability appear to be a compilation of parameters or factors that contribute to the vulnerability of a community or area to various types of disasters, particularly floods and landslides. The table is divided into five categories or domains of vulnerability, which are Physical, Social, Economic, Access to Drinking Water, and Psychological. Each category contains several indicators that are used to measure or assess the level of vulnerability of a community or area.

The indicators under the Physical domain include the occurrence of floods and landslides, severely damaged houses and plots, isolated areas, houses near high-slope areas, and houses near riverbanks. These indicators are related to the physical environment and infrastructure of a community and are significant contributors to the level of risk and vulnerability. The Social domain includes indicators related to the impact of disasters on vulnerable groups, such as Scheduled Castes/Tribes households affected, livelihoods affected, and dependent populations. These indicators highlight the social dimensions of vulnerability and the unequal distribution of the impacts of disasters on different groups within a community. The Economic domain includes livelihood-affected households, which emphasizes the economic impact of disasters on individuals and communities, particularly those whose livelihoods depend on vulnerable sectors such as agriculture, fishing, and small businesses. The Access to Drinking Water domain includes affected drinking water sources, which highlights the impact of disasters on the availability and accessibility of safe drinking water, which is essential for the survival and well-being of a community. The Psychological domain includes psychological stress, which is an indicator of the mental and emotional impact of disasters on individuals and communities, particularly in the aftermath of a disaster.

Figure 4 shows the identified clusters of the disaster area in Mananthavady town. The clusters have been identified based on the extent of damage caused by the disaster, including the number of affected households, buildings, and infrastructure. The clusters have been marked red colour circle dimension of each circle represents a different level of damage. The key provided on the map helps to identify the severity of damage in each cluster.

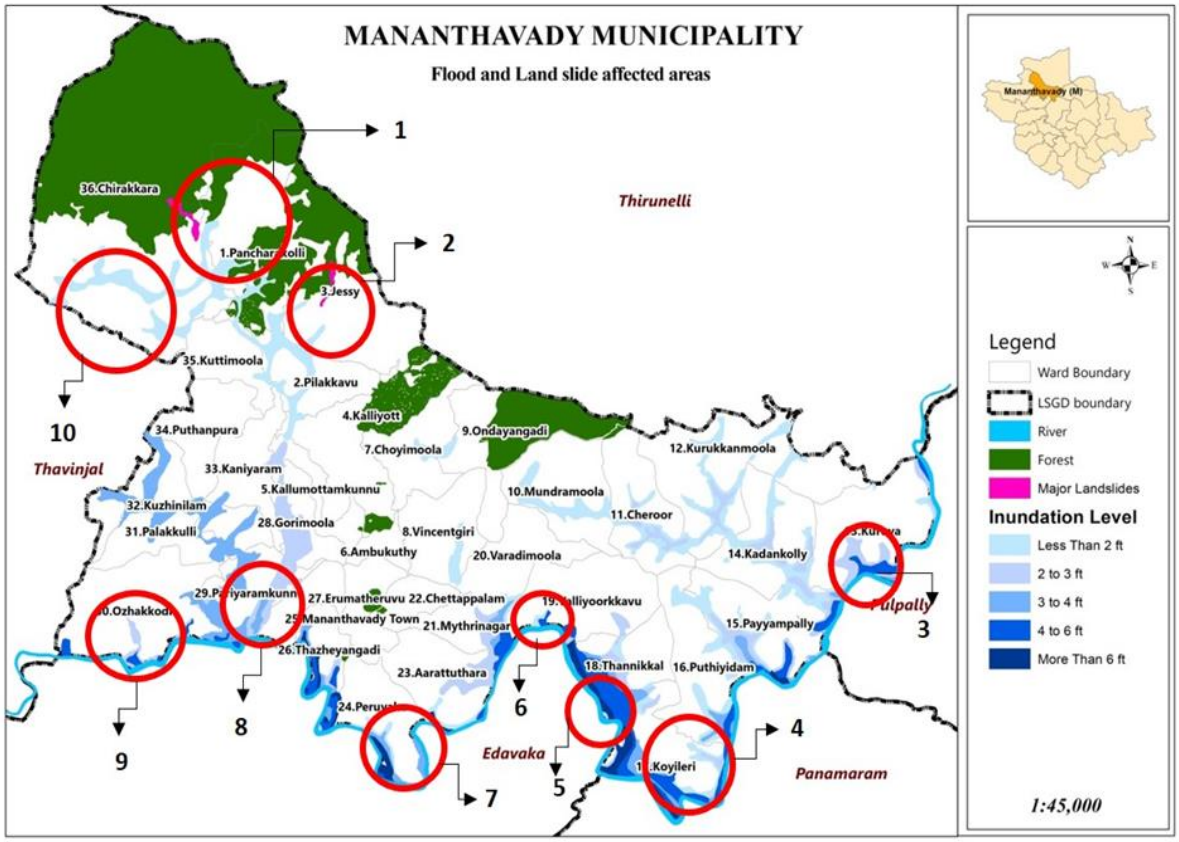


Figure 4. Identified clusters in Mananthavady Town

Table 2 represents the Weighted Scores of different parameters for different clusters. There are ten parameters in total, numbered from 1 to 10, and each parameter has its Weighted Scores for each of the 10 clusters, numbered from 1 to 10. The interpretation of the table varies based on the context in which it is presented, but in general, it can be used to compare the performance of different clusters across the parameters, and to identify which parameters have the highest impact on the overall scores.

Table 2. Magnitude Range of the Vulnerability Categories

Parameter	Cluster Number																			
	1	WT	WS	2	WS	3	WS	4	WS	5	WS	6	WS	7	WS	8	WS	9	WS	10	WS
Occurrence of flood and landslide	22	20.6	4.532	10.2	2.1012	11.5	2.369	34.5	7.107	28	5.768	85.1	17.531	75.2	15.491	82.1	16.913	55.7	11.474	100	20.6
% of severely damaged houses	6	20.6	1.236	13.2	2.719	7.8	1.607	13.2	2.719	18.5	3.811	11	2.266	2.1	0.433	12.5	2.575	4.3	0.886	6.8	1.401

% of severely damaged plots	Isolated areas	% of houses near high slope area	% of houses near riverbanks	% of SC/ST HHs affected	% of wage labour affected	% of dependent population	% of livelihood affected HHs	% of affected drinking water sources	% of Psychological stressed people	Average of values
23.1	0	85	0	43	85.3	69.4	29.5	12	60.4	
20.6	20.6	20.6	20.6	15	15	15	26.3	11.1	7.7	
4.7586	0	17.51	0	6.45	12.8	10.41	7.759	1.332	4.6508	71.4
4.4	100	94	0	14.6	55.6	69.6	38.8	50.4	99	
0.9064	20.6	19.36	0	2.19	8.34	10.44	10.2	5.594	7.623	90.1
59.6	0	22.4	0	25.6	45.7	70.6	13.5	23.6	2.45	
12.278	0	4.614	0	3.84	6.855	10.59	3.551	2.62	0.1887	48.5
83.4	100	0	90.5	94.5	98.5	65.4	3.8	100	23.5	
17.18	20.6	0	18.643	14.18	14.78	9.81	0.999	11.1	1.8095	119
89.5	100	0	95.1	65.5	70.6	78.5	18.8	89.5	2.45	
18.437	20.6	0	19.591	9.825	10.59	11.78	4.944	9.935	0.1887	115
41.9	0	0	67.1	19.8	23.7	78.9	29.7	80.7	56.2	
8.6314	0	0	13.823	2.97	3.555	11.84	7.811	8.958	4.3274	81.7
14.6	100	0	48.8	23.8	27.3	67.8	31	30.4	0.7	
3.0076	20.6	0	10.053	3.57	4.095	10.17	8.153	3.374	0.0539	79
25	100.6	0	9	18.9	60.9	65	9.7	76	1.1	
5.15	20.274	0	1.854	2.835	9.135	9.75	2.551	8.436	0.0847	80
4.3	0	0	46.8	26.1	22.7	66.7	30.4	69.7	1.2	
0.8858	0	0	9.6408	3.915	3.405	10.01	7.995	7.737	0.0924	56
56.7	100	0	86.7	31	23.6	73.1	68	38.2	0.5	
11.68	20.6	0	17.86	4.65	3.54	10.97	17.88	4.24	0.0385	113

Upon analyzing the data, it is evident that the occurrence of floods and landslides is highest in cluster number 5, with a weighted score of 100. This is followed by cluster numbers 7, 8, and 9, which also have high weighted scores, indicating a higher risk of flood and landslide occurrence. The percentage of severely damaged houses and plots is also high in cluster numbers 3 and 6, indicating the vulnerability of these areas to flood and landslide. The percentage of households near high slope areas is also high in clusters number 1, 2, and 3, and the percentage of households near riverbanks is high in clusters numbers 6 and 10, indicating the risk of flood and landslide in these areas.

The percentage of SC/ST households affected is high in cluster number 7, and the percentage of wage labour households affected is high in cluster numbers 1 and 5. The percentage of dependent population and livelihood-affected households are also high in cluster numbers 5 and 10, indicating the socio-economic vulnerability of these areas to the impact of flood and landslide. The percentage of affected drinking water sources is high in cluster numbers 4 and 7, indicating the risk of water contamination in these areas. Finally, the percentage of psychologically stressed people is high in cluster number 2, indicating the mental health impact of floods and landslides in these areas. The data suggests that cluster numbers 5, 7, 8, and 9 are at a higher risk of flood and landslide occurrence and their socio-economic impacts. The analysis can help in identifying areas that require immediate attention for mitigation and adaptation measures to reduce the risk and impact of flood and landslide.

Table 3. Vulnerability Levels of Clusters

Cluster No.	Location	Weighted Score of Vulnerability parameters (a)	Total number of affected people (b)	Total number of affected households (c)	Final Score (a+b+c)	Vulnerability Categories High (300+), Moderate (200-300), Low (<200)
1	Pancharakolli	71.4	31	20	122	Low
2	Jessy	90.1	198	70	358.1	High
3	Kuruva	48.5	78	35	161.5	Low
4	Choyimoola	119	259	58	436	High
5	Thannikkal	115	109	44	268	Moderate
6	Mythrinagar	81.7	52	23	156.7	Low
7	Peruvaka	79	130	61	270	Moderate
8	Pariyaramkunnu	80	92	35	207	Moderate
9	Ozhakkodi	56	140	44	240	Moderate
10	Chirakkara	113	174	88	375	High

Table 3 provides information on the total number of affected people, the total number of affected households, the final score, and vulnerability categories for ten different incidents. The first incident affected 31 people in 20 households, resulting in a low vulnerability score of 122. The second incident had a higher impact, with 198 people in 70 households affected, resulting in a high vulnerability score of 358.1. In contrast, the third incident only affected 78 people in 35 households, resulting in a low vulnerability score of 161.5. The fourth incident had the highest impact, with 259 people in 58 households affected, resulting in a high vulnerability score of 436. The fifth incident affected 109 people in 44 households, resulting in a moderate vulnerability score of 268. The sixth incident had a low impact, with 52 people in 23 households affected, resulting in a low vulnerability score of 156.7.

The seventh incident affected 130 people in 61 households, resulting in a moderate vulnerability score of 270. The eighth incident affected 92 people in 35 households, resulting in a moderate vulnerability score of 207. The ninth incident affected 140 people in 44 households, resulting in a moderate vulnerability score of 240.The final incident had the second-highest impact, with 174 people in 88 households affected, resulting in a high vulnerability score of 375. Overall, the table shows that incidents with a higher number of affected people and households generally result in higher vulnerability scores, indicating a higher level of vulnerability for the affected population.

7. Recommendations

Mitigation measures should be taken in cluster numbers 5, 7, 8, and 9 to reduce the risk of flood and landslide occurrence. These measures could include constructing or strengthening flood and landslide protection structures, improving drainage systems, and creating early warning systems for residents. In cluster numbers 3 and 6, where the percentage of severely damaged houses and plots are high, reconstruction and repair activities should be initiated. This will help to minimize the vulnerability of these areas to flood and landslide events. In cluster numbers 1, 2, and 3, where the percentage of households near high slope areas is high, there is a need for awareness campaigns to inform residents of the risk of flood and landslide occurrence. Residents should be advised to relocate to safer areas if possible or to take necessary precautions to protect themselves and their property. In cluster numbers 6 and 10, where the percentage of households near riverbanks is high, steps should be taken to reduce the risk of water contamination. This could involve setting up treatment plants or ensuring that residents have access to safe drinking water. In cluster number 7, where the percentage of SC/ST households affected is high, special attention should be given to ensure that these vulnerable communities have access to adequate resources and support during and after flood and landslide events. In cluster numbers 1 and 5, where the percentage of wage labour households affected is high, measures should be taken to ensure that these households have access to alternative livelihood options in the event of a disaster. In cluster numbers 5 and 10, where the percentage of dependent population and livelihood-affected households are high, interventions should be taken to support affected households in the recovery process. This could include providing temporary shelter, food, and medical assistance. In cluster numbers 4 and 7, where the percentage of affected drinking water sources is high, there is a need for regular monitoring and testing of water quality to prevent the spread of waterborne diseases. In cluster number 2, where the percentage of psychologically stressed people is high, psychosocial support should be provided to help individuals cope with the mental health impact of flood and landslide events. The analysis highlights the importance of taking a holistic approach to disaster risk reduction and management, which involves addressing both the physical and socio-economic vulnerabilities of communities. By implementing the above recommendations, it is possible to reduce the risk and impact of flood and landslide events and build more resilient communities.

The recommendations include mitigation measures in clusters 5, 7, 8, and 9, reconstruction and repair activities in clusters 3 and 6, awareness campaigns in clusters 1, 2, and 3, steps to reduce water contamination in clusters 6 and 10, special attention to vulnerable communities in cluster 7, alternative livelihood options for wage labour households in clusters 1 and 5, support for affected households in clusters 5 and 10, monitoring and testing of water quality in clusters 4 and 7, and psychosocial support in cluster 2. Overall, a holistic approach to disaster risk reduction and management is essential to build more resilient communities.

8. Conclusions

The study analyses the impact of a natural disaster on the town of Mananthavady in Kerala, India. The research focuses on the heavy rainfall and subsequent flooding that occurred in May 2018, which caused significant damage to infrastructure and homes, and resulted in the displacement of many residents.

The study uses a combination of qualitative and quantitative research methods to assess the impact of the disaster on the town, including interviews with residents, government officials, and NGO representatives, as well as surveys of affected households. The findings highlight the significant economic, social, and emotional impacts of the disaster on the affected community, including loss of income, damage to property and assets, and psychological distress and guides the local government and community to the disaster awareness, including their preparedness measures, relief and rehabilitation efforts, and recovery plans. The findings suggest that while the response was generally effective in addressing the immediate needs of the affected population, there were some gaps in the coordination and implementation of relief efforts, and the long-term recovery needs of the community were not fully addressed. The study concludes with recommendations for improving disaster preparedness, response, and recovery efforts, including the need for better coordination between government agencies and NGOs, the importance of involving affected communities in the planning and implementation of relief efforts, and the need for more comprehensive and sustainable recovery plans.

References

[1] UNISDR, "Sendai Framework for Disaster Risk Reduction 2015-2030." United Nations Office for Disaster Risk Reduction., 2015.
[2] M. E. Borsuk, R. E. Morss, and S. L. Cutter, "Understanding the Interplay between Hazards, Vulnerability, and Disaster Risk in Human Settlements.," in *Handbook of Disaster Research*, Springer, Cham, 2017.
[3] UN-Habitat, "Making Cities Resilient: My City is Getting Ready." United Nations Human Settlement Programme, 2015.
[4] "Census of India, Ministry of Home Affairs, Government of India," 2011. https://censusindia.gov.in/census.website/ (accessed Jan. 18, 2016).
[5] "Study of Landslide Prone Areas in Wayanad District." Kerala University, Wayanad, 2015. Accessed: Jan. 19, 2016. [Online]. Available: www.keralauniversity.ac.in/researchproject/projects/landslide-prone-areas-in-wayanad-district-kerala.
[6] NCESS, "Multi Zonation Map of Kerala," 2015. www.ncess.gov.in/publications/maps/multi-zonation-map-of-kerala. (accessed Jan. 21, 2016).
[7] S. Udayan, "Impacts of 2018 Floods on Infrastructure and Production Sectors in Wayanad District, Kerala: A Qualitative Assessment," *Int. J. Disaster Risk Sci.*, vol. 11, no. 2, pp. 311–322, 2020, doi: 10.1007/s13753-019-00221-3.
[8] NCESS, "Landslides in Wayanad: A Review." ncess.gov.in/publications/landslides-in-wayanad-a-review/. (accessed Jan. 21, 2018).
[9] R. K. Singh, A. Manoj, and L. Vijayan, "Hazard Zonation of Mananthavady Taluk, Wayanad District, Kerala," *Indian Geotech. J.*, vol. 47, no. 2, pp. 339–346, 2017.
[10] T. V. Rajan and P. K. Kalarikkal, "Climate Change and Disaster Risk Reduction in Wayanad District of Kerala, India: A Study," in *Climate Change, Disaster Risk and Vulnerability*, Springer, Cham, 2019, pp. 181–200.
[11] "Indian Meteorological Department," 2018. https://city.imd.gov.in/citywx/city_weather_test_try.php?id=30011 (accessed Jan. 25, 2018).
[12] "Official website of Mananthavady Municipality, Government of Kerala," 2042. https://mananthavadymunicipality.lsgkerala.gov.in/en/node/57 (accessed Jan. 28, 2018).
[13] M. Ratheesh and R. Baiju, "Review of landslide susceptibility mapping in Wayanad district, Kerala, India," *Environ. Earth Sci.*, vol. 79, no. 4, pp. 1–17, 2020, doi: doi:10.1007/s12665-019-8774-8.

IOP Conference Series: Earth and Environmental Science

PURPOSE-LED PUBLISHING™

PAPER • **OPEN ACCESS**

Mechanical performance and co2 footprint analysis: recycled aggregate polypropylene geopolymer concrete compared with conventional concrete

To cite this article: Petluru Prasanthi *et al* 2024 *IOP Conf. Ser.: Earth Environ. Sci.* **1409** 012024

View the article online for updates and enhancements.

You may also like

- Surface energy effect on nonlinear buckling and postbuckling behavior of functionally graded piezoelectric cylindrical nanoshells under lateral pressure
Xue-Qian Fang, Chang-Song Zhu, Jin-Xi Liu et al.
- Size-dependent thermo-electrical buckling analysis of functionally graded piezoelectric nanobeams
Farzad Ebrahimi and Erfan Salari
- Iterative image reconstruction algorithm analysis for optical CT radiochromic gel dosimetry
Steve Collins, Andy Ogilvy, Warren Hare et al.



This content was downloaded from IP address 47.247.77.11 on 27/11/2024 at 05:38

Mechanical performance and co_2 footprint analysis: recycled aggregate polypropylene geopolymer concrete compared with conventional concrete

Petluru Prasanthi*, Vijay Kumar Rayabharapu, Samanasa Krishna Rao, Ambati Supraja, Panthula Vamshi

Department of Civil Engineering, B V Raju Institute of Technology, Narsapur, Medak, Telangana State, India

Email: prasanthi.p@bvrit.ac.in

ABSTRACT. Geopolymer concrete (GPC) has gained significant awareness in recent years as an eco-friendly alternative to conventional concrete due to its lower CO_2 emissions and utilization of industrial waste materials. The cementitious material fly ash (FA), GGBS, silica fume (SF) with incorporation of polypropylene fiber (PF), recycled aggregates (RA) further promote the strength properties of geopolymer concrete, particularly in terms of ductility and crack resistance. Exploratory tests been conducted to assess the effects of various parameters including activator type, curing conditions, fiber content, and aggregate characteristics on the mechanical behaviour and CO_2 emissions of geopolymer concrete (GPC). The mechanical performance aspects like as compressive strength(45.7Mpa), flexural strength(4.78Mpa), and split tensile strength(4.12Mpa) were attain by optimum mix design GPC-FG where cement substituted with ratio of FA:GGBS:SF – 40:50:10 and compressive strength(50.4Mpa), flexural strength(5.51Mpa) and split tensile strength(4.99Mpa) were attain by optimum mix design of Polypropylene based GPC-FGP where cement substituted with ratio of FA:GGBS:SF:PF – 40:49:10:1. The optimal mix design GPC-FG and GPC-FGP are compared there is raise in compressive strength of 9.325%, flexural strength of 13.241%,split tensile strength 17.434% of GPC-FGP, along with CO_2 of polypropylene fiber-based geopolymer concrete with recycled aggregates as shown 60.01% reduction of CO_2 when compared with traditional concrete. The results demonstrate the potential of geopolymer concrete to achieve comparable or superior mechanical performance while significantly reducing CO_2 emissions compared to conventional concrete. This research adds to sustainable construction knowledge by showcasing geopolymer concrete's environmental benefits, mechanical strength, and potential applications in the industry and infrastructure development.

Keywords: Geopolymer concrete, Polypropylene fiber, Recycled Aggregates, Strength properties, CO_2 emissions

1. Introduction

Cement concrete is considered the world's second most resource-intensive material after potable water. Global usage of concrete is estimated at thirty billion tons annually [1]. The crucial and costly component of concrete is cement, serving as the binding agent. Cement industry production

Content from this work may be used under the terms of the Creative Commons Attribution 4.0 licence. Any further distribution of this work must maintain attribution to the author(s) and the title of the work, journal citation and DOI.
Published under licence by IOP Publishing Ltd

contributes approximately 5–7.5% of the world's CO_2 emission, with each ton of cement manufacturing releasing one ton of CO_2. This situation is concerning, necessitating urgent measures to decrease carbon dioxide (CO2) emissions from cement process production. [2][3].

In recent times, geopolymer binders have emerged as a substitute to traditional concrete. The term "geopolymer" was coined by Davidovits in 1978 to describe a non-crystalline alkali aluminosilicate or alkali-activated cement[4] [5]. The term geo - pertains to materials related to geology or industry like fly ash, slag, silica fume (SF) while polymer - signifies a sequence of molecules originating from identical units[5]. Geopolymers are substitute cement-like materials created through the recoil of an alkaline activator (such as KOH, NaOH, or soluble Na_2SiO_3) with aluminosilicate binder materials (like as silica fume (SF), fly ash (FA), metakaolin (M), iron slag, GGBS)[6] [7]. In recent times, there has been a surge in studies exploring optional cementitious materials due to the high claim for substances like GGBS and Fly ash. A study conducted a speculative investigation to assess the viability of low calcium-based wood ash as a substitute of fly ash in (GPC) geopolymer concrete[8]. Their outcome indicated that the optimal proportion of waste wooden ash was 32% of the whole binder material, leading to the highest compressive and flexural strengths[9]. Similarly, Shah et al. compute research on geopolymer concrete (GPC) based on GGBFS, using biomedical waste ash as a replacement[10]. The experiment ranged up to 10% ash content, showing a positive correlation between increased biomedical waste ash and compressive strength, a trend also observed in studies[11] [12].

Several researchers have signified that recycled aggregate (RA) would be effectively used as a replace for virgin aggregates in concrete production, achieving comparable performance to conventional structural concrete [13][14]. Nowadays, recycled aggregate based concrete is widely employed for both structural works and non-structural work purposes. It is been demonstrated that practicality extends to both commercial and technical aspects[15][16][17].

The carbon footprint is a common adopted method for evaluating the environmental effect of concrete production and its components, representing the absolute amount of carbon dioxide emissions and other greenhouse gases emits, expressed as CO2 equivalents. The research findings indicated that, as anticipated, carbon dioxide equivalent emissions experienced a slight decrease with the increased utilization of recycled aggregates. Furthermore, the study affirmed that cement has the most significant impact on greenhouse gas emits during the making phase of concrete, irrespective of whether recycled or virgin aggregates are employed.[18]

As many researchers' studies on recycled aggregate geopolymer concrete (GPC) where there is a decline in density and bond strength. This paper mainly focus on evaluation of polypropylene fiber based geopolymer concrete (GPC) were recycled aggregates (RA) from C, D waste are substituted with nominal aggregates. This paperwork insights the physical and structural properties of geopolymer concrete by adding fiber which promote good bond strength and crack resistance. It also aims to analyse the carbon footprint per m^3 . This research helps in further applications in construction industry and environmental benefits for future needs.

2. Raw Materials

In this study GGBS, Fly ash, silica fume, polypropylene fiber, recycled aggregates and alkaline solution are used as raw materials. Ground Granulated Slag (GGBS), also known simply as slag, is obtained as a yield matter during the production of iron metal in blast furnaces. GGBFS is widely used as a supplement of cementitious material in the making of concrete due to its pozzolanic and hydraulic properties. The physical effects of GGBS may vary up on how the slag is cooled. Slag is

off-white in colour, specific gravity of 2.9, fineness of 350 m^2/kg, density of 1100 kg/m^3 and surface area of 400-600 m^2/kg.

Fly ash is a micro fine powder made from the mineral matter in coal making process, and is generally tiny than OPC and lime. Fly ash is made up of silt-sized pieces, which are spherical, and commonly range in size from 10 and 100 microns. The fly ash is made up of oxides of silica, aluminium, iron oxide, and calcium. The specific gravity of fly ash is 2.5, surface area 900 m^2/kg, bulk density 2.3 g/m^3 and grey in colour.

Silica fume, also called micro(nano) silica or condensed silica, is a residue produced when making silicon metal or ferrosilicon alloys in electric arc furnaces. Silica fume particles are extremely fine, with most particles being less than 1 micron in size. It is typically dark grey to black in colour, with a powdery appearance. This fine particle size contributes to its high surface area and reactivity. It has a high density, usually ranging from about 2.2 to 2.3 grams per cubic centimetre (g/cm^3). Silica fume has a very high specific surface area, often exceeding 20,000 square meters per kilogram (m^2/kg). This large surface area enhances its pozzolanic reactivity when used in concrete.

Polypropylene fiber is manufactured through the polymerization of propylene gas. The process involves combining propylene monomers under controlled conditions, typically using catalysts, to form long chains of polypropylene molecules. These chains are then extruded and spun into fibers. Polypropylene fibers are usually white or translucent in color, although they can be produced in various colours. Polypropylene has a relatively low density, that is of 0.91 grams per cubic centimetre (g/cm^3). This makes it lightweight compared to many other fibers. Polypropylene fibers have good tensile strength, meaning they can withstand pulling forces without breaking easily.

Recycled aggregates are accomplished from the processing and recycling of construction and demolition waste materials. These waste materials include concrete rubble, asphalt, bricks, tiles, and other demolished building materials. The process involves crushing, screening, and sorting the waste materials to produce recycled aggregates suitable for use in construction applications. The density of recycled aggregates can vary widely depending on factors such as the different types of waste material and the degree of processing. Generally, recycled waste aggregates (RA) have a low density when compared to nominal aggregates, about 1.5 to 2.5 grams per cubic centimetre (g/cm^3). The specific gravity for recycled aggregates is 2.5 and surface area 5.98 cm^2/g. It is obtained from nearby demolished building which are passing through 20mm IS sieve.

Alkali activators are apparatus used in the preparation of geopolymers and alkali-activate materials (AAMs). These activators play a crucial role in initiating the chemical reactions that lead to the formation of strong, durable, and environmentally friendly cementitious materials. Alkali activators work by activating the amorphous aluminosilicate precursors present in materials like fly ash, slag, or metakaolin. This activation leads to the dissolution of silica (SiO_2) and alumina ($Al2O_3$) species, which then polymerize to form a three-dimensional network of polymeric chains. Alkaline solution used is a mixture of Na_2SiO_3 solution and NaOH solution. The NaOH in crystals from with 98% purity was also purchased from a retail market. The NaOH solution was prepared with a concentration of 12 M. The Na_2SiO_3 solution and the NaOH solution were blended together one day before use.

Table 1. Chemical Composition of Fly ash, Silica fume and GGBS

Material	Silica	Alumina	Iron Oxide	Lime	Magnesia	Titanium Oxide	Sulphur Trioxide	Loss on Ignition
Fly Ash	65.6	28.0	3.0	1.0	1.0	0.5	0.2	0.29

Silica fume	96	0.25	0.5	0.25	0.56	0.001	0.12	0.015
GGBS	30.61	16.24	0.584	34.48	6.79	-	1.85	2.1

3. Methodology

This study focusses on finding the outcome of using polypropylene fiber and recycled demolish aggregates on strength properties of polypropylene fiber based geopolymer concrete and compare with geopolymer concrete without polypropylene and traditional concrete.

The mechanism of geopolymerization involves the polycondensation reaction of geopolymeric precursors with alkali polysiliates. The precursors are aluminosilicate oxide and alkali polysiliates. The reaction yields a polymeric Si–O–Al bond. The initial material undergoes alkaline activation using a blend of ingredients: An alkali solution such as NaOH, and a silica-rich source like Na_2SiO_3. In the process of geopolymerization, Na+ plays a crucial role during the solidification phase. Thus, a greater concentration of Na+ leads to increased compressive strength in geopolymer concrete (GPC) and resistance to chemical attacks, abrasion, and weathering.

The following figure 1 shows process that represent the production of polypropylene based geopolymer concrete and its mix design procedure.

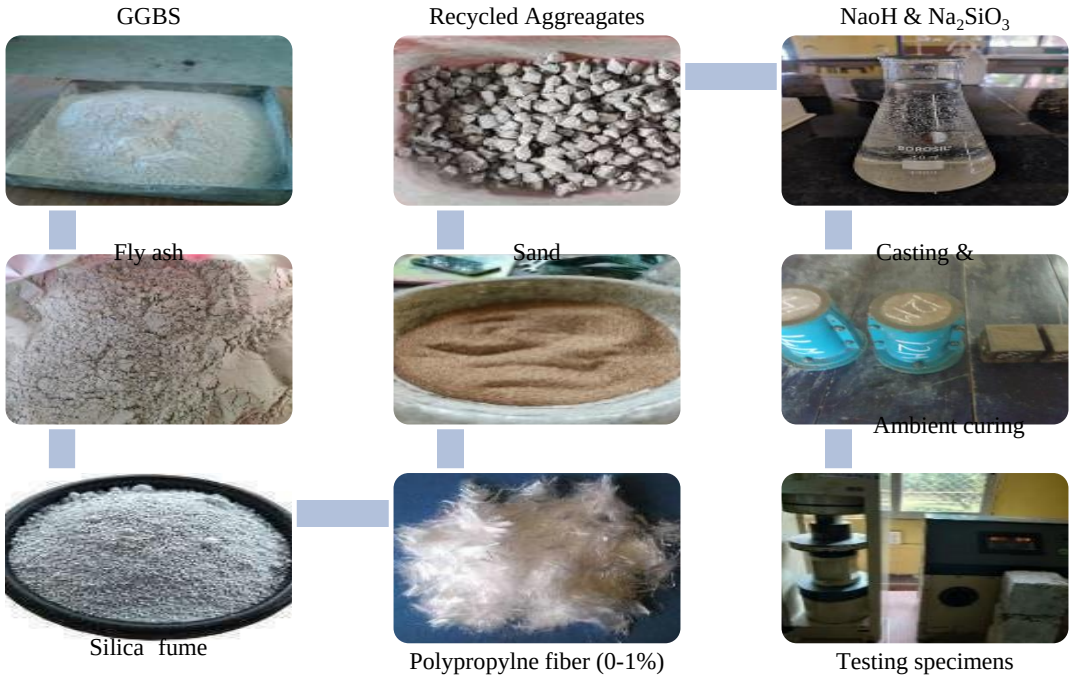


Figure 1. Production of polypropylene based geopolymer concrete

The traditional method of preparing geopolymer concrete involves manual mixing of dry components such as fine aggregates, recycled coarse aggregate, GGBS, fly ash, silica fume, and fibers. This dry mix is then combined with a calculated ratio of alkaline solution, comprising NaOH and Na_2SiO_3 solution mixed with water or a super-plasticizer. This alkaline solution is prepared an hour before casting. The below table 2 shows the mix ratios of various mix designs.

Table 2. Mix design of Geopolymer concrete per m^3 volume (%) for concrete of M40 grade

Mix Name	GGBS	Fly ash	Silica fume	Polypropylene fiber	RA (in g)	FA (in g)	NaOH (12M)	Na_2SiO_3 (in g)
G45F45SF10	45	45	10	-	310	160	51.85	103.7
G50F40SF10	50	40	10	-	310	160	51.85	103.7
G55F35SF10	55	35	10	-	310	160	51.85	103.7
G45F45SF9P1	45	45	9	1	310	160	51.85	103.7
G50F40SF9P1	50	40	9	1	310	160	51.85	103.7
G55F35SF9P1	55	35	9	1	310	160	51.85	103.7

To prepare the geopolymer concrete, the dry mix and the alkaline solution are hand-mixed thoroughly for five to ten minutes until a homogeneous mixture is achieved. Subsequently, the mixed concrete is poured into moulds of 150mm cube size in 3 equal layers. Every layer is compacted with rod strokes 25 times to ensure proper compaction, and the top layer of each mould is levelled. When casting is completed, the specimens are kept undisturbed for a minimum 24 hours post demoulding. This traditional method ensures that the geopolymer concrete is well-mixed, properly compacted, and allowed to set before testing or further use.

The same method is followed for preparing cylinders of 100mm diameter and height of 500mm for finding split tensile strength and prisms of 600mm x 100mm x 70mm size were used for finding flexural strength. All cast specimens are cured under ambient curing and tests done at 7 days, 14 days, and 28 days after curing.

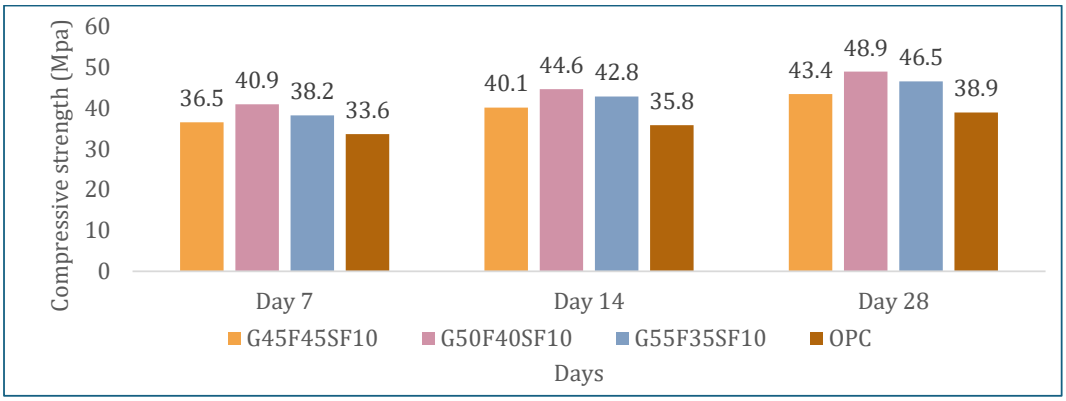


Figure 2. Compressive strength of GPC-FG without polypropylene fiber and OPC for 7, 14, 28 days (MPa)

4. Results and discussion

4.1. Compressive Strength

The outcome compressive strength testing showed in figure 3 of geopolymer concrete exhibited significantly greater compressive strength contrast to traditional concrete. The mean compressive strength of GPC-FGP with fiber determine to be 46.43 MPa, while traditional concrete specimens had an average compressive strength of 36.1 MPa. This represents a 22.24% increase in compressive strength for geopolymer concrete over traditional concrete.

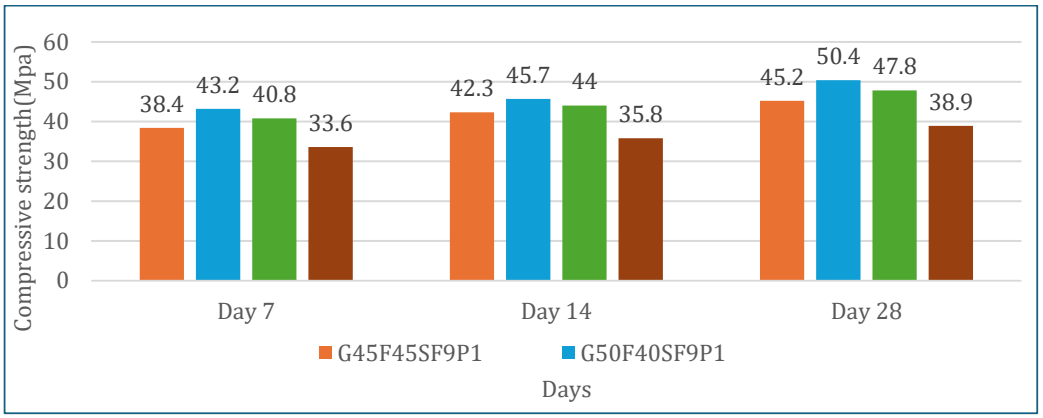


Figure 3: Compressive strength of GPC-FGP with polypropylene fiber and OPC for 7, 14, 28 days (MPa)

While geopolymer concrete with fiber has shown gradual greater compressive strength compared to geopolymer concrete without fiber. The mean compressive strength of GPC-FG without fiber was found to be 44.8 MPa, while GPC-FGP with fiber specimens had mean compressive strength of 46.43 MPa. This represents a 3.51% raise in compressive strength for GPC-FG without fiber over with fiber geopolymer concrete (GPC-FGP).

4.2. Split Tensile Strength

The outcome of the split tensile strength testing showed in figure 4 about geopolymer concrete exhibited significantly lesser tensile strength compared to traditional concrete. The mean tensile strength of GPC-FG without fiber compute to be 3.943 MPa, while traditional concrete specimens had mean tensile strength of 4.07 MPa. This represents 3.12% decline in tensile strength for geopolymer concrete (GPC-FG) over traditional concrete.

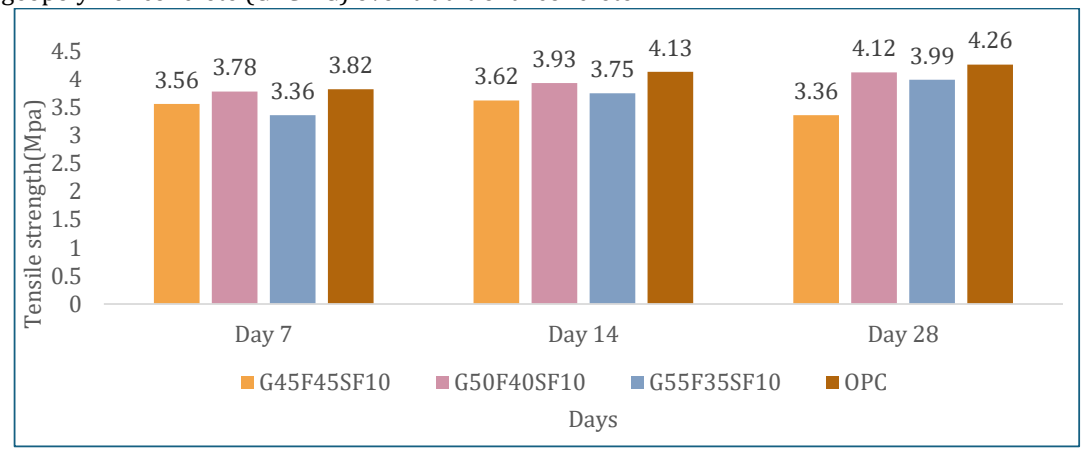


Figure 4. Split tensile strength of GPC without polypropylene fiber and OPC for 7, 14, 28 days (MPa)

The outcome of the split tensile strength testing shown in figure 5 about GPC-FGP exhibited significantly greater tensile strength contrast to traditional concrete. The mean tensile strength of GPC-FGP with fiber was found to be 4.24 MPa, while traditional concrete specimens had mean tensile strength of 4.07 MPa. This represents 4.176% increase in tensile strength for geopolymer concrete over traditional concrete.

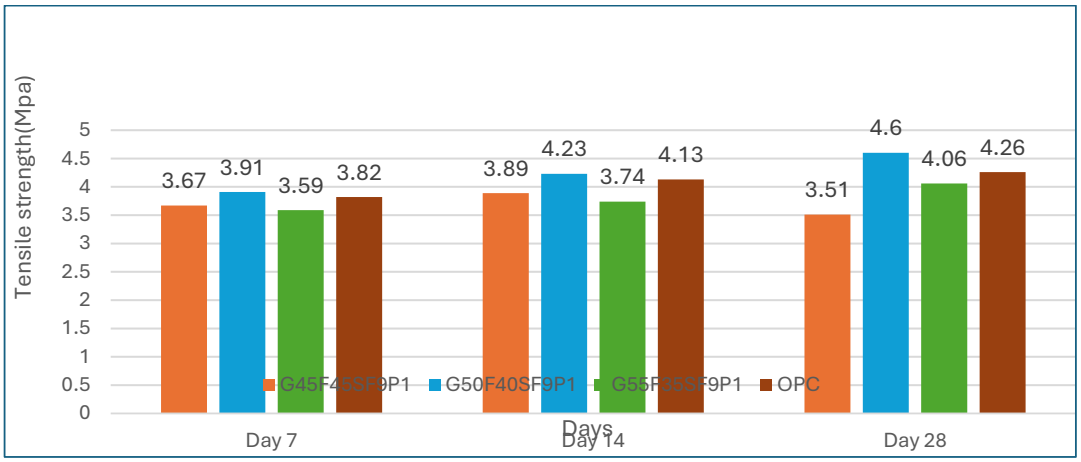


Figure 5: Split tensile strength of GPC-FG with polypropylene fiber and OPC for 7, 14, 28 days (MPa)

While geopolymer concrete with fiber has shown gradual greater tensile strength contrast to geopolymer concrete without fiber. An average tensile strength of GPC-FG without fiber was found to be 3.943 MPa, while GPC-FGP with fiber specimens had mean tensile strength of 4.24 MPa. This represents a 7.07% raise in tensile strength for GPC-FG without fiber over with fiber geopolymer concrete (GPC-FGP).

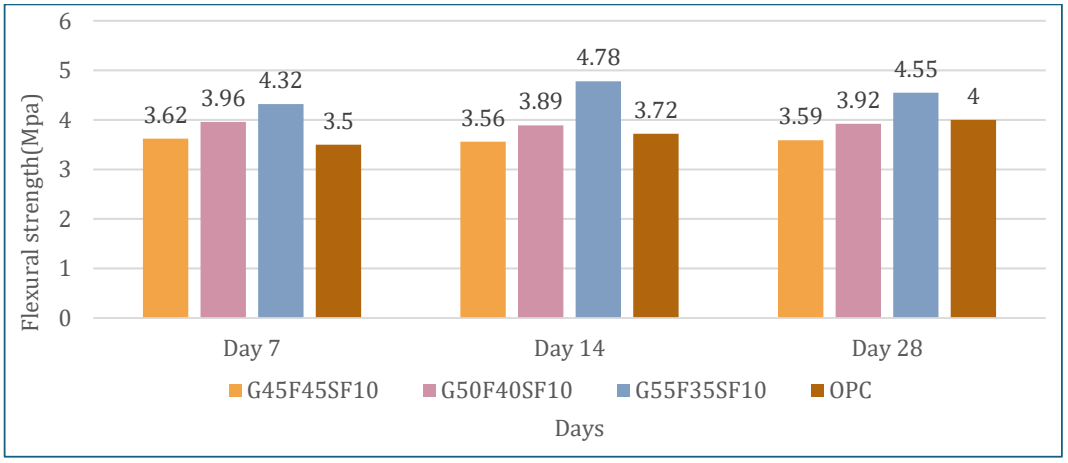


Figure 6. Flexural strength of GPC with polypropylene fiber and OPC for 7, 14, 28 days (MPa)

4.3. Flexural Strength

The outcome of the flexural strength testing showed in figure 6 that geopolymer concrete exhibited significantly higher flexural strength compared to traditional concrete. An average flexural strength of GPC-FG without fiber was found to be 4.02 MPa, while traditional concrete specimens had an average flexural strength of 3.74 MPa. This represents a 6.15% increase in flexural strength for geopolymer concrete (GPC-FG) over traditional concrete.

The outcome of the flexural strength testing showed in figure 7 that GPC-FGP exhibited significantly greater flexural strength compared to traditional concrete. The mean flexural strength of GPC-FGP with fiber compute to be 4.34 MPa, while traditional concrete specimens had

mean flexural strength of 3.74 MPa. This represents a 13.82% raise in flexural strength for geopolymer concrete over traditional concrete.

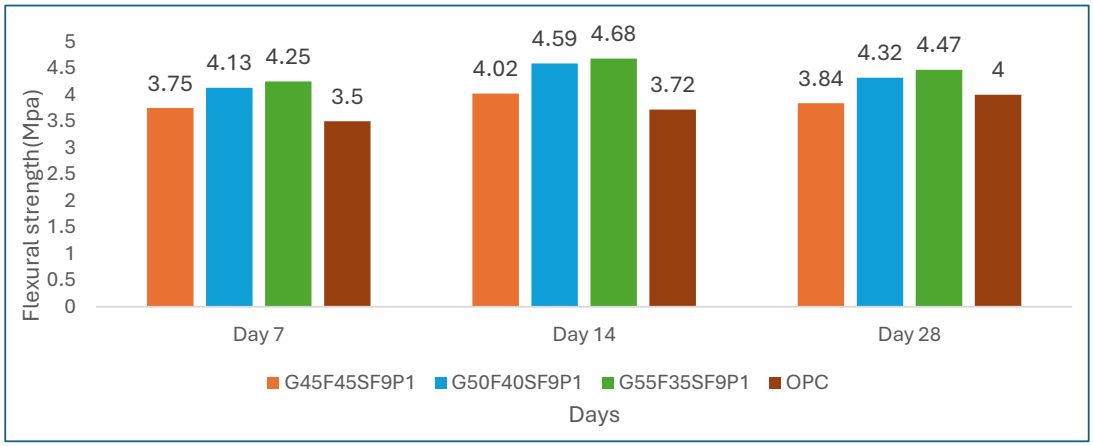


Figure 7. Flexural strength of GPC with polypropylene fiber and OPC for 7, 14, 28 days (MPa)

While geopolymer concrete with fiber has shown gradual greater flexural strength compared to GPC-FG without fiber. The mean flexural strength of GPC-FG without fiber was compute to be 4.02 MPa, while GPC-FGP with fiber specimens had mean flexural strength of 4.34 MPa. This represents a 7.37% raise in flexural strength for geopolymer concrete (GPC-FG) without fiber over with fiber geopolymer concrete (GPC-FGP).

From these findings, it shows that G50F40SF9P1 mix design has good chemical bonding that exhibits denser and more cohesive concrete matrix, contributing to higher compressive strength other than other mix designs. The curing regime used in this study ensured sufficient hydration and reaction kinetics, resulting in higher compressive strength values. The G50F40SF9P1 mix design has shown increase in density than other mix designs. Geopolymer concrete (G50F40SF9P1) typically has lower porosity compared to traditional concrete, as the geopolymerization process leads to the development of a more dense and less permeable microstructure. The workability of geopolymer concrete is enhanced when using recycled aggregates (RA) in a saturated dry surface condition. As amount concern to recycled aggregates increases, workability of the concrete also increases. While Polypropylene fibers act as crack arresters, helping to control and limit the propagation of cracks in geopolymer concrete. This reduces the risk of structural failure and improves overall integrity.

4.4. Carbon Footprint Analysis

First, the INECC paper used a method called Life Cycle Assessment (LCA) to calculate emissions from cement production in Mexico. They considered the entire process, from extracting raw materials to transporting the cement to the construction site. They used emission factors of 0.82 tons of CO_2 equivalent per ton of cement produced and 0.04 tons of CO_2 equivalent per ton of cement transported [19].

Next, Sabău et al. also used LCA to calculate emissions from concrete production in Europe. They looked at the entire supply chain, including raw material extraction, transportation, and concrete production. They used emission factors of 0.95 tons of CO_2 equivalent per ton of cement produced, 0.004 tons of CO_2 equivalent per ton of aggregate produced, and 0.06 tons of CO_2

equivalent per ton of concrete transported [20]. Thannimalay et al. took a slightly different approach, focusing on the production of sodium hydroxide, a key ingredient in concrete production. They used LCA to calculate emissions from sodium hydroxide production in Asia, using an emission factor of 0.28 tons of CO_2 equivalent per ton of sodium hydroxide produced [23]. Alsalman et al. used LCA to calculate emissions from concrete production in North America. They considered the entire supply chain, including raw material extraction, transportation, and concrete production. They used emission factors of 0.92 tons of CO_2 equivalent per ton of cement produced, 0.001 tons of CO_2 equivalent per ton of fly ash produced, and 0.05 tons of CO_2 equivalent per ton of concrete transported [24]. Finally, Yina et al. looked at the production of polypropylene fibers, which are often used in concrete production. They used LCA to calculate emissions from polypropylene fiber production in Asia, using an emission factor of 1.45 tons of CO_2 equivalent per ton of polypropylene fiber produced [26]. Each paper used different emission factors and boundaries, reflecting the specific context and location of the study. However, they all shared a common goal: to quantify the carbon footprint of concrete production and identify opportunities for reduction. Carbon footprint analysis for geopolymer concrete involves evaluating the environmental impact of producing geopolymer concrete, particularly focusing on carbon dioxide (CO_2) emissions and other greenhouse gases. The below-mentioned table 3 shows carbon assessment in terms of kg CO_2/m^3 of different mix design and materials.

Table 3. Carbon footprint analysis of GPC mix design and OPC (kg CO_2e per m^3)

Material	CO_2 of OPC (Kg CO_2e/m^3)	CO_2 of G45F45SF10 (Kg CO_2e/m^3)	CO_2 of G50F40SF10 (Kg CO_2e/m^3)	CO_2 of G55F35SF10 (Kg CO_2e/m^3)	CO_2 of G45F45SF9P1 (Kg CO_2e/m^3)	CO_2 of G50F40SF9P1 (Kg CO_2e/m^3)	CO_2 of G55F35SF9P1 (Kg CO_2e/m^3)	Reference
Cement	502.58	-	-	-	-	-	-	[19]
Coarse Aggregates	332	-	-	-	-	-	-	[20]
Recycled Aggregates	-	0	0	0	0	0	0	[20]
Sand	7.133	10.094	10.094	10.094	10.094	10.094	10.094	[20]
GGBS	-	145	140	135	145	140	135	[21]
Fly ash	-	0.012	0.015	0.014	0.012	0.015	0.014	[22]
NaOH	-	22.942	22.942	22.942	22.942	22.942	22.942	[23]
Na_2SiO_3	-	122.402	122.402	122.402	122.402	122.402	122.402	[24]
Silica fume	-	41.818	41.818	41.818	37.636	37.636	37.636	[25]
Polypropylene fiber	-	-	-	-	1.7	1.7	1.7	[26]
Total	841.71	342.268	337.271	332.27	339.786	334.78	329.788	

When comparing Ordinary Portland Cement (OPC) with various mix designs of GPC, computed that the CO_2 emissions are reduced. The mix design G45F45SF10 shows a CO_2 reduction of up to 59.33%, G50F40SF10 shows a CO_2 reduction of up to 59.93%, G50F40SF10 shows a CO_2 reduction of up to 60.52%, G45F45SF9P1 shows a CO_2 reduction of up to 59.63%, G50F40SF9P1

shows a CO_2 reduction of up to 60.225%, and G55F35SF9P1 shows a CO_2 reduction of up to 60.81%. These mix designs demonstrate a significant decrease in carbon emissions compared to OPC.

5. Conclusion

The conclusions drawn from the results can provide valuable insights for ongoing advancement of geopolymer concrete (GPC), aiming to enhance its properties for the benefit of the industry.

- The Strength properties of G50F40SF9P1 is greater than traditional concrete, and it increased due to polypropylene fiber content.
- The presence of recycled demolish aggregates in a saturated surface dry (SSD) condition enhances the workableness of geopolymer concrete (GPC), and as the quantity of recycled aggregates increases, so does the workability of the concrete.
- GGBS reduce voids, shrinkage cracks and fly ash potentially resist sulphates and alkali-aggregate reactions and improve overall performance.
- Silica fume improve abrasion resistance, bond strength and reduce permeability of geopolymer concrete compared to conventional concrete.
- CO_2 emissions decrease up to 60% compared to traditional concrete, these findings indicate that use of cementitious materials and recycled aggregates reduce carbon footprint emissions to a great extent.

References

[1] Concrete needs to lose its colossal carbon footprint, Nature 597 (2021). https://doi.org/10.1038/d41586-021-02612-5.
[2] N.K. Sharma, P. Kumar, S. Kumar, B.S. Thomas, R.C. Gupta, Properties of concrete containing polished granite waste as partial substitution of coarse aggregate, Constr Build Mater 151 (2017). https://doi.org/10.1016/j.conbuildmat.2017.06.081.
[3] N.B. Singh, B. Middendorf, Geopolymers as an alternative to Portland cement: An overview, Constr Build Mater 237 (2020). https://doi.org/10.1016/j.conbuildmat.2019.117455.
[4] J. Davidovits, Geopolymers and geopolymeric materials, Journal of Thermal Analysis 35 (1989). https://doi.org/10.1007/BF01904446.
[5] K.H. Younis, K.A. Salihi, T.K. Ibrahim, An overview of geo-polymer concrete including recycled aggregate, International Journal of Scientific and Technology Research 9 (2020).
[6] P. Duxson, A. Fernández-Jiménez, J.L. Provis, G.C. Lukey, A. Palomo, J.S.J. Van Deventer, Geopolymer technology: The current state of the art, J Mater Sci 42 (2007). https://doi.org/10.1007/s10853-006-0637-z.
[7] H. Assaedi, T. Alomayri, A. Siddika, F. Shaikh, H. Alamri, S. Subaer, I.M. Low, Effect of Nanosilica on mechanical properties and microstructure of PVA Fiber-Reinforced Geopolymer Composite (PVA-FRGC), Materials 12 (2019). https://doi.org/10.3390/ma12213624.
[8] K. Arunkumar, M. Muthukannan, A.S. Kumar, A.C. Ganesh, R.K. Devi, Cleaner environment approach by the utilization of low calcium wood ash in geopolymer concrete, Applied Science and Engineering Progress 15 (2022). https://doi.org/10.14416/j.asep.2021.06.005.
[9] A. Hassan, M. Arif, M. Shariq, Use of geopolymer concrete for a cleaner and sustainable environment – A review of mechanical properties and microstructure, J Clean Prod 223 (2019). https://doi.org/10.1016/j.jclepro.2019.03.051.
[10] A. Suresh Kumar, M. Muthukannan, I. Sri Krishna, Optimisation of bio medical waste ash in GGBS based of geopolymer concrete, in: IOP Conf Ser Mater Sci Eng, 2020. https://doi.org/10.1088/1757-899X/872/1/012163.
[11] A. Suresh Kumar, M. Muthukannan, R. Kanniga Devi, K. Arunkumar, A. Chithambar Ganesh, Reduction of hazardous incinerated bio-medical waste ash and its environmental strain by utilizing in green concrete, Water Science and Technology 84 (2021). https://doi.org/10.2166/wst.2021.239.

[12] S.K. Arunachalam, M. Muthiah, K.D. Rangaswamy, A. Kadarkarai, C.G. Arunasankar, Improving the structural performance of reinforced geopolymer concrete incorporated with hazardous heavy metal waste ash, World Journal of Engineering 19 (2022). https://doi.org/10.1108/WJE-01-2021-0055.
[13] K. Kalinowska-Wichrowska, D. Suescum-Morales, The experimental study of the utilization of recycling aggregate from the demolition of elements of a reinforced concrete hall, Sustainability (Switzerland) 12 (2020). https://doi.org/10.3390/su12125182.
[14] J. Tan, J. Cai, X. Li, J. Pan, J. Li, Development of eco-friendly geopolymers with ground mixed recycled aggregates and slag, J Clean Prod 256 (2020). https://doi.org/10.1016/j.jclepro.2020.120369.
[15] M. Behera, S.K. Bhattacharyya, A.K. Minocha, R. Deoliya, S. Maiti, Recycled aggregate from C&D waste & its use in concrete - A breakthrough towards sustainability in construction sector: A review, Constr Build Mater 68 (2014). https://doi.org/10.1016/j.conbuildmat.2014.07.003.
[16] M. Limbachiya, M. Seddik Meddah, Y. Ouchagour, Performance of Portland/silica fume cement concrete produced with recycled concrete aggregate, ACI Mater J 109 (2012). https://doi.org/10.14359/51683574.
[17] R.A. Robayo-Salazar, J.F. Rivera, R. Mejía de Gutiérrez, Alkali-activated building materials made with recycled construction and demolition wastes, Constr Build Mater 149 (2017). https://doi.org/10.1016/j.conbuildmat.2017.05.122.
[18] L.F. Jiménez, J.A. Domínguez, R.E. Vega-Azamar, Carbon footprint of recycled aggregate concrete, Advances in Civil Engineering 2018 (2018). https://doi.org/10.1155/2018/7949741.
[19] INECC, Inventario Nacional de Emisiones de Gases y Compuestos de Efecto Invernadero 1990-2015 en México, Instituto Nacional de Ecología y Cambio Climático (2018).
[20] M. Sabău, D. V. Bompa, L.F.O. Silva, Comparative carbon emission assessments of recycled and natural aggregate concrete: Environmental influence of cement content, Geoscience Frontiers 12 (2021). https://doi.org/10.1016/j.gsf.2021.101235.
[21] A. Aslani, C. Hachem-Vermette, R. Zahedi, Environmental impact assessment and potentials of material efficiency using by-products and waste materials, Construction Building Materials 378 (2023). https://doi.org/10.1016/j.conbuildmat.2023.131197.
[22] Y.R. Zhang, M.H. Liu, H.B. Xie, Y.F. Wang, Assessment of CO2 emissions and cost in fly ash concrete, in: Environment, Energy and Applied Technology - Proceedings of the 2014 3rd International Conference on Frontier of Energy and Environment Engineering, ICFEEE 2014, 2015. https://doi.org/10.1201/b18135-67.
[23] L. Thannimalay, S. Yusoff, N.Z. Zawawi, Life Cycle Assessment of Sodium Hydroxide, Aust J Basic Appl Sci 7 (2013).
[24] A. Alsalman, L.N. Assi, R.S. Kareem, K. Carter, P. Ziehl, Energy and CO2 emission assessments of alkali-activated concrete and Ordinary Portland Cement concrete: A comparative analysis of different grades of concrete, Cleaner Environmental Systems 3 (2021). https://doi.org/10.1016/j.cesys.2021.100047.
[25] M. Soomro, V.W.Y. Tam, A.C. Jorge Evangelista, Industrial and agro-waste materials for use in recycled concrete, in: Recycled Concrete: Technologies and Performance, 2022. https://doi.org/10.1016/B978-0-323-85210-4.00009-6.
[26] S. Yina, R. Tuladhar, M. Sheehan, M. Combe, T. Collister, A life cycle assessment of recycled polypropylene fibre in concrete footpaths, J Clean Prod 112 (2016). https://doi.org/10.1016/j.jclepro.2015.09.073.

Acknowledgements

The authors express deep gratitude towards B V Raju Institute of Technology, Narsapur, Medak, Telangana, India for providing all the facilities needed for the completion of research work.

IOP Conference Series: Earth and Environmental Science

PURPOSE-LED PUBLISHING™

PAPER • **OPEN ACCESS**

Enhancing sustainability through GIS mapping for groundwater quality analysis

To cite this article: Surisetti Vamsi Harischandra Prasad and Srinivas Tanuku 2024 *IOP Conf. Ser.: Earth Environ. Sci.* **1409** 012025

View the article online for updates and enhancements.

You may also like

- Impact of natural conditions and anthropogenic activities on groundwater quality in Puntang volcanic area, West Java, Indonesia.
R. Maria, T.Y.W.M Iskandarsyah, B.R. Suganda et al.
- Spatial quality of shallow groundwater in DAS Cijurey Regency of Majalengka, West Java
T Mutiara, E Kusratmoko and K Marko
- Evaluation of Trends for Iron and Manganese Concentrations in Shallow Groundwater, Jakarta City
Adelia Maria Julieta Parrangan, Yureana Wijayanti, Ernie Soekotjo et al.



This content was downloaded from IP address 47.247.77.11 on 27/11/2024 at 05:38

Enhancing sustainability through GIS mapping for groundwater quality analysis

Surisetti Vamsi Harischandra Prasad*[1] and Srinivas Tanuku[1]

[1]Department of Civil Engineering, GITAM University, Visakhapatnam, Andhra Pradesh, India.

*E-mail: vamsitanuku2@gmail.com

Abstract. The current study attempts to develop sustainability by utilizing Geographic Information System (GIS) technology by examining groundwater quality in Rajahmundry by dividing the region into 1 km × 1 km grids, resulting in 45 different areas. The grids are thoroughly dispersed, and groundwater samples have been collected from a variety of sources, including open wells, hand pumps, and bore wells, in each grid in order to assess water quality. The evaluation includes a physico-chemical parameter namely, pH, total alkalinity, TDS, total hardness, calcium hardness, magnesium hardness, chloride, nitrates, and sulphates. The purpose of this study is to create a map of the spatial distribution of these groundwater qualities using GIS in order to obtain a general understanding of the current state of the entire valorisation of groundwater resources. The current approach is novel in that it not only allows detecting the issues affecting water quality but also enables developing specific approaches for the sustainable management and protection of groundwater in Rajahmundry. Overall, through GIS mapping and conclusive water quality assessment, the study provides a significant input into the field of environmental science in terms of enhancing water sustainability practices.
Keywords. Geographic Information System (GIS), Groundwater, Sustainability

1. Introduction

Groundwater contamination is now one of the most pressing global health issues by causing many illnesses and deaths [1-3]. This however is most pronounced in India, where the rapid growth of industries, urbanization, and population have accelerated the release of effluents and pollutants into the environment [4-5]. Groundwater safety therefore requires that its constituents such as physical and chemical entities should fall within set limits for the particular use, to avoid offending effects to health. Therefore, groundwater pollution has been in the spotlight for many years. Revitalization of groundwater that was once contaminated is not a simple task – another argument for regular quality check and development of shielding strategies that would keep it safe from future contamination. The assessment of groundwater attributes comprises of physical and chemical parameters analysis. The most effective means of monitoring the groundwater quality is through the use of Geographic Information System (GIS) technology aided by the IDW interpolation method [7-12]. The approach has been reported to be capable of efficiently processing very big amounts of data, facilitating the creation of spatial distribution maps and projections that allow the identification of trends, correlations and sources of pollution. In this

Content from this work may be used under the terms of the Creative Commons Attribution 4.0 licence. Any further distribution of this work must maintain attribution to the author(s) and the title of the work, journal citation and DOI.
Published under licence by IOP Publishing Ltd

way it has been found to be a low-cost and time-saving method for analyzing water resources [13-14]. The goal is to leverage GIS interpolation techniques to evaluate the groundwater's fitness for human consumption, addressing the urgent need for comprehensive methods to safeguard our water supplies.

2. Materials and Methods

2.1. Study Area

Rajahmundry, officially referred to as Rajamahendravaram, stands as a prominent city within the state of Andhra Pradesh in India and functions as the administrative center of East Godavari district. The city covers about 45 square kilometres. The entire area of Rajahmundry was segmented into 45 grids, with each grid measuring 1 km by 1 km, utilizing topographic maps provided by the Town Planning Department of Rajahmundry. The information regarding sample locations is presented in Figure 1.

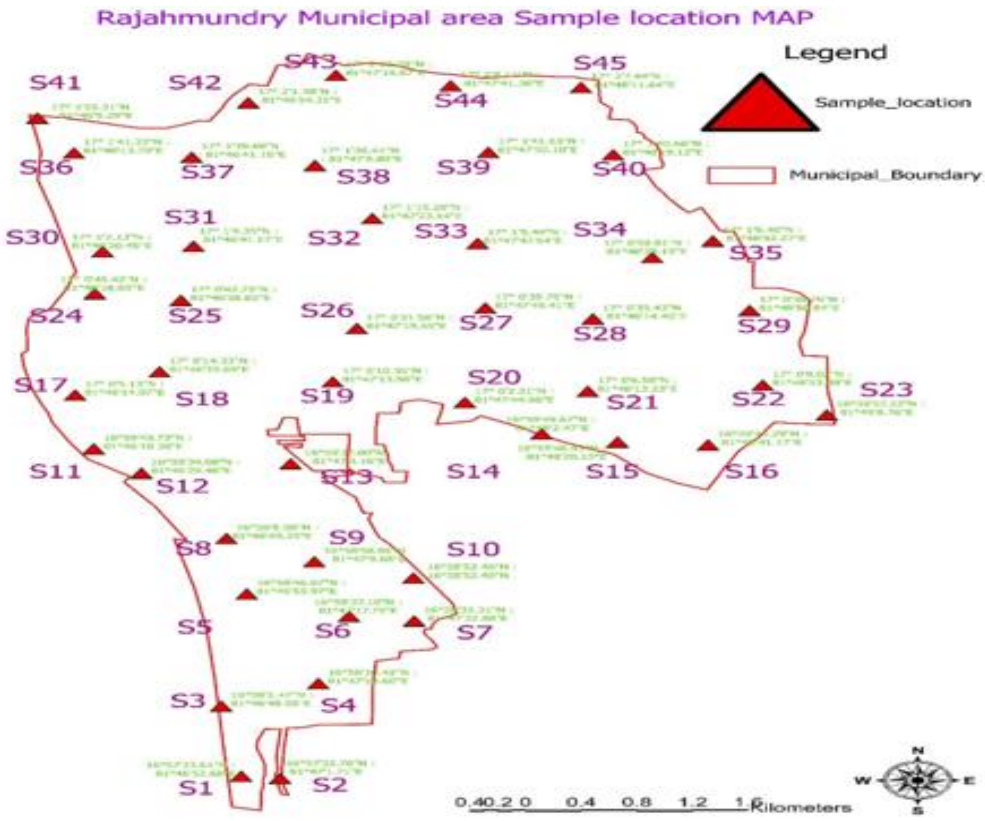


Figure 1. Map illustrating the sampling location sites within the study area

2.2. Sample Collection and Analysis

In order to conduct a comprehensive analysis of groundwater properties, a total of 45 samples were gathered during the Winter season in December 2023. A variety of sources, including hand pumps, bore wells inside designated grid regions, and open wells, were used to gather these samples. Each collected groundwater sample underwent a thorough analysis to evaluate several physicochemical parameters. In the present study, a total of nine ground water parameters were analyzed according to the test standard methods (APHA 2017) in the laboratory, except for unstable parameters such as hydrogen ion concentration (pH) and Total Dissolved Solids (TDS),

which were determined in situ using portable devices (pH-meter and TDS meter). Total Alkalinity (TA), Total Hardness (TH), Calcium (Ca^{2+}), Magnesium (Mg^{2+}), and Chloride (Cl^{-}) were analyzed using volumetric titrations. Nitrates (NO_3^{-}) and Sulphates (SO_4^{-}) were analyzed using Spectrophotometer.

3. Materials and Methods

3.1. pH

Most groundwater locations in the research region had pH values between 7.15 and 7.66, which is within the acceptable limit for drinking water quality. In site S10 and site S26, we spot relatively acidic condition; in S35, S36, S41, and S42, however, we notice alkaline readings. In this study, the region groundwater is generally safe to drink, based according to the map in Figure 2 which is showing the spatial distribution of pH value.

3.2. Total Alkalinity (TA)

The alkalinity total analysis for the groundwater in the study area shows extreme discrepancies, with sites such as S36 , S41, S44, S45 exhibiting alkalinity level exceptionally higher (644, 644, 644, 652) most likely meaning mineral present in high amount. Such practical initiatives as conducting assessments of water quality by location and doing ongoing monitoring (especially if the water quality is high somewhere) underline the incredible value of water resource management. S18 is the aberration as it has the total alkalinity of 611; so, there a need for a careful study and holistic water quality management plans in consideration from the alkalinity concentrations revealed in the spatial distribution map shown in figure 3, it is apparent that groundwater in the area studied appears to be safe for drinking despite seasonal fluctuations as the area is not under the effects of pollution or any other threat that affect the water quality.

3.3. Total Dissolved Solids (TDS)

In the *study* area's groundwater, the total dissolved solids (TDS) levels are widely varied, with S24, S25, S30, and S31 showing the highest values (798, 894, 934, and 938 mg/L). The mean of these values is approximately 896 mg/L, implying a relatively high concentration of minerals. This highlights the importance of continual and concentrated assessments of water quality, especially in areas where TDS is high, so that groundwater may be protected. TDS of 290 puts Site S10 in a need of detailed analysis and comprehensive management plans. In general, surface water is considered safe for drinking due to its low levels of dissolved solids which are demonstrated by the TDS spatial distribution map in Figure 4.

3.4. Total Hardness (TH)

In addition, among the various sites in the study area, some locations have very high TH values (i.e., S24, S25, S30, S31 ranging from 572, 584, 560, and 564 mg/L respectively). These measurements which are about 575 mg/L mean that many minerals are there that are responsible for the increase in hardness. This accentuates the fact that all measures related to groundwater quality should be targeted to water quality tests and ongoing monitoring, particularly the regions of water with high levels of hardness. A TH value of 336 in site S10 that is close to the TDS findings implies that this site should be further studied and managed to be exhaustive. Notwithstanding the fluctuations, the general groundwater level across the researched area is well below the maximum recommended hardness, qualifying it for drinking, depicted in the spatial distribution map of TH concentration in figure 5.

3.5. Calcium Hardness (Ca^{2+})

The analysis of Ca^{2+} in groundwater of areal observation reveals the value gap among the samples, in some locations, such as S24, S25, S30, and S31, show higher Ca2+ concentration (128, 131, 123, and 124 mg/L), respectively, while the general average of 127 mg/L, indicates This confirms how much needs to be done to preserve groundwater resources including, but not limited to, assessments of water quality, as well as monitoring, in the locations with high Ca^{2+} level. The Ca^{2+} reading value (=79) at Site S10 requires a detailed investigation and a total prudent administration. The report of the groundwater in research area shows that the water remains at desirable levels from the normal change and therefore it can be used for various functions by the impacted communities as shown by the figure 6 of the distribution map of Ca^{2+}.

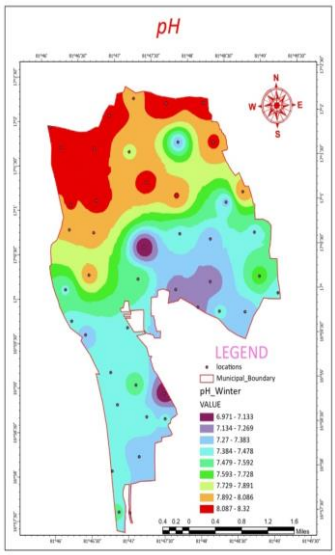


Figure 2. Spatial distribution of pH

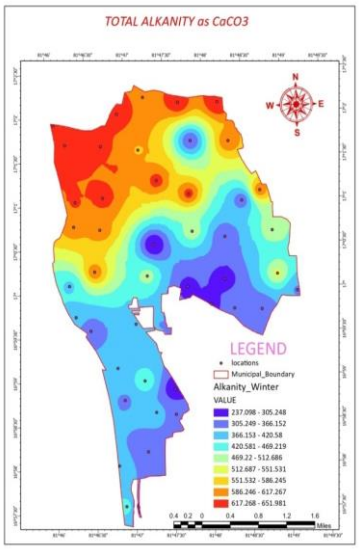


Figure 3. Spatial distribution of TA

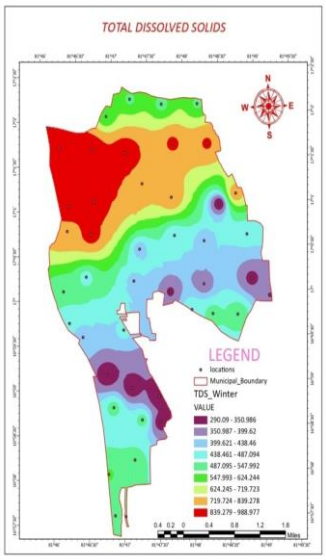


Figure 4. Spatial distribution of TDS

3.6. Magnesium Hardness (Mg^{2+})

The occurring Mg^{2+} values in all locations throughout the study area were varied. The actual highest concentrations were measured in S24. S25. S30. S31(61. 62, 61, 62 mg/L). Averagely, an amount of 61 mg/L representing the most active ions of magnesium, was measured in these localities. This highlights the significance of ongoing monitoring and focused evaluations of water quality, especially in locations with high Mg^{2+} concentrations, in order to protect groundwater resources. With a 34 mg/L Mg^{2+} content, site S10 necessitates extensive research as well as comprehensive management plans. Although there are some fluctuations, the Mg^{2+} spatial distribution map shown in figure 7 shows that, on the whole, the groundwater in the study region remains at acceptable levels, making it typically appropriate for a range of uses.

3.7. Chloride (Cl^-)

The groundwater examination of the study region shows a wide range of values for Chloride (Cl^-), with sites S24, S25, S30, and S31 showing particularly high readings (186, 194, 176, 185 mg/L). These measurements, which average about 185 mg/L, show that chloride ions are significantly present in these areas. This shows that the determination of water quality must be carried out with utmost care and regular monitoring during components near high Cl- in order to guard groundwater supplies. Site S10 has priority level owing to the fact that it is lower compared to the

outliers with chloride concentration of 76mg/L. This thus requires thorough research and several methods of management. It is worth noting that there could be some fluctuations. Figure 8 shows that the spatial Cl^- distribution map decently suggest the groundwater in the study area remain safe to use, allowing for various purposes.

3.8. Nitrates (NO_3^-)

The results of the groundwater analysis of the study area are well represented by the variation in Nitrate Levels (NO_3^-). Some sites S3, S31, S36, S42, S43, and S44 presents an average reading of 54,59,58,58,62, and 62 mg/L respectively. These data have an average of 57 mg/L, therefore you can understand that there are places with high nitrates and those with lower levels. The fact therefore implies the effectiveness of targeted testing of nitrate levels in water resources and routine monitoring, particularly in the areas with high nitrate presence, aiming to preserve the groundwater reserves. As contrasted to the other breakout, S10a has the NO_3^-level of 23 mg/L so that the rigger representation and respectively all-encompassing management will be thoroughly studied. The groundwater in our study areas may be occasionally changed but generally it continues to be well-satisfied; for that reason, this region is applicable for more than one use. This is indicated in Figure 9.

3.9. Sulphates (SO_4^-)

During the groundwater study that was done in the research site, the range of SO_4^- values was observed very broadly, for instance at sites 30, 31, 36, 42, 43, and 44, with some points having already high readings (51, 56, 65, 57, 56, and 55 mg/L). A distinct presence of sulphates may be seen in some areas, evident from these values which average around 55 mg/L. This further shows how needful it is to protect the groundwater by frequent water quality assessment plus regular monitoring in places with high SO_4^- levels. A thorough examination and comprehensive management methods are required for Site S10, which stands out among the outliers with a SO_4^- concentration of 28 mg/L. While there may be occasional variations, the groundwater in the research region generally remains adequate for a variety of uses, according to the spatial distribution map of SO_4^-displayed in Figure 10.

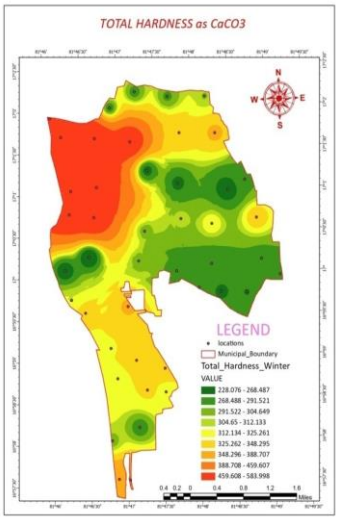


Figure 5. Spatial distribution of TH

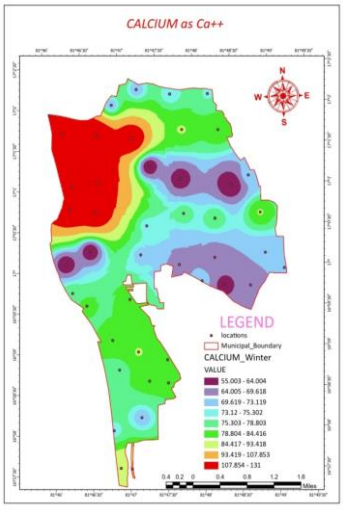


Figure 6. Spatial distribution of Ca^{2+}

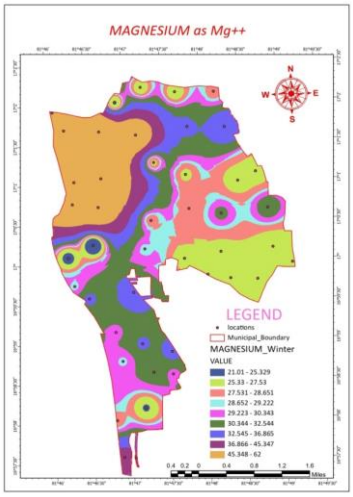


Figure 7. Spatial distribution of Mg^{2+}

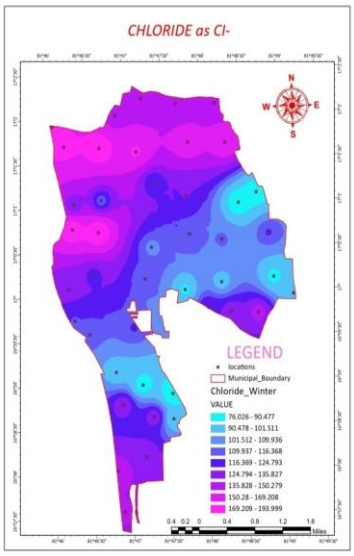


Figure 8. Spatial distribution of Cl^-

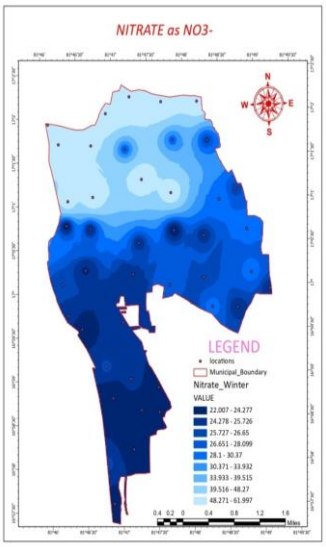


Figure 9. Spatial distribution of NO_3^-

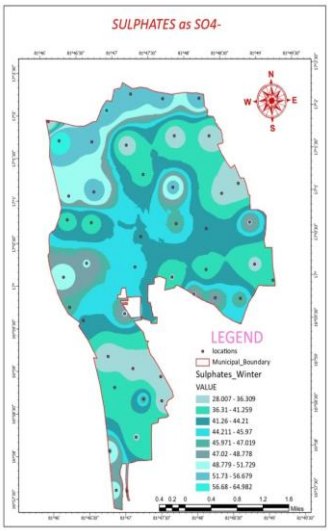


Figure 10. Spatial distribution of SO_4^-

4. Conclusions

From the findings and analysis of the 45 distinct areas, this study concludes that the use of the GIS technology to map and analyze the physico-chemical parameters can effectively contribute to improving the sustainability of the groundwater resources in Rajahmundry. Some of the major outcomes include the distribution of the groundwater quality within and outside the acceptable parameters of drinking water. Although much of the identified areas are well covered within the prescribed drinking water quality ranges, as captured earlier, this study demonstrates that there were intensive localized variations. This implies that there is a need for continuous monitoring, targeted assessments of the discrete areas of concern, and developing a management plan for the affected areas. The study makes a significant contribution to the field of environmental science by using GIS mapping to provide not only a detailed understanding of the spatial distribution of groundwater quality, but also insightful information for the sustainable management and protection of groundwater resources in Rajahmundry.

References

[1] Li, Q., Lu, L., Zhao, Q., & Hu, S. (2022). Impact of inorganic solutes' release in groundwater during oil shale in situ exploitation. Water, 15(1), 172.

[2] Wen, Z., Wang, Q., Ma, Y., Jacinthe, P. A., Liu, G., Li, S., ... & Song, K. (2024). Remote estimates of suspended particulate matter in global lakes using machine learning models. International Soil and Water Conservation Research, 12(1), 200-216.

[3] Qiu, D., Zhu, G., Bhat, M. A., Wang, L., Liu, Y., Sang, L., ... & Sun, N. (2023). Water use strategy of nitraria tangutorum shrubs in ecological water delivery area of the lower inland river: Based on stable isotope data. Journal of Hydrology, 624, 129918.

[4] Aravinthasamy, P., Karunanidhi, D., Subba Rao, N., Subramani, T., & Srinivasamoorthy, K. (2020). Irrigation risk assessment of groundwater in a non-perennial river basin of South India: implication from irrigation water quality index (IWQI) and geographical information system (GIS) approaches. Arabian Journal of Geosciences, 13, 1-14.

[5] Foster, T., & Willetts, J. (2018). Multiple water source use in rural Vanuatu: are households choosing the safest option for drinking?. International Journal of Environmental Health Research, 28(6), 579-589.

[6] Zhou, G., Tang, Y., Zhang, W., Liu, W., Jiang, Y., Gao, E., ... & Bai, Y. (2023). Shadow Detection on High-Resolution Digital Orthophoto Map (DOM) using Semantic Matching. IEEE Transactions on Geoscience and Remote Sensing.

[7] Hinge, G., Bharali, B., Baruah, A., & Sharma, A. (2022). Integrated groundwater quality analysis using Water Quality Index, GIS and multivariate technique: a case study of Guwahati City. Environmental Earth Sciences, 81(16), 412.

[8] Panneerselvam, B., Paramasivam, S. K., Karuppannan, S., Ravichandran, N., & Selvaraj, P. (2020). A GIS-based evaluation of hydrochemical characterisation of groundwater in hard rock region, South Tamil Nadu, India. Arabian Journal of Geosciences, 13, 1-22.

[9] Aravindan, S., Shankar, K., Ganesh, P., & Rajan, K. D. (2010). Groundwater geochemical mapping in hard rock area of Gadilam river basin using GIS technique, Tamil Nadu, India. Journal of Applied Geochemists, 12(2), 209-216.

[10] Soujanya Kamble, B., Saxena, P. R., Kurakalva, R. M., & Shankar, K. (2020). Evaluation of seasonal and temporal variations of groundwater quality around Jawaharnagar municipal solid waste dumpsite of Hyderabad city, India. SN Applied Sciences, 2, 1-22.

[11] Balamurugan, P., Kumar, P. S., Shankar, K., Nagavinothini, R., & Vijayasurya, K. (2020). Non-carcinogenic risk assessment of groundwater in southern part of Salem District in Tamilnadu, India. Journal of the Chilean Chemical Society, 65(1), 4697-4707.

[12] El Behairy, R. A., El Baroudy, A. A., Ibrahim, M. M., Kheir, A. M., & Shokr, M. S. (2021). Modelling and assessment of irrigation water quality index using GIS in semi-arid region for sustainable agriculture. Water, Air, & Soil Pollution, 232(9), 352.

[13] Guan, H., Huang, J., Li, L., Li, X., Miao, S., Su, W., ... & Huang, H. (2023). Improved Gaussian mixture model to map the flooded crops of VV and VH polarization data. Remote Sensing of Environment, 295, 113714.

[14] Dong, W., Yang, Y., Qu, J., Xiao, S., & Li, Y. (2023). Local information-enhanced graph-transformer for hyperspectral image change detection with limited training samples. IEEE Transactions on Geoscience and Remote Sensing, 61, 1-14

IOP Conference Series: Earth and Environmental Science

PURPOSE-LED PUBLISHING™

PAPER • **OPEN ACCESS**

Groundwater remediation techniques around Kodungaiyur dump yard

To cite this article: R. Aishwarya *et al* 2024 *IOP Conf. Ser.: Earth Environ. Sci.* **1409** 012026

View the article online for updates and enhancements.

You may also like

- SOLAR ACTIVE LONGITUDES FROM KODAIKANAL WHITE-LIGHT DIGITIZED DATA
Sudip Mandal, Subhamoy Chatterjee and Dipankar Banerjee
- Entropy for spherically symmetric, dynamical black holes from the relative entropy between coherent states of a scalar quantum field
Edoardo D'Angelo
- Kodama-like vector fields in axisymmetric spacetimes
Philipp Dorau and Rainer Verch



This content was downloaded from IP address 47.247.77.11 on 27/11/2024 at 05:39

Groundwater remediation techniques around Kodungaiyur dump yard

Aishwarya, R.[1*], Hemamathi, A.[2], Binu Sukumar[3] and Yuvaraj, M.[4]

[1,2,3] Department of Civil Engineering, R.M.K Engineering College, RSM Nagar, Gummidipoondi Taluk, Kavaraipettai, Tamil Nadu- 601206, India
[4] Proprietor, Skyrider Aerosolutions, Chennai, Tamil Nadu, India

[*]E-mail: raa.civil@rmkec.ac.in

Abstract. The groundwater around the Kodungaiyur dump yard, in Tamil Nadu, India, is polluted due to the percolation of leachate from the dumpsite. This paper proposes three remedial techniques to make the groundwater drinkable for the people living near the Kodungaiyur trash yard. Twelve bore wells around the Kodungaiyur dumpsite provided water samples for which the physicochemical parameters were measured. Moderately high concentrations of Total Hardness (TH), Total Alkalinity (TA), Chloride, Sulphate, Nitrate, Sodium, and Total Dissolved Solids (TDS) are present in the groundwater around the dump yard. The Physicochemical parameters of the samples tend to deviate from the standards prescribed by WHO and BIS. Therefore, remedial measures such as solar distillation, Activated Charcoal, and the Phytoremediation process are suggested to reduce the contaminants in the groundwater. The activated charcoal removes the unpleasant color of the water completely and makes the water clear and transparent through filtration. The solar distillation process does not affect the pH value and is reduced by 4.5% in the phytoremediation technique. Similarly, the level of chlorides is reduced by 99% in solar distillation and by 56% in the phytoremediation technique. Total hardness is reduced by 89.88% in the solar still process and 56.65% in the phytoremediation technique. Sodium is reduced by 99.88% in solar still and 57.03% in the phytoremediation technique. The economical and eco-friendly nature of the suggested techniques makes it sustainable for future generations.

Keywords: Groundwater, Solar distillation, Activated Charcoal, Phytoremediation

1. Introduction

The Corporation of Chennai is the largest generator of solid waste generated at a daily rate of 5400 metric tonnes. It has seven transfer stations and two landfill sites at Kodungaiyur and Perungudi [1]. Solid waste should be assorted, like recyclable, non-recyclable, compostable, hazardous, and non-hazardous waste. In the present system, the distinction is present only between the types of waste, like domestic waste, industrial waste, and construction rubble while, it is necessary to segregate the waste right from collection, transfer, and dumping. A separate collection system for e-waste has not been established so far and the majority of industrial and hospital waste also comes into the corporation system while it is the responsibility of the generator. By 2026, approximately 6590 tonnes of solid trash will be generated within the local body regions of CMA, including Chennai town, based on the current per capita generation of solid

Content from this work may be used under the terms of the Creative Commons Attribution 4.0 licence. Any further distribution of this work must maintain attribution to the author(s) and the title of the work, journal citation and DOI.
Published under licence by IOP Publishing Ltd

waste of 4248 tonnes [2]. The ecosystem has been contaminated as a result of the immoral handling of municipal solid waste, which has contaminated both surface and groundwater. Residents who live close to the trash yard now have to deal with very poor water quality. Under present garbage disposal techniques, the transit of debris from breakdown after its creation is unavoidable. The amount and types of pollutants produced in the landfill, as well as its closeness to the groundwater basin, significantly influence the degree to which groundwater is harmed. Leachate penetrates the subsurface and the effluent gas is released into the atmosphere during the trash disposal process. Rainwater gathered on the landfill during precipitation seeps into the earth, where it collects both organic and inorganic materials.

Many leachable materials will be released into the land throughout the decomposition process because organic and inorganic chemicals leach into the bottom even before the disposal procedures. Leachate, or tainted water, is the result of accumulated chemical substances polluting the water. Leachate from municipal landfills seeps into the ground and contains highly concentrated complicated effluents. It has dissolved organic matter, inorganic substances like calcium, magnesium, sodium, potassium, iron, sulfates, and chlorides, and xenobiotic organic materials that cast doubt on the groundwater's suitability for human consumption. Heavy metals are also absorbed by the percolating water before it enters the aquifer system. The dense, metallic elements that exist in lower amounts in water but are extremely dangerous and have a tendency to collect are referred to as heavy metals in water, also known as trace metals. Industrial wastes from mining sites, manufacturing and metal finishing companies, home sewer water, and road runoff are anthropogenic sources of heavy metals.

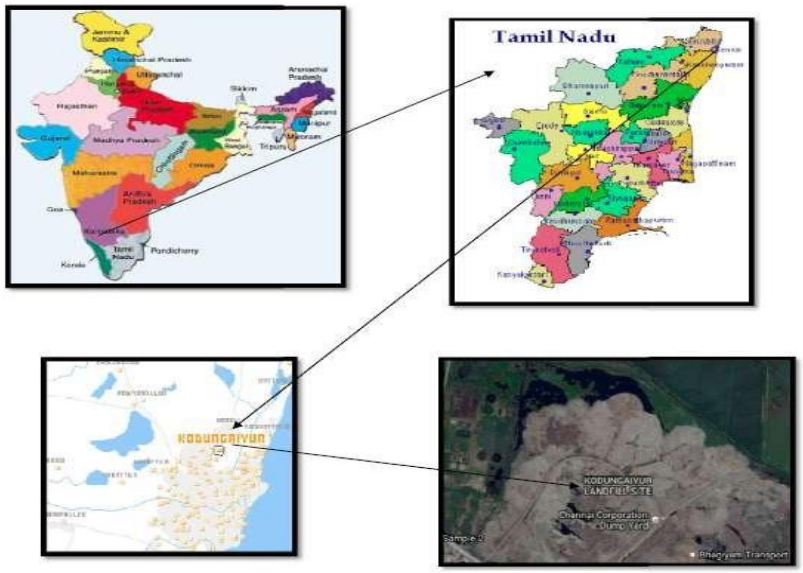


Figure 1. Study area.

2. Study area

The water quality is evaluated by determining the physical-chemical parameters for the water samples collected from the residences around the dump yard. An attempt was made to check the effectiveness of the remedial techniques in the reduction and removal of the parameters within permissible limits as explained in the following sections.

In Chennai, Tamil Nadu, India, there is a residential neighbourhood called Kodungaiyur. Within the Chennai District, it falls under the Perambur Taluk. A sizable region, Kodungaiyur is bounded to the north by Manali, to the east by Korukkupet, to the west by Madhavaram Milk Colony and Madhavaram, to the southwest by Perambur, and the south by MKB Nagar (Vysarpadi). National Highway 16 (NH 16) touches this area in the southwest of Moolakadai. As seen in Figure 1, Kodungaiyur's latitude and longitude are 13.140961°N and 80.248175°E, respectively. Kodungaiyur is home to a large number of educational institutions as well as businesses like Indian Oil Corporation, Madras Refinery Limited, and Madras Fertilizer Limited. The largest landfill in the city is Kodungaiyur, which has been attended to by Chennai Corporation since 1987. The Greater Chennai Corporation states that the 269-acre dump yard has been in operation for more than 35 years and receives 2600–2800 metric tonnes of rubbish per day [3]. The dumpsite is surrounded by the Buckingham Canal on the north and the Bay of Bengal on the west, both of which slope towards the terrain. This open dump yard lacks lining facilities to stop leachate percolation, which hurts groundwater. The Kodungaiyur dump closure was a demand made by residents of north Chennai during the Assembly elections of 2016 and 2021. It violates the MSW guidelines established by the Ministry of Environment and Forests and has numerous negative repercussions on the local population. Depending on their priorities, the people living in the Kodungaiyur area rely on both private water supplies and groundwater. A questionnaire survey demonstrates that a growing amount of contamination prevents most people from having access to groundwater.

2.1. Testing protocol

Twelve water samples were taken in and around the Kodungaiyur trash yard to investigate the contamination of the groundwater. Following sampling, the water samples are subjected to an analysis of their various physico-chemical characteristics in accordance with Indian Standards (IS3025). Common tests performed on any water sample include Chlorides, pH, Electrical Conductivity, Sulfates, COD, BOD, Total Hardness, Total Dissolved Salts and Total Alkalinity [4]. It facilitates understanding of the fundamental physical properties. Table 1 and 2 displays the test findings that were collected.

3. Groundwater remediation techniques

Groundwater remediation is the process of removing pollutants from groundwater. The moderately high concentrations of Total Hardness (TH), Total Alkalinity (TA), chloride, sulphate, nitrate, sodium, Total Dissolved Solids (TDS), and iron in the groundwater in the proximity of the dump yard deteriorate its quality for drinking and other domestic purposes. It is clear that leachate significantly affects groundwater quality in the vicinity of the dumpsite because there is no natural or other explanation for the elevated quantity of these pollutants. The percolation of leachate is unavoidable due to the heavier garbage load on the dumpsite. This creates the necessity for treating the groundwater to make it potable. The quality of groundwater was found to improve with some of the recommended techniques which include the solar distillation process, Activated Charcoal, and Phytoremediation process.

Table 1. The concentration of Physico-chemical in water samples.

Location	1	2	3	4	5	6	7	8	9	10	11	12
pH	7.37	6.99	7.3	7.25	7.46	7.31	7.34	7.11	7.53	7.25	7.48	8.04

COD	(mg/L)	498.304	10911.908	4984.26	273.5	24	28	20	12	8	24	12	8
BOD	(mg/L)	527.793	11656.811	5176.67	273.125	5	6	4	4	5	5	6	4
Conductivity	(µs/cm)	888	16820	9120	647	1350	1697	609	3130	2540	5410	3460	2210
Total hardness	(mg/L)	557.282	12401.714	5369.08	272.75	388	344	142	374	718	880	324	596
Chlorides	(mg/L)	260	3949	1475	110	180	310	120	550	625	1225	575	325
Sulphates	(mg/L)	468.815	10167.005	4791.85	273.875	19	9	40	216	112	254	372	307
TDS	(mg/L)	425	12443	6641	335	811	962	350	1861	1556	3253	2109	1467
Calcium	(mg/L)	586.771	13146.617	5561.49	272.375	133	97	34	101	162	186	65	170
Magnesium	(mg/L)	616.26	13891.52	5753.9	272	14	25	14	29	76	101	39	42
Sodium	(mg/L)	704.727	16126.229	6331.13	270.875	95	174	50	598	260	898	772	298
Potassium	(mg/L)	4	38	51	4	22	28	2	38	19	44	45	19
Alkalinity	(mg/L)	645.749	14636.423	5946.31	271.625	477	456	138	541	254	721	392	329
Nitrate	(mg/L)	675.238	15381.326	6138.72	271.25	5	6	2	8	12	13	11	4

Table 2. Comparison of Physico-chemical parameters with TNPCB and BIS Standards.

Parameters	pH	Conductivity	TDS	Chlorides	Sulphates	COD	BOD	Hardness	Calcium	Magnesium	Total alkalinity	Nitrate	Sodium	Potassium
Minimum	6.99	609	335	110	9	4	4	69	16	7	64	2	50	2
Maximum	8.04	16820	12443	3949	372	236	71	2113	324	317	721	140	1649	51
TNPCB tolerance limits	Min	6.5	-	-	-	-	-	-	-	-	-	-	-	-
	MAx.	8.5	-	-	-	-	-	-	-	-	-	-	-	-
BIS Standards	6.5-8.5	-	500	250	200	-	-	300	75	-	200	45	-	-
Effects of undesirable limits	Taste	-	Gastro intestinal effect	Taste affected	Laxative effect	-	-	Scale formation	Scale formation	Scale formation	Boiled rice turns yellow	Blue baby syndrome	-	-

3.1. Solar Distillation

This process removes impurities like salts, heavy metals as well as microbiological organisms [5]. It is a passive solar distiller that solely needs sunshine to operate. Solar still will offer enough drinking water for family and cooking purposes. Figure 2, The base of the solar still is made of a Galvanized Iron box of dimensions (3' x 2' x6") painted in black on the inside to absorb heat. The frame is screwed along the sides of the G.I. box to support the top cover. The top cover is the route from which radiation emerges on the basin's surface. The top of the G.I. box is covered using fibreglass of thickness 4mm. Fibreglass cover is selected for its features like transparency to solar radiation, non-absorptivity to water, and clean and smooth surface. As the moisture-laden air rises to the sloping sheet of comparatively cool fibreglass attached to the box, water condenses out in the form of small droplets that cling to the fibreglass as in Figure 3. As these droplets get heavier, they roll down the fibreglass to the collection tube at the bottom and then out to the water-collecting container.



Figure 2. Experimental setup of Solar Still

3.2. Phytoremediation

One of the most extensively studied topics in the world is phytoremediation, which recycles nutrients from aquatic plants to treat water pollution. It is a promising bioremediation method. Aquatic macrophytes store heavy metals and harmful nutrients, which helps to maintain the proper oxygen balance. A wide range of aquatic floating macrophytes with rapid growth rates and low maintenance requirements have been suggested for wastewater bioremediation. Azolla pinnata, Figure 4, one of the macrophytes that include duckweed and water fern, is used in bioremediation to remove toxins from soils, sludge, sediments, surface water, and groundwater. Fast-growing Azolla pinnata is a free-floating water fern that can thrive even in the absence of nitrogen in the surrounding water. Normally, Azolla pinnata is grown in paddy fields or shallow water bodies. It contains 25 to 30 percent protein, 10 to 15 percent of minerals, and 7 to 10 percentage of amino acids, bioactive substances, and biopolymers. It can remove Hg, Cd, Pb, Cr, As, Ag, Pt, and Au from water [6].



Figure 3. Collection of treated water from solar still



Figure 4. Growth of Azolla pinnata during remediation process

3.3. Activated Carbon filter

Carbon filtering is a filtration method that gets rid of contaminants and pollutants by using an activated carbon bed and chemical adsorption. The mechanism of action of activated carbon is based on the principle of adsorption, in which the molecules of pollutants present in the fluid are drawn into the pores of the carbon substrate. The location and size of pores determine how efficient AC filtering is. When carbon pores are big enough to let impurities adsorb onto them, filtration happens. AC filters are frequently the best option for removing large molecules and organic substances. The rate of adsorption will often be higher at lower temperatures and pH values. The duration of time of contact of the contaminants with the AC filter also influences the adsorption process. A higher volume of active carbon and a slower filter rate will improve the effectiveness of the filter. As seen in Figure 5, Three layers are formed using coarse aggregate, fine sand, and activated charcoal. The bottom-most layer which acts as the bed to the top charcoal layer is formed using cotton which allows only the water and all other sediments to be retained. The second layer is the activated charcoal layer which acts as the filter media. It works under the adsorption process where all the sediments and other constituents are adsorbed. The third layer is made of finer sand which helps in removing coarser particles. The topmost layer is the coarse aggregate which also acts as a filter media for granular particles. [7]



Figure 5. Treated water sample using Activated carbon filter

4. Results and Discussion

4.1. Groundwater quality data

The water samples collected are analysed for various Physicochemical parameters and heavy metal content. It is essential to assess the stability of groundwater for drinking and other domestic purposes Table 2 summarizes the analytical results of the groundwater samples and compares the parameters of groundwater quality with the Tamilnadu Pollution Control Board (TNPCB) and the Bureau of Indian Standards (BIS) [8]. The comparison makes clear that some of the chemical components are more than what is safe to consume. The quality of groundwater is affected due to the presence of landfills, open dumps, use of fertilizer, disposal of industrial wastes, mining activities, absence of underground drainage system, continuous burning of Municipal Solid Waste (MSW) etc. In the study area, the major reason for water contamination is the presence of an open dump and the burning of waste which causes the leachate to percolate deep down into the ground [9].

4.2. Physicochemical parameters

One of the most important operational water quality factors is pH. According to the TNPCB (Tamilnadu Pollution Control Board) and the BIS (Bureau of Indian Standards), the ideal pH value is between 6.5 and 8.5. Water is considered basic and prone to scaling if its pH is higher than 7. Acidic water (pH less than 7) can lead to corrosion. The pH values in the groundwater data that were gathered ranged from 6..99 to 8.04. Since the pH level near the Kodungaiyur dump yard is within allowable bounds, it is deemed suitable for residential usage. Dissolved solids are defined as the concentration of mineral content dissolved in water. Brackish water is defined as subsurface water with a TDS content of more than 1000 mg/l. According to TNPCB regulations, TDS may not exceed 500. The TDS value in the Kodungaiyur region is between 335 and 12443 mg/l. S2 had the greatest total dissolved solids concentration, according to the findings. In numerous areas in Kodungaiyur, it was found that the TDS content exceeded allowable limits.

Sodium is the main component in bodily fluids and an important nutrient. When ingested by food and drinking water, sodium doesn't affect people in typical amounts. It is very soluble when it leaches into groundwater from the terrestrial environment or when saltwater intrusion from coastal regions and road salt occurs. The EPA advises taking 500 mg or more of sodium daily for optimal health. It is also not advised for those with heart problems to consume excessive amounts of sodium. The World Health Organization recommends a maximum allowable value of 200 mg/l of salt in drinking water. The salt contents in this study, which range from 50 to 1649 mg/l, are higher than the allowable limits. S3 has a high percentage of sodium. The presence of bicarbonates and carbonates of calcium and magnesium is what causes hardness in water. According to TNPCB,

hardness is only found within the limit at three sampling sites (300 mg/l). Extremely hard water can cause scaling inside tanks and pipes and is not recommended for residential use. The amount of chloride in natural water varies depending on the geological conditions. Chloride concentrations can result from the leaching of saline wastes into the soil, and the disposal of industrial waste, or sewage. A high percentage of chloride gives drinking water a salty taste. Water quality statistics show that the range of chloride level is 110 mg/l to 3949 mg/l. The optimal limit, according to TNPCB, is 250 mg/l. Chloride is prevalent in large amounts. It is imperative that action be done to reduce its content to the required amount. Potassium is abundant in the environment, including natural streams, and is a necessary element for human health. Groundwater from the research region has a gradually varying potassium level, ranging from 4 mg/l to 50 mg/l. If potassium chloride is utilized in water softeners to regenerate ion exchange, then serious health problems could result from the treatment. High-risk patients with kidney disease, coronary artery disease, hypertension, etc. are processed by these.

Many minerals, such as barite, epsomite, and gypsum, naturally include sulphates. These dissolved minerals add to the mineral composition of many groundwater resources. Water at the Kodungaiyur trash yard has a sulphate content ranging from 10 mg/l to 350 mg/l. According to TNPCB regulations, the maximum allowable limit for sulfate content in water are 400 mg/l. The water is therefore within acceptable bounds. The overabundance of sulfate ions in drinking water causes digestive issues, diarrhea, and unpleasant odors. The most significant property of water is its alkalinity, which is the capacity to counteract acidic qualities. The ideal limit for total alkalinity, according to BIS guidelines, is 200 mg/l. The Kodungaiyur waste yard's water quality standards demonstrate the difference in alkalinity levels between samples. The range is 64–721, mg/l. The water so above the tolerance limit. The taste of the water is significantly affected by its high alkalinity level, rendering it unfit for human consumption. Legumes, plant detritus, animal excrement, and the atmosphere are the principal sources of nitrate in water. A bitter taste is added to the water and causes physiological irritation in humans when there is nitrate content present. In humans, water from shallow wells with more than 45 mg/l can produce methemoglobinemia, sometimes known as "blue baby syndrome." One of the main causes of the increased nitrate concentration is also dumpsites. The maximum amount of nitrate allowed in water, according to TNPCB, is 20 mg/l. The nitrate level in the study area varies from 2 to 140 mg/lt. In S2, nitrate concentration is observed to be high.

4.3. Effect of groundwater remediation

Performance investigation of the proposed technologies was carried out through measurements of different parameters of water after treatment. From the water quality test results it is evident that S2 & S3 have a higher amount of contamination. Hence S2 is chosen to carry out the performance analysis for the technologies suggested. The higher concentrations of total hardness, total alkalinity, chlorides, sodium, total dissolved solids, and pH found near dumpsite deteriorate the quality for drinking and other domestic purposes. After the treatment process, the samples are subjected to physical and chemical tests [10] to determine the quality of treated water as shown in Table 3. Appropriate comparisons are made among the recommended technologies to categorize the implementation of processes based on the level and efficiency of the contaminants [11]. Table 4 shows the percentage reduction of contaminants in groundwater samples after treatment and it also correlates with the efficiency of each technique.

Table 3. Drinking water parameters after remediation.

Parameters	Before treatment	After treatment

	Sample Site: S2	Phytoremediation using Azolla pinnata	Solar distillation
pH	6.99	6.67	6.99
Conductivity	16820	7967	1574
TDS	12443	2263	1251
Total alkalinity	382	84	37
Total hardness	2113	726	213
Chloride	3949	1727	434.39
Sodium	1631	700	1.9572

From the above table, it is evident that major contaminants like hardness, total alkalinity, Sodium, Chloride and total dissolved solids are greatly reduced in Solar still and the Phytoremediation process. Solar still is capable of reducing contaminants within the permissible limits. A higher amount of sodium contamination in the groundwater in the proximity of the dumpsite can be reduced through the distillation process.

Since the discharge of water through the distillation process is low, it can still provide enough water for drinking and cooking needs for a family. Solar still is an appropriate site-specific technology that requires no electricity to run, easy to use and maintain. The phytoremediation process using a floating fern Azolla pinnata can be recommended in areas where the hardness and the TDS content of the groundwater are high. The Azolla pinnata plant is suspended in a collection tank which absorbs all the contaminants and gives us potable water. Since it is a floating fern it will not cause any clogging problem during the supply. It is one of the efficient and economical ways of treating water. Activated charcoal filters are effective in the reduction of chlorine, sediments, volatile organic compounds, taste and odour from water. From the analysis of treated water quality parameters, it is evident that AC is not efficient in removing minerals, salts and dissolved inorganic compounds which are higher in concentrations in the study area. Therefore, this AC filter is not much recommended for treating groundwater near Kodungaiyur.

Table 4. Efficiency of each technique in reducing contaminants.

Parameters	Reduction (%) after the treatment of water samples	
	Phytoremediation	Solar water distillation
pH	04.49	No change
Conductivity	52.63	90.64
TDS	81.81	89.94
Total alkalinity	77.85	90.14
Total hardness	65.64	89.88
Chloride	56.25	89.00
Sodium	57.03	99.88

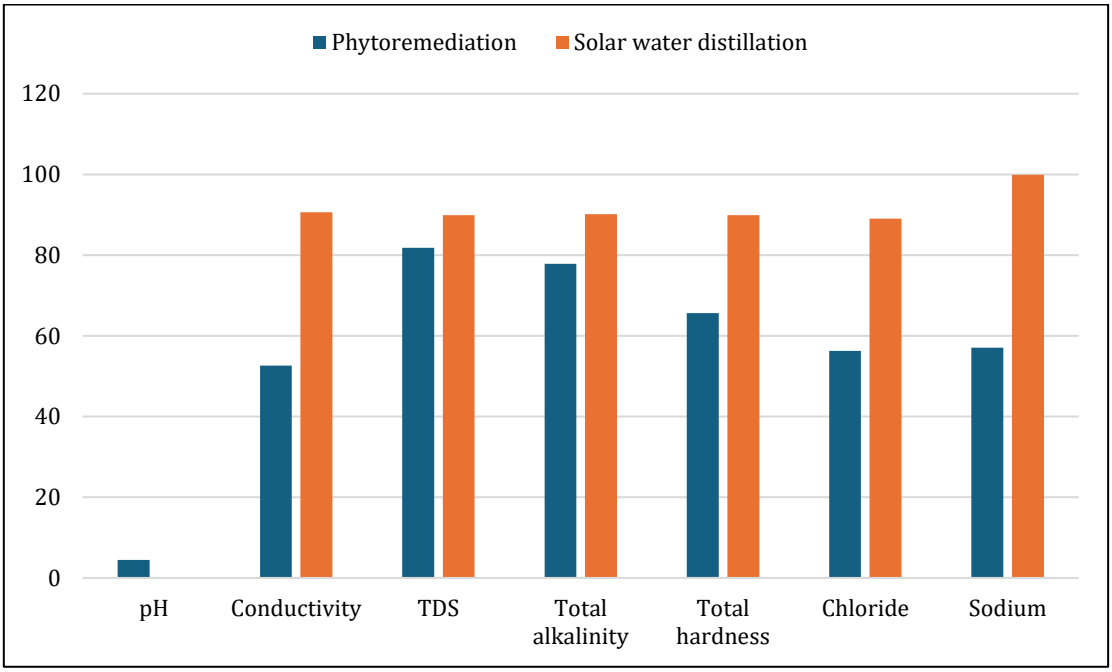


Figure 6. Comparison of test results after treatment with Phytoremediation and Solar water distillation

5. Conclusion

The criteria that deviate from the TNPCB norms the most are sodium, total hardness, TDS, and chloride. These factors hurt the unfitness of the water to drink. While the quantity of certain contaminants is not higher than that of drinking water, the condition of groundwater poses a serious risk to human health. Hence the treatment techniques for particularly affected parameters are focused and suggested. For the samples with high sodium content, the solar water distillation process proves to be more efficient than the other methods. Similarly, for the groundwater samples with high hardness and heavy metal content phytoremediation technique seems to be more effective. For water with high turbidity content activated carbon filter is more effective. Hence, from the test results obtained, it is prominent that each technique is effective and efficient in reducing the particular deviated parameters in the affected water samples. The survey conducted by the questionnaire around Kodungaiyur locality depicts that majority of the population is affected by the contaminated groundwater qualities. Hence, if the suggested remedial techniques are incorporated at each residence, the groundwater can be used effectively despite its contamination. Further, the economic and eco-friendly nature of the techniques suggested makes it sustainable for future generations.

References

[1] Apoorva Ramaswamy, "Impact of the Kodungaiyur dump hard on health: findings from the health service provider's study", Citizen consumer and Civil Action group, Blogs, 2019. https://www.cag.org.in/blogs/impact-kodungaiyur-dump-hard-health-findings-health-service-providers-study.

[2] Laasya Shekhar, 2019, "Nearly a third of Kodungaiyur residents have difficulty breathing, but no action on waste dump", Citizen consumer and Civil Action group, Blogs.

[3] Afroz Khan, 2020, "Destruction of marshlands due to garbage dumping", Citizen consumer and Civil Action group, Newsletter.

[4] R Aishwarya. "Assessment of Spatial Distribution of Physico-Chemical Parameters of Groundwater around Kodungaiyur Dump yard", J. Phys.: Conf. Ser. 2070 012215, 2021. https://iopscience.iop.org/article/10.1088/1742-6596/2070/1/012215 .
[5] Zargistalukder and Avizitebasak foisal (2013), "Design and performance evaluation of solar water distillation plant", Global journal of researches in engineering (volume 13, Issue 1, 2013).
[6] Dr.T.MuraliKrishna, Dr.V.Sivasubramanian, Ms.K.Divya, Ms.J.Christina Shiny, Ms.S.Kalaivani, "Treatment and analysis of Industrial Effluent using Phytoremediation Technology", Test Engineering and Management, ISSN: 0193-4120, Volume 82, 2020.
[7] A. Hemamathi, Binu Sukumar, R. Aishwarya, A. Kruthikameenakshy, V. Nivetha, J. Pradhiksha, B. Rashika, "Treatment of textile waste water using activated carbon method", Materials Today: Proceedings, 2023, ISSN 2214-7853, https://doi.org/10.1016/j.matpr.2023.10.027.
[8] Chavan.B.L and Zambare.N.S, "Physiochemical Analysis of Groundwater samples in Sholapur City, Maharastra ,India", International journal Research Civil Engineering Archit.Des. ,vol.2,no.3,pp.712,2014, https://www.researchgate.net/publication/268059050_Physicochemical_Analysis_of_Groundwater_Samples_in_Solapur_City_Maharashtra_India.
[9] Aishwarya R, Faizuneesa A, Hemamathi A, Ramshankar P, Yuvaraj M. Correlation Study of Physico-Chemical Parameters and Water Quality Index Around Kodungaiyur Dumping Ground, IOP Conf. Series: Earth and Environmental Science, https://doi:10.1088/1755-1315/1084/1/012061.
[10] Agrawal PR, Singhal S, Sharma R. Heavy Metal Contamination in Groundwater Sources. Groundwater Geochemistry: Pollution and Remediation Methods. 2021 Jun 25:57-78, https://doi.org/10.1002/9781119709732.ch4
[11] Aishwarya R, Hemamathi A, Binu S, Suvetha V (2023) Investigation and Indexing of Eco-Toxic Metals in the Groundwater Around the Kodungaiyur Dumpsite. Indian Journal of Science and Technology 16(13): 998-1006. https://doi.org/ 10.17485/IJST/v16i13.1405.

Acknowledgements

We are grateful to the residents who live near the Kodungaiyur dump yard for their cooperative efforts in gathering water samples and completing the survey.

IOP Conference Series: Earth and Environmental Science

PURPOSE-LED PUBLISHING™

PAPER • **OPEN ACCESS**

Innovative HDPE plastic aggregates in concrete: enhancing sustainability

To cite this article: Ratod Vinod Kumar and Dhondy Rupesh Kumar 2024 *IOP Conf. Ser.: Earth Environ. Sci.* **1409** 012027

View the article online for updates and enhancements.

You may also like

- Recycling of Waste Plastic into Fine-Grained Concrete Without Strength Reduction
M Chekanovich, S Romanenko and Ya Andriievska
- Different plastic-bag type photobioreactor for biomass production of *Chlorella* species
Yu Pei Chen, Yao Hsin Huang and Hsiang Chin Huang
- Mathematical modeling of rotating disk states
E V Semka, M A Artemov, Y N Babkina et al.



This content was downloaded from IP address 47.247.77.11 on 27/11/2024 at 05:39

Innovative HDPE plastic aggregates in concrete: enhancing sustainability

Ratod Vinod Kumar[1*] and Dhondy Rupesh Kumar[1]

[1]Department of Civil Engineering University College of Engineering, Osmania University, Hyderabad, India.

[*]E-mail: vinodrathod918@osmania.ac.in

Abstract. In the pursuit of sustainable construction practices, the integration of recycled materials into concrete production emerges as a pivotal strategy. This research delves into the integration of recycled High-Density Polyethylene (HDPE) plastic aggregates into concrete mixes, with the aim of bolstering both the mechanical properties and ecological sustainability of concrete structures. The study meticulously examines the compressive, tensile, and flexural strengths, along with Young's Modulus of Elasticity, of concrete specimens incorporating recycled HDPE plastic aggregates. Notably, a water-to-cement (w/c) ratio of 0.25 was employed in the concrete mix formulation, optimizing the material's performance. The plastic aggregates utilized in this study were meticulously prepared, comprising 50% recycled HDPE plastic and 50% sand, resulting in a balanced 1:1 ratio for the first type, while the second type featured a 1:2 ratio. Through rigorous experimentation and analysis, the findings elucidate the transformative potential of recycled HDPE plastic aggregates in reshaping conventional concrete production paradigms. This research underscores the viability of recycled HDPE plastic aggregates as a sustainable substitute for traditional aggregates, offering a compelling avenue for reducing environmental impact while enhancing structural integrity. The implications of this study extend beyond the laboratory, signalling a paradigm shift towards more environmentally conscious construction practices. As the construction industry continues to grapple with sustainability challenges, the integration of recycled materials such as HDPE plastic aggregates holds immense promise for fostering a greener and more resilient built environment.

Key words. Sustainable construction, Recycled materials, HDPE plastic aggregates, Concrete production, Environmental impact.

1. Introduction

The global construction industry faces a pressing challenge: how to reconcile the ever-growing demand for infrastructure with the imperative of environmental sustainability. In response to this challenge, there has been a growing interest in the integration of recycled materials into concrete production as a means of reducing environmental impact and enhancing sustainability. Among these materials, recycled High-Density Polyethylene (HDPE) plastic aggregates have garnered attention for their potential to revolutionize concrete production practices. Concrete, as one of the most widely used construction materials, plays a significant role in shaping the built environment. Conventional methods of manufacturing concrete predominantly depend on natural aggregates, including sand and gravel. These resources, however, are limited in supply and

Content from this work may be used under the terms of the Creative Commons Attribution 4.0 licence. Any further distribution of this work must maintain attribution to the author(s) and the title of the work, journal citation and DOI.
Published under licence by IOP Publishing Ltd

contribute significantly to environmental deterioration during extraction and transportation phases. Recognizing this issue, researchers and industry practitioners have turned their focus towards alternative materials, such as recycled HDPE plastic aggregates, to address sustainability concerns.

This research investigates the utilization of recycled HDPE plastic aggregates in concrete mixes with the aim of improving both mechanical properties and ecological sustainability. By incorporating recycled HDPE plastic aggregates into concrete mixes, the study seeks to mitigate the environmental impact associated with traditional aggregates while enhancing the performance of concrete structures.

The experimental investigation meticulously examines the compressive, tensile, and flexural strengths, as well as Young's Modulus of Elasticity, of concrete specimens containing recycled HDPE plastic aggregates. In addition to assessing mechanical properties, the study explores the feasibility of utilizing recycled HDPE plastic aggregates[1] as a sustainable substitute for traditional aggregates in concrete production. Through a detailed analysis of experimental findings and existing literature, this research aims to elucidate the transformative potential of recycled HDPE plastic aggregates in reshaping conventional concrete production paradigms.

Furthermore, the implications of this study extend beyond the laboratory, signalling a broader shift towards more environmentally conscious construction practices. As sustainability becomes an increasingly prominent concern in the construction industry, the integration of recycled materials such as HDPE plastic aggregates offers a promising avenue for fostering a greener and more resilient built environment. Thus, this research contributes to the ongoing discourse on sustainable construction practices and underscores the importance of innovation in addressing environmental challenges facing the construction industry.

2. Materials and methodology

2.1. Cement

The cement utilized in this study was 53-grade Ordinary Portland Cement, adhering to the specifications outlined in IS 12269-2013[2].The physical requirements are outlined in relevant standards, with detailed findings presented in Table 1

Table 1. Laboratory test results of Cement

Property	Results	Limits as per IS 12269-2013	Test method
Fineness (Retained 90 mm).	Less than 1%	Max 10%.	IS4031(P1)-1996[3].
Specific Gravity	3.14		IS 4031(P11)-1988[4].
Soundness by Le-Chatelier's	5mm	Max 10mm.	IS 4031(P3)-1988[4].
Initial -setting time	61min	min 30min.	IS 4031(P5)-1988[5].
Final setting time	335min	Max 600min	
Standard consistency	34%		IS 4031(P4)-1988[5]

2.2. Fine aggregate

The fine aggregates used are natural river sand shown in Table 2 and the properties of fine aggregate(sand) conform to Zone II of IS 383 having a fineness modulus of 2.61.

Table 2. Laboratory test results of Fine Aggregates.

Test	Results	Limits	Reference code	Test Method
Specific Gravity	2.63		IS 383–2016[6]	IS 2386 (P3) 1963[7]

Water-absorption%.	0.80%	Max 2%	IS 383–2016[6]	
Particle passing 75 mm.	1.1%	Max 15%	IS 383–2016[6]	IS 2386 (P1) 1963[5]

2.3. Coarse aggregates

Plastic-Sand Aggregates: - 1:1 plastic-sand Aggregates (one part of plastic means 50% of plastic and 1 part of sand means 50% of sand (500grams of plastic 500grams of sand)), 1:2 plastic-sand Aggregates (one part of plastic and 2parts of sand (means 500grams of plastic 1000grams of sand)), Figure 1 illustrates a flowchart delineating the step-by-step process involved in preparing plastic sand aggregate. The foundational material utilized for manufacturing plastic aggregate is HDPE (High-density polyethylene), procured from a local supplier specializing in the collection and treatment of various waste plastics within the vicinity. Waste plastic High-Density Polyethylene (HDPE) was sourced from the AADILAXMI plastic manufacturing plant situated in KUKATPALLY-Hyderabad. The treatment process encompasses collection, purification, shredding, melting, pelletizing, and ultimately, powdering to attain the final form. As part of the process, fillers comprising sand with median particle sizes ranging between 4.75 to 75μm were incorporated.

The particle size distribution was meticulously calculated, and based on this distribution, the fineness modulus of the corresponding material was determined. Fine aggregate Natural River sand, readily available in the market, was utilized. It passes through a 4.75 mm IS sieve, adhering to grading zone II of IS 383:1970, and exhibits a specific gravity of 2.61 (IS 2386 Part III, 1963), with a relative bulk density of 1460. The aggregates were prepared by heating 500 grams of HDPE in a locally available metallic iron TAWA[1], commencing from room temperature at 27°C. The HDPE was then heated further until melted, reaching temperatures ranging between 294 to 339°C. Initially, 500 grams of sand were taken for 1:1 mix, followed by an additional 1000 grams for 1:2 mix, and mixed into the molten HDPE until a homogeneous dark paste was achieved. Subsequently, this mixture was poured onto a concrete base, and after a period of air drying, the material was broken into small pieces, resulting in aggregate sizes ranging from 4.75 to 20mm. The aggregates were then moulded into the necessary shapes, with the formed sizes ranging from 1mm to 20mm.

Table 3. Physical properties of RPSCA aggregate

Physical Property	1:1-RPSCA	1:2-RPSCA
Aggregate impact value.	4.56	1.8
Abrasion value.	7.08	8.34
Flakiness index.	13.9	14.44
Elongation index.	14.8	14.13
Bulk Density(kg/m3) (ASTM C330-99: Table-2).	709	738
Absorption (%).	0.450	0.602
Particle Shape.	Sub angular	Sub angular
Type.	Crushed	Crushed
Nominal Maximum Size(mm).	20	20
Surface Texture.	Partially rough/ porous	Partially rough/ porous
Specific Gravity (IS:2386-1963).	1.60	1.68
Colour.	brown	brown

Table 4. Plastic-Sand (1:1) Sieve analysis for formed coarse aggregate.

Sieve size. ASTM and (IS)	Weight retained weight.	Cumulative weight retained. (g)	Cumulative percentage retained. (%)	Cumulative percentag	Cumulative percentage	Cumulative percentage	Remarks

	(g) A	B	(B*100/5000) =C	e passing (100-C)	standard value (IS code 383-1978)[6] (%)	standard value AST M C-33[8] (%)	
37.5(40) mm	0.00	0.00	0	100	100	100	Satisfied
19(20) mm	206	206	4.1	95.9	85-100	90-100	Satisfied
9.5(10) mm	3699	3905	78.1	21.9	0-20	10-50	Unsatisfied
4.75mm	613	4518	90.4	9.6	0-5	0-15	Satisfied
Pan	465	4983	99.7	0.3	0	00	Satisfied

Table 5. Plastic-Sand (1:2) Sieve analysis for formed coarse aggregate.

Sieve size. ASTM and (IS)	Weight retained weight. (g) A	Cumulative weight retained. (g) B	Cumulative percentage retained. (%) (B*100/5000) =C	Cumulative percentage passing (100-C)	Cumulative percentage standard value [6] (%)	Cumulative percentage standard value [8] (%)	Remarks
37.5(40) mm	0.00	0.00	0.00	100	100	100	Satisfied
19(20) mm	160	160	3.2	96.8	85-100	90-100	Satisfied
9.5(10) mm	3777	3937	79.04	20.96	0-20	10-50	Satisfied
4.75mm	678	4615	92.65	7.35	0-5	0-15	Satisfied
Pan	368	498	100	0.00	00	00	Satisfied

2.4. Superplasticizer

The superplasticizer utilized in this study was obtained from Fosroc Chemicals India Pvt. Ltd. The specific chemical, known as Conplast SP430, adheres to both BS 5075 Part 3 and ASTM C494[9] standards, qualifying as Type A and Type F, respectively. Conplast SP430 is characterized as a chloride-free, super plasticizing admixture formulated with carefully selected sulphonated naphthalene polymers. It is supplied in the form of a brown solution, readily dispersible in water. Typically, for concrete requiring high workability, the recommended dosage range falls between 0.70 to 1.30 Liters per 100 kilograms of cementitious material.

Table 6. Properties of Superplasticizer

Appearance	Brown liquid
Specific gravity-	Typically, 1.20 at 20°C
Chloride content-	Nil to BS 5075
Air entrainment-	Typically, less than 2% additional air is entrained at normal dosages
Alkali content-	Typically, less than 72.0 g. Na2O equivalent/litre of admixture. A fact sheet on this subject is available.

3. Methodology of work

Determining the appropriate water-to-cement (w/c) ratio and superplasticizer dosages is critical, considering both workability and strength requirements[10]. Mix design adhered to the guidelines outlined in ACI211.2-98[11]. Aiming to achieve optimal workability within the range of 25–50 mm while maintaining desirable strength levels. Workability was assessed using the slump test. Initially, trial mixes were conducted using a w/c ratio of 0.25 to ascertain the dosage capacity of the superplasticizer. A dosage of 1.0% superplasticizer was found suitable for conventional concrete mixtures with a w/c ratio of 0.25, based on the results obtained. Subsequently, cubical Molds conforming to IS: 10086–1982[5], with dimensions of 150 mm on each side, were prepared. Compressive strength tests were performed on specimens containing two types of aggregates. This systematic approach ensures that the concrete mixture meets mechanical properties.

3.1. The procedure for designing elaboration mixtures.

- **Stage 1:** Selection and Fixation of the Water-Cement Ratio: In this research, a water-cement ratio of 0.25 was utilized. Determining the appropriate water-cement ratio involves considering various parameters, including strength requirements, and finishing characteristics. Due to the variability in strength produced by different aggregates and cement types under the same water-cement ratio, establishing a relationship between the water-cement ratio and strength is crucial. While precise data may be lacking, conservative values from IS 10262-2019 guidelines (Free w/c ratio vs. 28-day compressive strength ratio curve)[1] are often employed for Portland cement concrete. The strength of any type of concrete is primarily governed by the water-cement ratio. While standard mix designs typically utilize a water-cement compressive strength curve to estimate the water-cement ratio, this study proposes a novel relationship for plastic aggregate concrete.
- **Stage 2:** Modifying Water Content: The water content in concrete, denoted as "w" in kg/m3, is crucially determined by the requirements outlined in ACI 211-98[11] and the desired workability specific to the project at hand. Typically, the free water content for non-air-entrained concrete ranges between 187 kg/m3 and 237 kg/m3[1]. Incorporating 1.0% superplasticizer, such as sulfonated naphthalene polymer concrete mix, has been shown to effectively decrease water content by up to 25%.
- **Stage 3:** Calculation of Cement Content: The cement content ("c" in kg/m3) for each mixture can be calculated using the equation (a), assuming the water-cement ratio from Stage 1.
  Cement content (kg/m^3)} = w /(w/c)
- **Stage 4:** Identification of Coarse and Fine Aggregates: In this procedure, the coarse aggregates are constituted by plastic sand aggregates, while the fine aggregates comprise natural river sand. The determination of the total aggregate quantity follows the absolute volume approach. Two distinct types of coarse aggregates were employed, conforming to ASTM C330/C330M[8] and ASTM C33 combined grading specifications, maintaining a water-cement ratio of 0.25. Typically, non-air-entrained concrete retains approximately 2% entrapped air. The volume of coarse aggregate required per unit volume of concrete is influenced by its nominal maximum size and the fineness modulus of the standard weight fine aggregate. The volume of aggregate is computed by multiplying the volume of coarse aggregate by its oven-dry loose weight per cubic meter.
- **Stage 5:** Estimation of Fine Aggregate Content: After estimating all concrete materials except fine aggregate in Stage 4, the difference is used to determine the amount of fine aggregate required. This calculation considers the air content of the concrete and the specific gravity of the lightweight plastic coarse aggregate. While the estimate for concrete

weight per m3 may be approximate, the mix proportions allow for easy adjustment based on test batches.

- **Stage 6:** Testing of Recycled Plastic Aggregate Mixtures: Test mixes are prepared using proportions obtained from the technique. Several strength tests should be conducted on concrete prepared with recycled plastic aggregate to evaluate its fresh and strength properties effectively.

4. Results and discussion

During the initial stage of concrete preparation, great care was taken to ensure its uniformity and stability, thereby preventing any potential segregation or handling issues. Visual assessment confirmed that the concrete exhibited no signs of segregation or bleeding. Utilizing the provided table, the dosage of superplasticizer was meticulously calculated. It was observed that the amount of superplasticizer required to achieve workable high-strength concrete with plastic aggregates was minimal. The decreased requirement for superplasticizers can be linked to the subangular form of the aggregates, potentially improving the concrete's ease of handling.

Table 7. Mix details for the developed concrete

w/c ratio	Sample type	Cement-Kg/m^3	Water Kg/m^3	Fine-aggregate Kg/m^3	Coarse aggregate Kg/m^3	Superplasticizer Kg/m^3
0.25	1:1-RPSCA	568	187	865	709	5.68
	1:2 -RPSCA	568	178	824	738	5.68

Estimations suggest that the plastic densities of lightweight concrete containing synthetic aggregates range between 2155 and 2223 kg/m3, whereas standard concrete densities typically fall within the range of 2200-2600 kg/m3. This observation underscores the potential of fully replacing the coarse aggregates of regular concrete with recycled plastic sand. Structural lightweight concrete is commonly categorized based on its air-dry density and wet density, as outlined in most guidelines.

Table 8. Densities of the developed concrete.

w/c ratio	Sample-type	Fresh-Density (kg/m^3)	Air-dry Density (kg/m^3)
0.25	1:1-RPSCA	2223	2213
	1:2-RPSCA	2165	2155

4.1. Compressive strength

To ensure structural integrity, structural lightweight concrete must possess a minimum compressive strength of 17 MPa. ASTM C 330 serves as the benchmark standard, delineating the manufacturing specifications required for such products. Comparison of Compressive Strength Results for Recycled HDPE Plastic Aggregates. In the assessment of concrete's mechanical properties, compressive strength is a key indicator of its structural performance. This study aims to compare the compressive strength results of concrete specimens prepared with recycled High-Density Polyethylene (HDPE) plastic aggregates in two different ratios: 1:1 (1 part plastic to 1 part sand) and 1:2 (1 part plastic to 2 part sand). The water-to-cement (w/c) ratio for both mixes was maintained at 0.25. Concrete specimens were cast using recycled HDPE plastic aggregates in the specified ratios, ensuring consistent mixing and compaction procedures. After the curing period, the compressive strength of each specimen was determined through the application of axial loads until failure using a compression testing machine. The compressive strength (F) of each concrete specimen was calculated using the standard formula and the strength results for the two mixes are as follows: -

- For the 1:1 ratio mix: F = 35.68 MPa and
- for the 1:2 ratio mix: F = 33.33 MPa.

The comparison of compressive strength results indicates that the concrete mix with a 1:1 ratio of recycled HDPE plastic aggregates to sand exhibited slightly higher compressive strength (35.68 MPa) compared to the mix with a 1:2 ratio (33.33 MPa). This difference in compressive strength may be attributed to the varying proportions of plastic aggregates in the mixes, leading to differences in the packing density and interfacial bonding within the concrete matrix. the compressive strength test results suggest that the mix with a 1:1 ratio of recycled HDPE plastic aggregates to sand achieved slightly higher compressive strength compared to the mix with a 1:2 ratio. However, both mixes demonstrated satisfactory compressive strength values, indicating the viability of recycled HDPE plastic aggregates as a sustainable alternative in concrete production.



Figure 1. Compressive strength of concrete cubes

4.2. Splitting tensile strength

Split Tensile Strength Results for Recycled HDPE Plastic Aggregates The split tensile test is a fundamental method used to evaluate the tensile strength of concrete specimens. In this study, we compare the split tensile strength results of concrete specimens prepared with recycled High-Density Polyethylene (HDPE) plastic aggregates in two different ratios: 1:1 (1 part plastic to 1 part sand) and 1:2 (1 part plastic to 2 parts sand). The water-to-cement (w/c) ratio for both mixes was maintained at 0.25 Concrete cylinders were cast using recycled HDPE plastic aggregates in the specified ratios. The mix proportions were carefully controlled to ensure consistency and accuracy. After curing for the prescribed duration, the concrete cylinders underwent the split tensile test to determine their tensile strength.

The split tensile strength (fct) of each concrete specimen was calculated using the standard formula and the split tensile strength results for the two mixes are as follows

- For the 1:1 ratio mix: f_{ct} = 3.35 MPa
- For the 1:2 ratio mix: f_{ct} = 2.85 MPa

The comparison of split tensile strength results indicates that the concrete mix with a 1:1 ratio of recycled HDPE plastic aggregates to sand exhibited a higher tensile strength (3.35 MPa) compared to the mix with a 1:2 ratio (2.85 MPa). This difference in tensile strength can be attributed to the varying proportions of plastic aggregates in the mixes. the split tensile test results demonstrate that the mix with a 1:1 ratio of recycled HDPE plastic aggregates to sand yielded superior tensile strength compared to the mix with a 1:2 ratio. These findings highlight the importance of optimizing aggregate proportions in concrete mix design to achieve desired mechanical properties. Further research could explore additional mix ratios and variations in the

properties of recycled HDPE plastic aggregates to identify the optimal combination for enhancing concrete performance.

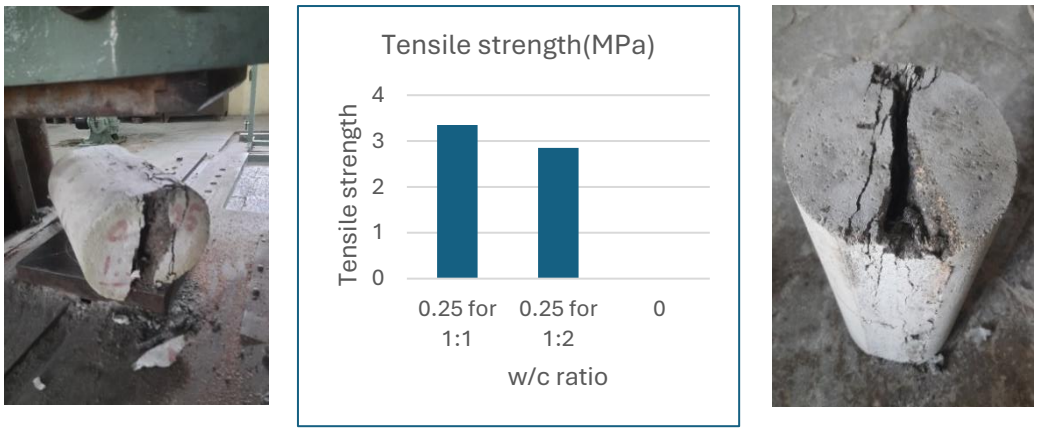


Figure 2. Split tensile test of cylinders.

4.3. Flexural strength

In assessing the performance of concrete in flexural applications, the flexural strength test provides crucial insights into its ability to withstand bending stresses. This study aims to compare the flexural strength results of concrete specimens prepared with recycled High-Density Polyethylene (HDPE) plastic aggregates in two different ratios: 1:1 (1 part plastic to 1 part sand) and 1:2 (1 part plastic to 2 parts sand). The water-to-cement (w/c) ratio for both mixes was maintained at 0.25. Concrete beams were cast using recycled HDPE plastic aggregates in the specified ratios, ensuring uniform mixing and compaction techniques.

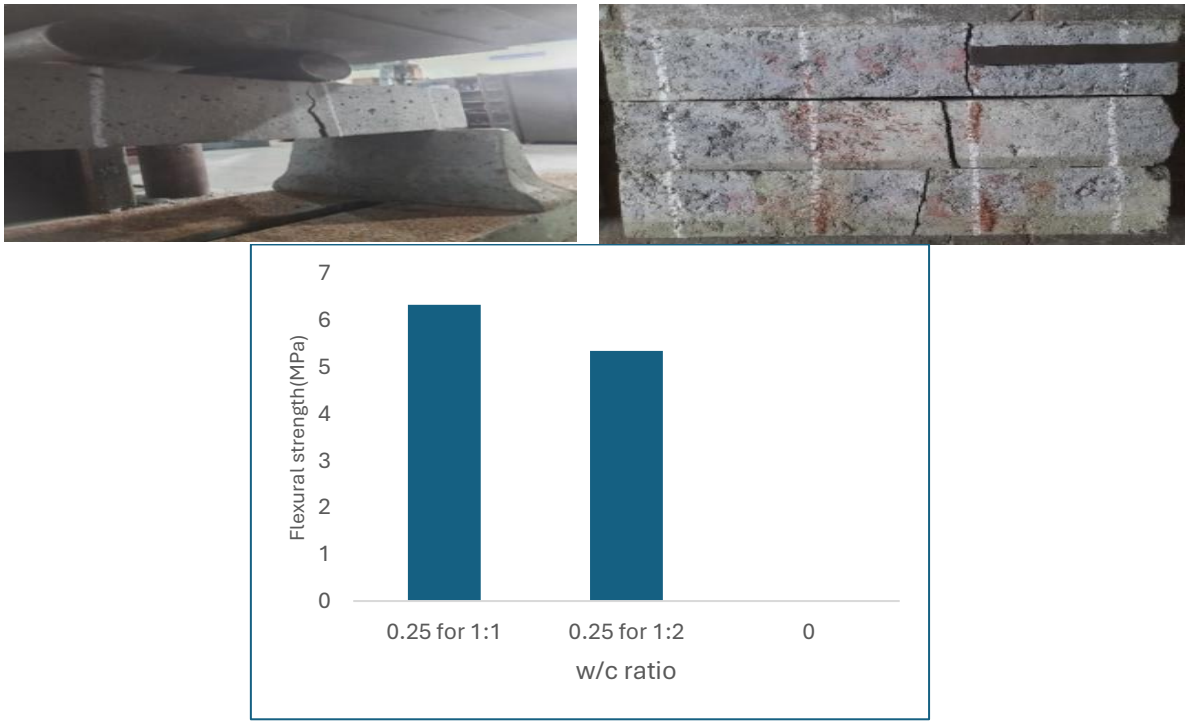


Figure 3. Flexural strength test of prisms

After the curing period, the flexural strength of each beam was determined through the application of a three-point loading system until failure. The flexural strength (F) of each concrete beam was calculated using the standard formula the results for the two mixes are as follows:

- For the 1:1 ratio mix: F=6.335F=6.335 MPa
- For the 1:2 ratio mix: F=5.35F=5.35 MPa

The comparison of flexural strength results reveals that the concrete mix with a 1:1 ratio of recycled HDPE plastic aggregates to sand exhibited higher flexural strength (6.335 MPa) compared to the mix with a 1:2 ratio (5.35 MPa). This difference in flexural strength may be attributed to variations in the distribution and packing of plastic aggregates within the concrete matrix, influencing the beam's resistance to bending stresses. the flexural strength test results suggest that the mix with a 1:1 ratio of recycled HDPE plastic- sand aggregates achieved higher flexural strength compared to the mix with a 1:2 ratio. These findings highlight the importance of optimizing aggregate proportions in concrete mix design to enhance flexural performance.

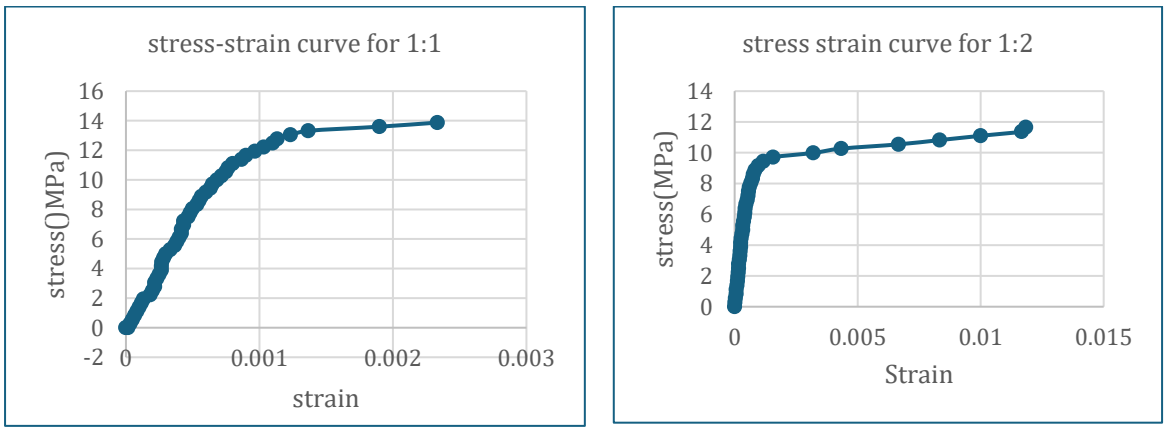
4.4. Youngs modulus of elasticity

Plotting Data on a Stress-Strain Curve: Start by plotting the stress on the y-axis and the strain on the x-axis, use a special function (scatter with smooth lines and markers or just the line) to accurately plot the data, Identifying the Elastic and Plastic Regions: Locate the elastic region, where a perfect straight line is present, this elastic region represents the linear relationship between stress and strain. Calculating Young's Modulus: Select the data corresponding to the elastic region, add a linear trendline to this data, and display the equation on the chart, The gradient of the trendline equation yields the Young's Modulus in megapascals, to convert to gigapascals, simply divide by a thousand. Measurement Validation: The accuracy of the obtained Young's Modulus can be verified using the r-squared value. A value close to 1 indicates a good regression line.

4.5. Key Elements from the Figures

Equation of the Line: - The equation "y = 12948x + 0.5905" suggests a linear relationship between stress (y) and strain (x), This equation likely represents the linear regression line fitted to the elastic region of the stress-strain curve, where "y" represents stress and "x" represents strain, Coefficient of Determination (R-squared):- The value "R^2 = 0.961" indicates the coefficient of determination, which measures how well the linear regression line fits the data points, A high R-squared value close to 1 suggests a strong fit of the regression line to the data points in the elastic region, Implications and Interpretation-The equation of the line and the R-squared value indicate that the Figure illustrates the process of identifying the elastic region, fitting a linear regression line, and calculating Young's Modulus from the stress-strain data.

To calculate Young's Modulus from the provided Figure and data, we can utilize the equation of the fitted linear regression line. The equation "y = 12948x + 0.5905" indicates the relationship between stress (y) and strain (x). Based on this equation, Young's Modulus can be determined from the coefficient in front of the strain (x), which is 12948, Therefore, the Young's Modulus value obtained from the Figure and data is 12948 megapascals, this value provides critical insight into the material's stiffness and elastic behaviour under load.



Figures 4. stress-strain curves for 1:1 and 1:2 concrete

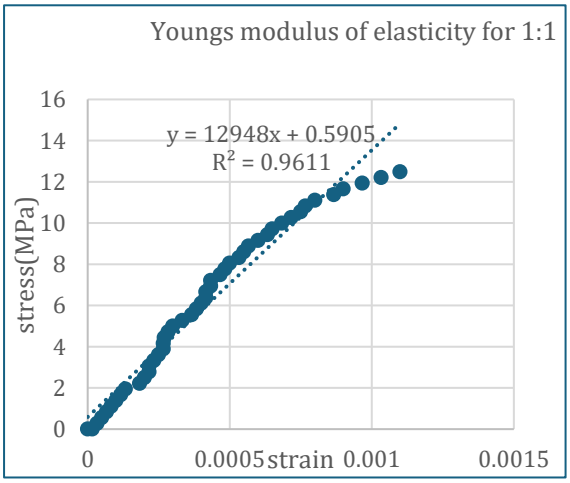


Figure 5. Youngs modulus of Elasticity for 1:1

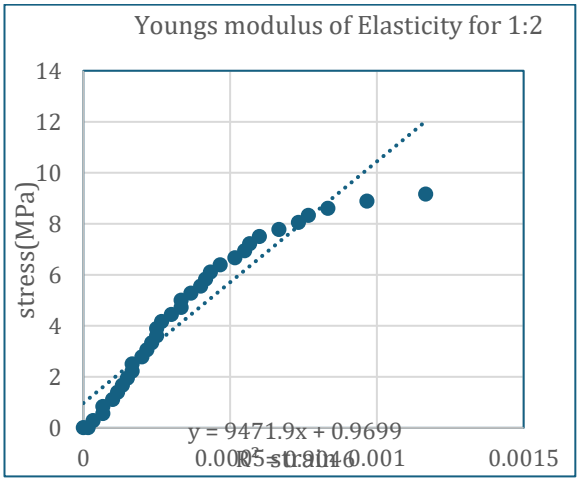


Figure 6. Youngs modulus of Elasticity for 1:2

From the given equation, it appears that the relationship between stress (y) and strain (x) is defined by the equation y = 9471.9x + 0.9699. Therefore, the Young's Modulus value obtained from the Figure and data is 9471.9MPa. The R^2 value is also given as 0.9046, which indicates the goodness of fit of the regression line to the data points. The R^2 value, also known as the coefficient of determination, indicates the proportion of the variance in the dependent variable that is predictable from the independent variable(s). In this case, an R^2 value of 0.9046 suggests that approximately 90.46% of the variability in the dependent variable (stress) can be explained by the independent variable (strain).

5. Conclusion

The research findings underscore the potential of recycled plastic aggregates as a sustainable alternative in concrete production, offering both environmental and technical advantages. The successful integration of RPSCA into concrete mixtures demonstrates promising mechanical properties, indicating its feasibility for widespread adoption in construction projects. Further optimization of mix designs and comprehensive life cycle assessments are recommended to fully realize the environmental benefits and long-term durability of RPSCA-concrete composites.

Overall, this research contributes to the advancement of sustainable construction practices and reinforces the imperative of innovation in addressing global environmental challenges.

In summary, the comprehensive evaluation of concrete specimens incorporating recycled High-Density Polyethylene (HDPE) plastic aggregates across compressive, tensile, and flexural strength tests has provided valuable insights into their mechanical performance. For compressive strength, the results demonstrated that the mix with a 1:1 ratio of recycled HDPE plastic aggregates to sand achieved slightly higher compressive strength compared to the mix with a 1:2 ratio. This highlights the importance of optimizing aggregate proportions to enhance concrete's ability to withstand axial loads. Regarding tensile strength, the mix with a 1:1 ratio of recycled HDPE plastic aggregates to sand exhibited superior tensile strength compared to the mix with a 1:2 ratio. This underscores the significance of aggregate composition in enhancing concrete's resistance to tensile stresses. In terms of flexural strength, the concrete mix with a 1:1 ratio of recycled HDPE plastic aggregates to sand also achieved higher flexural strength compared to the mix with a 1:2 ratio. This emphasizes the importance of proper distribution and packing of plastic aggregates to improve concrete's ability to withstand bending stresses. Obtaining Young's Modulus from a stress-strain curve involves careful analysis of the elastic region and the application of regression analysis to derive the material's Young's Modulus. This value is pivotal in understanding the stiffness and elastic behaviour of a material under tensile or compressive loads.

Overall, the findings suggest that recycled HDPE plastic aggregates have the potential to enhance various mechanical properties of concrete when carefully incorporated into mixed designs. Further research into optimizing mix proportions and investigating long-term durability will contribute to advancing the use of recycled materials in sustainable construction practices.

References

[1] R. Vinod Kumar and D. D. Rupesh Kumar, “Recycled plastic (HDPE) coarse aggregate manufacturing method and performance in concrete,” *Mater. Today Proc.*, vol. 92, pp. 1304–1309, 2023, doi: 10.1016/j.matpr.2023.05.489.

[2] IS-12269:, “Specification for 53 grade ordinary Portland cement,” *Bur. Indian Stand.*, p. New Delhi,India, 1987, [Online]. Available: https://law.resource.org/pub/in/bis/S03/is.12269.b.1987.pdf

[3] IS 4031-1 (1996): Methods of physical tests for hydraulic cement, Part 1: Determination of fineness by dry sieving [CED 2: Cement and Concrete]

[4] IS 4031-11 (1988): Methods of physical tests for hydraulic cement, Part 11: Determination of density and IS 4031-3 (1988): Methods of physical tests for hydraulic cement, Part 3: Determination of soundness [CED 2: Civil Engineering].

[5] IS 4031-5 (1988): Methods of physical tests for hydraulic cement, Part 5: Determination of initial and final setting times [CED 2: Civil Engineering].

[6] IS:383, “Specification for Coarse and Fine Aggregates From Natural Sources for Concrete,” *Indian Stand.*, pp. 1–24, 1970.

[7] IS 2386- Part III, “Method of Test for aggregate for concrete. Part III- Specific gravity, density, voids, absorption and bulking,” *Bur. Indian Stand. New Delhi*, p. (Reaffirmed 2002), 1963.

[8] ASTM C33, “Standard specification for concrete aggregates, ASTM C 33-86,” *Annu. B. ASTM Stand.*, vol. i, 2AD.

[9] ASTM C494-99, “C494 - 99 Standard Specification for Chemical Admixtures for Concrete,” *ASTM Int.*, vol. 04, pp. 1–9, 2013.

[10] P. K. Akarsh, S. Marathe, and A. K. Bhat, “Influence of graphene oxide on properties of concrete in the presence of silica fumes and M-sand,” *Constr. Build. Mater.*, vol. 268, no. xxxx, 2021, doi: 10.1016/j.conbuildmat.2020.121093.

[11] S. G. Barton *et al.*, “Standard Practice for Selecting Proportions for Structural Lightweight Concrete (ACI 211 . 2-98) Reported by ACI Committee 211,” *Aci 211.2-98*, vol. 98, no. Reapproved, pp. 1–18, 1998.

IOP Conference Series: Earth and Environmental Science

PURPOSE-LED PUBLISHING™

PAPER • **OPEN ACCESS**

Enhancing concrete performance and sustainability through carbonation curing: Effects of fly ash incorporation and mechanical properties evaluation

To cite this article: P. Joyson Silva *et al* 2024 *IOP Conf. Ser.: Earth Environ. Sci.* **1409** 012028

View the article online for updates and enhancements.

You may also like

- pH sensor using aniline blue and functionalized nylon for monitoring the final stage of concrete carbonation
Hoseong Jeong, Byung Jun Jung, Jae Hyun Kim et al.
- Comparative study of direct solid-gas carbonation and direct aqueous carbonation for carbon capture and storage
Jack Wang
- Mitigating CO_2 emissions of concrete manufacturing through CO_2-enabled binder reduction
Tae Lim, Brian R Ellis and Steven J Skerlos



This content was downloaded from IP address 47.247.77.11 on 27/11/2024 at 05:39

Enhancing concrete performance and sustainability through carbonation curing: Effects of fly ash incorporation and mechanical properties evaluation

Joyson Silva, P.[1*], Binu Sukumar[1], Hemamathi, A.[1], Ram Shankar, P.[1], Bommu Aakash[1], Janda Chaithanya[1] and Shanmugam, P. B.[1]

[1]Department of Civil Engineering, R.M.K. Engineering College, Kavaraipettai – 601 206, Tanil Nadu, India.

[*]jsp.civil@rmkec.ac.in

Abstract. This research paper intends to assess the characteristics of various concrete samples exposed to carbonation curing. Carbonation curing is a technique used to quicken the solidifying process of concrete by exposing it to carbon dioxide. Concrete treated with carbonation exhibits mechanical and durability properties superior to those treated with moisture. In this study, carbonation-treated concrete was prepared by initially pre-curing and then subjecting it to carbonation curing. The research encompassed testing different properties of concrete specimens treated with carbonation, including compressive strength, tensile strength, and carbonation resistance. The addition of Fly Ash (FA) is renowned for enhancing the durability of reinforced concrete as supplementary contentious materials. In this investigation, concrete cubes were prepared with and without partial substitution of cement by Fly Ash and were encased in plastic covers tightly sealed to prevent air ingress, undergoing carbonation in a controlled environment. Results revealed that the compressive strength of carbonation-treated concrete exceeded that of moisture-cured concrete by 15% to 20% at the same age. These findings indicate that carbonation curing holds promise for enhancing concrete performance in specific applications.

Keywords- Concrete; Carbonation curing; Mechanical properties; Fly Ash

1. Introduction

Carbonation curing is a process that can be used to enhance the strength and durability of concrete structures. It involves the absorption of carbon dioxide by the cementitious materials in the concrete, resulting in the formation of calcium carbonate. “Carbonation” of concrete is defined as the chemical reaction between the products of hydration of the concrete and the Co2 Present in the atmosphere [1, 2]. During the carbonation curing process, the hardening process of concrete is accelerated and its mechanical and durability properties are also improved [3,4,5,6,7,8,9]. Ashraf and Tian (2016) examined the viscoelastic traits of carbonated cementitious matrices, revealing the formation of silica gel and calcium carbonate as wollastonite reacted with CO2. Their findings highlighted the role of silica gel in enhancing concrete's strength, durability, and porosity. Zhang and Shao (2016) observed higher initial strength and lower chloride content in carbonated concrete, despite developing cracks in marine environments, leading to reinforced concrete rusting. Sakai et al. (2016) found that carbonated belite-rich cement and ethylene vinyl acetate (EVA) copolymer enhanced concrete's bending strength and

Content from this work may be used under the terms of the Creative Commons Attribution 4.0 licence. Any further distribution of this work must maintain attribution to the author(s) and the title of the work, journal citation and DOI.
Published under licence by IOP Publishing Ltd

toughness. Zhang, Cai, and Shao (2017) emphasized CO2 diffusion's preference in carbonation curing, while Cabral, Nakanishi, and Fiorelli (2017) proposed accelerated carbonation as a sustainable method to enhance construction materials' durability and resilience. Various methods exist for performing carbonation in concrete, including enclosed chamber, flow-through, injection, autoclave, and combination methods. Among these, the plastic sheet wrapping method is adopted in this experiment for its simplicity, cost-effectiveness, and ease of implementation. Plastic sheet wrapping aids in retaining moisture and increasing CO_2 concentration around the concrete, thereby promoting the carbonation process and yielding a stronger and more durable end product.

This paper aims to assess the physical properties of carbonated concrete specimens compared to conventionally prepared concrete and those impregnated with fly ash, focusing on their compression and split tensile strengths. The integration of fly ash into concrete not only reduces the carbon footprint but also contributes to the carbonation curing process [2,10]. This is attributed to the reactive materials present in fly ash, facilitating the formation of calcium carbonate and additional calcium silicate hydrate, thereby enhancing concrete strength and durability.

2. Mechanism behind using plastic sheets for carbonation curing of concrete

Retaining Moisture: Concrete includes a substantial amount of water when it is first poured and set. The chemical processes that take place during the curing process require this water. The concrete may, however, lose moisture through evaporation while it dries. This may cause the carbonation process to take longer and weaken the finished product's strength. The plastic sheets serve as a barrier, ensuring that the concrete stays wet during the curing process and prevents moisture from evaporating. By covering the concrete with plastic sheets, the moisture in the concrete is retained, which helps to keep the concrete moist and promotes the carbonation process.

Increasing CO_2 Concentration: Carbon dioxide is an essential component of the carbonation process. During the curing process, CO_2 reacts with the calcium compounds in the concrete, forming calcium carbonate. This process increases the strength and durability of the concrete. By covering the concrete with plastic sheets, the concentration of CO_2 around the concrete can be increased. The plastic sheets help to trap CO_2 around the concrete, ensuring that it remains in contact with the concrete and promoting the carbonation process.

In general, using plastic sheets during the carbonation curing process of concrete helps in the formation of a more regulated environment for the concrete, which supports the carbonation process and gives a stronger and more durable end product.

Table 1. Mix Proportion

W/C ratio	Fly ash replacement %	Cement (kg)	Fly ash (kg)	Fine aggregate (kg)	Coarse aggregate (kg)
0.45	0	432.55	0	619.49	1089.61
0.45	30	302.95	129.76	619.49	1089.61

3. Preparation of Specimens

To evaluate the effectiveness of the carbonation in concrete, the experimentation involved casting cube and cylinder concrete specimens using both conventional mix design and a mix design that incorporated fly ash as a cementitious material. The concrete was prepared according to the mix proportion shown in Table 1. First all the specimens were pre cured under room temperature for

24 hours then removed from the moulds and wrapped with plastic sheets. A set of these specimens were kept for carbonation-curing and other for conventional curing.



Figure 1. Plastic sheets wrapped concrete specimens

4. Experimental Investigation

In this experimental investigation, the efficacy of carbonation curing facilitated by plastic sheet wraps was evaluated. Carbonation curing, a process involving the absorption of carbon dioxide by cementitious materials, enhanced the strength and durability of concrete structures. The study focused on utilizing plastic sheet wraps to create a controlled environment conducive to carbonation. Tests conducted included compression tests, split tensile tests, and carbonation tests. These tests were crucial for assessing the mechanical properties and carbonation resistance of the concrete specimens subjected to this curing method. Insights into the effectiveness of plastic sheet wraps in promoting carbonation curing and improving the performance of concrete structures were gained through systematic analysis of the results obtained from these tests.

5. Results

5.1. Compression Test

The test results of cube compressive strength of conventional curing and carbonation curing was shown in Table 2 and the graphical variations were shown in Figure 1.

Table 2. Compressive Strength

% Fly Ash	Conventional Curing Compressive Strength (MPa)		Carbonation Curing Compression Strength (MPa)	
	7 Days	28 Days	7 Days	28 Days
0	19.16	31.28	20.47	33.29
30	13.42	25.12	15.43	24.64

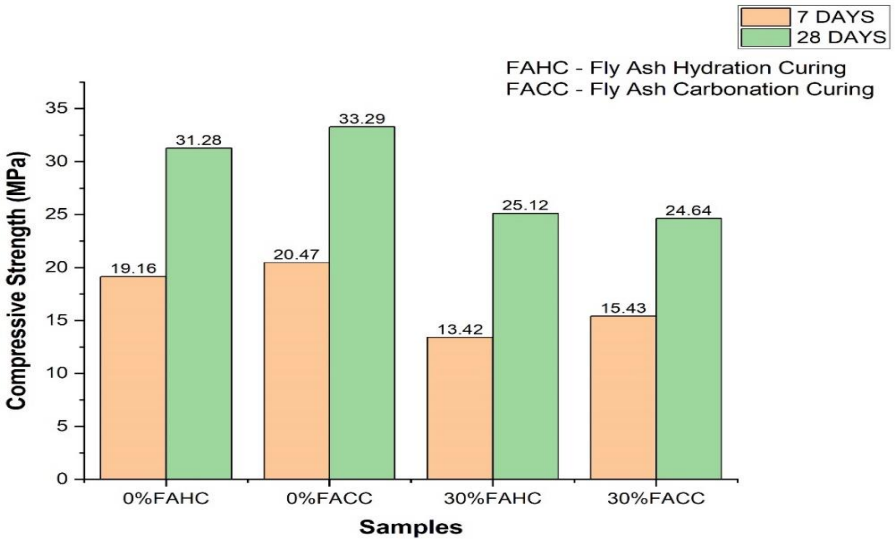


Figure 2. Comparison of Compressive Strength of Specimens

Cube specimens were tested at the ages of 7 days and 28 days. Six cubes of each specimen were tested for every mixture. The ages of 7 days and 28 days are significant milestones in concrete curing, representing early and later stages of the hardening process, respectively. By testing cube specimens at these specific ages, we aimed to evaluate the progression of concrete strength over time and assess the effectiveness of various curing methods employed.

5.2. Split Tensile Test

Table 3. Split Tensile Strength

% Fly Ash	Conventional Curing Compressive Strength (MPa)		Carbonation Curing Compression Strength (MPa)	
	7 Days	28 Days	7 Days	28 Days
0	1.56	2.02	1.61	2.18
30	1.14	2.18	1.28	2.30

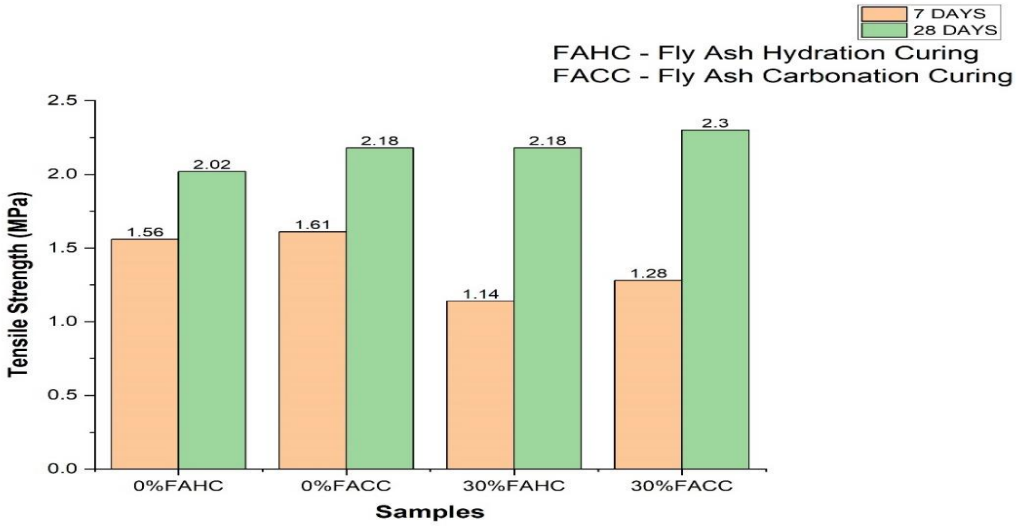


Figure 3. Comparison of Split Tensile Strength of Specimens

In this study, split tensile tests conducted on concrete specimens to understand how different curing methods and materials affect the tensile strength of concrete over time, contributing to the development of more resilient and reliable concrete structures. The test results are mentioned in the Table 3 and Figure 3.

5.3. Carbonation Test

After removing the test specimens from the plastic sheets at 7 days and 28 days, they were subjected to compression testing. Subsequently, the specimens were examined to assess carbonation depth. A hammer was utilized to break the surface of each specimen, and the resulting powder was brushed off. Next, phenolphthalein solution was sprayed over the cut region. The appearance of a purple colour indicated the non-carbonated zone, while the absence of colour change signified the presence of a carbonated zone refer Figure 4. The term "carbonated zone" in concrete refers to a region that has undergone a reaction with carbon dioxide in the air, leading to the formation of calcium carbonate through interaction with calcium hydroxide present in the concrete.



Figure 4. carbonation test sample

6. Conclusions

The effectiveness of carbonation curing was evaluated by analysing the carbonation depth in concrete samples, and strength properties of the concrete specimens by compression test and split tensile strength test. Overall effectiveness of the carbonation curing is a promising technique for improving the quality and sustainability of concrete over conventionally cured concrete. Fly ash as a cementitious material has shown to be effective in laboratory tests. Fly ash is a recyclable product so by reducing the amount of cement used and increasing the rate of carbonation, fly ash can help make concrete more sustainable and durable. By the study it is also evident that there is slight increase of 15-20% compression strength of carbonated concrete specimen over conventional concrete specimens. Plastic bags are being used as a medium for undergoing carbonation treatment in concrete, in place of an accelerated carbonation curing chamber. This method has been successful in facilitating the carbonation curing process, resulting in an increase in the strength and durability of the concrete. The overall carbonation depth of the concrete specimens was found to be less than 10mm upon measurement, indicating a positive result for carbonation curing.

References

[1] A Pravalika and N Venkat Rao, "Effect of Carbonation on the Properties of Concrete" International Journal of Civil Engineering and Technology (IJCIET), Volume 9, Issue 7, July 2018.
[2] Tiefeng Chen , Mengjie Bai, Xiaojian Gao," Carbonation curing of cement mortars incorporating carbonated fly ash for performance improvement and CO2 sequestration", Journal of CO2 Utilization, July 2021.
[3] Monkman S., Shao Y. Integration of carbon sequestration into curing process of precast concrete. Can. J. Civ. Eng. 2010;37:302–310. doi: 10.1139/L09-140.
[4] Yixin S., Xiaolu L. Early-age carbonation curing of concrete using recovered CO2. Concr. Int. 2011;33:50–56.
[5] Rostami V., Shao Y., Boyd A.J., He Z. Microstructure of cement paste subject to early carbonation curing. Cem. Concr. Res. 2012;42:186–193. doi: 10.1016/j.cemconres.2011.09.010.
[6] Rostami V., Shao Y., Boyd A.J. Durability of concrete pipes subjected to combined steam and carbonation curing. Constr. Build. Mater. 2011;25:3345–3355. doi: 10.1016/j.conbuildmat.2011.03.025.
[7] Shao Y., Rostami V., He Z., Boyd A.J. Accelerated Carbonation of Portland Limestone Cement. J. Mater. Civ. Eng. 2014;26:117–124. doi: 10.1061/(ASCE)MT.1943-5533.0000773.
[8] El-Hassan H., Shao Y. Early carbonation curing of concrete masonry units with Portland limestone cement. Cem. Concr. Compos. 2015;62:168–177. doi: 10.1016/j.cemconcomp.2015.07.004.
[9] Zhan B., Poon C., Shi C. CO2 curing for improving the properties of concrete blocks containing recycled aggregates. Cem. Concr. Compos. 2013;42:1–8. doi: 10.1016/j.cemconcomp.2013.04.013.
[10] Duo Zhang, S.M.ASCE, Xinhua cai and Yixin shao," Carbonation Curing of Precast Fly Ash Concrete", Journal of Materials in Civil Engineering. 2016, Volume 28, Issue 11. https://doi.org/10.1061/(ASCE)MT.1943-5533.0001649.

IOP Conference Series: Earth and Environmental Science

PURPOSE-LED PUBLISHING™

PAPER • **OPEN ACCESS**

Revolutionizing concrete construction: Harnessing the potential of low-shrinkage over-burnt clay bricks as sustainable coarse aggregate

To cite this article: J. Selwyn Babu and D. Hemanth 2024 *IOP Conf. Ser.: Earth Environ. Sci.* **1409** 012029

View the article online for updates and enhancements.

You may also like

- Experimental Analysis of Composite Paver Block Using Bagasse Ash and Crushed Clay Brick
Anant Kumar, Abhigyan Shakar, Mayush Lonhare et al.
- Physical and Mechanical Properties of Bodymill Sludge (BS) Incorporated Into Fired Clay Brick
Aeslina Abdul Kadir, Ahmad Shayuti Abdul Rahim, Mohd Ikhmal Haqeem Hassan et al.
- Comparison of Fly Ash Based (AAC) Block and Clay Bricks for Structure and Strength Properties
V Singh, V Behl and V Dahiya



This content was downloaded from IP address 47.247.77.11 on 27/11/2024 at 05:40

Revolutionizing concrete construction: Harnessing the potential of low-shrinkage over-burnt clay bricks as sustainable coarse aggregate

Selwyn Babu, J.[1] and Hemanth, D.[1*]

[1]Department of Civil Engineering, Malla Reddy Engineering College (A), Maisammaguda, Gundlapochampally (v), Medchal, 500100, Telangana, India.

[*]E-mail: devollahemanth@gmail.com

Abstract. This paper presents a study on the feasibility of using low-shrinkage over-burnt clay bricks as a sustainable coarse aggregate in concrete mixes. The research encompasses a thorough evaluation of mechanical and durability properties to assess the performance of these mixes in structural and durable applications. Mechanical strength tests, including compressive strength, split tensile strength, flexural strength, and modulus of elasticity, were conducted to evaluate structural behaviour. The results indicate that the mix with 30% brick aggregate replacement demonstrated competitive compressive strength at 28 days, showing promise for structural use. Additionally, split tensile strength, flexural strength, and modulus of elasticity displayed favourable trends over time, suggesting improved structural performance. Durability properties assessment focused on concrete bond strength, water absorption, permeable voids, sorptivity, and resistance to chloride diffusion. The mix with 30% replacement exhibited the highest bond strength at 28 days and the lowest water absorption, indicating enhanced durability. Sorptivity values showed reduced water absorption rates, particularly for mixes with higher replacement levels, highlighting improved resistance to moisture ingress. Resistance to chloride diffusion varied with replacement levels, with the 30% replacement mix demonstrating satisfactory performance. Overall, the concrete mixes with varying levels of brick aggregate replacement, particularly the 30% replacement mix, exhibited favourable performance across mechanical and durability tests. These findings suggest the potential of low-shrinkage over-burnt clay bricks as a sustainable alternative in concrete production, offering enhanced structural strength and durability for sustainable construction practices.

Keywords: over- burnt clay brick aggregates, mechanical, durability.

1. Introduction

Concrete, pivotal in modern construction, boasts unparalleled versatility and enduring durability. Yet, its production poses environmental concerns due to heavy reliance on natural resources like sand and gravel, leading to habitat destruction, pollution, and carbon emissions [17][20]. Addressing this, researchers and industry experts are exploring sustainable alternatives to reduce concrete's environmental impact while preserving its mechanical and durability properties [2][6]. One promising avenue involves using alternative aggregates from industrial by-products or recycled materials [3][4], aligning with circular economy principles and sustainable development

Content from this work may be used under the terms of the Creative Commons Attribution 4.0 licence. Any further distribution of this work must maintain attribution to the author(s) and the title of the work, journal citation and DOI.
Published under licence by IOP Publishing Ltd

[15]. Low-shrinkage over-burnt clay bricks, derived from subjecting clay bricks to higher firing temperatures, have emerged as a compelling alternative aggregate [13]. Their reduced porosity and enhanced mechanical properties offer benefits like improved strength, durability, and sustainability when used in concrete mixes [5]. This study aims to evaluate their feasibility and efficacy as sustainable coarse aggregates in concrete [19], comprehensively assessing mechanical (compressive, split tensile, flexural strengths, modulus of elasticity) and durability properties (bond strength, water absorption, permeable voids, sorptivity, resistance to chloride diffusion) [10][16][17]. Systematic experimentation with varying brick aggregate replacements will determine optimal blends for desired characteristics [5]. Through rigorous testing and statistical analysis [9], this research aims to provide valuable insights for concrete producers, engineers, and policymakers, promoting sustainable practices and innovation in the construction industry [4]. This exploration sets the stage for understanding the potential impact of sustainable material choices on concrete construction.

2. Material Characterizations and Mix Preparation

Prior to the concrete formulation, all components of the mixture underwent rigorous pre-testing in accordance with established standards [16][19][24]. Comprehensive laboratory testing was conducted on both aggregates and the binder, which, in this case, is Portland cement [22]. These tests aimed to ascertain essential parameters and ensure the quality and compatibility of the components in the concrete mixture.

2.1. Preliminary Assessment of Concrete Components

2.1.1. Cement

Ordinary Portland Cement (OPC) used in Indian construction adheres to IS 269:2015 standards. The specific gravity of OPC is 3.15, with a Blaine fineness of 380 m^2/kg [20]. The consistency of the cement paste is 30% using the Vicat apparatus [20]. The initial setting time is 30 minutes, and the final setting time is 280 minutes [17], and the compressive strength at 28 days is typically around 53 MPa [21].

2.1.2. Fine Aggregate (Sand)

Natural River sand conforming to IS 383:2016 [24] has a specific gravity of 2.65 [22] and a fineness modulus of 2.7. To ensure optimal performance in concrete mixes, the moisture content of the sand is kept below 5%.

2.1.3. Coarse Aggregate

The coarse aggregate, which is typically crushed stone or gravel, conforms to IS 383:2016 specifications [24]. Figure 2. displays the grading curve of aggregates, illustrating their particle size distribution. The specific gravity of the coarse aggregate ranges from 2.8 [6].

2.1.4. Water

Clean potable water meeting IS 456:2000 standards [15] is essential for concrete mixing. The recommended water-cement ratio for normal strength concrete ranges from 0.5 to 0.6 [18]. The mixing water temperature is typically maintained between 20°C to 30°C [6].

2.1.5. Low-Shrinkage Over-Burnt Clay Bricks (Sustainable Coarse Aggregate)

Selected over-burnt bricks surpass class 7.5's 4.5 MPa compressive strength requirement [3][8][19], with lower water absorption (around 18%) than the specified 20% [9][12]. Minimal

efflorescence and acceptable warpage at 0.8/100 times the length is noted [1][15]. They exhibit a 25% impact resistance [3] and a crushing value of about 10%, complementing their strength [16]. These bricks undergo unique kiln firing [8] and can be crushed for aggregate, albeit generating dust during screening [12].

2.1.6. Chemical Admixture - CONPLAST SP 430

The incorporation of CONPLAST SP 430, a high-performance superplasticizer, aligns with IS: 9103-1999 [19] and ASTM C494 standards [21]. Recognized for reducing water content by up to 30%, CONPLAST SP 430, derived from chloride-free sulfonated naphthalene polymers, enhances workability without compromising strength.

Table 1. Chemical compositions

Sample	Chemical composition (%)									
	SiO_2	Al_2O_3	CaO	Fe_2O_3	MgO	SO_3	K_2O	Na_2O	Other	Loss on ignition
OPC 53 Grade	23.00	5.00	62.00	3.50	1.76	2.85	-	-	2.38	1.92
COBB	45.00	30.00	10.60	11.20	3.10	1.20	-	-	Varies	6.5
Traditional CA	72.00	12.60	1.80	2.40	1.42	Varies	2.62	3.42	Varies	Varies
Traditional FA	90.10	5.22	1.10	1.05	0.95	Varies	1.23	1.00	Varies	Varies

2.2. Concrete Batching and Mixing Procedures

Concrete production begins with meticulous material selection (cement, aggregates, water, admixtures) [14][21], followed by precise proportioning based on the mix design using equipment like weigh batchers and mixers for accuracy [14]. Transit mixers aid in transportation and prevent segregation. Curing for hydration [18] and regular maintenance/calibration [14] are crucial. Figure 3 outlines the sequential steps: material selection, batching, mixing, transportation, placement, curing, and maintenance for quality production. In a study on crushed Overburnt Brick (COBB) concrete blends [2][11], six conventional mixes with varying cement content were prepared alongside COBB mixes gradually replacing natural stone aggregate at intervals of 0-50% [14]. Consistent cement, filler, water amounts were maintained [8], and Superplasticizer (SP) was added to COBB concrete for workability and sustainability [19][21].

2.3. Conventional Mix Design

Conventional concrete mix designs for 1 cubic meter strictly adhere to precise values per Indian standard practices [25], incorporating essential ingredients as per established norms [20]. Maintaining a water-to-cement ratio of 0.5 to 0.6 ensures structural integrity and optimal performance [12], with a targeted compressive strength of 20-30 MPa aligning with industry standards [18]. Table 2 outlines Mixture Composition, forming a foundational framework for consistent quality and durability [5]. Adhering to the specified water-to-cement ratio balances workability and strength, guaranteeing structural robustness for diverse construction needs [4], showcasing commitment to quality and compliance with Indian standards in concrete mix design.

Table 2. Mixture Composition of conventional concrete

Mix Scenario	Cement	Fine Aggregate	Coarse Aggregate	Water (0.5 to 0.6)
Standard Concrete Mix	360	720	1440	195
Higher Cement Ratio Mix	432	720	1440	245
Lower Cement Ratio Mix	288	720	1440	172
Standard Mix with Enhanced Workability	360	720	1440	200
Economical Mix with Reduced Cement Ratio	324	720	1440	190
High-Strength Mix with Increased Cement Ratio	540	720	1440	324

2.4. Overburnt Mix Design with Various Percentages

Mix designs for 1 cubic meter of Overburnt Brick (COBB) concrete follow Indian standard practices [4], considering various proportions of crushed Overburnt Brick as per established norms [26]. The water-to-cement ratio is carefully maintained between 0.5 and 0.6, with a targeted compressive strength ranging from 20 to 30 MPa [17]. Each COBB mix systematically replaces natural stone coarse aggregate, from 0% to 50% [22]. Table 4 outlines the Crushed Overburnt Mix scenario [22]. This systematic approach ensures COBB concrete maintains structural integrity and meets desired performance criteria [16]. Incorporating varying percentages of crushed Overburnt Bricks (Table 3) [22] allows for exploring sustainable alternatives while adhering to recognized standards [6][16][22]. The specified water-to-cement ratio and compressive strength range create a reliable framework for producing COBB concrete with necessary workability and strength, aligning with industry standards.

Table 3. Ratio of Coarse Aggregate for Replacement Concrete Blends (W/C=0.49)

Blend Classification in Concrete	Blend Identification	Ratio of Coarse Aggregate in Blend (kg/m^3)
Traditional	C1 to C6	1440
Substituting 0% with COBB Aggregate	M1	0
Substituting 10% with COBB Aggregate	M2	144
Substituting 20% with COBB Aggregate	M3	288
Substituting 30% with COBB Aggregate	M4	432
Substituting 40% with COBB Aggregate	M5	576
Substituting 50% with COBB Aggregate	M6	720

Table 4. Mixture Composition of Crushed Overburnt Mix

Mix Scenario	Cement (kg)	Fine Aggregate (kg)	Coarse Aggregate (Crushed Overburnt Mix kg)	Granite Stone (kg)	Water (lit)
Standard Mix (0% Replacement)	360	720	0	1440	195
Mix with 10% Replacement in Higher Cement Mix Ratio	432	720	144	1296	245

Mix with 20% Replacement in Lower Cement Mix Ratio	288	720	288	1152	172
Mix with 30% Replacement in Standard mix with enhanced workability	360	720	432	1008	200
Mix with 40% Replacement in Economical Mix with Reduced Cement Ratio	324	720	576	864	190
Mix with 50% Replacement in High-Strength Mix with Increased Cement Ratio	540	720	720	720	324

2.5. The test Specimens for Each Mix

The concrete testing program adheres to industry standards [1][16][17]. It employs various specimen types: 100mm cubes for compression testing (IS 1199 - 1959), 150mm diameter, 300mm height cylinders for split tension testing (IS 516 – 1959), 100mm x 100mm x 500mm prisms for flexure testing (IS 5816 – 1999), and 150mm diameter, 300mm height cylinders for modulus of elasticity testing (IS 516 – 1959). Bond strength, water absorption, and sulphate attack are assessed using 100mm cubes following ASTM and IS standards, while sorptivity and Rapid Chloride Penetration Test (RCPT) are done on 100mm diameter, 50mm thick slices following ASTM standards. This program evaluates concrete properties like compressive and tensile strength, flexural strength, modulus of elasticity, bond strength, water absorption, and durability comprehensively.

3. Concrete Assessment and Tests with Results

Initial properties of fresh concrete, crucial for workability and performance, require tailored parameters during mix design [17]. Assumed unit weight for cementitious materials, typically 1100 kg/m^3, adjusts based on actual material properties [19]. A consistent 12 ml/kg superplasticizer dosage, with potential variations, improves workability [16]. Initial slump values, 50-100 mm, indicate baseline workability, increasing to 100-150 mm post-superplasticizer for enhanced ease of placement [17][16].

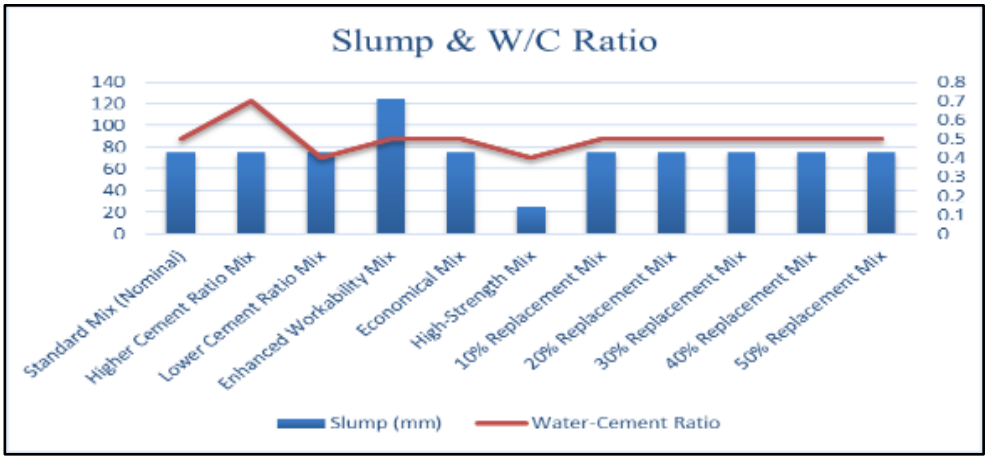


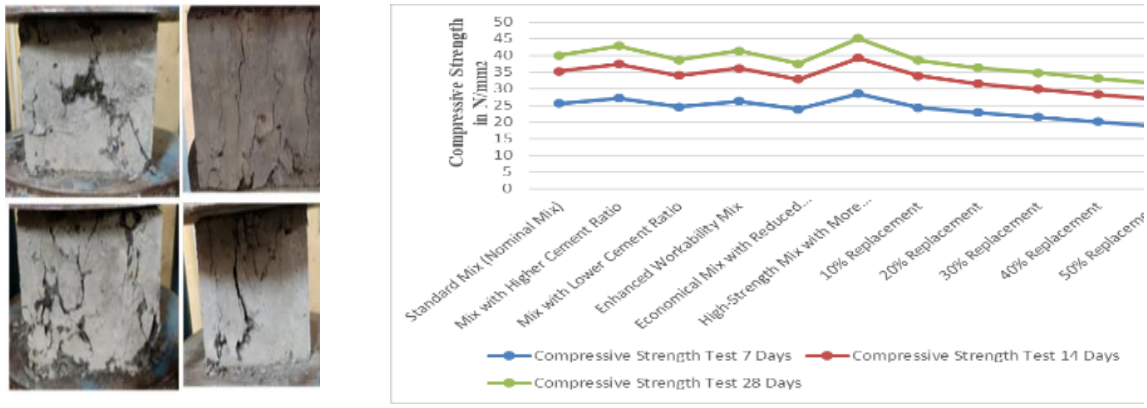
Figure 1. Correlation Between Slump and Water–Cement Ratio

Figure 1 illustrates concrete workability and slump values across diverse mix compositions and additives [13]. Standard and high cement content mixes show improved workability, with slumps of 110-120 mm. Low cement content with a low-range superplasticizer increases from 25 mm to 100 mm, demonstrating superplasticizer effectiveness [12]. The mix designed for enhanced workability with a mid-range superplasticizer maintains a balanced slump [17]. An economical mix using a medium-range superplasticizer reaches 105 mm from 50 mm. High-strength mixes with very high-range superplasticizers achieve 130 mm from 100 mm. COBB-infused concrete increases from 60 mm to 120 mm post-superplasticizer.

3.1. Mechanical property Assessment of concrete

3.1.1. Compressive Strength Test

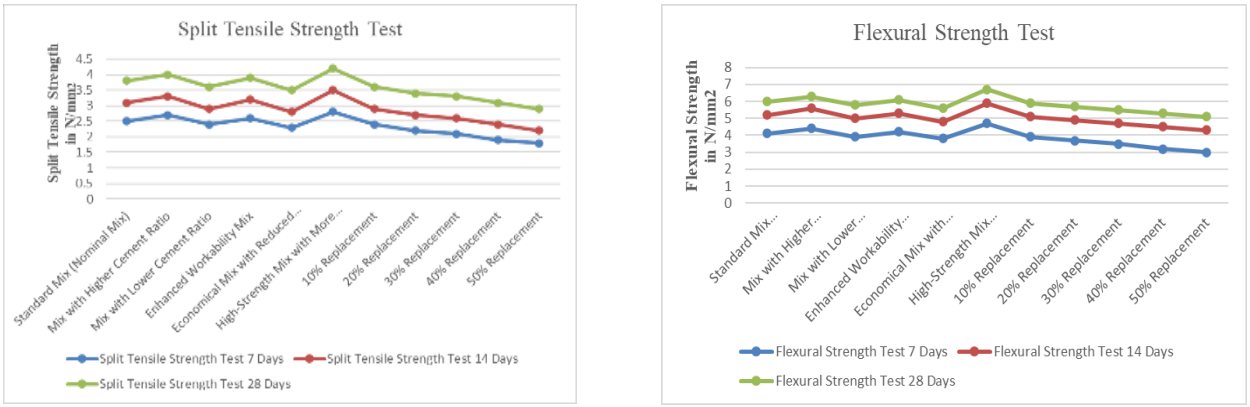
The compressive strength tests were conducted on Conventional and COBB-infused concrete specimens over 7, 14, and 28 days [12][17]. The Standard Mix showed strengths of 25.6 MPa (7 days), 35.2 MPa (14 days), and 40 MPa (28 days) [8]. The Mix with Higher Cement Ratio exhibited strengths of 27.1 MPa (7 days), 37.4 MPa (14 days), and 42.8 MPa (28 days) [13][18]. The Mix with Lower Cement Ratio had strengths of 24.5 MPa (7 days), 33.9 MPa (14 days), and 38.6 MPa (28 days) [7][9]. The Enhanced Workability Mix showed strengths of 26.2 MPa (7 days), 36.1 MPa (14 days), and 41.3 MPa (28 days) [13]. The Economical Mix with Reduced Ratio exhibited strengths of 23.8 MPa (7 days), 32.8 MPa (14 days), and 37.5 MPa (28 days) [10]. The High-Strength Mix had strengths of 28.5 MPa (7 days), 39.2 MPa (14 days), and 45.1 MPa (28 days) [18]. COBB-infused mixes and replacements at 10%, 20%, 30%, 40%, and 50% showed varying strengths [10][14][19].



(a) (b)

Figure 2. (a). Various Failure patterns in concrete Cubes (b). 7 days, 14 days and 28 days Compressive Strength

Our findings consistently showed increasing compressive strength over time in both Conventional and COBB-infused concrete mixes [19]. Figure 2(b) illustrated the impact of mix composition on compressive strength trends, particularly burnt clay brick replacement. Figure 2(a) highlighted failure patterns during compressive strength tests, stressing the need to consider material composition and curing duration for optimal strength [5]. These results emphasize the importance of such considerations for enhancing concrete strength in diverse applications. Further research in this area promises advancements in concrete technology, leading to more durable structures in the future.



(a) (b)

Figure 3. 7 days, 14 days and 28 days (a) split tensile strength and (b) flexural strength test

3.1.2. Split tensile strength and Flexural strength

Split tensile and flexural strength tests were conducted on Conventional and COBB-infused concrete specimens following IS: 5816 – 1970 standards using a 4000 kN compression testing machine [10][14][19]. Standard Mix showed split tensile strengths of approximately 2.5 MPa, 3.1 MPa, and 3.8 MPa at 7, 14, and 28 days, respectively, with flexural strengths of 4.1 MPa, 5.2 MPa, and 6 MPa (Figure 3) [7][11]. Mixes with different cement ratios, workability enhancements, and replacements at 10%-50% exhibited varying tensile and flexural strengths [1][18]. The replacements demonstrated progressive improvements in both split tensile and flexural strengths over curing periods [7].

3.1.3. Modulus of elasticity test

The Modulus of Elasticity (MOE) Test assesses concrete stiffness and resistance to deformation, with results measured in GPa at 7, 14, and 28 days. The Standard Mix exhibited an MOE of 31.2 GPa at 28 days, reflecting baseline stiffness [22]. Mixes with higher cement content achieved higher MOE values, such as 31.8 GPa for the High-Cement Mix [16]. Conversely, lower cement ratios resulted in slightly reduced MOE, as seen in the Economical Mix with 30.2 GPa [25]. Replacement scenarios with burnt clay bricks showed varying MOE values, with higher replacements leading to decreased elasticity, e.g., 28.3 GPa at 50% replacement [22]. Overall, MOE increased over time, indicating progressive stiffness development [22], depicted visually in Figure 9 for Modulus of Elasticity trends (Figure 4).

Table 5. Mechanical Strength Characteristics

Mix Scenario	Compressive Strength Test			Split Tensile Strength Test			Flexural Strength Test			Modulus of Elasticity Test		
	7 Days	14 Days	28 Days	7 Days	14 Days	28 Days	7 Days	14 Days	28 Days	7 Days	14 Days	28 Days
Standard Mix (Nominal Mix)	25.6	35.2	40	2.5	3.1	3.8	4.1	5.2	6	28.5	29.7	31.2
Mix with Higher Cement Ratio	27.1	37.4	42.8	2.7	3.3	4	4.4	5.6	6.3	29.1	30.3	31.8
Mix with Lower Cement Ratio	24.5	33.9	38.6	2.4	2.9	3.6	3.9	5	5.8	28	29.2	30.7

Enhanced Workability Mix	26.2	36.1	41.3	2.6	3.2	3.9	4.2	5.3	6.1	28.8	30	31.5
Economical Mix with Reduced Ratio	23.8	32.8	37.5	2.3	2.8	3.5	3.8	4.8	5.6	27.5	28.7	30.2
High-Strength Mix with More Cement	28.5	39.2	45.1	2.8	3.5	4.2	4.7	5.9	6.7	29.6	30.8	32.3
10% Replacement	24.3	33.8	38.5	2.4	2.9	3.6	3.9	5.1	5.9	27.8	29	30.5
20% Replacement	22.8	31.4	36.2	2.2	2.7	3.4	3.7	4.9	5.7	27.2	28.4	29.9
30% Replacement	21.5	29.9	34.7	2.1	2.6	3.3	3.5	4.7	5.5	26.7	27.9	29.4
40% Replacement	20.1	28.3	33.1	1.9	2.4	3.1	3.2	4.5	5.3	26.1	27.3	28.8
50% Replacement	18.7	26.8	31.6	1.8	2.2	2.9	3	4.3	5.1	25.6	26.8	28.3

3.1.4. Pull-Out Test for Concrete Bond Strength

The Pull-Out Test assesses concrete-aggregate bond strength, critical for evaluating mix effectiveness across curing periods [12]. The Standard Mix showed gradual bond strength improvement from 18 MPa (7 days) to 25 MPa (28 days) [14]. A higher cement ratio yielded superior bonds (20-28 MPa) [12], while lower ratios exhibited slower strength development (16-23 MPa) [19]. The Enhanced Workability Mix maintained consistent gains (19-26 MPa) [5]. Economical and High-Strength Mixes balanced cost-saving with robust bonds (17-24 MPa, 22-30 MPa) [16][19]. Incorporating 10-50% replacement materials yielded varying bonds (14-27 MPa) [1][22]. These results, detailing bond evolution over time, inform tailored mix designs for durability, as depicted in Figure 5 for visual bond strength trends [12][6].

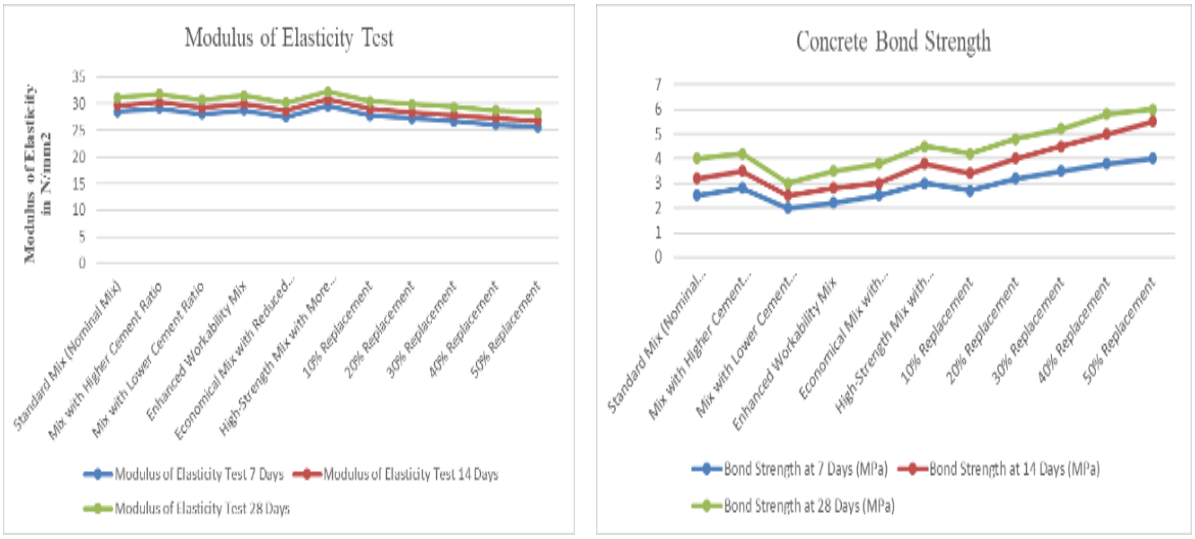


Figure 4 and 5: 7 days, 14 days and 28 days visual representation of Modulus of elasticity and bond strength development trends

3.2. Durability Properties Assessment of concrete

3.2.1. Water Absorption Capacity and Volume of Permeable Voids Assessment

The Water Absorption Capacity Test evaluates concrete's water absorption at 7, 14, and 28 days, presenting insights into porosity evolution [1][11]. The Standard Mix showed incremental absorption and void development, typical during curing [16][18]. Conversely, the Mix with Higher Cement Ratio demonstrated lower absorption and stable void volumes [11]. The Mix with Lower Cement Ratio exhibited slightly higher absorption and voids, while the Enhanced Workability Mix displayed excellent resistance and durability [6]. The Economical Mix and High-Strength Mix maintained moderate to low absorption, emphasizing their water-resistant properties [9][5]. Replacement scenarios showed varying impacts on absorption, with higher percentages leading to increased porosity and water ingress [12][3]. Figure 6 visually represents these absorption trends and Volume of Permeable Voids, highlighting material composition's role in sustainable construction [8]. This comprehensive analysis aids in designing eco-friendly and durable concrete mixes.

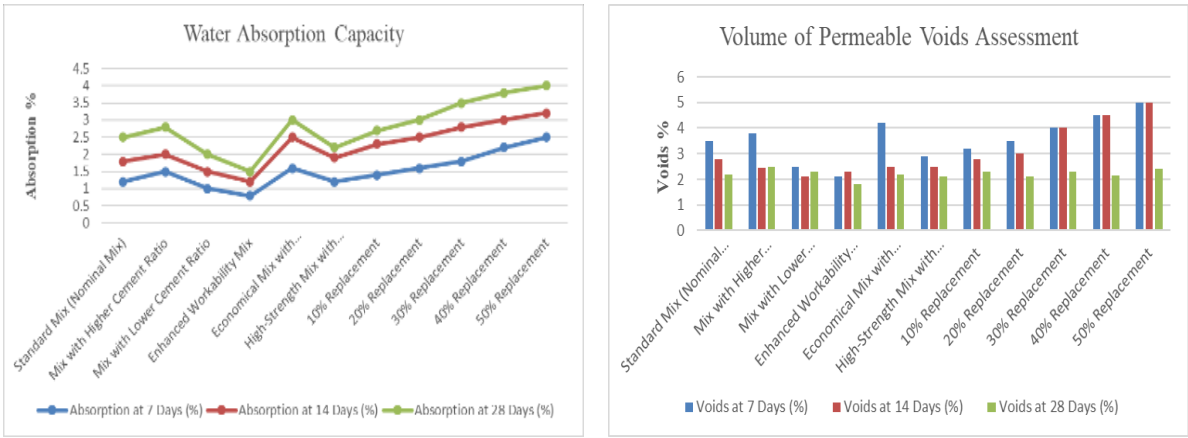


Figure 6. 7 days, 14 days and 28 days visual representation of water absorption and the Volume of Permeable Voids Assessment trends

Table 6. Durability Strength Characteristics

Mix Scenario	Bond Strength (MPa)			Water Absorption (%)			Volume of Permeable Voids (%)		
	7 Days	14 Days	28 Days	7 Days	14 Days	28 Days	7 Days	14 Days	28 Days
Standard Mix (Nominal Mix)	2.5	3.2	4	1.2	1.8	2.5	3.5	2.8	2.2
Mix with Higher Cement Ratio	2.8	3.5	4.2	1.5	2	2.8	3.8	3	2.5
Mix with Lower Cement Ratio	2	2.5	3	1	1.5	2	2.5	2	2
Enhanced Workability Mix	2.2	2.8	3.5	0.8	1.2	1.5	2.7	2.3	1.8
Economical Mix with Reduced Ratio	2.5	3	3.8	1.6	2.5	3	4.2	4	2.2
High-Strength Mix with More Cement	3	3.8	4.5	1.2	1.9	2.2	2.9	2.5	2.9
10% Replacement	2.7	3.4	4.2	1.4	2.3	2.7	3.2	2.8	3.2
20% Replacement	3.2	4	4.8	1.6	2.5	3	3.5	3	3.5

30% Replacement	3.5	4.5	5.2	1.8	2.8	3.5	4	4	4
40% Replacement	3.8	5	5.8	2.2	3	3.8	4.5	4.5	4.5
50% Replacement	4	5.5	6	2.5	3.2	4	5	5	5

3.2.2. Sorptivity

The Sorptivity Test evaluates concrete water absorption over 7, 14, and 28 days, indicating material porosity and durability [6]. The Standard Mix showed decreasing sorptivity, reflecting improved water resistance over time [9]. Conversely, the Mix with Higher Cement Ratio exhibited consistently lower sorptivity rates, indicating superior durability [11]. The Mix with Lower Cement Ratio had slightly higher sorptivity but within acceptable limits, showing improved resistance with curing [14]. The Enhanced Workability Mix and High-Strength Mix displayed excellent water resistance, maintaining low sorptivity rates [22][9]. Replacement scenarios showed varying sorptivity impacts, with higher percentages leading to increased water absorption [4][13]. Figure 7 visually represents these trends, indicating COBB concrete's favourable reduction in sorptivity over time. This reduction suggests enhanced durability and reduced water permeability, essential for sustainable construction practices.

3.2.3. Chloride Diffusion Analysis (RCPT) and Interpretation

This article explores Chloride Diffusion Analysis using the Rapid Chloride Penetration Test (RCPT) to assess concrete mixes with low-shrinkage burnt clay bricks as coarse aggregates. The Standard Mix exhibited good chloride resistance, essential for durability [19]. Mix variations showed differing penetration rates, with higher cement ratio mixes displaying moderate resistance [22]. Lower cement ratios indicated potential risks requiring mitigation [14]. The Enhanced Workability Mix demonstrated effective protection [10]. The Economical Mix showed acceptable performance [9]. The High-Strength Mix displayed good to excellent resistance, crucial for aggressive environments [15]. Replacement scenarios showed varying impacts on chloride penetration [13][16], emphasizing the need for monitoring and remedial actions. Figure 8 visually represents these trends. These insights aid in optimizing mixes and implementing protective measures for enhanced concrete durability in chloride-rich settings [20].

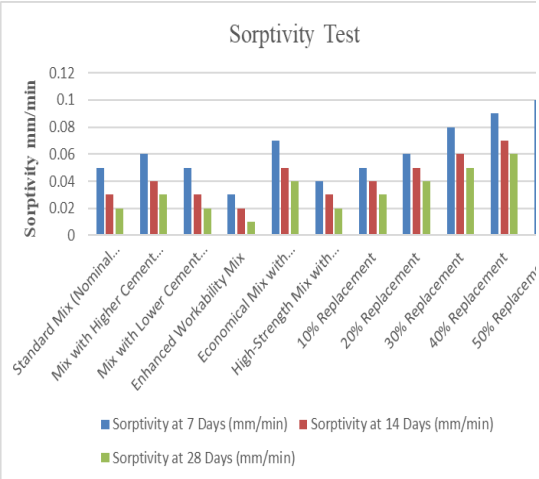


Figure 7 Sorptivity of Concrete

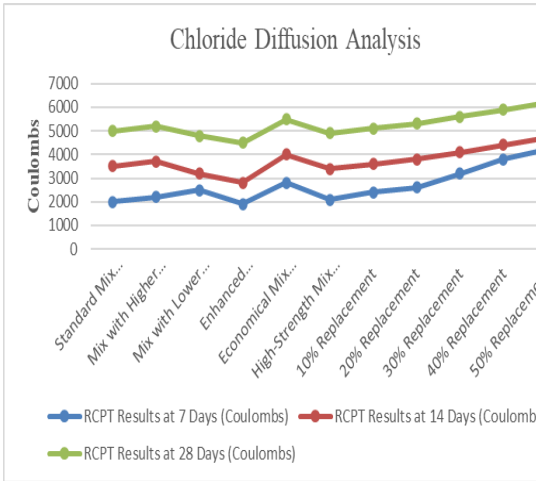


Figure 8. 7 days, 14 days and 28 days chloride diffusion analysis

Table 7. Characteristics of Sorptivity and RCPT

Mix Scenario	Sorptivity (mm/min)	RCPT (Coulombs)

	7 Days	14 Days	28 Days	7 Days	14 Days	28 Days
Standard Mix (Nominal Mix)	0.05	0.03	0.02	2000	3500	5000
Mix with Higher Cement Ratio	0.06	0.04	0.03	2200	3700	5200
Mix with Lower Cement Ratio	0.05	0.03	0.02	2500	3200	4800
Enhanced Workability Mix	0.03	0.02	0.01	1900	2800	4500
Economical Mix with Reduced Ratio	0.07	0.05	0.04	2800	4000	5500
High-Strength Mix with More Cement	0.04	0.03	0.02	2100	3400	4900
10% Replacement	0.05	0.04	0.03	2400	3600	5100
20% Replacement	0.06	0.05	0.04	2600	3800	5300
30% Replacement	0.08	0.06	0.05	3200	4100	5600
40% Replacement	0.09	0.07	0.06	3800	4400	5900
50% Replacement	0.1	0.08	0.07	4200	4700	6200

3.3. Microstructure

Microstructure analysis of innovative concrete compositions, featuring low-shrinkage over burnt clay bricks as sustainable coarse aggregate, employed various techniques, including XRD and FESEM, to validate their unique properties. The experimental procedures for these analyses are detailed below.

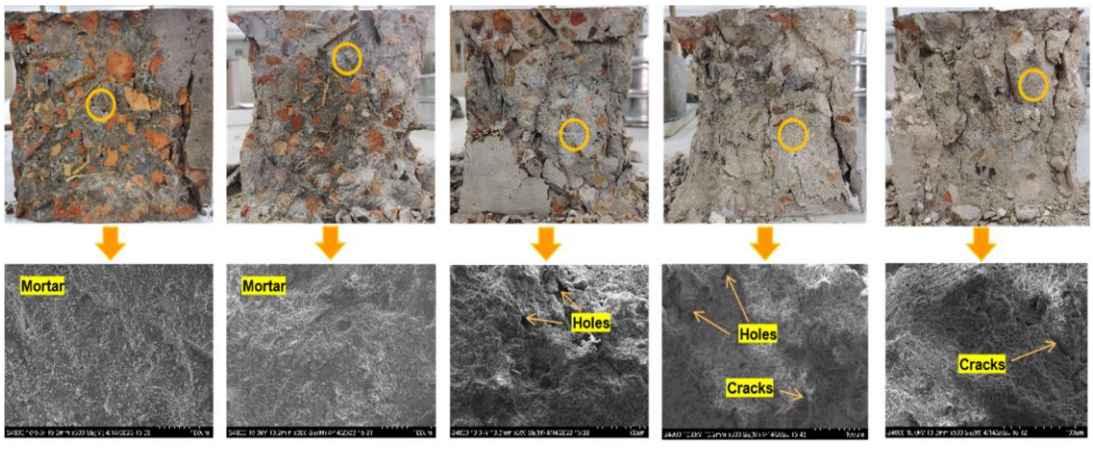


Figure 9. Displays FESEM images of concrete specimens

3.3.1. Field Emission Scanning Electron Microscopy (FESEM) Imaging

The Nova Nano SEM 450 was instrumental in producing FESEM images of innovative concrete mixes [20]. This facilitated observation of cement paste phases and the inter-transitional zone with low-shrinkage burnt clay brick aggregates [16][23]. The process involved precision cutting (10 × 10 × 10 mm) [21], wet-grinding using a Buhler disc [16], acetone cleaning to remove dust [16][17], and oven-drying at 100°C [22]. These steps were crucial for clear FESEM images, revealing microstructural features in sustainable coarse aggregates. Figure 9 presents FESEM

images of 28-day cured samples, with a red line marking the Interfacial Transition Zone (ITZ) [12]. ITZ quality influences concrete's mechanical and durability performance, visible through FESEM's magnifications, detailing ITZ, aggregate distribution, voids, microcracks, and Calcium Silicate Hydrate (CSH) gel formation [12]. This comparative analysis, including the control mix, evaluates the impact of Crushed Over Burnt Bricks on cement concrete [2], enhancing understanding of mechanical and durability traits [12].

4. Conclusion

This study investigates the innovative use of low-shrinkage over burnt clay bricks as sustainable coarse aggregate in concrete, offering valuable insights into concrete performance. In terms of mechanical strength tests, compressive strength consistently increased over time for all mixes, highlighting their structural robustness. Notably, the 30% replacement mix exhibited competitive compressive strength at 28 days, indicating its potential for structural applications. Additionally, split tensile strength and flexural strength displayed similar upward trends, indicating overall favourable structural behaviour. The modulus of elasticity also improved over time across all mixes, further emphasizing their structural integrity.

Moving on to durability properties, concrete bond strength improved with curing time across all replacement levels, with the 30% replacement mix showing the highest bond strength at 28 days. Water absorption decreased over time, with replacement mixes demonstrating enhanced resistance compared to standard and higher cement ratio mixes. Particularly, the 50% replacement mix exhibited the lowest water absorption rate. Voids assessment revealed a reduction over time for most mixes, with the 30% replacement mix consistently showing lower permeable voids. Sorptivity values indicated a slower rate of water absorption for mixes with higher replacement levels, indicating improved water resistance. Resistance to chloride diffusion varied with replacement levels, with mixes having higher replacements generally showing satisfactory to good resistance, and the 30% replacement mix demonstrating satisfactory performance.

Looking ahead, concrete mixes with replacement levels, especially the 50% replacement mix, demonstrated favourable performance across multiple tests. Their enhanced bond strength, reduced water absorption, lower permeable voids, and improved resistance to chemical and chloride attacks suggest their suitability for structural and durable applications. Considerations such as structural applications, durability, sustainability through material replacement, project-specific factors, and further testing under specific environmental conditions should guide optimal mix selection to ensure long-term performance and resilience of concrete structures.

5. References

[1] Padmini, A. K., Ramamurthy, K., & Mathews, M. S. (2001, December). Behaviour of concrete with low-strength bricks as lightweight coarse aggregate. *Magazine of Concrete Research*, *53*(6), pp. 367–375. https://doi.org/10.1680/macr.53.6.367.40798

[2] Ramos, Yober Ostherlen Mantari, et al. “Mechanical Analysis of Concrete Using Over-burnt Bricks as Coarse Aggregate.” *Civil Engineering and Architecture*, vol. 12, no. 2, Horizon Research Publishing Co., Ltd., Mar. 2024, pp. 814–21. *Crossref*, doi:10.13189/cea.2024.120211.

[3] Yang, Jian, et al. “Concrete With Recycled Concrete Aggregate and Crushed Clay Bricks.” *Construction and Building Materials*, vol. 25, no. 4, Elsevier BV, Apr. 2011, pp. 1935–45. *Crossref*, doi:10.1016/j.conbuildmat.2010.11.063.

[4] Duna, Samson, and Fwangmun Wamyil. “Performance of Concrete Using Burnt Waste Plastic as Partial Replacement for Coarse Aggregate.” *Archives of Current Research International*, vol. 9, no. 1, Sciencedomain International, Jan. 2017, pp. 1–11. *Crossref*, doi:10.9734/acri/2017/35706.

[5] Ranjan, Rajeev, and Anubhav Rai. "To Study the Properties of Concrete Mix on Partial Replacement of Coarse Aggregate With Burnt Bricks." *International Journal of Innovative Research in Engineering and Management*, vol. 10, no. 3, Innovative Research Publication, June 2023, pp. 1–4. *Crossref*, doi:10.55524/ijirem.2023.10.3.1.

[6] Debieb, Farid, and Said Kenai. "The Use of Coarse and Fine Crushed Bricks as Aggregate in Concrete." *Construction and Building Materials*, vol. 22, no. 5, Elsevier BV, May 2008, pp. 886–93. *Crossref*, doi:10.1016/j.conbuildmat.2006.12.013.

[7] Auta, Samuel Mahuta, and Tasiu Hassan. "Effect of Waste Burnt Bricks as Coarse Aggregate on the Compressive Strength of Ligth Weight Re-Vibrated Concrete." *IOP Conference Series: Materials Science and Engineering*, vol. 955, no. 1, IOP Publishing, Nov. 2020, pp. 012037. *Crossref*, doi:10.1088/1757-899x/955/1/012037.

[8] Damdelen, O. "Investigation of 30% Recycled Coarse Aggregate Content in Sustainable Concrete Mixes." *Construction and Building Materials*, vol. 184, Elsevier BV, Sept. 2018, pp. 408–18. *Crossref*, doi:10.1016/j.conbuildmat.2018.06.149.

[9] Zhao, Yasong, et al. "Utilization of Waste Clay Bricks as Coarse and Fine Aggregates for the Preparation of Lightweight Aggregate Concrete." *Journal of Cleaner Production*, vol. 201, Elsevier BV, Nov. 2018, pp. 706–15. *Crossref*, doi:10.1016/j.jclepro.2018.08.103.

[10] Abdul Hakim, Mohammad Yasir, et al. "Physical and Mechanical Properties of Concrete Using Recycled Clay Bricks as Coarse Aggregate." *American Journal of Engineering and Applied Sciences*, vol. 15, no. 1, Science Publications, Jan. 2022, pp. 88–100. *Crossref*, doi:10.3844/ajeassp.2022.88.100.

[11] Sajid Saleem, et al. "Exploratory Study of Machine Crushed Over Burnt Brick as Coarse Aggregate in Concrete Hollow Blocks." *International Journal of Engineering Research And*, vol. V6, no. 02, ESRSA Publications Pvt. Ltd., Jan. 2017. *Crossref*, doi:10.17577/ijertv6is020008.

[12] Hu, Jiong, and Kejin Wang. "Effect of Coarse Aggregate Characteristics on Concrete Rheology." *Construction and Building Materials*, vol. 25, no. 3, Elsevier BV, Mar. 2011, pp. 1196–204. *Crossref*, doi:10.1016/j.conbuildmat.2010.09.035.

[13] Idrees, Maria, et al. "Sustainable Production of Low-Shrinkage Fired Clay Bricks by Utilizing Waste Plastic Dust." *Alexandria Engineering Journal*, vol. 68, Elsevier BV, Apr. 2023, pp. 405–16. *Crossref*, doi:10.1016/j.aej.2023.01.040.

[14] Pinchi, S., et al. "Use of Recycled Broken Bricks as Partial Replacement Coarse Aggregate for the Manufacturing of Sustainable Concrete." *IOP Conference Series: Materials Science and Engineering*, vol. 758, no. 1, IOP Publishing, Feb. 2020, pp. 012039. *Crossref*, doi:10.1088/1757-899x/758/1/012039.

[15] Mohammed Umar, Usmani, and K. Muthusamy. "Potential of Waste Material as Coarse Aggregates for Lightweight Concrete Production: A Sustainable Approach." *CONSTRUCTION*, vol. 3, no. 1, Universiti Malaysia Pahang Publishing, June 2023, pp. 87–114. *Crossref*, doi:10.15282/construction.v3i1.9217.

[16] T, Kibriya. "Sustainable Construction – High Strength Concrete With Crushed Burnt Clay Brick Waste Aggregates." *International Journal for Research in Applied Science and Engineering Technology*, vol. 6, no. 1, International Journal for Research in Applied Science and Engineering Technology (IJRASET), Jan. 2018, pp. 194–200. *Crossref*, doi:10.22214/ijraset.2018.1031.

[17] Zhang, Huan, et al. "Autogenous-shrinkage Model for Concrete With Coarse and Fine Recycled Aggregate." *Cement and Concrete Composites*, vol. 111, Elsevier BV, Aug. 2020, pp. 103600. *Crossref*, doi:10.1016/j.cemconcomp.2020.103600.

[18] Fathifazl, Gholamreza, et al. "Creep and Drying Shrinkage Characteristics of Concrete Produced With Coarse Recycled Concrete Aggregate." *Cement and Concrete Composites*, vol. 33, no. 10, Elsevier BV, Nov. 2011, pp. 1026–37. *Crossref*, doi:10.1016/j.cemconcomp.2011.08.004.

[19] Indian Standards Institution. (1999). IS 9103:1999 - *Concrete Admixtures* - Specifications. Bureau of Indian Standards.

[20] Indian Standards Institution. (2015). IS 269:2015 - *Ordinary Portland Cement* - Specification. Bureau of Indian Standards.

[21] ASTM International. (n.d.). ASTM C494/C494M - *Standard Specification for Chemical Admixtures for Concrete*. ASTM International.

[22] Indian Standards Institution. (2000). IS 456:2000 - *Code of Practice for Plain and Reinforced Concrete*. Bureau of Indian Standards.

[23] Indian Standards Institution. (1992). IS 1077:1992 - *Common Burnt Clay Building Bricks* - Specification. Bureau of Indian Standards.

[24] Indian Standards Institution. (2016). IS 383:2016 - *Specification for Coarse and Fine Aggregates from Natural Sources for Concrete*. Bureau of Indian Standards.

Acknowledgments

The author expresses sincere gratitude to the Principal, Malla Reddy Engineering College(A), Hyderabad, for generously granting permission to conduct the research and the unwavering support and excellent facilities provided by the university in the successful completion of the study. Special appreciation is reserved for friends whose steadfast support significantly contributed to the collaborative effort, making this project an enriching and rewarding experience.

IOP Conference Series: Earth and Environmental Science

PURPOSE-LED PUBLISHING™

PAPER • **OPEN ACCESS**

Effect of infill walls on seismic performance of RC framed buildings

To cite this article: Y. Bala Balaji *et al* 2024 *IOP Conf. Ser.: Earth Environ. Sci.* **1409** 012030

View the article online for updates and enhancements.

You may also like

- Numerical study on masonry infill wall by using in-plane element and joint interface with RC frame
Mochamad Firmansyah Sofianto, Muhammad Imaduddin and Berkat Cipta Zega
- The effects of 3D printing designs on PLA polymer flexural and fatigue strength
Pham Son Minh, Van-Thuc Nguyen, Tran Minh The Uyen et al.
- Dual-energy CT evaluation of 3D printed materials for radiotherapy applications
Gabriel P Fonseca, Behzad Rezaeifar, Niklas Lackner et al.



This content was downloaded from IP address 47.247.77.11 on 27/11/2024 at 05:40

Effect of infill walls on seismic performance of RC framed buildings

Y. Bala Balaji[1*], S. A. V. Prasad[1] and B. Kavitha[1]

[1]Department of Civil Engineering, National Institute of Technology Warangal, Telangana-506004, India

[*]E-mail: balabalaji0722@gmail.com

Abstract. Infill walls are masonry walls constructed to fill the gaps between the structural frames. In structural analysis, these walls are considered non-structural members as they do not participate in the load transfer mechanism. These walls offer considerable resistance in terms of a diagonal strut when the bounding frame experiences lateral loads. This study focuses on the effect of infill walls on the seismic parameters by modelling different infill wall configurations of G+6 buildings by considering the infill resistance as a pin-jointed strut using SAP2000 software. The results from the response spectrum analysis of these models emphasized the importance of infill walls and their configuration in the seismic resistance of buildings.

Keywords. Diagonal strut, infill wall, SAP2000

1. Introduction

In order to take care of structures to earthquake loads, we need to consider the effect of the earthquakes on the design process based on our understanding of their characteristics. But although it is necessary to design for these earthquake events in many parts of the country, it seems uneconomical. So seismic design philosophy has been developed over the years. The objective of this seismic design is to constrain the damage to the structure. The structures are designed in such a way that every structure should resist minor earthquakes without damage, moderate earthquakes with minor structural damage, and severe earthquakes with minor structural damage but without collapse. Still, we need to understand the behaviours of buildings under earthquakes for various requirements like plan and vertical irregularities, infill wall interaction, etc.

For the purpose of privacy, the space between the frames of beams and columns is covered by a masonry wall. These walls are called infill walls. These walls are constructed after the building frame made of reinforced concrete has gained sufficient strength. So, these walls possess a weak joint between the frame and the wall, thereby causing separation from each other. As a result of this separation, the stresses are concentrated at the corners of the frame and fail. These infill walls were assumed not to take part in any kind of load transfer in the structure. So, these walls are just considered a dead weight in the structure, and the dead load of the walls is directly applied to the beams. This assumption is reasonably valid for gravity loads, but it is not valid under the application of lateral loads caused by wind and earthquake forces. Upon the application of lateral force, these walls offer considerable resistance to lateral forces. These infill walls enhance the strength and stiffness of the structures. The additional stiffness due to the infills will

Content from this work may be used under the terms of the Creative Commons Attribution 4.0 licence. Any further distribution of this work must maintain attribution to the author(s) and the title of the work, journal citation and DOI.
Published under licence by IOP Publishing Ltd

modify, influence, and alter the dynamic behaviours of the structure, resulting in a change in structural response.

As per IS 1893-2016, the time period is different for different types of buildings, like steel buildings, reinforced concrete buildings, and buildings with lateral load-resisting members. The empirical expressions suggested for calculating time periods only depend on the height and plan dimensions of the building. So, these equations neglect the stiffness offered by the infill walls and estimate larger values of natural time periods. Higher time periods indicate lower base shear and other parameters. Upon considering the stiffness of infill walls, the time period reduces and attracts more base shear force. So, the equivalent static method cannot estimate the time period of structures accurately. On the other hand, the response spectrum method is a dynamic analysis method. It considers the stiffness offered by the infill walls and estimates the response of the structure more accurately than the equivalent static method. So, in the present work, the response spectrum method has been adopted to analyze the models with different infill wall configurations along the height of the building.

In the present work, the G+6 rectangular building plan is considered and analyzed with and without considering the infill wall. The buildings are modelled in SAP 2000 software by considering different possible infill wall configurations in elevation under the response spectrum method. Shear walls and steel bracings are also considered along with the infill walls and analyzed for seismic performance.

2. Literature Study

The interaction of masonry infill walls with the building frame by assuming infill walls as a “diagonal struct” and “equivalent diagonal structs” has been studied in the past [1, 12, 18, 19]. Stafford et al. (1969) proposed the contact length between frame and infill by considering the relative stiffness of the infill and frame and their material properties [20]. In 1974, Mainstone proposed an empirical equation to calculate the equivalent width of the struct by considering the relative stiffness of the infill and the frame and their material properties [16, 21]. According to Paulay et al., the width of the wall in contact should be less than that of the full infill wall as the lateral force increases, separation of frame and infill occurs, and the contact length between the frame and infill is reduced [14]. Altogether, the results of elastic analysis show that the presence of non-structural masonry infill walls can modify the global seismic behaviour of framed buildings to a large extent [9, 10]. Considering infill walls as a diagonal strut increases stiffness and reduces the time period, which results in an increase in maximum base shear during an earthquake [5]. Razzaghi (2015) performed a nonlinear response history analysis to investigate the effect of infill wall arrangements in RC dual frames [17]. Qian (2017) observed that the initial stiffness of the structure increased nine times for the infill wall frame than the bare frame and also showed a large increase in the load-resisting capacity in the large deformation stage [15]. Li (2019) used macro models with one, two, and three strut models, as well as a modified three strut macro model, to predict the progressive collapse behaviour of RC infilled frames [11]. The analytical studies of different multi-story RC buildings with different shear wall positions for better performance are also found in the literature [2, 3, 22].

Based on the literature study, it was found that many researchers have performed experimental studies and found that infill walls contribute to an increase in stiffness to a large extent. Some researchers have proposed empirical formulas to predict the response of infill walls inside the bare frame. There is very little literature available on base shear, storey displacements, and storey drifts when infill walls are considered as a diagonal strut. Also, the effect of infill walls

on seismic parameters is not focused so far when the infill walls are configured irregularly on different floors.

3. Methodology

3.1. Infill Walls

For the dynamic study of R.C. frames with masonry infills, many techniques have been developed that incorporate simplifying assumptions about the stiffness and strength of the material. Various empirical structures have been advised by numerous national and international standards. Different methods of modelling these infill walls are available, like micro- and macro-modelling. Micromodel Ing includes modelling the infill wall as a finite element model. Since the infill wall is a composite member, micro-modelling is a complex and tedious procedure. In the macro-modelling procedure, the infill wall is modelled as a diagonal strut with equivalent width and thickness equal to the width of the wall, which includes all the material properties and stiffness properties of the infill wall material and the bounding frame. The modelling procedure is presented below. In the present study, the equivalent width of the diagonal struct is calculated as per IS 1893-2016 guidelines. Figure 1 provides a typical view of the infill wall.

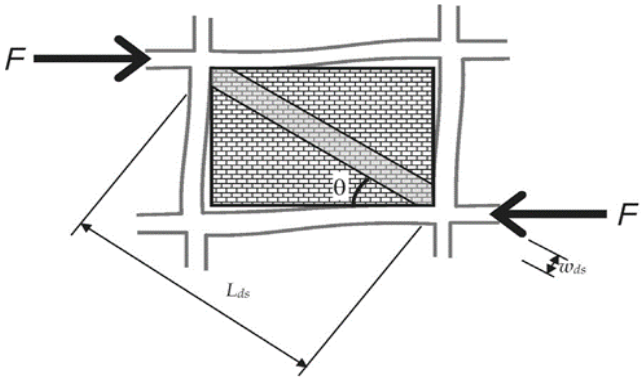


Figure 1. Equivalent diagonal strut of infill wall (Taken from IS:1893-2016 [6])

The equation for the width of an equivalent diagonal struct is given by

$$w_{ds} = 0.175 \propto_h{}^{-0.4} L_{ds} \quad (1)$$

$$\propto_h = h\left[\sqrt[4]{\frac{E_m t.\sin 2\theta}{4.E_f.I_c.h}}\right] \quad (2)$$

where,
L_{ds}= Diagonal length of the infill wall
t = thickness of infill wall
E_m= Young's modulus of infill wall material
E_f=Youngs modulus of bounding frame
I_c= Moment of inertia of the column
h = height of infill wall
θ= angle of inclination of diagonal strut with horizontal
The modulus of elasticity or young's modulus of infill wall material is given by

$$E_m = 550.f_m \quad (3)$$

$$f_m = 0.433.f_b^{0.64}.f_{mo}^{0.36} \quad (4)$$

f_m = compressive strength of masonry prism in MPa
f_b = compressive strength of brick in MPa.
f_{mo} = compressive strength of mortar in MPa.

3.2. Structural Modelling

In this study, a G+6 reinforced cement concrete-framed building with a 16 m x 12 m area in plan dimension with 4 bays in the X direction with 4 m bay spacing and 3 bays in the Y direction with 4 m bay spacing is considered. The general, sectional, and seismic properties, along with loads acting on the structure, are provided in Table 1. The RC beams and columns are modeled as frame elements, whereas slabs are modeled as area elements. The live loads and floor finish loads acting on the floor and roof slabs are taken from [7, 8]. A special moment resisting frame is considered for the building, confirming ductile detailing. The building is assumed to have a 5% damping ratio, is situated on medium soil, and is used for residential purposes.There are totally 7 models considered in this work and their results are compared with respect to a bare frame model (M1), which is shown in Figure 2.

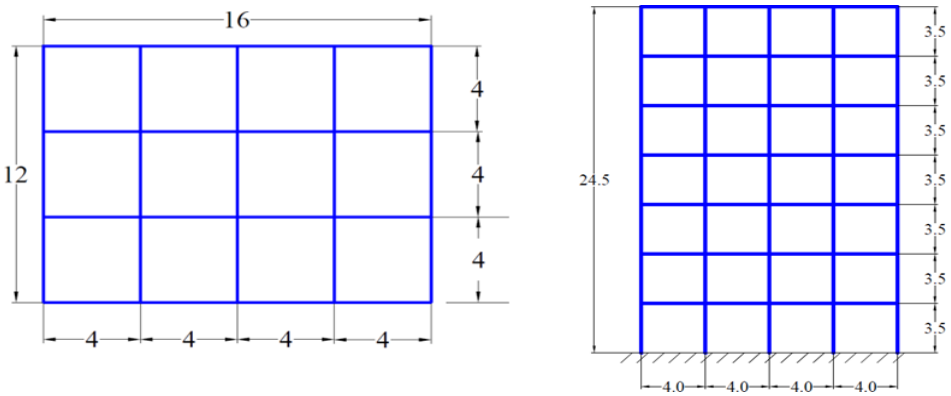


Figure 2. Plan (left side) and elevation (Right side) of the bare frame model (M1).

Infill walls are modeled as an equivalent pin jointed diagonal struct within the RCC. As per the macro-modeling concept, the infill wall is assumed to be acting as a diagonal struct and the width of struct is estimated using code provisions. In the present study, the equivalent width of the diagonal struct is calculated as per IS 1893-2016 guidelines. In this study, brick masonry infill walls are considered, and the properties of the brick masonry infill walls are provided in Table 2. The values of the compression strength of brick masonry and its modulus of elasticity have been obtained from the experimental results of researchers [23]. The infill wall modeled as a diagonal strut (M2) has been shown in Figure 3.

To understand the performance of buildings for different infill wall configurations in vertical directions, three models have been considered. In model 3 (M3), the ground floor is modeled without infill walls, and all other floors are modeled with infill walls, as shown in Figure 4. In model 4 (M4), both the ground floor and the first floor are modeled without infill walls, and all others floors are modelled with infill wall. Figure 5 illustrates the elevation of the M4.

Table 1. Properties of the building models considered in the study.

Type	Properties	Dimensions/Value
General Properties	No. of stories	7
	Typical floor height	3.5m
	Grade of concrete	M20
	Grade of steel reinforcement	Fe415
	Parapet wall height	1m
	Density of infill material	19.8 kN/m3
Sectional Properties	Size of the Beam	0.3m*0.45m
	Size of the Column	0.45m*0.45m
	Thickness of Slab	150mm
Loads acting on Structure	Live load on floors	3 kPa
	Live load on roof	1.5 kPa
	Floor finish load on all floors	1 kPa
	External wall load	13.89 kN/m
	Internal wall load	9.05 kN/m
	Parapet wall load	2.98 kN/m
Seismic Properties	Seismic zone	IV
	Soil type	II
	Zone factor	0.24
	Response reduction factor (RF)	5
	Importance factor(I)	1

These variations are considered to explain the formation of soft storey because of the absence of infill walls on lower floors. In model 5 (M5) alternate floors are modeled with infill walls and other floors are modeled without infill walls, shown in Figure 6. In all the above models, infill walls are modeled as diagonal pin joined strut element with eccentric back connection. In model 6 (M6) the infill walls are modelled as cross bracing, shown in Figure 7. In 7 model (M7) shear walls are adopted at the corner along with the infill walls as shown in Figure 8. In model 8 steel bracings have been provided at the corner bays throughout the height of the building.

Table 2. Properties of the building models considered in the study.

Properties	Values
Thickness of external wall	230mm
Thickness of internal wall	150mm
Diagonal length of struct	4.68m
Height of infill wall	3050mm
Youngs modulus of concrete	22360 MPa
Youngs modulus of infill wall	3300 MPa
Angle of inclination	40.667^{o}
Width of diagonal struct of external wall	535mm
Width of diagonal struct of internal wall	560 mm

The elevation of model 8 (M8) has been shown in Figure 9. All the above-mentioned models are analyzed for seismic response by using the response spectrum method in SAP2000 (V23.2.0) software. These results will be compared for seismic performance like base shear, top storey displacements, storey drifts and storey stiffness.

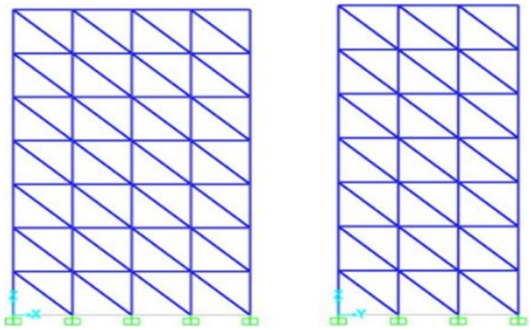


Figure 3. Elevation of infill wall model (M2)

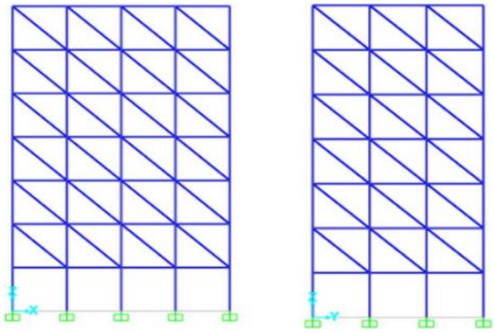


Figure 4. Ground floor without infill (M3)

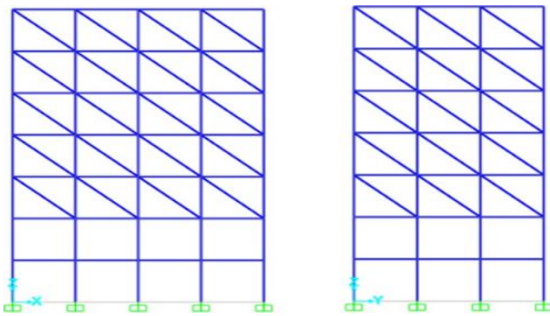


Figure 5. Ground floor and first floor without walls (M4)

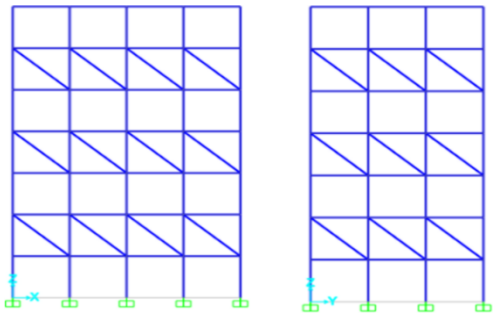


Figure 6. Alternate floors without infill walls (M5)

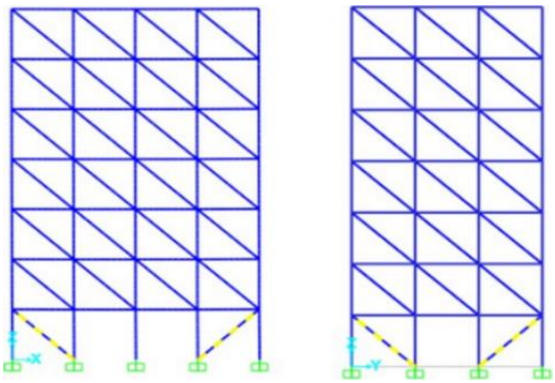


Figure 7. Steel bracings at ground floor corners(M6)

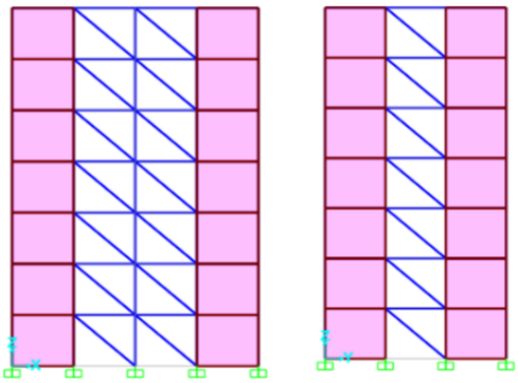


Figure 8. Shear walls at corners along with fill walls (M7)

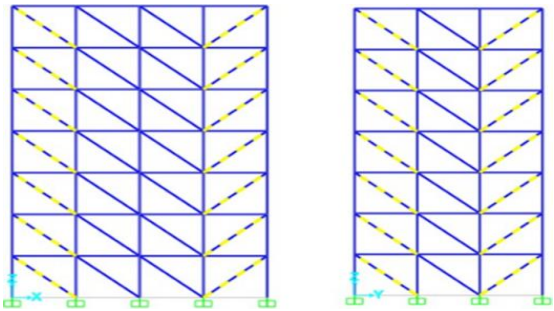


Figure 9. Steel bracings at the corners bays along with infill walls (M8)

4. Results and discussion

The models are modeled and analyzed using response spectrum analysis. The seismic parameters considered for the comparison are the natural time periods of the building, base shear experienced by the structure, top-storey displacement, storey drift ratio, storey stiffness, and storey overturning moment.

4.1. Natural Time period

The natural time periods of the models are obtained after performing modal analysis. The reported time periods correspond to the first mode of the structure and are the highest of all other modes. Comparing the results (Figure 10), it is observed that the natural time period is reduced for all the models that have infill walls and lateral load-resisting elements. Model 7 recorded the least time period with 0.374 seconds, with a 70% reduction because of the presence of the shear wall. Considering model 2, the presence of infill walls throughout the building has greatly influenced the natural time period, with a 45% reduction compared with the bare frame model. Observing models 3, 4, and 5, the absence of infill walls at the bottom floors brings a time period nearly equal to that of the bare frame, which means the presence of infill walls on the top floors doesn't alter the time period very much. For model 6, the reduction in time period is about 60% compared with the bare frame. Providing steel bracings at the corner bays of Modal 8 has reduced the time period by 48%.

4.2. Base shear

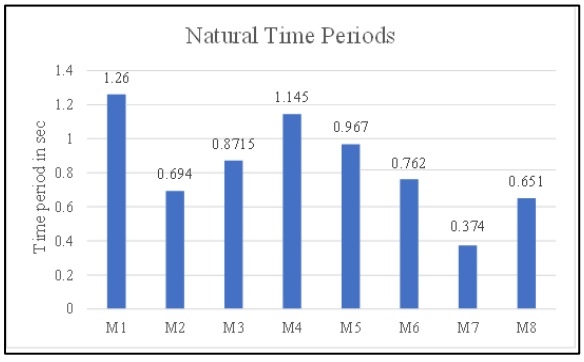


Figure 10. Variation of Natural Time periods in Models

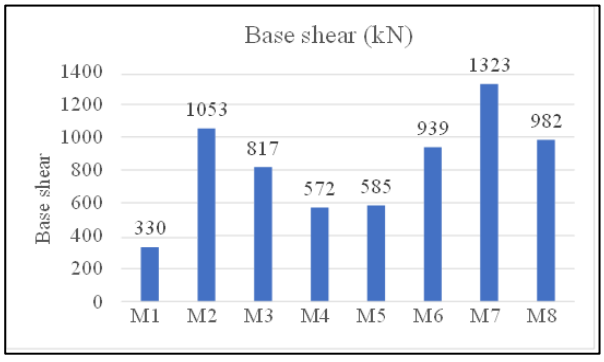


Figure 11. Variation of Maximum base shear for considered models

The base shear acting at the base of the structure is considered for the response spectrum load case in both directions, and the maximum values have been reported here. Comparing the base

shear values of all the models, as shown in Figure 11, the values are higher for every model than those of a bare frame model. Modal 7 recorded the highest base shear value due to the presence of shear walls at the corners. The base shear value is increased by four times that of the bare frame model. Considering model 2, the presence of infill walls throughout the height of the building has considerably increased base shear three times.

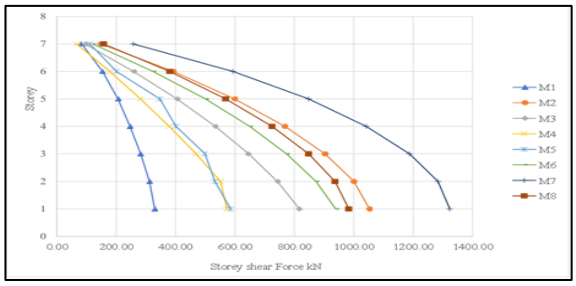


Figure 12. Storey Shear Force in X- Direction

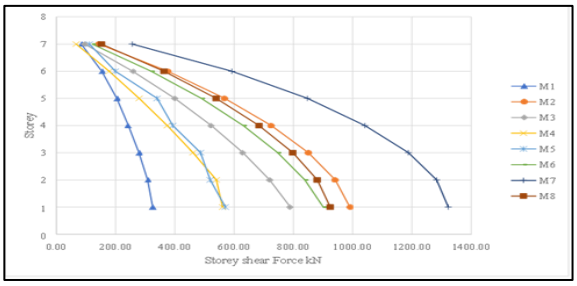


Figure 13. Storey Shear Force in Y- Direction

The storey shear force is shown in Figures 12 and 13. Observing models 4 and 5, base shear increased by around 70%, but for model 3, base shear increased by around 150%. This indicates the presence of infill walls at the lower stories highly influences base shear, and the arrangement of infill walls in the top storey has a lesser impact on base shear. For model 6, the base shear is increased by 185%. For model 8, the base shear is increased by 200% compared to the bare frame. Upon observing models 2 and 8, the performance of infill walls throughout the buildings is almost similar to that of the building, which has steel braces just at the outer corners of the building.

4.3. Top Storey Displacement

The variation of Storey Displacements and Storey Stiffness in both X and Y directions are shown in Figures from 15 to 18. The top-story displacements for all the models are adopted for the response spectrum load case for both directions, and the maximum values are considered, which were observed in the y direction. Top-storey displacements for the response spectrum load case are provided in Table 3. Comparing the top-story displacements as shown in Figure 14, the maximum displacements are observed to be almost the same in both directions. The maximum top-story displacements are reduced for all the models when compared with the bare frame model. Model 7, which has a shear wall at the corners records the lowest displacement with a 74% reduction from the bare frame model. Considering model 2, the presence of infill walls has greatly affected top-story displacements, with a 48% reduction in their value. Modal 4 and Modal 5 have around a 35% reduction, and Model 3 has around a 40% reduction in top-storey displacement. For modal 6 and modal 8, the top storey displacement has been reduced by 44%.

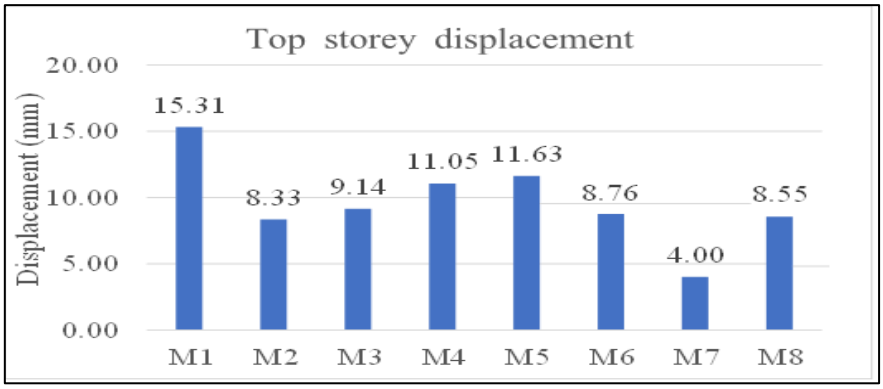


Figure 14. Variation of Top Storey Displacements for considered models

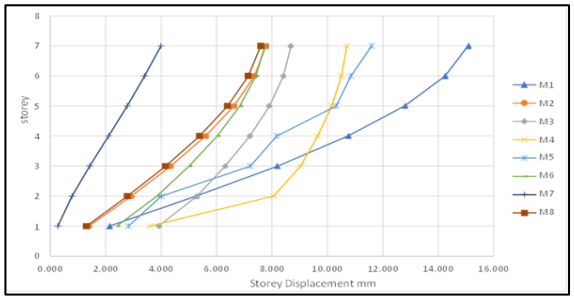


Figure 15. Storey Displacement in X-Direction

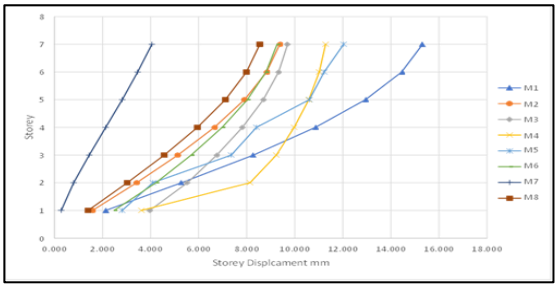


Figure 16. Storey Displacement in Y-Direction

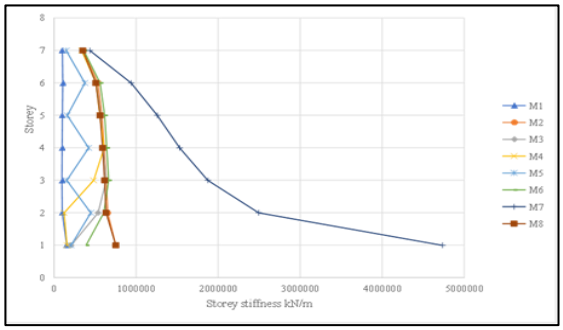


Figure 17. Storey Stiffness in X- Direction

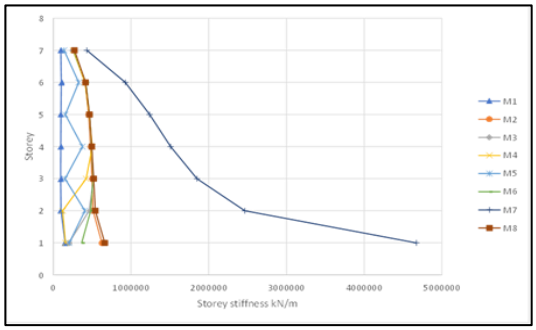


Figure 18. Storey Stiffness in Y- Direction

5. Conclusions

From the results, it can be seen that the maximum decrease in the time period of the structure is 45% for the building in which all floors have infill walls. The absence of infill walls at the bottom floors doesn't affect the natural time period much. Providing steel bracings at the corners of the building reduces the natural time period by 44%, which is almost equal to that of the infill wall model. From the results, the presence of infill walls throughout the building resulted in an increase of base shear by 200%. The presence of infill walls at the bottom of the building highly influences seismic response and increases base shear considerably. From the results, the presence of infill walls greatly reduces maximum top storey displacements by 48%. Bottom floors without infill walls lead to an overall 35% decrease in top-storey displacement and increase base shear by 70%. Discontinuity of infill walls along height may lead to more storey displacements than that of the bare frame model. Displacement at the bottom floors has increased by 175% for models without infill walls at the bottom floors. This means that out of the total top storey displacement, a huge amount of displacement occurs at the bottom floor, causing a soft storey effect. Storey drift ratio is maximum for buildings in which bottom floors are modelled without infill walls, and storey drift ratio is increased by 45% compared to the bare frame model. For model 4, where infill walls are absent in both ground and first-floor storeys, stiffness is reduced by 75% for the first floor. Also, in every model where infill walls are absent, the stiffness of the floor is reduced by more than 50%, which leads to a soft-storey effect.

In any case, if infill walls are to be avoided only on certain floors, they must be properly analyzed and designed to take care of unusual storey displacement demand and stiffness reduction so as to avoid soft storey effects. Providing steel bracings in the corner of the building may restrict the excessive displacement demand due to the soft-storey effect, and the stiffness of the building will increase. It can be seen that the base shear value is increased to a large extent,

which leads to an increase in column axial forces. An additional percentage of steel may be required to withstand these extra axial forces caused by an increase in base shear.

References

[1] A. Panagiotis G, Antoniou, ST and Sophianopoulos, Dimitris S and Chrysostomou ch 2011 Mathematical Macromodeling of Infilled Frames: State of the Art Journal of Structural Engineering 137 1508-1517.
[2] Anes Babu, Chandan Kumar Patnaikun and D. B. K.V.G.D 2017 Effect of Steel Bracings on RC Framed Structure International Journal of Mechanics and Solids 12 97-112.
[3] Ashish Kumar Gupta, Dr. Saleem Akhtar and Dr. Aslam Hussain 2020 Analysis of a Tall Building with Shear Wall of RCC and Steel Plate International Journal of Engineering Research & Technology (IJERT) 9 308-314.
[4] Basha, Syed Humayun, Kaushik and Hemant, B 2015 Evaluation of Non-linear Material Properties of Fly Ash Brick Masonry under Compression and Shear Journal of Materials in Civil Engineering 27 8-10.
[5] C. Rajesh, R. Kumar and S. Kandru 2014 Seismic Performance of RC Framed Buildings With & Without Infill Walls International Journal of Engineering research and Technology 3 2278-0181.
[6] Indian Standard, Criteria for Earthquake resistant design of structures (part 1) - Code of Practice (IS: 1893-2016).
[7] Indian Standard, Code of Practise for Design Loads for Buildings and Structures - Code of Practice (IS: 875-1987).
[8] Indian Standard, Code of Practice for Design Loads for Buildings and Structures (part 1) - Code of Practice (IS: 875-1987).
[9] Kaushik, Hemant B, Durgesh C and Jain 2007 Stress-strain Characteristics of clay brick masonry under uniaxial compression Journal of materials in Civil Engineering 19 728-739.
[10] Korkmaz and k. armagan 2007 Earthquake assessment of RC structures with Masony infill walls International Journal of science & Technology 155-164.
[11] Li, Shuang, Kose, Mehmet Metin and Shan, Sidi 2019 Modeling Methods for Collapse Analysis of Reinforced Concrete Frames with Infill Walls Journal of Structural Engineering 145.
[12] M. Holmes 1961 Steel frames with brickwork and concrete infilling 19 473-478.
[13] Murty, CVR, Sudhir K and Jain 2000 Beneficial influence of masonry infill walls on seismic performance of RC frame buildings.
[14] Paulay, Thomas and Priestley, MJ 1992 Seismic Design of Reinforced Concrete and Masonry Buildings, vol. 768, Wiley New York.
[15] Qian, Kai and Li, Bing 2017 Effects of Masonry Infill Wall on the Performance of RC Frames to Resist Progressive Collapse Journal of Structural Engineering 143.
[16] R. J. Mainstone 1974 Supplementary note on the stiffnesses and strengths of infilled frames, Building Research Establishment, Building Research Station.
[17] Razzaghi, MS and Javidnia, M 2015 Evaluation of the effect of infill walls on seismic performance of RC dual frames International Journal of Advanced Structural Engineering (IJASE) 7 49-54.
[18] S. Polyakov 1959 Masonry in framed buildings, Gosudarstvennoe izdatel'stvo Literatury postroitel'stvu i arkhitekture.
[19] Samoila and M. Diana 2012 Analytical Modelling of Masonry Infills Moment 1000 1-10.
[20] Stafford, Smith, Bryan and Carter, C 1969 A method of analysis for infilled frames Proceedings of the institution of civil engineers 44 31-48.
[21] T. tahsin, D. Cigdem, b. meril, Baris and O. Guney 2014 Evaluation of the Predictive Models for Stiffness, Strength, and Deformation Capacity of RC Frames with Masonry Infill Walls Journal of Structural Engineering 140.
[22] Vikas Govalkar, S. P. J. and G. N. G. 2014 Analysis of Bare Frame and Infilled Frame with International Journal of Recent Technology and Engineering (IJRTE) 3 67-72.

IOP Conference Series: Earth and Environmental Science

PURPOSE-LED PUBLISHING™

PAPER • **OPEN ACCESS**

Development of lightweight bricks using agricultural and industrial waste

To cite this article: R. R. Dighade *et al* 2024 *IOP Conf. Ser.: Earth Environ. Sci.* **1409** 012031

View the article online for updates and enhancements.

You may also like

- Seismic analysis of vertically irregular RCC high-rise buildings: A study with provision of FVD at various locations
Batchu Ramanjaneyulu, Achina Prasad, keshagoni Satish et al.
- The performance of arabica coffee farmers in implementing good agricultural practices in Aceh Tengah, Indonesia
A H Hamid, Q N Siregar, V Zikria et al.
- Impact of nano-silica on the mechanical properties of lightweight concrete
N Alghrairi, F N A Aziz, S A Rashid et al.



This content was downloaded from IP address 47.247.77.11 on 27/11/2024 at 05:40

Development of lightweight bricks using agricultural and industrial waste

R. R. Dighade[1*], J. D. Sakhare[1], S. S. Mujumdar[1], L. W. Bhimte[1], V. M. Bansod[1], A. S. Pachpole[1] and T. Y. Rukhamode[1]

[1]Department of Civil Engineering, Yeshwantrao Chavan College of Engineering, Nagpur-441110, Maharashtra, India

[*]E-mail: rajendradighade@gmail.com

Abstract The construction industry is undergoing a notable shift towards environmental sustainability, driving the innovation of construction materials that are robust, lightweight, and eco-friendly. this study delves into the formation of lightweight bricks, with a focus on their mechanical properties, thermal insulation capabilities, and environment-imperative agricultural and industrial waste material. In response to the environmental imperative to reduce reliance on clay and other raw materials in construction, this study investigates the utilization of flower waste, iron ore, chaff, and wheat husk, in the production of lightweight bricks. This alternative material offers a sustainable solution to mitigate the environmental impact of traditional brick manufacturing processes. Through a systematic evaluation of physical properties, materialistic properties, and thermal performance the study provides insights into the feasibility and efficacy of incorporating chaff and wheat husk into brick production. The findings offer practical recommendations for the development of environment-friendly construction materials contribute to the conservation of natural resources and the promotion of sustainable building practices.

1. Introduction

The construction sector, a cornerstone of the global economy, plays a pivotal role in shaping the urban fabric [1,3,4,7,11]. In order to address these issues, it becomes important to produce building materials that are both environmentally sustainable and commercially feasible. As public knowledge of the benefits of sustainable practices grows, the building sector must innovate new materials that balance environmental responsibility with business feasibility. In particular, conventional clay bricks have long been preferred in buildings due to their strength and longevity, although they do have certain disadvantages. [1,4,7,9,11] Because of their weight, manufacturing requires a lot of energy, heavy materials are produced, and transportation expenses are frequently substantial. Moreover, the extraction of raw materials for conventional bricks contributes to ecological degradation. In response, there is a growing need for innovative and sustainable solutions that can reduce the environmental impact of the construction industry while preserving the structural integrity and essential properties of building materials [1-11]. To address this dilemma, scientists and business leaders have looked at a number of strategies for creating lightweight building materials that maximize environmental benefits and improve energy efficiency. Using agricultural waste in addition to industrial waste is one such strategy that makes use of this recently created environmentally acceptable aggregate [1-9]. The goal of the study article is to create lightweight bricks from industrial leftovers and agricultural trash. An inventive way to solve environmental issues and advance sustainable building methods is the creation of lightweight bricks made from industrial and agricultural waste. [1-11].


Content from this work may be used under the terms of the Creative Commons Attribution 4.0 licence. Any further distribution of this work must maintain attribution to the author(s) and the title of the work, journal citation and DOI.
Published under licence by IOP Publishing Ltd

Several waste materials were investigated in this study as possible additions to conventional brick-making techniques. The goal of the project is to create lightweight bricks out of industrial and agricultural wastes such as wheat husk, iron ore, flower waste, and chaff. The evaluation of these bricks' mechanical behaviour, thermal performance, material properties, and overall environmental sustainability receives particular emphasis. One potential method for producing ecological, structurally sound, and lightweight bricks is to use agricultural waste like wheat husk and chaff. By maximizing the use of leftover resources, this strategy encourages resource efficiency and advances sustainable building techniques.

2. Materials and proportion

The materials used for constructing the bricks are waste materials generously collected from the environment, due to their properties like availability, abundance, materialistic properties etc. The chosen materials, which include iron ore, wheat husk, chaff, flower waste ash, and chaff, are readily available in significant amounts and can be used to make bricks without depleting natural resources. Thus, by making use of these plentiful waste materials, we can produce environmentally friendly bricks that support sustainable construction practices, lessen waste and its impact on the environment, and support the circular economy by repurposing industrial byproducts in an environmentally friendly way.

2.1. Flower waste

The flower waste was gathered and allowed to sun dry for approximately one to two weeks before undergoing controlled combustion to produce ash. In general, flowers are organic materials, and their combustion temperature typically ranges from around 300°C to 600°C (570°F to 1110°F). The temperature provided was 990ºF. However, this temperature range can vary based on the specific composition of the flowers and the efficiency of the combustion process.

Table 1. Proportion used for flower waste brick construction

S. No.	Material used	Soil (gm)	Proportion	
			Fly Ash (gm)	Material (gm)
1.	Flower	1100	660	440 (20%)
	Waste	1160	440	600 (30%)
		1300	-	880 (45%)

Table 2. Proportion used for flower waste brick construction using lime as binder

S. No.	Material used	Soil (gm	Lime	(gm)	Proportion	
					Fly Ash (gm)	Material (gm)
1.	Flower	1100	330		330	440 (20%)
	Waste	1160	220		220	600 (30%)

2.2. Iron Ore

Iron ore ash is a byproduct of steel production processes and is typically composed of fine particles that are left after the combustion or smelting of iron ore. It was ensured that the iron ore ash

obtain meets the required specifications for use in brick manufacturing, such as particle size distribution and chemical composition.

Table 3. Proportion used for iron ore brick construction

S. No.	Material used	Soil (gm)	Proportion	
			Fly Ash (gm)	Material (gm)
1.	Iron ore	1500	260	440 (20%)
		1400	260	800 (40%)
		1340	-	600(30%)

2.3. Chaff

Chaff refers to the husk or outer layer of grains that are separated during threshing or winnowing. Chaff is often considered a waste product for agriculture and industrial purpose. Using chaff for brick construction can mitigate its environmental impact by repurposing a waste product into a valuable building material.

Table 4. Proportion used for chaff brick construction

S. No.	Material used	Soil (gm)	Proportion	
			Fly Ash (gm)	Material (gm)
1.	Chaff	1320	-	880 (20%)
		1120	-	1020(30%)
		920	-	1120(40%)

2.4. Wheat Husk

The protective outer coating of wheat grains that is removed during threshing is called wheat husk, sometimes referred to as wheat straw. As a byproduct of harvesting and processing wheat, wheat husk is widely accessible. Bricks and solar panels made of eco-friendly materials can be made from wheat husk. Using wheat husk for a variety of uses can encourage sustainable farming methods and help cut down on waste in agriculture. Utilizing wheat husk for value-added products can also help preserve resources by lowering the need for conventional materials.

Table 5. Proportion used for wheat husk brick construction

S. No.	Material used	Soil (gm)	Proportion	
			Fly Ash (gm)	Material (gm)
1.	Wheat husk	1320	-	880(20%)
		1120	-	1020(30%)
		920	-	1120(40%)

2.5. Binder selection: Lime

Lime has a lengthy history of demonstrated effectiveness and has been used as a binder in construction for millennia. There are several advantages to using lime as a binder in the production of bricks, including environmental friendliness, durability, sustainability, and thermal

efficiency. Lime is added to the brick mixture to create environmentally friendly bricks that satisfy structural and environmental standards. [2,3,7,8,9]

2.6. Methodology

Bricks that are eco-friendly, lightweight, and structurally sound must be produced using a number of crucial production processes. First, careful material preparation is essential. Here, materials such as flower waste, iron ore, chaff, and wheat husk are chosen in order to guarantee that the finished bricks have the desired acoustic qualities. Second, a thorough mix design is created to ascertain the ideal proportions of waste products from agriculture and industry. This stage guarantees a homogenous mixing, which is necessary for consistent qualities and attributes in the finished product. Thirdly, the binder is carefully chosen, fly ash and lime are the main ingredients since they are readily available and economically viable. These binders are essential for keeping the particles together and creating a coherent structure while reducing production costs and environmental effects. The slurry is then meticulously shaped into brick forms using moulds with standardized diameters to guarantee compliance with current building codes. The moulds dimensions, which are usually fixed at 190x90x90 mm, correspond to the common brick measurements used in construction procedures. Another crucial step in the production process is curing, which is a controlled drying and hardening process that improves the strength and longevity of the bricks. Lastly, the bricks are strengthened even further by exposure to sunshine for a predetermined amount of time, usually ten days, though the precise amount of time may vary based on variables including weather, humidity, and brick thickness. With an emphasis on performance and sustainability, these combined techniques help produce high-quality, eco-friendly bricks appropriate for a range of construction applications. [2,3,6,7,9]

3. Tests and Experiments

3.1. Methodology for tests

3.1.1. Compressive strength test

The greatest axial load that a brick can bear before failing or deforming is indicated by its compressive strength, which is an essential characteristic in structural engineering and building. This key factor, which is commonly expressed in megapascals (MPa) or pounds per square inch (psi), determines which bricks are suitable for what uses. A universal testing machine (UTM) is used in a standard testing technique to ascertain this strength. Compressive strength is determined by subjecting representative brick samples to controlled loading until they fail. The greatest load that can be sustained is then used. Bricks compressive strength is assessed using a painstaking process that guarantees precise testing and perceptive analysis.

After choosing representative samples, the bricks are put horizontally between a universal testing machine's (UTM) platen and subjected to progressively higher compressive loads. The crucial cracking point, where the first indications of structural compromise appear, can be found by tracking the applied force. If the test is continued past this stage and brick failure is indicated by more splitting, crushing, or cracking, it is over. The measurement of compressive strength—which is essential for determining whether a brick is suitable for use in construction—is made possible by computing the maximum load sustained. This thorough method, which includes determining the breaking point, improves comprehension of the behaviour of bricks under stress and aids in the development of well-informed decisions for building projects. [12,13].



Figure1. Compressive Strength testing



Figure2. Development of cracks

3.1.2. Water Absorption test

Bricks must undergo a water absorption test to ascertain their porosity and absorbability, which is necessary to ascertain whether or not the bricks are suitable for a given construction work. To guarantee correct shape, a number of representative bricks are first gathered, and any evident flaws are checked out. To determine each brick's original dry mass, it is weighed separately. The bricks are then oven dried at temperatures between 105 and 110 degrees Celsius, and they are kept there until they have a constant weight, which normally takes around 24 hours. To determine the final dry mass, the samples are taken out and weighed once more.

After that, the dried bricks are submerged in purified water for a predetermined amount of surface water is wiped off, and their ultimate wet weight is measured while they are still wet. Next, using the given formula and taking into account the difference between the final wet and dry weights, determine the water absorption %.

The following formula determines the proportion of water absorbed: Initial weight * 100 / (Final weight - Initial weight). One important measure of the porosity of the bricks is the water absorption percentage that was achieved. Carefully carrying out the water absorption test guarantees a comprehensive evaluation of the porosity and absorption properties of bricks, facilitating well-informed decision-making throughout building projects. [12,13].



Figure 3. Submerging Bricks in water



Figure 4. Weighing of Bricks

3.2. Elongation test

A number of measurements can be made in order to fully evaluate brick size and possible elongation or deformation properties. First, twenty representative bricks are selected for testing. Vertical orientation is used to measure these bricks. Using a tape measure or ruler, the bricks are first arranged into a row and placed vertically on their ends. A comparison of the measurements from these orientations offers important information about possible differences in brick dimensions. Any variations between vertical measurements show how the brick behaves under various loading scenarios and orientations. Factors like material qualities, production tolerances, and environmental impacts can be responsible for these differences.

The data gathered from these measurements can be analyzed to provide a thorough understanding of the elongation or deformation characteristics of the bricks. Although this method provides a simple way to evaluate dimension differences according to orientation, it is important to recognize its limits, especially with regard to accuracy and precision. Standardized testing procedures and specialized equipment are advised for assessments that are more accurate. However, this method offers a preliminary understanding of how bricks behave in various orientations, which is helpful for planning construction projects and choosing building materials.[12].

$$Formula\ used\ for\ calculation\ = \frac{Length\ of\ standard\ brick - Length\ of\ manufactured\ brick}{\text{Length of manufacturing bricks}} X100$$



Figure 5. Elongation Test on Bricks

3.3. Efflorescence test

For the efflorescence test, which is designed to soak only a section of the brick, an observation area with a glass cover that is cylindrical in shape offers control. A thorough selection and cleaning process is used to prepare representative brick samples for placement inside the glass cover. Just a 25 mm portion of the brick is immersed in distilled or deionized water when using precision immersion. When the glass cover is sealed, the immersion period—which usually lasts 24 to 72 hours—is kept at a constant humidity level. To enable regulated circumstances, the brick samples are air-dried inside the sealed environment after soaking. Efflorescence is only observed on the drenched part; deposits that are white or grey are noted. Brick susceptibility is evaluated by rating and analyzing efflorescence severity using a standardized scale.

For documentation purposes, test results—including ratings and observations—are carefully documented. This technique guarantees accurate and consistent test results while enabling focused efflorescence examination. [12,13].



Figure 6. Efflorescence test



Figure 7. Sulphate formation on Bricks

4. Results and discussion

4.1. Results for flower waste

The inadequate bonding between the ash from flower waste and clay or lime resulted in poor cohesiveness, which caused fissures and structural instability in the clay bricks that were formed from flower waste. The bricks were lightweight, but after drying at room temperature, they appeared to contain fissures. The brick creations, which were made entirely of clay without the addition of lime and flower waste, likewise failed rather rapidly; after being constructed and allowed to dry in the sun, they began to show noticeable fractures after around four to five hours. Surprisingly, this failure happened even though there was no lime present, suggesting that other reasons, such as poor material compatibility, miscommunication, or a lack of structural integrity, could be the cause of future problems. More testing was just not done since the first obvious cracks appeared during the early phases of brick manufacturing and sun drying. We have really come to the conclusion that flower waste doesn't seem to be acceptable at all as a material for brick construction, based on all of these observations as well as the difficulty to achieve total structural integrity.

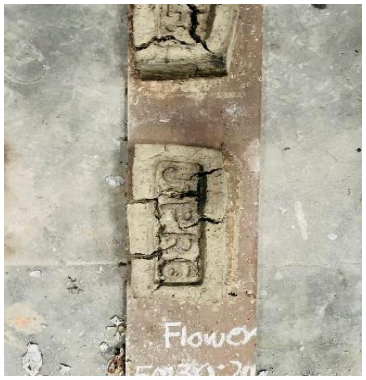


Figure 8. Formation of Early Cracks on Flower Waste Bricks



Figure 9. Formation of Early Cracks on Iron Ore Bricks

4.2. Results for iron ore

For a variety of reasons, the bricks made with iron ore during the first phase also failed. The development of fractures following sun drying was cited as the reason for the failure of ion ore bricks, indicating that iron ore ash might not mix well with other ingredients in the brick mixture, resulting in poor bonding and structural instability. These bricks also lacked the intended lightweight quality; the measured weight was greater than that of a regular brick. It was discovered that the mixture's lack of binders, incorrect ratios, and poor bonding were the causes of the fissures' early creation. Because of the early onset of cracks, experiments were subsequently halted, and it was determined that waste from stainless steel facilities could not be used to create lightweight bricks.

4.3. Results for chaff and wheat husk

Wheat husk and chaff had noticeably better results than flower and iron ore waste. The resulting wheat husks and chaff showed characteristics like binding, strength, structural integrity, and suitable size and shape. These bricks had the desired level of hardness and were sound. The prepared bricks also fulfilled all requirements and were lightweight. The compressive strength and water absorption findings met standard values and were satisfactory.

4.3.1. Results for Water absorption

Table 6. Water absorption test results

S. Nos	Material used	Proportion Used		
		20%	30%	40%
1	Chaff	14%	21%	16.7%
2	Wheat Husk	16.5%	20.5%	22%

A brick with a higher water absorption capacity will have a lower overall strength. The water absorption capacity of first-class bricks should not exceed 20% of their weight. Our bricks' water absorption was less than the specified levels. In particular, the water absorption ranged from around 16% for chaff bricks to about 15% for wheat husk bricks.

4.3.2. Results for Compressive strength

Table 7. Compressive strength test results

S. No.	Material used	Proportion Used		
		20%	30%	40%
1	Chaff	3.4N/mm^2	3.5N/mm^2	3.8N/mm^2
2	Wheat Husk	3.3N/mm^2	3.6N/mm^2	3.2N/mm^2

The composition, production method, and intended application of the bricks can all have a significant impact on their compressive strength. That being said, common bricks typically have compressive strengths ranging from about 3.5 N/mm^2 to 7.5 N/mm^2 [12,13]. Using a Universal Testing Machine (UTM) to test the compressive strength of wheat husk and chaff bricks, the average compressive strength of the chaff bricks was discovered to be approximately 3.5 N/mm^2 (Table 7). This number is within the normal range for ordinary bricks' compressive strength.

Table 8. Compressive Efflorescence test results

S. No.	Material used	Proportion Used		
		20%	30%	40%
1	Chaff	Heavy	Moderate	Slight
2	Wheat Husk	Heavy	Slight	Moderate

4.3.3. Results for Efflorescence test

Efflorescence under 10% of the brick area refers to the slight presence of deposit. Until 50% refers to moderate deposit and a deposit more than 50% refers to the heavy deposition of sulphate [12,13] (Table 8). In our favour, many various proportion bricks showed various results mentioned above.

Table 9. Elongation test results

S. No.	Material used	Result
1	Chaff	3.26%
2	Wheat Husk	3.11%

4.3.4. Results for elongation test

Elongation test results (Table 9) were obtained using the formula mentioned in Indian standard codes. The test results showed fairly precise values and met our standard specifications. The elongation test, also known as the tensile elongation test, is a common mechanical test conducted to measure the amount of deformation a material undergoes when subjected to tensile forces. This test helps evaluate the ductility, strength, and deformation behaviour of materials.

5. Result and discussion

Following a battery of performance testing, we have determined that wheat husk and chaff are eco-friendly materials that may be used to make bricks. Our investigation indicates that these materials can successfully replace traditional bricks, including defining all necessary parameters and delivering precise outcomes. Using wheat husk and chaff also encourages sustainable building techniques and minimizes waste. Not only can building expenses be minimized but also the ecological footprint can be greatly lowered by using these alternative materials.
In summary, chaff and wheat husk offer a practical and environmentally responsible brick-building material that also happens to be reasonably priced.

6. Conclusions

The development of lightweight bricks using upward methodologies has been completed. The utilization of flower waste, iron ore, chaff, and wheat husk in varying proportions to create different types of bricks was achieved. Comparing and analyzing the performance of bricks made from different materials, including flower waste, iron ore, chaff, and wheat husk results showed that using chaff and wheat husk as construction materials presents a compelling alternative to conventional options, offering eco-friendly and sustainable solutions.
Incorporating chaff and wheat husk into brick production indeed presents a range of compelling advantages, making them a sustainable and eco-friendly alternative to conventional brick materials. The utilization of chaff and wheat husk as agricultural byproducts reduces waste, contributing to environmental sustainability by repurposing these materials. These agricultural byproducts are often inexpensive or even free, as they are waste products, leading to potential cost savings in brick production. Bricks made with chaff and wheat husk tend to be lightweight, making them easier to handle and transport. Additionally, this characteristic can potentially reduce the structural load on buildings, offering advantages during construction and transportation.

Overall, the utilization of chaff and wheat husk in brick production not only aligns with sustainable construction practices but also offers remarkable benefits in terms of cost savings, handling ease, energy efficiency, and environmental impact, making them an attractive option for environmentally conscious construction projects.

References

[1] Swati S.Mane, Abhijit Kamate Experimental study on utilization of waste material in brick manufacturing Vol-7 Issue-5 2021 IJARIIE-ISSN(O)-2395-4396
[2] S.P. Raut, R.V. Ralegaonkar , S.A. Mandavgane Development of sustainable construction material using industrial and agricultural solid waste: A review of waste-create bricks 14 April 2011
[3] R R Dighade , International Conference on Recent Advances in Materials and Manufacturing (ICRAMM 2023)
[4] Ashwita Dalvi, Sachin Adapat, Aditi Patil, Shantanu Patil, Vinayak Mali, Research and development of brick using waste material, 07 July 2022
[5] N.K. Arif Ameeni, S.S.S. Koshik , Utilization of Plastic waste in bricks as eco-friendly material, December 2020 to April 2021.
[6] Gousiya Sayyed, Vishal Sardar, Sharwary Zade, Shabdagandha Tambe, Anuradha Ugile, Manufacturing of bricks by using industrial and agricultural waste
[7] Abang AA, Chandra S. Waste materials used in concrete manufacturing. New Jersey (USA): Noyes Publications Westwood; 1977.
[8] D. Rajput, S. S. Bhagade, S. P. Raut, R. V. Ralegaonkar, and S. A. Mandavgane, "Reuse of cotton and recycle paper mill waste as building material construction and building materials," Construction and Building Materials, vol. 34, pp. 470– 475, 2012.
[9] B.Fuller, Fafitis and L. Santamaria, ''Structural Properties of a new material of waste paper '', ASCE Civil Engineering, Vol. 76, No.5, May 2006, pp.72-77.
[10] Rai M (1978) Low-cost building materials using industrial and agricultural wastes. 2:213–221
[11] ,Ananthakrishnan C P1, Arun H J 'Experimental Investigation on Light Weight Concrete Block' second International Research Journal of Engineering and Technology (IRJET)
[12] IS 3495 (Part 1-4):1992 "Methods of tests of burnt clay building bricks, Part 1: Determination of compressive strength"
[13] IS 1077:1992 "Common burnt clay building bricks - Specification".

Acknowledgments

First and foremost, we express our sincere gratitude to the officials of the Department of Civil Engineering at Yeshwantrao Chavhan College of Engineering, Nagpur, for granting us permission to utilize the lab facilities. Additionally, we extend our thanks to the Minar Hydro Plant and Rukhmode Wheatmill for their prompt assistance in collecting waste materials and providing necessary permissions and facilities. We also appreciate the nearby temples for their cooperation in this initiative.

IOP Conference Series: Earth and Environmental Science

PURPOSE-LED PUBLISHING™

PAPER • **OPEN ACCESS**

Analysis and Design of Floating Concrete and its Applications

To cite this article: Vijay Kumar Rayabharapu *et al* 2024 *IOP Conf. Ser.: Earth Environ. Sci.* **1409** 012032

View the article online for updates and enhancements.

You may also like

- Alternating Current Impedance Electrochemical Modeling of Lithium-Ion Positive Electrodes
Dennis Dees, Evren Gunen, Daniel Abraham et al.
- Ideal Hexagonal Order: Formation of Self-Organized Anodic Oxide Nanotubes and Nanopores on a Ti–35Ta Alloy
Wei Wei, Steffen Berger, Nabeen Shrestha et al.
- A STACKED SEARCH FOR INTERMEDIATE-MASS BLACK HOLES IN 337 EXTRAGALACTIC STAR CLUSTERS
J. M. Wrobel, K. E. Nyland and J. C. A. Miller-Jones



This content was downloaded from IP address 47.247.77.11 on 27/11/2024 at 05:41

Analysis and Design of Floating Concrete and its Applications

Vijay Kumar Rayabharapu[1*], Prasanthi Petluru[1], Kavya Sudha Pallapu[1] and Bharat Sai Mella[1]

[1]Department of Civil Engineering, B V Raju Institute of Technology, Narsapur, Medak, Telangana, India

*Email: vijaykumar.r@bvrit.ac.in

Abstract. The main object of this paper is to experimentally explore the optimal design of lightweight aggregate concrete, considering its compressive strength and density. This Project deals with the development of Floating type of concrete by using less weighted aggregates such as expanded clay, perlite, vermiculite, EPS beads etc. The usage of light weight aggregates has drastically reduced the overall mass of concrete when compared to nominal concrete. However, attaining the characteristic strength of nominal concrete was indeed a challenge. Numerous concrete test cubes of size 0.15×0.15×0.15 m3 were cast using cementitious materials and aggregates of different proportions and their characteristic compressive strength was tabulated. The appropriate mix design having adequate compressive strength and floating property was selected. This mix had a density of 866.63 kg/m^3 and a compressive strength of 12.45 MPa which is quite optimal in comparison to the rest of the mixes.

Keywords. lightweight aggregate concrete, compressive strength, mix design

1. Introduction

The Present world is witnessing construction of very challenges and difficult civil engineering structures. Researchers all over the world are attempting to develop low density or light weight concreteor floating concrete by using different admixtures in concrete up to certain properties. Floating concrete consists of cement, water, aggregates, and admixtures (both physical and chemical). Unlike traditional Portland cement concrete (whose density is about 2400kg/m3), floating concrete contains light aggregates and certain admixtures which makes the composite lighter. The density of the floating concrete ranges from 600kg/m3 to 1000kg/m3 enabling it to float on water. Floating concrete can be putto use in several structures. Its service life is generally expected to be as long as 50 to 100 years with preferably a low maintenance cost. They are ideal for applications as floating emergency release bases in earthquake level countries. One of the best approaches to lessen the heaviness of the structure is by utilizing the lightweight aggregate solid which is the most plausible strategy in decreasing the heaviness of the structure. Floating concrete is a sort of light weight solid which is light in weight and the thickness is additionally not exactly the thickness of water.

Content from this work may be used under the terms of the Creative Commons Attribution 4.0 licence. Any further distribution of this work must maintain attribution to the author(s) and the title of the work, journal citation and DOI.
Published under licence by IOP Publishing Ltd

2. Literature Review

S Pradeep et al [1] used rice husk ash, micro silica, and microspheres to examine the characteristics of lightweight concrete canoes. An admixture to replace some of the cement in structuralmortar has been revealed: rice husk ash, an industrial by- product from boilers for parboiling rice. The mechanical and durability behaviour of mortars is improved by adding micro silica. Othman M et al (2020) performed an experiment to create lightweight concrete for structural use using LECAand EPA. By performing cube compressive test and UPV test, various mixes' densities, concrete quality,and strength are evaluated. The experiment was divided into two phases. The first phase variable was thepercentage of LECA replacing the typical coarse aggregate, the second phase variable being the percentage of EPA replacing the sand proportion. The LECA replacements make up 60% of the ideal concrete mix, and the EPA replacements make up 50%.

Jayakumar, et al [3) studied the addition of metakaolin to silica fume and fly ash increased the pozzolanic nature of the concrete mix and had a significant impact on the early strength development. Stanton [4] showed that lightweight concrete made with Poraver can result in concretethat is suitable for structural use.

3. Methodology

The methodology for the experimentation to be carries out to obtain the objectives are given as a followchart in the figure below:

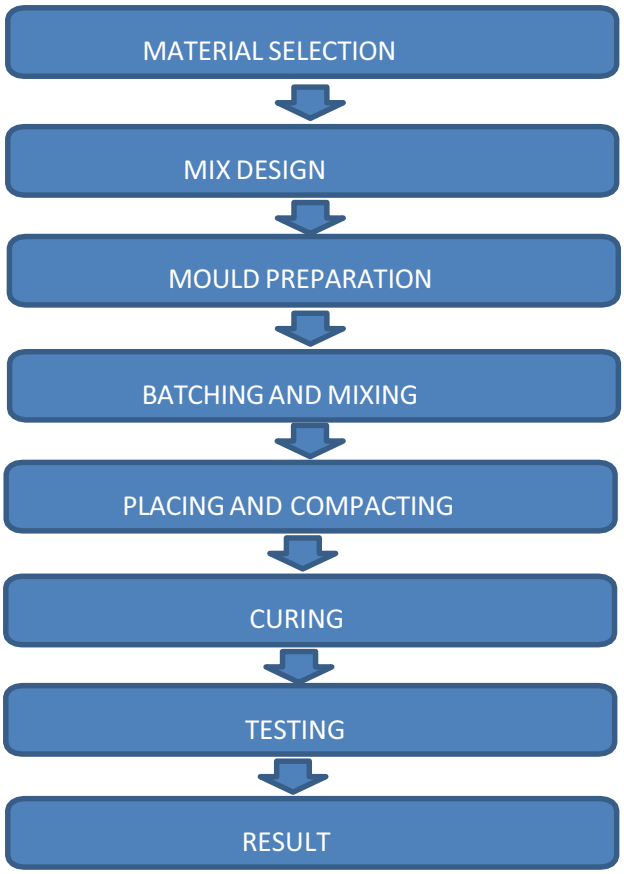


Figure 1. The methodology for the experimentation

4. Materials

4.1. Cement

Cement is a powdery material made from a mixture of compounds, primarily limestone, and clay with adensity of 1400 kg/m^3. Its higher-than-water density is the primary reason why it has been partially replaced with other materials of comparatively lower density. When mixed with water, it forms a paste that hardens over time through a chemical process known as hydration main components of cement are compounds of calcium, silicon, aluminium, and iron. The most common type of cement, Portland cement, is made by heating a mixture of limestone (calcium carbonate) and clay (silicon oxide, aluminium oxide, and iron oxide) to a high temperature (about 1450°C) and then grinding the resulting clinker (Figure 2).

The main chemical compounds found in cement are: Calcium oxide (CaO): Also known as lime, it is the main component of cement and gives it its bindingproperties. Silicon dioxide (SiO2): Known as silica, it gives cement its strength and durability. Aluminium oxide (Al2O3): Known as alumina, it helps to control the setting time of cement. Iron oxide (Fe2O3): Known as iron oxide, it gives cement its colour and can also help to control the setting time. Tricalcium aluminate (C3A): Responsible for the initial setting of cement, it forms a hydration product called aluminates. Dicalcium silicate (C2S): Responsible for the early strength development of cement,it forms a hydration product called Belite. Tricalcium silicate (C3S): Responsible for the majority of the strength development of cement, it forms a hydration product called Alice.

Table-1: Chemical composition of Cement

Components	Percentage (%)
Silica (SiO_2)	22
Calcium Oxide (CaO)	62
Aluminium Oxide (Al_2O_3)	5
Iron Oxide (Fe_2O_3)	3
Magnesium Oxide (MgO)	6
Sodium Oxide (Na_2O)	2

4.2. Silica fume

Silica fume, also known as micro silica, is a by-product of the main benefits of using Poraver as a lightweight aggregate production of silicon metal or ferrosilicon alloys. It is a very fine powder, with particle sizes typically around 1 micron, that is composed mainly of silicon dioxide (SiO_2). To enhanceits properties, silica fume is added to the concrete as a supplementary cementitious material (SCM). When added to concrete, it reacts with the calcium hydroxide (CH) produced by the hydration of cementand forms additional cementing compounds such as calcium silicate hydrate (C-S-H). This leads to an increase in the strength and durability of the concrete, as well as reduced permeability and improved resistance to chemical attack. Silica fume also increases the workability of the concrete, which makes iteasier to place and finish. It also helps to reduce the amount of water needed in the mix, which can leadto increased strength and durability. Silica fume is typically added to the concrete at a dosage of around5-10% by weight of cement. It is usually stored in silos, and it can be added to the concrete mixer at thetime of batching (Figure 3).



Figure 2. Cement



Figure 3. Silica Fume

4.3. Fine aggregates

4.3.1. Poraver

Poraver is a brand of expanded glass granules used as a lightweight aggregate in construction. It is made from recycled glass that is heated to a high temperature, causing it to expand and form small beads. Poraver replaces traditional aggregate materials such as sand, gravel, and crushed stone in concrete, mortars, and grouts. It is also used as insulation and filler material in various building materials (Figure 3).

Table 2. Physical properties of Poraver

Dimensions Of Poraver	0.1 - 0.3
Bulk Density (kg/m^3)	400 ± 60
Cracking force (KN)	24
Chemical Reaction (PH)	9 - 12
Thermal conductivity (W/mK)	0.7
Melting point (^{o}C)	700
Colour	Creamy white

The main benefits of using Poraver as a lightweight aggregate include:

- Reduced weight: Poraver has a lower density than traditional aggregate materials, which can reduce the weight of the final product. This can be beneficial for structures such as bridges, buildings, and precast products.
- Increased insulation: Poraver's low thermal conductivity provides improved insulation properties,which can help to reduce energy consumption in buildings.
- Increased fire resistance: Poraver is non-combustible and can increase the fire resistance of the final product.
- Increased workability: Poraver's round shape and smooth surface can improve the workability ofthe concrete or mortar, making it easier to place and finish.
- Increased sustainability: Poraver is made from recycled glass and is a sustainable alternative to traditional aggregate materials, as it helps to reduce waste and pollution.



Figure 4. Poraver (0.1 - 0.3mm)

4.4. Coarse aggregates

4.4.1. Lightweight clay aggregate (LECA)

Lightweight expanded clay aggregate (LECA) is a lightweight aggregate made by heating clay to around 1,200 °C (2,190 °F) in a rotary kiln. The resulting spheres have a honeycomb structure inside, which gives them a high surface area-to-volume ratio and excellent thermal insulation properties. They are used in a wide range of construction applications, including lightweight concrete, insulation, and hydroponics. LECA is an environmentally friendly and sustainable building material, as it is made from natural clay and can be recycled after use. LECA can be used as a replacement for traditional coarse commonly used in the production of concrete. It is a chemical aggregate in concrete, which makes the concrete lighter and admixture that is added to the concrete mix to improve the properties of the concrete. Because of its high surface area to volume ratio and excellent thermal insulation properties, LECA is often used as insulation in walls, roofs, and floors. It has good water retention anddrainage properties and can be used in the canoe for ballast and to maintain the buoyancy of the canoe. It can also be used as insulation to keep the canoe cool during the hot weather (Figure 5).

Table 3. Physical Properties of Leca

Physical Properties	Values
Size	10mm
Dry Density (kg/m3)	415
Absorption (%)	20
Specific Gravity	0.62



Figure 5. Light Weight Expanded Clay Aggregate (LECA)(8 - 12 mm)



Figure 6. Polypropylene fibre

4.4.2. Polypropylene fibres

Strongcrete Polypropylene Fibre is a type of synthetic fiber that issued as a reinforcement in concrete construction. It is made from polypropylene, which is a thermoplastic polymer. The fibers are added tothe concrete mix in small amounts, typically at a dosagerate of around 0.5 - 1.5 kg/m3 of concrete. The fibres help to improve the concrete's strength and ductility and reduce cracking by distributing stress evenly throughout the concrete. They also can be used to reduce the overall weight of the structure. Additionally, polypropylene fibers are corrosion resistant and can be used in aggressive environments (Figure 6).

4.4.3. Superplasticizer

Polycarboxylate ether (PCE) is a type of superplasticizer. PCE is a high-range water-reducing admixture and is a non-air-entraining type of superplasticizer. PCE works by reducing the amount ofwater required to produce a certain level of workability in the concrete mix. This allows for less water in the mix, resulting in stronger and more durable concrete. The reduction in the water-cementratio improves the strength, durability, and impermeability of the concrete. The dosage of PCE superplasticizer opted as 0.9% of total cementitious materials. It should be noted that it is important to use the correct dosage of PCE to avoid overdosing, which can lead to reduced workability and increased setting time (Figure 7).



Figure 7. Polycarboxylate ether

Table 4. Relationship between percentage of materials and Density

Materials	Percentage (%)	Density (1m³)
CEMENT	80	384
METAKAOLIN	10	48
SILICA	10	48
LECA	40	78.6
PUMICE	60	200.13
PERLITE	40	35.2
TOTAL:		**866.6**

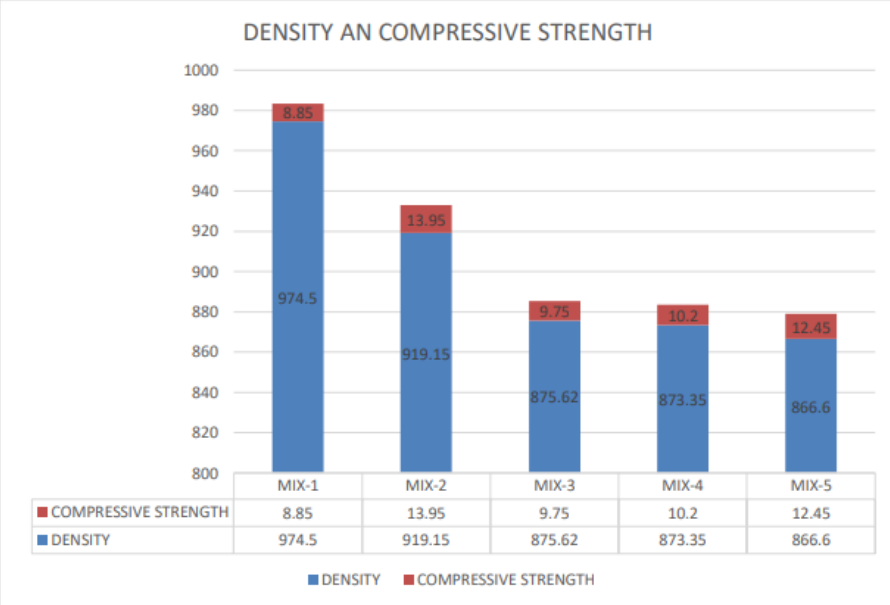


Figure 8. Relation between Density and Compressive strength

4.5. Mix Design

The Figure 8 shows the relationship between density and compressive strength across five different concrete mixes (MIX-1 to MIX-5). MIX-1 has the highest density at 974.5 kg/m^3 but a relatively lower compressive strength of 8.85 MPa, indicating that higher density does not always correlate with greater strength. MIX-2 stands out with the highest compressive strength at 13.95 MPa, despite having a lower density (919.15 kg/m^3) than MIX-1. MIX-3 and MIX-4 show moderate compressive strengths (9.75 MPa and 10.2 MPa, respectively) with similar densities of around 875.6 to 873.4 kg/m^3, suggesting a consistency in performance within that range. A general trend observed is a trade-off between density and compressive strength, with MIX-2 exemplifying that high strength can be achieved without maximizing density. Finally, MIX-5 shows a balance between properties, achieving a compressive strength of 12.45 MPa with a density of 866.6 kg/m^3, demonstrating that optimizing for strength may come at the cost of reduced density.

5. Conclusions:

- Density of the Materials can be reduced by using Lightweight materials as alternating to make theconcrete a Floating concrete.
- The less density is obtained in mix-5 and the high compressive strength obtained in mix-5.
- The strength of the concrete mix-5 is high because poraver replacement is high.

- Higher replacements of poraver reduced the density of concrete by maintaining high compressive strength.
- The compressive strength of Floating concrete is less than Conventional concrete.
- The Density of Floating Concrete by given Mix Design is less than 1000 kg/m2.
- Finally, we conclude that the proportions of mix-5 are optimal for us to use as a floating application.
- Application from same mix is made and it is floating on water.
- It is also possible to made Boat by the Concrete i.e., Floating Concrete, which gives the more benefit such as Cost saving, Reduces the use of Timber, For Rescue operation.
- The future scope of the work is to check the durability of floating concrete.

6. References

[1] P. Sivanantham, D. Pugazhlendi, and S. Dheepak, "Rice husk ash based cementitious material for concrete canoe," IOP Conference Series Materials Science and Engineering, vol. 912, 09/30 2020, DOI: 10.1088/1757-899X/912/6/062004

[2] M. Othman, A. Sarayreh, R. Abdullah, N. Sarbini, M. Yassin, and H. Ahmad, "Experimental study on lightweight concrete using lightweight expanded clay aggregate (LECA) and expanded perlite aggregate (EPA)," Journal of Engineering Science and Technology, vol. 15, no. 2, pp. 1186-1201, 2020.

[3] Jayakumar, S., Kurian, A., Zachariah, F.T. and Navin, P., 2020. Construction of Concrete Canoe Using Light Weight Aggregates. International Journal of Engineering Research and, 9 IS 456:2000 code book

[4] M. Stanton, "Preliminary Design Guidelines for Poraver-Based Lightweight Concrete," Engineering, Material Science, 2016. doi: DOI:10.15760/HONORS.367

[5] Entrekin, R.C. and Porter, B.A., 1986. Design and Construction of the Concrete Canoe California I! Marine Technology, 23(3), pp.271-275.

[6] Schmitt, S.B., 2006. The Vanderbilt Concrete Canoe Design Project: The Little Engine that Canoed. Vanderbilt Undergraduate Research Journal, 2(1).

[7] Leczovics, P. and Sugár, V., 2013. Concrete Canoe: A Complex Concrete Technology. YBL Journal of Built Environment, 1(2), pp.43-55.

[8] Malik Mehran Manzoor et al. (2018): “development of light wight “, Civil Engineering Portal,2014

IOP Conference Series: Earth and Environmental Science

PURPOSE-LED PUBLISHING™

PAPER • **OPEN ACCESS**

Treatment of wastewater using rice husk ash

To cite this article: Vijay Kumar Rayabharapu *et al* 2024 *IOP Conf. Ser.: Earth Environ. Sci.* **1409** 012033

View the article online for updates and enhancements.

You may also like

- Agro waste reinforcement of metal matrix composites, a veritable sustainable engineering achievement, or an effort in futility? A critical review
Festus Ben and Peter A Olubambi
- Comparative study using different external sources of aluminum on the zeolites synthesis from rice husk ash
Marcos Antonio Klunk, Mohuli Das, Sudipta Dasgupta et al.
- Physicochemical signatures of nanoparticle-dependent complement activation
Dennis G Thomas, Satish Chikkagoudar, Alejandro Heredia-Langner et al.



This content was downloaded from IP address 47.247.77.11 on 27/11/2024 at 05:41

Treatment of wastewater using rice husk ash

Vijay Kumar Rayabharapu[1*], Manjunatha, B.[1] Prasanthi Petluru[1] and Bharat Sai Mella[1]

[1]Department of Civil Engineering, B V Raju Institute of Technology, Narsapur, Medak, Telangana, India

*Email: vijaykumar.r@bvrit.ac.in

Abstract. Water is a critical issue in the present world. Agricultural development, industrialization, and urbanization cause the drying up of most river basins in India and elsewhere further resulting in severe water shortages. In most cities in India, the estimated amount of sewage generated is around 40000 million liters per day (MLD). However, the sewage treatment capacity is only a mere 11786 MLD. To address this problem, several cost-effective and sustainable wastewater treatment methods are being researched. One such method is adsorption using Rice Husk Ash (RHA), an industrial by-product abundantly available at a very low cost. This study aimed to identify the effectiveness of activated carbon for the reduction of chemical oxygen demand (COD), Biological Oxygen Demand (BOD) total dissolved solids (TDS), total suspended solids (TSS), colour, turbidity from municipal wastewater by using RHA. A set of four samples were selected and analyzed under both conditions: (1) before treatment with RHA and (2) after treatment with RHA. Our analysis showed that the addition of RHA as a coagulant to wastewater treated it efficiently as evident from the results obtained in the aforementioned laboratory tests.

Keywords: rice husk ash, wastewater treatment methods, coagulant

1. Introduction

Water is essential for sustaining life and almost all human activities, namely, domestic, and industrial use, irrigation to meet the growing demand for food and fibre, electricity generation, mobility, recreation, etc. Typical water sources include rainwater, surface water, groundwater, and recycled water.

1.1. Wastewater Production

As per Central Public Health & Environmental Engineering Organization (CPHEEO) estimates, about 70-80% of total water supplied for domestic use is generated as wastewater. As per CPCB estimates, the total wastewater generation from Class I cities (498) and Class II (410) towns in the country is around 35,558 and 2,696 MLD respectively. The installed sewage treatment capacity is just 11,553 and 233 MLD, respectively. Maharashtra, Delhi, Uttar Pradesh, West Bengal, and Gujarat are the major contributors of wastewater (63%; CPCB, 2007). It is projected that by 2050, about 48.2 BCM (132 billion litres per day) of wastewater (with a potential to meet 4.5% of the total irrigation water demand) will be generated thereby further widening this gap.

Content from this work may be used under the terms of the Creative Commons Attribution 4.0 licence. Any further distribution of this work must maintain attribution to the author(s) and the title of the work, journal citation and DOI.
Published under licence by IOP Publishing Ltd

1.2. Wastewater Treatment

The water supply for any purpose contains organic materials, minerals, chemicals, and manmade pollutants making it unfit for use. Thus, to address this issue, different water treatment methods have been developed to allow our water supply to be safe to drink. Primarily, any wastewater treatment procedure includes:

- Coagulation/ Flocculation, where liquid aluminium sulphate or alum and/or polymer is added to water which causes the dirt particles to coagulate. These aggregated dirt particles are then removed through flocculation.
- Sedimentation, in which water is allowed to stand still for a certain detention period causing the heavy suspended particles to settle down and leaving clear water above.
- Filtration, where the water is passed through filters to restrain the unwanted particles present within.
- Disinfection, where water is made free of disease-causing microbes.

2. Literature Review

Amaruzzaman [1] and Vinod K. Gupta (2011) studied the use of RHA as Low-Cost adsorbents in water and wastewater treatment. They presented a brief review on the role of RHA in the removal of various pollutants from wastewater. Swarnalakshmi [2] compared the role of RHA as an adsorbent with an advanced oxidation process by removing selected contaminants like Acid Orange 7, Amoxicillin, Metformin, and Carbamazepine. Sadon [3] revealed that RHA can be used as an adsorbent to adsorb water pollutants mainly heavy metals like Fe, Mn, Cd, Pb, Zn, Cu, and Cr (VI) and textile dyes like Direct F. Scarlet, ever direct Orange – 3GL, Direct Blue – 67, Direct Red – 31, Direct Orange – 26, and Crystal Violet from wastewater. Vivek Ganvir [4] published a paper on the removal of fluoride from drinking water using RHA coated with aluminium hydroxide. Zahid Naeem [5] studied the treatment of municipal wastewater using RHA and Kikar Charcoal as Activated Carbon and provided the corresponding comparative analysis. Uttarini Pathak [6] employed RHA as an adsorbent to remove pollutants in wastewater from a dairy industry and provided a detailed analysis of the treatment efficiency, thermodynamics, kinetic modelling, and isotherms. Camila Emanuelle [7] used water filtration systems embedded with RHA as a means to treat wastewater and as a substitute for industrial activated carbon. They have produced significant results in terms of colour, turbidity, BOD, COD, etc.

3. Methodology

3.1. Introduction

Rice husk is an industrial by-product obtained from the outer coverings of rice grains that is an abundantly available waste material. It contains about 30%–50% of organic carbon. Rice husk constitutes about 20% of the weight of rice and its composition is as follows: cellulose (50%), lignin (25%–30%), silica (15%–20%), and moisture (10%–15%). The bulk density of rice husk is low and lies in the range of 90–150 kg/m^3. RHA (Figure 2) is obtained by incinerating rice husks. Every 100 kg of husks burnt in a Muffle furnace at 500°C for 1 hour will yield about 25 kg of RHA. This residue is rich in silicates. Rice husk, due to its high cellulose and lignin content, can be used as a source of carbons to produce activated carbon which is an excellent adsorption agent. Further, RHA is a good super-pozzolan that can be used in the preparation of special concrete mixes.



Figure 1. Rice Husk



Figure 2. Rice Husk Ash (RHA)

3.2. Sample Collection

For the purpose of study, a set of 4 samples from various sources of wastewater were collected as follows.

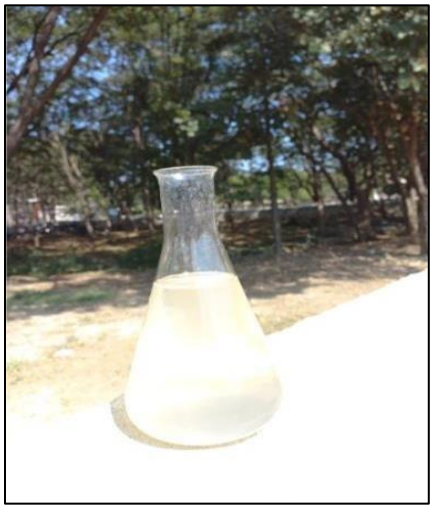


Figure 3. Sample-1 Drainage Water, Narsapur



Figure 4. Sample-2 Wastewater from Sewage Treatment Plant, BVRIT, Narsapur



Figure 5. Sample-3 Effluent from a rice mill, Narsapur



Figure 6. Sample-4 Laundry Wastewater

3.3. Testing Procedure

Each sample has been classified into two categories: (1) Samples before RHA treatment and (2) Samples after RHA treatment. Consequently, they were subjected to various laboratory tests to determine parameters like pH, chloride content, dissolved oxygen (DO), TDS, turbidity, BOD and COD.

4. Results

4.1. pH Test

Table 1. pH Test Results

Sample No.	pH Value Before Treatment	pH after treating with RHA
Sample -1 (Drainage water Narsapur)	7.47	8.19
Sample -2 (Sewage Water @ BVRIT college)	7.85	8.24
Sample -3 (Rice Mill Effluent)	8.2	8.0
Sample -4 (Laundry Wastewater)	9.5	8.1

4.2. Chloride Test

Table 2. Chloride Test Results

Sample No.	Chloride content before treatment (mg/l)	Chloride content after treating with RHA (mg/l)
Sample -1 (Drainage water Narsapur)	495.73	214.54
Sample -2(Sewage Water @ BVRIT college)	424.36	196.35
Sample -3 (Rice Mill Effluent)	197.39	105.32
Sample -4 (Laundry Wastewater)	363.28	171.26

4.3. Dissolved Oxygen Test

Table 3. Dissolved Oxygen Test Results

Sample No.	DO content before treatment (mg/l)	DO content after treating with RHA (mg/l)
Sample -1 (Drainage water Narsapur)	5.8	4.2
Sample -2 (Sewage Water @ BVRIT college)	6.1	5.6
Sample -3 (Rice Mill Effluent)	1.2	0.9
Sample -4 (Laundry Wastewater)	4.8	4.2

4.4. Total Dissolved Solids

Table 4. Total Dissolved Solids Test Results

Sample No	TDS before Treatment (mg/l)	TDS after Treating with RHA (mg/l)
Sample -1 (Drainage water Narsapur)	1090	185
Sample -2(Sewage Water @ BVRIT college)	1158	221
Sample -3 (Rice Mill Effluent)	685	162
Sample -4 (Laundry Wastewater)	856	159

4.5. Turbidity

Table 5. Turbidity results

Sample No	Turbidity before treatment. (NTU)	Turbidity after treating with RHA. (NTU)
Sample -1 (Drainage water Narsapur)	103	11
Sample -2(Sewage Water @ BVRIT college)	114	14
Sample -3 (Rice Mill Effluent)	263	49
Sample -4 (Laundry Wastewater)	145	40

4.6. BOD Test

Table 6. BOD Results

Sample No	BOD before treatment (mg/l) 5 days @ 27ºc	BOD after treating with RHA.
Sample -1 (Drainage water Narsapur)	225	26
Sample -2(Sewage Water @ BVRIT college)	230	28
Sample -3 (Rice Mill Effluent)	460	74
Sample -4 (Laundry Wastewater)	145	8

4.7. COD Test

Table 7. COD Test Results

Sample No	COD before treatment (mg/l)	COD after treating with RHA (mg/l)
Sample -1 (Drainage water Narsapur)	1083	122
Sample -2(Sewage Water @ BVRIT college)	1152	152
Sample -3 (Rice Mill Effluent)	1380	130
Sample -4 (Laundry Wastewater)	3460	679

5. Conclusions

Table 8. Consolidated Test Results

Sample no		pH	Chloride content (mg/l)	DO (mg/l)	Turbidity NTU	TDS	BOD	COD
Sample 1	Before Treatment	7.47	495.732	5.8	103	1090	225	1083
	After Treatment	8.19	214.54	4.2	11	185	26	122
Sample 2	Before Treatment	7.85	424.36	6.1	114	1158	230	1152
	After Treatment	8.24	196.35	5.6	14	221	28	152
Sample 3	Before Treatment	8.2	197.39	1.2	263	685	460	1380
	After Treatment	8	105.32	0.9	49	162	74	130
Sample 4	Before Treatment	9.5	363.28	4.8	145	856	145	3460
	After Treatment	8.1	171.26	4.2	40	159	8	679
BIS Standards for Drinking Water		6.5-8.0	<250	6.5–8.0	1-5	500	5-30	<250
Irrigation water Standards		5.5-9	70-350	>5	-	2100	100	-

The results of the study indicate the potential use of RHA as an adsorbent for the reduction of various parameters like pH, Turbidity, Chloride content, COD, BOD etc and effectively treat wastewater. It is observed that these exceptional results are due to presence of high concentration of silicates in RHA. The treated water can thus be used for domestic and irrigation purposes.

After treating five different wastewater samples with RHA, the following observations have been made:

- Sample-1 (Drainage Water) & Sample-2 (Water from STP) showed the best results in comparison with the other samples. With further treatment, these samples can be used for drinking purposes.
- Sample-3 (Rice Mill Effluent), Sample-5 (Granite Industry Effluent) and Sample -5 (Laundry Wastewater) can be used for irrigation and/or discharged into water bodies.
- All samples have given significant results after treatment with RHA. As evident from the results obtained, it can be concluded that RHA is one of the best, cost-effective adsorbent that can be employed while treating different kinds of wastewater.

6. References

[1] Ahmaruzzaman, M., & Gupta, V. K. (2011). Rice husk and its ash as low-cost adsorbents in water and wastewater treatment. Industrial & Engineering Chemistry Research, 50(24), 13589-13613.

[2] Swarnalakshmi, K. S., Chinnaiyan, P., Nivetha, S., & Nair, A. S. (2018). Use of rice husk ash as an adsorbent to remove contaminants in water and comparison with advanced oxidation process–a study. Materials Today: Proceedings, 5(11), 24248-24257.

[3] Sadon, F. N., Ibrahem, A. S., & Ismail, K. N. (2012). An overview of rice husk applications and modification techniques in wastewater treatment. J Purity Utility Reaction Environ, 1, 308-34.

[4] Ganvir and Kalyan Das Published paper on Removal of fluoride from drinking water using aluminium hydroxide coated rice husk ash, Research Gate- Volume 185, Issue 2-3, 30 January 2011

[5] Zahid, Ibrar, S. Asadullah, Najam Malghani, Zahid Naeem, Mohammad Saddam, Muhammad Amin Siddique, Faisal Mushtaq, and A. Waqas. "Municipal wastewater treatment using rice husk and kikar charcoal as activated carbon." In Int. Res. Symp. Eng. Adv, vol. 2016, pp. 56-59. 2016.

[6] Pathak, U., Banerjee, A., Das, S. K., Roy, T., & Mandal, T. (2022). Wastewater Types, Characteristics and Treatment Strategies. Recent Trends and Innovations in Sustainable Treatment Technologies for Heavy Metals, Dyes and Other Xenobiotics, 1.

[7] Camila Emanuelle Mendonca Viana, Jose Wilmar da Silveira Neto, & Khaldoon A. Mourad. (2016). Using rice husks in water purification in Brazil. International Journal of Environmental Planning and Management, 2(3), 15-19

[8] Anuj Kumar, Subhajit Singah and others presented research paper on Simultaneous recovery of silica and treatment of rice mill wastewater using rice husk ash: An economic approach Received 12 November 2014.

[9] Anjitha.A, Duithy Goerge has published paper on Comparative Study Using Rice Husk and Its Ash as Natural Coagulants in Wastewater Treatment on International Journal of Scientific & Engineering Research Dated – 4th April 2016.

[10] Jose Wilmar da Silveira Neto and Khaldoon A. Mourad Published paper on AISCIENCE International Journal of Environmental Planning and Management regarding Using Rice Husks in Water Purification in Brazil. Vol 1, No. 3, 2016.

[11] Riyanto, Rury Astuti and Bayu ismoyo mukti presented a research paper on Simple preparation of rice husk activated carbon (RHAC) and applications for laundry and methylene blue wastewater treatment the year 2017 on AIP conference proceedings.

[12] S. Sharada, B. Sahithi, V. Pradeep kumar, D. Akhileswar and B. Samatha presented paper on Treatment of Effluent from Granite Cutting Plant by Using Natural Adsorbents like Rice Husk Carbon and Saw Dust Carbon on International Journal of Engineering Research and Development in the year 2015.

IOP Conference Series: Earth and Environmental Science

PURPOSE-LED PUBLISHING™

PAPER • **OPEN ACCESS**

Seismic analysis of vertically irregular RCC high-rise buildings: A study with provision of FVD at various locations

To cite this article: Batchu Ramanjaneyulu *et al* 2024 *IOP Conf. Ser.: Earth Environ. Sci.* **1409** 012034

View the article online for updates and enhancements.

You may also like

- Analytical study on seismic response of RC and steel structures with fluid viscous dampers
Y Subasini and C G Sivakumar
- The damping effect Analysis of viscous damper in eccentric concrete frame structure
Zhou Fang, Qiuyue Zhang, Chongge Wang et al.
- Enhancing Seismic Resistance of G+10 MSB by Introducing FVD System
T S D Phanindranath, K V G D Balaji and P Markandeya Raju



This content was downloaded from IP address 47.247.77.11 on 27/11/2024 at 05:41

Seismic analysis of vertically irregular RCC high-rise buildings: A study with provision of FVD at various locations

Batchu Ramanjaneyulu*, Achina Prasad, keshagoni Satish, Tirukovela Sai Keertan and Jagadeesh Bommisetty

Department of Civil Engineering, CVR College of Engineering, Hyderabad, Telangana, India, 501510.

*E-mail: ramanji139@gmail.com

Abstract: Irregular buildings are a significant part of urban infrastructure, often resulting from architectural, functional, and economic constraints. Among these, structures embracing vertical irregularities are predominantly receptive to dynamic loads, with earthquakes being the most damaging event. The dynamic forces acting on a structure during an earthquake generate vibrations and increase the energy within the structure. The primary role of a structure is to withstand these lateral loads and transmit them to the foundation. To enhance the seismic performance of such structures, various energy dissipation systems are employed to absorb and dissipate the released energy, thereby improving the building's response to earthquake forces. This study focuses on the use of Fluid Viscous Dampers (FVDs) to dissipate energy from the structure. It involves a comparative analysis of effect due to inclusive and non-inclusiveness of fluid viscous dampers at various locations for Set-Back and Step-Back type vertical irregular high-rise buildings. The analysis aims to study key response parameters such as modal time-period, storey displacement, mode type, storey shear, torsional irregularity, and storey drift using ETABS software. The primary objective is to enhance understanding of the seismic behaviour of high-rise reinforced concrete structures with vertical irregularities and Fluid Viscous Dampers (FVDs) at different locations.

Keywords: Vertical irregularity, Lateral load, Energy dissipation, Fluid Viscous Dampers (FVD).

1. Introduction

1.1 General

In modern urban landscapes, irregular buildings are a common sight, reflecting the diverse interests and needs of stakeholders involved in their planning and construction, including owners, architects, engineers, contractors, and regulatory authorities. These structures often exhibit varying distributions of mass, stiffness, and strength vertically, posing significant challenges, especially in seismic regions like India's hill slopes. Recent seismic events in the country have underscored the vulnerability of reinforced concrete frame buildings on hilly

Content from this work may be used under the terms of the Creative Commons Attribution 4.0 licence. Any further distribution of this work must maintain attribution to the author(s) and the title of the work, journal citation and DOI.
Published under licence by IOP Publishing Ltd

terrain, highlighting the urgent need for robust structural solutions. Hillside buildings face unique design and construction challenges due to their irregular configurations and foundation levels. During seismic events, these challenges are amplified, leading to notable responses such as storey displacement, storey drift, torsional irregularity, and storey shear. Addressing these responses is critical to ensuring the structural integrity and safety of the buildings during seismic events.[1-5]

To enhance the seismic resilience of hillside structures, structural engineers must employ innovative design strategies and rigorous analysis techniques. Collaborative efforts among stakeholders are essential to integrating seismic resilience measures seamlessly into the design and construction processes. By addressing the specific challenges posed by irregular buildings in seismic-prone areas, engineers can contribute significantly to creating safer and more resilient urban environments. [10-17,19]

1.2 Vertical Irregular Buildings

The vertical irregular buildings are the use of setback or step-back configurations. Setback buildings have upper floors that are smaller in area than the lower floors, creating terraces or recessed areas as the building rises. Step-back buildings, on the other hand, feature distinct setbacks at various levels, resulting in a cascading or tiered appearance [3,7]. These design elements not only enhance the visual appeal of the building but also serve functional purposes such as providing outdoor spaces, optimizing views, and improving natural light penetration.

By identifying and addressing the vertical irregularities in the design and construction process, engineers can enhance the seismic resilience of vertical irregular buildings and ensure the safety of occupants and surrounding communities. Through a combination of innovative architectural design and rigorous structural engineering principles, vertical irregular buildings continue to push the boundaries of modern architecture while prioritizing safety and functionality. [13-17]

1.3 Fluid Viscous Dampers

Thick dampers comprise a chamber containing silicone liquid, separated by a cylinder and steel piston. Activation happens as liquid flows between chambers via small openings. Compression moves liquid from chamber 2 to 1, while tension reverses it. Pressure drop across the hole creates strain on the cylinder head, generating damping force. These dampers effectively reduce both pressure and displacement during ground movement, as they respond to velocity, out of phase with structural stresses. With easy installation, adaptability, and compatibility, they're widely applied in design and retrofitting, especially in earthquake-prone areas for tall buildings. [1,6,18,23,26,31-32]

Fluid Viscous Dampers (FVDs) are used because…

- Effective in Energy Dissipation
- Reduction of Structural responses
- Improved Stability and control
- Protection of Non-Structural members
- Cost-Effective Retrofitting

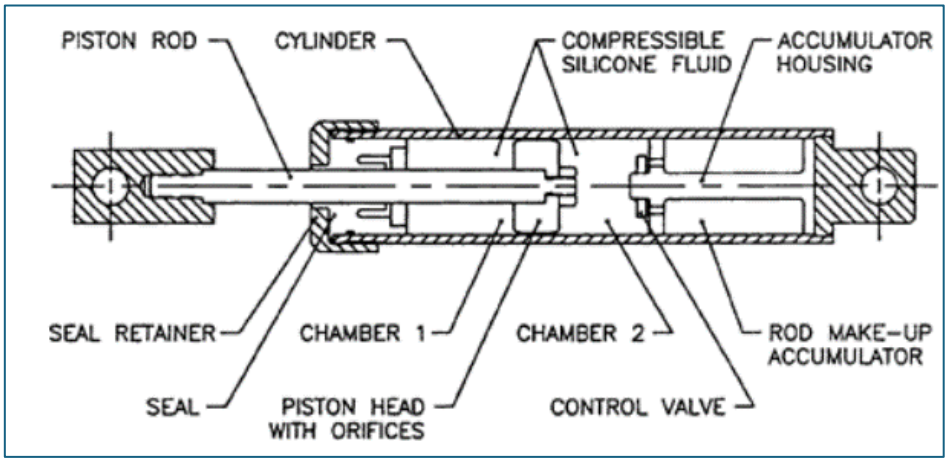


Figure 1. Fluid Viscous Dampers

1.4 Wind Static Analysis

Wind static analysis is a method used to evaluate the effects of wind loads on buildings and structures, particularly in regions where wind forces can pose significant challenges to structural integrity. Structures that are built taller than 10 stories require extra steel for horizontal framework. In wind static analysis, the magnitude and distribution of wind loads acting on a structure are determined based on established codes and standards, such as IS 875:2015 in India. For buildings with vertical irregularities, such as setbacks or variations in height, wind static analysis becomes even more crucial. Engineers consider factors such as building height, shape, orientation, and surrounding terrain to accurately calculate wind loads. The analysis involves determining the wind pressure coefficients for different parts of the building and applying them to the structural elements to assess their response. In regions where wind speeds can exceed 30m/s, as specified in IS 875:2015, wind static analysis is particularly important to ensure structural safety and stability. By conducting wind static analysis, engineers can optimize structural designs, select appropriate materials, and implement mitigation measures to minimize the risk of structural failure and ensure the safety and durability of buildings and structures subjected to wind loads. [28]

1.5 Equivalent Static Analysis

The Equivalent Static Method is a simplified approach used in seismic analysis to estimate the response of buildings and structures to seismic forces. In the Equivalent Static Method, seismic parameters such as the seismic zone, soil type, building height, and structural characteristics are used to determine a set of equivalent static forces that represent the effects of seismic loading. Unlike dynamic methods, which consider the time-varying nature of seismic ground motions, the Equivalent Static Method treats seismic forces as static loads applied instantaneously to the structure. The method simplifies the analysis by assuming that the structure responds linearly to the applied forces and neglects the effects of damping, resonance, and higher modes of vibration. Despite its simplifications, the Equivalent Static Method is widely used in seismic design and retrofitting projects due to its ease of application and conservative nature. Engineers can quickly estimate the seismic demands on a structure and design appropriate lateral force-resisting systems to ensure structural integrity and occupant safety. [29-30]

1.6 Time History Analysis

Time history analysis involves studying the dynamic response of a structure at each moment in time when subjected to specific ground motion scenarios. It allows for the direct or nonlinear assessment of how the structure reacts dynamically to loads, which may vary over time. The dynamic equilibrium equations, represented by $K^*u(t) + C^*(d/dt)\,u(t) + M^*(d2\,/dt2)\,u(t) = r(t)$, are solved using either modal or direct integration methods. [29-30]

In this study GAZLI ground motion data is taken.

Description of GAZLI Earthquake:

GAZLI 1976-05-17 02:58:40(UTC)

UTC Station: RU.GAZ

Region: Uzbekistan

Magnitude: 6.8

Latitude: 40.3810 N

Longitude: 63.4720 E

Depth: 10 km

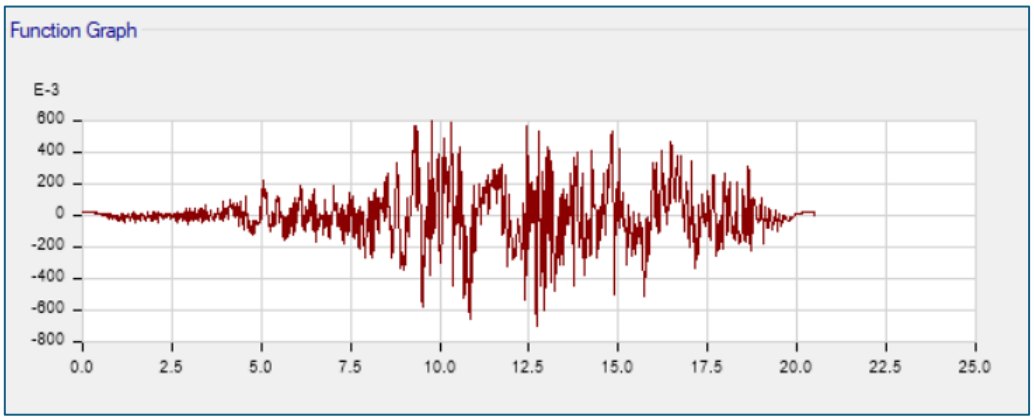


Figure 2. Time History function of GAZLI earthquake (Acceleration vs Time)

1.7 Objectives of the Study

The objectives of the current study are…

- To Evaluate the seismic performance of High-rise Vertical Irregular Buildings having Set-Back and Step-Back with FVD at Various locations.
- To Analyse the effectiveness and positioning of the fluid viscous dampers and compare those results of the seismic responses of the building.
- To study variations in Seismic response parameters such as Time period, Storey Shear, Storey Displacement, Storey Drift for structures with Vertical Irregularity with and without FVD.

2. Methodology

2.1 General description of the building models

Eight models of sixteen-story (G+15) structures representing vertical irregular buildings, including Set-Back (SB) and Step-Back Buildings (SBB) are simulated using ETABS-2021 software. The models incorporate variations with and without Fluid Viscous Dampers (FVDs) installed at different locations.

In this study, the differents Buildings are modeled and analyzed vertical irregular buildings, such as Set-Back (SB) and Step-Back (SBB) structures, incorporating Fluid Viscous Dampers

(FVDs) at various locations. Each building model includes columns, beams, and structural slabs. All models are subjected to equivalent static analysis based on IS 1893-2016, time history analysis using GALZI ground motion, and wind static analysis following IS 875-2015 (part 3), utilizing ETABS (2021) software. The dimensions of beams, columns, and slabs adhere to IS 456-2000 standards. Our design accounts for dead load, live load, seismic load, and wind load resistance, with load combinations considered during the analysis and design of all building models.[27-30]

Table 1. Types of Building models considered.

S.NO	SET-BACK BUILDING
1	Without FVD
2	With FVDs at Corners
3	With FVDs at Middle
4	With FVDs at Middle and Corners in Alternative Floors
5	Without FVD
6	With FVDs at Corners
7	With FVDs at Middle
8	With FVDs at Middle and Corners in Alternative Floors

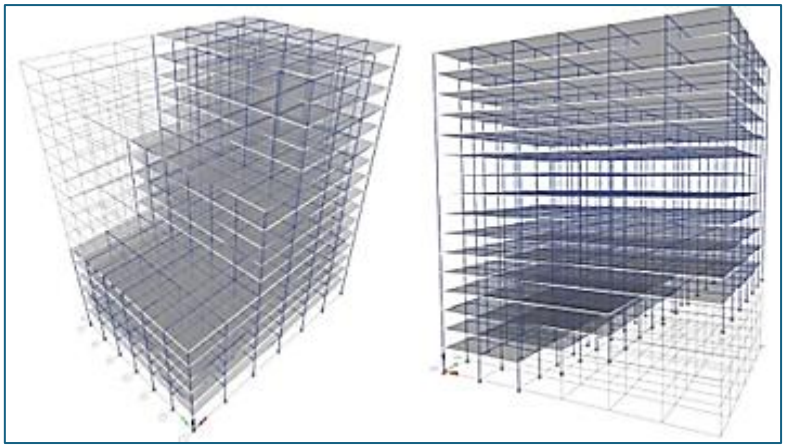


Figure 3. 3D modelling of Set-Back and Step-Back Buildings without FVD

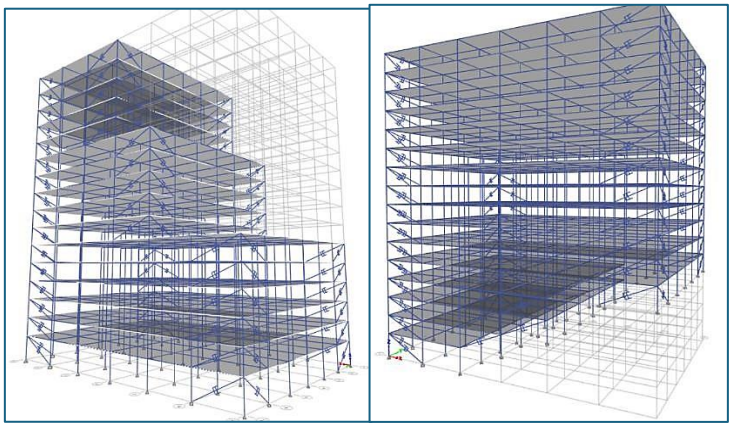


Figure 4. 3D modelling of Set-Back and Step-Back Buildings with FVDs at Corners

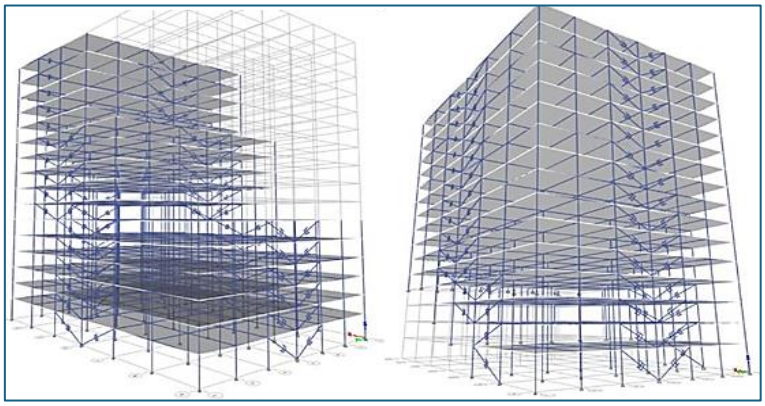


Figure 5. 3D modelling of Set-Back and Step-Back Buildings with FVDs at Middle

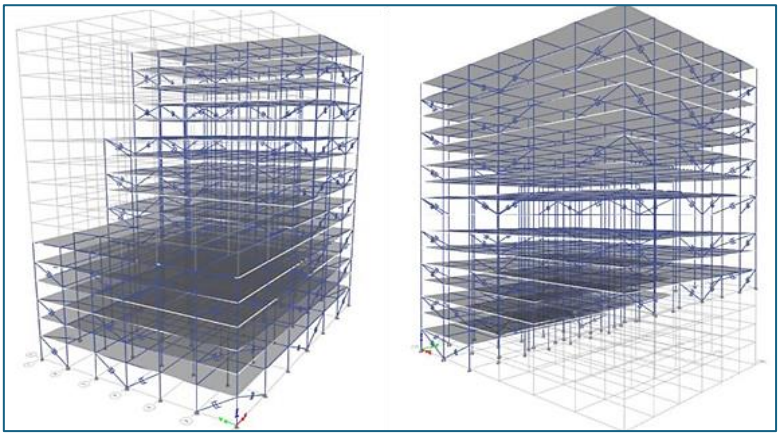


Figure 6. 3D modelling of Set-Back & Step-Back Buildings with FVDs at middle and corners in Alternative floors

2.2 Geometric properties of the Structures

The Structural and material properties are considered as per IS 456-2000. The following table explains the detailed description of the building models.[27]

Table 2. Structural properties of the building models

Description	Details
Type of structure	Residential
Size of Building	42m X 35m
No. of Stories	16(G+15)
No. of Bays in X-direction	6
No of Bays in Y-direction	6
Bay length in X-direction	7m
Bay length in Y-direction	5m
Base Storey height	4 m

Typical Storey height	3.2 m
Grade of Concrete	M30
Grade of steel	Fe500
Density of Concrete	25 KN/m^2
Density of Masonry wall	19 KN/m^2
Thickness of Slab	200 mm
Size of Beam	400 mm X 800 mm
Size of Column	700 mm X 900 mm
Imposed load	3.5 KN/m^2
Floor finish	2 KN/m^2
Dead load	Calculated by ETABS
Thickness of Outer Walls	230 mm
Thickness of Inner Walls	115 mm
Slope of Step-Back Building	26^0

2.3 Wind load parameters of the Structures

1. Design Wind Pressure, Vz = Vb * k1 * k2 * k3 * k4
   Wind speed, Vb = 50 m/s
   Risk coefficient factor, k1 = 1, IS 875 (part 3): 2015, Clause 6.3.1
   Terrain category, k2 = 1, IS 875 (part 3): 2015, Clause 6.3.2.1
   Topography factor, k3 = 1 (Θ < 3°) IS 875 (part 3): 2015, Clause 6.3.3
   Cyclonic Important factor, k4 = 1.3, IS 875 (part 3): 2015, Clause 6.3.4
2. Design pressure, Pz = 0.6 * Vz2 Pd = ka * kc * kd * Pz
   ka is obtained from Clause 7.2.2, IS 875 (Part 3) 2015
   kc is obtained from Clause 7.3.3.13, IS 875 (Part 3) 2015
   kd is obtained from Clause 7.2.1, IS 875 (Part 3) 2015
   Design Wind Force, F = (Cpe – Cpi) * Ae * Pd
   From IS 875 Part 3, 2015, Clause 7.3.2, pg no:11, Internal Pressure Coefficients are obtained.
   From IS 875 (Part 3), 2015, Table 5, pg no: 13, Externals Pressure Coefficients are obtained.

2.4 Seismic load parameters of the Structures

Soil Type = Medium
Frame system = Special Moment Resisting Frame (SMRF)
Response reduction factor = 5
Seismic Zone Factor = 0.36 (Zone-V)
Importance factor = 1.2
Seismic Weight = DL+0.5LL

3. Results and analysis

3.1 Results of Set-Back Buildings

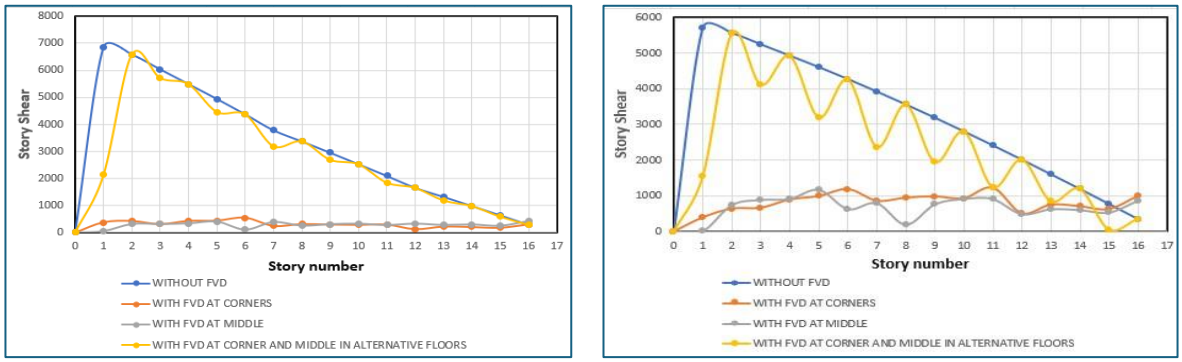


Figure 7. Storey Shear variation under Wind load in X and Y-directions respectively

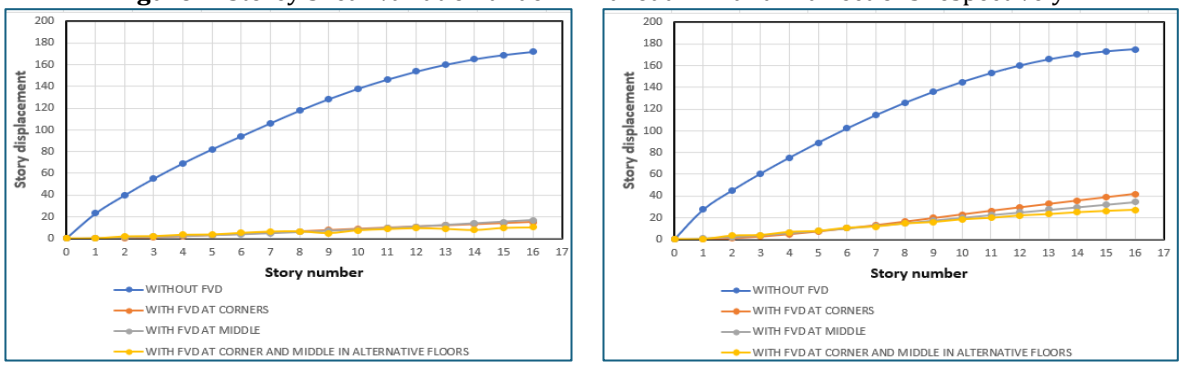


Figure 8. Storey displacement variation under Wind load in X and Y-directions respectively

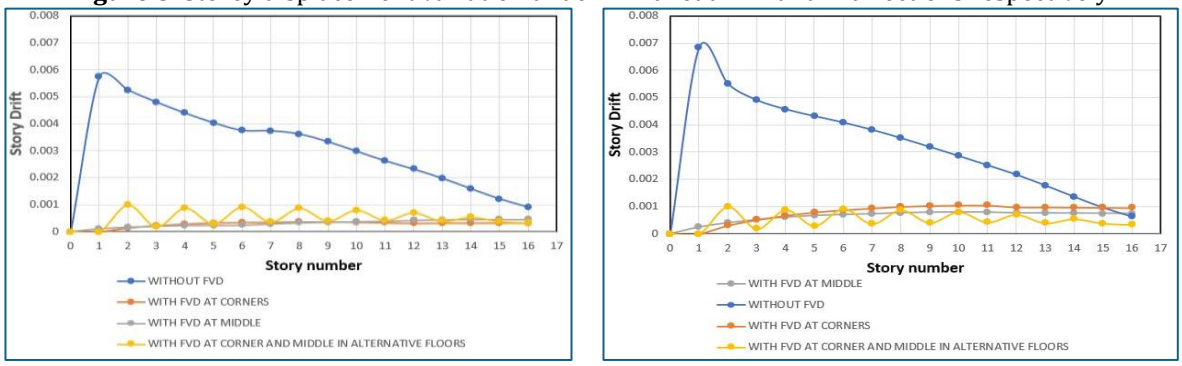


Figure 9. Storey drift variation under Wind load in X and Y-directions respectively

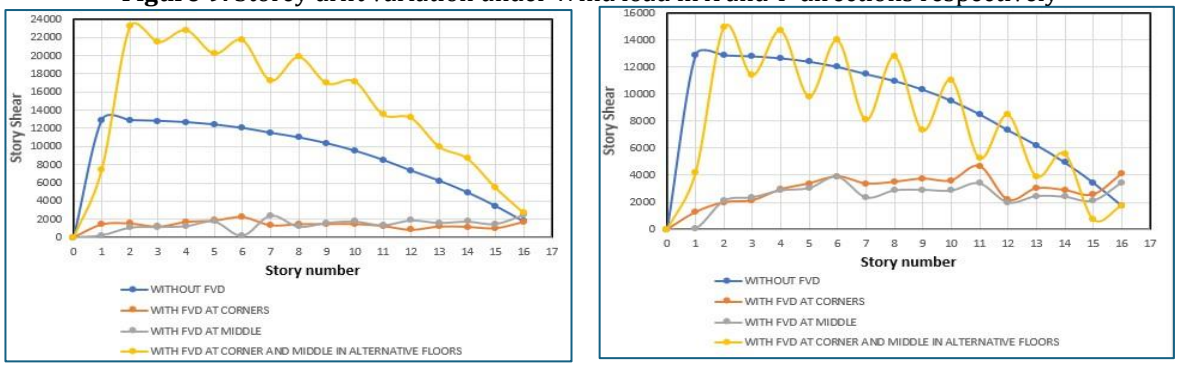


Figure 10. Storey Shear variation under static Earthquake load in X and Y-directions

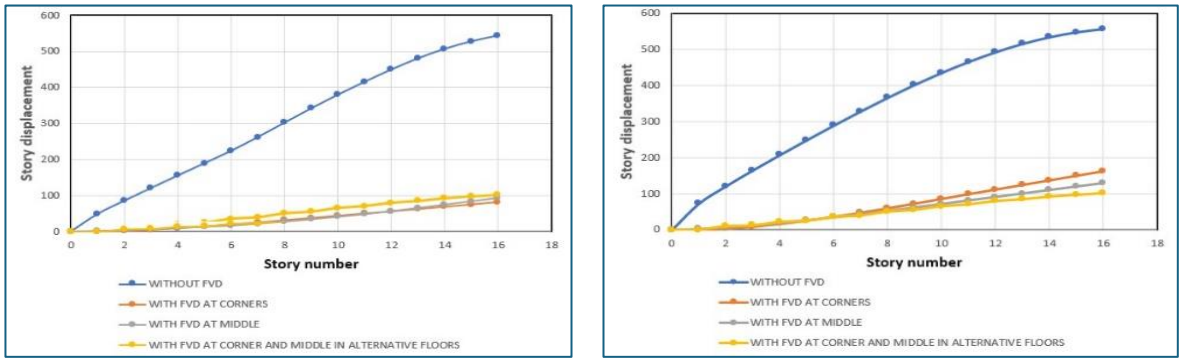


Figure 11. Storey displacement variation under static Earthquake load in X and Y-directions

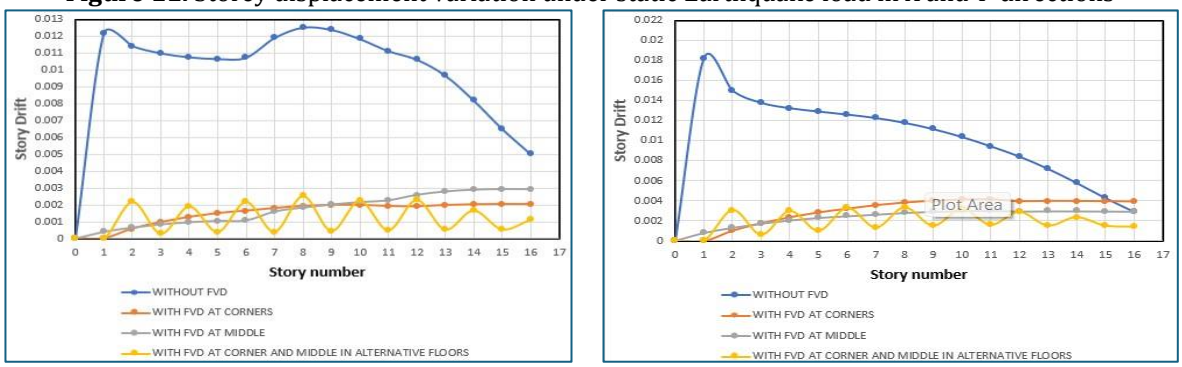


Figure 12. Storey drift variation under static Earthquake load in X and Y-directions

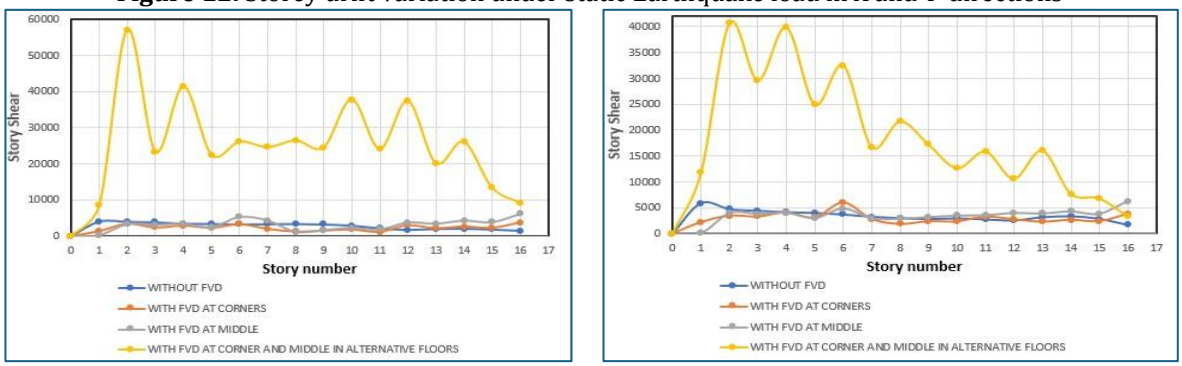


Figure 13. Storey Shear variation under GAZLI Earthquake in X and Y-directions

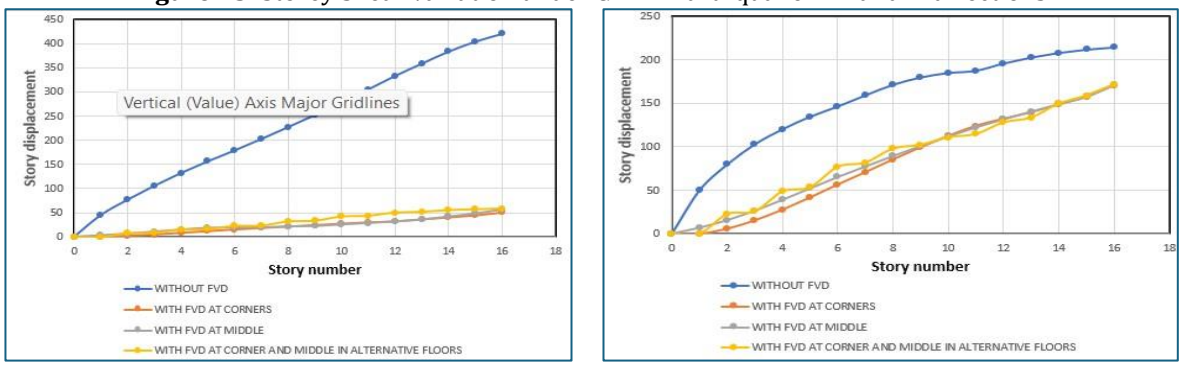


Figure 14. Storey displacement variation under GAZLI Earthquake in X and Y-directions

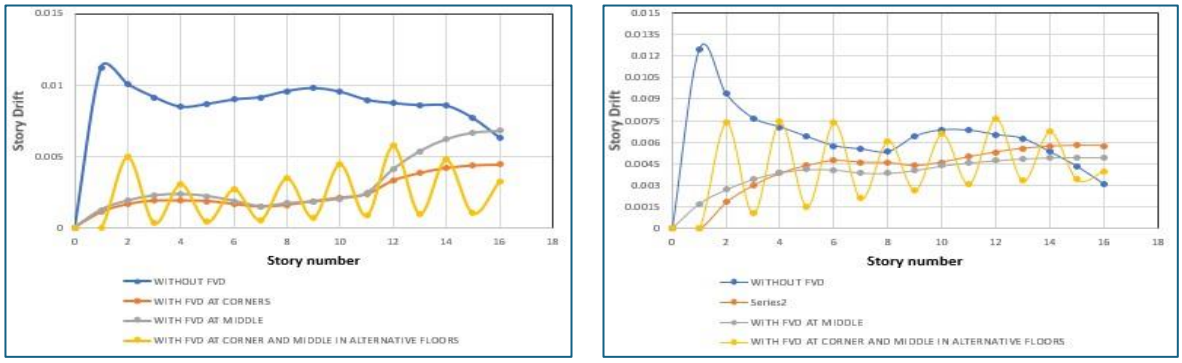


Figure 15. Storey drift variation under GAZLI Earthquake in X and Y-directions

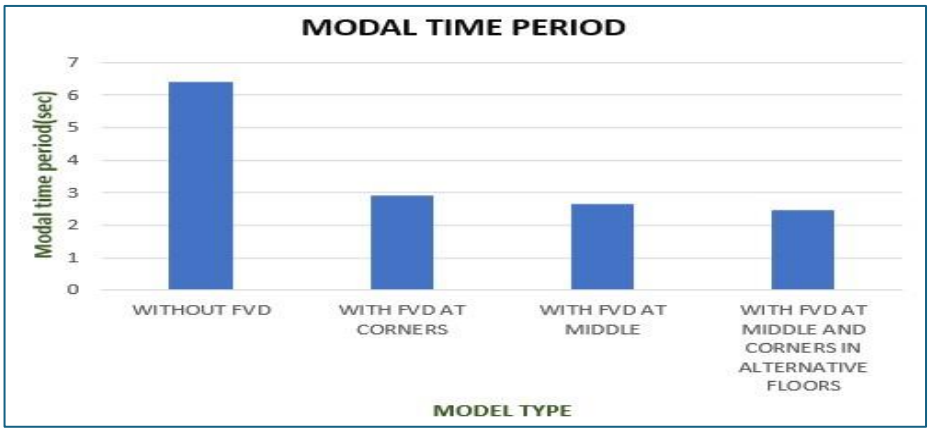


Figure 16. Variation of time period for different SET-BACK models

Table 5. Torsional irregularity in X-direction under earthquake loads

Model	Horizontal Displacement at one end	Horizontal Displacement at another end	Ratio	Result
Without FVD	543.443	464.222	1.17	No Torsional Irregularity
With FVD at Corners	81.571	72.818	1.12	No Torsional Irregularity
With FVD at Middle	65.051	56.738	1.14	No Torsional Irregularity
With FVD at Corners and Middle in Alternative floors	61.925	50.526	1.22	No Torsional Irregularity

Table 6. Torsional Irregularity in Y-direction under earthquake loads

Model	Horizontal Displacement at one end	Horizontal Displacement at another end	Ratio	Result
Without FVD	402.424	194.738	2.06	Extremely Torsional Irregular

With FVD at Corners	47.310	33.583	1.4	Slightly Torsional Irregular
With FVD at Middle	71.617	50.349	1.42	Slightly Torsional Irregular
With FVD at Corners and Middle in Alternative floors	65.321	44.870	1.45	Slightly Torsional Irregular

Table 7. Type of 1st mode in modal analysis of SET-BACK Buildings

Model	RX	Type
Without FVD	18.6%	Rotational mode
With FVD at Corners	8.3%	Rotational mode
With FVD at middle	8.2%	Rotational mode
With FVD at Corners and middle in alternate Floors	11.5%	Rotational mode

In this comprehensive analysis, meticulously compared building models equipped with Fluid Viscous Dampers (FVDs) to those without FVDs. Notably, the introduction of FVDs yielded significant reductions in maximum storey shear under various loading conditions. Placing FVDs at corners and middle floors, both separately and alternately, led to distinct reductions in storey shear, with reductions of 85.45%, 73.16%, and 49.97% under wind static analysis, and 86.72%, 75.36%, and 42.15% under earthquake static and dynamic analysis, respectively. These findings highlight the effectiveness of strategic FVD placement strategies.

Furthermore, our investigation revealed that building models with FVD arrangements at middle and corners, particularly at alternative floors, exhibited extreme storey shear compared to other configurations. This finding underscores the importance of strategic FVD placement to mitigate structural vulnerabilities.

Examining story displacement, there are noteworthy reductions under earthquake and wind forces across all directions with the introduction of FVDs. Placing FVDs at corners, middle floors, and alternately resulted in reductions of around 80% in story displacement, indicating consistent effectiveness in dampening displacement. Moreover, the risk of structural failure was substantially mitigated with FVD installation, ensuring enhanced structural resilience.

In terms of storey drift, the results indicated that while models without FVDs exceeded drift limits, FVD arrangements effectively controlled drift within acceptable bounds, albeit not consistently in time history analysis. Among these arrangements, FVDs positioned at middle floors demonstrated superior performance.

Torsional irregularity is predominantly observed in the Y-direction, was effectively mitigated by specific FVD placement strategies, highlighting the role of FVDs in enhancing structural stability.

Finally, our analysis revealed notable reductions in modal time period with the introduction of FVDs, with reductions of 3.46s, 3.756s, and 3.932s with FVD placement at corners, middle, and corners and middle in alternative floors, respectively, underscoring their efficacy in enhancing structural response dynamics. Additionally, FVD placement influenced modal behaviour, with corner and middle arrangements exhibiting slightly superior results in rotational modes.

3.2 Results of Step-Back Buildings

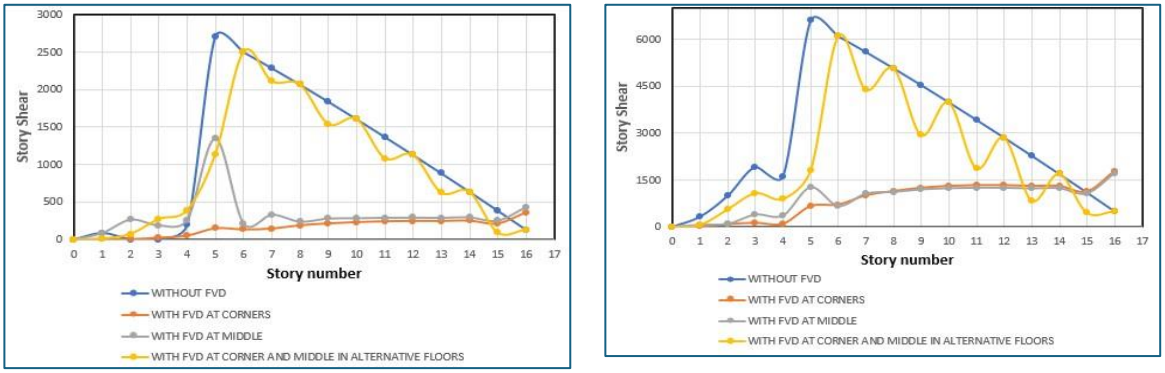


Figure 17. Storey Shear variation under Wind load in X and Y-directions respectively

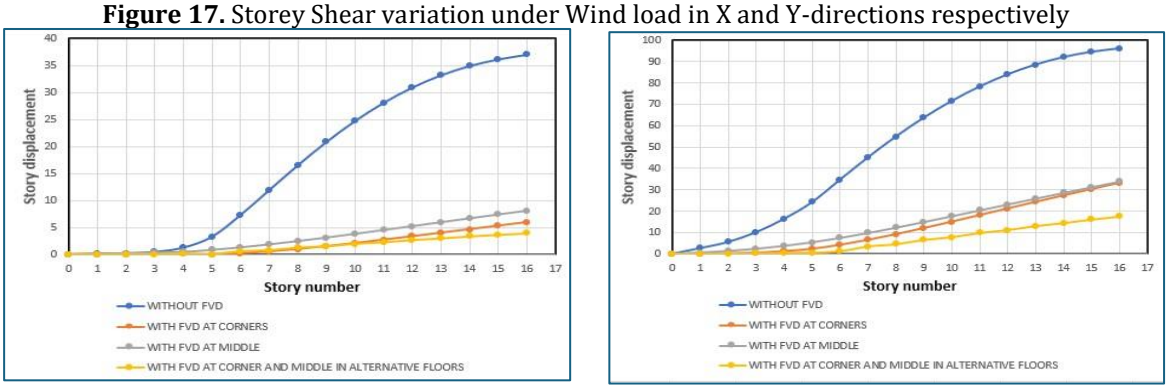


Figure 18. Storey displacement variation under Wind load in X and Y-directions respectively

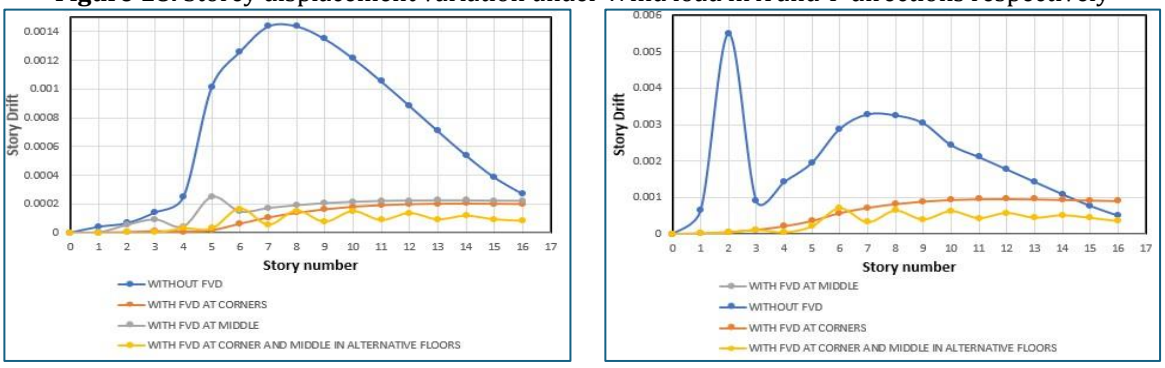


Figure 19. Storey drift variation under Wind load in X and Y-directions respectively

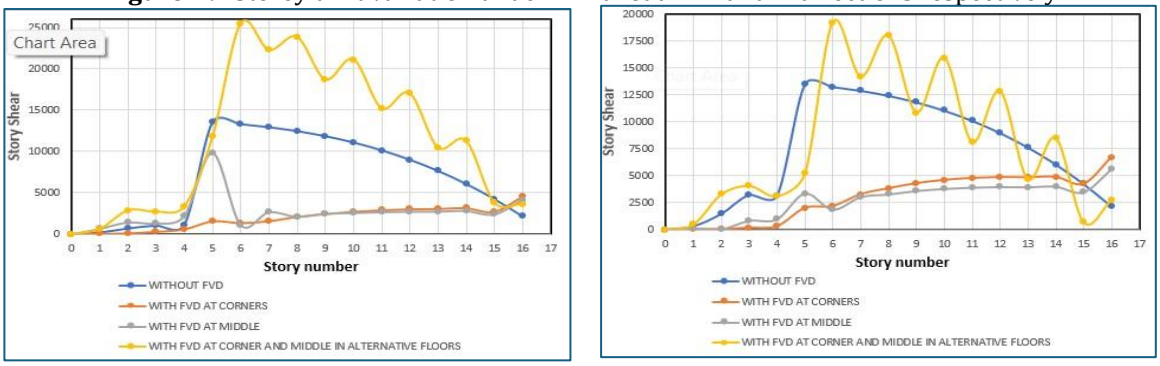


Figure 20. Storey Shear variation under static Earthquake load in X and Y-directions

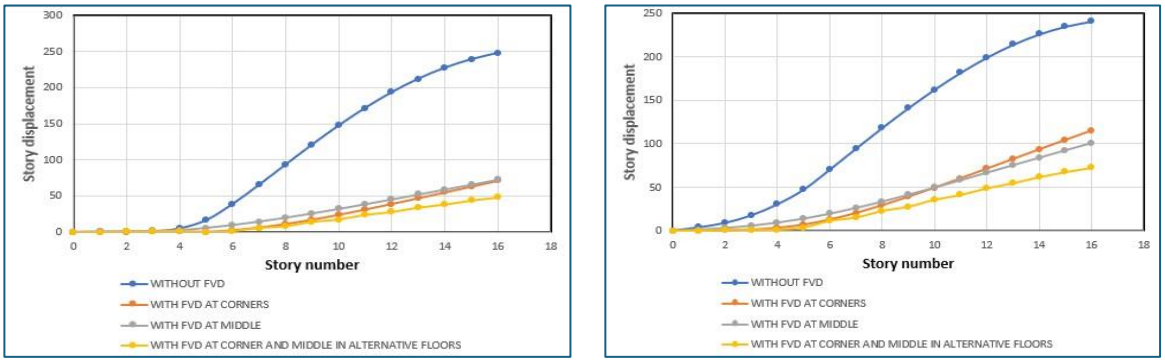


Figure 21. Storey displacement variation under static Earthquake load in X and Y-directions

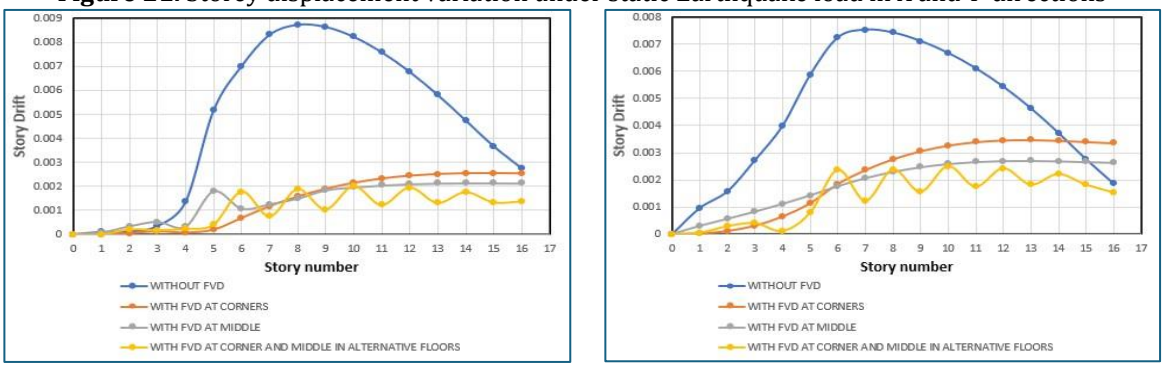


Figure 22. Storey drift variation under static Earthquake load in X and Y-directions

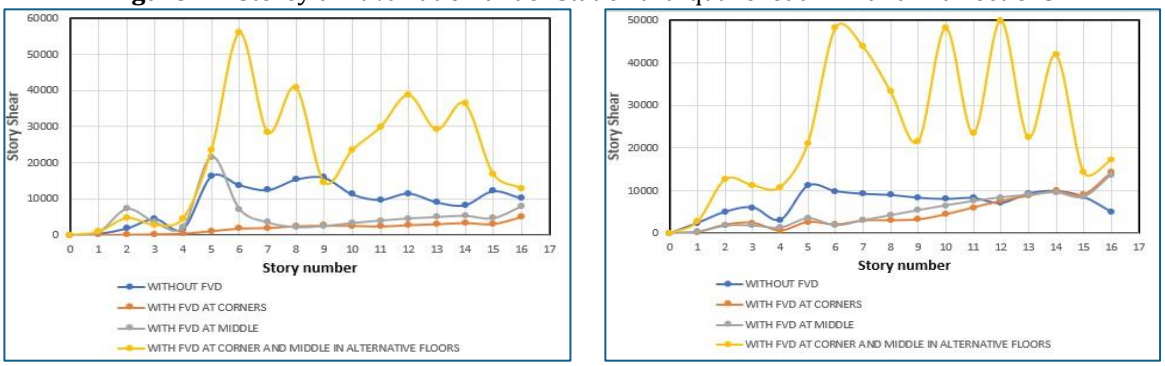


Figure 23. Storey Shear variation under GAZLI Earthquake in X and Y-directions

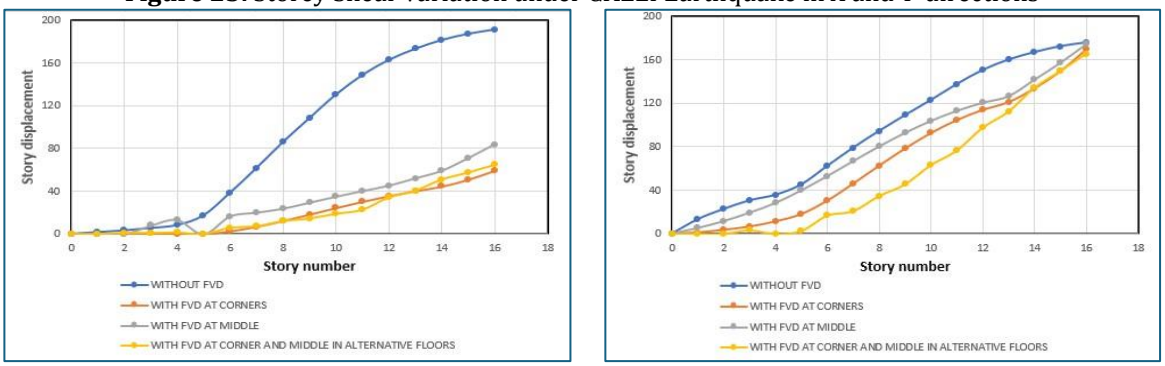


Figure 24. Storey displacement variation under GAZLI Earthquake in X and Y-directions

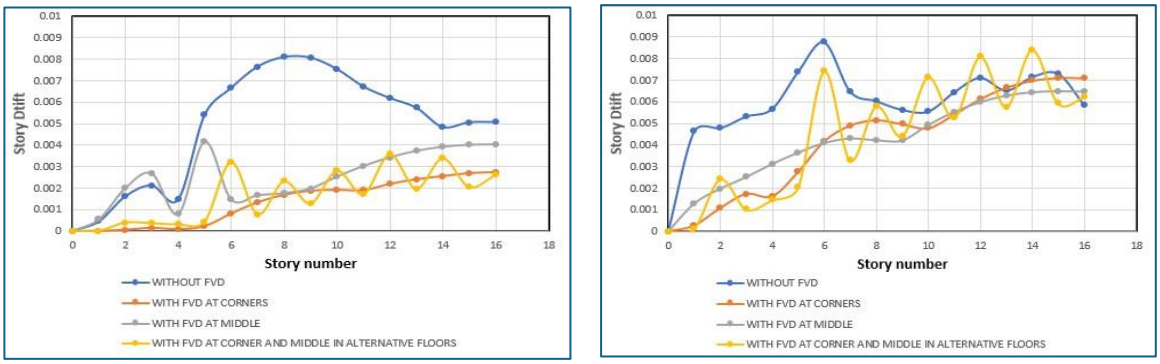


Figure 25. Storey drift variation under GAZLI Earthquake in X and Y-directions

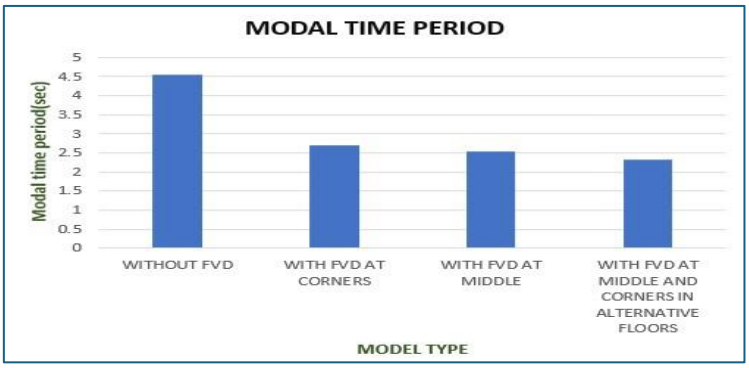


Figure 26. Variation of time period for different STEP-BACK models

Table 8. Torsional Irregularity in X-direction under wind loads

Model type	Horizontal displacement at one end	Horizontal displacement at another end	Ratio	Result
Without FVD	36.995	36.995	1	Extremely Torsional Irregular
With FVD at Corners	5.91	5.91	1	No Torsional Irregularity
With FVD at Middle	8.073	8.073	1	No Torsional Irregularity
With FVD at Corners and Middle in Alternative floors	4.945	4.945	1	Slightly Torsional Irregular

Table 9. Torsional Irregularity in Y-direction under wind loads

Model	Horizontal Displacement at one end	Horizontal Displacement at another end	Ratio	Result
Without FVD	45.025	24.907	1.81	Extremely torsional Irregular
With FVD at Corners	33.028	24.639	1.34	No Torsional irregularity
With FVD at Middle	21.789	12.685	1.71	Torsional Irregular
With FVD at Corners and Middle in Alternative floors	14.372	11.777	1.22	No Torsional Irregularity

Table 10. Torsional Irregularity in X-direction under earthquake loads

Model	Horizontal Displacement at one end	Horizontal Displacement at another end	Ratio	Result
Without FVD	247.82	247.82	1	No Torsional Irregularity
With FVD at Corners	71.42	71.42	1	No Torsional Irregularity
With FVD at Middle	72.69	72.69	1	No Torsional Irregularity
With FVD at Corners and Middle in Alternative floors	60.22	60.22	1	No Torsional Irregularity

Table 11. Torsional Irregularity in Y-direction under earthquake loads

Model	Horizontal Displacement at one end	Horizontal Displacement at another end	Ratio	Result
Without FVD	70.374	32.898	2.14	Extremely Torsional Irregular
With FVD at Corners	49.399	34.290	1.44	Slightly Torsional Irregular
With FVD at Middle	68.35	42.963	1.59	Slightly Torsional Irregular
With FVD at Corners and Middle in Alternative floors	67.776	56.279	1.20	No Torsional Irregularity

Table 12. Type of 1st mode in modal analysis of STEP-BACK Buildings

Model	RX	Type
Without FVD	0%	Translational mode
With FVD at Corners	0.4%	Translational mode
With FVD at middle	0.038%	Translational mode
With FVD at Corners and middle in alternate Floors	0.1%	Translational mode

In this analysis, Author conducted a comparative assessment of building models equipped with Fluid Viscous Dampers (FVDs) against those without FVDs. This examination revealed substantial reductions in maximum storey shear across various loading scenarios. Placing FVDs at corners led to reductions of 77.91%, 58.4%, and 37.2% under wind static analysis, earthquake static, and dynamic analysis, respectively. Similarly, FVD placement at middle floors resulted in reductions of 69.5% and 43.07% under wind and earthquake static analysis, with a slight increase of 14% observed. Additionally, combining FVDs at corners and middle floors in alternative arrangements yielded reductions of 73.5% and an increase of 13%, and a significant increase of 262%.

However, building models with FVD arrangements at middle and corners, particularly at alternative floors, exhibited extreme storey shear compared to other configurations, underscoring the need for careful FVD placement strategies. In terms of storey displacement, FVD installation led to reductions of at least 80% under earthquake and wind forces in both X and Y directions, ensuring enhanced structural stability and reducing the risk of failure. Notably, FVD arrangements demonstrated consistent efficacy across various placement strategies.

Further analysis revealed that while models without FVDs exceeded permissible drift limits, FVD arrangements effectively controlled drift within acceptable bounds. Among these arrangements, FVDs positioned at middle floors demonstrated superior performance, mitigating torsional irregularities and enhancing structural stability. Moreover, FVD installation resulted in notable reductions in modal time periods, with reductions of 1.862s, 2.009s, and 2.211s with FVD placement at corners, middle, and corners and middle in alternative floors, respectively. Additionally, the observation of translational modes as the first mode in both normal and FVD-equipped buildings indicated structural safety against rotational modes, as per structural dynamics principles.

4. Conclusions

In the investigation of the seismic behaviour of G+15 structures, specifically SET-BACK and STEP-BACK buildings, the comprehensive analysis was conducted with and without Fluid Viscous Dampers (FVDs) at various locations. Employing wind-static analysis, earthquake-static analysis, and time history analysis, several following key findings are summarized:

Time history analysis for both SET-BACK and STEP-BACK buildings did not yield anticipated results for Storey drift in X and Y directions. However, apart from Storey drift, the results from time history analysis indicated structural safety in terms of Storey displacement and Torsional irregularity.

The Storey shear experienced by the buildings saw significant increases ranging from 200% to 300% in time history analysis for both building types equipped with FVDs at middle and corner locations in alternative floors.

Torsional irregularity in the X-direction was not observed in any of the models under wind and earthquake loads, indicating stability in this aspect.

For SET-BACK Buildings:

- The Buildings without FVDs exhibited extreme storey drift and storey displacement under wind and earthquake forces.
- Placing FVDs at Corners demonstrated favourable outcomes across various parameters such as storey shear, storey displacement, storey drift, time period, modal analysis, and torsional irregularity, albeit with slightly higher storey drift values in time history analysis in the Y-direction compared to other arrangements.

For STEP-BACK Buildings:

- Normal buildings without FVDs and those with alternative FVD arrangements exhibited extreme torsional irregularity exclusively in the Y-direction under wind and earthquake forces, which was effectively mitigated by FVD placement.
- All three arrangements showed similar results for storey displacement, storey drift, torsional irregularity, and modal time period. However, the arrangement involving FVDs at corner and middle in alternative floors showcased superior performance in terms of storey drift, storey shear, modal time period, storey displacement, modal analysis, and torsional irregularity compared to other configurations.

References

[1] Ravitheja, A. (2016). Seismic evaluation of multi-storey RC buildings with and without fluid viscous dampers. Global Journal of Researches in Engineering: E, Civil and Structural Engineering, 16(1), Version 1.0. Global Journals Inc. (USA).

[2] Nalawade, S. S. (2003). Seismic analysis of buildings on sloping ground (M.E. Dissertation). University of Pune, Pune.
[3] Deshpande, C. A., & Mohite, P. M. (2014). Effect of sloping ground on step-back and setback configurations of R.C.C. frame building (M.E. Dissertation). Rajarambapu Institute of Technology Rajaramnagar, Maharashtra.
[4] Kumar, S., & Paul, D. K. (2017). Analyzing the seismic behaviour of setback buildings by using E-TABS.
[5] Singh, Y., Gade, P., Lang, D. H., & Erduran, E. (2012). Seismic behaviour of buildings located on slopes—An analytical study and some observations from the Sikkim earthquake of September 18, 2011.
[6] Rakhimol, S., & Cheriyath, S. (2018). Seismic response control of irregular shaped RCC buildings by using nonlinear viscous damper.
[7] Mohammad, Z., Baqi, A., & Arif, M. (2017). Seismic response of RC framed buildings resting on hill slopes. Procedia Engineering, 100-108.
[8] Chhetri, S., & Adhikari, S. (2021). Seismic performance of step back, step back-set back, and set back buildings in sloping ground base.
[9] Ghosh, R., & Debbarma, R. (2017). Performance evaluation of setback buildings with open ground storey on plain and sloping ground under earthquake loadings and mitigation of failure. International Journal of Advanced Structural Engineering, 97-110.
[10] Keertan, T. S., Kumar, S., & Bommisetty, J. (2023). Seismic performance evaluation of RC tall buildings irregular in plan with varied location of fluid viscous damper: A comparative study.
[11] Birajdar, B. G., & Nalawade, S. S. (2004). Seismic analysis of buildings resting on sloping ground.
[12] Ras, A., & Boumechra, N. (2017). Seismic energy dissipation study of linear fluid viscous dampers in steel structure design. Journal of Constructional Steel Research, 4, 189–249.
[13] Prajapati, A., & Parikh, K. B. (2021). Parametric study on step-back and step back-set back building on sloping ground.
[14] Ghosh, R., & Debbarma, R. (2019). Effect of slope angle variation on the structures resting on hilly region considering soil-structure interaction. International Journal of Advanced Structural Engineering, 67-77.
[15] Kavya, G. S., Ramesh, B. M., & Ramesh, P. S. (2018). Seismic performance of step-back and step back-set back building resting on a hill slope. International Research Journal of Engineering and Technology, 575-582.
[16] Kumar, K., Gupta, S., & Kumari, S. (2018). Dynamic study of step back and set back building. International Journal of Civil Engineering and Technology, 9, 185-190.
[17] Mohammed Irfan, A. Z., & Patil, V. B. (2018). Seismic analysis of multistoried building on sloping ground with ground soft storey and top soft storey. International Journal of Technical Innovation in Modern Engineering & Science, 4, 441-450.
[18] Guo, W., Xu, J., Xu, W., & Di, Z. (2014). Seismic upgrade of existing buildings with fluid viscous dampers: Design methodologies and case study.
[19] Sawant, A. G., & Ghugal, Y. M. (2018). Seismic analysis of buildings resting on sloping ground. International Journal of Advanced Research in Science and Engineering, 7, 345-357.
[20] Halkude, S. A., Kalyanshetti, M. G., & Ingle, V. D. (2013). Seismic analysis of buildings resting on sloping ground with varying number of bays and hill slopes. International Journal of Engineering Research & Technology, 2(12).
[21] Rohini, B., Gowri, C. L., & Jyothirmayee, T. (2018). Analysis of 2D frame (G+10) building on sloping ground. Journal of Emerging Technologies and Innovative Research, 5, 37-44.
[22] Deng, P., Li, X., Dong, W., & Tai, L. (2014). Seismic analysis of L-shaped irregular plane frame structure with viscous dampers. Applied Mechanics and Materials, 501-504, 1547-1550.
[23] Whittle, K. J., Williams, S. M., Karavasilis, L. T., & Blakeborough, A. (2012). A comparison of viscous damper placement methods for improving seismic building design. Journal of Earthquake Engineering, 4, 78-95.

[24] Vijaya Narayanan, A. R., Goswami, R., & Murty, C. V. R. (2012). Performance of RC buildings along hill slopes of Himalayas during 2011 Sikkim earthquake. EERI Newsletter, EERI Special Earthquake Report, February, 1-14.
[25] Choudhury, T., & Kaushik, H. B. (2017). Seismic fragility of open ground storey RC frames with wall openings for vulnerability assessment. Engineering Structures, 155, 345-357.
[26] Miyamoto, K. H., & Gilani, S. J. (2012). The effectiveness of viscous dampers for structures subjected to large earthquakes. Journal of Engineering Science, 5, 389-493.
[27] Bureau of Indian Standards (BIS). (2000). IS 456: Code of practice for plain and reinforced concrete (4th ed.). New Delhi, India.
[28] Bureau of Indian Standards (BIS). (1987). IS 875 (Part 3): Code of practice for design loads (other than earthquake) for buildings and structures. New Delhi, India.
[29] Bureau of Indian Standards (BIS). (2002). IS 1893 (Part 1): Criteria for earthquake resistant design of structures. New Delhi, India.
[30] Bureau of Indian Standards (BIS). (2016). IS 1893 (Part 1): Criteria for earthquake resistant design of structures – General provisions for buildings. New Delhi, India.
[31] Kumar, C. V., Ganesh, A., Bommisetty, J., Varun, L. M., Saibaba, A. N., & Ravinder, R. (2022). Evaluation of response spectrum and equivalent static analysis for recognizing the safest position of floating columns by ETABS in Zone V. In 2022 International Conference on Computational Intelligence and Sustainable Engineering Solutions (CISES) (pp. 209-216). Greater Noida, India.
[32] Farhan, M. A., & Bommisetty, J. (2019). Seismic analysis of multistoried RCC buildings regular and irregular in plan. International Journal of Engineering Research & Technology, 8(11), 115–121.

IOP Conference Series: Earth and Environmental Science

PURPOSE-LED PUBLISHING™

PAPER • **OPEN ACCESS**

Optimal placement of shear wall in multistorey buildings on sloping ground

To cite this article: N. C. Ghangare *et al* 2024 *IOP Conf. Ser.: Earth Environ. Sci.* **1409** 012035

View the article online for updates and enhancements.

You may also like

- Evaluation of Internal Forces and Support Reaction of Column and Shearwall in 15th Building Design
D R Wiyono, R Milyardi and Y A Pranata
- Response analysis of a multi-story building structure with a variety of horizontal irregularities and shear wall geometries
A H Prathama, M Teguh and F Saleh
- Literature review of seismic performance of double-layer steel plate-concrete composite shear wall with stiffeners
Chungang Wang, Shengkai Liu, Yong Chen et al.



This content was downloaded from IP address 47.247.77.11 on 27/11/2024 at 05:42

Optimal placement of shear wall in multistorey buildings on sloping ground

N. C. Ghangare[1*], S. S. Meshram[1] and V. U. Wasalwar[1]

[1]Department of Civil Engineering, Yeshwantrao Chavan College of Engineering, Nagpur, Maharashtra, India

*Email: nandinighangare@gmail.com

Abstract. High-rise buildings most frequently use shear wall systems as one of their lateral load-resisting techniques. The great plane stiffness and strength of shear walls allow them to withstand significant horizontal loads and gravity stresses, making them particularly valuable in many structural engineering applications. The main objective of this research project is to identify the optimal position for shear walls in multistorey buildings with sloping terrain. A ten-story RCC building located in a zone IV seismically active location and slopes. An earthquake load is calculated using the comparable static technique with IS 1893 (PART–I):2016. The software utilized for these assessments was STAAD Pro V8i. An extensive investigation was carried out to examine several factors, including average displacement, period, story shear, story drift, reinforcement reduction, and G+10 story building on sloping terrain. Including shear walls has become indispensable in multistorey buildings to effectively withstand lateral forces. A comparison between the bare frame structure and the shear wall applied structure is shown.

1. Introduction

The rapid development of the world has led to the creation of high-rise skyscrapers, with framed structures being the preferred option. However, the frame structure is influenced by both lateral and vertical loads, which can lead to significant overturning moments at the base of a structure. This is the primary reason for structural failure in seismic zones, where the structure was not designed for these stresses. To ensure the construction of buildings in earthquake-prone zones, reinforcing percentages are increased, making the construction heavy and unfeasible. Therefore, it is crucial to thoroughly examine seismic stresses and the influence of lateral loads on structural elements.[1]

India's rapid industrial growth and urbanization have accelerated real estate development in hilly terrain. Construction on sloping ground is necessary due to the lack of plain ground. Natural disasters like earthquakes, wind forces, and uneven settlement loads can cause high-rise buildings to bend and twist. Shear walls are essential for maintaining stability and stiffness in multistorey structures.[2]

In the context of a multistorey building, specifically a ten-story structure denoted as G+10, located in Zone 4 with medium soil conditions, the optimal placement of shear walls assumes heightened significance. The Equivalent Static Method (ESM) serves as a foundational approach for analyzing seismic forces and designing structures to withstand such forces. In Zone 4,

Content from this work may be used under the terms of the Creative Commons Attribution 4.0 licence. Any further distribution of this work must maintain attribution to the author(s) and the title of the work, journal citation and DOI.
Published under licence by IOP Publishing Ltd

characterized by high seismic activity, the ESM provides a rational and practical framework for evaluating the dynamic response of buildings and determining the requisite measures for seismic resistance. [3]

The interaction between sloping ground and the structural configuration of the building introduces unique challenges that necessitate a comprehensive understanding of geological, geotechnical, and structural principles the strategic placement of shear walls entails a judicious balance between structural efficiency, architectural aesthetics, and seismic resilience. [4]. The location of the shear wall becomes vital because the building on sloping land is asymmetrical about one of the principal axes. [5]. The location of the shear wall that will provide the greatest resistance to lateral forces must be chosen carefully [6]. The earth's tectonic plates move or tremble as a result of a sudden release of energy in the lithosphere. Since Bangladesh is situated between major fault lines, a major earthquake would cause massive damage. The capital city of Bangladesh, Dhaka, is prone to earthquakes and has sustained significant losses as a result of unplanned development. The city's high population density, nearby buildings, uncontrolled construction, and other infrastructural deficiencies make it vulnerable to impending earthquakes [19].

1.1. Equivalent static analysis

To mitigate the effects of earthquake ground movement, this method describes a series of forces building up on a structure, typically represented by a seismic design response spectrum. This is only true if the structure is low-rise and doesn't rotate significantly when the ground shifts. Given the structure's normal recurrence, which is either defined or described by the building rules, the response is examined from a design response spectrum. By employing pieces to symbolize higher structures for certain higher modes and low degrees of mobility, this method is extended in various construction standards. Modification factors that reduce the design forces are applied by various regulations to depict impacts resulting from the building yielding.

1.2. Limitations of Equivalent Static Analysis

There are restrictions on the usage of this approach about:

- High seismic zones and structure height
- Structures with vibration modes higher than the basic mode.
- Structures with notable variations in mass and stiffness over their height

1.3. Sustailability

When it comes to the best location of shear walls in tall buildings on sloping terrain, sustainability entails incorporating long-term durability, environmental effect, and structural efficiency into the design and construction phases. Here's how this scenario may take sustainability into account.

- Structural Efficiency-Material Optimization: By placing shear walls in the best possible way, you may minimize the quantity of materials used overall by reducing the requirement for excess. This may result in a decrease in the carbon footprint caused by the manufacture and delivery of building supplies like steel and concrete.
- Environmental Impact-Site-Specific Design: A design phase that takes into account the slope and other geographical characteristics can limit land disturbance and lessen the impact on nearby ecosystems. This might entail placing terraces, retaining walls, or other earth-stabilization methods next to the shear walls.
- Aesthetics and Community Impact-Community and Social Impact: Taking into account a building project's social effect is another aspect of sustainable construction. The neighborhood benefits when a structure is sturdy and safe, especially in places where

natural disasters are common. By taking these things into account, engineers and architects may help create structures that are long-term sustainable and ecologically responsible in addition to being structurally sound and useful.

2. Experimental and materials

An asymmetric office building structure with an L-shaped layout and ten stories made of reinforced concrete, situated on a mountainous terrain with irregular and uneven ground surface, is the subject of this examination. By a similar static analysis approach, the considered zone is IV under the medium soil condition. The below listing includes the plan's dimensions and elevations shown in Figure 1.

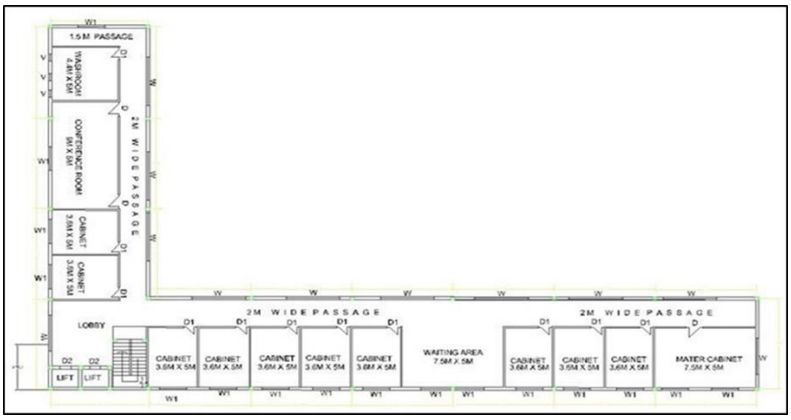


Figure 1. Architectural plan of building (2D PLAN)

2.1 Description of Building

For analytical purposes, the construction under consideration in this study is meant to operate as a practical office building. The architecture of the G + 10-story structure will be asymmetrical. utilizing three-depth grids to give the sloping ground structure. The building will have an overall length of 30 meters in the Z direction and 52.5 meters in the X direction. The entire width of the building will be 7.5 meters. In a Y orientation, the building will stand 24 meters tall overall. M30-grade concrete and Fe500 steel have been used. The details of the building's specifications are explained in greater detail below.

2.2 Structural Parameters

The geometric shape of the construction is understood to be an asymmetrical or "L"-shaped building. Because of the sloping site on which it is situated, the structure will have three distinct heights. There are two columns in Grid 01, each three metres above the ground. The sixteen columns that comprise Grid 03 are positioned one meter above the floor, while Grid 02 consists of four sets of columns that are two meters above the floor. We are thinking of this structure as a multi-story office building because we are creating it with pragmatism in mind. Because the multi-story building is made of RC frames, its primary beam structure is 7.5 m by 7.5 m. Secondary beams that are meant to rest on the primary beam structure further divide the primary beam grid into 3.75 m x 3.75 m grids. The secondary beams in the grid design will effectively cross at the same level. There will be four main grids in the vertical (Z) direction and seven primary grids in the horizontal (x) direction that make up the structure. Situated on the Sloping Ground, it comprises G+7 levels in the Y direction. All of the beams, excluding the lift and staircase, will

measure 230 mm by 600 mm; the lift shaft and staircase beams will be 230 mm by 450 mm. Column measurements will be between 300 x 450 mm and 300 x 750 mm; lift and staircase columns will have dimensions of 230 x 400 mm. The depth of the RCC slab will be 135 mm.

2.3 Framing Plan

The primary beam in this framing plan, as depicted in Figure 2. is indicated by the green beams, while the orange beams indicate the positioning of the secondary beams, which are resting on the primary beams and intersecting at the same elevation or passing through each other at the same height. The columns' locations within the building are indicated by the green rectangular boxes.

2.4 Modelling and Analysis

Below two models are shown in Figure 3 with a shear wall and without a shear (bare frame) wall in 3D view.

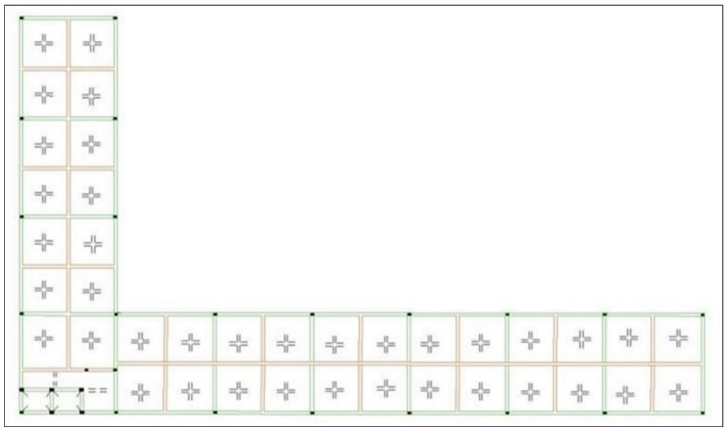


Figure 2. 2-D framing plan of structure

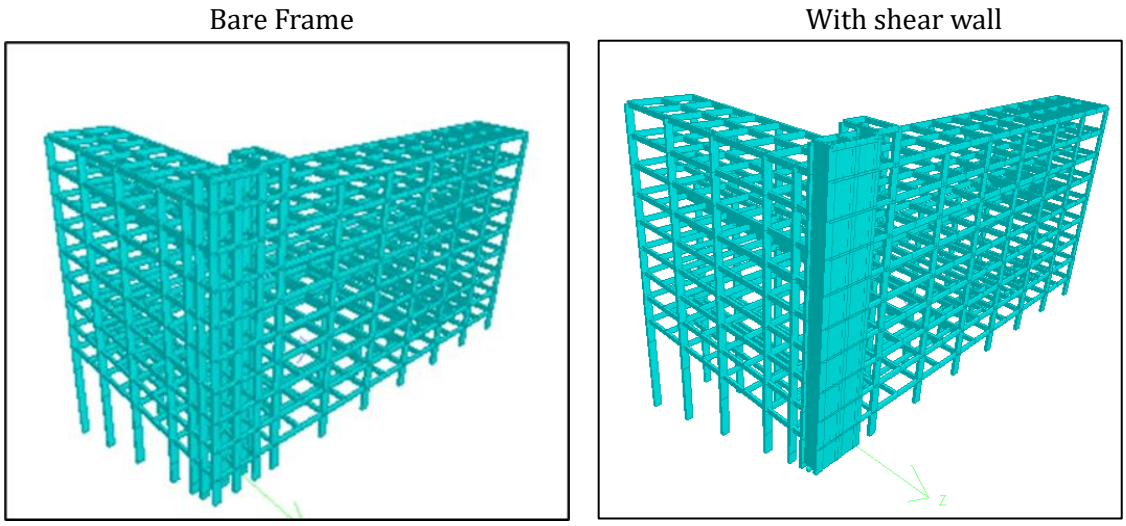


Figure 3. 3D View of the model (Rendering)

3. Results and discussion

The results for the seismic assessment of the G + 10 Reinforced Concrete office building are occupied from the STAAD Pro software as given in the following points:

3.1 Seismic Parameter Results

1. Base Shear

The maximum lateral force that is anticipated to result from seismic ground acceleration at the base of the building is known as base shear. The graphs for base shear in the x and z directions for bare frames and shear walls with shear walls are displayed in Figure 4, Table 1, and Figure 5, respectively.

Bare Frame

```
**********************************************************
*                                                        *
* TIME PERIOD FOR X 1893 LOADING =    2.39640 SEC        *
* SA/G PER 1893=    0.568, LOAD FACTOR= 1.000            *
* VB PER 1893=    0.0136 X    64229.24=     874.83 KN    *
*                                                        *
**********************************************************
```

```
**********************************************************
*                                                        *
* TIME PERIOD FOR Z 1893 LOADING =    2.65745 SEC        *
* SA/G PER 1893=    0.512, LOAD FACTOR= 1.000            *
* VB PER 1893=    0.0123 X    64229.24=     788.89 KN    *
*                                                        *
**********************************************************
```

With shear wall

```
**********************************************************
*                                                        *
* TIME PERIOD FOR X 1893 LOADING =    2.34997 SEC        *
* SA/G PER 1893=    0.579, LOAD FACTOR= 1.000            *
* VB PER 1893=    0.0139 X    61209.83=     850.18 KN    *
*                                                        *
**********************************************************
```

```
**********************************************************
*                                                        *
* TIME PERIOD FOR Z 1893 LOADING =    2.60240 SEC        *
* SA/G PER 1893=    0.523, LOAD FACTOR= 1.000            *
* VB PER 1893=    0.0125 X    61209.83=     767.71 KN    *
*                                                        *
**********************************************************
```

Figure 4. Base Shear

Table 1. Base Shear

Bare Frame		With shear wall	
For X Direction	874.83 KN	For X Direction	850.18 KN
For Z Direction	788.89 KN	For Z Direction	767.71 KN

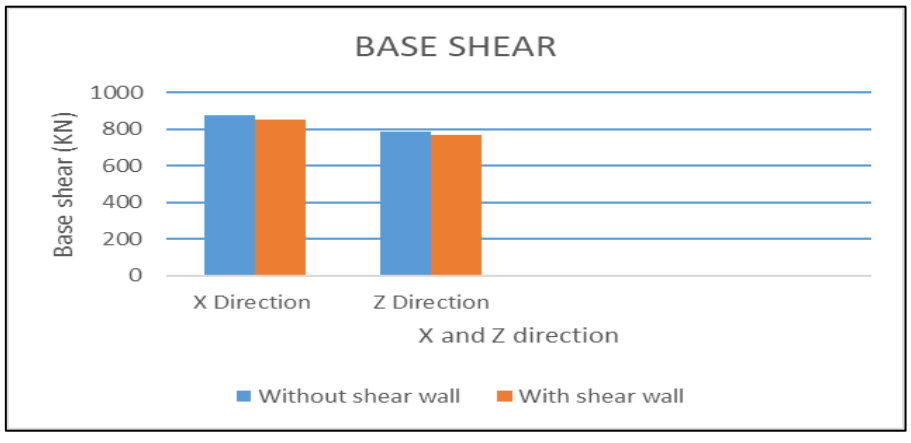


Figure 5. Base Shear

2. Fundamental Period

The building's Fundamental Natural Period T is defined as the amount of time (measured in seconds) required for one full cycle of free vibration or one full back-and-forth motion. Table 2 and Figure 6 display the basic period results for both the without and with shear walls in the x and z directions.

Table 3. Fundamental Time Period

Bare Frame		With shear wall	
For X Direction	2.39 secs	For X Direction	2.34 secs
For Z Direction	2.65 secs	For Z Direction	2.60 secs

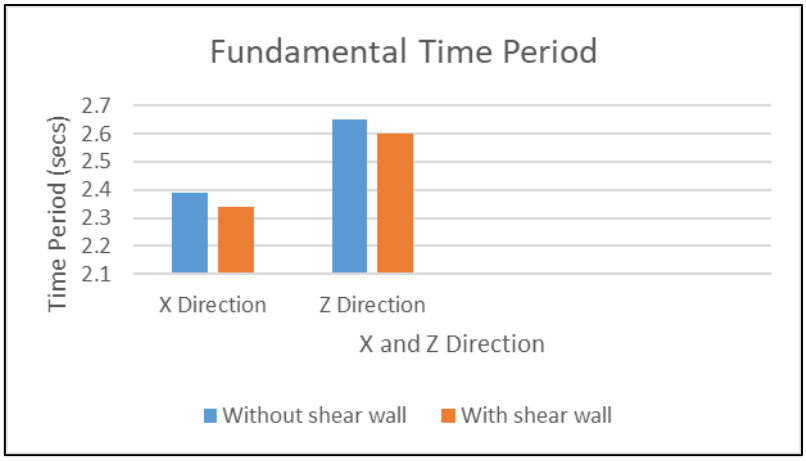


Figure 6. Fundamental Time Period

3. Maximum Storey Displacement

The extent of lateral story displacement depends on the height and slenderness of the building. As the height of a building increases, it becomes more flexible and vulnerable to lateral loads. The research will provide the outcomes of storey displacement in all the zones with varying sloping inclined conditions. The results for maximum storey displacement without and with the shear wall are shown in Figure 7.

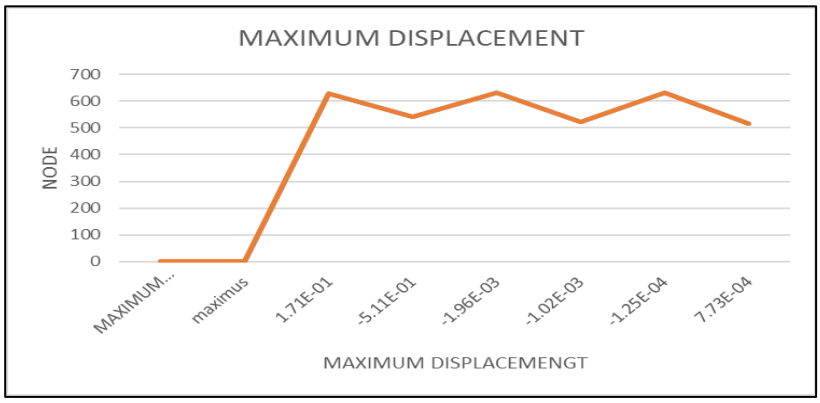


Figure 7. Maximum Storey Displacement

4. Storey Drift

A level that is moved laterally concerning a level above or below it is referred to as "story drift". The drift limit does not apply to a single-story building intended to allow for storey drift. Regarding any other level, IS 1893 (Part 1): 2016 states that the storey drift cannot be greater than 0.004 times the storey height. The storey drift, for example, should not be more than 12 mm if the storey height is 3000 mm, which is more than the minimal restriction of 1.958 mm. Zero in the absence of a shear wall. Figure 8 and Table 3 illustrate the average displacement and storey drift with a shear wall.

5. With shear wall

Table 4. Avg. displacement and Storey Drift

Storey	Height	Avg. displacement(cm)		Drift(cm)	
		X	Z		
1	0	0.9613	0.8802	1	0
2	3.3	0.8549	1.0940	2	3.3
3	6.6	1.756	2.0318	3	6.6
4	9.9	2.149	2.5582	4	9.9
5	13.2	2.5111	3.0212	5	13.2
6	16.5	2.8311	3.4015	6	16.5
7	19.8	3.093	3.6795	7	19.8
8	23.1	3.1423	3.8410	8	23.1
9	25.6	2.1676	2.2906	9	25.6
10	26.10	2.445	2.5509	10	26.10

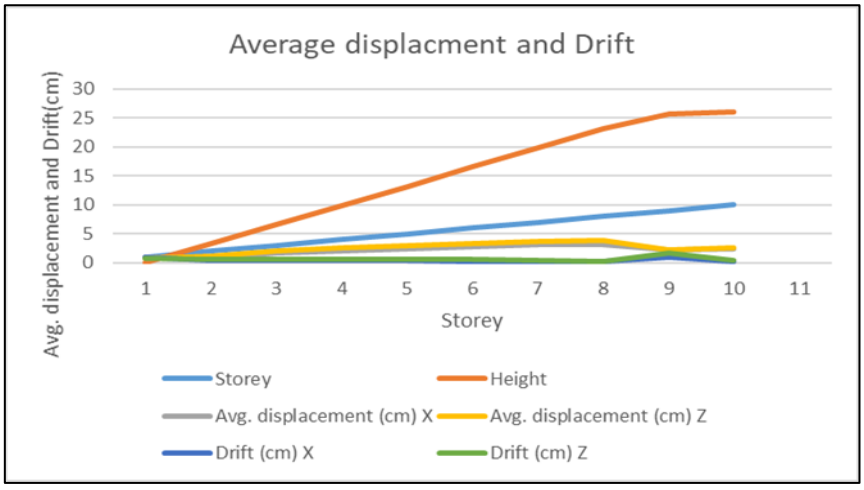


Figure 8. Avg. displacement and Storey Drift

3.2 Design Result of Beam

A beam must be designed in a certain way to guarantee that the loads it is supposed to support are safe. Below is a general process outline:

1. Determine Loads

Dead load: Constant loads brought on by the structure's own weight.

Live load : Variable load ,People, furniture, cars, etc.
Natural load factors : Include snow, wind, and earthquakes.
2. Select Beam Material
Concrete: Usually used for large, stiff constructions.
Steel: Used frequently for long-span, high-strength applications.
Wood: Frequently utilized in modest business or residential structures.
3. Choose a Beam Type
Simply Supported: Supported at both ends.
Cantilever: Fixed at one end, free at the other.
Continuous: Supported at more than two points.
4. Initial Sizing
Estimate the beam size based on standard guidelines or empirical formulas. For instance, for steel beams, the depth can be roughly 1/20 to 1/30 of the span.
5. Structural Analysis
Calculate Reactions: Determine support reactions using static equilibrium equations.
Shear Force and Bending Moment Diagrams: Plot the shear force and bending moment distribution along the beam.
Maximum Shear Force (Vmax) and Maximum Bending Moment (Mmax): Identify the peak values.
6. Design for Shear
Shear Stress (τ) = $V \times Q / I \times b$,
where:
V = Shear force,
Q = First moment of area,
I = Moment of inertia,
b= Width of the beam.
Ensure \tauτ is less than the allowable shear stress for the material.
7. Design for Bending
Bending Stress (σ) = $M \times y / I$
where:
M = Bending moment,
y = Distance from the neutral axis to the outermost fiber,
I = Moment of inertia.
Ensure \sigmaσ is less than the allowable bending stress for the material.
8. Check Deflection
Calculate the deflection using the appropriate formula based on beam type and loading.
Ensure deflection is within the permissible limits (often L/360L/360 for live loads, where LL is the span length).
9. Design for Stability
Check for lateral-torsional buckling in slender beams, especially in steel beams.
Provide lateral bracing if necessary.
10. Detailing
Specify the dimensions, reinforcements, connections, and other necessary details.
Ensure that the beam can be constructed as per design specifications.
11. Review and Optimization
Double-check calculations for errors.
Optimize the design for cost, material usage, and constructability if needed.

12. Code Compliance
Ensure the design meets relevant building codes and standards (e.g., AISC, ACI, Eurocode).

1. Shear Force
The force that causes a surface to deform or slide when applied parallel or tangentially. Shear force in bare frame and with the shear wall are shown in Table 4 and Figure 9.

Table 5. Shear force of beam No.522

	Bare Frame	With shear wall
Fy	-0.101 KN	-0.130 KN
Mz	0.113 KNm	0.146 KNm

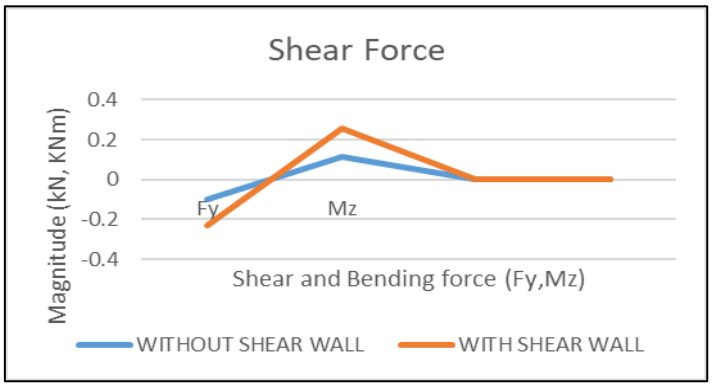


Figure 9. Shear force of beam No.522

2.Deflection
Beam deflection is the term used to describe how a beam will deflect when a force is applied in a specific direction. Deflection in bare frame and with shear wall is shown in table 5 and figure 10.

Table 6. Deflection diagram of beam No.522

Bare Frame	With shear wall
11.720 mm	9.134 mm

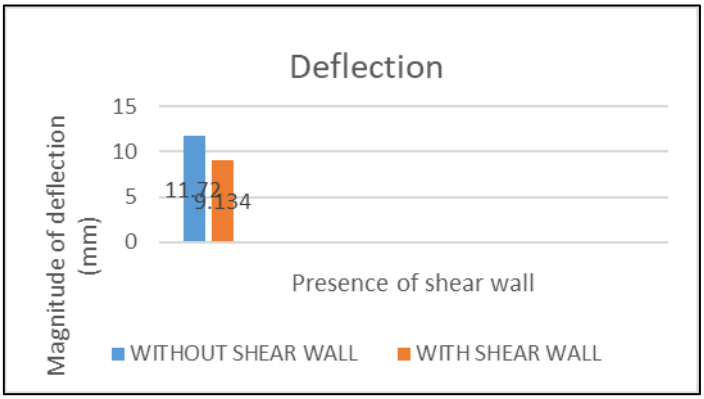


Figure 10. Deflection of beam No.522

4. Conclusions

Research has been done on the response of an effective shear arrangement to a multistorey building situated on sloping terrain.

The Equivalent Static Method was applied to the analysis and design of a G+10 building in seismic zone IV with medium soil conditions. The STAAD Pro V8i program was used to apply loadings in compliance with IS regulations.

When a shear wall is installed, base shear decreases by 22.915 KN or 2.29%, and the fundamental period correspondingly decreases by 0.05 sec. When a shear wall is positioned, deflection decreases by 2.586 mm, and shear bending increases, and vice versa.

The building's design base shear reduction is significantly impacted by the shear wall's shape and placement.

Compared to the shorter portion of the building, the longer portion is primarily influenced by the design base shear.

References

[1] U. P. Ankit Dane, "Effective Positioning of Shear Wall in G+5 Storey Building on Sloping Ground," International Journal of Engineering and Advanced Technology (IJEAT), vol. 9, no. 2, p. 5, 2019.

[2] A. S. Sripriya Arjun, "A Study on Dynamic Characteristics of RC Buildings on hilly slopes," International Journal of Science and Research (IJSR), vol. 5, no. 7, p. 4, 2016.

[3] A. T. Q. Tarun Magendra, International Journal of Trend in Research and Development, vol. 3, p. 7, 2016.

[4] D. A. M. B. a. P. S. S. Sagar D. Parbat, "Positioning of Shear Wall In L- Shaped Unsymmetrical Building onThe Sloping Ground.," IJISET - International Journal of Innovative Science, Engineering & Technology, vol. 8, no. 4, p. 9, 2021.

[5] P. k. V. R. M H Mohammadi, "The effective placing of Shear Wall for Seismic Resistance of G+5 Story building on sloping Ground," IOP Conf. Series: Earth and Environmental Science, p. 11, 2023.

[6] D. S. B. Ms. Sunita D. Kamble, "Seismic Performance of the Building Resting on Sloping Ground with Shear Wall," International Journal of Engineering Research & Technology (IJERT), p. 4, 2016.

[7] Arjun S. and Arathi S. (2016), "A Study on Dynamic Characteristics of RC Buildings on Hill slopes", International Journal of Science and Research (IJSR) ISSN (Online): 2319-7064 Index Copernicus Value (2013): 6.14 | Impact Factor (2015): 6.391

[8] Bhavesh R. S. et al. (2018), "Seismic Behaviour of Flat Slab Building with Shear Wall According to I. S. 1893 2016", International Journal of Civil Engineering and Technology (IJCIET) Volume 9, Issue 5, May 2018, pp. 955–963, Article ID: IJCIET_09_05_105

[9] Bongilwar R. et al. (2018), "Significance of Shear Wall in Multi-Storey Structure with Seismic Analysis", IOP Conf. Series: Materials Science and Engineering 330 (2018) 012131 doi:10.1088/1757-899X/330/1/012131.

[10] Dipak M. K. and Mukund M. P. (2017), "Study of Base Shear, Storey Shear and Base Moment on Multistorey Building for Different Seismic Zones", International Journal of Engineering Science and Computing, June 2017 Research Article Volume 7 Issue No.6.
[11] Doijad S. and Bhalchandre S. (2015), "Seismic Behaviour of RC Buildings Constructed on Plain and Sloping Ground with Different Configuration of Shear Walls", Journal of Civil Engineering and Environmental Technology Print ISSN: 2349-8404; Online ISSN: 2349-879X; Volume 2, Number 10; April-June, 2015 pp. 59-65
[12] V.V.B.L.N.D. Vara Prasad, Mrs T. Sujatha, Mrs J. Supriya-, "Optimum Location of a Shear Wall in High Rise U-Shape Building", International Journal of Engine
[13] Hirde S. K. and Charjan S. T. (2009), "Effect of various positions of reinforced concrete shear walls on seismic performance of building having soft bottom storey", ISSE Journal, Volume 11-1.
[14] Kamal V. S. and Kharole S. K. (2020), "Seismic Analysis of RC Building on Sloping Ground with Shear Wall", International Journal for Research in Engineering Application & Management (IJREAM) ISSN: 2454-9150 Vol-06, Issue-06.
[15] Kasi K. M. et al. (2016), "Study on Seismic Performance of Buildings Resting on Sloping Grounds with and without Shear Wall", International Journal of Engineering and Management Research Page Number: 90-94, ISSN (ONLINE): 2250-0758, ISSN (PRINT): 2394-6962 90 Copyright © 2016. Vandana.
[16] M H Mohammadi, P kumar, V Rishi (2022), "The effective placing of Shear Wall for Seismic Resistance of G+5 Story building on sloping Ground", IOP Conference Series: Earth and Environmental CASF-2022.
[17] Prasad Ramesh Vaidya, (2015) "Seismic Analysis of Building with Shear Wall on Sloping Ground", International Journal of Civil and Structural Engineering Research ISSN 2348-7607 (Online) Vol. 2, Issue 2, pp: (53-60), Month: March 2015.
[18] Pinaki and A.K. Dwivedi (2022) , "Comparison of Seismic Response of Multi-Storey Building Having Shear Walls Without Opening onSTAAD-PRO and ETAB", IOP Conf. Series: Materials Science and Engineering SCTACE-2022.
[19] Chowdhury Zubayer Bin Zahid, Shahriar Alam, Azmain Fahik, Minhaz Imran Khan and Tarek Uddin Mohammed, "Different orientations of shear wall in a reinforced concrete structure to control drift and deflection", Journal of Physics: Conference Series CONCET-2022.
[20] RS Maili O. et (2008), "Study of RC Shear Wall System in a 56-Storey RC Tall Building", The 14th World Conference on Earthquake Engineering October 12-17, 2008, Beijing, China.

IOP Conference Series: Earth and Environmental Science

PURPOSE-LED PUBLISHING™

PAPER • **OPEN ACCESS**

Harnessing piezoelectric sensors for electricity generation from speed breaker

To cite this article: A. A. Girde *et al* 2024 *IOP Conf. Ser.: Earth Environ. Sci.* **1409** 012036

View the article online for updates and enhancements.

You may also like

- Analytical solution for fractional order temperature distribution in two dimensional multilayer composite circular discs
N.J. Wange, M.N. Dandale and Vinod Waikar
- Enhancing crop protection through smart autonomous pesticide spray bot in sustainable agriculture
Ashish Meshram, Anil Vanalkar, Kavita A. Meshram et al.
- FTIR spectral analysis of glycine doped ammonium dihydrogen phosphate (ADP) crystal
A Z Khan, Z S Khan, S Patle et al.



This content was downloaded from IP address 47.247.77.11 on 27/11/2024 at 05:42

Harnessing piezoelectric sensors for electricity generation from speed breaker

A. A. Girde[1], A. A. Farsole[2], H. P. Deshmukh[3], M. P. Umate[4], N. A. Rai[5], S. S. Lanjewar[6], M. S. Bhagat[7*]

[1-6] Undergraduate Students, Department of Civil Engineering, Yeshwantrao Chavan College of Engineering, Nagpur, 441110. Maharashtra, India
[7]Assistant Professor, Department of Civil Engineering, Yeshwantrao Chavan College of Engineering, Nagpur, 441110. Maharashtra, India

*E-mail: msbciv@gmail.com

Abstract. The population of India is increasing drastically. In 2024, it has reached 140 crores, which leads to more energy consumption. The energy generated from conventional sources is limited and non-renewable. Also, due to urbanization, the energy demand is increased tremendously. So, there is a need to generate energy through renewable sources. One of the effective ways to generate renewable energy is by using piezoelectric cells. Piezoelectric cells are the cells that can generate electric charge through mechanical stress. The mechanical stress is generated on the roads, especially on the road breakers. This mechanical stress is created by vibrations of the vehicles on the speed breaker which will induce electrical energy. By installing piezoelectric cells beneath the speed breaker, the generated mechanical energy can be converted into electrical energy. The generated electricity can be utilized for street lighting, traffic signals, etc. It helps in generating clean and renewable energy from vehicular motion, leading to sustainable development.

1. Introduction

Electrical power has become the basic need of every human being. Every appliance electronic goods, institutional facilities, industrial machinery, medical equipment, etc, run on electrical power. Life could be miserable without electricity. A world without electricity could not be imagined. Conventional sources of energy like coal, fossil fuels, and LPG are depleting day by day. The tremendous increase in population needs electrical energy for their survival. Also, industrial and institutional requirements for energy are increasing drastically. To meet the demands of society renewable energy is the only effective economic solution. In India, the sunshine hours are more than 12 hours and hence the solar radiation can be converted into electrical power. Another source of renewable energy is Refuse Derived Fuels (RDF).

In India, the development of road transportation has changed significantly due to Pradhan Mantri Gram Sadak Yojana (PMGSY). Due to such an initiative, the road transportation has been improved. Most of the roads are converted to rigid pavements with finished smooth road surfaces, with less friction. This leads to higher speed of the vehicle moving on such roads. Hence, there is a need of frequent speed breakers on the roads. In general, speed breakers on city roads are typically spaced between 100 to 200 meters [1]. Also, roads are an important part of the human living environment, is built for passing vehicles and the increasing demands of growing traffic have led to tremendous changes in the function of roads [2].

Content from this work may be used under the terms of the Creative Commons Attribution 4.0 licence. Any further distribution of this work must maintain attribution to the author(s) and the title of the work, journal citation and DOI.
Published under licence by IOP Publishing Ltd

Nowadays Population is increasing drastically, the development of roads is enhanced, also urbanization leads to more financial stability and people are capable of keeping more vehicles. This leads to increased load on the roads. As, roads have become an integral part of every human being, and are used extensively, it is applying gigantic pressure on the earth's surface. In turn, the earth's surface gives a reaction that is not being utilized. If it is used, then a large amount of reaction pressure can be used effectively. Also, annually the motor vehicles rate is increased at about 20% during the last decades [3]. Thus, any technology that uses the road transportation system will be economical and feasible.

The last decade has witnessed significant advances in energy harvesting technologies as a possible alternative to provide a continuous power supply for small, low-power devices in applications, such as wireless sensing, data transmission, actuation, and medical implants [4]. The energy is harvested by using piezoelectric transducers from moving vehicle excitations [5]. By placing piezoelectric sensors underneath a road, the vibrations produced by vehicles would be converted into electricity, which helps in enlightening signs and lights [6]. Piezoelectric devices, used for harvesting the vibrational energy of roads and walkways due to traffic, can produce a competitive, clean energy source, that is predictable, and locally storable [7].

Piezoelectric sensors offer a revolutionary approach to electricity generation by harnessing kinetic energy from sources like speed breakers. These sensors are strategically placed beneath the road surface to convert the mechanical pressure generated by vehicles passing over them into electrical energy. This innovative technology presents a sustainable solution for urban areas, where vehicular traffic is dense. By utilizing existing infrastructure, piezoelectric sensors not only generate electricity but also contribute to reducing carbon emissions and promoting renewable energy practices. Implementing this system could significantly enhance energy efficiency for a greener, more sustainable future in urban environments.

Renewable Energy is currently one of the most important research topics. The form and source of energy have changed continuously over the last century. Nowadays it is a challenge to produce enough energy to support human activities and minimize the environmental impact. This challenge is for researchers to look for alternative energy sources apart from the current widely used fossil energy sources. These fossil energy sources are known for their pollution and depletion issues. Interest in harvesting ambient energy has increased considerably during the last few decades [8].

Thus, it is seen that urbanization and high living standards demand more Energy requirements. Also, developments have increased the vehicular load and improvements in road infrastructure increased the speed of vehicles. To control the speed of vehicles speed breakers are installed at 100-200 m.

2. Literature Review

Various literatures related to harvesting energy have been reviewed. The referred literature includes energy harvesting by converting mechanical energy into electrical energy. The literature has been classified into various categories depending on the method of generating the energy.

Various methods include: -

- Energy generation from piezoelectric sensors or vibration of moving vehicle.
- Energy generation from Renewable energy sources includes Refuse Derived Fuels (RDF) and Incineration.

2.1. Energy generation from piezoelectric sensors or vibration of moving vehicle

A piezoelectric material, such as Lead Zirconate Titanate (PZT) is widely used in piezoelectric sensors due to its ability to convert mechanical stress or energy into electrical energy [9]. Piezoelectric materials are crystalline in form, which may capture and transform kinetic energy into useful electrical energy by putting piezoelectric sensors beneath a speed breaker [10].

According to researchers, the use of piezoelectric cells or sensors for the generation of sustainable energy gives a clearer picture of the challenges and advantages of piezoelectric materials as a means of power generation support material [11]. Mechanical strain energy from human movement and infrastructure can be harvested using piezoelectric transducers to generate electrical energy. Various factors that affect the output power of piezoelectric generators, are a type of sensor, packing density, applied strain, electronic circuitry, storage device, and load [12].

An empirical study on piezoelectric sensors was conducted to optimize the resources, constraints, and possibilities of piezoelectric sensors in producing electricity from speed breakers, followed by a suggestion for a sustainable electricity development strategy [13]. Piezoelectric sensors generate electricity due to vertical deflection caused by the speed breaker when an oncoming vehicle passes over it which results in the release of electrical energy [14].

Comparing piezoelectric sensors to traditional energy sources reveals several benefits. Piezoelectric materials have high power densities. First of all they generate energy consistently regardless of external influences because they function independently of weather. Also, as they are decentralized, they are more efficient overall because they minimize the transmission losses that come with centralized electricity networks. Additionally, when in operation, piezoelectric systems produce no pollutants or greenhouse gases, having a negligible environmental impact. This environmentally beneficial feature supports international initiatives to slow down climate change and switch to sustainable energy sources [15].

To optimize energy capture, the sensors are placed strategically at busy places like roads and intersections. In the last several years, harvesters have proposed a large number of applications, such as industrial applications, medical implants, embedded sensors in buildings and bridges, and regenerative shock absorbers to absorb and generate electricity [16]. Harvested energy from ambient vibrations, such as winding, human motion, vehicles, machines, and buildings, etc, have been organized as an efficient way to supply green energy to wireless sensor nodes, which can be implemented by using electromagnetic, electrostatic, and piezoelectric transduction mechanisms to convert mechanical energies into electricity [17].

Another option for producing electricity sustainably from speed breakers is by using piezoelectric sensors. A vehicle weighing 1,000 kg going up a height of 10 cm on such a rumble strip produces approximately 0.98-kilowatt power [19].

Piezoelectric sensors capture the kinetic energy from speed breakers to generate electricity through renewable sources without any type of environmental effects [20]. The generated power through vibration energy harvested depends on the transducer used for the electro-mechanical energy conversion. The lifespan of the infrastructure and its optimal operation are guaranteed by routine maintenance information to assess the effectiveness and efficiency of the system in producing electricity [21].

2.2. Energy generation from Renewable energy sources

In recent years, there has been an increased focus on using renewable energy sources to meet the growing need for power while cutting carbon emissions and decreasing dependency on

fossil fuels. As the demand of fossil fuel is enormously increasing over time, the future will focus on generating power using non-renewable energy sources [19]. Energy can also be generated from Refused Derived Fuels (RDF) and Incineration.

2.2.1. Refused Derived Fuels (RDF)
Refused Derived Fuels (RDF) are the fuels produced from combustible components from industry and Municipality. It is dried, baled, and then finally burned to produce electricity [19].

2.2.2. Incineration
Incineration is the process of direct controlled burning of waste in the presence of oxygen at temperatures of about 800°C and above, liberating heat energy, gases and inert ash. Net energy yield depends upon the density and composition of the waste [19].

3. Methodology

3.1. Methodology adopted

3.1.1. Selection of a site for installing a speed breaker
For installing the sensors, appropriate places like junctions or residential neighbourhoods, where there is a lot of traffic and where there are noticeable zones for reduced vehicle speeds are selected.

3.1.2. Selection of piezoelectric sensors
The piezoelectric sensors should be selected based on information on vehicular traffic in the selected area.

3.1.3. Formation of an array of piezo-electric sensors
The piezoelectric sensors should be connected in the array for placing it inside the breakers. All the 36-volt piezoelectric sensors were connected in the array.

3.1.4. Fixation of the array inside the speed breaker
The arrays of piezoelectric sensors are fixed inside the breakers.

3.1.5. Installation of speed breaker on the selected site.
The speed breakers are then installed on the selected road.

3.1.6. Installation of a monitoring system
A monitoring system is to be installed to monitor the vehicular traffic, pressure applied by the vehicles, energy production and identify damage or problems with the sensors.

3.2. Methodology applied

3.2.1. Selection of a site for installing a speed breaker.
In the present study, the college campus was selected, as it has high vehicular traffic of an average of 2000 vehicles per day.

3.2.2. Selection of piezoelectric sensors.
After a detailed literature survey, for heavy vehicular traffic of 2000 vehicles per day, a 35mm piezoelectric cell producing a voltage of 4-6 volts is selected. Hence 35mm piezoelectric sensor cells producing a voltage of 4-6 volts are used in the present study as shown in Figure 1 and the expanded view is shown in Figure 2.

3.2.3. Formation of an array of piezo-electric sensors.
All 35mm piezoelectric sensor cells producing a voltage of 4-6 volts were connected in an array as shown in Figure 3.

3.2.4. Fixation of the array inside the speed breaker.
The prepared arrays of piezoelectric sensors were fixed inside the breakers.

3.2.5. Installation of speed breaker on the selected site.
The speed breakers were then installed on roads inside the college campus.

3.2.6. Installation of a monitoring system
A monitoring system is installed to monitor the vehicular traffic; pressure applied by the vehicles, energy production and identify damage or problems with the sensors.
The entire harnessing process is shown in Figure 4.

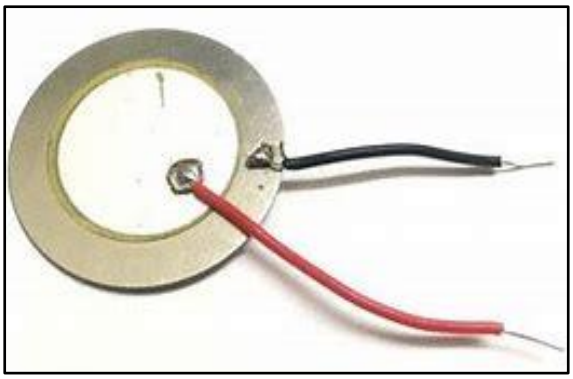


Figure 1. Piezoelectric Sensor Plate

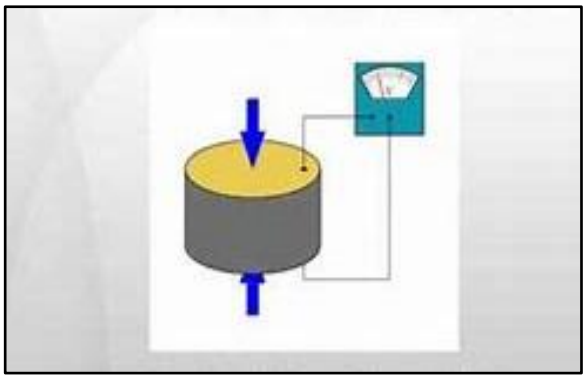


Figure 2. Expanded view of Sensor Plate

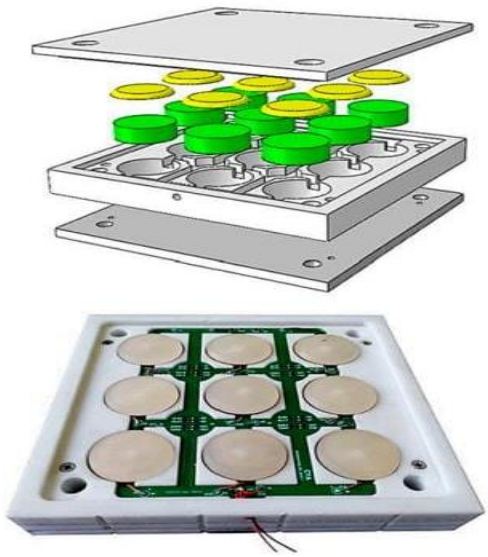


Figure 3. Arrays of piezoelectric sensors

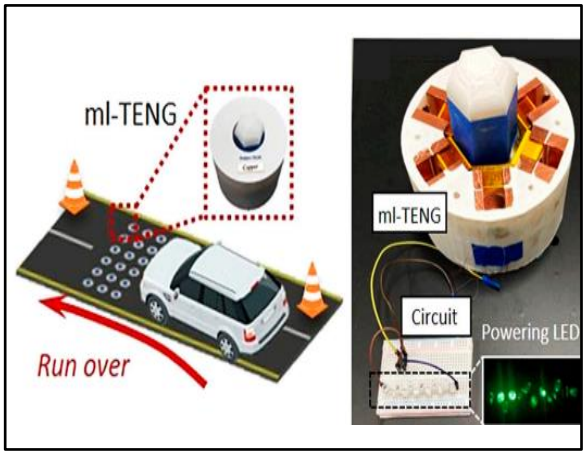


Figure 4. Harnessing process

4. Result & Discussion

The system that is installed on the college campus reports vehicle type and vehicular traffic (%) as tabulated in **Table 1** and is shown in **Figure 5.**

Table 1. Vehicle Type and Vehicular Traffic (%)

Types of Vehicles	Vehicular Traffic (%)
Two-Wheeler (Bikes)	50
Four-Wheeler (Cars)	40
Heavy Vehicles	2
Others	8

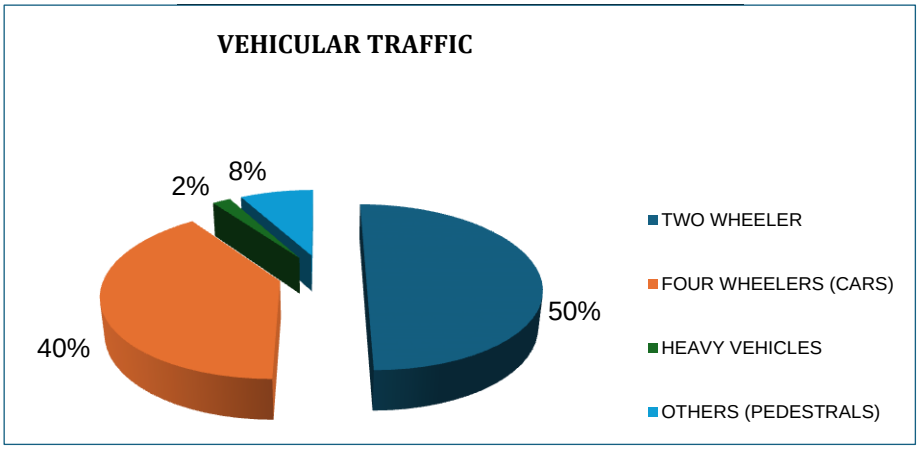


Figure 5. Vehicle type and vehicular traffic (%)

Figure 5, represents the total number of vehicles passing through a college campus. It is found that the vehicular traffic of two-wheelers is 45%, four-wheelers is 30 %, heavy vehicles is 15% and pedestrian and other is 10 %.

Table 2. Vehicle Type and Voltage Generation

Types of Vehicles	Voltage Generation (Volts/50 nos. Vehicle Pass)	Vehicular Traffic (%	Total number of vehicles passing in college campus (2000)	Total voltage generated in college campus
Two Wheelers	17	50	0. 5x2000=1000	17x1000/50=340
Four Wheelers (Cars)	104	40	0.40x2000= 800	104x800/50=1664
Heavy vehicles	>1000	2	0.02x2000=40	1000x40/50=800
Others Vehicles	2	8	0.08x2000=160	2x160/50=6.4
Total				2810.4 volts

Thus, it is seen that by using Piezoelectric Sensors 2810.4 volts can be generated daily on the college campus which can be used for enlightening about 24 street lights during the night daily.

5. Conclusions

The various conclusions drawn from the above study are as under:

- In India, the development of road transportation has changed significantly due to Pradhan Mantri Gram Sadak Yojana (PMGSY). Hence, there is a need for frequent speed breakers on the roads.
- The increasing load of vehicles on roads can be used for the generation of energy from piezoelectric sensors or vibration of moving vehicles.
- It is seen that a total of 50 passes of two-wheelers, four-wheelers, heavy vehicles, and others can generate 17, 104, 1000, and 2 volts respectively.
- Vehicular traffic for two-wheelers, four-wheelers, heavy vehicles, and others is found to be 50%, 40 %, 2%, and 8 % respectively.
- The voltage generation from 50 passes of two-wheelers, four-wheelers, heavy vehicles, and others in college campuses is found to be 340, 1664, 800, and 6.4 respectively.
- The voltage required for lighting a street light is 120 volts. The total voltage generated is 2810.4 volts. Hence 23 street lights in the college campus can be enlightening.
- The campus is 14 acres and there are many connecting roads, so constructing a speed breaker with sensors is a complicated task.
- These types of piezoelectric generators are suitable as they are more reliable and have long operating life. The illumination of street lights is done with the help of the proposed piezoelectric generator.
- The present study is carried out for a sample of one road breaker, but energy stored at one location can be utilized for local lighting only. More numbers of road breakers are required to get the advantage of energy harnessing from piezoelectric sensors.

6. References

[1] irc.gov.in.099.1988.pdf, 05.03.2024.
[2] W. Jiang, Y. Huang and A. Sha, 2018 “A review of eco-friendly functional road materials”, *Constr. Build. Mater.*, vol. 191, pp. 1082–1092.
[3] R. D. Sharma, S. Jain, K. Singh, 2011, "Growth rate of Motor Vehicles in India - Impact of Demographic and Economic Development ", *Journal of economics and social studies*, Vol. 1, no. 2. Pp. 137-153.
[4] H. Liu, J. Zhong, C. Lee, S.W. Lee, L. Lin, 2018, “A comprehensive review on piezoelectric energy harvesting technology: materials, mechanisms, and applications”, *Appl. Phys. Rev.* 5 (4), 041306.
[5] H. J. Xiang, J. J. Wang, Z. F. Shi, and Z. W. Zhang, 2013, “Corrigendum: Theoretical analysis of piezoelectric energy harvesting from traffic induced deformation of pavements,” *Smart materials structures.* 22, 095024
[6] [6]https://inhabitat.com/piezoelectric-energy-generating-roads-proposed-for-california/, 05.03.2024.
[7] J.Q. Sun, T.B. Xu, A. Yazdani, 2023, “Ultra-High Power Density Roadway Piezoelectric Energy Harvesting System”, Energy Research and Development Division, Final Project Report, Department of Mechanical Engineering, University of California.
[8] A. Harb, 2011, Energy harvesting: State-of-the-art , Renewable Energy, 36, PP. 2641–2654
[9] R. Kour, A. Charif, 2016 “Piezoelectric Roads: Energy Harvesting Method Using Piezoelectric Technology”. *Innov. Energy Res.*, *5*, 1–6.
[10] H. Sodano, D. Inman, G. Park, 2004, A Review of Power Harvesting from Vibration using Piezoelectric Materials *The Shock and Vibration Digest*, 36(3), Pp.197-205
[11] Jeffrey R. Alverto-Suazo, Julio R. Garcfa-Cabrera, 2019, Piezoelectricity: a literature review for power generation support, MATEC Web of conferences, 293(6):05004, 7th Asia Conference on Mechanical and Materials Engineering
[12] D. Kumar, P. Chaturvedi and N. Jejurikar, 2014, Piezoelectric Energy Harvester Design and Power Conditioning, IEEE Students’ Conference on Electrical, Electronics and Computer Science.

[13] J. Xiao, X. Zou, W. Xu, 2017, ePave: A Self-Powered Wireless Sensor for Smart and Autonomous Pavement. *Sensors*, 17, 10, 2207; doi:10.3390/s17102207.
[14] B. R. Sandhya, A. Unnikrishnan, A. K. Akshaya, 2018, "Energy Harvesting through Speed Breakers Using Piezoelectric materials", *International Journal of Innovative Research in Science, Engineering and Technology*, Vol 7, Issue 6, pp. 210-213.
[15] E. Lefeuvre, M. Lallart, C. Richard, D. Guyomar, 2010, "Piezoelectric Material Based Energy Harvesting Devices: Advance of SSH Optimization Techniques (1999–2009)"; *Piezoelectric Ceramics,* Intech Open: London, UK,; ISBN 978-953-307-122-0. Pp.165-185.
[16] L. Costanzo, M. Vitelli, 2020, "Tuning Techniques for Piezoelectric and Electromagnetic Vibration Energy Harvesters", *Energies*, 13, 527, https://doi.org/10.3390/en13030527.
[17] H. Qin, S. Mo, X. Jiang, S. Shang, P. Wang, Y. Liu, 2022, "Multimodal Multidirectional Piezoelectric Vibration Energy Harvester by U-Shaped Structure with Cross-Connected Beams", *Micromachines*, *13*(3), 396.
[18] R. D. Sharma, S. Jain, K. Singh, 2011,"Growth rate of motor vehicals in India", *Journal of economics and social studies*, vol.1, Issue 6,
[19] S. Srivastava, A. Asthana, 2011, "Produce electricity by the help of speed breakers," *Journal of Engineering Research and Studies*" Vol.II, issue 1, pp.163-165.
[20] Y. Sun, J. Chen, X. Li, Y. Lu, S. Zhang, Z. Cheng, Flexible piezoelectric energy harvester/sensor with high voltage output over wide temperature range, Nano Energy 61 (2019) 337-345,
[21] Y.Levron, D. Shmilovitz and S. L. Martinez, 2011, "A Power Management Strategy for Minimization of Energy Storage Reservoirs in Wireless Systems with Energy Harvesting". *IEEE Transactions on Circuits and Systems,* Regular Papers, 58, 633-643

IOP Conference Series: Earth and Environmental Science

PURPOSE-LED PUBLISHING™

PAPER • **OPEN ACCESS**

Properties and eco-cost effectiveness of concrete containing waste blast furnace slag and demolition waste

To cite this article: Rajib Kumar Majhi *et al* 2024 *IOP Conf. Ser.: Earth Environ. Sci.* **1409** 012037

View the article online for updates and enhancements.

You may also like

- Cyclic behavior of Ground Granulated Blast Furnace Slag (GGBFS) concrete beams
H Fikri, Y P Krisologus, R Permana et al.
- The effect of Ground Granulated Blast Furnace Slag (GGBFS) on Portland cement type II to compressive strength of high quality concrete
N Puspita, A I Hani'a and M Fauzi
- Mechanical Properties of Ground Granulated Blast Furnace Slag Made Concrete
Kishan Lal Jain, Lokendra Singh Rajawat and Gaurav Sancheti



This content was downloaded from IP address 47.247.77.11 on 27/11/2024 at 05:42

Properties and eco-cost effectiveness of concrete containing waste blast furnace slag and demolition waste

Rajib Kumar Majhi[1], Saine Sikta Dash[1*], Madhusmita Moharana[1], Shiv Sankar Das[2]

[1]Department of Civil Engineering, Centurion University of Technology & Management, Odisha-752050, India
[2]School of Management, Centurion University of Technology and Management, Odisha–752050, Odisha, India

*E-mail: sainesikta.dash@cutm.ac.in

Abstract. This work aims to develop eco-friendly, cost-effective concrete using ground granulated blast furnace slag (GGBFS) and recycled coarse aggregate (RCA). Seven concrete mixes are prepared with different combinations of RCA and GGBFS. Properties like 28-day compressive strength, rapid chloride permeability and abrasion resistance have been studied. Physical and microstructural investigations have been carried out to justify the variation in the properties. Moreover, environmental impact and cost-effective analyses are performed. It is found that the strength of concrete mix with 50% RCA and 45% GGBFS closely satisfies the desired strength for M25 grade concrete. Also, the mix has shown good resistance against abrasion and chloride permeability. Physical examination reveals that ITZ has played a significant role in the strength variation. Similarly, microstructural investigation reveals that the formation of voids due to RCA and the filling of the voids by GGBFS are the two phenomena responsible for variation in durability. Further, the negative environmental impacts and cost of concrete can be reduced up to 62.93% and 11.9%, respectively, compared to the control concrete using RCA and GGBFS. Since this mix provides desired strength and durability, environmental benefit and cost benefit over normal concrete, this concrete becomes eco-cost efficient**.**

Keywords: Compressive strength; Chloride permeability; abrasion resistance; Cost-effectiveness; Environmental impact; Ground granulated blast furnace slag; Recycled coarse aggregate.

1. Introduction

Nowadays, infrastructural development has significantly increased the demand for concrete usage in the construction sector. Despite concrete being a good building material, its extensive use has many negative impacts on the ecosystem. In this context, the sustainability of concrete is one of the most challenging topics and the keen interest of worldwide researchers. On the other hand, there have been issues with the solid waste accumulation and their proper disposal. For instance, the enormous generation of industrial by-products and C&D wastes has not only created land problems. Still, it is also liable for contaminating the soil, water, air and thereby human health. For minimizing these issues, use of C&D waste along with industrial by-products together in concrete production is going to be a sustainable approach. Therefore, recycled coarse aggregate (RCA) derived from C&D wastes and ground granulated blast furnace slag (GGBFS), a steel industry by-

Content from this work may be used under the terms of the Creative Commons Attribution 4.0 licence. Any further distribution of this work must maintain attribution to the author(s) and the title of the work, journal citation and DOI.
Published under licence by IOP Publishing Ltd

product, has been chosen for this study to produce sustainable concrete. RCA is a processed version of waste concrete that differs from NCA with respect to its porous nature, having two phases (mortar and aggregate) and old interfacial transition zone (ITZ). A schematic diagram of RCA is shown in Fig. 1.

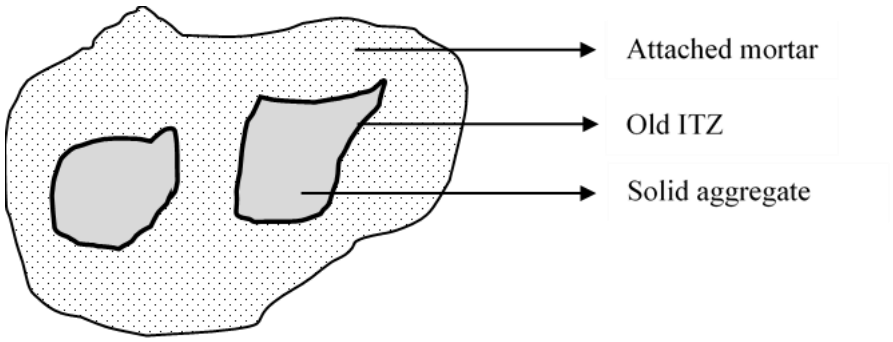


Figure 1. Schematic presentation of RCA

Previous research has revealed that RCA-incorporated concrete or recycled aggregate concrete (RAC) is inferior to natural aggregate concrete (NAC) in terms of mechanical and durability properties (Xiao et al., 2022). Similarly, GGBFS is a steel industry by-product broadly used by cement manufacturers as supplementary cementitious material (SCM). As per the literature (Siline, 2022), GGBFS possess self-hydration property, which in other terms is known as latent hydraulic property. In addition, it has certain pozzolanic properties also. As a result of which GGBFS is well known for imparting good long-term strength and durability to the concrete-based structures. As far as the application of GGBFS in RAC in concerned, a limited numbers of investigations (Ann et al., 2008; Kou et al., 2011; Cakir et al., 2014; Majhi et al., 2018; Majhi and Nayak, 2019) have been conducted to study its limited characteristics.

Most spectacularly, Majhi et al. (2018) have extensively studied the various physical, mechanical and non-destructive characteristics of RCA-GGBFS incorporated concrete (GGBFS based RAC) of different combinations. Out of sixteen different combinations of RCA and GGBFS, six mixes incorporated with high volume of RCA or both RCA and GGBFS (50% RCA & 0% GGBFS, 100% RCA & 0% GGBFS, 50% RCA & 40% GGBFS, 50% RCA & 60% GGBFS, 100% RCA & 40% GGBFS, 100% RCA & 60% GGBFS) found to satisfy the 28 days target compressive strength requirement of different grades of concrete such as M25, M20 and M15 as per IS 10262 (2009). Moreover, the use of GGBFS reduces the higher water absorption and volume of voids associated with RAC. Hence, the authors (Majhi and Nayak, 2019) have extended their earlier work (Majhi et al., 2018) to study the acid and sulphate attack characteristics of the above mentioned six concrete mixes. Lenka et al. (2021) also studied the various properties of RAC incorporated with blast furnace slag as replacement of fine aggregate. The study's findings show that these characteristics of RAC reduces with increase in GGBFS content.

On the other side, environmental impact (EI) associated with concrete is mainly dependent on the huge cement production and aggregate quarrying processes. For instance, it is evident that EI can be reduced up to 23% by using 100% RCA in concrete (Evangelista and de Brito, 2007). Besides, Marinkovic et al. (2010) have found that inclusion of 50% RCA in concrete is the optimum from cost/environment benefit point of view. However, inclusion of RCA beyond 50% can cause an increase in both cost and EI, irrespective of the advantages of using RCA. Likewise, Estanqueiro et al. (2018) have also revealed the benefits of RCA incorporated concrete in comparison with NCA incorporated concrete in context of land use and other environmental aspects. Furthermore,

Wijayasundara et al. (2018) have reported that concrete with 100% RCA can achieve 29% net cost benefit in comparison to that of NAC. On the other side related to GGBFS, it has been found that inclusion of GGBFS up to 40% in concrete can cause 22% reduction in CO2 emissions (Flower and Sanjayan, 2007). Research work of Li et al. (2016) on GGBFS based concrete reports a remarkable reduction in environmental factors like abiotic depletion & land utilisation by 73% and 42%, respectively. Likewise, Chen et al. (2019) have reported that GGBFS based concrete can save up to 9% energy and can lower the CO2 emission up to 19% in comparison with the Portland cement-based concrete. It is to mention that few studies have examined cost-effectiveness of employing GGBFS in concrete from a financial perspective. (Song et al., 2019).

From the above literature survey related to utilisation of RCA and GGBFS in concrete, it is realised that though most of the properties of GGBFS based RAC have already been investigated, there are some essential durability properties like rapid chloride permeability and abrasion resistance that need to be looked into. Moreover, the sustainability and cost effectiveness of GGBFS based RAC are yet to be established. Hence, an effort has further been extended to study the durability, environment impact and cost-effectiveness of the seven concrete mixes mentioned in the experimental programme.

2. Experimental Program

2.1. Materials

2.1.1. Binders

In the current experimental study, grade 43 OPC in compliance with IS: 269 (2015) was employed as the primary binder. In addition, locally purchased GGBFS was used as replacements of OPC. The results of the chemical analyses, physical and mechanical characteristics of OPC and GGBFS are furnished in Table 1. With respect to the chemical properties, GGBFS is having more silica and alumina content than OPC, which justifies its pozzolanic nature. Lime saturation factor (LSF) of GGBFS is also very low (0.26) as compared to OPC (0.97) due to very less CaO content, which indicates very low activity of GGBFS in comparison to OPC. Physical properties reveal that GGBFS consist of very tiny and fine particles than OPC particles that justifies its filling ability in the cement concrete composites.

2.1.2. Aggregates

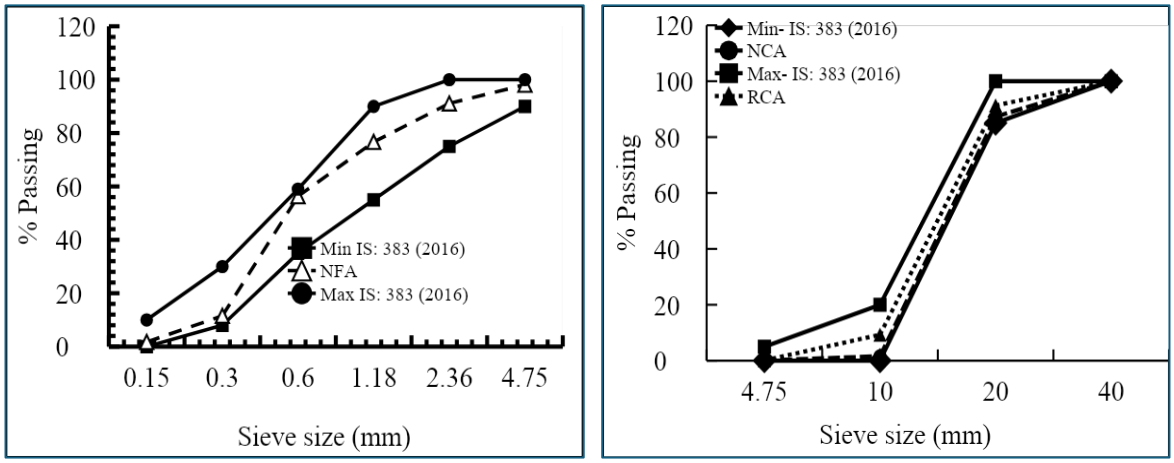
Siliceous type sand obtained from nearby river was employed as natural fine aggregate (NFA). Further, crushed 20 mm granite chips were used as NCA. For RCA, 20 mm chips prepared by crushing the demolished railway sleepers were employed. The grading curves of all aggregates shown in Fig. 2 are found to satisfy the ranges stated by IS 383 (2016). Other properties furnished in Table 2 indicate that in comparison to NCA, RCA possess lower values for specific gravity as well as higher values for moisture/absorption. Even though the strength properties of RCA are inferior to those of NCA, the values are found to be within the specified limits of IS: 383 (2016).

Table 1. Properties of binders

Chemical compounds	OPC	GGBFS
SiO2	19.55	36.58
Al2O3	5.74	16.18
Fe2O3	4.34	6.17

CaO	62.7	33.13
MgO	0.55	7.03
SO3	3.75	0.03
Na2O	0.34	0.05
K2O	0.33	0.03
Loss of ignition	1.6	0.8
Insoluble residue	0.2	-
Free CaO	0.9	-
LSF	0.97	0.26
Specific gravity	3.12	2.80
Fineness (cm2/g)	3200	5100
Consistency (%)	33	29
Initial setting time (min)	145	215
Final setting time (min)	365	465
28 days Mortar strength (MPa)	44.0	-

* Note: LSF=CaO/(2.8SiO2 + 1.2Al2O3 + 0.65Fe2O3)



(a) NFA (b) NCA & RCA

Figure. 2. Grading curves of aggregates

2.1.3. Water

The water utilized in the current experiment to make the concrete was impurity-free and complied with IS: 10500 (2012).

Table 2. Aggregates properties

Properties	NFA	RCA	NCA	IS: 383 limits
Loose density (kg/m^3)	1540	1345	1580	-
Compact density (kg/m^3)	1660	1480	1810	-
Specific gravity (No unit)	2.65	2.45	2.85	-
Absorption (%)	0.80	4.60	0.40	-

Moisture (%)	0.20	1.60	0.00	-
Fineness modulus (No unit)	3.21	6.94	7.00	
Impact strength (%)	-	21.80	15.40	45
Abrasion (%)	-	30.40	17.20	50
Crushing strength (%)	-	29.50	17.70	45
Flakiness (%)	-	25.40	28.80	35
Elongation (%)	-	22.50	27.70	35

2.2. Concrete mix proportion

Seven different concrete mixes total, each developed for M 25 grade in accordance with IS: 10262 (2019), one of which was control mix (normal concrete). Another six mixes were made by combining 0%, 45%, and 65% GGBFS as OPC replacement to each of the 50% and 100% RCA based concrete. Effective water-binder ratio (w/b) was maintained at 0.48 – 0.50. All aggregates were used in saturated surface dry (SSD) condition as per IS: 10262 (2019). So, ensure extra water was added, which was calculated based on the free moisture and water absorption of aggregates. This extra water is soaked by the dry aggregates and, hence, doesn't alter the effective w/b. At the same time the slump values of all mixes were ensured in the range 75±5 mm. Table 3 provides a summary of the specific mix proportions.

Table 3. Mix designations and mix proportions for one cubic meter of concrete for concrete mixes

Mix	%RCA	%GGBFS	Cement (kg)	NCA (kg)	RCA (kg)	NFA (kg)	GGBFS (kg)	Water (kg)	Effective w/b	Extra Water for SSD (kg)	SP (kg)	Slump (mm)
R0G0	0	0	390	1190	0	700	0	195	0.5	4.76	0	80
R50G0	50	0	390	600	548	700	0	187	0.48	29.8	3.1	75
R50G45	50	45	215	600	548	700	175	187	0.48	29.8	3.1	80
R50G65	50	65	137	600	548	700	253	187	0.48	29.8	3.1	85
R100G0	100	0	390	0	1096	700	0	187	0.48	54.8	3.1	70
R100G45	100	45	215	0	1096	700	175	187	0.48	54.8	3.1	75
R100G65	100	65	137	0	1096	700	253	187	0.48	54.8	3.1	80

2.3. Casting and curing of concrete specimens

Homogenous fresh concrete was produced for every mix by mixing the ingredients like OPC, GGBFS, fine and coarse aggregate followed by the required quantity of water in the concrete mixer. After that using a slump cone, the slump value of the freshly produced concrete was determined. Thereafter, the fresh concrete was poured in the required moulds and removed from the mould after 24 ± 1 h. After removal specimens underwent submerged water curing at a room temperature of 27±2 ^{0}C up to 28 days. After 28 days, the specimens were taken out of the curing tank and different tests were performed.

2.4. Testing methodology

2.4.1. Compressive strength

Concrete cubes of 150 mm in size were tested at 28 days using a regular compression testing machine with a 2000 kN capacity, applying a steady compressive force of 14 MPa/minute till failure as stated in IS: 516 -Part 1/Sec 1 (2021).

2.4.2. Rapid chloride permeability test (RCPT)

The rapid chloride permeability test (RCPT) was performed as per ASTM C1202 (2022) standard was used to perform on saturated specimens (circular disc specimens of 50 mm height x 100 mm diameter) aged 28 days and 90 days. Over the course of six hours, the total charge passing through the specimens was measured. In the test one end of the specimen was exposed in NaCl solution and the other end in NaOH solution and a potential difference of 60 V dc was maintained across their ends as displayed in Figure 3.



Figure 3. RCPT Test Setup

2.4.3. Abrasion resistance

In this investigation, the abrasion resistance of the concrete mixes was tested using the Bohme device (Fig. 4) as per TS EN14157 (2017). The specimens' abrasion value was determined using Bohme and Wide-Wheel abrasion equipment. In this test cubical specimen (71x71x71 mm) was given to 0.06 N/mm2 pressure on a spinning drum with abrasive added underneath the sample. The abrasion value of the sample was calculated as the % weight loss after the desired number of rotation cycles. So, the spinning drum was rotated continuously (88 rotations in one cycle) and the weight of the samples was recorded after every 4th cycle up to the 16th cycle. Finally, all the weights taken were expressed in percentage weight loss with respect to the initial weight of the specimen.



Figure 4. Abrasion resistance test set up

2.4.4. Physical and microstructural investigation

For physical examination, the concrete cube was fractured into two halves by a special arrangement in the compression testing machine using two steel bars at the top and bottom of the cube. Thereafter, the fractured surface of the cube was examined with the naked eye with respect to the pattern of failure i.e., by cleaving of aggregates or by popping out of aggregates.

Microstructural investigation was done in Scanning Electron Microscope (SEM). The small fractured pieces of concrete after its compressive strength were collected. These fractured pieces were then coated with gold coating and placed under the SEM stub and binary images were taken at different magnifications.

2.4.5. Cost effectiveness

In order to evaluate the cost effectiveness of the GGBFS based RAC mixes, the base rates of the materials including transportation charges as given in Schedule of Rates (2017) of "Works Department, Govt. of Odisha, India vide File no. 07556900012013-13827/W, dated- 16.09.2017" were considered. The base costs for ingredients like GGBFS/RCA were not mentioned in the Schedule of Rates (2017). So, in the case of GGBFS, its market price was taken as its base cost. Further, the processing and transportation charges were added and considered as base cost of RCA. Accordingly, cost of all the component materials at the destination (University Batching Plant) were computed per kilogram. Using this material cost/kg, the costs for all mixes were determined and the cost effectiveness analysis has been performed.

2.4.6. Environmental impact

The different environmental aspects considered in this study were ADP- "Abiotic depletion potential", GWP- "Global warming potential", ODP- "Ozone depletion potential", POCP- "Photochemical ozone creation potential", AP- "Acidification potential" and EP- "Eutrophication potential". Data on the effects of each component used to make 1 m3 of concrete on different environmental characteristics were gathered from the literature. Using these inventory data, the

environmental impacts were calculated for each concrete mix and compared with respect to those of the control concrete.

3. Results and discussion

3.1. Compressive strength

The variation of compressive strength of HV GGBFS based RAC mixes in contrast with normal concrete at 28 days is presented in Fig. 5. The control concrete (R0G0) has the compressive strength value 34.6 MPa at 28 days. Replacement of NCA by RCA at 50% and 100% level results in a decrease in the strength i.e., 3.5% and 12.1%, respectively as compared to R0G0. This trend of decrease in strength of RAC mixes (R50G0 and R100G0) is a very well-known phenomenon caused by the inferiority of RCA and has been witnessed in many studies (Majhi et al., 2018; Majhi and Nayak, 2019).

Further, cement replacement with HVGGBFS at 45% and 65% level to RAC mixes also results in a remarkable reduction in compressive strength. This reduction is up to 18.5% with 50% RAC and 30.1% with 100% RAC in comparison to R0G0. From the preliminary investigation with respect to the composition and properties of materials like RCA and HVGGBFS, the reason for the remarkable strength reduction is found convincing. It is to mention that GGBFS, being a low hydraulicity material with very low lime saturation factor (LSF), have very low binding capacity as compared to cement. When GGBFS is replaced with cement in a high volume i.e., HVGGBFS, there is a tremendous loss of binding capacity of the resulting binder. As a result, when the HVGGBFS based binder is used in RAC there is reduction in strength. Hence, both the lower hydraulic activity of HVGGBFS and inferiority of RCA are responsible for the remarkable strength reduction as compared to normal concrete.

Apart from the variations in the strength, it is noteworthy that some of the HVGGBFS based RAC mixes such as R50G45, R50G65 and R100G45 have achieved the strength nearly equal or greater than 26.6 MPa, which is the target strength for M20 grade concrete as per IS 10262 (2019). Similarly, the strength corresponding to R50G45 (31.4 MPa) very closely satisfies the target strength required for M25 concrete (31.6 MPa) according to the codal provision. Hence, from a compressive strength viewpoint the above-mentioned concrete mixes can be considered suitable for normal structural works.

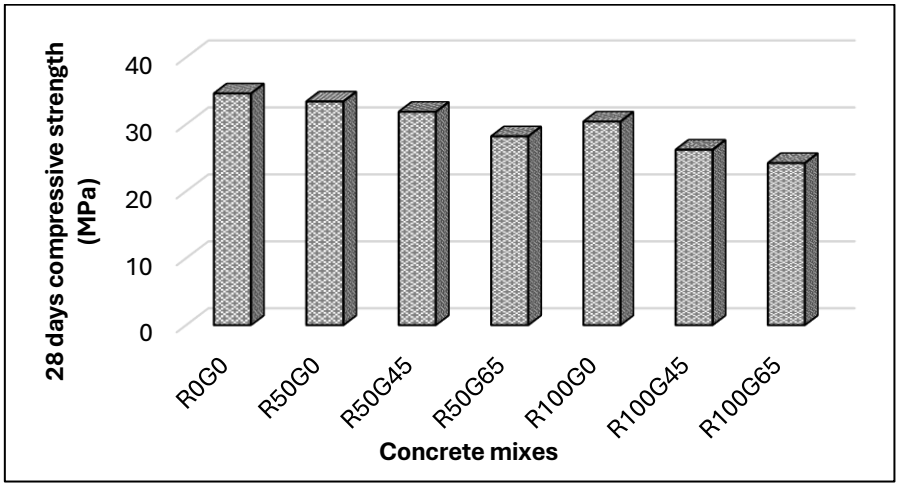


Figure 5. Compressive strength variation

3.2. Physical and Microstructural investigation

The hypothesis mentioned in the previous section in support of the strength variation of the concrete mixes due to inclusion of RCA and HVGGBFS is verified from both physical as well as microstructural investigations. For physical investigation, the concrete specimens were fractured and the failure surfaces of the respective mixes (Fig. 6) have been examined in detail. The fractured surface of R0G0 reveals that in most of the places cleaving of the coarse aggregate occurred and in certain places popping out of the aggregates is also observed (Fig. 6a). This indicates a strong mortar as compared to the strength of ITZ, due to which the failure in R0G0 specimen is a combined action of both transition zone and aggregate failure. When 45% GGBFS is incorporated with 50% RAC (R50G45), the fracture surface indicates comparatively less cleaving of aggregates than popping out of aggregates (Fig. 6b), which indicates that with replacement of 45% GGBFS there is decrease in the mortar strength causing more popping out of aggregates. Along with reduced mortar strength, the old ITZ of the RCA is also responsible for the popping out mechanism occurring in the concrete specimen. Similarly, when 65% GGBFS incorporated with 50% RCA (R50G65), it is observed that the specimen failed without clearly demonstrating aggregate cleavage, but rather aggregate popping out (Fig. 6c). This indicates weak ITZ and weak mortar due to inclusion of 65% GGBFS and 50% RCA.

A detailed investigation concerning the microstructure of the HVGGBFS paste phase is conducted to explore the hydration mechanism of the HVGGBFS-based binder. The Scanning Electron Microscope (SEM) images of the mortar paste of the HVGGBFS-based RAC mix (50% RCA) are shown in Fig. 7. The figure reveals the hydration compounds formed in both types of paste phases. According to the SEM micrograph of R0G0, i.e., control mix (Fig. 7a), CSH gel and calcium hydroxide are distributed throughout the sample and arranged well, providing the concrete a compact structure. Therefore, R0G0 has a better strength than other GGBFS-based RAC mixes. In the case of R50G45, a reduction in the formation of CSH is noticed (Fig. 7b), which is due to delayed GGBFS hydration and a decrease in OPC content. However, including GGBFS has contributed to a compact microstructure in the concrete sample.



(a) Fractured specimen of R0G0



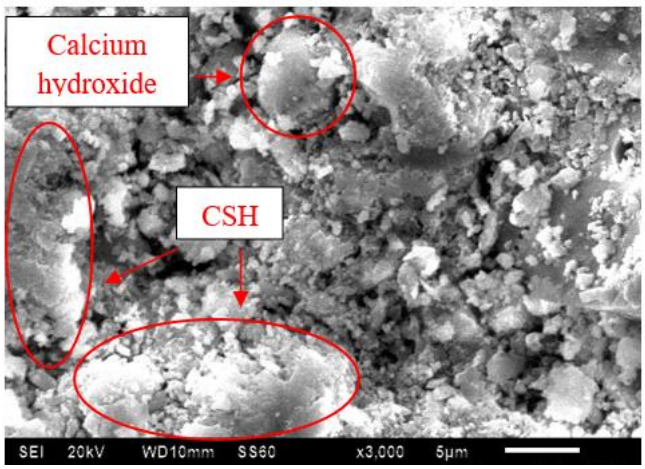
(b) Fractured specimen of R50G45



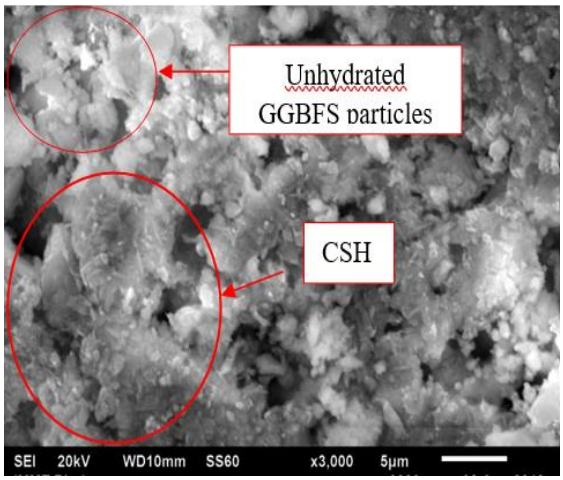
(c) Fractured specimen of R50G65

Figure 6. Photographs of the fractured surfaces of the concrete mixes

Similarly, in the case of R50G65 Figure 7 (c) does not show any formation of CSH. Un-hydrated particles of GGBFS, however, are distributed evenly throughout the sample. So, the dispersion of un-hydrated GGBFS and the nonexistence of calcium hydroxide both confirm the time-consuming pozzolanic reaction and instant filling action in the specific concrete sample of R50G65. A similar phenomenon has also been observed when 45% and 65% GGBFS are introduced to 100% RAC. So, the corresponding micrographs have not been discussed here in detail.



(a) SEM micrograph corresponding to R0G0



(b) SEM micrograph corresponding to R50G45



(c) SEM micrograph corresponding to R50G65

Figure 7. (a,b,c).SEM Micrographs (5µm scale) of R0G0, R50G45 & R50G65

3.3. Resistance to Rapid Chloride Permeability

Fig. 8 shows the variation of total charge passed (coulombs) in the rapid chloride permeability test for all the concrete mixes at a curing period of 28 days. The discussion focuses on comparing and contrasting the trends followed by the total charge passed for various combinations. The charge passed for the control mixture (R0G0) is 4628 C. With increased RCA content to 50% and 100%, the electric charge passed increases, which are found as 5473 C for R50G0 and 6284 C for R100G0, respectively. However, when HVGGBFS is incorporated into the RAC mixes in further steps, the total charge passed is found to decline at all levels of HVGGBFS, i.e., 45% and 65%. The increase/decrease in charge passed is directly related to the compactness of the matrix inside the specimen of the respective concrete mixes. For instance, the figure (Fig. 9) indicates the overall compactness through 50µm scale SEM micrographs of the concrete mixes R50G0, R50G45 and R50G65.

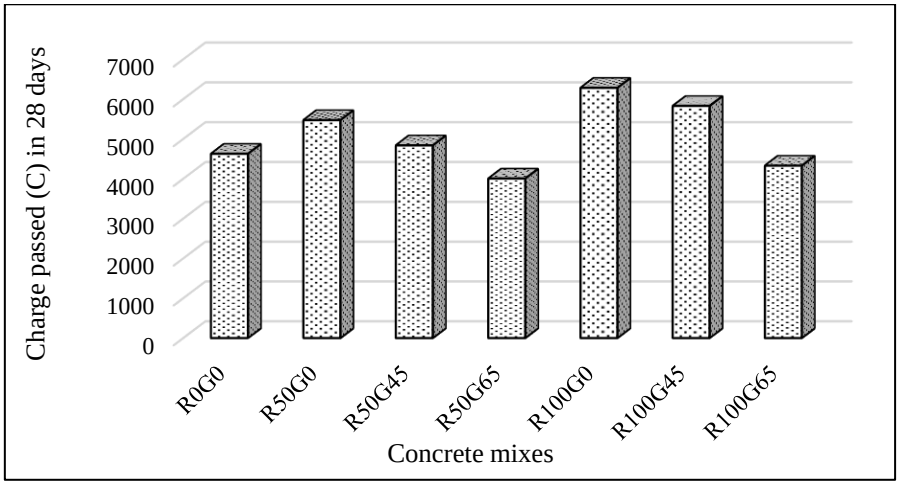
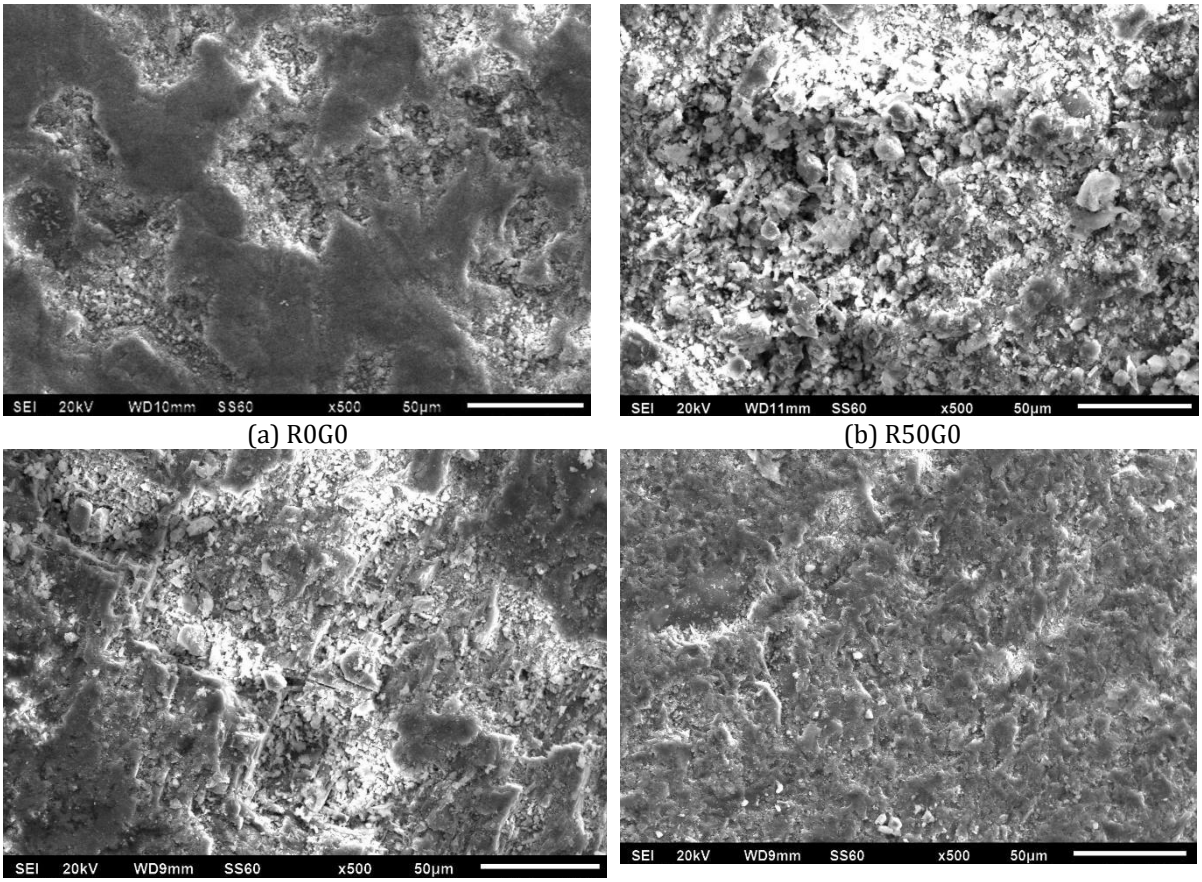


Figure 8. Variation in total charge passed



(a) R0G0 (b) R50G0

(c) R50G45 (d) R50G65

Figure 9. SEM Micrographs (50µm scale) of R0G0, R50G0, R50G45 & R50G65

The figures shown have witnessed the variation in the compactness with the inclusion of 50% RCA and further inclusion of HVGGBFS. The micrograph of R0G0 showed a dense microstructure while the same for R50G0 shows loose microstructure as compared to R0G0. However, the microstructure was found to be improved with inclusion of 45% and 65% GGBFS, which can be seen from the micrographs corresponding to R50G45 and R50G65. These changes in the dense to loosen microstructure due to addition of RCA and again loose to dense microstructure due to addition of GGBFS can be related to the chemical and physical phenomena occurring inside the matrix. When RCA is substituted, its porous microstructure is replaced with the pre-existing compact microstructure, which is a physical phenomenon. Besides, the adhered mortar of RCA contains un-hydrated cement particles, which in addition to the actual cement increases the amount of formation of calcium hydroxide in the mix and after the calcium hydroxide leaches out its occupied space becomes voids. This chemical phenomenon occurred due to RCA. Similarly, when GGBFS is substituted, the particles of GGBFS fill the voids of the RAC mix causing the increasing compactness through the physical mechanism. Besides, the calcium hydroxide formed inside the matrix has been utilized by GGBFS through pozzolanic reaction to create secondary CSH, which is a chemical phenomenon that occurred due to GGBFS addition. According to Amiri and Hatami (2022) RCA substitution in concrete increases the chloride ion migration rate. However, GGBFS mitigates the detrimental impacts of RCA by enhancing hydration products. An earlier study by Lin et al. (2021) also reported that incorporating high volume (higher than 45%) of

GGBFS in RAC can greatly reduce the chloride-ion ingress, which could be due to the contribution of the pozzolanic character of GGBFS.

Apart from the variations, the amount of charge passing through the HVGGBFS based RAC mixes like R50G45 and R50G65 are very close to that of R0G0. Hence, the interpretation of the results with the witnessed discussion concludes that the mixes, R50G45 is the most suitable mix for normal structural works in saline environments.

3.4. Abrasion Resistance

Fig. 10 displays the variances in abrasion test for all mixes at 28 days as a function of percent weight loss. As observed, % variation of weight loss shows the same increasing trends for all mixes with respect to the increase in number of cycles. The figure indicates that the % weight loss significantly increases with increase in RCA content and is drastic for mixes with 100% RCA. Previous study (Yuksel, 2007) indicates that abrasion resistance has a link with porosity and contact area between specimen & abrasive disc. It is to mention that the RCA incorporated concrete experiences more porosity as compared to the normal aggregate concrete due to the porous nature of the RCA. Since the RCA-incorporated concrete has higher porosity, it decreases the contact area, which causes rapid abrasion.

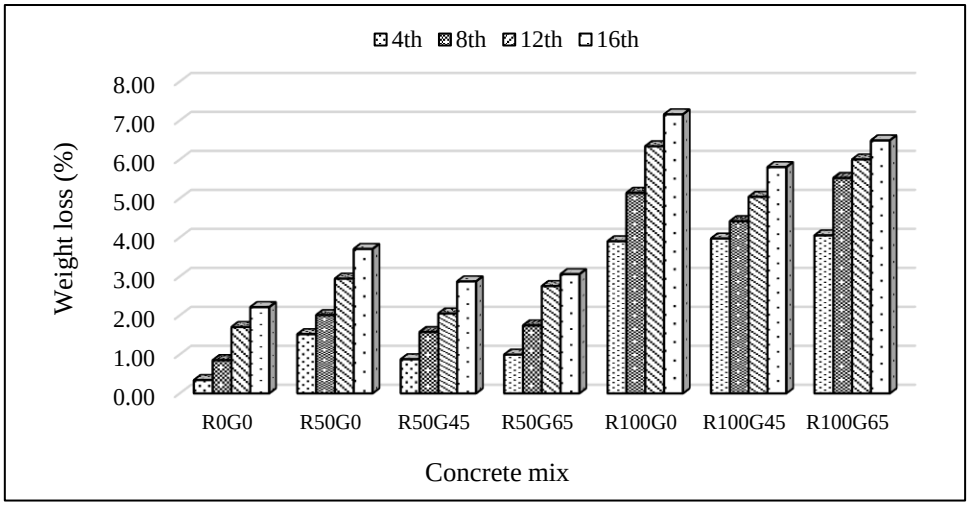


Figure 10. Variation in % weigh loss with respect the abrasion cycle

On the other hand, Fig. 10 depicts that the % weight loss of the HVGGBFS based RAC mixes (i.e., R50G45, R50G65, R100G45 and R100G65) are lower than those of the respective RAC mixes (R50G0 and R100G0). It indicates that the incorporation of GGBFS to the RAC mixes tends to decrease the extent of % weight loss caused by RCA. This is due to the reduction in porosity of the RAC mixes as tiny GGBFS particles filled up the voids. The reduction in porosity offered more contact area between concrete and the abrasive rotating disc, which minimizes the rapid abrasion. However, beyond 45% GGBFS content a small increment in the abrasion value is seen. This could be due to the loss of binding in the concrete as a high fraction of cement is replaced by GGBFS. So, even though there is a compact structure, the loss of binding causes easy segregation under the action of abrasion.

According to Shou-kai et al. (2020) in case of RCA based concrete, the abrasion resistance is optimal at 50% RCA substitution level. Similarly, as per Rashad et al. (2020), in case of GGBFS concrete, the abrasion resistance is optimal at 45%- 50% GGBFS content. It noteworthy that in the present study, HVGGBFS based RAC mixes (R50G45 and R50G65) has certainly experienced %

weight loss closer to that of the control concrete (R0G0). The abrasion value of these mixes after 16th cycle is 2.87% and 3.07%, which is very close to that of conventional concrete (2.21%).

3.5. Cost effectiveness

The cost effectiveness describes the relation between % savings in cost of one cubic meter concrete and its 28 days compressive strength. First of all, the cost of 1 cum concrete corresponding to all concrete mixes has been calculated. For this the individual materials cost including transportation charges have been calculated following the Schedule of rates (2017), Govt. of Odisha, India. The materials costs in INR are found as: OPC/ton = 6644; GGBFS/ton = 3844; NFA/m3 = 554; NCA/m3 = 1445.63; and RCA/m3 = 1917. Accordingly, the unit rate of the different materials is calculated and used for calculation of the cost of concrete. It can be noticed that the cost of RCA is higher than NCA. It actually varies directly with the transportation distance between its source and the batching plant. In this case the transportation distance of RCA is much more than NCA. The cost of different concrete mixes calculated using the base rates of the materials mentioned in the previous section is furnished Table 4.

Table 4. Cost evaluation of concrete mixes in INR

		OPC	GGBFS	NCA	RCA	NFA	Total cost
Cost/kg (INR)		6.64	3.84	0.91	1.42	0.36	
Cost of concrete mixes/cubic meter (INR)	R0G0	2590	0	1083	0	252	3925
	R50G0	2590	0	546	778	252	4166
	R50G45	1428	672	546	778	252	3676
	R50G65	910	972	546	778	252	3457
	R100G0	2590	0	0	1556	252	4398
	R100G45	1428	672	0	1556	252	3908
	R100G65	910	972	0	1556	252	3690

The cost effectiveness of HVGGBFS based RAC mixes in conjunction to their respective compressive strength is graphically shown in Fig. 11. The % cost saving of HVGGBFS based RAC with regard to normal concrete are calculated and shown in Y-axis. The corresponding compressive strength values in MPa are shown in X-axis.

From Figure 11, it is observed that while the costs of RCA based concrete mixes i.e., R50G0 and R00G0 are much higher than that of the normal mix (R0G0), their strength values are shown to be less than the normal mix. The increased base cost of RCA, as mentioned above, is the cause of the cost rise. Similar to the prior discussion, the decline in strength is brought on by the lower quality of RCA. In spite of the fact that the strength of RAC has decreased by introducing GGBFS, its cost has also decreased in contrast to that of conventional concrete. It is evident from Figure 11 that all mixes excluding R50G0 and R100G0 have shown up to 11.9% cost savings with respect to the control mix. However, it is worth mentioning that implementation of a mobile recycling plant for producing RCA can tremendously reduce the cost of HVGGBFS based RAC mixes in comparison to normal concrete. In spite of the cost variations of these concrete mixes, R50G45 closely satisfies the desired strength for M25 grade concrete and exhibits strength that is comparable with that of the conventional concrete. Because of its cost effectiveness, equivalent strength, and waste utilisation compared to the conventional concrete, the mix R50G45 is therefore considered to be sustainable concrete.

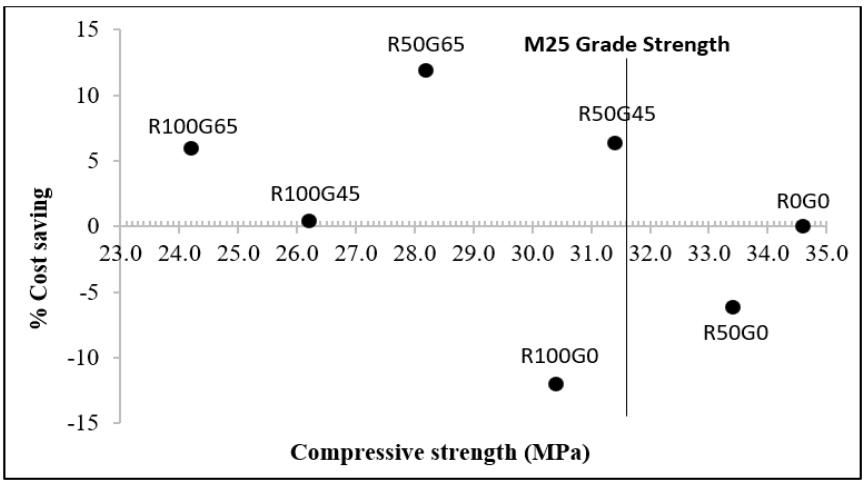


Figure 11. Cost-benefit analysis

3.6. Environmental impacts

The impact of the HVGGBFS-based RAC mixes on various environmental aspects has been calculated using the inventory data. In this study, the quantified inventory data related to the various environmental aspects have yet to be calculated. However, to realise the environmental impact of the mixes, the inventory data have been taken from the available literature (Table 5). Using the data, the percentage reduction in the impacts of the HVGGBFS-based RAC mixes in regard to normal concrete is calculated and shown in Fig. 12.

Table 5. Environmental impact data related to concrete ingredients

Material/kg	Author	ADP kg Sbeq	GWP kg CO_2eq	ODP kg CFC-11 eq	POCP kg C_2H_4eq	AP kg SO_2eq	EP kg PO_4eq
OPC	Kurda et al. (2018)	3.84×10-03	9.28×10-01	9.48×10-08	7.53×10-05	2.56×10-03	3.51×10-04
NFA	Kurda et al. (2018)	3.31×10-10	9.88×10-03	1.72×10-11	2.81×10-06	4.59×10-05	1.09×10-05
NCA	Kurda et al. (2018)	1.08×10-09	2.45×10-02	2.44×10-10	7.84×10-06	1.45×10-04	3.19×10-05
RCA	Park et al. (2019)	1.61×10-05	2.95×10-02	4.69×10-10	1.26×10-05	2.94×10-05	5.45×10-06
GGBFS	Kim et al. (2016)	4.56×10-05	5.20×10-02	1.14×10-8	1.30×10-05	1.73×10-04	6.39×10-05
Water	Kurda et al. (2018)	1.58×10-11	1.34×10-04	5.94×10-12	4.98×10-08	3.88×10-08	9.71×10-07

First of all, it is evident from Fig. 12 that, with the exception of the concrete mixes R50G0 and R100G0, the impact of the other four mixes is significantly lower than that of R0G0 in terms of all environmental factors. The ADP, GWP, ODP, and POCP for R50G0 and R100G0 are found to be higher than those for R0G0. It is important to note that the remaining four concrete mixes show ADP, GWP, ODP, and POCP values that are lower than those of the conventional concrete by 16.26 to 62.93%. So, it is noticeable that the concrete containing only RCA, but without GGBFS have exhibited inferior performances in terms of ADP, GWP, ODP, and POCP. Hazardous gas emissions during the production and shipment of RCA could be the cause for this degraded performance.

Nevertheless, despite the negative consequences of RCA, concrete mixes with GGBFS have shown a considerable reduction in ADP, GWP, ODP, and POCP. This is owing to the fact that compared to RCA manufacture, the increase in ADP, GWP, ODP, and POCP, is greater in the case of OPC manufacturing due to the air being contaminated by CO_2, CO, NO_2, etc.

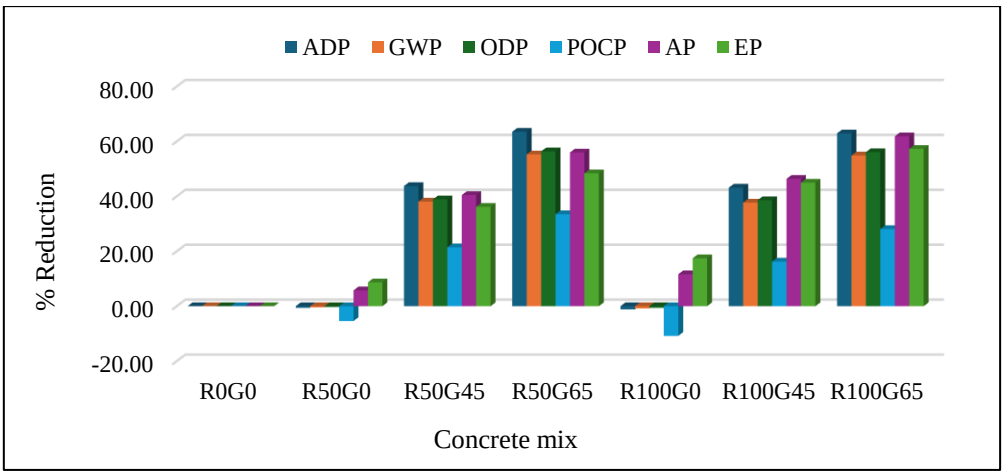


Figure 12. Reduction in EIs of mixes with respect to R0G0

The decreases in AP and EP in all mixes, however, are lower than those for the conventional concrete. This is due to the fact that AP and EP referred to the ecosystems' polluted state, in which excessive soil and water fertilisation has resulted in a rise in biomass growth, that is primarily brought on by the excessive accumulation of solid waste produced during the cement/aggregate production. Therefore, the better performance regarding AP and EP can be attributed mostly by utilising both RCA and GGBFS in concrete.

As it can be seen from the discussion, the environmental impact of concrete incorporated with high volumes of RCA and GGBFS can be greatly reduced. These mixes preserve the ecological balance and environmental soundness while conserving an equivalent number of natural resources. Additionally, a significant amount of solid waste is used in creating these concrete mixes, which helps to address the issue of waste disposal.

4. Conclusions

- The 28-day compressive strength of concrete decreases with an increase in both RCA and GGBFS contents. In spite of this trend, it is noteworthy that some of the HVGGBFS-based RAC mix, such as R50G45, R50G65, and R100G45, have achieved a strength nearly equal to or greater than 26.6 MPa, which is the target strength for M20 grade concrete as per IS 10262 (2019). Similarly, the strength of R50G45 (31.4 MPa) very closely satisfies the target strength required for M25 grade concrete (31.6 MPa) as per the codal provision. Hence, from a compressive strength point of view, the concrete mixes can be considered suitable for normal structural works.
- The physical examination concludes that the HVGGBFS-based RAC specimens failed mostly due to popping out of aggregates from the mortar bond. This indicates the existence of poor bonding and weak ITZ in the matrix. Similarly, the microstructural (SEM) investigation reveals that an increase in RCA content increases the surplus calcium hydroxide that is liable

for the formation of voids inside the concrete. However, the inclusion of GGBFS has minimised the voids and increased the compactness of the HVGGBFS-based RAC mixes.

- RCPT results reveal that the total charge passed through the concrete increases with an increase in RCA, while it reduces with HVGGBFS. This is justified by the microstructural investigation that RCA creates voids in the concrete, but GGBFS fills the voids. In spite, the charge passes through the HVGGBFS-based RAC mixes like R50G45 and R50G65 are very close to that of R0G0. Hence, the interpretation of the results with the witnessed discussion concludes that the mix R50G45 is the most suitable for normal structural works in saline environments.
- Abrasion value is triggered with RCA inclusion due to decreases in the contact area of the concrete with the abrasive rotating disc. Contrarily, incorporating GGBFS up to 45% to the RAC mixes tends to decrease the extent of abrasion caused by RCA due to an increase in the contact area. However, beyond 45% GGBFS content, a small increment in the abrasionvalue is seen, which could be due to the loss of binding in the concrete as a high fraction of cement is replaced by GGBFS. Despite this, concrete mixes with 50% RCA and GGBFS (R50G45 and R50G65) have certainly experienced abrasion closer to that of the control concrete (R0G0).
- The use of RCA increases the cost of concrete. However, using GGBFS results in lower costs. As a result, the high-volume RCA and GGBFS-containing concrete mixes outperform the control mix in cost.
- Incorporating RCA has less of a favourable impact on AP and EP and more of a negative impact on ADP, GWP, ODP, and POCP. However, the usage of GGBFS has demonstrated remarkable EI minimisation in all respects. As a result, using high-volume RCA and GGBFS together in concrete significantly reduces EI in all ways.

References

[1] Amiri, M., &Hatami, F. 2022 Prediction of mechanical and durability characteristics of concrete including slag and recycled aggregate concrete with artificial neural networks (ANNs) *Construction and Building Materials* **325** 126839
[2] ASTM C1202, 2022 Standard Test Method for Electrical Indication of Concrete's Ability to Resist Chloride Ion Penetration American Standard for Testing of Materials Farmington Hills USA
[3] Çakır, Ö., 2014 Experimental analysis of properties of recycled coarse aggregate (RCA) concrete with mineral additives *Construction and Building Materials* **68** 17–25
[4] Chen, X., Wang, H., Najm, H., Venkiteela, G., Hencken, J., 2019 Evaluating engineering properties and environmental impact of pervious concrete with fly ash and slag *Journal of Cleaner Production* **237** 117714
[5] Estanqueiro, B., Dinis Silvestre, J., de Brito, J., Duarte Pinheiro, M., 2018 Environmental life cycle assessment of coarse natural and recycled aggregates for concrete *European Journal of Environmental and Civil engineering* **22** 429–449
[6] Evangelista, L., de Brito, J., 2007 Mechanical behavior of concrete made with fine recycled concrete aggregates *Cement Concrete Composite* **29** 397–401
[7] Flower, D.J.M., Sanjayan, J.G., 2007 Greenhouse gas emissions due to concrete manufacture. International Journal of Life Cycle Assessment **12**, 282
[8] IS 516 (Part 1/Sec 1), 2021 Indian Standard Hardened Concrete —Methods of Test, Part 1 Testing of Strength of Hardened Concrete, Section 1 Compressive, Flexural and Split Tensile Strength, *Bureau of Indian Standards* New Delhi
[9] IS: 10262, 2009 Indian Standard Concrete Mix Proportioning – Guidelines *Bureau of Indian Standards* New Delhi
[10] IS: 10262, 2019 Indian Standard Concrete Mix Proportioning — Guidelines *Bureau of Indian Standards* New Delhi
[11] IS: 10500, 2012 Indian Standard, Drinking Water – Specification Bureau *of Indian Standards* New Delhi
[12] IS: 269, 2015 Indian Standard Ordinary Portland cement – Specification *Bureau of Indian Standards* New Delhi

[13] IS: 383, 2016 Indian Standard Specification for coarse and fine aggregate from natural sources *Bureau of Indian Standards* New Delhi
[14] K.Y. Ann, H.Y. Moon, Y.B. Kim, J. Ryou, 2008 Durability of recycled aggregate concrete using pozzolanic materials Waste management **28** 993–999
[15] Kim, T., Tae, S., Chae, C., Choi, W., 2016 The environmental impact and cost analysis of concrete mixing blast furnace slag containing titanium gypsum and sludge in South Korea *Sustainability* **8** 502
[16] Kurda, R., Silvestre, J.D., de Brito, J., 2018 Toxicity and environmental and economic performance of fly ash and recycled concrete aggregates use in concrete: A review *Heliyon* **4**, e00611
[17] Lenka, B. P., Majhi, R. K., Singh, S., &Nayak, A. N. 2021 Eco-friendly and cost-effective concrete utilizing high-volume blast furnace slag and demolition waste with lime *European Journal of Environmental and Civil Engineering* 1–23
[18] Li, Y., Liu, Y., Gong, X., Nie, Z., Cui, S., Wang, Z., Chen, W., 2016 Environmental impact analysis of blast furnace slag applied to ordinary Portland cement production *Journal of Cleaner Production* **120** 221–230
[19] Lin, S. K., & Wu, C. H. 2021 Improvement of Bond Strength and Durability of Recycled Aggregate Concrete Incorporating High Volume Blast Furnace Slag *Materials* 14**(13)** 3708
[20] Majhi, R.K., Nayak, A.N., 2019 Bond, durability and microstructural characteristics of ground granulated blast furnace slag based recycled aggregate concrete *Construction and Building Materials* **212** 578–595
[21] Majhi, R.K., Nayak, A.N., Mukharjee, B.B., 2018 Development of sustainable concrete using recycled coarse aggregate and ground granulated blast furnace slag *Construction and Building Materials.* **159** 417–430
[22] Marinković, S., Radonjanin, V., Malešev, M., Ignjatović, I., 2010 Comparative environmental assessment of natural and recycled aggregate concrete Waste management 30 2255–2264
[23] Park, W.-J., Kim, T., Roh, S., Kim, R., 2019 Analysis of life cycle environmental impact of recycled aggregate *Applied Science* **9**, 1021
[24] Rashad, A. M., &Sadek, D. M. 2020 Influence of different particle sizes of blast-furnace slag as a fine aggregate on concrete's mechanical strength and abrasion resistance *Silicon* **12(10)**, 2365-2373
[25] S. Kou, C. Poon, F. Agrela, 2011 Comparisons of natural and recycled aggregate concretes prepared with the addition of different mineral admixtures *Cement Concrete Composite* **33** 788–795
[26] Schedule of Rates 2017 of *Works Department, Govt. of Odisha, India* File no. 07556900012013-13827/W, dated-16.09.2017
[27] Shou-kai, C. H. E. N., Zheng-nan, Z. H. A. N. G., Yong-jie, Z. H. E. N. G., Lei, G. U. O., &Lun-yan, W. A. N. G. 2020 Experimental Study on Impact-abrasion Resistance of Recycled Aggregate Pervious Concrete Journal *of Yangtze River Scientific Research Institute* 37**(7)** 153
[28] Siline, M. 2022 Efficiency of incorporating Algerian ground granulated blast furnace slag as a supplementary cementitious material: a review *Innovative Infrastructure Solutions* **7(1)** 1-12
[29] Song, W., Yi, J., Wu, H., He, X., Song, Q., Yin, J., 2019 Effect of carbon fiber on mechanical properties and dimensional stability of concrete incorporated with granulated-blast furnace slag Journal *of Cleaner Production* 238 117819
[30] TS EN14157, 2017 Natural stone: Determination of the abrasion resistance *Turkish Standards Institution*
[31] Wijayasundara, M., Mendis, P., Crawford, R.H., 2018 Net incremental indirect external benefit of manufacturing recycled aggregate concrete *Waste Management* **78** 279–291
[32] Xiao, J., Poon, C. S., Wang, Y., Zhao, Y., Ding, T., Geng, Y. & Li, L. 2022 Fundamental behaviour of recycled aggregate concrete–Overview I: strength and deformation *Magazine of Concrete Research* 1-12
[33] Yuksel I, Bilir T, Ozkan O 2007 Durability of concrete incorporating non-ground blast furnace slag and bottom ash as fine aggregate Building and Environment **42**(7) 2651–2659

Acknowledgement

The authors acknowledge the Indian and Institute of Minerals and Materials Technology, Bhubaneswar, Odisha for providing the necessary laboratory facilities for conducting the Microstructural investigations.

IOP Conference Series: Earth and Environmental Science

PURPOSE-LED PUBLISHING™

PAPER • **OPEN ACCESS**

Utilization of e-waste as a partial replacement of coarse aggregate in concrete

To cite this article: Pawan Hinge *et al* 2024 *IOP Conf. Ser.: Earth Environ. Sci.* **1409** 012038

View the article online for updates and enhancements.

You may also like

- Awareness of Reuse Reduce Recycle & Dispose of E-Waste in Chennai
R Ganesan, B Ramesh and Charan Teja
- An Integrated and Sustainable Model for E-Waste Management for Pune City Households
Viraja Bhat and Yogesh Patil
- Current status of household e-waste management in Jakarta, Indonesia
H Soesanto, M S Maarif, S Anwar et al.



This content was downloaded from IP address 47.247.77.11 on 27/11/2024 at 05:42

Utilization of e-waste as a partial replacement of coarse aggregate in concrete

Pawan Hinge[1], Keshar Thakur[1], Rutuja Humane[1], Vibhati Tikle[1*], Aditya Shrirame[1], Suraj Chafle[1], Umesh Dharammali[1] and Rohan Rathod[1]

[1]Department of Civil Engineering, Yeshwantrao Chavan College of Engineering, Nagpur, 441110. Maharashtra, India

*Email: vibhatiofficial24@gmail.com

Abstract. One of the fastest waste streams to generate and amass is electronic garbage, or "E-waste," which is growing exponentially. This is a result of the development and expansion of other technical sectors as well as the information technology industry. In many places, improper handling such as open burning of e-waste and uncontrolled landfill disposal accelerates the release of greenhouse gases (GHG) into the sky, which is a direct cause of global warming. It presents serious worldwide environmental challenges. There is a thirty percent increase in the production of electronic waste, or "E-waste". 90% of e-waste is collected and 70% is recycled in India, where the informal sector handles the majority of E-waste management. Important steps must be taken for the treatment of E-waste to decrease the volume of waste and reuse it for other purposes. This paper gives a review of how the repurposed E-waste used as a partial replacement in concrete affects the various properties of concrete.

Keywords. E-waste, Concrete, Greenhouse gases, Global warming

1. Introduction

E-waste is being produced on a massive scale these days due to the rapid growth and development of the information and technology sector, as well as its advancements. This is due to the interconnectedness and relevance of all technical sectors, as well as their combined growth, even in the absence of recycling and a decrease in the amount of electronic trash produced.

A variety of materials, including chips, motherboard components, fuses, circuits, plastics, printed circuit boards (PCBs), and other hard-core components, can be found in e-waste. When e-waste is disposed of to the environment, poisonous and dangerous compounds and metals including lead (Pb), cadmium (Cd), mercury (Hg), and nickel (Ni) leak out into subterranean water bodies and contaminate the soil and water. This ultimately has detrimental, deadly health effects. Concrete trash generation is a problem as well as the generation of E-waste. several concrete buildings that are revealed annually. Furthermore, it is primarily run by the cutthroat unorganized sector. This unofficial industry salvages outdated electronics for replacement parts and makes profitable repairs. As per the research presented by the India Cellular & Electronics Association (ICEA), 90% of e-waste collection and 70% of recycling in India takes place in the informal sector. Furthermore, the improper disposal of e-waste exposes people to direct exposure, which deteriorates both the global ecology and climate. Inappropriate treatment, such as open burning

Content from this work may be used under the terms of the Creative Commons Attribution 4.0 licence. Any further distribution of this work must maintain attribution to the author(s) and the title of the work, journal citation and DOI.
Published under licence by IOP Publishing Ltd

of e-waste and uncontrolled landfill disposal, accelerates the release of greenhouse gases (GHG) into the atmosphere in many places, which directly contributes to global warming and has an impact on environmental creatures. Cut down on the production of e-waste by practicing wise maintenance and procurement. Donate the working electrical equipment to someone else or reuse it yourself.

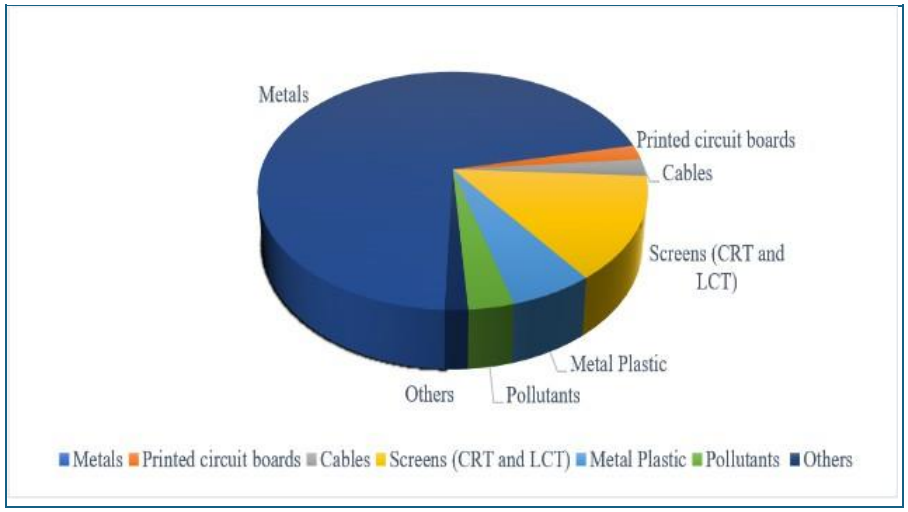


Figure 1. Composition of materials in E-waste

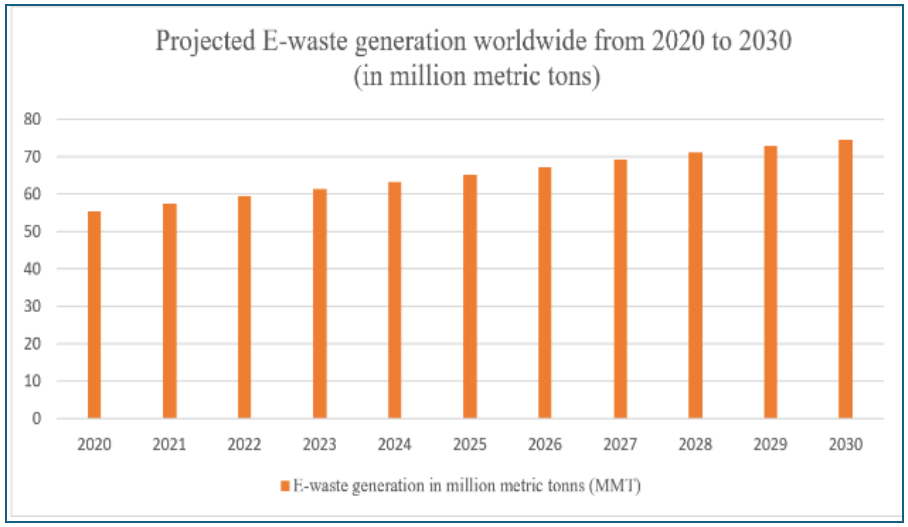


Figure 2. E-waste generation

The parts that are beyond repair should be recycled. As a long-term strategy to lessen the massive production of E-waste, the 3Rs are the best pre-disposal and minimal trash-generating techniques. This document provides information on the use of E-waste in concrete as a partial substitute for coarse aggregate with a size of 10 mm. This is done to improve strength and durability because coarse aggregate and e-waste have similar qualities. lowers the heat of hydration and lessens bleeding and segregation as well. The replacement is carried out as 5%, 10%, 15%, and 20% by volume in this paper. Casts included specimens for compression, tensile, and flexural stresses, such as cubes. Specimens are put through a variety of tests to determine their strengths. We saw sufficient strengths at 15% replacement in this project.

1.1. Components of E-wastes

The components of e-waste used are chips, motherboards, and hard plastic components like keyboards and mice.

1.2. Advantages of using E-waste in concrete

- Utilizing e-waste in concrete offers a sustainable solution for managing e-waste, diverting it from landfills, and reducing the environmental impact related to disposal.
- This material is chemically resistant and lighter in weight than regular materials.
- E-waste comes in various sizes and compositions, allowing for customized concrete mix designs to optimize pozzolanic properties based on specific requirements.

2. Development of sustainable construction using e-waste concrete

2.1. Methodology

The e-waste was collected from the local e-waste recycling plant and was converted into coarse aggregates by separating and crushing. After crushing, 10 mm size e-waste aggregates are used for replacement. High-quality OPC 53-grade cement was used. Initial tests were performed on the collected raw materials and e-waste to assess the physical properties. The concrete mix design of M45 grade was prepared as per IS 10262-2019. The largest acceptable diameter for coarse aggregate is 20 mm. The highest permitted water-cement ratio is 0.255. Cement has a specific gravity of 3.15, while coarse aggregate has a specific gravity of 2.79. Additionally, fine aggregate has a specific gravity of 2.67, and E-waste has a specific gravity of 2.11. By using this data different mix designs were prepared for control mix and 5%, 10%, 15% & 20% replacement of 10mm size coarse aggregate by E-waste. The slump cone test was performed to check the workability of the concrete. Coarse aggregates were replaced by various percentages by volume of e-waste.

The casting is done in different shapes as cubes, cylinders, and beams. Destructive tests such as Compressive, Flexural, and split tensile strength tests are performed on 7 days, 14 days, and 28 days cured specimens. Non–non-destructive test “Rebound Hammer” performed for 28 days cured specimens. Acid attack test performed for 28 days cured cubes. For Acid attack tests on concrete specimens, HCl acid is used as 2% by volume.

2.2. Material used

2.2.1. Cement

Cement is a primary binding agent in concrete, it is responsible for holding the mixture together. When water is added to cement, it triggers a chemical reaction known as hydration. This process forms a paste that coats the surface of the aggregates, gradually hardening to create a strong and durable material. Ordinary Portland Cement, conforming to specifications for 53 grade OPC (ordinary Portland cement) as per IS 12269-2013 was used in this study.

2.2.2. Water

Water plays a crucial role in concrete by initiating the hydration process of cement. It is essential for forming the cement paste that binds the aggregates together and contributes to concrete's workability. Normal tap water and consumable water were utilized in this research.

2.2.3. Aggregates

Aggregates are inert filler materials comprising coarse and fine aggregates. Coarse aggregates provide strength and stability to the concrete mix, while fine aggregates, such as sand, fill the spaces between larger particles and improve workability. Well-graded aggregates with a variety

of sizes and shapes optimize particle packing and interlocking, resulting in denser and stronger concrete. Natural sand typically passes through a 4.75 mm filter to include fine particles, whereas nominally sized coarse aggregates are kept in 10 mm and 20 mm sieves.

2.2.4. E-waste

The e-waste is used as a partial replacement for 10mm size coarse aggregate in the forms of motherboard chips, hardcore keyboard plastic, PVC plastic, etc. The e-waste was collected from an e-waste recycler.

2.2.5. Admixtures

Admixtures are specialty chemicals added to concrete mixes to modify the fresh or hardened properties. They offer a range of benefits, including improved workability, enhanced durability, and water-cement ratio. Polycarboxylate ether base (Admixture) was used in this research.

3. Results and comparison

3.1. Physical Properties

3.1.1. Cement

The cement has a 97% fineness, 2 mm soundness, 32% consistency, 75 minutes initial setting time, and 450 minutes final setting time, making it reliable for general construction due to its high grinding level, minimal expansion, and long-term stability.

3.1.2. E-waste

E-waste, with a specific gravity of 2.11, is lightweight and resistant to impact and wear and tear, making it suitable for construction applications. Its impact value of 4% and abrasion value of 5.98 demonstrate its durability and toughness, making it a suitable alternative to traditional aggregates.

3.1.3. Aggregates

Sand, with a specific gravity of 2.67, is a fine aggregate with a density of 2.79, its bulking percentage of 42% indicates a significant volume increase due to moisture content, crucial for concrete mixes, while coarse aggregate has a higher specific gravity of 2.79.

3.2. Workability of concrete

To find out the workability of the concrete Slump cone test is performed on freshly prepared concrete. The increase in the percentage replacement of e-waste in concrete results in a decrease of the workability of the concrete. Concrete with the right workability ensures that it can be properly placed and compacted without bleeding and segregation. This test helps in determining the amount of water needed for proper workability.

Table 1. Compression strength test

Types of cubes	Compressive Strength (7 days)		Compressive Strength (14 days)		Compressive Strength (28 days)	
	N/mm^2	Average	N/mm^2	Average	N/mm^2	Average
Control mix	29.33 33.33 36.44	33.03	43.11 36.00 48.44	42.52	47.11 49.33 48.00	48.15
5% replacement	37.78 32.89 35.56	35.41	40.44 36.89 43.56	40.30	48.00 53.33 53.33	51.55

	34.67		40.00		47.22	
10% replacement	35.11	33.78	39.11	39.56	48.44	48.18
	31.56		39.56		48.89	
	33.33		42.22		46.22	
15% replacement	34.22	33.92	39.55	38.51	47.56	46.85
	34.22		33.77		46.78	
	28.00		34.67		42.55	
20% replacement	28.44	28.29	36.80	35.66	42.23	42.22
	28.44		35.50		41.78	

3.3. Compressive strength test

Cube specimens of 150 x 150 x 150 mm size were produced to measure the compressive strength. following 7, 14, and 28 days of curing following surface drying, the compressive strength of specimens is assessed.

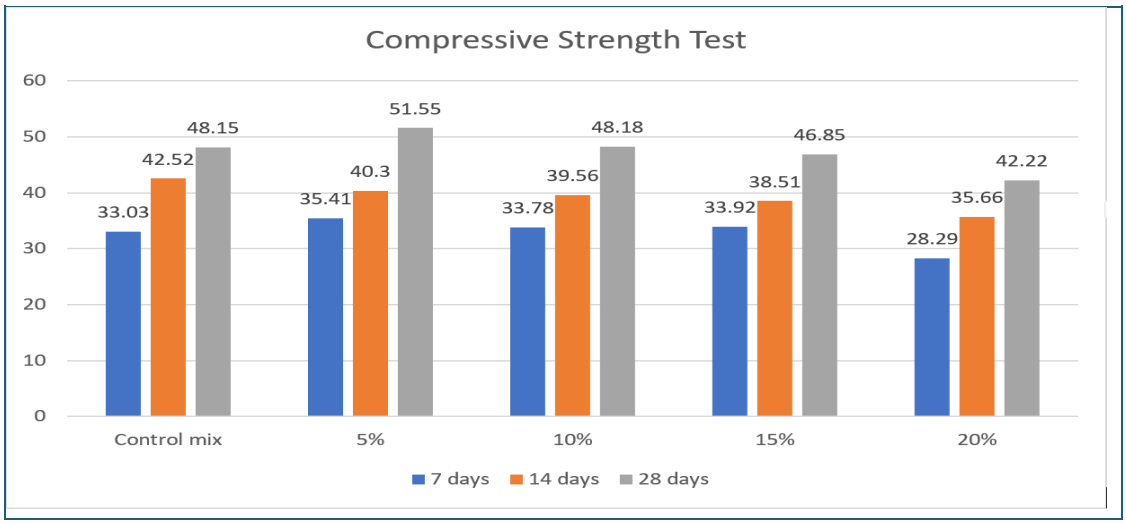


Figure 3. Compressive strength comparison

3.4. Flexural strength test

To determine the Flexural strength, 500×100×100mm beam specimens were cast. After the concrete specimens have been surface dried and allowable to cure for 28 days, their flexural strength is measured.

Table 2. Flexural strength test

Types of beams	Flexural Strength N/mm²	Average(N/mm²)
	7.0	
Control mix	9.0	8.73
	10.20	
	9.20	
5% replacement	5.20	7.20
	7.20	
	7.20	
10% replacement	6.0	6.73
	7.0	
	7.60	
15% replacement	8.0	8.53
	10.0	
20% replacement	3.0	2.33

2.0
2.0

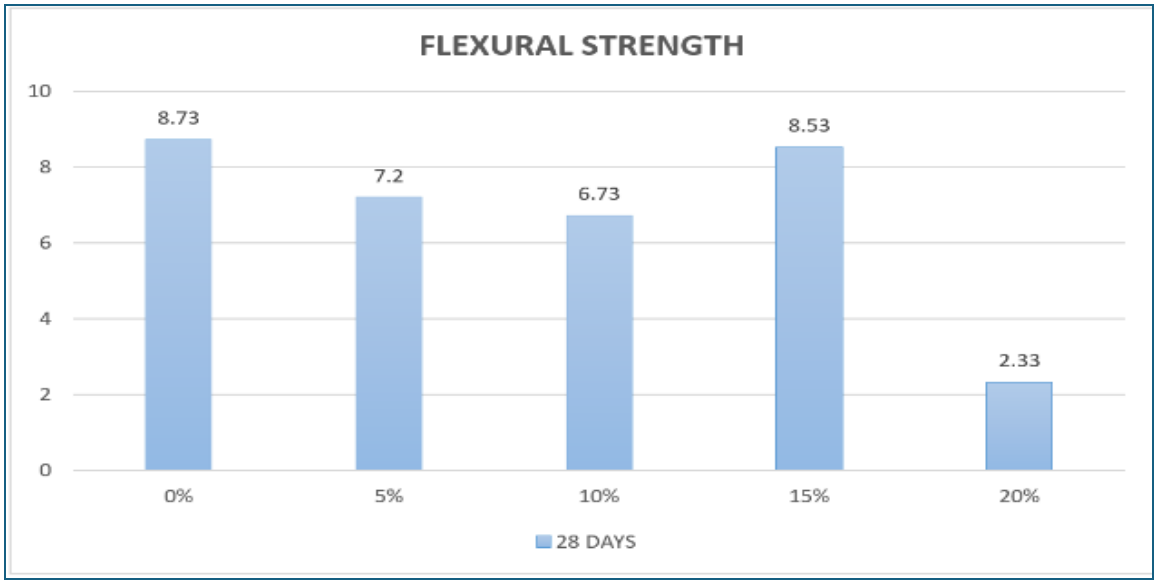


Figure 4. Flexural Strength test comparison

3.5. Split tensile test

Cylinder specimens of 150 mm in diameter and 300 mm in height were cast to measure the split tensile strength. After surface drying for 28 days, the tensile strength of specimens is measured.

Table 3. Split tensile test

Types of cylinders	Tensile Strength	
	N/mm^2	Average (N/mm^2)
Control mix	3.96	3.30
	3.11	
	2.89	
5% replacement	2.97	3.39
	3.67	
	3.56	
10% replacement	4.12	3.96
	3.67	
	4.10	
15% replacement	3.53	4.0
	3.96	
	4.52	
20% replacement	2.82	2.28
	1.76	
	2.26	

3.6. Water absorption test

The water absorption test is performed to c the amount of water absorbed by the concrete specimen under controlled conditions. The specimens were cured for a total of 28 days, after being dried condition, weighed, and again cured for 28 days. This way it shows the actual water absorption after gaining maximum strength after 28 days.

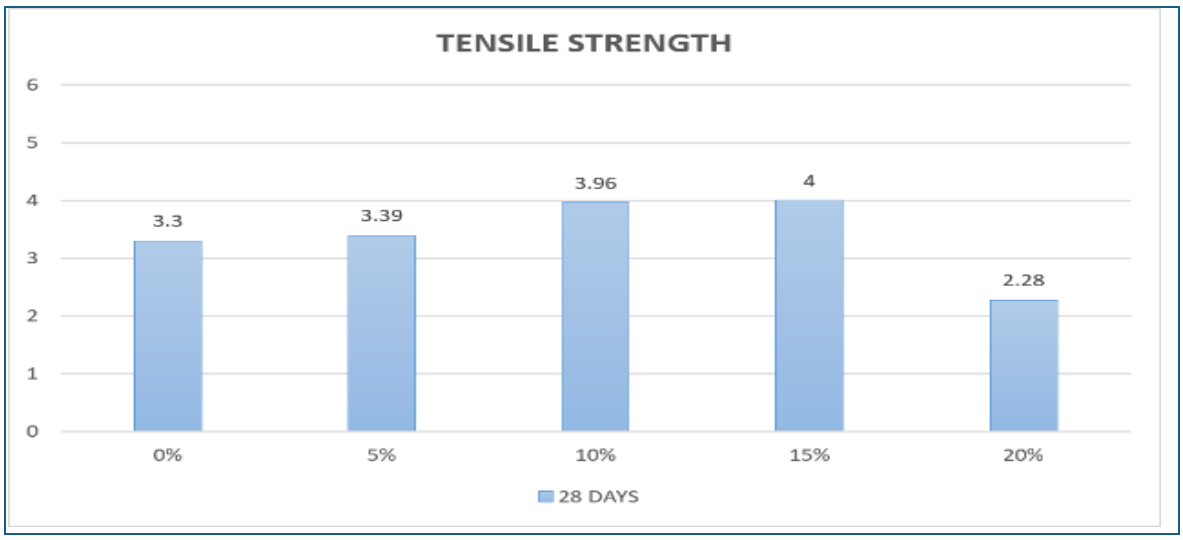


Figure 5. Tensile strength comparison

Table 4. Water absorption test

Mix Designation	Weight of cubes (Kg)		Water absorbed. (%)
	Dry weight	After 28 days of curing	
Control Mix	8.58	8.68	1.13
5% replacement	8.68	8.70	1.2
10% replacement	8.79	8.91	1.3
15% replacement	8.56	8.68	1.4
20% replacement	8.50	8.64	1.6

3.7. Acid attack test

The purpose of conducting an acid attack test on concrete is to assess its resistance to deterioration when exposed to an acidic environment. This helps to determine the suitability of concrete for structures in industries or locations where acid exposure is expected, ensuring durability and safety over time. Acid attack test performed for 28 days cured specimens. For the Acid attack test on concrete specimens, HCl acid is used only 2% by volume.

Table 5. Acid attack test

Mix Designation	Compressive Strength of cubes after acid attack (N/mm^2)	Average Compressive Strength (N/mm^2)
Control Mix	46.33 45.27 47.92	46.51
5% replacement	45.17 43.79 45.32	44.76

	44.72	
10% replacement	43.22	43.61
	42.90	
	42.12	
15% replacement	41.33	41.23
	40.22	
	39.72	
20% replacement	41.13	39.86
	38.73	

3.8. Rebound Hammer test.

An alternative name for the rebound hammer is the Schmidt hammer. The compressive strength can be fast and simply determined using the rebound hammer test, an NDT (non-destructive) method of testing.

Understanding the compressive strength is facilitated by the Rebound Hammer Test. In general, a concrete structure with a higher rebound value is stronger and longer-lasting. On the other hand, a smaller rebound value can point to possible problems with the strength or quality of the concrete.

Table 6. Rebound hammer test

Mix Designation	Specimen	Avg. rebound number of 4 surfaces	Average rebound number	Compressive strength (N/mm^2)	
				Maximum	Minimum
Control Mix	Cube1	40.7,41.7,41,40	40.85	41.50	30.50
	Cube2	40.3,39.8,40.1,39.9	40	41	29.00
	Cube3	40.2,38.7,39.7,40	39.65	41.5	29.50
5% replacement	Cube1	41,40.8,41.2,40.6	40.90	42.50	30.50
	Cube2	40.9,39.9,39.8,41.5	40.525	42.25	30.25
	Cube3	41.2,40.7,41.7,39.9	40.875	42.4	30.40
10% replacement	Cube1	41.7,42,41.2,43	41.975	42.0	30.00
	Cube2	42.8,43.2,41.9,42	42.475	42.5	30.50
	Cube3	42.9,43,42,42.7	42.65	42.3	30.30
15% replacement	Cube1	43.8,43.5,44,43.6	43.725	44.00	32.00
	Cube2	44.7,44.2,43.9,44	44.2	44.1	32.10
	Cube3	45,44.2,44,43.9	44.275	44.2	32.2
20% replacement	Cube1	40,38,40.1,38.22	39.85	41	29.50
	Cube2	40,38.7,39.9,39.2	39.45	40.50	28.50
	Cube3	39.7,40.2,40.7,38.9	39.89	40.8	28.8

4. Discussion

This study revealed that incorporating e-waste up to 15% gives good compressive and flexural strength of concrete compared to conventional mixtures. Workability, however, tends to decrease with increasing e-waste content.

The improved strength observed with moderate e-waste inclusion can be attributed to the denser interfacial bond formed between the e-waste particles and the cement paste due to the rougher texture of the recycled material. Additionally, some research suggests that the presence of certain elements in e-waste like iron might contribute to a pozzolanic reaction, further strengthening the concrete matrix.

E-waste utilization in concrete offers a dual benefit reducing the environmental impact of e-waste disposal and potentially lowering the demand for natural aggregates. Additionally, the

enhanced strength properties achieved with optimal e-waste content could lead to the development of lightweight concrete with improved structural performance.

Further research is necessary to optimize e-waste content for various concrete strengths and functionalities. Studies on the long-term behavior of e-waste concrete under different environmental conditions are crucial. Notably, the incorporation of e-waste has been shown to augment the split tensile strength of cylinders, compressive strength cubes, and flexural strength of beams. This innovative approach not only addresses the pressing E-waste problem but also contributes to the development of high-performance and eco-friendly construction materials.

In this specific project, a concrete mix of M45 grade was utilized, incorporating a superplasticizer (Polycarboxylate ether Base). The cement used was of 53-grade quality. Various percentages of e-waste were introduced as replacements for traditional coarse aggregates, including 5%, 10%, 15%, and 20%. To analyze the effect of E-waste partial replacement on concrete properties, we can examine the variations in the test results about the control mix (0% replacement). Here are the changes for each parameter.

The study assessed the cube's compressive strength, cylinder's tensile strength, and beam's flexural strength of concrete mixes incorporating varying e-waste proportions of (5%, 10%, 15%, and 20%) across varying curing periods: 7, 14, and 28 days. We found the materials used in this research, to give suitable results for compressive and tensile strengths. So, further research should be needed for flexural strength.

The results above indicate how the addition of E-waste as a partial substitute affects the various properties of concrete. Notably, the maximum improvement is observed when the replacement rate reaches 15%, indicating an optimal balance between e-waste incorporation and concrete performance. This finding underscores the potential of e-waste as a practical replacing aggregate material in concrete, it offers a dual advantage, encompassing both environmental benefits and structural enhancement.

5. Conclusion

The current study finds the following conclusions on the consequence of e-waste as a partial substitute for coarse aggregate in concrete mixtures:

- Comparing results with conventional concrete after 28 days, it is detected that the average compressive strength of concrete is greater than characteristic compressive strength up to 15% replacement of the coarse aggregate by e-waste.
- Comparing results with conventional concrete after 28 days, it is detected that the average flexural strength of the concrete reaches 8.53 MPa when 15% of the coarse aggregate is replaced by e-waste.
- By comparing results with conventional concrete after 28 days, it is detected that the average tensile strength of the concrete reaches 4 MPa when 15% of the coarse aggregate is replaced by e-waste.
- By conducting a water absorption test at 28 days, it was determined that the concrete can absorb up to 1.6 % of its water content in the water absorption test.
- The maximum decrease in compressive strength observed is 3.40%, 13.17%, 9.48%, 11.99%, and 5.58% for control mix, 5%, 10%, 15%, and 20% replacement as compared to Compressive strength test results.
- The rebound hammer test shows the maximum strength of the cubes with a 15% replacement, reaching a maximum value of 44.20 MPa.
- Replacing more than 15% of the waste with any size of e-waste is deemed impracticable and ineffective for construction

References

[1] P. Muthupriya and B. Vignesh Kumar (2022), Experimental Investigation on Concrete with E-waste - A Way to Minimize Solid Waste Deposition, ResearchGate
[2] Bibek Kumar Gupta, Dr. Sandeep Singh (2021), Experimental Investigation on concrete containing E-waste as coarse aggregate, COSMEC
[3] Mr. R. Srinivas Prabhu, N. Chakravarthy, S. Gokulajay, C. Kuppuraj, B. Sharan (2020) Experimental Investigation on Partial Replacement of Coarse Aggregate with E-Waste, IRJET-V716820
[4] Arivalagan S (2019), Experimental Study on the Properties of Green Concrete by Replacement of E-Plastic Waste as Aggregate, Science Direct.
[5] Aravind B Sagar (2022), An experimental laboratory study on utilization of e-waste as a partial replacement of fine aggregates in concrete
[6] Ms. Roopa M, R Das, Sanjana M and Thungashree B S (2022), Study on Partial Replacement of E-Plastic Waste as Coarse Aggregates, Research Gate
[7] Saurav Dixit, Rishab Arora, Kaushal Kumar, Shweta Bansal (2021), Replacing E-waste with coarse aggregate in architectural engineering and construction industry, Research Gate
[8] Muhammad Irshad Qureshi, Muhammad Farrukh Javaid, Afnan Ahmad, Sibghat Ullah Khan (2021), An experimental study on the mechanical and durability properties assessment of E-waste concrete, Journal of Building Engineering 38 (2021) 102177.
[9] S. Bharani, G. Rameshkumar, J. Manikandan, T. Balayogi, M. Gokul (2021), Experimental investigation on partial replacement of steel slag and E-waste as fine and coarse aggregate, Research Gate
[10] S Bharani (2021), Mechanical properties of concrete as partial replacement of coarse aggregate by e-waste, IOP Conf. Series: Materials Science and Engineering 1145

IOP Conference Series: Earth and Environmental Science

PURPOSE-LED PUBLISHING™

PAPER • **OPEN ACCESS**

Navigating Cityscapes: Innovations in Urban Mobility and Infrastructure

To cite this article: Priyanka Kumaravel and R. Velkennedy 2024 *IOP Conf. Ser.: Earth Environ. Sci.* **1409** 012039

View the article online for updates and enhancements.

You may also like

- The complex method of estimation of highway maintenance quality taking into account the International Roughness Index
E V Zhustareva and V I Bochkarev
- Sensitivity analysis of road roughness on transportation costs
Fardzanela Suwarto, Anjang Nugroho, Riza Susanti et al.
- Economically and environmentally informed policy for road resurfacing: tradeoffs between costs and greenhouse gas emissions
Darren Reger, Samer Madanat and Arpad Horvath



This content was downloaded from IP address 47.247.77.11 on 27/11/2024 at 05:43

Navigating Cityscapes: Innovations in Urban Mobility and Infrastructure

Priyanka Kumaravel[1*] and R. Velkennedy[2]

Department of Civil Engineering, Thiagarajar College of Engineering, Madurai, Tamil Nadu, India.

*Email: priyankakumaaravel@gmail.com

Abstract. The nature and broadening of road transportation infrastructure influence a nation's ability to grow sustainably. Due to the combined impacts of poor maintenance and structural weaknesses to meet the demands of an increase in traffic intensity and loads, India's enormous network of existing roads, which were built at considerable expense, is starting to exhibit signs of distress failure before the design period. Maintenance directly affects a pavement's longevity. The Pavement Maintenance Management System (PMMS) is a scientific strategy for assessing the current state of pavement in a specific area. To provide a more flexible approach that allows tasks to be accomplished more successfully, this project intends to provide a Pavement Maintenance Management System that provides an organized approach for the maintenance, improvement, and operation of city pavements and tools. As part of this study, an initial survey is carried out from Thanakankulam to Thiruparankundram. The World Bank created HDM-4, a software program that may be used internationally to identify the best repair itinerary for highway pavements. To identify the Pavement Quality Index and associated techniques, the HDM-4 tool will conduct further investigations.

Keywords – Pavement management, distress failures, pavement condition survey, HDM-4 tool.

1. Introduction

The standard of living, the strength of the social structure, and the continuation of economic and commercial operations are all impacted by the effectiveness and quality of the road surface. Roadway deterioration and failure may be brought on by ageing, excessive usage, and poor management. Hence, the preservation and maintenance of roadways should be regarded as a subject of considerable national importance [1]. The "Pavement Management" program is designed to improve the quality and performance of pavements while simultaneously cutting costs, and employing effective management practices. A Pavement Management System functions as a specialized asset management tool that is specifically engineered to uphold the maintenance of roadways. The Pavement Maintenance Management System encompasses a collection of tools that facilitate the decision-making process by assessing and conserving pavement to maintain a satisfactory level of functionality for a pre-established period. Integrating Pavement Maintenance Management Systems with Highway Development and Management (HDM-4) models enhances road infrastructure management [2]. PMMS focuses on short-term maintenance, while HDM-4

Content from this work may be used under the terms of the Creative Commons Attribution 4.0 licence. Any further distribution of this work must maintain attribution to the author(s) and the title of the work, journal citation and DOI.
Published under licence by IOP Publishing Ltd

considers long-term lifecycle costs. This correlation optimizes decision-making by combining immediate repairs with future planning.

2. Pavement Maintenance Management System Fundamentals and Ideas

A Pavement Management System (PMS) is an asset management tool specifically designed for effective road maintenance, forming part of a larger asset management system. It offers objective data for analysis, aiding road managers in making consistent, cost-effective, and legally sound decisions regarding pavement preservation. While not making final decisions, a PMS establishes the groundwork for a comprehensive understanding of potential outcomes from various choices [3]. According to the Federal Highway Administration, a PMS encompasses defined procedures for collecting, analyzing, maintaining, and reporting pavement data, assisting decision-makers in determining optimal strategies for maintaining pavements in serviceable condition at minimal cost over a specified period. The benefit of a PMS lies in its ability to present information clearly and intelligibly, empowering users to make informed management decisions for their roads.

A Pavement Maintenance Management System (PMMS) provides a systematic, objective, and consistent approach to assessing current and future pavement conditions. It helps manage paving maintenance costs more efficiently. Pavement maintenance is perceived as a means to effectively repair and treat specific roadway pavement systems (FAA, 2006). PMMS can be applied at both project and network levels [4]. At the project level, it focuses on implementing rehabilitation techniques in specific areas, while at the network level, it aims to maintain the entire network while optimizing available funding. By maximizing funding utilization, each pavement maintenance system aims to enhance the effectiveness of pavement treatment and restoration. PMMS commonly utilizes the Pavement Condition Index (PCI) to assess present and future pavement quality and conducts cost-effectiveness studies on various maintenance and restoration options.

2.1. Types of Pavement Maintenance Management Systems

Pavement maintenance can be divided into two categories:

- Preventive maintenance aims to avoid or mitigate further damage to the pavement.
- Structural maintenance involves repairing or improving the structural integrity of the pavement.

Depending on the nature and extent of the pavement distress that has to be treated, a particular maintenance approach or procedure may be employed. Several maintenance procedures would need to be used for the distressed pavement to yield excellent results. For instance, with medium severity levels of transverse or longitudinal cracking, a surface treatment like a chip seal or slurry seal normally comes after crack filling or sealing. Pavement sealant can be used to alleviate alligator cracking temporarily, but full-depth patches must be installed once the distressed portion of pavement is removed for a more long-lasting fix. When utilities or drainage infrastructure placed beneath the pavement needs to be changed, some maintenance procedures are necessary [5]. A full-depth patch must be placed to repair the lost pavement, which was cut into the pavement to access these services. Since these patches may provide extra ports of entry for water into the pavement structure, they must be appropriately placed. The aesthetic appeal of the pavement and the riding qualities can both be impacted by the patches.

2.2. Levels of Pavement Maintenance Management Systems

Pavement management is capable of being implemented on two different levels. They are as follows

- Project level and
- Network level.

2.2.1. Network level

All pavements under city municipality control are evaluated as part of network-level management. The basic objective of network-level management is to create a prioritized pavement repair program for the whole agency that will result in the greatest benefit with the lowest overall cost within the given budgetary limits. Additionally, compared to project-level management, network-level management relies more on approximations. Answers to queries about short- and long-term budget requirements as well as the general state of the network (both now and in the future) are provided at the network level. Additionally, network-level management aids in determining which pavement sections should receive repair, rehabilitation, or both. The aforementioned sort of evaluation frequently relies on a basic level of inspection, which consists predominantly of visual inspection of an individual component of each pavement section in the network.

2.2.2. Project level

Project-level management is focused on a specific place and often follows network-level analysis in local agencies. After discovering a part requiring repairing at the network level, an engineering investigation is carried out at the project level. Since the data gathered at the network level typically lacks the information needed to make specific decisions for each project design, a more thorough evaluation is required through this analysis [6]. More testing, like as visual inspection, non-destructive testing, and coring testing, is frequently carried out during a project-level examination to provide additional information regarding the state of the pavement and the reason for degradation. Management decisions are made at the project level on the most economical maintenance and rehabilitation options for a specific pavement segment. Normally, the assessment at the project level is examined more thoroughly than at the network level. The pavements that were identified during the network-level analysis as candidates for maintenance and repair measures are evaluated further. For pavement examination, a larger sampling rate is frequently employed. In the project level, other testing methodologies such as texture and roughness testing, may be used depending on the specific requirements.

Problem identification

- Inadequate Road System to Handle Traffic Demand.
- Ineffective network maintenance procedures.
- Financial restrictions on decision-makers.
- Road geometry flaws, as well as poor construction and maintenance techniques
- Improper Planning
- The need for appropriate planning and resource management.

2.3. About HDM-4

The systematic approach of Highway Development Management (HDM-4) offers numerous benefits for highway infrastructure planning, design, and maintenance. It integrates traffic patterns, pavement conditions, and economic factors to enable effective decision-making. Figure 1 provides a comprehensive overview of the HDM-4 software.HDM-4 evaluates design and maintenance techniques for cost-effectiveness and resource allocation while enhancing the long-term performance and sustainability of roadway assets, thus reducing life-cycle costs. Additionally, it improves road safety by identifying and addressing hazards [7]. Overall, HDM-4 optimizes highway network management, ensuring sustainability, safety, and economic efficiency.

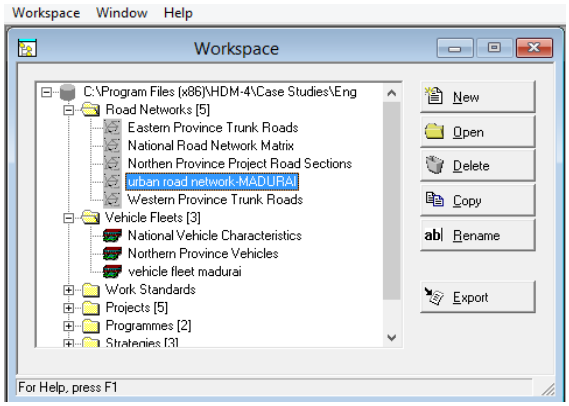


Figure 1. Software Overview

2.4. Need for Implementation of PMMS Using HDM-4 in Madurai

Implementing a Pavement Management and Maintenance System (PMMS) with HDM-4 in Madurai offers significant benefits to road maintenance. It enables systematic data collection and analysis, prioritizing maintenance activities based on pavement condition and optimizing resource allocation. Additionally, HDM-4 aids in developing cost-effective maintenance strategies by predicting pavement deterioration and recommending timely interventions, thus reducing long-term expenses. Moreover, PMMS with HDM-4 enhances sustainability by minimizing environmental impact through optimized maintenance, extending pavement lifespan, and promoting responsible infrastructure management. Furthermore, it enhances accountability and transparency by providing data-driven insights for effective decision-making and resource allocation. In summary, PMMS with HDM-4 implementation in Madurai improves road maintenance efficiency, sustainability, and overall infrastructure quality.

3. Literature Review

To build a current understanding of the subject, this literature review analyses interprets, and critically assesses the body of prior research. A summary of the literature review on the pavement maintenance management system is given, and the references are cited after the paper. Numerous studies on the subject were gathered and examined. This chapter discusses a few of the papers.

The sustainable development of any country depends upon the type and quantum of road transportation infrastructure provided [15]. The massive growth in traffic makes daily transportation planning in both urban and rural areas more and more challenging.2.6-kilometer state highway route that passes through Belgaum city was investigated. The following study was conducted: The chosen road length was divided into 3 portions of lengths of 1 km, 0.65 km, and 0.95 km, respectively, for data collecting and the subsequent processes. To determine the number of cars using the route, a traffic volume analysis was conducted. Road geometry was studied to determine its rise, fall, and horizontal curvature. Using the program HDM-4, the data gathered is utilized to offer the maintenance necessary for the various road networks. The best maintenance approach necessary for the design life is advised for execution after many alternative techniques have been studied.

A study on the Patiala city road network was conducted [1] to provide a powerful system for the analysis of pavement management and investment strategies for the maintenance of the huge urban road network. 52 road sections in Patiala city were analyzed for strategy and program using the HDM-4 software, of which 5 manageable pavement sections are discussed in detail based on

various characteristics. The HDM-4 tool uses data on current road conditions, traffic volume, and composition in addition to a deterministic approach for data input and processing to predict road conditions.

Shashi Bhushan et al., [11] conducted a Distress survey on Bangalore City's outer ring road. They were afterward, figuring out the kind and degree of damage it had experienced. Many alternative maintenance procedures were recommended based on the scientific analytical tool HDM-4 created by the World Bank. The best maintenance strategy is then chosen from the available maintenance strategies for a particular urban route.

R. Sudhakar [12] discussed various maintenance treatments that are being practiced in India for urban roads. The field engineers now choose the sort of treatment at random and without any kind of scientific foundation. In this study, an advanced and cutting-edge scientific instrument called HDM-4 created by the World Bank is used to determine the best maintenance strategy for urban roads among the different possibilities suggested by the Government of India's requirements.

3.1. Recent Trends and Comparison of HDM-4

Recent trends in Pavement Management Systems (PMS) emphasize the integration of advanced technologies like Machine Learning and GIS for more efficient data collection and analysis. Sustainability and resilience have become focal points, with a focus on eco-friendly materials and designs capable of withstanding extreme weather. When comparing HDM-4 with newer systems, HDM-4's comprehensive approach stands out, incorporating traffic patterns, pavement conditions, and economic factors to optimize decision-making. It excels in evaluating design and maintenance techniques, predicting pavement deterioration, and ensuring long-term sustainability. However, newer systems offer advantages in user interface and accessibility, featuring user-friendly interfaces and cloud-based platforms for easier data sharing and collaboration. Additionally, they boast advanced analytics and predictive modeling capabilities for more accurate pavement performance predictions and targeted maintenance strategies. While HDM-4 remains respected, the industry is moving towards technologically advanced and user-friendly systems that provide enhanced pavement analysis, decision-making, and sustainability features.

4. Methodology

The project's workflow is described in a flow diagram that is part of the methodology. Problem identification explains the current problems with road maintenance. The PMMS technique is critically assessed in the literature, which also offers study methodologies. Primary details like visual examination, the length and kind of the road, and measurements of distress failures such as potholes, rutting, ravelling, and cracking are all part of the data-collecting process [8]. The program is called Highway Development and Management (HDM-4) which analyses data. The HDM-4 will be used to get the findings, and the road network will be used for a distress survey. A schematic diagram is used to illustrate this technique, as shown in Figure 2. Validation of HDM-4 pavement deterioration models involves comparing expected and observed distresses, with data obtained in subsequent time series. This study aimed to validate calibrated distress models using various statistical techniques. This study utilized these methodologies to validate and adjust the HDM-4 models.

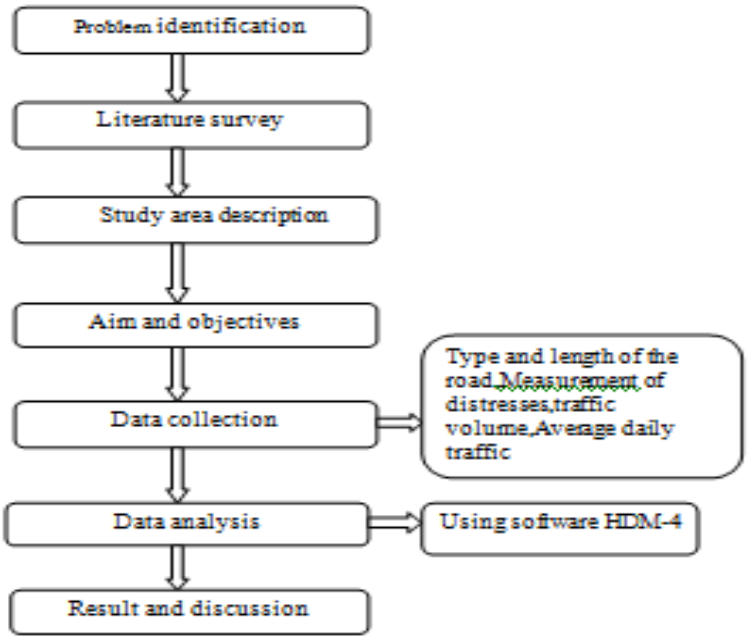


Figure 2. Research Methodology

4.1. Study Area Description

4.1.1. Road network in Madurai

The City Corporation is responsible for maintaining a total of 1572.38 kilometers of streets and lanes. These include B.T., CC, Metal Roads, Sand Roads, Stone Cut, and Tile Paved Roads. Figure 3 displays the road map of Madurai, which offers a thorough and detailed representation of the city's transportation network.

- There are bituminous roads for 947.94 km.
- Madurai is traversed by the National Highways NH 7, NH 45B, NH 208, and NH 49. The city is traversed by the state roads SH-32, SH-33, and SH-72, which connect different areas of the Madurai district.



Figure 3. Road map of Madurai

22.58 km of highways with tile and stone pavement. The following tables 1 and 2 provide information on the lengths and types of roads. Figure 4 depicts the road network connecting Thanakankulam and Thiruparankundram. It highlights the main routes and linkages between these two regions, focusing on important roads.

Table 1. The total length of roads is based on materials.

S.No	Roads	Length in km
1.	Bituminous Tar Roads	947.94
2.	Stone cut and tiles paved roads	22.58
3.	Sand roads	207.52
4.	Cement Concrete Roads	268.99
5.	Metal roads	125.50
	Total	1572.38

Source: https://maduraicorporation.co.in/aboutus/roads

Table 2. The total length of roads is based on the type of roads.

Roads	Length in km
Internal road	239.66
Ring road	27.20
Bus route road	162.87
Total	532.22

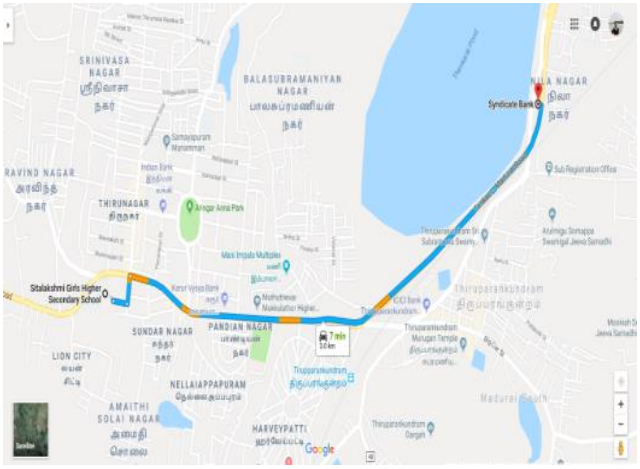


Figure 4. Road network from Thanakankulam to Thiruparankundram

4.2. Data Collection

Additionally, information on the breadth, length, structural parts, maintenance histories, traffic patterns, and soil conditions was obtained from records. An inventory of streets is one of the database's primary advantages. It included a pavement condition assessment and evaluation of every roadway to determine structural degradation, surface deterioration/condition, riding quality, skid resistance, potholes, and associated information [9]. The gathering of information on vehicle fleet characteristics, such as traffic volume and axle load, is used to analyze traffic patterns across all pavement sections [10]. Figure 5 shows the data collection flow chart, which organizes data collection, processing, and analysis for accurate and trustworthy results.

4.2.1. Preliminary survey

- Conducted in route: Thirunagar to Periyar Bus Stand
- Distress survey carried out on GST Road
- Starting point: Thanakankulam (near Sitalakshmi Girls hr. School)
- Ending point: Periyar Bus Stand
- Length of the road details were collected as shown in Table 3.
- Type of material: Asphalt bitumen

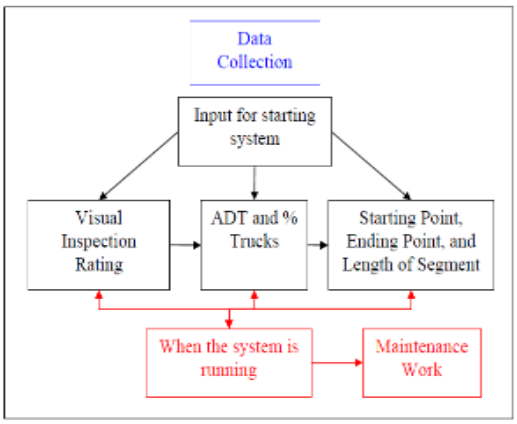


Figure 5. Data collection flow chart

Table 3. Details of urban roads in Madurai City.

S. No.	Name of the Road	Direction		Length(km)
		From	To	
1	Madurai to thenkasiroad	Sitalakshmi Girl'sHigher Secondary School	Thirunagar Second Stop	0.8
2	Madurai to Thirumangalam GST road	Thirunagar Second Stop	Thirunagar 1st stop	2.2
3	Thirunagar Main Road	Thirunagar 1st stop	Harveypatti	1.7
4	Harveypatti Main Road	Harveypatti	Thiruparankundram	1.5
5	Madakulam Main Road	Tce stop	Moolakarai	1.8
6	Moolakarai	Mannar college	Pasumalai	0.7
7	Pasumalai	Pasumalai	Pykara	0.85
8	Pykara	Pykara	Alagappan Nagar	0.6
9	Alagappan nagar	Alagappan nagar	Palanganatham	0.5
10	Palanganatham	Palanganatham	Vasantha Nagar	0.5
11	Vasantha nagar	Vasantha nagar	Andalpuram	0.26

4.2.2. Visual inspection

- Conducted in route: Thirunagar to Periyar Bus Stand
- Distress survey is carried out on GST Road

Identified distress includes:

- Potholes
- Cracking
- Rutting
- Ravelling

4.2.3. Pavement Condition Survey

Pavement condition data is typically collected using two primary methods: manual and automated. In addition, with automated data collection, data is analyzed using either fully automated or semi-automated procedures.

4.2.4. Manual surveys

These surveys involve workers strolling or driving at slow speeds to visually check pavement conditions. Manual surveys do not require specialized technology and can provide a plethora of information about the types, intensities, and quantities of distress; nevertheless, data collection is labour and time-consuming [11]. Due to the lengthy data-gathering process involved in manual surveys, there is an increased risk of injury to both the data collection staff and the general traveling public. To ensure appropriate data quality, raters for manual surveys need to be well-educated. Some organizations demand certification. Figure 6 reveals that road conditions have worsened in the section from Thanakankulam to Thiruparankundram and need advancement.



Figure 6. Distress identified in the stretch-Thanakankulam to Thiruparankundram

4.3. Automated surveys

Automated surveys include automated machinery that measures pavement deterioration using images and/or noncontact sensors. (For example, surface cracking, roughness, rutting, and faulting). Automated surveys may be carried out at or close to traffic speeds with the least amount of exposure to the data-collecting crew and the least amount of disruption to the general traveling public [12].

4.3.1. Fully automated processing-

Employs software to understand variances in greyscale to find cracks and other surface abnormalities. Distress diagnosis (kind, severity, and extent) is performed in this manner without the need for human interaction.

4.3.2. Semi-automated processing

Detection of discomfort (kind and intensity), which needs human interaction to quantify. Computer workstations and specialized software are used to do analysis.

Figure 7 illustrates how the pavement condition rating evaluates the current condition of road surfaces by categorizing them according to criteria such as wear, damage, and general integrity.

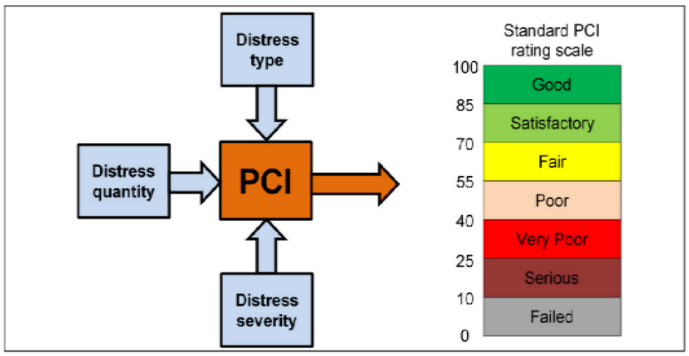


Figure 7. Pavement condition rating

5. Key concepts of strategy analysis

An HDM-4 Strategy Analysis develops a medium-to-long-term investment strategy for selected Sections: set optimization criteria and budget constraints for each Strategy Analysis as shown in Figure 8. Max NPV, Max IRI, and Minimize Cost for Target IRI are optimization strategies. The investment option combines Section Maintenance and Improvement Standards. Select Sections from a predetermined Road Network or construct a Network Matrix when defining a Strategy Analysis [13]. You can build numerous sample Sections using aggregate parameters to reflect the Road Network being examined using the Network Matrix option.

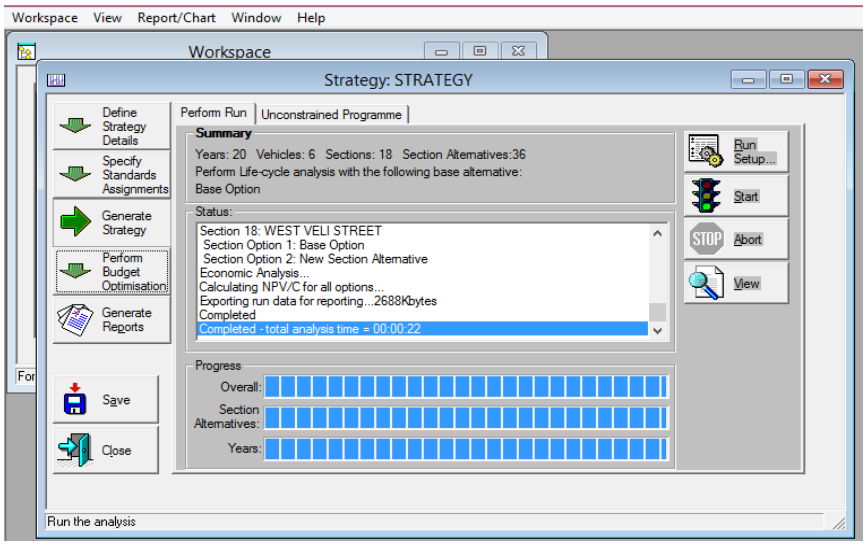


Figure 8. Strategy analysis-generate strategy

The output, as mentioned in Table 4, presents the priority ranking of road sections and the optimal Maintenance and Rehabilitation (M & R) approach for each segment. This provides a strategic framework for infrastructure management. Utilizing HDM-4 for strategic analysis enables a comprehensive assessment of road projects, ensuring that decisions are made based on reliable data and thorough economic, environmental, and social factors. This results in enhanced and persistent administration and growth of road networks.

Table 4 Output: Priority ranking of road sections and best M & R strategy for each section.

Section name	Section ID	Priority Ranking (based on highestNPV)	Best M&R Strategy
Periyar	UR 10	10	Resealing + overlay
Pasumalai	UR 05	9	Resealing+Overlay
Palanganatham	UR 09	8	Resealing+Overlay
Madurai to Thirumangalam GST road	UR 02	7	Resealing+Overlay
Madurai to Thenkasi road	UR 01	6	Thin overlay
Thirunagar main road	UR 03	5	Thin overlay
Pykara	UR 07	4	Thin overlay
Moolakarai	UR 08	3	Routine maintenance
Madakulam main road	UR 06	2	Routine maintenance
Harveypatti main road	UR 04	1	Routine maintenance

6. Conclusion

In India, PMMS is crucial for optimizing road infrastructure management. It systematically gathers data on pavement conditions, enabling prioritized maintenance interventions and cost-effective resource allocation. This proactive approach extends road asset lifespan, reduces accidents, and enhances transportation efficiency. In a rapidly developing country like India, PMMS plays a vital role in building resilient, sustainable, and high-quality road networks essential for progress and economic growth [14]. Economic analysis-driven interventions minimize lifecycle costs, enabling cost savings and stimulating economic activity by facilitating smoother transportation and reducing overall costs. Environmentally sustainable maintenance practices mitigate infrastructure impact, promoting resilience and safety, while fostering long-term planning for sustainable infrastructure management, ensuring continued prosperity and development. From the analysis, the following conclusions were drawn:

- Strategy analysis is necessary to estimate expenditures for medium to long-term periods (5-40 years) while considering budget constraints, maintenance standards, and road usage scenarios.
- Economic analysis, conducted with a 12% discount rate (by Clause 7.8, IRC: SP: 30), assessed selected roads' performance indicators including surface distress, user costs, safety levels, and environmental impacts. It predicted key economic metrics like Net Present Value (NPV) for the road network over the analysis period. Routine maintenance emerges as the optimal investment for sections UR 04, UR 08, and UR 06. Meanwhile, 'Thin Overlay (25 mm BC) and resealing' and 'Overlay (40 mm BC)' are recommended for the remaining sections, based on maximizing NPV criteria.
- "Namma Saalai" is a mobile application developed by the Government of Tamil Nadu, providing real-time updates on road conditions and traffic, alongside information on nearby facilities like petrol pumps and hospitals, allowing users to report road issues or accidents. It aims to enhance road safety, improve traffic flow, and elevate the travel experience across Tamil Nadu. Conversely, PMMS in India plays a vital role in systematically managing pavement conditions and infrastructure. PMMS enables prioritized maintenance interventions and cost-effective resource allocation,

extending road asset lifespan, reducing accidents, and enhancing transportation efficiency [15]. Furthermore, PMMS contributes to long-term planning for sustainable infrastructure management, fostering resilience and economic growth. While "Namma Saalai" addresses immediate road-related concerns, PMMS ensures the longevity, safety, and economic viability of road infrastructure, making it crucial for overall road network management and development.

References

[1] Amritpal Singh, Annu, "The role of HDM-4 in developing pavement maintenance management systems (PMMS) for the Patiala city road network", *International Journal of Emerging Technology and Innovative Engineering Volume I, Issue 7, July 6, 2015.*

[2] Bandara and M. Gunaratne, current and future pavement maintenance prioritization based on rapid visual condition evaluation**,** *journal of Transportation Engineering / March/April 2001;127:116-123.*

[3] Chalise DN. Roads Board, Nepal: A Sustainable Approach to Road Maintenance Management, *Transport and Communication Bulletin for Asia and the Pacific*, No. 75, 2005.

[4] Fareed M.A. Karim, Dr. Khaled Abdul Haleem Rubasi, and Dr. Ali Abdo Saleh. The Road Pavement Condition Index (PCI) Evaluation and Maintenance: A Case Study of Yemen, *Organization, Technology, and Management in Construction 2016; 8: 1446–1455.*

[5] Hamad Al-Ajami, "Pavement maintenance management systems", *Civil and Environmental Research, ISSN 2224-5790, Vol.7, No.5, 2015.*

[6] Jendia S, Al Hallaq M. Development of Pavement Maintenance Management System (PMMS) for Gaza City, *J Islamic University of Gaza* (Series of Natural Studies & Engineering), 2005; 13(1): 119–138p.

[7] Milaa Murshan, Monicaba Vala, A review on gis-based pavement maintenance management system for urban corridors, *International Journal of Advance Engineering and Research Development Volume 4, Issue 3, March - 2017.*

[8] Mounesh R T, Rohit V A, Prakash R H, Shivaprasad C N, Pavement Maintenance and Management of Urban Roads Using HDM 4, *International Journal of Engineering Technology, Management and Applied Sciences, May 2015, Volume 3, Issue 5, ISSN 2349-4476.*

[9] Sarsam S. Visual Evaluation of Asphalt Concrete Surface Condition using an Expert System VEACPSC, *Indian Highways* IRC. 38(9), 2010.

[10] Sarsam SI, Mohammed IA, Burhan AM. Using Pavement Automated Monitoring System in Prioritization of Maintenance Decisions, *Int J Constr Eng Plann. IJCE J Pub*. 2015; 1(1): 1–13p.

[11] Shashi Bhushan Girimath, Dr.Venkat Chilukuri,Prof. T. G. Sitharam, Dr. Krishnamurthy, "Pavement Management System for Urban Roads", *IJSRD - International Journal for Scientific Research & Development Vol. 2, Issue 03, 2014.*

[12] S*udhakar. R,* Pavement Maintenance Management System for Urban Roads Using HDM-4, *Indian Geotechnical Society Chennai chapter (2009).*

[13] Raid R.A. Almuhanna, "Using PAVER 6.5.7 and GIS program for pavement maintenance management for selected roads in Kerbala city"**.** *Case Studies in Construction Materials 8 (2018) 323–332.*

[14] Tanuj Chopra, Manoranjan Parida, Naveen Kwatra, Jyoti Mandhani, "Development of Pavement Maintenance Management System (PMMS) of Urban Road Network Using HDM-4 Model", *International Journal of Engineering & Applied Sciences (IJEAS), Vol.9, Issue 1(2017) 14-31.*

[15] Vinod Mashyal, "Pavement Maintenance and Management of urban roads by using HDM- 4", *International Research Journal of Engineering and Technology (IRJET),2018.*

Acknowledgment

The authors express their gratitude to the Thiagarajar College of Engineering (TCE) for supporting us in carrying out this research work. Also, the financial support from TCE under the Thiagarajar Research Fellowship scheme (File.no: TRF/Jul-2023/02) is gratefully acknowledged.

IOP Conference Series: Earth and Environmental Science

PURPOSE-LED PUBLISHING™

PAPER • **OPEN ACCESS**

Shear capacity enhancement of slab-column joint of a flat slab system

To cite this article: Manoj Tangudu *et al* 2024 *IOP Conf. Ser.: Earth Environ. Sci.* **1409** 012040

View the article online for updates and enhancements.

You may also like

- Numerical Analysis of Shear Strength Behavior of self-compact reinforced concrete Two-way Bubble Deck Slab with Shear Reinforcement
Ibrahim S. I. Harba and Mais A. Hammed
- Strength prediction of a bottle-shaped strut for evaluating the shear capacity of reinforced concrete deep beam
Avinash Kumar and R S Jangid
- Effect of Shear Reinforcement on Punching Shear Capacity of Reinforced Concrete Flat Plates
Osama Mohamed and Rania Khattab



This content was downloaded from IP address 47.247.77.11 on 27/11/2024 at 05:43

Shear capacity enhancement of slab-column joint of a flat slab system

Manoj Tangudu[1], Jagadeesh Bommisetty[1], Tirukovela Sai Keertan[1] and P.V.V.S.S.R. Krishna[2]

[1]Department of Civil Engineering, CVR College of Engineering, Hyderabad, Telangana, India, 501510.
[2]Department of Civil Engineering, Gokaraju Rangaraju Institute of Engineering & Technology, Hyderabad, Telangana, India, 500090.

E-Mail: manoj.tangudu03@gmail.com

Abstract. The need for beam-less space structures has been increasing globally in recent times to meet the demand new construction method is being used popularly known as Flat slab. Flat Slab has many advantages such as ease of application of formwork, more space to occupy, and shorter duration for construction. Implementing efficient load-bearing structures is an often-underestimated measure with enormous saving potential compared to conventional, but rather criteria such as construction costs the possibility of integrating building services components must be socially sustainable including safety, functionality, and adaptability. To construct commercial buildings mostly Flat slabs are economical compared with conventional slabs. The present work involves finding out the equivalent space framework with slab and column elements to reduce the effect of shear. Outcomes of RC Slab-Column joints with Shear Reinforcement from FE (Finite Element) analysis are presented. Three Interior Slab-Column Joints were modelled and analyzed in ANSYS. One slab specimen is without drop and shear reinforcement the second specimen is with drop and without shear reinforcement and the third specimen is without drop and with shear reinforcement. Similarly, three Exterior and three Edge Joints were modelled and analysed. In this study, the enhancement of principal stress, shear stress, principal strain, and shear strain of the slab-column assemblies by provision of shear reinforcement were discussed. The provision of shear reinforcement at slab-column assembly exhibited a maximum shear stress reduction of 42% at the edge joint.

Keywords: Flat slab; Slab-column joint; ANSYS; Shear reinforcement; Column drop, Sustainable infrastructure.

1. Introduction

An RC Slab without beams directly supported on columns is a Flat slab. The loads on the Flat slab directly transfer to the supporting columns. Flat slabs are advantageous for many of these reasons, including low construction costs, good acoustic sound insulation, low overall depth, and the ability to integrate building services as inserts. Their production has been optimized for

Content from this work may be used under the terms of the Creative Commons Attribution 4.0 licence. Any further distribution of this work must maintain attribution to the author(s) and the title of the work, journal citation and DOI.
Published under licence by IOP Publishing Ltd

decades to have more sustainability and reduce the use of materials. Three types of systems such as Flat slab with column head and drop panel; Flat slab without column head and with drop panel; Flat slab with column head and without drop panel are in the construction practice of flat slabs. The critical occurrence in flat slabs that might cause a brittle breakdown in punching shear failure. In the design of Flat Slabs, care needs to be taken in cases like a) To reduce the maximum central deflections, the sub- frame method needs to be adopted for structure layout design and implementation, and the use of at least two parallel column strips is another method of assessing mid-panel deflection, b) reinforcements are mandatory to decrease the punching shear in thin type flat slabs c) yield line output is the better optimization method for Main reinforcement compared to remaining design methods. The primary issue with flat slabs is the large load concentration at the slab-column connection, which can lead to punched shear failure. As of now, there is no methodology to check the slab column joint. Although there are several models available, the issue of column-slab junction effective strength has not been resolved. This is because of the limitations of statistical regression and the complexity of the phenomenon involved. Lower stiffness of slab-column leads to relatively large deflections compared to beam-column and also there will be a reduction in shear capacity in and around the column. Many investigators used and proposed various kinds of shear reinforcements, including bent-up bars, stirrups, shear heads, and shear studs, in studies assessing shear-reinforced concrete slabs.

It is proposed to develop a simple model representing the performance of slab-column assemblies to assess the safety of the slab-column assemblies in a framed structure. The model to be proposed shall be simple, amenable, and adaptable with the conventional structural analysis packages dealing with discrete structures with the provision of shear reinforcement. The main objective is to study the influence of shear reinforcement on Flat slab with the help of nine models namely S1:Interior Flat slab without a drop and shear reinforcement; S2: Interior Flat slab with drop and without shear reinforcement; S3: Interior Flat slab without a drop and with shear reinforcement; S4: Exterior Flat slab without drop and shear reinforcement; S5: Exterior Flat slab with drop and without shear reinforcement; S6: Exterior Flat slab without a drop and with shear reinforcement; S7:Edge Flat slab without drop and shear reinforcement; S8:Edge Flat slab with drop and without shear reinforcement; S9: Edge Flat slab without drop and with shear reinforcement.

2. Previous Investigations

Mengzhu Diao, et.al., [1] the investigation yielded outcomes pertaining to the given structural conditions, the punching deformations of Downward Punching Shear-1 and Upward Punching Shear-1 were identical. Jinrong Liu, et.al [2] created RC flat plates and progressive collapse analysis was done on a macro model slab-column connection. M. Hasan Meisami et.al., [3] developed a method to mitigate the occurrence of brittle failures that involve the utilization of advanced strengthening techniques. It was observed that the maximum loading and deformation capabilities are improved due to the same. Long Nguyen-Minh, et.al., [4] observed a considerable improvement in shear and cracking resistance of the SFRC slab column connections due to the impact of fiber quantity. Priya, S. Greeshma, and K. N. Suganya[5] evaluated the performance of connections subjected to axial and lateral loads were examined using the finite element program ANSYS (Version 11), The findings indicate that the slab-column joint experiences the highest levels of stress and deformation, as evidenced by the results obtained. Ronaldo B. Gomes and Paul E. Regan [6] investigated the punching failure influenced by shear reinforcement on. Aikaterini S. Genikomsou, and Maria Anna Polak [7] a novel numerical modeling strategy was proposed to

simulate and analyze shear-reinforced slabs incorporating shear bolts. Alex M.D. de Sousa, et.al., [8] indicated that the presence of a UHPFRC layer in the slab compression zone near the column has been shown to enhance the punching and deformation capacities. Soliman Alkhatib and Ahmed Deifalla [9] claimed that the First Order Second Moment approach is a more straightforward method of analysis and that important variables such as model correctness, effective slab depth, and compressive strength of concrete were noted. Tung D. Dang, et.al., [10] the deep beams' shear resistance can be significantly enhanced by incorporating steel fibers, increasing by up to 55%. Additionally, the utilization of steel fibers can effectively reduce shear crack width by up to 68%.

Flat slabs with drop buildings have a high natural period compared to flat slabs without drop [11]. The resistance of the beam mechanism under collapse was significantly enhanced by increasing the beam height [12]. The installation of double stirrups around the column stub could reduce joint damage and increase punching shear and post-punching strengths by 15% and 9%, respectively [13]. Two distinct corner reinforcement configurations were tried on the specimens: first with torsional strips and then without torsional strips. [14]. The first high loads were caused by observed punching shear failures, which were all swiftly followed by a quick load decline [15]. In flat slab constructions, the column may fail due to the unexpectedly high loads caused by a significant increase in moment and shear force at the nearby slab-column connections. [16]. The capacity improvement was not significant with the inclusion of continuous bottom reinforcement through a column. Basic test parameters were studied parametrically: slab length, effective depth, reinforcement ratio, column aspect ratio, gravity load ratio, and boundary condition [18]. Using ABAQUS software, the slab has been simulated, and the model has been calibrated against developed experimental results. [19]. Three samples were examined, with one lacking shear reinforcement and the remaining two possessing shear reinforcement in the form of studs arranged either radially or orthogonally [20].

Introduced an innovative method by utilizing double-headed studs with large diameters as shear dowels to reinforce slabs against efficiently punching shear. [21]. The punching shear behavior of the SFRC slab-column joint was studied with the help of unbonded tendons [22]. Four distinct shear reinforcement dispositions were tested on eight slabs, and the findings indicate that the arrangement of shear reinforcement corresponded to the punched shear capacity of the transverse reinforced slabs [23]. The presence of the inserted beams improved the specimens' resistance to both flexural and suspension mechanisms [24]. The RC beam-slab substructures are characterized by a compressive arch action of the longitudinal beams and flexural mechanism of the transverse beam, which is used to generate progressive collapse resistance of the substructures [25]. Fiber volume content has an impact on how flat slabs punch and shear [26]. An experimental program by M. E. Shoukry et,al., [27] ten simply supported slabs were tested by subjecting each to a single, rising focused load. The evaluation of the results indicated their accuracy when compared to the equations proposed by the conventional literature. Pedram Zohrev et.al., [28] focused on the key punching shear region and the applicability of two punching shear models, it was determined how to best employ ultrahigh-performance concrete (UHPC) in flat slabs. The results revealed that full-depth UHPC application increases punching shear capacity by 70%. Aikaterini S. Genikomsou & Maria Anna Polak [29,30] studied the failure modes under static and fictitious dynamic loadings by performing nonlinear FE analyses. The study and presentation of RCSC connections with shear reinforcement were conducted through FE analysis and associated ultimate loads, and crack patterns to experimental findings. A novel numerical

modeling approach has been suggested, which involves a comparison of rectangular and radial shear reinforcement layouts.

From the studies, it was observed that continuous slabs have a larger punching shear capability than isolated slabs [31]. The findings by Graeme J. Milligan et.al., [32]. show that column rectangularity is not only dependent on column aspect ratio and worsens as the minimum column dimension to effective slab depth ratio rises. High-rise constructions must have reinforced concrete slabs; however, these slabs experience punching shear failure that can have disastrous effects. In the study by M. Navarro et.al., [33], Non-linear numerical models are utilized in ABAQUS to study and replicate the effect of punching shear on concrete flat slabs, incorporating bolt retrofits.. According to the study, a shear-bolt radial pattern with a suggested spacing of five times the shear bolts' diameter is best for retrofitting slab-to-column connections. The study conducted by Graeme J. Milliganst.al.,[34] revealed that the rectangularity of the column significantly affects the punching shear capacity, with the severity of this impact increasing as the column aspect ratio increases.

The punching shear behaviour of isolated RC flat slabs modified using different UHPFRC (ultrahigh-performance fiber-reinforced concrete) layouts is examined in the work performed by Demewoz W. Menna and Aikaterini S. Genikomsou [35]. A hybrid damaged plasticity-based model is used to suggest and assess two ideal retrofitting configurations. Slab-column connections analysis and parametric studies are used to validate the model. The study discovers that the improved thickness of the UHPFRC covering enhances punching shear capacity but lowers displacement at maximum resistance. Due to the quantity of UHPFRC being lowered and the slab's increased ductility, using UHPFRC just in key regions may be more efficient and cost-effective.

Due to their simplicity in placing, speedy construction, and shallow structural floor depth, flat slabs are frequently used in the construction of multi-story buildings. But at slab-column connections, they are susceptible to punching shear, a failure mechanism that happens suddenly. For modelling the punching shear response of composite NC (Normal Concrete)/UHPC flat slabs with no shear reinforcement, a non-linear finite element (FE) model was created by Majid M.A. Kadhim et.al., [36]. The impact of slab thickness, column size, UHPC area, and compressive strength was examined, and the model's validity was checked against experimental findings. The investigation reveals an increase in punching shear capacity as the UHPC zone expands in size. Additionally, the hybrid slab behavior is significantly affected by the ratio of UHPC concrete compressive strength to NC.

In the study investigated by Micael M.G. Inácio et.al., [37] the study team assessed the effectiveness of reinforced high-strength concrete (HSC) flat slabs in resisting punching under monotonic vertical stress. Four specimens were evaluated using HSC, while one was tested with NSC. The HSC was limited to a thin layer in the compressive zone. The punching strength values from this method were outstanding, virtually matching those of a slab that was cast in HSC. Based on essential shear cracks, the punching shear in slabs without transverse reinforcement was understood and a novel failure criterion was created that, even with low reinforcement ratios, reliably captures punching shear failures in experimental testing [38]. With a low coefficient of variance, this method produces outcomes that are superior to those produced by existing design codes. According to parametric research, the slab's span, not its thickness, determines the punching shear strength. The study conducted by W.S.A. Nana et.al., [39] examined the shear behavior of RCC slabs at full size that lack shear reinforcement when subjected to concentrated stresses close to longitudinal supports in nuclear structures. It assesses how numerous factors, such as slab depth, loading plate length, compression strength, bottom longitudinal

and transverse reinforcement, and the shear behaviour of the slabs are influenced by the compressive strength and size of the concrete aggregate. Nine full-scale slabs were employed in the experimental campaign, and the study's three-dimensional modelling and calibration were done using Abaqus software. The experimental findings and the suggested numerical model agreed well. The study conducted by L.F. Maya et.al., [40] predicts the punching strength and behavior of reinforced concrete slabs that are reinforced with steel fibers and conventional reinforcement, utilizing a mechanical model. Antonio Marí et.al., [41] performed punching tests on 560 concentric loaded slabs equipped and not equipped with shear reinforcement, and A mechanical model for the determination of punching shear strength was developed. The design parameters, including the critical perimeter position and the punching reinforcement's effective stress, are given physical significance by the model. As it can be observed from the literature, the enhancement of stress and strain-carrying capacity of the slab-column joint in interior, exterior, and edge slabs requires more research and this article mainly focuses on the effect of shear reinforcement, and drop in flat slab-column systems.

3. Materials

For the input of material properties in the ANSYS software, experimental investigations were performed. The reinforcement sample was tested under UTM for Young's modulus and found to be 210 GPa. OPC 53 grade cement as binder, River sand available in the laboratory as Fine aggregate, and Gravel as coarse aggregate were used as materials for mixing of concrete specimens. The physical properties were tested according to Indian Standards and mentioned below in Table 1.

Table 1. Physical properties.

S. No	Property	Test Results
Cement		
1.	Fineness	6%
2.	Specific gravity	3.00
3.	Soundness	3mm
River Sand		
1.	Fineness Modulus	3.08
2.	Bulk Density	1643.3 kg/m3
3.	Specific gravity	2.59
Gravel		
1.	Fineness Modulus	6.41
2.	Bulk Density	1413.3 kg/m3
3.	Specific gravity	2.43

Mix proportions were calculated for M20 grade concrete by fixing the cement content to 350 kg per cubic meter of concrete and a water-to-binder (w/b) ratio of 0.5 as per the codes IS:10262-2019 and IS:456-2000. 3 cubes and 6 cylinders specimens were cast and results of hardened properties such as compressive strength obtained are as shown below in Table 2.

Table 2. Hardened properties of M20 grade concrete

S. No	Property	Test Results
1.	Compressive Strength of Cube after 28 days of curing	27.8 N/mm^2
2.	Compressive Strength of Cylinder after 28 days of curing	24.5 N/mm^2
3.	Young's Modulus	24372 N/mm^2

4. Analytical Study

The beam-column joint of the flat slab system was modelled and analyzed. The column is of circular cross-section. Nine models have been analyzed at the Interior Joint, Exterior Joint, and Edge Joint. Each of them belongs to three categories, one is a flat slab column joint without drop and shear reinforcement, the second is a flat slab column joint with shear reinforcement and without drop and the Third model is a flat slab with drop and without shear reinforcement. The purpose of the tests was to evaluate the effect of shear reinforcement in flat slabs at different locations. The modelled beam-column joints of the flat slab system representing S1:Interior flat slab-column joint without drop and without shear reinforcement; S2 Interior flat slab-column joint with drop and without shear reinforcement; S3 Interior flat slab-column joint with shear reinforcement and without drop; S4: Exterior flat slab-column joint without drop and shear reinforcement; S5: Exterior flat slab-column joint with drop and without shear reinforcement; S6: Exterior flat slab-column joint with shear reinforcement and without drop; S7: Edge flat slab-column joint without drop and shear reinforcement; S8: Edge flat slab-column joint with drop and without shear reinforcement; S9: Edge flat slab-column joint with shear reinforcement and without drop can be seen from the figures 1 to 9 respectively.

Each slab panel modelled is 1000mm X 1000mm X 200mm along with a column of 230mm diameter and 500mm height. For all the models, the column bottom is fixed, and slab edges are provided symmetry conditions to simulate the continuity of edges for the related models. A nominal slab reinforcement is provided in all the models as 12 mm diameter bars at 120mm c/c and the column reinforcement is provided as 12mm diameter bars are provided and ties of 8mm diameter to the column. Shear reinforcement of 12mm diameter with 8mm diameter ties are provided as ring formation around the column reinforcement with size, D/2+d/2 Where D is the depth of the Flat Slab and d is the diameter of the column.

Before meshing the model, it is important to know about the free meshing and mapped meshing options. A free mesh has no restrictions in terms of the element shape it contains and the pattern of the mesh. A mapped area mesh contains either only quadrilateral or triangular elements, while a mapped volume mesh contains tetrahedron or hexahedron elements. In addition, a mapped mesh has a regular pattern, with obvious rows of elements. To mesh the beams, columns, and beam-column joints set the mesh attributes such as element type and material number, etc. By using the mesh tool mesh the geometry of the structure with the mapped volume mesh. The 1-meter x 1-metre length slab and column of 230mm diameter size and 500mm height were auto-meshed.

Input Provided:
Concrete Grade: M20
Grade of Steel: Fe415 N/mm2
Width of Slab (b): 1000 mm
Depth of Slab (D): 200 mm
Length of Column (L): 500mm
Diameter of Column (d):230mm
Clear cover of the reinforcement:25mm
Young's modulus (Es) of steel: 210GPa
Young's Modulus (Ec) of concrete:5000√(f_ck)

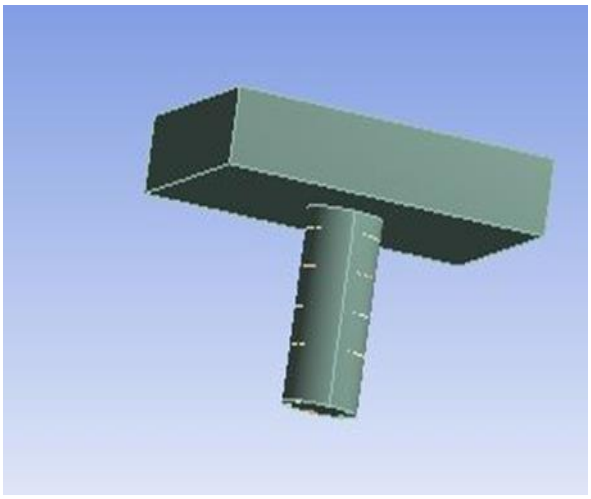


Figure 1. S1: Interior flat slab-column joint without *drop* and without shear reinforcement.

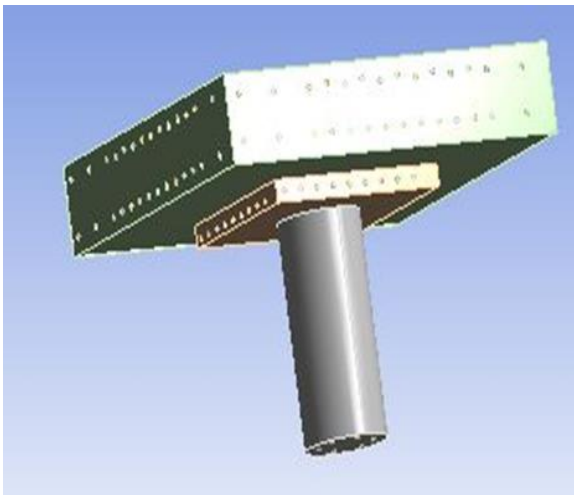


Figure 2. S2: Interior flat slab-column joint with drop and without shear reinforcement.

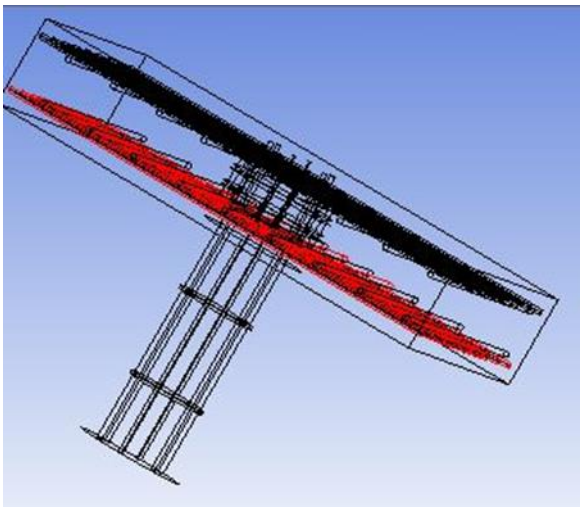


Figure 3. S3 Interior flat slab-column joint with shear reinforcement and without drop.

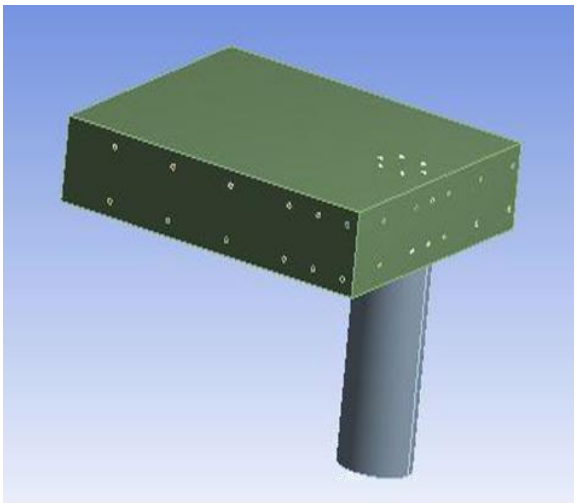


Figure 4. S4: Exterior flat slab-column joint without drop and without shear reinforcement.

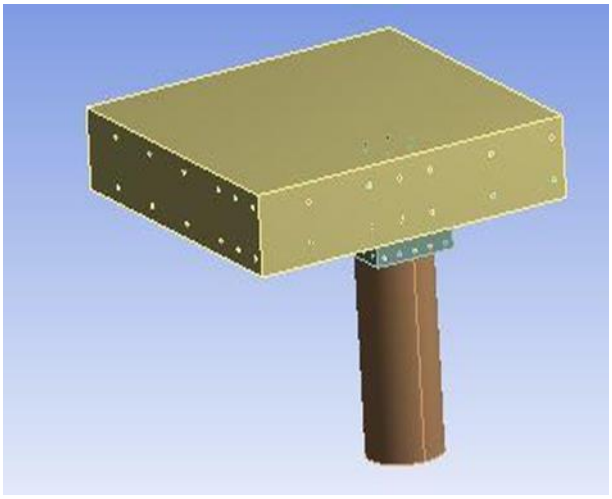


Figure 5. S5: Exterior flat slab-column joint with drop and without shear reinforcement.

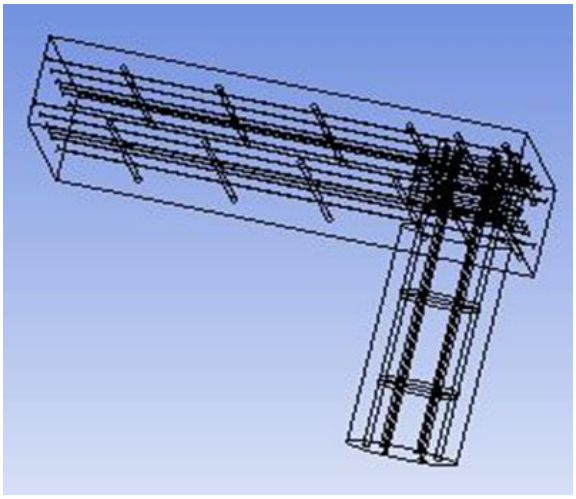


Figure 6. S6: Exterior flat slab-column joint with shear reinforcement and without drop.

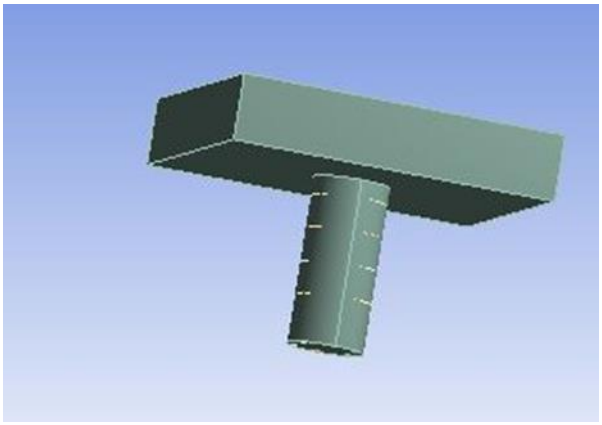


Figure 7. S7: Edge flat slab-column joint without drop and without shear reinforcement.

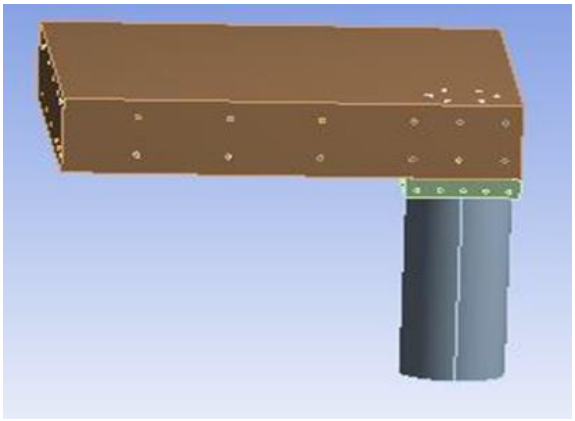


Figure 8. S8: Edge flat slab-column joint with drop and without shear reinforcement.

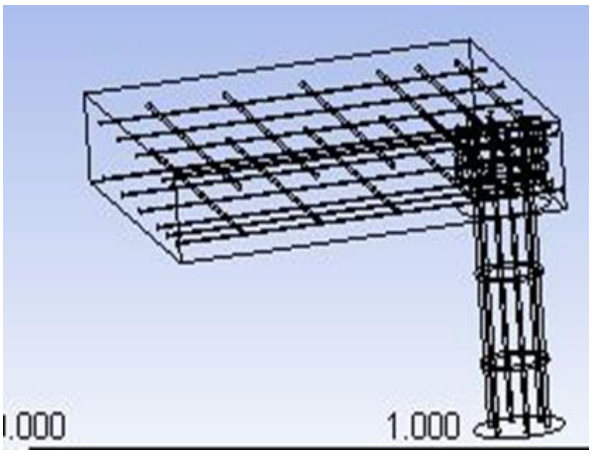


Figure 9. S9: Edge flat slab-column joint with shear reinforcement and without drop.

5. Results and Discussions

Due to the provision of shear reinforcement in the Flat slab, there seems to be an advantage in both the shear stress and principal stress that is shown in the following Tables 3 to 6. Based on the analytical studies carried out on Flat Slab-column joint models using finite element analysis, the following observations are made:

- By incorporating shear reinforcement into Interior Flat slab column joints, there's a decrease in Maximum Principal stress by approximately 33.09% and 21% respectively, while comparing Flat slab column joints with and without a drop.
- Similarly, in Exterior Flat slab column joints, the inclusion of shear reinforcement leads to a reduction of about 30% and 11% in Maximum Principal stress comparing Flat slab column joints with and without a drop.
- For Edge Flat slab column joints, the implementation of shear reinforcement results in a decrease of about 19% and 20% respectively in Maximum Principal stress comparing Flat slab column joints with and without a drop.
- Moreover, the introduction of shear reinforcement in Interior Flat slab column joints leads to a reduction of approximately 13% and 14% respectively in Maximum Shear stress compared to Flat slab column joints with and without a drop.
- In Exterior Flat slab column joints, the incorporation of shear reinforcement results in a decrease of about 12% and 10% respectively in Max Shear stress compared to Flat slab column joints with and without a drop.
- Similarly, for Edge Flat slab column joints, the utilization of shear reinforcement leads to a reduction of about 19% and 20% respectively in Maximum Shear stress compared to Flat slab column joints with and without a drop.

By adding shear reinforcement to the Interior, Exterior, and Edge panels of Flat slab column joints, there is a consistent reduction in both Maximum Shear and Maximum Principal strains compared to joints without such reinforcement. The reduction in Maximum Shear strain ranges from approximately 14% to 19%, while the decrease in Maximum Principal strain ranges from around 11% to 26%. The incorporation of shear reinforcement within Interior, Exterior, and Edge Flat slab column joints has proven to be a remarkably effective strategy. When compared to joints lacking such reinforcement, the observed reductions in both Maximum Shear and Maximum Principal strains are notable and consistent. Impressively, these enhancements demonstrate reductions ranging between approximately 11% to 26% in Maximum Principal strain and 14% to 19% in Maximum Shear strain, affirming the robustness and efficacy of shear reinforcement in managing strain levels across diverse column joint configurations in flat slab structures. This underlines the significance of this method as a means to fortify and optimize structural integrity in various real-world applications.

Table 3. Maximum principal stress variation.

S. No.	Type of Slab	Flat slab without drop and shear reinforcement	Flat slab with drop and without shear reinforcement	Flat slab without a drop and with shear reinforcement
1.	INTERIOR FLAT SLAB	3.66	2.45	1.94
2.	EXTERIOR FLAT SLAB	2.70	1.9	1.69
3.	EDGE SLAB	2.42	1.98	1.55

Table 4. Maximum shear stress variation.

S.No.	Type of Slab	Flat slab without drop and without shear reinforcement	Flat slab with drop and without shear reinforcement	Flat slab without drop and with shear reinforcement
1.	INTERIOR FLAT SLAB	4.56	3.98	3.43
2.	EXTERIOR FLAT SLAB	4.67	4.14	3.74
3.	EDGE SLAB	3.91	2.73	2.21

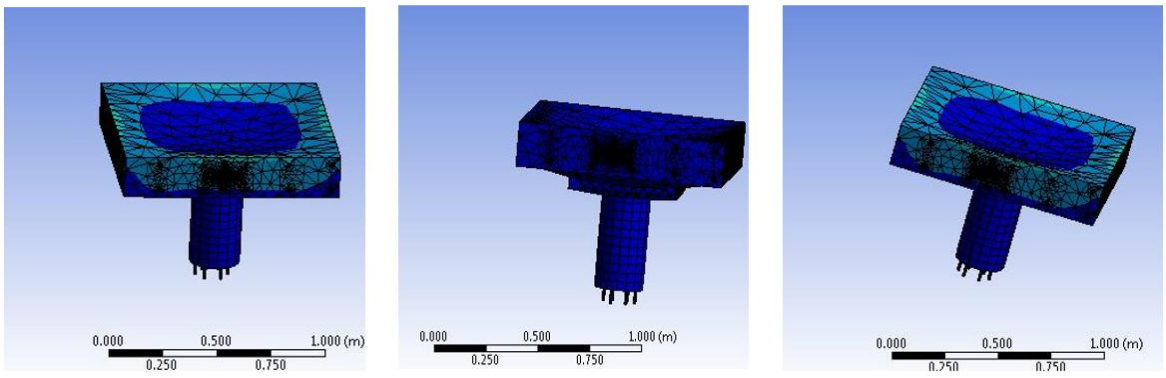
Table 5. Maximum principal strain variation.

S.No.	Type of Slab	Flat slab without drop and without shear reinforcement	Flat slab with drop and without shear reinforcement	Flat slab without drop and with shear reinforcement
1.	INTERIOR FLAT SLAB	2.59	2.15	1.80
2.	EXTERIOR FLAT SLAB	2.56	1.98	1.46
3.	EDGE SLAB	2.25	1.97	1.76

Table 6. Maximum shear strain variation.

S.No.	Type of Slab	Flat slab without drop and without shear reinforcement	Flat slab with drop and without shear reinforcement	Flat slab without drop and with shear reinforcement
1.	INTERIOR FLAT SLAB	3.28	2.80	2.40
2.	EXTERIOR FLAT SLAB	2.56	2.15	1.76
3.	EDGE SLAB	2.74	2.36	1.98

With the introduction of slab drop and the shear reinforcement, the magnitude of Maximum principal stress is reduced by about 33.09% and 47% respectively in the Interior Flat slab column joint, reduced by about 30% and 38% respectively in the Exterior Flat slab column joint, reduced by about 19% and 34%respectively in Edge Flat slab column joint. Figures 10 to 12 show the maximum principal stress contours obtained in ANSYS in all the 9 slab models.

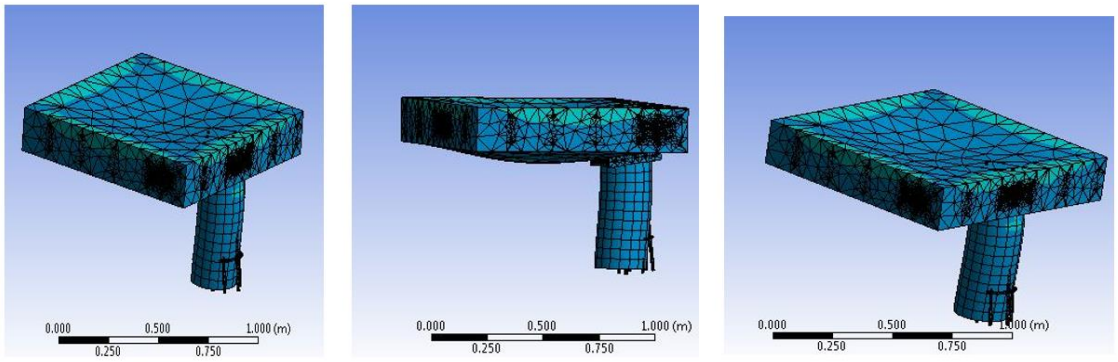


S1: Interior Flat Slab without drop and without shear reinforcement

S2 Interior Flat Slab with drop and without shear reinforcement

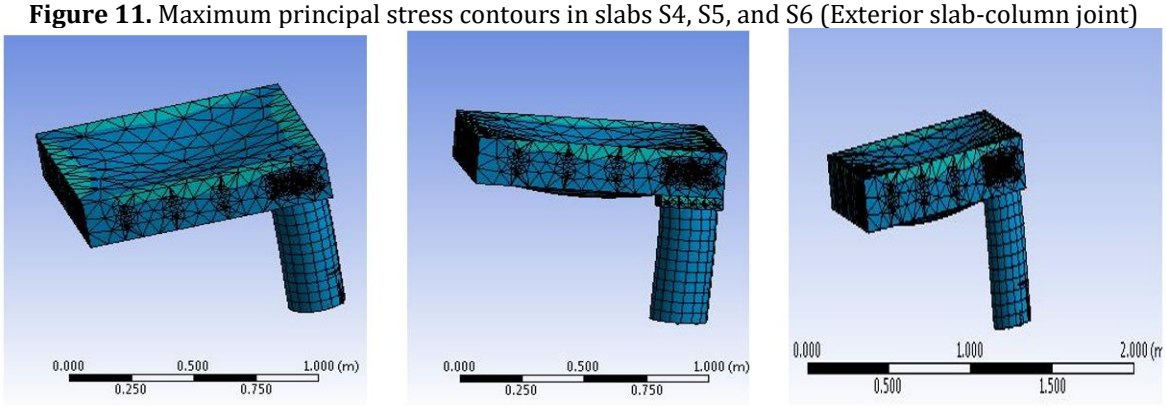
S3:Flat slab without drop with shear reinforcement

Figure 10. Maximum principal stress contours in slabs S1, S2, and S3 (Interior slab-column joint)



S4 Exterior Flat Slab without drop and without shear reinforcement **S5 Exterior Flat Slab with drop and without shear reinforcement** **S6: Exterior Flat Slab without drop and with shear reinforcement**

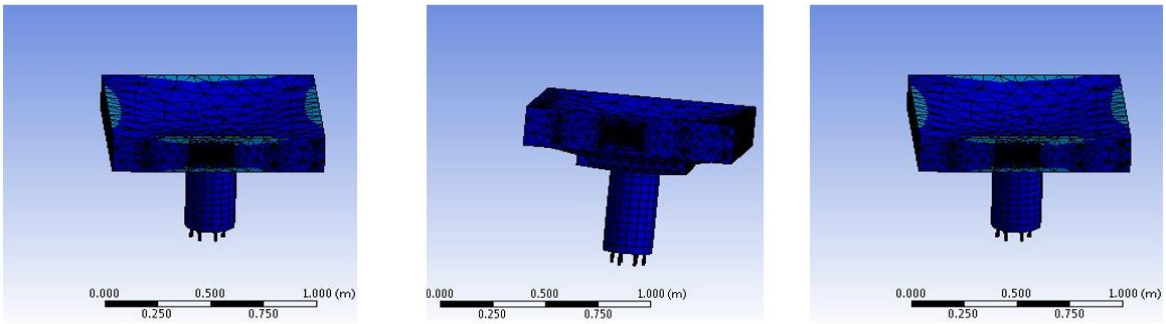
Figure 11. Maximum principal stress contours in slabs S4, S5, and S6 (Exterior slab-column joint)



S7 Edge Flat Slab without drop and Without shear reinforcement **S8 Edge Flat Slab with drop and without shear reinforcement** **S9 Edge Flat Slab without drop and with shear reinforcement**

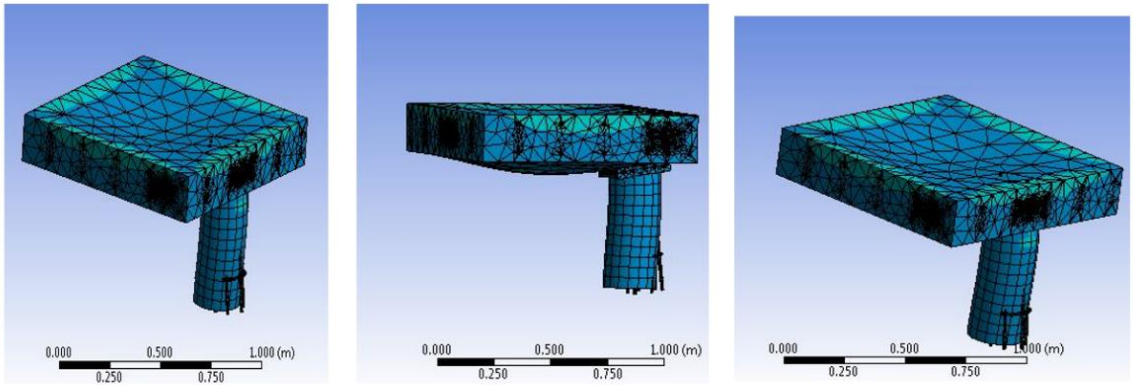
Figure 12. Maximum principal stress contours in slabs S7, S8, and S9 (Edge slab-column joint)

As it can be observed from the figures 10 to 12, the inclusion of shear reinforcement and column drop significantly reduces the maximum principal stress in the slab-column joint at different locations. With the introduction of slab drop and the shear reinforcement, the magnitude of Maximum Shear stress is reduced by about 13% and 25% respectively in Interior Flat slab column joint, reduced by about 12% and 21% respectively in Exterior Flat slab column joint, reduced by about 31% and 42% respectively in Edge Flat slab column joint. Figures 13 to 15 represent contours of maximum shear stress for all the 9 slab models.



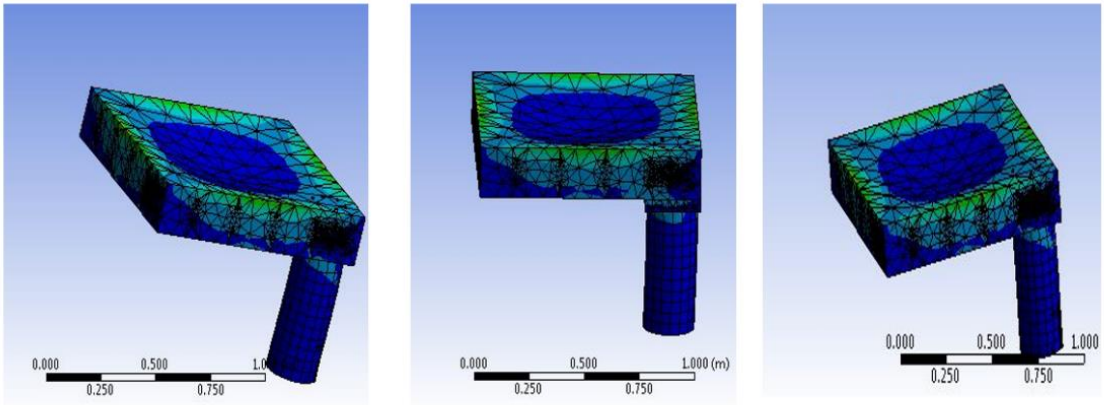
S1 Flat Slab without drop and without shear reinforcement **S2 Flat Slab with drop and without shear reinforcement** **S3 Flat Slab with drop and without shear reinforcement**

Figure 13. Maximum shear stress contours in slabs S1, S2, and S3 (Interior slab-column joint)



S4 Exterior Flat Slab without drop and without shear Reinforcement **S5 Exterior Flat Slab with drop and without shear reinforcement** **S6: Exterior Flat Slab without drop and with shear reinforcement**

Figure 14. Maximum shear stress contours in slabs S4, S5, and S6 (Exterior slab-column joint)



S7 Flat Slab without drop and without Reinforcement **S8 Flat Slab with drop and without shear Reinforcement** **S9 Flat Slab with drop and without shear Reinforcement**

Figure 15. Maximum shear stress contours in slabs S7, S8, and S9 (Edge slab-column joint)

As it can be observed from Figures 10 to 12 and 13 to 15, the inclusion of shear reinforcement and column drop significantly reduces the maximum shear stress in the slab-column joint at different locations. With the introduction of slab drop and the shear reinforcement, the magnitude of Maximum Principal strain is reduced by about 17% and 30% respectively in the Interior Flat slab column joint, reduced by about 23% and 43%respectively in the Exterior Flat slab column joint, reduced by about 13% and 22% respectively in Edge Flat slab column joint. With the introduction of slab drop and the shear reinforcement, the magnitude of Maximum Shear strain is reduced by about 15% and 27% respectively in the Interior Flat slab column joint, reduced by about 16% and 31%respectively in the Exterior Flat slab column joint, reduced by about 14% and28% respectively in Edge Flat slab column joint.

6. Conclusions

- The insights derived from the preceding chapter underscore a notable enhancement in the shear capacity at the junctions of Flat-slab and columns across various scenarios, primarily attributable to the inclusion of slab drop and shear reinforcement.
- Upon meticulous observation, it becomes apparent that the introduction of a slab drop yielded a decrease in maximum principal stress within a range of 18.18% to 33.06%.

Interestingly, the application of shear reinforcement displayed an even more significant impact, showcasing a reduction in principal stress spanning between 35.95% to 46.99%, with the most pronounced effect noted at the interior panel.

- Similarly, in the realm of maximum shear stress, the provision of a slab drop led to a reduction ranging from 12.72% to 30.18%, particularly significant at the edge panel. Yet, with the implementation of shear reinforcement, an even more substantial reduction in the range of 24.78% to 43.48% was observed, showcasing its effectiveness, especially at the edge panel.
- In summary, the comparative assessment underscores the enhanced effectiveness of flat slab-column joints strengthened by shear reinforcement. This improvement is evident in various aspects such as principal stress, principal strain, shear stress, and shear strain, when compared to joints featuring a slab drop.
- The comprehensive finite-element analysis delineated herein provides valuable insights into the nuanced behaviour and potential failure modes of flat-slab column joints across various locations. However, it's imperative to underscore the necessity for meticulous modelling of concrete and shear reinforcement to ensure the precision and fidelity of these findings. Such refined modelling techniques hold promise in offering strategies to augment the shear capacity across diverse concrete types and grades.

Declaration of Competing Interests

The authors declare that they have no known competing financial interests or personal relationships that could have appeared to influence the work reported in this paper.

Credit Author Statement

Tangudu Manoj: Conceptualization, Supervision, Modelling, Writing – Original draft & revision, Data curation &validation; Jagadeesh Bommisetty: Conceptualization, Supervision, Methodology, Writing – Original draft & revision; Tirukovela Sai Keertan: Conceptualization, Supervision, Writing – Original draft & revision, Data validation, Data curation; P.V.V.S.S.R. Krishna: Conceptualization, Supervision, Writing – Original draft & revision, Data validation, Data curation.

7. References

[1] Mengzhu Diao, Yi Li and Xinzheng Lu,Post-Punching Mechanism of Slab-Column Joints Subjected Upward and Downward Punching Shear Actions, Structures Conference 2018, American Society of Civil Engineers. doi:10.1061/9780784481349.023

[2] M. Hasan Meisami, Davood Mostofinejad, and Hikaru Nakamura, Punching Shear Strengthening of Two-Way Flat Slabs with CFRP Grids,2013, American Society of Civil Engineers. DOI: 10.1061/(ASCE)CC.1943-5614.0000443.

[3] Long Nguyen-Minh, MariánRovňákand Toan Tran-Quoc, Punching Shear Capacity of Interior SFRC Slab-Column Connections, Journal of Structural Engineering © ASCE / MAY 2012 / 613, DOI: 10.1061/(ASCE)ST.1943-541X.0000497.

[4] P. R. Walker, P. E.Regan, Corner column-slab connections in concrete flat plates, Journal of Structural Engineering,Vol. 113, No. 4, April, 1987.©ASCE, https://doi.org/10.1061/(ASCE)0733-9445(1987)113:4(704).

[5] M. Priya,S.Greeshma, K. N. Suganya, Finite Element Analysis of Slab-Column Joint Under Lateral Loading, Asian Journal of Civil Engineering (BHRC) VOL. 16,no. 2 (2015) Pages 291-300.

[6] Ronaldo B. Gomes, Paul E. Regan,Punching resistance of RC Flat slabs with shear Reinforcement, Journal of Structural Engineering /JUNE 1999, https://doi.org/10.1061/(ASCE)0733-9445(1999)125:6(684).

[7] Aikaterini S.Genikomsou, Maria Anna Polak, Finite-Element Analysis of Reinforced Concrete Slabs with Punching Shear Reinforcement, July 2016, American Society of Civil Engineers, https://doi.org/10.1061/(ASCE)ST.1943-541X.0001603.

[8] Alex M.D. de Sousa, Eva O.L. Lantsoght, Aikaterini S. Genikomsou, Pablo A. Krah and Mounir K. El Debs, Behavior and punching capacity of flat slabs with the rational use of UHPFRC: NLFEA and analytical predictions, Engineering Structures 244 (2021) 112774, https://doi.org/10.1016/j.engstruct.2021.112774.

[9] Soliman Alkhatib and Ahmed Deifalla, Punching Shear Strength of FRP-Reinforced Concrete Slabswithout Shear Reinforcements: A Reliability Assessment, Polymers 2022, 14, 1743. https://doi.org/10.3390/polym14091743

[10] Tung D. Dang, Duong T. Tran, Long Nguyen-Minh and Ayman Y. Nassif, Shear resistant capacity of steel fibres reinforced concrete deep beams: An experimental investigation and a new prediction model, 2021 Institution of Structural Engineers.Published by Elsevier Ltd., https://doi.org/10.1016/j.istruc.2021.05.091.

[11] Sanjay P N,Umesh Mahesh S S, Mahesh Prabhu K, Behaviour of Flat Slab RCC Structure Under Earthquake Loading, International Journal of Engineering Research & Technology, May 2014, Vol. 3 Issue 5,.DOI : 10.17577/IJERTV3IS051624.

[12] Lu, X., Lin, K., Li, Y., Guan, H., Ren, P., & Zhou, Y. (2017). Experimental investigation of RC beam-slab substructures against progressive collapse subject to an edge-column-removal scenario. Engineering Structures, 149, 91-103, http://dx.doi.org/10.1016/j.engstruct.2016.07.039.

[13] Yang, Y., Li, Y., Guan, H., Diao, M., & Lu, X. (2021). Enhancing post-punching performance of flat plate-column joints by different reinforcement configurations. Journal of Building Engineering, 43, 102855, https://doi.org/10.1016/j.jobe.2021.102855.

[14] Ma, F., Gilbert, B. P., Guan, H., Xue, H., Lu, X., & Li, Y. (2019). Experimental study on the progressive collapse behaviour of RC flat plate substructures subjected to corner column removal scenarios. Engineering Structures, 180, 728-741, https://doi.org/10.1016/j.engstruct.2018.11.043.

[15] Ma, F., Gilbert, B. P., Guan, H., Lu, X., & Li, Y. (2020). Experimental study on the progressive collapse behaviour of RC flat plate substructures subjected to edge-column and edge-interior-column removal scenarios. Engineering Structures, 209, 110299, https://doi.org/10.1016/j.engstruct.2020.110299.

[16] Qian, K., & Li, B. (2015). Load-resisting mechanism to mitigate progressive collapse of flat slab structures. Magazine of concrete research, 67(7), 349-363, https://doi.org/10.1680/macr.14.00293.

[17] Russell, J. M., Owen, J. S., & Hajirasouliha, I. (2015). Experimental investigation on the dynamic response of RC flat slabs after a sudden column loss. Engineering Structures, 99, 28-41, http://dx.doi.org/10.1016/j.engstruct.2015.04.040.

[18] Choi, K. K., & Kim, J. C. (2015). Nonlinear model simulating load–deformation relationship of flat plate structures. Engineering Structures, 85, 26-35, http://dx.doi.org/10.1016/j.engstruct.2014.12.008.

[19] Navarro, M., Ivorra, S., & Varona, F. B. (2018). Parametric computational analysis for punching shear in RC slabs. Engineering Structures, 165, 254-263, https://doi.org/10.1016/j.engstruct.2018.03.035.

[20] Dam, T. X., & Wight, J. K. (2016). Flexurally-triggered punching shear failure of reinforced concrete slab–column connections reinforced with headed shear studs arranged in orthogonal and radial layouts. Engineering structures, 110, 258-268, http://dx.doi.org/10.1016/j.engstruct.2015.11.050.

[21] Cantone, R., Fernández Ruiz, M., Bujnak, J., & Muttoni, A. (2019). Enhancing punching strength and deformation capacity of flat slabs. ACI structural journal, 116(ARTICLE), 261-274, https://doi.org/10.14359/51716842.

[22] Nguyen-Minh, L., Rovňák, M., Tran-Ngoc, T., & Le-Phuoc, T. (2012). Punching shear resistance of post-tensioned steel fiber reinforced concrete flat plates. Engineering Structures, 45, 324-337, http://dx.doi.org/10.1016/j.engstruct.2012.06.027.

[23] Caldentey, A. P., Lavaselli, P. P., Peiretti, H. C., & Fernandez, F. A. (2013). Influence of stirrup detailing on punching shear strength of flat slabs. Engineering Structures, 49, 855-865, http://dx.doi.org/10.1016/j.engstruct.2012.12.032.

[24] Diao, M., Li, Y., Guan, H., Lu, X., Xue, H., & Hao, Z. (2021). Post-punching mechanisms of slab–column joints under upward and downward punching actions. Magazine of Concrete Research, 73(6), 302-314, https://doi.org/10.1680/jmacr.19.00217.

[25] Yu, J., Luo, L., & Li, Y. (2018). Numerical study of progressive collapse resistance of RC beam-slab substructures under perimeter column removal scenarios. Engineering Structures, 159, 14-27, https://doi.org/10.1016/j.engstruct.2017.12.038.

[26] Nguyen, T. N., Nguyen, T. T., & Pansuk, W. (2017). Experimental study of the punching shear behavior of high-performance steel fiber reinforced concrete slabs considering casting directions. Engineering Structures, 131, 564-573, http://dx.doi.org/10.1016/j.engstruct.2016.10.031.

[27] Shoukry, M. E., Tarabia, A. M., & Yassin, A. M. (2022). Punching shear strength of ultra-high-performance fibre concrete slab–column connections. Proceedings of the Institution of Civil Engineers-Structures and Buildings, 175(8), 644-656, https://doi.org/10.1680/jstbu.19.00201.
[28] Zohrevand, P., Yang, X., Jiao, X., & Mirmiran, A. (2015). Punching shear enhancement of flat slabs with partial use of ultrahigh-performance concrete. Journal of Materials in Civil Engineering, 27(9), 04014255, https://doi.org/10.1061/(ASCE)MT.1943-5533.0001219.
[29] Genikomsou, A. S., & Polak, M. A. (2015). Finite element analysis of punching shear of concrete slabs using damaged plasticity model in ABAQUS. Engineering structures, 98, 38-48, http://dx.doi.org/10.1016/j.engstruct.2015.04.016.
[30] Genikomsou, A. S., & Polak, M. A. (2016). Finite-element analysis of reinforced concrete slabs with punching shear reinforcement. Journal of Structural Engineering, 142(12), 04016129, DOI: 10.1061/(ASCE)ST.1943-541X.0001603.
[31] Genikomsou, A. S., & Polak, M. A. (2017). 3D finite element investigation of the compressive membrane action effect in reinforced concrete flat slabs. Engineering Structures, 136, 233-244, http://dx.doi.org/10.1016/j.engstruct.2017.01.024.
[32] Milligan, G. J., Polak, M. A., & Zurell, C. (2020). Finite element analysis of punching shear behaviour of concrete slabs supported on rectangular columns. Engineering Structures, 224, 111189, https://doi.org/10.1016/j.engstruct.2020.111189.
[33] Navarro, M., Ivorra, S., & Varona, F. B. (2020). Parametric finite element analysis of punching shear behaviour of RC slabs reinforced with bolts. Computers & Structures, 228, 106147, https://doi.org/10.1016/j.compstruc.2019.106147.
[34] Milligan, G. J., Anna Polak, M., & Zurell, C. (2021). Impact of column rectangularity on punching shear strength: Code predictions versus finite element analysis. Journal of Structural Engineering, 147(2), 04020331, DOI: 10.1061/(ASCE) ST.1943-541X.0002889.
[35] Menna, D. W., & Genikomsou, A. S. (2021). Punching shear response of concrete slabs strengthened with ultrahigh-performance fiber-reinforced concrete using finite-element methods. Practice Periodical on Structural Design and Construction, 26(1), 04020057, DOI: 10.1061/(ASCE)SC.1943-5576.0000546.
[36] Kadhim, M. M., Saleh, A. R., Cunningham, L. S., & Semendary, A. A. (2021). Numerical investigation of non-shear-reinforced UHPC hybrid flat slabs subject to punching shear. Engineering Structures, 241, 112444, https://doi.org/10.1016/j.engstruct.2021.112444.
[37] Inácio, M. M., Lapi, M., & Ramos, A. P. (2020). Punching of reinforced concrete flat slabs–Rational use of high strength concrete. Engineering Structures, 206, 110194, https://doi.org/10.1016/j.engstruct.2020.110194.
[38] Muttoni, A. (2008). Punching shear strength of reinforced concrete slabs without transverse reinforcement. ACI structural Journal, 105(ARTICLE), 440-450, DOI: 10.14359/56428.
[39] Nana, W. S. A., Bui, T. T., Limam, A., & Abouri, S. (2017, May). Experimental and numerical modelling of shear behaviour of full-scale RC slabs under concentrated loads. In Structures (Vol. 10, pp. 96-116). Elsevier, http://dx.doi.org/10.1016/j.istruc.2017.02.004.
[40] Maya, L. F., Ruiz, M. F., Muttoni, A., & Foster, S. J. (2012). Punching shear strength of steel fibre reinforced concrete slabs. Engineering Structures, 40, 83-94, http://dx.doi.org/10.1016/j.engstruct.2012.02.009.
[41] Marí, A., Cladera, A., Oller, E., & Bairán, J. M. (2018). A punching shear mechanical model for reinforced concrete flat slabs with and without shear reinforcement. Engineering Structures, 166, 413-426, https://doi.org/10.1016/j.engstruct.2018.03.079.

IOP Conference Series: Earth and Environmental Science

PURPOSE-LED PUBLISHING™

PAPER • OPEN ACCESS

Rehabilitation and restoration of the historic church using the conventional method

To cite this article: D. Monica and D. Brindha 2024 *IOP Conf. Ser.: Earth Environ. Sci.* **1409** 012041

View the article online for updates and enhancements.

You may also like

- Study of the structure and chemical composition of the protective coating of a fist stage gas turbine blade after regenerative heat treatment
D I Davidov, N V Kazantseva, N I Vinogradova et al.
- Effect of protective coating on random birefringence variations in anisotropic optical fibres in response to temperature changes
S.K. Morshnev, V.P. Gubin, N.I. Starostin et al.
- Highly Dense Mn-Co Spinel Coating for Protection of Metallic Interconnect of Solid Oxide Fuel Cells
Sung-Il Lee, Jongsup Hong, Hyoungchul Kim et al.



This content was downloaded from IP address 47.247.77.11 on 27/11/2024 at 05:43

Rehabilitation and restoration of the historic church using the conventional method

Monica, D.[1*] and D. Brindha[1]

[1] Department of Civil Engineering, Thiagarajar College of Engineering, Madurai, Tamil Nadu, India

[*]E-mail: monikad@student.tce.edu

Abstract. This abstract outline the restoration process of St. Michael and All Angels Church, which was constructed in the Thoothukudi region of Tamil Nadu in 1883. The church is a significant landmark and an important example of local ecclesiastical architecture. The project aims to use a methodical restoration approach to preserve the building's historical and architectural identity. The first step in the process is to identify any structural deficiencies, which will then be addressed using traditional techniques. Traditional materials will also be used to replace any damaged parts, such as timber fittings, stained glass windows, and decorative elements, to maintain authenticity. The building will be assessed using a standard penetration radar test (GPR). The restoration work will use lime mortar consisting of lime (CaO), sand (SiO2), and juice extract from gall nut and jaggery, similar to the existing structure. The roof will be restored using a 5-layer protective coating. Special measures will be taken to preserve the historic significance of the building.

Keywords. Rehabilitation, Conventional Method, Lime Mortar, Grouting, Protective Coating.

1. Introduction

Bishop Sargent consecrated the St. Michael and All Angels church on St. Andrew's Day, November 30th, 1883. The church, originally built by Reverend H. B. Norman, was 152 feet long and 63 feet wide, with an altar standing four feet high and a designated choir area. The people of Muldaur later added a 193-foot tower with seven floors to the church, topped with a crown stone featuring a gold cross. This new church tower was dedicated on September 29th, 1929. The research delves into the obstacles and possibilities of sustainable building restoration in Brazil, emphasizing the importance of addressing regulatory, technical, and financial aspects to advance sustainable rehabilitation projects in the nation [1]. The study delved into sustainable practices in the restoration of heritage buildings by conducting a detailed analysis of a specific case [2][3]. This source probably talks about the significance of utilizing traditional materials and methods when restoring and renovating heritage structures to preserve their authenticity and historical precision [4]. The researchers emphasized the importance of balancing conservation values and modern restoration techniques [5]. The significance of this topic stems from the fast urban growth in many Asian cities, leading to difficulties in preserving cultural heritage and improving living conditions in their old city centers [6] [7]. This resource

Content from this work may be used under the terms of the Creative Commons Attribution 4.0 licence. Any further distribution of this work must maintain attribution to the author(s) and the title of the work, journal citation and DOI.
Published under licence by IOP Publishing Ltd

provides guidelines and criteria for renovating historic buildings while incorporating modern amenities and technologies [8]. The case study highlights the significance of rehabilitating historical buildings with suitable construction methods and exploring potential alternative approaches to ensure their preservation [9]. The document offers advice on repointing mortar joints in old masonry buildings, emphasizing the need to use suitable materials and methods to maintain the historical authenticity of the structure [10]. Non-destructive testing (NDT) methods are crucial in assessing the condition of heritage structures without causing any damage. Given the significant number of historically important buildings, it is essential to use NDT techniques to preserve and manage these architectural treasures [11][12][13]. Non-destructive evaluation techniques can be used to preserve ancient masonry buildings and maintain architectural heritage [14]. The research highlights the importance of combining field observations and laboratory experiments to inform restoration decisions [15]. NDT techniques and FTIR analysis gave insights into bridge conditions, aiding the development of maintenance plans [16]. Experts emphasized the importance of non-destructive testing in maintaining heritage buildings. They pointed out methods such as ground-penetrating radar, infrared thermography, and ultrasonic testing as valuable tools for preserving historical structures [17]. Ground Penetrating Radar (GPR) is often used to assess and evaluate historic structures. It helps uncover concealed flaws, structural irregularities, and decay without causing any damage to the building [18]. Utilizing local limestone for restoring heritage buildings, such as in the case of the Frumoasa Monastery project, is crucial for preserving their historical significance [19]. The results showed that this type of mortar is long-lasting, works well with traditional materials, is user-friendly, and effectively preserves and rejuvenates stone buildings [20]. The study examined ancient mortar practices in Crete and suggested restoration mortar guidelines for current structures. The research proposed tailored formulas for restoration mortars to maintain historical building integrity [21]. The focus of the restoration project is to preserve the historical and architectural identity of the church by using traditional techniques. Any structural deficiencies are identified and addressed with traditional methods, while damaged parts are replaced with traditional materials such as timber fittings, stained glass windows, and decorative elements to maintain authenticity. The restoration plan includes a preliminary assessment using the Ground penetration radar test (GPR), and the use of lime mortar containing lime, sand, and natural extracts to match the existing structure. Additionally, the church's roof is restored with a 5-layer protective coating, underscoring the importance of preserving historic buildings.

2. Site investigation

Site investigation for health monitoring of structures is a thorough evaluation that strives to comprehend the condition and behaviour of a structure over a while. It typically involves a variety of techniques, such as visual inspections, non-destructive testing, and structural analysis. Through these methods, engineers collect data on factors like material properties, structural integrity, and environmental influences to assess the overall health of the structure. Visual inspection is the most effective way to evaluate the structural soundness of a building and identify any typical distress symptoms and associated problems. Upon visual inspection, it was discovered that the building has severe external damage, but it is still strong enough to bear loads. Therefore, only retrofitting is needed to ensure its safety.

2.1. Assessment of building damages during the site visit:

Monitoring the health of the church's structure provides valuable insights for guiding maintenance and rehabilitation efforts, ensuring its preservation for future generations to cherish. After completing the site investigation, it was discovered that the interior walls of the church had suffered severe damage and the bricks were exposed. The ceiling of the church had also deteriorated, with mortar falling off. The dome of the church had been damaged due to weathering conditions and cracks were also noted on its surface. Some common signs of masonry problems are as follows the bulging of the wall suggests that there has been some movement. Cracks in the wall indicate that there has been shifting within the structure. Straining is a sign of too much moisture present. Crumbling is a result of moisture seeping in due to low-quality brick or sandblasting. Paint blistering is a sign that moisture is trapped beneath the paint. Cracks in the mortar show that the cement is too rigid and is breaking off during freeze-thaw cycles.



Figure 1. Church inner celling area



Figure 2. Brick wall inside the building area

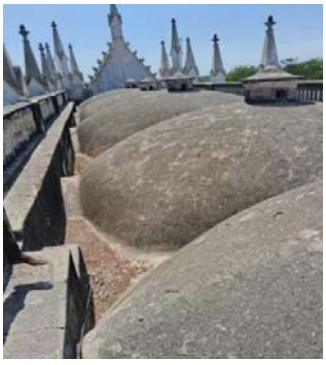


Figure 3. Domes affected due to dampness

2.2. Tastings to be performed

Lime content test: The lime content test is an important process used to determine the amount of lime present in a sample of mortar. Lime is a crucial ingredient in traditional mortar mixes, providing workability, plasticity, and aiding in the binding of other materials like sand and water. To perform the test, a sample of the mortar is collected and prepared with care. The mortar sample is then mixed with a known quantity of hydrochloric acid (HCl) under controlled conditions. The acid reacts with lime in the mortar, producing carbon dioxide gas as a byproduct. The volume of gas generated during the reaction is measured using a suitable apparatus, such as a gas burette or a gas collection system. The lime content in the mortar can be calculated using stoichiometric principles based on the volume of gas produced. This test is crucial for evaluating the quality and composition of mortar mixes, particularly in historic preservation projects where traditional lime-based mortars are commonly used. Based on the test result, the raw material for repair work is selected as the lime content that matches the existing lime mortar used in the church.

GP radar scanning: Ground Penetrating Radar (GPR) testing is a non-destructive method used to assess the condition of structures by sending electromagnetic waves into the ground or structures and analyzing changes in material properties. It can detect defects like cracks, voids, delamination, and corrosion in concrete structures. GPR creates detailed images of the subsurface, allowing engineers to visualize potential issues without causing damage. By analyzing reflections and

diffractions of electromagnetic waves, GPR can identify defects based on variations in signal characteristics such as amplitude, travel time, and waveform. Defects like voids, delamination, cracks, and corrosion can be detected by observing irregular wave patterns or discontinuities in the GPR data.

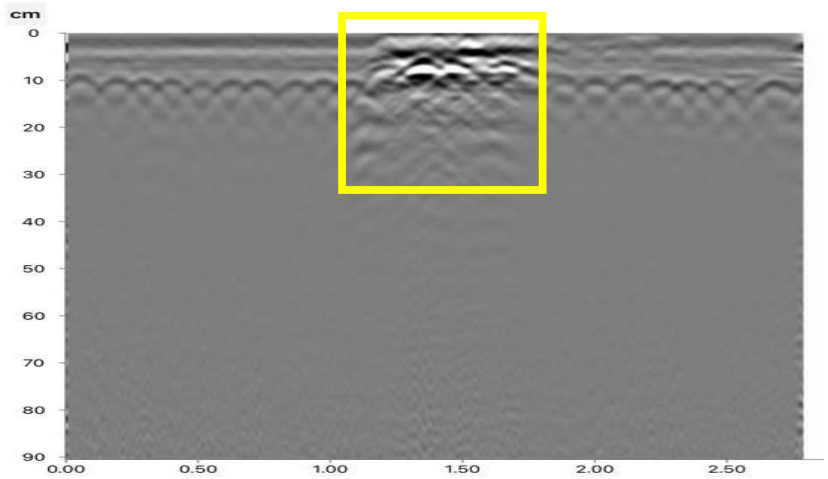


Figure 4. Image obtained from GPR test

2.3. Summary of test results

- Lime is an essential component of traditional mortar mixes. It contributes to the plasticity and workability of the mixture and helps bind other materials like sand and water. When selecting materials for a new mix, opting for ones with similar properties to the substrate enhances the bonding between the two.
- Ground Penetrating Radar (GPR) testing is an important technique for monitoring the health of structures. It provides a non-destructive and efficient way of assessing their condition, which contributes to their safety, longevity, and resilience. When using GPR, it may be revealed that there are voids inside the wall that need to be filled in order to ensure the safety of the structure.

3. Methodology for executing repair work

The methodology for executing repair work on an old church involves a structured approach to ensure efficiency, quality, and preservation of the structure's historical integrity.

- Cleaning
- Chipping
- Grouting
- Supporting member
- Plastering
- Waterproofing for roof

3.1. Cleaning

- Clear the work area of any obstacles and protect surrounding features from damage.

- If needed, erect scaffolding or other access equipment for safe and efficient work.
- Address any immediate structural concerns that may compromise the safety or stability of the building.
- Use temporary supports or shoring where necessary to stabilize weakened or damaged structural elements.

3.2. Chipping

Chipping off loose mortar is an essential step in repairing an old church. This process helps to maintain the structural integrity and aesthetic appeal of the building. The chipping of the loosened mortar was achieved using breakers that produced minimal vibrations. To inspect the mortar joints, use a probing tool and a small hammer that vibrates less. Gently tap along the joints while listening for any hollow or loose-sounding areas. Before you begin the repair work, clean the area around the deteriorated mortar joints using a stiff brush or compressed air to remove loose debris and dirt.

3.3. Grouting

Grouting is a process of filling gaps and crevices, particularly in masonry and construction work. It is used to enhance the structural stability of buildings and prevent water leakage. Depending on the grout type and project requirements, applying a sealer may be necessary to enhance its durability and stain resistance.



Figure 5. Pipe inserted for grouting



Figure 6. Grout mixture (lime+cement+cebex100)

For the purpose of grouting, a combination of cebex100 resin, lime, and cement is used. To make the mixture, 10g of cebex100 resin is added to every 50kg of lime. Pipes are then inserted into the wall through pre-made holes at defined intervals to fill voids and cracks. The grouting mixture is made up of a proper mix of lime, cement, and cebex100 resin. A pump is connected to one end of the pipe and the grout mixture is injected under specified pressure. The grouting process continues until the mixture flows out of the other end of the pipe and is then sealed with a combination of cement and lime.

3.4. Supporting member

Shear key: Shear key bars provide extra resistance against shear forces and improve structural performance under different loading conditions. Properly designing and installing them is essential

for guaranteeing the safety and longevity of the structure. In this particular structure, a shear key bar with a diameter of 10mm is used.

Wire mesh: A wire mesh with a size of 50x50mm and a diameter of 8mm is being used. A shear key bar and wire mesh arrangement are a construction technique used to increase the strength and stability of concrete structures. It involves the placement of horizontal steel bars (shear key bars) in the concrete, which are then covered with a layer of wire mesh. This arrangement helps to distribute the weight and force evenly, preventing the concrete from cracking or breaking under stress.



Figure 7. Shear key bar and wire mesh arrangement



Figure 8. Preparation of extract water from gallnut and jaggery powder

3.5. Plastering

Lime mortar has been a popular choice in traditional masonry construction for centuries. When restoring old buildings, lime mortar helps maintain their historical authenticity and preserves the traditional craftsmanship and architectural character of the structure. Properly applied lime mortar can enhance the long-term durability and performance of old buildings. Its breathable and flexible nature allows for natural moisture management and reduces the risk of moisture-related deterioration, such as spalling, efflorescence, and salt damage. Lime mortar also ages gracefully over time, developing a natural patina that adds to the character of historic buildings. To make lime mortar,

lime is used as the raw material. The plaster is a mixture of lime, water extracted from gallnut, and jaggery. The gallnut and jaggery are taken in equal amounts and ground to a powder form, which is then soaked in water for one month. For the preparation of mortar, extracted water from the gallnut and jaggery is used along with lime.

4. Waterproofing for roof

4.1. Dome & terrace area waterproofing work

The construction task involves providing and laying a high-quality waterproofing and heat insulation system on an existing roof slab. The system should consist of five layers of elastomeric material that is cold-applied and heat reflective. The total system thickness should be between 1500 to 1800 microns, as directed by the Engineer in Charge and as per the manufacturer's specifications. The task also includes fixing roof leaks through the use of a five-layer treatment with MIX GUARD HR-5-layer system elastomeric waterproofing and heat reflective coating. The rate quoted should cover surface preparation unless a separate item is available in the schedule.

4.2. General material specifications

- Density: 1.2 gm/cc
- Solids content 80% + 2% by weight
- Tensile strength ASTM D 412-87: 6.0 N/Sq.mm
- Water penetration D/N 1048: No leak at 7 bars (+side)
- Adhesion to substrate ASTM D 4541: >1.2 N/Sq.mm
- Water vapour transmission ASTM E 96: 19 g/Sqm/day
- Crack bridging ASTM C836: Cracks up to Max 2mm width in slab/plastering to be taken care
- Application temperature: 5 to 50 C.
- Solar reflectance value: 84% to 87% (ASTM E-903).

4.3. Surface preparation

- Cleaning the whole area with a wire brush. Chipping all loose/dead mortar thoroughly.
- Cleaning the entire area with high pressure water jetting to remove all loose particles/grease/oil/dust/dirt/curing compounds etc.
- Surface cracks must be filled with Mix build AP and wide cracks must be cut and repaired with Mix build SR polymer modified repair mortar.

4.4. Application of mix guard hr five-layer system with brush

(i) First layer – mix prime AC-100:

The base primer coat shall be applied by utilizing Mix Prime AC 100 compound, created through the combination of Mix Prime AC-100, water, and cement at a volume ratio of 2:1:3 [Mix prime AC 100: Water: Cement]. This mixture should be applied using a slow speed drill with a paddle, ensuring a sufficient thickness to effectively cover any holes, pores, or cracks at a rate of 0.75 litre per square meter.

(ii) Second layer – MIXMAT GFM:
The synthetic fibre reinforced mesh, known as Mix mat GFM, will be placed on the wet primer [MIXPRIME AC 100] and left to dry for a duration of 6 to 8 hours. A minimum of 100mm overlap is required at the joints. The Mix mat GFM mesh must meet the technical requirements outlined in the manufacturer's datasheet.
(iii) Third layer – mix prime AC:
In the research report, it is recommended to apply one coat of Mix Prime AC water-based acrylic primer, using undiluted material, over the mesh at a rate of 0.25 Kg/Sqm. The primer should be allowed to dry for 6 hours.
(iv) Fourth layer – mix guard HR (Base coat):
Two coats of Mix Guar HR acrylic-based waterproof and weatherproof coating should be applied at a rate of 0.15 Kg/Sq.m [with undiluted material]. Each coat should be allowed to dry for 6 hours. The second coat should be applied at a right angle to the first coat.
(v) Fifth layer – mix guard HR XTRA (Top coat):
Apply two layers of Mix Guard HR extra acrylic-based fibre reinforced waterproof coating, using undiluted material at a rate of 0.15 Kg/Sqm for each layer. Each layer must be allowed to dry for 6 hours. The film thickness of the second layer must be at least 1500 microns. It is crucial to ensure that the final surface is smooth and uniform, with no visible mesh from the top.

5. Conclusion

Renovating an old church through conventional methods is a meticulous and rewarding process that entails blending historical preservation with structural enhancements to ensure the longevity and continued functionality of the sacred space. The rehabilitation project is designed to uphold the historical significance of the church while addressing its structural deficiencies and functional requirements. This goal is accomplished through the careful application of traditional construction techniques, in conjunction with modern engineering standards.

- A combination of a vibrator breaker and sandblasting was utilized to remove the loose and damaged mortar.
- During the grouting process, lime, cement, and Cebex100 are mixed to fill the voids and cracks.
- To reinforce and stabilize the existing masonry construction of an old church, shear key bars, and wire mesh arrangements can be incorporated by structural engineers and contractors during its rehabilitation. This enhances the structure's resilience to external forces and extends its lifespan for future generations to appreciate and enjoy.
- Lime mortar, made from raw lime and water extract from gallnut and jaggery, can be adjusted to the desired consistency. When rehabilitating an old church, the use of lime mortar offers numerous advantages, such as historical authenticity, compatibility with historic materials, increased durability, breathability, and moisture control. Furthermore, the use of lime mortar simplifies repair and maintenance tasks while also promoting environmental sustainability.
- The domes of the church were restored by applying a high-quality waterproofing and heat insulation system onto the existing roof slab. This system consists of five layers of elastomeric material that is cold-applied and heat-reflective, with a total system thickness ranging from 1500 to 1800 microns.

References

[1] E. L. Qualharini, L. H. C. Oscar, and M. R. Da Silva, "Rehabilitation of buildings as an alternative to sustainability in Brazilian constructions," *Open Engineering*, vol. 9, no. 1, pp. 139–143, 2019, doi: 10.1515/eng-2019-0017.

[2] S. Sandbhor and R. Botre, "A SYSTEMATIC APPROACH TOWARDS RESTORATION OF HERITAGE BUILDINGS-A CASE STUDY," *IJRET: International Journal of Research in Engineering and Technology*, [Online]. Available: http://iscarsah.icomos.org/content/principles].

[3] Y. Kantheepan *et al.*, "Rehabilitation of Historical Building-A Case Study."

[4] S. R. Subramaniam, "A Review on Repair and Rehabilitation of Heritage Buildings," *International Research Journal of Engineering and Technology*, 2016, [Online]. Available: www.irjet.net

[5] J. Radnić, D. Matešan, and A. Abaza, "Restoration and Strengthening of Historical Buildings: The Example of Minceta Fortress in Dubrovnik," *Advances in Civil Engineering*, vol. 2020, 2020, doi: 10.1155/2020/8854397.

[6] U. Department of the Interior National Park Service Technical Preservation Services, "The Secretary of the Interior's Strandards for the Treatment of Historic Properties With Guidelines For Preserving, Rehabilitating, Restoring & Reconscructing Historic Buildings."

[7] T. Yee Sing and S. Yoh, "Rehabilitation Methods and Revitalization Strategies in the Old Inner-City Areas of Rapid Growth Cities in Asia," *Urban and Regional Planning Review*, vol. 3, no. 0, pp. 1–20, 2016, doi: 10.14398/urpr.3.1.

[8] S. Pescari, L. Budău, and C. B. Vîlceanu, "Rehabilitation and restauration of the main façade of historical masonry building –Romanian National Opera Timisoara," *Case Studies in Construction Materials*, vol. 18, Jul. 2023, doi: 10.1016/j.cscm.2023.e01838.

[9] C. Natarajan, S.-E. Chen, and M. Syed, "Rehabilitation and Preservation of the St. Lourdes Church, Tiruchirappalli," *Journal of Performance of Constructed Facilities*, vol. 24, no. 3, pp. 281–288, Jun. 2010, doi: 10.1061/(asce)cf.1943-5509.0000101.

[10] R. C. Mack and J. P. Speweik, "2 PRESERVATION BRIEFS Repointing Mortar Joints in Historic Masonry Buildings."

[11] S. K. Verma, S. S. Bhadauria, and S. Akhtar, "Review of Non-destructive Testing Methods for Condition Monitoring of Concrete Structures," *Journal of Construction Engineering*, vol. 2013, pp. 1–11, Apr. 2013, doi: 10.1155/2013/834572.

[12] L. Binda and C. Maierhofer, "Strategies for the assessment of historic masonry structures."

[13] C. W. Wong, "Applications of Non-destructive Tests for Diagnosis of Heritage Buildings: Case Studies from Singapore and Malaysia."

[14] M. E. Kaplan *et al.*, "Non-destructive Evaluation Techniques for Masonry Construction Preservation Architecture Non-destructive evaluation techniques can be of significant value in historic preservation projects."

[15] B. Yildizlar, B. Sayin, and C. Akcay, "A Case Study on the Restoration of A Historical Masonry Building Based on Field Studies and Laboratory Analyses," *International Journal of Architectural Heritage*, vol. 14, no. 9, pp. 1341–1359, Oct. 2020, doi: 10.1080/15583058.2019.1607625.

[16] G. Kilic, "Condition assessment of different historic bridges using Non Destructive Techniques (NDT) with FTIR analysis in Izmir after the Samos Island earthquake," *Herit Sci*, vol. 10, no. 1, Dec. 2022, doi: 10.1186/s40494-022-00746-x.

[17] B. Tejedor, E. Lucchi, D. Bienvenido-Huertas, and I. Nardi, "Non-destructive techniques (NDT) for the diagnosis of heritage buildings: Traditional procedures and futures perspectives," *Energy and Buildings*, vol. 263. Elsevier Ltd, May 15, 2022. doi: 10.1016/j.enbuild.2022.112029.

[18] G. W. Tuckwell, "NDT of historic buildings using GPR," *Insight: Non-Destructive Testing and Condition Monitoring*, vol. 47, no. 8, pp. 491–493, Aug. 2005, doi: 10.1784/insi.2005.47.8.491.

[19] C. Onuțu, D. Ungureanu, D. N. Isopescu, N. Vornicu, and I. A. Spiridon, "Sourcing Limestone Masonry for the Restoration of Heritage Buildings: Frumoasa Monastery Case Study," *Materials*, vol. 15, no. 20, Oct. 2022, doi: 10.3390/ma15207178.

[20] S. Kröner, M.-T. Doménech-Carbó, and X. Mas-Barberà, "HYDRAULIC LIME MORTAR IN THE AMBIT OF STONE RESTORATION: EVALUATION OF APPLICABILITY," 2010.

[21] A. Moropoulou, P. Noni Maravelaki-Kalaitzaki, and A. Bakolas, "Historic mortar technologies in Crete and guidelines for compatible restoration mortars," 1998. [Online]. Available: https://www.researchgate.net/publication/292408802

Acknowledgment

The author expresses their gratitude to Thiagarajar College of Engineering (TCE) for supporting us to carry out this research work. Also, the financial support from TCE under Thiagarajar Research Fellowship scheme (File.no: TRF/Jul-2023/01) is gratefully acknowledged.

IOP Conference Series: Earth and Environmental Science

PURPOSE-LED PUBLISHING™

PAPER • **OPEN ACCESS**

Experimental Investigation on Reactive Powder Concrete Designed with Micro silica and Alccofine1203

To cite this article: Ahmadshah Abrahimi and V. Bhikshma 2024 *IOP Conf. Ser.: Earth Environ. Sci.* **1409** 012042

View the article online for updates and enhancements.

You may also like

- Effect of High Contain Sustainable Steel Fiber on Properties of Reactive Powder Concrete
N M F Aljalawi
- Behavior of Reinforced Reactive Powder Concrete Two-Way Slabs with Openings
Ola Adel Qasim
- Analytical Equation for Stress-Strain Relationship in compression for Reactive Powder Concrete
Suaad Khaleel I. Al-Fadhli



This content was downloaded from IP address 47.247.77.11 on 27/11/2024 at 05:43

Experimental Investigation on Reactive Powder Concrete Designed with Micro silica and Alccofine1203

Ahmadshah Abrahimi[1*], V. Bhikshma[1]

[1]Department of Civil Engineering, University College of Engineering, Osmania University, Hyderabad, India.

*E-mail: ahmadshah.eng786@yahoo.com

Abstract. This study investigates the incorporation of micro silica and alccofine1203 as supplementary cementitious materials (SCM) in Reactive Powder Concrete (RPC). Optimization of normal RPC mix is performed using the modified Andreassen model by the Elkem Material Mix Analyzer (EMMA), alongside experiments involving 0–30% SCM replacement and different quartz sand size combinations. Rigorous assessments cover compressive strength, density, splitting tensile strength, flexural strength, and flow diameter. The study underscores the effectiveness of the modified Andreassen model and suggests a blend of 10% micro silica and 20% alccofine1203 in RPC under normal curing conditions. The study achieved 127 MPa, 18 MPa, and 10 MPa compressive strength, flexural strength, and splitting tensile strength, respectively, by utilizing a blend of micro silica and alccofine. These values show 5%, 7%, and 9% increments, respectively, compared to the maximum values of only micro silica (20%) and alccofine1203 (20%) mixes. The study also identifies the impact of high-content (>2%) superplasticizer on early strength as well as the role of mixing duration, particularly in low-speed mixers for RPC.

1. Introduction

Rapid advancements in the technology of concrete have given rise to an innovative substance known as Reactive Powder Concrete (RPC). This ultra-high-performance concrete (UHPC) is distinguished by its extraordinary mechanical properties and notable ductility, which are attained using innovative procedures to improve its microstructure [1].

RPC is characterized by high contents of cement (800–1100 kg/m^3) and silica fume (150–300 kg/m^3), which cause some serious consequences [2]. Cement, for example, is unsuitable due to the heat of hydration, which eventually results in thermal cracking caused by a significant temperature difference between an element's surface and inside [3],[4]. Moreover, silica fume is connected with rising prices and scarcity when utilized in large quantities, especially in poor nations [4]. Additionally, silica fume has been shown to have significant impacts on the autogenous shrinkage of concrete caused by internal water consumption during hydration [5]. This causes large internal stresses, which generate micro-cracking and affect the durability of concrete. RPC's low water content makes it more susceptible to autogenous shrinkage than regular concrete [6].

As a result, many investigations tried to employ other materials to partially or completely substitute cement and silica fume. Several materials, including silica fume [7], [8], [9], GGBS

Content from this work may be used under the terms of the Creative Commons Attribution 4.0 licence. Any further distribution of this work must maintain attribution to the author(s) and the title of the work, journal citation and DOI.
Published under licence by IOP Publishing Ltd

[10], [11], [12], fly ash [8], [13], phosphorous slag [14], glass powder [15], limestone powder [16], rice husk ash [17], and white rice husk ash [18], have been used in RPC, and their performances have been investigated.

This study incorporates alccofine1203 and micro silica in conjunction with cement, as well as high-content silica sand (quartz sand) in different sizes. Alccofine1203 has almost similar characteristics to cement, including a higher level of fineness that promotes faster hydration, increased impermeability, and a strong pozzolanic reactivity [10].

Some past studies have investigated alccofine for the production of ultra-high-performance concrete (UHPC). A study [11] discovered that UHPC made from alccofine had higher 28-day compressive strength (132 MPa), flexural strength (31 MPa), and splitting tensile strength (15 MPa) than a control mix that only had silica fume. A blend of alccofine with fly ash was utilized in another study [12] for developing high-strength concrete, which indicates that a 30% replacement of cement with 10% alccofine and 20% fly ash yields higher compressive strength (80 MPa), flexural strength (6 MPa), and splitting tensile strength (6 MPa) compared to control mixtures. Despite prior recommendations advocating a blend of 10% silica fume and 10% alccofine for high-performance concrete, cautionary notes on strength reduction with higher alccofine percentages due to dilution effects are reported [19]. RPC's high binder concentration may result in a limited diluting impact.

Despite existing knowledge, there is a notable scarcity of studies regarding the incorporation of high-content (>20%) alccofine into RPC, particularly blends with micro silica. As a result, the purpose of this research is to look into the fresh and hardened properties of RPC containing high-content alccofine as well as a combination of alccofine and micro silica under normal curing conditions.

2. Materials

This study used grade 53 OPC, which has a specific gravity of 3.11 and a surface area of 2830 cm^2/gr. The accompanying micro silica surface area was determined to be 19886 m^2/kg, with silica content higher than 90 (wt%). For obtaining low W/B ratio, polycarboxylate ether superplasticizer (PCE), specifically “Tam Cem11, was utilized. Cement substitution was carried out utilizing Ultrafine Ground Granulated Blast Furnace Slag (UGGBS), denoted as alccofine1203, possessing a Blaine fineness of 12000 cm^2/g, a specific gravity of 2.86, and particle size distribution parameters: d (0.1) = 1.38 μm, d (0.5) = 4.13 μm, d (0.9) = 11 μm. Additionally, three distinct sizes of quartz sand (QA: 2-400 μm, QB: 4-600 μm, QC: 100-1000 μm) with particle size distributions drawn in Figure 2 were utilized in this study. The chemical composition of RPC ingredients has been detailed in Table 1.

Table 1. Physical properties and chemical composition of RPC ingredients.

Components	Cement	Alccofine (Wt.%)	Micro silica	Quartz Sand
Sio_2	21.03	34.45	98.73	98.1
Fe_2O_3	5.67	0.31	0.07	0.05
Al_2O_3	4.03	13.45	0.1	0.66
CaO	64.19	40.8	0.1	<0.1
MgO	0.88	6.1	0.2	<0.1
SO_3	2.86	2.73	0.1	-
K_2O	0.2	0.31	0.4	<0.1
Na_2O	0.12	0.14	-	<0.1
Loss of Ignition	1.02	-	0.3	-
Specific gravity	3.11	2.86	2.2	2.6

3. Research Method

This research is structured in two distinct phases. In the initial phase RPC proportions were deduced from existing literature, followed by optimization using the Elkem Material Mix Analyzer (EMMA). In the subsequent phase, an experimental program was conducted to investigate the fresh and hardened properties of the RPC, utilize supplementary cementitious materials (alccofine and micro silica) along with various size combinations of quartz sand. A four-stage mixing procedure was followed, as shown in Figure 3.

3.1 Phase-1: Proportions optimization

The initial mix proportions, as outlined in [20], have been fine-tuned to suit locally available materials through the utilization of the Elkem Material Mix Analyzer (EMMA) .

Developed by Elkem Company, EMMA refines mix proportions by leveraging optimal packing density models (Andreassen and modified Andreassen), and incorporating particle size distribution data. In this investigation, modified Andreassen model was used because of finely textured nature of the mix resulting from the presence of fine particles.

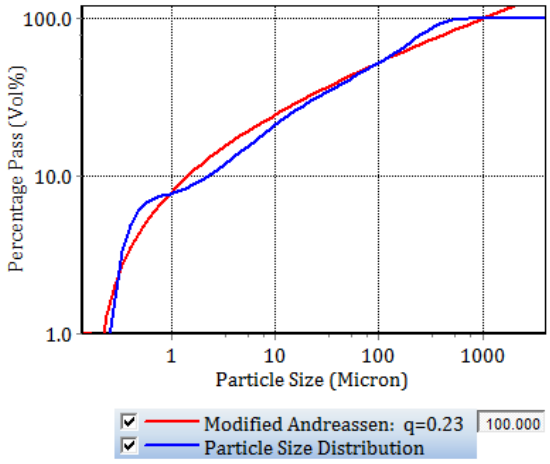


Figure 1. Mix optimization adjusted in EMMA.

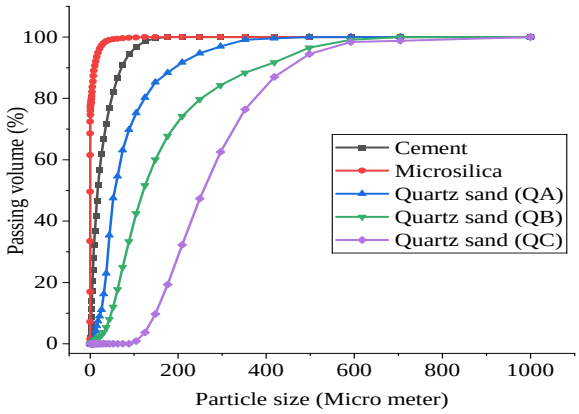


Figure 2. Particle size distribution of ingredients.

This model takes into account both maximum and minimum particle sizes in conjunction with the distribution coefficient "q" as defined by the formula:

$$\text{CPFT}=A=\left(\frac{(d-do)}{(D-d0)}\right)^{q} x100 \quad (1)$$

Where “CPFT” represents the cumulative (volume) percentage finer than, “d” is the particle size, “d_0” is the minimum particle size, “D” is the maximum particle size, and “q” is the distribution coefficient or exponent. The selected exponent "q" was set at 0.23 based on literature [21] due to the very fine particle sizes of ingredients. The optimized curve, derived after adjustment to the particle size distribution in EMMA, is shown in Figure 1, and the resulting proportions are detailed in Table 2.

Where “CPFT” represents the cumulative (volume) percentage finer than, “d” is the particle size, “d_0” is the minimum particle size, “D” is the maximum particle size, and “q” is the distribution coefficient or exponent. The selected exponent "q" was set at 0.23 based on literature [21] due to the very fine particle sizes of ingredients. The optimized curve, derived after adjustment to the particle size distribution in EMMA, is shown in Figure 1, and the resulting proportions are detailed in Table 2.

2.2 Phase-2: Experimental program

Table 2. Mix proportions optimized in EMMA for different w/b ratios.

Mix	Cement (kg/m³)	Micro silica (kg/m³)	W/B Ratio	Quartz Sand (QB) (kg/m³)	Quartz sand (QC) (kg/m³)	Super plasticizer (% of Binders)
A1- 0.18	850	170	0.18	390	690	1.5
B1- 0.20	850	170	0.20	390	690	1.5
C1- 0.22	850	170	0.22	390	690	1.5
D1-0.24	850	170	0.24	390	690	1.5

Stage No.1: Mixing binders in dry form for 2 minutes.	**Stage No.2:** Addition of 80% water with total superplasticizer, mixing for 6 minutes.
Stage No.3: Addition of quartz sand and mixing for 6 minutes.	**Stage No.4:** Add the rest of the 20% water and stir for 6 minutes.

Figure 3. Mixing procedure

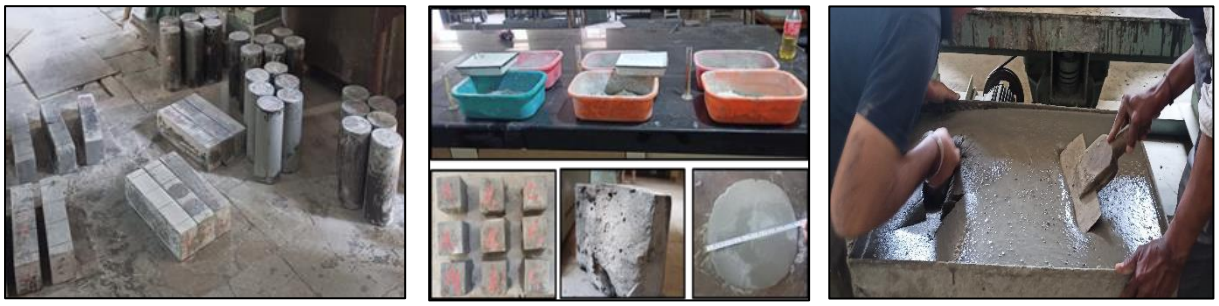


Figure 4. Experimental work photos.

In this phase, an initial investigation was undertaken on the w/b ratio started within the range of 0.18-0.24, as detailed in Table 2**.** Additionally, the mixing procedure, mixing time (15, 20 minutes), and fresh properties were systematically assessed. Subsequently, in the second stage of the experimentation, alccofine1203 was added at varying proportions of 20%, 30% and a blend of 10% micro silica and 20% alccofine. This substitution was carried out in conjunction with different combinations of quartz sand sizes, as delineated in Table 3. A water-to-binder ratio of 0.18 and a superplasticizer dosage of 1% (mass % of binders) were employed. The flow table test was completed according to "ASTM C1437" norms. Specimens of (100x100x100) mm cubes, (150x300) mm cylinders, and (100x100x500) mm prisms were cast for each mix to assess compressive strength, splitting tensile strength, and flexural strength, respectively. Density measurements were obtained after 28 days under surface-dry condition.

Table 3. Mix proportions of RPC incorporating micro silica, alccofine, and combinations of quartz sand.

Mix	Cement (kg/m³)	Supplementary cementitious material (% of cement mass)		Quartz sand (kg/m³)		
		MS (%)	AL (%)	QA	QB	QC
1MS20	850	20	-	390	690	-
2MS20		20	-	-	390	690
3MS20		20	-	430	-	690
1AL20		-	20	430	690	-
2AL20		-	20	-	480	690
3AL20		-	20	480		690

1AL30	-	30	330	690	-
2AL30	-	30	-	370	690
3AL30	-	30	370	-	690
1MS+AL	10	20	300	690	-
2MS+AL	10	20	-	350	690
3MS+AL	10	20	350	-	690

MS; Micro silica, AL; Alccofine1203, SP; Superplasticizer, QA; Quartz sand (2-400μm), QB; Quartz sand (4-600 μm), QC; Quartz sand (100-1000 μm), W/B: water to binder ratio.

3. Results and discussions

3.1 Effect of water to binder ratio

Figure 5 illustrates that a lower water-to-binder ratio (0.18) exhibits superior performance in 28-day compressive strength (110 MPa) and density (2250 kg/m^3) compared to other ratios, however low water-to-binder ratio resulted in a notable decrease in workability. Consequently, an elevated content (up to 2%) of superplasticizer was employed in the initial trials to enhance workability. It is important to note that the excessive use of superplasticizer negatively impacted the early hardening of RPC.

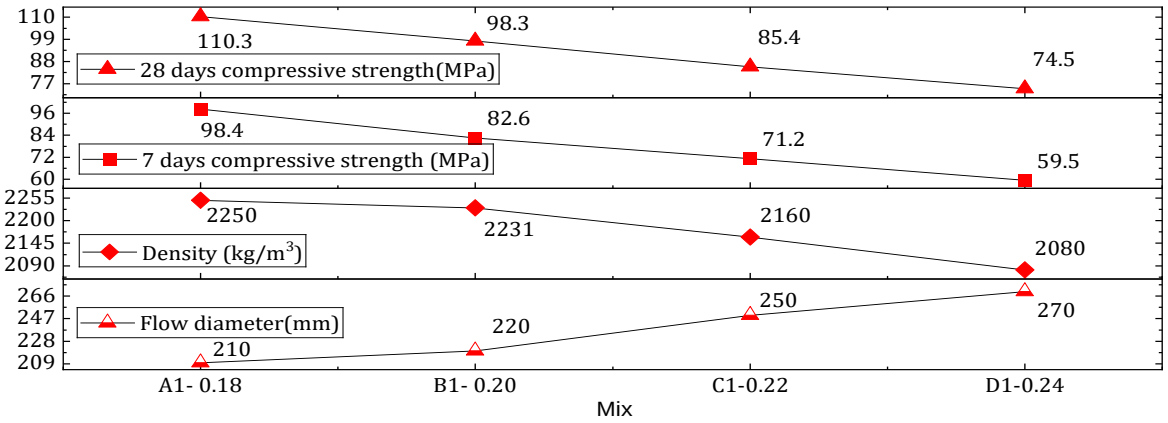


Figure 5. Fresh and hardened properties of RPC mixes adjusted in EMMA for different w/b ratios.

3.2 Density

According to the literature, reactive powder concrete is known for its high density (more than 2200 kg/m^3) which is attributed to its uniformity and compact microstructure. Nevertheless, during the initial trials, the densities exhibited a significant decrease, hence adversely affected the strength characteristics. The discrepancy can be attributed to factors such as increased water content, a slow mixing speed of 25 RPM, and a brief mixing time of 15 minutes, which hindered the efficient homogenization of small particles. These issues were resolved by extending the duration of mixing and utilizing less water.

Mix optimization plays a crucial role in developing a high-density mixture, which significantly affects the overall performance of RPC. The results shown in Figure 6 demonstrate higher densities and better mechanical properties for mixes 2MS20, 2AL20, 2AL30, and 2MS+AL, which were optimized by EMMA. The study also shows that alccofine-based mixes have higher densities and flowability compared to those containing only microsilica, as depicted in Figure 6. The greater specific gravity and glassy surface of alccofine compared to microsilica are the reasons for this attribution.

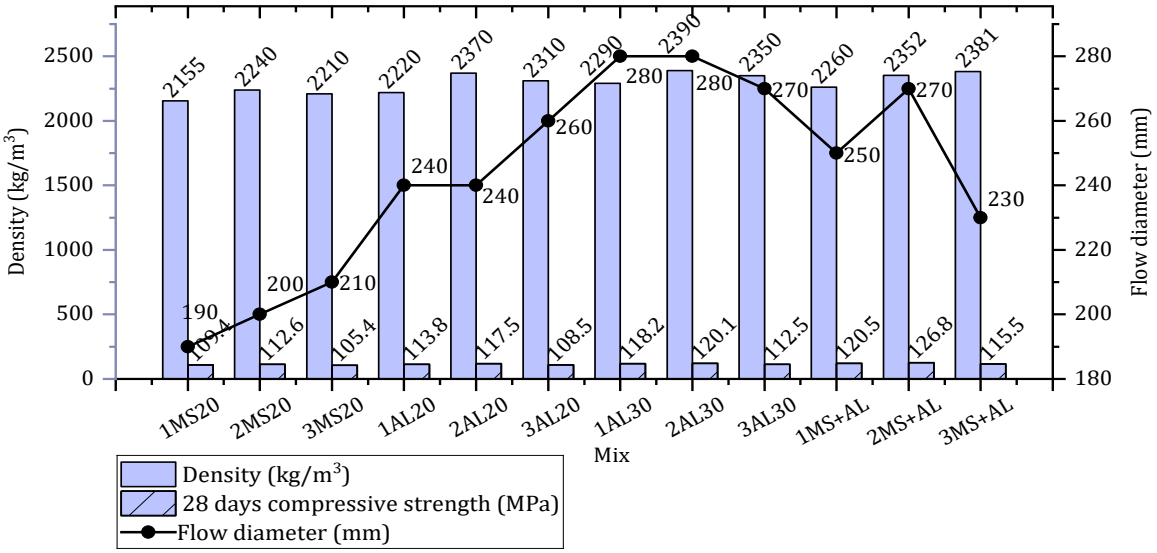


Figure 6. Fresh and hardened properties for microsilica and alccofine based mixes.

3.3 Compressive strength

In Figure 7, the compressive strength (117.5 MPa) goes up by only 4% for the mix with 20% alccofine (2AL20) compared to the same mix with 20% microsilica (2MS20). In addition, the alccofine-based mix (2AL20) gained 96% compressive strength only after 7 days, which is a 5% increment compared to the microsilica-only mix (2MS20). The results indicate higher compressive strength at both 7 and 28 days for the (QB+QC) quartz sand combinations optimized by EMMA. It illustrates the effectiveness of the modified Andreassen model in RPC mix design. Mixing with a blend of 10% microsilica and 20% alccofine (2MS+AL) indicates the highest compressive strength of 127 MPa at 28 days. This shows an 11%, 7%, and 5% increment as compared to the mixes containing 20% microsilica (2MS20), 20% alccofine (2AL20), and 30% alccofine (2AL30), respectively.

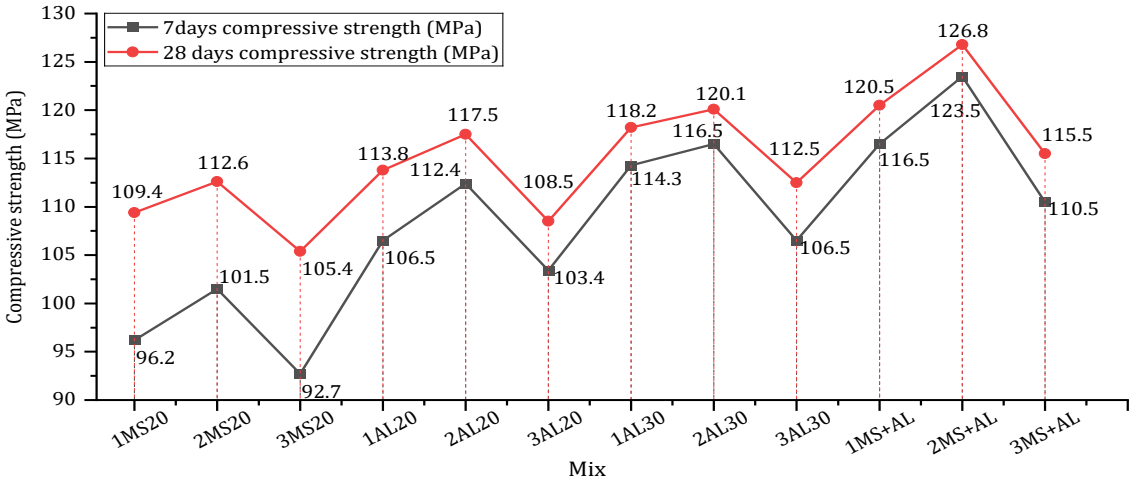


Figure 7. Compressive strength results.

Furthermore, the blended mix reaches 97% of its compressive strength in 7 days, demonstrating early strength growth and rapid hydration. The compressive strength values

between the two time intervals are quite close, which emphasizes the rapid rise in strength. This confirms that mixing alccofine with microsilica is beneficial.

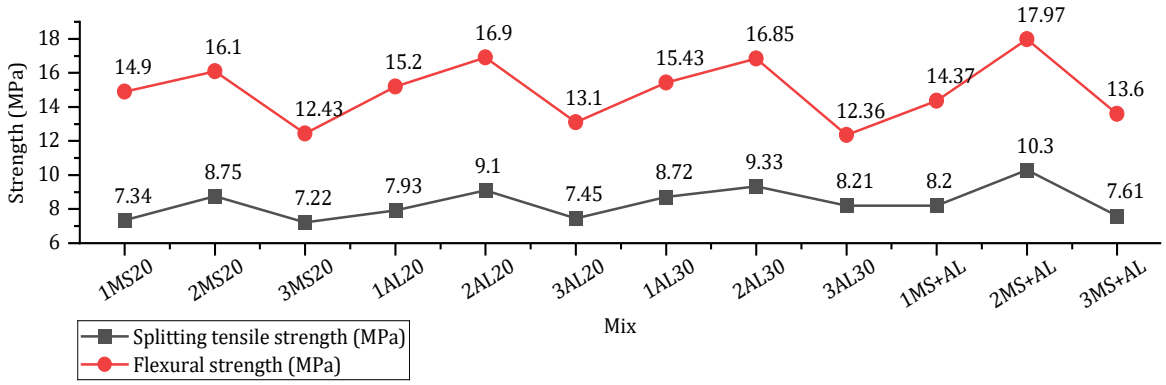


Figure 8. Flexural and splitting tensile strength results.

3.3 Flexural and splitting tensile strength

The results in Figure 8 show better flexural and splitting tensile strengths (16.9 MPa and 7.93 MPa) for the 20% alccofine mix (1AL20) compared to the 20% microsilica mix (1MS20). Nevertheless, there is no substantial alteration in the strength when the alccofine percentage exceedes 20%. The results also show better performance, with a tensile strength of 10.3 MPa and a flexural strength of 17.97 MPa for a mix of 10% alccofine and 20% microsilica. This is the mix that EMMA optimized (2SMS+AL). This represents a significant improvement (10%, 6%, and 7%) in flexural strength and (15%, 12%, and 9%) in tensile strength over the mixes 1AL20, 1MS20, and 2Al30, respectively.

4. Conclusions

From the results and discusions, below findings could be summarized:

- The study demonstrated that the sand size combination (QB+QC) optimized by EMMA had superior strength properties in comparison to other combinations. Furthermore, the use of an optimizing model (Modified Andreassen) greatly contributed to improving RPC strength and density.
- This study also found that a blend of 10% microsilica and 20% alccofine performed well in RPC compared to separate microsilica and alccofine. The mix (2MS+AL) gained an early 7-day compressive strength of 124 MPa as well as a 28-day strength of 127 MPa. The 28-day strength showed 11%, 7%, and 5% increments compared to 2MS20, 2AL20, and 2AL30 mixes, respectively.
- The study confirmed that the same volume of alccofine (20%) gained better early compressive strength (96% of 28-day strength in 7days) and had higher 28-day compressive strength (117 MPa) compared to microsilca mixe (113 MPa). Additionally, the 30% alccofine mix showed the highest flow diameter (280 mm) compared to others.
- High-content alccofine (20 and 30%) improved flexural and tensile properties; however, the blend mix (2MS+AL) gained the highest flexural and splitting tensile strengths (18 MPa and 10 MPa, respectively). It shows a 10% and 15% improvement compared to only the microsilica mix (1MS20), respectively.

- Due to high-content binders and a low water-to-binder ratio, workability is always a challenging task in RPC; therefore, superplasticizer plays a significant role in it. This study found that using a high-content (>2%) superplasticizer could significantly affect early strength development.
- The mixing procedure for reactive powder concrete is another important parameter, particularly with a low-speed mixer. This study found that mixing time (20 minutes) resulted in higher strength characteristics and workability.

References

[1] P. Richard and M. Cheyrezy, "Composition of reactive powder concretes," *Cem. Concr. Res.*, vol. 25, no. 7, pp. 1501–1511, 1995, doi: 10.1016/0008-8846(95)00144-2.

[2] S. Ahmed, Z. Al-dawood, F. Abed, and M. Abdul, "Impact of using different materials , curing regimes , and mixing procedures on compressive strength of reactive powder concrete - A review," *J. Build. Eng.*, vol. 44, no. September, p. 103238, 2021, doi: 10.1016/j.jobe.2021.103238.

[3] K. H. Yang, G. D. Moon, and Y. S. Jeon, "Implementing ternary supplementary cementing binder for reduction of the heat of hydration of concrete," *J. Clean. Prod.*, vol. 112, pp. 845–852, 2016, doi: 10.1016/j.jclepro.2015.06.022.

[4] M. Vigneshwari, K. Arunachalam, and A. Angayarkanni, "Replacement of silica fume with thermally treated rice husk ash in Reactive Powder Concrete," *J. Clean. Prod.*, vol. 188, pp. 264–277, 2018, doi: 10.1016/j.jclepro.2018.04.008.

[5] E. Ghafari, S. A. Ghahari, H. Costa, E. Júlio, A. Portugal, and L. Durães, "Effect of supplementary cementitious materials on autogenous shrinkage of ultra-high performance concrete," *Constr. Build. Mater.*, vol. 127, pp. 43–48, 2016, doi: 10.1016/j.conbuildmat.2016.09.123.

[6] J. Mo, Z. Ou, X. Zhao, J. Liu, and Y. Wang, "Influence of superabsorbent polymer on shrinkage properties of reactive powder concrete blended with granulated blast furnace slag," *Constr. Build. Mater.*, vol. 146, pp. 283–296, 2017, doi: 10.1016/j.conbuildmat.2017.04.105.

[7] D. Mostofinejad, M. R. Nikoo, and S. A. Hosseini, "Determination of optimized mix design and curing conditions of reactive powder concrete (RPC)," *Constr. Build. Mater.*, vol. 123, pp. 754–767, 2016, doi: 10.1016/j.conbuildmat.2016.07.082.

[8] Y. Peng, S. Hu, and Q. Ding, "Preparation of reactive powder concrete using fly ash and steel slag powder," *J. Wuhan Univ. Technol. Mater. Sci. Ed.*, vol. 25, no. 2, pp. 349–354, 2010, doi: 10.1007/s11595-010-2349-0.

[9] H. Yazici, H. Yiğiter, A. Ş. Karabulut, and B. Baradan, "Utilization of fly ash and ground granulated blast furnace slag as an alternative silica source in reactive powder concrete," *Fuel*, vol. 87, no. 12, pp. 2401–2407, 2008, doi: 10.1016/j.fuel.2008.03.005.

[10] A. Nadiger and M. K. Madhavan, "Influence of Mineral Admixtures and Fibers on Workability and Mechanical Properties of Reactive Powder Concrete," *J. Mater. Civ. Eng.*, vol. 31, no. 2, pp. 1–12, 2019, doi: 10.1061/(asce)mt.1943-5533.0002596.

[11] G. Gautham Kishore Reddy and P. Ramadoss, "Influence of Alccofine incorporation on the mechanical behavior of ultrahigh performance concrete (UHPC)," *Mater. Today Proc.*, vol. 33, no. xxxx, pp. 789–797, 2020, doi: 10.1016/j.matpr.2020.06.180.

[12] B. Sagar and M. V. N. Sivakumar, "Mechanical and Microstructure Characterization of Alccofine Based High Strength Concrete," pp. 795–813, 2022.

[13] Z. Wu, C. Shi, and W. He, "Comparative study on flexural properties of ultra-high performance concrete with supplementary cementitious materials under different curing regimes," *Constr. Build. Mater.*, vol. 136, pp. 307–313, 2017, doi: 10.1016/j.conbuildmat.2017.01.052.

[14] Z. Yunsheng, S. Wei, L. Sifeng, J. Chujie, and L. Jianzhong, "Cement & Concrete Composites Preparation of C200 green reactive powder concrete and its static – dynamic behaviors," vol. 30, pp. 831–838, 2008, doi: 10.1016/j.cemconcomp.2008.06.008.

[15] N. A. Soliman and A. Tagnit-Hamou, "Development of ultra-high-performance concrete using glass powder – Towards ecofriendly concrete," *Constr. Build. Mater.*, vol. 125, pp. 600–612, 2016, doi: 10.1016/j.conbuildmat.2016.08.073.

[16] W. Huang, H. Kazemi-Kamyab, W. Sun, and K. Scrivener, "Effect of cement substitution by limestone on the hydration and microstructural development of ultra-high performance concrete (UHPC)," *Cem. Concr. Compos.*, vol. 77, pp. 86–101, 2017, doi: 10.1016/j.cemconcomp.2016.12.009.

[17] H. Huang, X. Gao, H. Wang, and H. Ye, "Influence of rice husk ash on strength and permeability of ultra-high performance concrete," *Constr. Build. Mater.*, vol. 149, pp. 621–628, 2017, doi: 10.1016/j.conbuildmat.2017.05.155.

[18] S. H. Kang, S. G. Hong, and J. Moon, "The use of rice husk ash as reactive filler in ultra-high performance concrete," *Cem. Concr. Res.*, vol. 115, no. September, pp. 389–400, 2019, doi: 10.1016/j.cemconres.2018.09.004.

[19] B. Sankar and P. Ramadoss, "Experimental and Statistical Investigations on Alccofine Based Ternary Blended High- performance Concrete," vol. 35, no. 08, pp. 1629–1640, 2022.

[20] S. Grzeszczyk and G. Janus, "Reactive powder concrete with lightweight aggregates," *Constr. Build. Mater.*, vol. 263, p. 120164, 2020, doi: 10.1016/j.conbuildmat.2020.120164.

[21] R. Yu, P. Spiesz, and H. J. H. Brouwers, "Cement & Concrete Composites Development of an eco-friendly Ultra-High Performance Concrete (UHPC) with efficient cement and mineral admixtures uses," vol. 55, pp. 383–394, 2015, doi: 10.1016/j.cemconcomp.2014.09.024.

IOP Conference Series: Earth and Environmental Science

PURPOSE-LED PUBLISHING™

PAPER • **OPEN ACCESS**

Study on strength and durability characteristics of geopolymer fly ash sand

To cite this article: Pupalwad Arti Sudam *et al* 2024 *IOP Conf. Ser.: Earth Environ. Sci.* **1409** 012043

View the article online for updates and enhancements.

You may also like

- Utilization of River Sand as a Substitution and Addition of Cement to Increase The Shear Strength of Clay Soil
G F Risva, Y Apriyanti and B D A Sandy
- Thermal and durability characteristics of optimized green concrete developed using slag powder and pond ash
Jeyaprakash Maheswaran, Maheswaran Chellapandian, Nakarajan Arunachelam et al.
- Economic and environmental impacts of sand mining activities at sadang river Pinrang Regency, South Sulawesi
Didi Rukmana, Darmawan Salman, Ilham Alimuddin et al.



This content was downloaded from IP address 47.247.77.11 on 27/11/2024 at 05:43

Study on strength and durability characteristics of geopolymer fly ash sand

Pupalwad Arti Sudam[1]*, K. Srinivas[1], V. Ankitha[1], Ch. Nihalini[1], Suresh, Y.N.S.[1] and Chinmay Battini[1]

[1]Department of Civil Engineering, VNR Vignana Jyothi Institute of Engineering & Technology, Hyderabad, Telangana, India

*Email: artisudam_p@vnrvjiet.in

Abstract. As the construction industry undergoes rapid growth, the deteriorating reserves of river sand have emerged as a critical issue, given its essential role in construction activities. The extraction of sand exacerbates this problem, leading to adverse consequences such as riverbank erosion, harm to aquatic ecosystems, and a decline in the water table. To sustain the construction sector, there is an urgent need for alternative sustainable granular materials. However, the durability characteristics of these substitutes in civil engineering applications remain uncertain. This research focuses on developing alternative sustainable granular materials to replace fine aggregates traditionally sourced from river sand. The study aims to demonstrate the preparation of new sustainable granular material using fly ash and compare its properties with those of river sand (RS), highlighting their significance and practical applications in civil engineering. The synthesized artificial fly ash sands are examined extensively for their physical properties (such as specific gravity, water absorption, specific surface area (SSA), and particle size distribution), chemical properties [including pH, electrical conductivity (EC), and total dissolved solids (TDS)], engineering properties [like cohesion (C), angle of shearing resistance(Φ), compression strength, and hydraulic conductivity], and durability properties [covering leaching, lime reactivity, and turbidity]. The previous research experiments have demonstrated that the results of this study hold significant value for professionals in the industry, as well as for academics and researchers. The synthesized geopolymer sand showed a similar strength compared to river sand. Moreover, these findings strengthen the feasibility of utilizing synthetic alternatives to river sand across a range of civil engineering applications.

Keywords: Geopolymer fly ash sand (GFAS), River sand (RS), Strength and durability properties, Fly ash (FA)

1. Introduction

Due to huge construction activities, the demand for river sand has been increasing rapidly causing adverse effects on the environment. Hence, there is a requirement to replace river sand with alternatives that are environmentally sustainable and can meet the future demand for fine aggregates in concrete [1]-[4]. The UNEP report suggests that the global use of aggregates is estimated to be between 25.9 billion and 29.6 billion tons annually. Given the escalating environmental issues and the depletion of natural resources, geopolymer fine aggregates have emerged as a promising alternative to natural aggregates [4]-[6]. In addition to this, In India, the

Content from this work may be used under the terms of the Creative Commons Attribution 4.0 licence. Any further distribution of this work must maintain attribution to the author(s) and the title of the work, journal citation and DOI.
Published under licence by IOP Publishing Ltd

extensive production of fly ash, which is more than 200 million tons per year at present could increase to about 900 million tons per year over the next 20 years [7]. However, only approximately 40% of fly ash is currently utilized for applications like brick block making, pavement construction, cement, and asbestos manufacturing, with the remainder being disposed of in landfills [8],[9]. Fly ash-based geopolymer production involves the mixing of fly ash with an alkaline solution, leading to a process called geopolymerization, which can take place simultaneously. [1],[8],[10].

Many researchers have investigated the incorporation of geopolymer fly ash sand as a substitute for conventional fine aggregate in their concrete mixtures. Experiments were conducted on the pH, water absorption, specific gravity, particle size distribution, direct shear test, and compression test of mortar made with geopolymer fly ash sand (GFAS). The results showed that GFAS mortar achieved nearly identical strength to regular sand mortar after 28 days. Only a few applications of geopolymer fly ash sand as a fine aggregate have been explored in the past [2], [3], [6]. It was suggested that both Class C geopolymer fly ash and Class F geopolymer fly ash have potential as replacements for natural sand in construction activities [4]. These applications include the building of sustainable structures, road construction jointing and repairs, precast concrete production, embankment material, and pipe backfilling material.

This study aims to assess the durability of geopolymer fly ash sand in comparison to natural river sand. In addition, it aimed to figure out the ideal molarity of geopolymer fly ash sand (8M, 10M, and 12M) to substitute conventional granular material as river sand. Investigating the geopolymer fly ash sand's durability qualities in mortar mix can provide important information about how well-suited it is for a variety of applications, such as industrial flooring, pavements, dams, bridges, and highways.

2. Materials employed in the present study

Fly ash sourced from the Singareni thermal power plant, alkaline activators like sodium hydroxide (NaOH) and sodium silicate (Na2SiO3) were used to create geopolymer fly ash sand (GFAS).

To determine the chemical composition of the fly ash, a mixture comprising 4 grams of fly ash and 1 gram of nitrocellulose was prepared using isopropyl alcohol [2]. After being ready, the sample was placed into a small metal dish. An X-ray fluorescence (XRF) analysis was performed, and the results are presented in Table 1, fly ash was classified as class F due to its CaO content of 4.85%, which is below 10% [2]. The sodium hydroxide and sodium silicate used were sourced from a nearby industry, with their specifications detailed in Tables 2 and 3, respectively. The river sand was procured from the local construction industry, and its characteristics are being compared with those of GFAS.

Table 1. Analysis of Fly Ash Chemical Composition

Elements	(% by weight)
SiO_2	58.38
Al_2O_3	23.69
Fe_2O_3	8.80
CaO	4.85
K_2O	2.89
TiO_2	2.70
SO_2	1.48
Others	0.56
LOI	0.07

Table 2. Specifications of Sodium Hydroxide

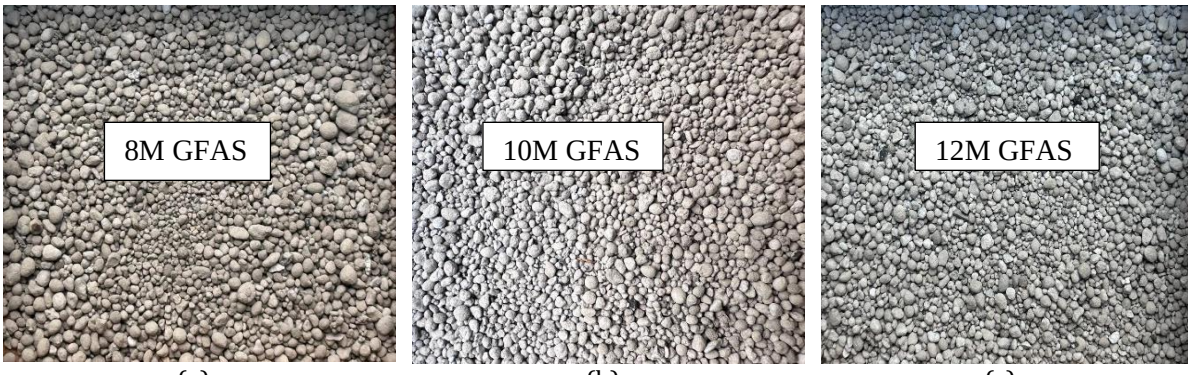
Parameters	Quantity (%)
Minimum assay (Acidmetric)	97%
Carbonate (as Na2CO3)	2%
Chloride (Cl)	0.12%
Sulphate (SO4)	0.04%
Zinc (Zn)	0.02%
Potassium(K)	0.1%
Iron (Fe)	0.006%
Silicate (SiO2)	0.05%

Table 3. Specifications of Sodium silicate

Parameters	Quantity (%)
pH	8 to 14
Assay of Na_2O	7.5-8.5%
Assay (as SiO_2)	25-28%
Weight per ml 20°C	1.35 g/ml

3. Synthesis of GFAS

Geopolymer fly ash sand granules were created by heating fly ash at 100°C to ensure complete dryness. An optimized geopolymer liquid solution, comprising 8M, 10M, and 12M GFAS alkaline activators mixed with sodium silicate and sodium hydroxide in a 1:1 ratio, was thoroughly blended. The fly ash and alkaline activator (geopolymer liquid solution) were mixed in a solid-to-liquid ratio of 3:1 for 15 minutes, resulting in a dry mixture. The granules were then oven-dried at 100°C for 1 hour to complete the polymerization process. Afterward, the oven-dried particles were allowed to cool at room temperature for 24 hours. Subsequently, the granules were sieved through a 4.75mm sieve and subjected to characterization for their physical, chemical, engineering, and durability properties, which were then compared with those of river sand (RS) [2]– [4], [6].



(a) (b) (c)

Figure 1. Geopolymer fly ash sand (a) 8M GFAS (b) 10M GFAS and (c) 12M GFAS

4. Results and discussions

The specific gravity of 8M GFAS,10M GFAS, and 12M GFAS was determined as per [11] and are less than river sand this is due to improper binding during gepolymerization [2]–[4] and is shown in Table 4. The water absorption of GFAS was determined as per [11] which were then compared to

river sand (RS), it may be because of the binding of alkaline activator to fly ash which results in its porous nature [2], [4], [6]. Grain size distribution is done for 8M,10M,12M GFAS, and RS [12] , and results showed that GFAS was classified as Zone I and RS as Zone II. According to [13], the specific surface area of GFAS was performed as per[14] and 10M GFAS reported to be 3.65 m^2/g, which is less than 8MGFAS and 12M GFAS, implying that 10M is the appropriate quantity for gepolymerization of fly ash into granules and like RS and reported in Table 4.

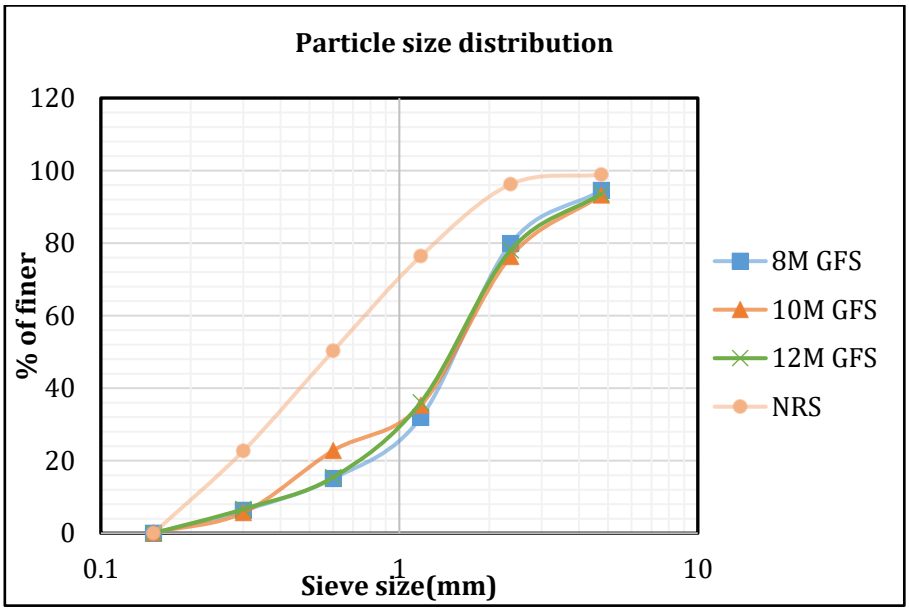


Figure 2. Particle size distribution of 8M,10M,12M GFAS, and RS

Table 4. Properties of GFAS and RS

Parameter	8M GFAS	10M GFAS	12M GFAS	RS
Physical property				
Specific gravity	2.20	2.45	1.80	2.66
Water absorption (1%)	5.34	5.02	5.51	2.57
Specific surface area (m^2/g)	4.58	3.65	4.2	1.21
Sand Classification	Zone I	Zone I	Zone I	Zone II
Chemical property				
pH	11.58	11.69	11.94	7.65
EC (µs/ppm)	59.3	65.8	71.1	32.8
TDS (µs/ppm)	4.2	5.4	6.8	3.8
Turbidity (NTU)	39.7	35.9	28.5	14.1
Engineering property				
Friction angle(ϕ°)	35.75	39.35	38.65	26.01
Cohesion(C)	0.25	0.29	0.36	0.71
Hydraulic conductivity(cm/sec)	0.012	0.013	0.016	0.018

The pH values of GFAS sand, as determined in accordance with [15], are higher compared to RS, attributed to the inclusion of alkaline activator in GFAS, with results presented in Table 5. The

findings indicate that GFAS granules exhibit higher alkalinity (pH=11.58-11.94) due to the incorporation of alkaline activators, in contrast to river sand (pH=7.65). According to [16], the electrical conductivity (EC) of GFAS was measured and reported to be higher (59.3-71.1) compared to RS (32.8) due to the presence of more of dissolved solids, indicating a higher concentration of Total Dissolved Solids (TDS) (4.2-6.8) than RS (3.8) due to the presence of more soluble particles [17]. GFAS displays elevated electrical conductivity and a higher TDS concentration, with results presented in Table 4. A direct shear test was conducted for GFAS and RS to determine the friction angle, as outlined in [18], under normal stresses of 0.5 kPa, 1kPa, and 1.5 kPa, with the samples subjected to shear as depicted in Figure 4. It was perceived that GFAS exhibited excellent friction angle of (35.75°-39.35°) due to the dense packing of granules displaying angularity and could be considered as ideal angular particles in comparison with RS (26.01°) [2]–[4]. The hydraulic conductivity of GFAS (0.01-0.016 cm/sec), conducted in accordance with [19] per the IS code, exhibited similar permeability characteristics to that of RS (0.018 cm/sec). The compressive strength of the cubes was assessed by casting them with dimensions of 70.6 mm x 70.6 mm x 70.6 mm, using a cement: sand ratio of 1:3, with a water-cement (w/c) ratio of 0.45 for river sand mortar and 0.9 for geopolymer fly ash sand mortar [3], [4], [6]. After casting, the cubes were allowed to cure at room temperature before being submerged in tap water for 28 days. Subsequently, compression tests were conducted on each cube at intervals of 3, 7, and 28 days [20]. It was noted that after 28 days of curing, the compressive strength of GFAS surpassed that of RS, as illustrated in Figure 3.

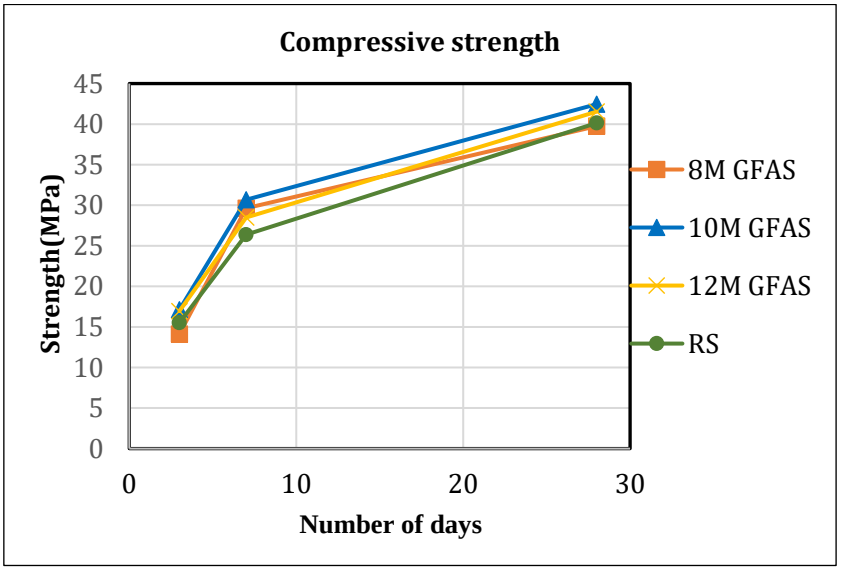


Figure 3. Compressive strength of GFAS and RS

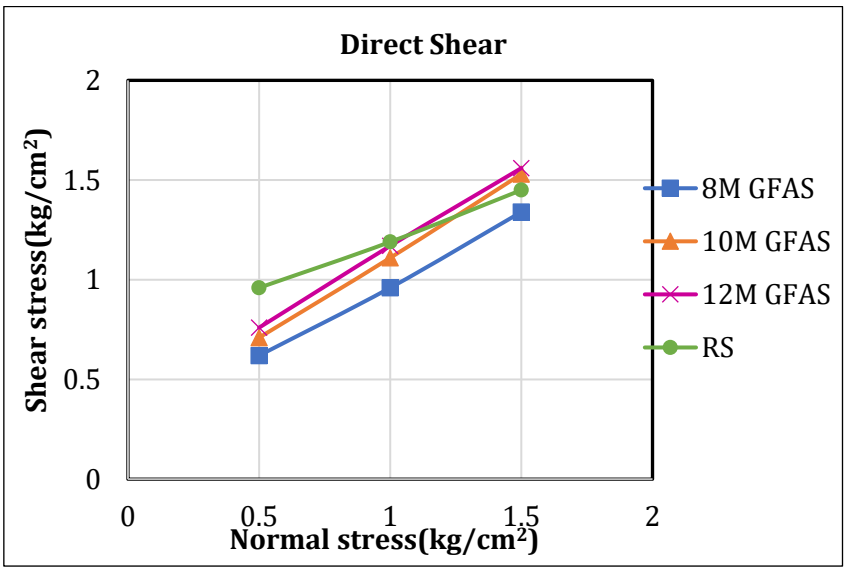


Figure 4. Direct shear test on GFAS and RS

Leaching experiments were performed on 8M,10M, and 12M GFAS in comparison with RS for a time interval of 15 minutes[16], [21]. It was observed that alkaline activators start leaching into the water slowly till 60 minutes of time duration and later it becomes stable implying that there will not be a dissolution of alkaline binders into the water as presented in Figure 5. The pH indicates that the material's leaching behaviour will eventually stabilize. Electrical conductivity values decrease after 60 minutes and become stable demonstrating no further dissolution of ions into water as shown in Figure 6.

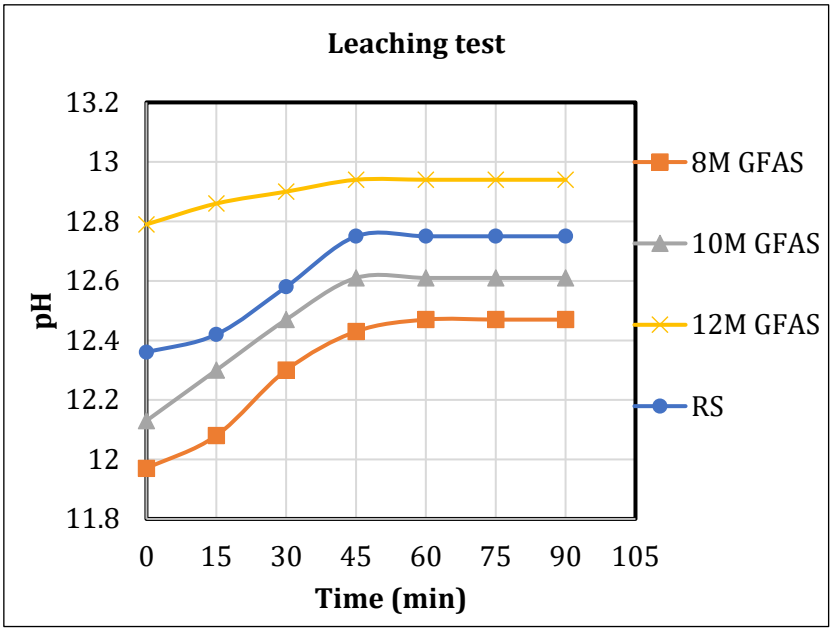


Figure 5. pH variation showing 8M,10M,12M GFAS, and RS

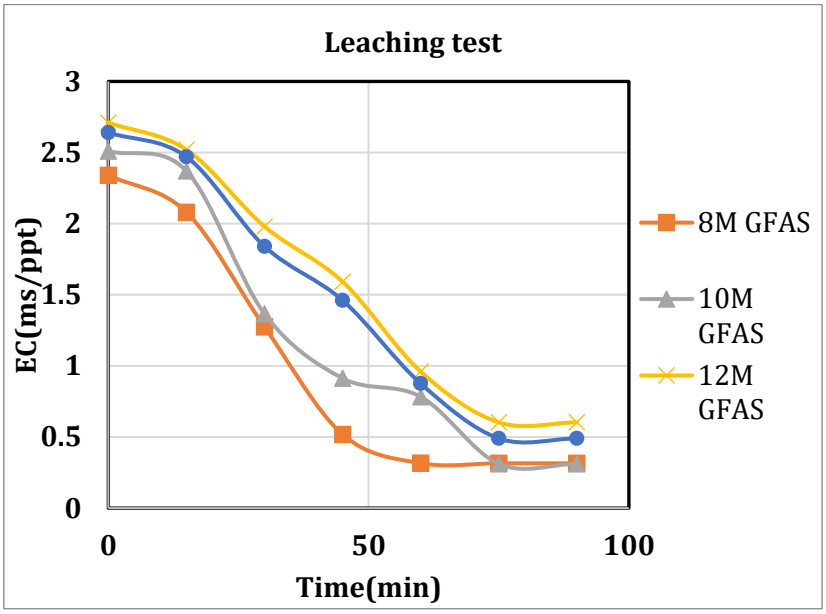


Figure 6. EC variation showing 8M,10M,12M GFAS, and RS

The lime reactivity was evaluated by [22] over time, it was found that the electrical conductivity (EC) values of GFAS decreased while those of RS increased as shown in Figure 7. After thirty to forty minutes, neither substance reacted with lime. Furthermore, with time, GFAS's pH values ascended while RS dropped as shown in Figure 8.

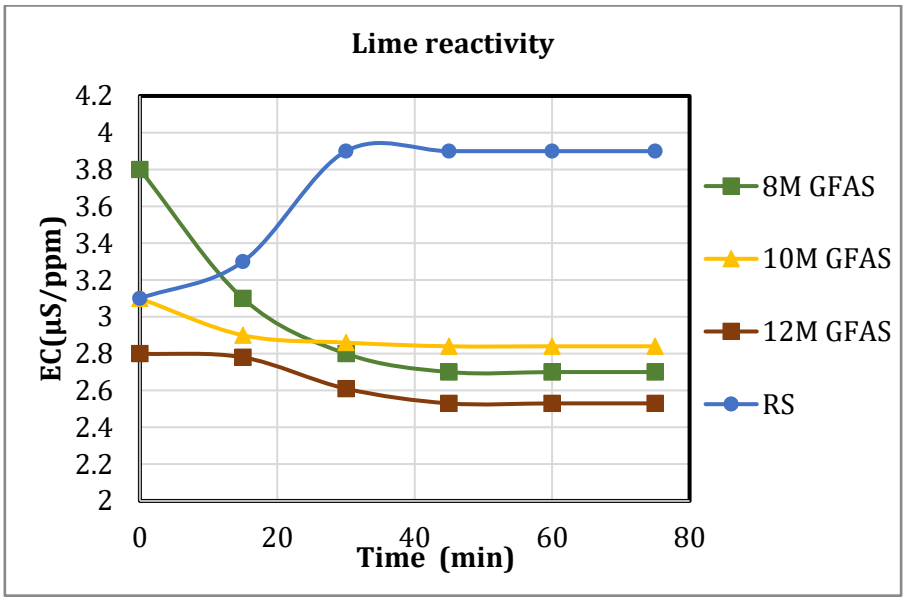


Figure 7. EC variation showing 8M,10M,12M GFAS, and RS

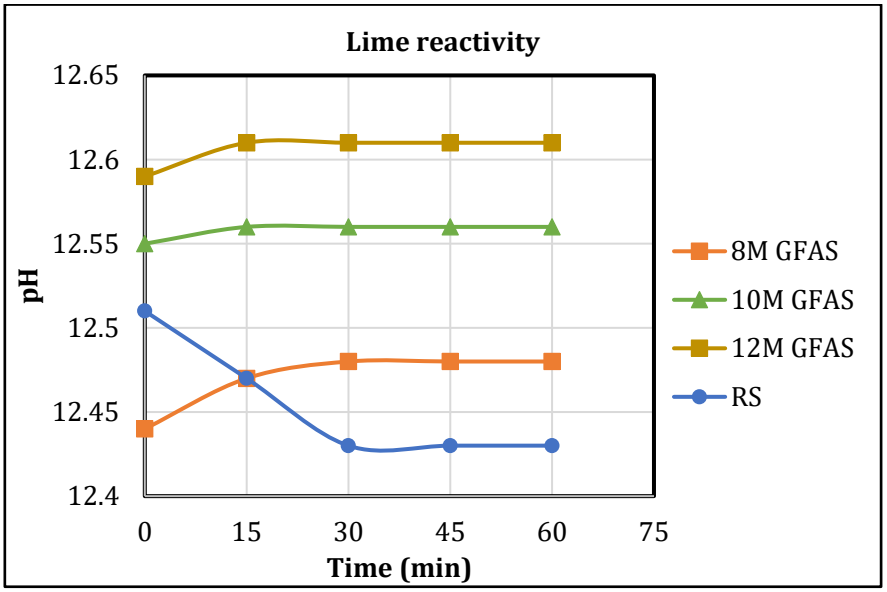


Figure 8. pH variation showing 8M,10M,12M GFAS, and RS

4. Conclusions

GFAS granules with molarities of 8M, 10M, and 12M were prepared by combining fly ash with an alkaline activator in a 3:1 ratio. The physical, chemical, engineering, and durability properties were examined to compare GFAS and RS and determine which molarity among 8M, 10M, and 12M yields the best results. Physical properties such as specific gravity, grain size distribution, water absorption, and specific surface area (SSA) of GFAS and RS were investigated. The specific gravity of 10M GFAS (2.45) was superior to that of 8M GFAS (2.20) and 12M GFAS (1.80) but slightly lower than RS (2.66). The particle size distribution of both GFAS and RS was classified as poorly graded (SP), with Cc values lower than 4. GFAS was categorized as Zone I, while RS was categorized as Zone II. Water absorption for 8M, 10M, and 12M GFAS was 5.34%, 5.02%, and 5.51%, respectively, which exceeded that of RS (2.57%). Water absorption was notably better in 10M GFAS, possibly due to its higher porosity. The specific surface area (SSA) of 10M GFAS (3.65) was the highest among the GFAS granules but surpassed RS (1.21), likely due to the synthesis process increasing SSA.

Chemical properties such as pH, electrical conductivity (EC), total dissolved solids (TDS), and turbidity for GFAS exhibited comparable values with RS. Engineering properties like compressive strength were higher for GFAS compared to RS after 28 days of curing. GFAS granules demonstrated denser packing and greater angle of shearing resistance than RS. Leaching and lime reactivity tests confirmed that synthesized GFAS granules react for one hour without subsequent dissolution of alkaline activators in water. GFAS mortar achieved similar compressive strength to RS mortar after 28 days of curing and may continue to increase over time.

References

[1] D. D. M. Kumar and K. Asha, “Formulation of Fly Ash Geopolymer Sand (FGPS) as a Sustainable Alternative to Natural River Sand,” no. 5, pp. 5–8, 2018.

[2] P. A. Sudam, M. Heeralal, and K. Srinivas, “Strength Characteristics of Geopolymer Synthetic Sand Using Fly Ash,” J. Mater. Civ. Eng., vol. 35, no. 6, 2023, doi: 10.1061/jmcee7.mteng-14200.

[3] U. S. Agrawal, S. P. Wanjari, and D. N. Naresh, “Characteristic study of geopolymer fly ash sand as a replacement to natural river sand,” Constr. Build. Mater., vol. 150, pp. 681–688, 2017, doi: 10.1016/j.conbuildmat.2017.06.029.

[4] S. Parvathy S, A. K. Sharma, and K. B. Anand, "Comparative study on synthesis and properties of geopolymer fine aggregate from fly ashes," Constr. Build. Mater., vol. 198, pp. 359–367, 2019, doi: 10.1016/j.conbuildmat.2018.11.231.
[5] B. Dong, C. Chen, G. Wei, G. Fang, K. Wu, and Y. Wang, "Fly ash-based artificial aggregates synthesized through alkali-activated cold-bonded pelletization technology," Constr. Build. Mater., vol. 344, no. April, p. 128268, 2022, doi: 10.1016/j.conbuildmat.2022.128268.
[6] S. M. Rao and I. P. Acharya, "Synthesis and Characterization of Fly Ash Geopolymer Sand," J. Mater. Civ. Eng., vol. 26, no. 5, pp. 912–917, 2014, doi: 10.1061/(asce)mt.1943-5533.0000880.
[7] Y. Sato, "Fly Ash as an Attractive Material," Concr. J., vol. 56, no. 3, pp. 260–260, 2018, doi: 10.3151/coj.56.3_260.
[8] A. Yousuf, S. O. Manzoor, M. Youssouf, Z. A. Malik, and K. Sajjad Khawaja, "Fly Ash: Production and Utilization in India-An Overview," J. Mater. Environ. Sci, vol. 2020, no. 6, pp. 911–921, 2020.
[9] A. Kumar and D. Kumar, "Use of Sintered Fly Ash Aggregates as Coarse Aggregate in Concrete," Int. J. Civ. Eng., vol. 1, no. 4, pp. 13–19, 2014, doi: 10.14445/23488352/ijce-v1i4p103.
[10] A. T and J. A, "Experimental Study on Mechanical Properties of Sintered Fly Ash Aggregate in Concrete," Int. J. Trend Sci. Res. Dev., vol. Volume-3, no. Issue-3, pp. 203–215, 2019, doi: 10.31142/ijtsrd21679.
[11] IS 2386- Part III, "Method of Test for aggregate for concrete. Part III- Specific gravity, density, voids, absorption and bulking," Bur. Indian Stand. New Delhi, p. (Reaffirmed 2002), 1963.
[12] IS:2720 (Part 4), "Indian Standard, Methods of Test for Soils, Part 4: Grain Size Analysis," Bur. Indian Stand. New Delhi, India., vol. Reaffirmed, no. 2006, pp. 1–38, 1985.
[13] IS:383, "Specification for Coarse and Fine Aggregates From Natural Sources for Concrete," Indian Stand., pp. 1–24, 1970.
[14] B. of Indian Standards, "IS 11578 (1986): Method for determination of specific surface area of powder and porous particle using low temperature gas adsorption techniques."
[15] IS:2720 (Part 26), "Indian Standard Method of Test for Soils: Determination of pH Value," pp. 1–10, 1987.
[16] B. 23 Soil Engineering Sectional Committee, "Indian standard determination of the specific electrical conductivity of soils - method of test," Bur. Indian Stand., pp. 1–10, 2000, [Online]. Available: https://law.resource.org/pub/in/bis/S06/is.14767.2000.pdf
[17] IS 3025 (Part 16), "IS 3025-16 (1984): Methods of sampling and test (physical and chemical) for water and wastewater, Filterable residue (total dissolved solids), BIS, New Delhi.," 1984.
[18] I. S. BIS, "2720 Methods of test for soils, Part 13: Direct shear test," Bur. Indian Stand. New Delhi, India., vol. Reaffirmed, no. 2002, pp. 1–12, 1986.
[19] Bureau of Indian Standards, "Methods of test for soils, determination of water content dry density relation using light compaction," IS 2720 (Part VII-1980), pp. 1–16, 2011.
[20] BIS, "Preparation and Use of Masonry Mortar," Bur. Indian Stand. IS 2250, New Delhi, 1981.
[21] B. 23 Soil Engineering Sectional Committee, "Indian Standard Method of tests for soil: Part 26 Determination of pH value," Bur. Indian Stand., pp. 1–14, 2002, [Online]. Available: https://ia801003.us.archive.org/9/items/gov.in.is.2720.26.1987/is.2720.26.1987.pdf
[22] IS: 1727, "Methods of test for pozzolanic materials," Bur. Indian Stand. New Delhi New Delhi, no. February, pp. 1–55, 2013.











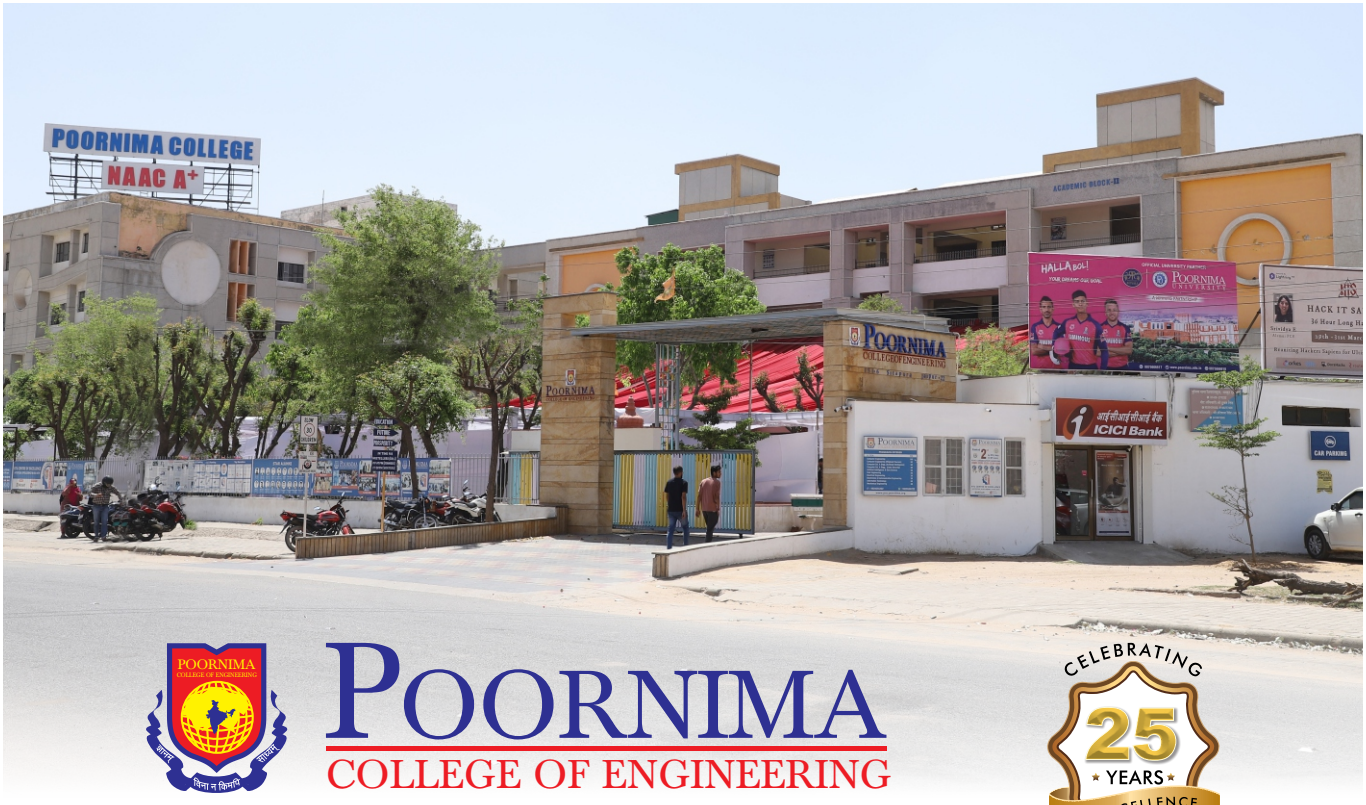




VASAVI COLLEGE OF ENGINEERING, HYDERABAD, INDIA

(Private Un-aided Non-minority Autonomous Institution)
ACCREDITED BY NAAC WITH 'A++' GRADE
Affiliated to Osmania University and Approved by AICTE

44 YEARS OF EXCELLENCE



POORNIMA
COLLEGE OF ENGINEERING

Affiliated to RTU, Kota • Approved by AICTE & UGC under 2(f) • NAAC A+ Accredited

CELEBRATING 25 YEARS OF EXCELLENCE

ISI-6 RIICO Institutional Area, Sitapura, JAIPUR – 302022 (Rajasthan), INDIA
Website: www.pce.poornima.org